ROLE OF BIFIDOBACTERIA IN HUMAN AND ANIMAL HEALTH AND BIOTECHNOLOGICAL APPLICATIONS

EDITED BY: María Esteban-Torres, Douwe Van Sinderen, Gabriele Andrea Lugli, Abelardo Margolles, Lorena Ruiz and Marco Ventura

PUBLISHED IN: Frontiers in Microbiology

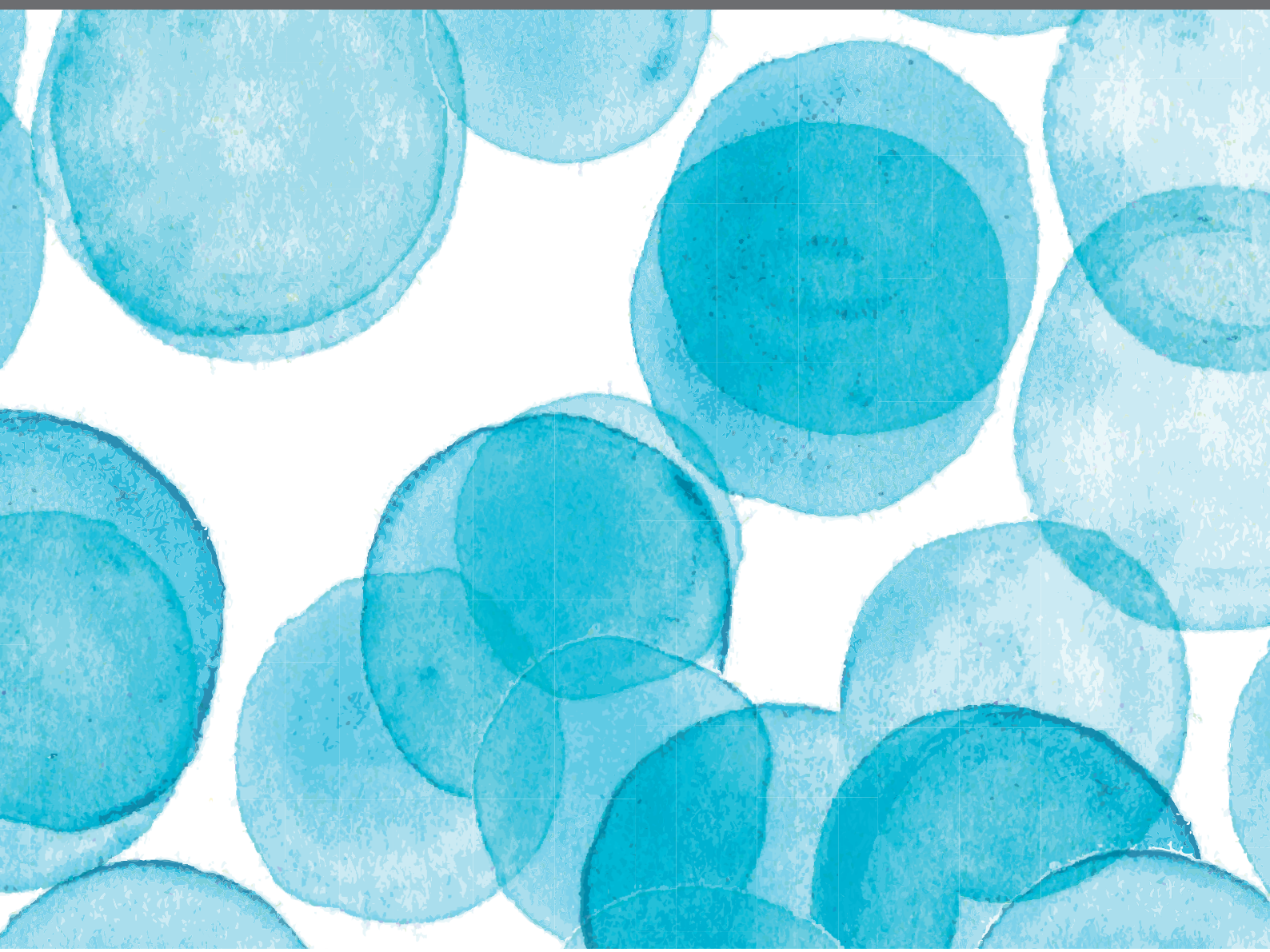

frontiers Research Topics

ISSN 1664-8714
ISBN 978-2-88971-955-6
DOI 10.3389/978-2-88971-955-6

About Frontiers

Frontiers is more than just an open-access publisher of scholarly articles: it is a pioneering approach to the world of academia, radically improving the way scholarly research is managed. The grand vision of Frontiers is a world where all people have an equal opportunity to seek, share and generate knowledge. Frontiers provides immediate and permanent online open access to all its publications, but this alone is not enough to realize our grand goals.

Frontiers Journal Series

The Frontiers Journal Series is a multi-tier and interdisciplinary set of open-access, online journals, promising a paradigm shift from the current review, selection and dissemination processes in academic publishing. All Frontiers journals are driven by researchers for researchers; therefore, they constitute a service to the scholarly community. At the same time, the Frontiers Journal Series operates on a revolutionary invention, the tiered publishing system, initially addressing specific communities of scholars, and gradually climbing up to broader public understanding, thus serving the interests of the lay society, too.

Dedication to Quality

Each Frontiers article is a landmark of the highest quality, thanks to genuinely collaborative interactions between authors and review editors, who include some of the world's best academicians. Research must be certified by peers before entering a stream of knowledge that may eventually reach the public - and shape society; therefore, Frontiers only applies the most rigorous and unbiased reviews.
Frontiers revolutionizes research publishing by freely delivering the most outstanding research, evaluated with no bias from both the academic and social point of view. By applying the most advanced information technologies, Frontiers is catapulting scholarly publishing into a new generation.

What are Frontiers Research Topics?

Frontiers Research Topics are very popular trademarks of the Frontiers Journals Series: they are collections of at least ten articles, all centered on a particular subject. With their unique mix of varied contributions from Original Research to Review Articles, Frontiers Research Topics unify the most influential researchers, the latest key findings and historical advances in a hot research area! Find out more on how to host your own Frontiers Research Topic or contribute to one as an author by contacting the Frontiers Editorial Office: frontiersin.org/about/contact

ROLE OF BIFIDOBACTERIA IN HUMAN AND ANIMAL HEALTH AND BIOTECHNOLOGICAL APPLICATIONS

Topic Editors:
María Esteban-Torres, University College Cork, Ireland
Douwe Van Sinderen, University College Cork, Ireland
Gabriele Andrea Lugli, University of Parma, Italy
Abelardo Margolles, Spanish National Research Council (CSIC), Spain
Lorena Ruiz, Institute of Dairy Products of Asturias, Spain
Marco Ventura, University of Parma, Italy

Citation: Esteban-Torres, M., Van Sinderen, D., Lugli, G. A., Margolles, A., Ruiz, L., Ventura, M., eds. (2021). Role of Bifidobacteria in Human and Animal Health and Biotechnological Applications. Lausanne: Frontiers Media SA. doi: 10.3389/978-2-88971-955-6

Table of Contents

frontiers in Microbiology

EDITORIAL
published: 08 November 2021
doi: 10.3389/fmicb.2021.785664

Editorial: Role of Bifidobacteria in Human and Animal Health and Biotechnological Applications

Maria Esteban-Torres[1*†], *Lorena Ruiz*[2,3], *Gabriele Andrea Lugli*[4,5], *Marco Ventura*[4,5], *Abelardo Margolles*[2,3] *and Douwe van Sinderen*[1*]

[1] School of Microbiology, APC Microbiome Ireland, University College Cork, Cork, Ireland, [2] Department of Microbiology and Biochemistry, Institute of Dairy Products of Asturias, IPLA-CSIC, Villaviciosa, Spain, [3] Functionality and Ecology of Beneficial Microbes (MicroHealth) Group, Instituto de Investigación Sanitaria del Principado de Asturias, Oviedo, Spain, [4] Laboratory of Probiogenomics, Department of Chemistry, Life Sciences and Environmental Sustainability, University of Parma, Parma, Italy, [5] Microbiome Research Hub, University of Parma, Parma, Italy

OPEN ACCESS

Edited by:
Giovanna Suzzi,
University of Teramo, Italy

Reviewed by:
Paola Mattarelli,
University of Bologna, Italy

***Correspondence:**
Maria Esteban-Torres
m.esteban@iata.csic.es
Douwe van Sinderen
d.vansinderen@ucc.ie

†Present address:
Maria Esteban-Torres,
Department of Biotechnology, Institute of Agrochemistry and Food Technology, National Research Council (IATA-CSIC), Valencia, Spain

Specialty section:
This article was submitted to Food Microbiology, a section of the journal Frontiers in Microbiology

Received: 29 September 2021
Accepted: 20 October 2021
Published: 08 November 2021

Citation:
Esteban-Torres M, Ruiz L, Lugli GA, Ventura M, Margolles A and van Sinderen D (2021) Editorial: Role of Bifidobacteria in Human and Animal Health and Biotechnological Applications. Front. Microbiol. 12:785664. doi: 10.3389/fmicb.2021.785664

Keywords: probiotics, bifidobacteria, gut microbiome, prebiotics, biotechnology

Editorial on the Research Topic

Role of Bifidobacteria in Human and Animal Health and Biotechnological Applications

The gut microbiota is a dynamic community playing a key role in maintaining and supporting host health (Zheng et al., 2020). The interactions between the gut microbiota and the host are complex and perturbations by different causes may result in a variety of diseases including infections, inflammatory bowel disease, metabolic syndrome, neurodegenerative disorders and malignancy (Zheng et al., 2020). In humans, members of *Bifidobacterium* genus are among the most abundant colonizers of the gut of healthy infants (Milani et al., 2017) and persist throughout adulthood at lower relative abundance with a further reduction in the elderly (Arboleya et al., 2016).

Certain bifidobacterial strains with purported health-promoting properties in the host are being commonly used as probiotics. These benefits include protection against pathogens, modulation of the host immune system, provision of nutrients and vitamins, among various other reported beneficial activities (O'Callaghan and van Sinderen, 2016; Wong et al., 2020). Based on these findings, it seems clear that the complex interactions between human host and bifidobacteria play a key role in health and disease.

The present Research Topic entitled "*Role of Bifidobacteria in Human and Animal Health and Biotechnological Applications*" is comprised of 11 articles. These scientific articles expand our knowledge on the interactions of bifidobacteria (and their metabolites) with its host, and their application as probiotics to improve human and animal health. Here, we summarize some of the scientific highlights of the articles published in this special issue.

Bifidobacteria metabolize a variety of complex carbohydrates that through their metabolic end products also provide nutrients to the host. This remarkable metabolic behavior reflects the importance of carbohydrate utilization as part of bifidobacterial gut colonization and persistence. The current knowledge of bifidobacterial carbohydrate metabolism is reviewed, with a focus on plant poly-/oligosaccharide degradation (Kelly et al.). Many so-called non-digestible glycans specifically stimulate growth of particular bifidobacterial strains and/or species. Among them, galacto-oligosaccharides (GOS) are widely used as prebiotics in infant nutrition. Ambrogi et al. showed that the enzyme BgaE, from *Bifidobacterium longum* subsp. *longum* NCIMB 8809, is suitable for *in vitro* GOS synthesis using lactose as the starting substrate. This work highlights the potential of bifidobacterial enzymes to be exploited for the development of dietary prebiotics.

Another feature of bifidobacterial metabolism with potentially important health implications is the *in situ* production of vitamins. Solopova et al. applied comparative genomics and phylogenomic analysis to investigate the acquisition and distribution of riboflavin (vitamin B2) biosynthesis-associated genes across the genus *Bifidobacterium*. The authors generated spontaneous riboflavin-overproducing variants of *Bifidobacterium longum* subsp. *infantis* ATCC 15697, which were also shown to increase vitamin B_2 concentration in a fecal fermentation system, thereby providing promising data for application of this isolate as a functional food ingredient.

Commensal bacteria colonize the gut and by doing so offer protection against pathogens. Mechanisms of gastrointestinal protection by probiotic bacteria against infection involve modulation of intestinal epithelial barrier function. The application of trans-epithelial electrical resistance (TEER) has been used by Yuan et al. to evaluate the effect of bifidobacteria on intestinal epithelial layers when damaged by pathogenic *Escherichia coli*.

The production of extracellular layers, such as exopolysaccharide (EPS), by certain bifidobacteria taxa, allows them to overcome gastrointestinal challenges and to persist for longer periods in the gut (Hidalgo-Cantabrana et al., 2014). EPS produced by bacteria with probiotic traits has been associated with protective immunomodulatory effects (Delgado et al., 2020). In this context, some of the mechanisms underpinning the involvement of bifidobacterial EPS in immune cell response were investigated in more detail by Hickey et al.

Alterations in gut bacteria and their metabolites on several inflammatory and immune processes have been associated with carcinogenesis and tumor etiology (Fong et al., 2020). The current development of microbiome-based therapies has focused on the role of particular bifidobacterial species in cancer immunotherapy as reviewed here (Longhi et al.).

Probiotics are believed to become a potent tool to modify the composition of the gut microbiome and to benefit host health in multiple ways. As part of this Research Topic, several papers discuss the use of bifidobacterial strains as probiotics. For example, the use of *Bifidobacterium bifidum* JCM 1254 to treat antibiotic-induced dysbiosis was studied (Ojima et al.). The administration of the bifidobacterial strain resulted in the reduction of gut inflammation in mice without recovering gut microbiome diversity. This positive effect in the gut only occurs when proinflammatory species-induced gut inflammation (Ojima et al.).

To exert a probiotic effect, a bacterial strain may need to colonize and persist in the host. In the clinical trial carried out by Horigome et al. in low birth weight infants, the oral administration of *Bifidobacterium breve* M-16V allowed its gut colonization for several weeks post-administration and appeared to improve gut microbiota formation. In addition, bifidobacteria isolated from dogs were characterized *in vitro* and *in vivo* for potential use to support canine health (Jang et al.).

The period immediately following birth is crucial for the appropriate development of the gut microbiota and infant development (Turroni et al., 2020). In recent years, scientific efforts have tried to explain how commensal bacteria are established in the infant gut. Breast milk is a factor driving the transfer of functionally important commensal bacteria from mother to infant, specially *Bifidobacterium* species that efficiently colonize the infant gut. Yan et al. explored the co-occurrence of *Bifidobacterium* phylotypes in mother–breast milk–infant triads. The authors describe that the *gro*EL gene is an effective target for in depth resolution of *Bifidobacterium* communities. This approach allowed the assignment of *Bifidobacterium* phylotypes in mother–infant pairs.

To shed light on probiotic features and gut adaptation of bifidobacteria more mechanistic and functional analysis are needed through embracing different "omics" approaches in combination with novel/existing molecular tools, technologies and models. Members of the genus *Bifidobacterium* are notoriously recalcitrant to genetic manipulation due to presence of Restriction-Modification (R-M) systems. In this regard, a novel genetic tool for bifidobacterial targeted mutagenesis, based on a synthetic vector (pFREM28) lacking known *B. breve* R-M motifs, was described and validated by Hoedt et al.. This approach can be applied to design synthetic plasmids to target other genetically inaccessible bifidobacterial species. Additionally, an adapted plasmid expressing mCherry with OVA (pMG-mCherry-OVA) for bifidobacteria was developed to study bifidobacterial-host interactions in both *in vitro* and *in vivo* studies (Hickey et al.).

In summary, the integration of various approaches to determine the presence and functionality of bifidobacteria in the gut are crucial to improve our understanding of the complex interactions between the human (gut) and (health-promoting) bifidobacteria. Future probiotic interventions directed to modulate gut microbiota will lead to "next-generation" probiotic bifidobacterial strains in functional food and nutraceutical industries.

AUTHOR CONTRIBUTIONS

MET and DS wrote and edited the manuscript. All authors have made substantial contributions to the article and approved the manuscript for publication.

FUNDING

DS and MET are members of APC Microbiome Ireland, which is a research center funded by the Science Foundation Ireland (SFI), through the Irish Government's National Development Plan. The authors and their work were supported by SFI (Grant SFI/12/RC/2273), Irish Research Council Postdoctoral Fellowship (GOIPD/2017/1302) and MSCA-IF (Grant number 898088). LR has received funding from the Spanish State Research Agency RTI2018-095021-J-I00 (funded by MCIU/AEI/FEDER, UE).

ACKNOWLEDGMENTS

The editors would like to thank the authors for their contributions, and all the reviewers for their effort, expertise and constructive suggestions that significantly contributed to the quality of this Research Topic.

REFERENCES

Arboleya, S., Watkins, C., Stanton, C., and Ross, R.P. (2016). Gut bifidobacteria populations in human health and aging. *Front. Microbiol.* 7:1204. doi: 10.3389/fmicb.2016.01204

Delgado, S., Sánchez, B., Margolles, A., Ruas-Madiedo, P, and Ruiz, L. (2020). Molecules produced by probiotics and intestinal microorganisms with immunomodulatory activity. *Nutrients* 12:391. doi: 10.3390/nu12020391

Fong, W., Li, Q., and Yu, J. (2020). Gut microbiota modulation: a novel strategy for prevention and treatment of colorectal cancer. *Oncogene* 39, 4925–4943. doi: 10.1038/s41388-020-1341-1

Hidalgo-Cantabrana, C., Sánchez, B., Milani, C., Ventura, M., Margolles, A., and Ruas-Madiedo, P. (2014). Genomic overview and biological functions of exopolysaccharide biosynthesis in *Bifidobacterium* spp. *Appl. Environ. Microbiol.* 80, 9–18. doi: 10.1128/AEM.02977-13

Milani, C., Durante, S., Bottacini, F., Casey, E., Turroni, F., Mahony, J., et al. (2017). The first microbial colonizers of the human gut: composition, activities, and health implications of the infant gut microbiota. *Microbiol. Mol. Biol. Rev.* 81, e00036–e00017. doi: 10.1128/MMBR.00036-17

O'Callaghan, A., and van Sinderen, D. (2016). Bifidobacteria and their role as members of the human gut microbiota. *Front. Microbiol.* 7:925. doi: 10.3389/fmicb.2016.00925

Turroni, F., Milani, C., Duranti, S., Lugli, G. A., Bernasconi, S., and Margolles, A. (2020). The infant gut microbiome as a microbial organ influencing host well-being. *Ital. J. Pediatr.* 46:16. doi: 10.1186/s13052-020-0781-0

Wong, CB., Odamaki, T., and Xiao, J.Z. (2020). Insights into the reason of Human-Residential Bifidobacteria (HRB) being the natural inhabitants of the human gut and their potential health-promoting benefits. *FEMS Microbiol. Rev.* 44, 369–385. doi: 10.1093/femsre/fuaa010

Zheng, D., Liwinski, T., and Elinav, E. (2020). Interaction between microbiota and immunity in health and disease. *Cell Res.* 30, 492–506. doi: 10.1038/s41422-020-0332-7

Conflict of Interest: The authors declare that the research was conducted in the absence of any commercial or financial relationships that could be construed as a potential conflict of interest.

Publisher's Note: All claims expressed in this article are solely those of the authors and do not necessarily represent those of their affiliated organizations, or those of the publisher, the editors and the reviewers. Any product that may be evaluated in this article, or claim that may be made by its manufacturer, is not guaranteed or endorsed by the publisher.

frontiers in Microbiology

ORIGINAL RESEARCH
published: 18 June 2020
doi: 10.3389/fmicb.2020.01349

Bifidobacterium bifidum Suppresses Gut Inflammation Caused by Repeated Antibiotic Disturbance Without Recovering Gut Microbiome Diversity in Mice

Miriam N. Ojima[1], Aina Gotoh[1]*, Hiromi Takada[1], Toshitaka Odamaki[2], Jin-Zhong Xiao[2], Toshihiko Katoh[1] and Takane Katayama[1]*

[1] Division of Integrated Life Science, Graduate School of Biostudies, Kyoto University, Kyoto, Japan, [2] Next Generation Science Institute, Morinaga Milk Industry Co., Ltd., Zama, Japan

OPEN ACCESS

Edited by:
Zhongtang Yu,
The Ohio State University,
United States

Reviewed by:
Elena Igorevna Ermolenko,
Institute of Experimental Medicine (RAS), Russia
Jeff David Galley,
The Ohio State University,
United States

***Correspondence:**
Miriam N. Ojima
ojima.nozomi.78a@st.kyoto-u.ac.jp
Aina Gotoh
aina.g1985@gmail.com

Specialty section:
This article was submitted to Microbial Symbioses, a section of the journal Frontiers in Microbiology

Received: *02 February 2020*
Accepted: *26 May 2020*
Published: *18 June 2020*

Citation:
Ojima MN, Gotoh A, Takada H, Odamaki T, Xiao J-Z, Katoh T and Katayama T (2020) Bifidobacterium bifidum Suppresses Gut Inflammation Caused by Repeated Antibiotic Disturbance Without Recovering Gut Microbiome Diversity in Mice. Front. Microbiol. 11:1349. doi: 10.3389/fmicb.2020.01349

The gut microbiome is a dynamic community that significantly affects host health; it is frequently disturbed by medications such as antibiotics. Recently, probiotics have been proposed as a remedy for antibiotic-induced dysbiosis, but the efficacy of such treatments remains uncertain. Thus, the effect of specific antibiotic-probiotic combinations on the gut microbiome and host health warrants further research. We tested the effect vancomycin, amoxicillin, and ciprofloxacin on mice. Antibiotic administration was followed by one of the following recovery treatments: *Bifidobacterium bifidum* JCM 1254 as a probiotic (PR); fecal transplant (FT); or natural recovery (NR). Each antibiotic administration and recovery treatment was repeated three times over 9 weeks. We used the Shannon Index and Chao1 Index to determine gut microbiome diversity and assessed recovery by quantifying the magnitude of microbial shift using the Bray-Curtis Index of Dissimilarity. We determined the community composition by sequencing the V3–V4 regions of the 16S ribosomal RNA gene. To assess host health, we measured body weight and cecum weight, as well as mRNA expression of inflammation-related genes by reverse-transcription quantitative PCR. Our results show that community response varied by the type of antibiotic used, with vancomycin having the most significant effects. As a result, the effect of probiotics and fecal transplants also varied by antibiotic type. For vancomycin, the first antibiotic disturbance substantially increased the relative abundance of inflammatory species in the phylum Proteobacteria, such as *Proteus*, but the effect of subsequent disturbances was less pronounced, suggesting that the gut microbiome is affected by past disturbance events. Furthermore, although gut microbiome diversity did not recover, probiotic supplementation was effective in limiting cecum size enlargement and colonic inflammation caused by vancomycin. However, for amoxicillin and ciprofloxacin, the relative abundances of proinflammatory species were not greatly affected, and consequently, the effect of probiotic supplementation on community structure, cecum weight, and expression of inflammation-related genes was comparatively negligible.

These results indicate that probiotic supplementation is effective, but only when antibiotics cause proinflammatory species-induced gut inflammation, suggesting that the necessity of probiotic supplementation is strongly influenced by the type of disturbance introduced to the community.

Keywords: gut microbiome, *Bifidobacterium bifidum*, probiotics, antibiotic disturbance, vancomycin

INTRODUCTION

The ecological balance maintained by the gut microbial community is significant in establishing and maintaining host health. Previous studies show strong relationships between the gut microbiome and the host's metabolism (reviewed by Rowland et al., 2018), nutrition (Yatsunenko et al., 2012), and immune function (Round and Mazmanian, 2009; Kau et al., 2011). On the other hand, dysbiosis, or a disturbance in the healthy microbiome, is linked to a variety of health issues such as obesity (Ley et al., 2005), diabetes (Qin et al., 2012; Kostic et al., 2015), asthma (Stokholm et al., 2018), and inflammatory bowel disease (IBD) (Petersen and Round, 2014). Though relatively stable over time (Faith et al., 2013), the gut microbiome experiences frequent disturbance, and the long term effects of repeated disturbance remain relatively understudied.

Disturbances to the gut microbiome can be caused by events such as the consumption of a high-fat diet (He et al., 2018), jet lag (Thaiss et al., 2014), and use of medications, especially antibiotics (Theriot et al., 2014). While antibiotics are important in combating diseases caused by pathogenic bacteria, they not only affect the target pathogen, but also the other beneficial and commensal species in the gut (Jernberg et al., 2007). Overuse of antibiotics can also lead to major clinical problems, such as the emergence of antibiotic-resistant strains (Levy and Marshall, 2004), weight gain (Cho et al., 2012; Gerber et al., 2016) and antibiotic-associated diarrhea (Hogenauer et al., 1998; Wiström et al., 2001; Elseviers et al., 2015). Furthermore, repeated antibiotic use has been reported to alter the composition of the gut microbiome long term (Dethlefsen and Relman, 2011).

Recent studies have suggested that the use of probiotics, or live microbes exogenously administered for therapeutic purposes, is a promising remedy for antibiotic-induced dysbiosis (Korpela et al., 2016; Ekmekciu et al., 2017). Probiotics have become increasingly popular — with a compound annual growth rate (CAGR) of 7.0%, the global probiotics market is expected to reach 63 billion USD by 2023 (Global Market Insights, 2016). However, the efficacy of such probiotic remedies remains debated, as many probiotic strains do not remain in the gut long term and are usually shed within 1–2 weeks (reviewed by Suez et al., 2019). Furthermore, a recent study suggested that probiotics may inhibit, rather than promote, recovery, while autologous fecal microbiome transplants were more effective (Suez et al., 2018).

Fecal microbiome transplants (FMT) have been used as a treatment for severe antibiotic-induced dysbiosis (Shahinas et al., 2012) and provide relatively rapid recovery from dysbiosis (Suez et al., 2018). However, despite increasing reports of successful treatments, the methodology is unstandardized (Goldenberg et al., 2018), and challenges for clinical implementation remain. Furthermore, several side effects, such as weight gain and diarrhea, have been reported (Alang and Kelly, 2015). In 2019, a death from an infection caused by *Escherichia coli* strains that produce extended-spectrum β-lactamase (ESBL) after FMT was reported (U.S. Food and Drug Administration, 2019). While recent studies on both probiotics and FMT suggest a therapeutic potential for microbiome-based treatments, studies often report conflicting results, indicating a need for further research.

One of the difficulties with probiotics research is the variety of probiotic strains available, leading to variability in reported results. For example, species in the genus *Bifidobacterium* are often used in probiotic therapies, but purported effects can vary not only at the species level but also at the strain level. When formula-fed infants were given either *Bifidobacterium longum* subspecies *infantis* (*B. infantis*) or *Bifidobacterium animalis* subspecies *lactis*, *B. infantis* was more effective in increasing fecal bifidobacteria and decreasing γ-Proteobacteria due to its superior ability to colonize the infant gut (Underwood et al., 2013). In a study by Gotoh et al. (2018), the addition of different *Bifidobacterium bifidum* strains to fecal cultures increased fecal bifidobacteria, but the ability of *B. bifidum* to increase the prevalence of other bifidobacterial species varied by strain (Katoh et al., 2020).

Many studies utilize a single combination of broad-spectrum antibiotics and pre-made probiotic blends; thus, the effect of specific antibiotic-probiotic combinations remains relatively understudied. The type, intensity, and frequency of disturbance is an important factor that shapes ecological communities and their response to subsequent recovery treatments. Therefore, we introduced a repeated disturbance to the gut microbiome with three types of antibiotics that have different bacterial targets and modes of action: vancomycin, amoxicillin, and ciprofloxacin. As a probiotic, we used *Bifidobacterium bifidum* JCM 1254, an infant-gut associated, altruistic species that extracellularly degrades complex sugars, such as human milk oligosaccharides (HMOs) and mucin *O*-glycans (Gotoh et al., 2018; Katoh et al., 2020). We present here a comparative analysis of the repeated antibiotic disturbance on the gut microbiome and the effect of probiotics on recovery in a lab-controlled experiment using mouse models.

MATERIALS AND METHODS

Animals and Housing

We purchased 40 female C57BL/6 mice from Japan SLC, Inc. (Shizuoka, Japan) at 8–10 weeks of age. Mice were housed individually in polycarbonate cages with bedding and given free access to drinking water and a basal diet, Oriental MF (Oriental

TABLE 1 | Summary of antibiotics used in the experiment.

Antibiotic	Class	Bacterial target	Mode of action	Dosage
Amoxicillin	Penicillin	Moderate spectrum	Inhibition of cell wall biosynthesis	0.22 mg/mL
Ciprofloxacin	Fluoroquinolone	Broad-spectrum, Gram-negatives	Inhibition of DNA replication	0.19 mg/mL
Vancomycin	Glycopeptide	Gram-positives	Inhibition of peptidoglycan synthesis	0.25 mg/mL

TABLE 2 | Treatment groups. Antibiotics were given to mice based on dosages described in **Table 1**.

Treatment group	Antibiotics	Recovery
Control		
A	Amoxicillin	Natural recovery (NR)
AB	Amoxicillin	*B. bifidum* JCM1254 (PR)
AF	Amoxicillin	Fecal transplant (FT; from control)
P	Ciprofloxacin	Natural recovery (NR)
PB	Ciprofloxacin	*B. bifidum* JCM1254 (PR)
PF	Ciprofloxacin	Fecal transplant (FT; from control)
V	Vancomycin	Natural recovery (NR)
VB	Vancomycin	*B. bifidum* JCM1254 (PR)
VF	Vancomycin	Fecal transplant (FT; from control)

Natural recovery groups were administered PBS on each treatment day. Groups given probiotics as a recovery treatment were administered 10^9 CFUs of B. bifidum per day. For fecal transplants, a mixture of fresh feces collected from age-matched control mice were suspended in PBS at a concentration of 40 mg/mL. After vortexing, the mixture was allowed to settle and the supernatant was administered.

Yeast Co., Ltd., Tokyo, Japan), under controlled conditions of humidity (70%), lighting (12-h light/dark cycle), and temperature (22°C). The experiment began after a 2-week acclimation period. The protocols of the experiment were approved by the Kyoto University Animal Experimentation Committee (Lif-K18009 and Lif-K19022). Animal experiments were performed from August 21, 2018, to June 17, 2019.

Antibiotics

Three types of antibiotics, vancomycin hydrochloride (Nacalai Tesque Inc., Kyoto, Japan), amoxicillin (LKT Laboratories, Inc., Minnesota, United States), and ciprofloxacin (LKT Laboratories, Inc., Minnesota, United States) were administered in drinking water for mice to ingest *ad libitum*. Concentrations of each antibiotic were calculated and adjusted for mice based on human dosages suggested by the US Food and Drug Administration (GlaxoSmithKline, 2006; Baxter Healthcare, 2007; Bayer HealthCare, 2017). We selected these antibiotics for their varied spectrum of activity and reported effects on the gut microbiome (**Table 1**).

Experimental Design

Mice were divided into 10 groups (**Table 2**), with one control group and nine different antibiotic-recovery combinations, with four biological replicates per group. We determined the sample size based on power analyses and the resource equation approach (Arifin and Zahiruddin, 2017). Each group received antibiotics (vancomycin, amoxicillin, or ciprofloxacin) in drinking water for 7 days (antibiotics week). After antibiotics were administered, mice were switched to normal water without antibiotics and were given one of the following recovery treatments for 7 days (treatment week): natural recovery (NR); *Bifidobacterium bifidum* JCM 1254 as a probiotic (PR); or fecal transplant from control mice (FT). The treatment week was followed by 7 days with no treatments to allow the mice to recover (recovery week). During the treatment week and recovery week combined, we allowed the mice to recover from antibiotic administration for 14 days, as past studies have reported that the gut microbiome recovers within 1–2 weeks after disturbance (David et al., 2014; MacPherson et al., 2018). This was repeated three times for a total of three 3-week phases (**Figure 1**). Mice in the control were provided with water without antibiotics throughout the 9-week experiment.

To prepare for probiotic administration, Gifu Anaerobic Medium (GAM, Nissui Pharmaceutical, Tokyo, Japan) was inoculated with *B. bifidum* each day, from glycerol stocks stored at −80°C, and incubated at 37°C overnight. From the overnight cultures, bacterial suspensions were diluted in phosphate-buffered saline (PBS) at a concentration of 10^9 CFU per 200 μL. We then administered 200 μL of the bacterial suspensions to each mouse via oral gavage daily during the treatment weeks. For fecal transplants, a mixture of fresh feces collected from age-matched control mice were suspended in PBS at a concentration of 40 mg/mL and vortexed for 3 min. We then allowed the mixture to settle, and 200 μL of the supernatant was given to the mice via oral gavage daily during the treatment weeks. Mice in the control and NR groups were given 200 μL of PBS via oral gavage daily during the treatment weeks.

We also measured body weight as an indicator of feed intake and health. Fecal samples were collected from each mouse at the end of each week and stored at −30°C, and freeze-dried within a few days of collection. Freeze-dried fecal samples were stored at −30°C until use for DNA extraction. At the end of the experiment, animals were humanely euthanized by cervical dislocation. Immediately after death, a midline incision was made to exteriorize the intestine and cecum. Cecum weight was measured, and intestinal tissue samples were stored in RNA*later* (Invitrogen, Taastrup, Denmark) at 4°C until use.

DNA Extraction

Freeze-dried fecal samples were placed in 2 mL plastic tubes with one stainless steel bead and approximately 200 mg of 0.1 mm zirconia beads and vigorously shaken for 10 min at 1500 rpm using the Shake Master NEO (Bio Medical Science, Tokyo, Japan) before extraction, as described previously (Sakanaka et al., 2019). Genomic DNA was extracted using a Qiagen QIAamp® DNA Fast Stool Mini Kit (Hilden, Germany) according to the manufacturer's instructions. Extracted DNA samples were stored at −30°C until use.

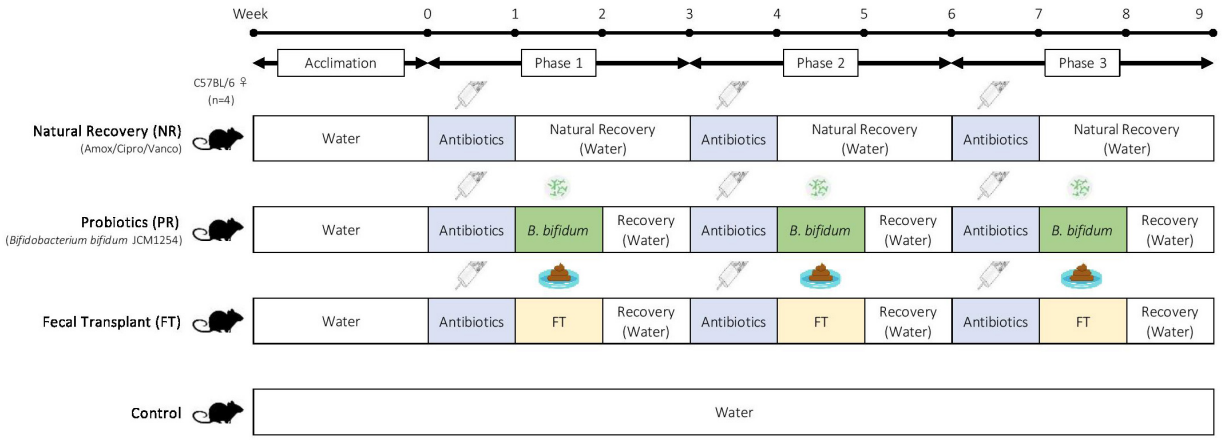

FIGURE 1 | Experimental design. Adult female C57BL/6 mice were used in this experiment, with four biological replicates per group. After 2 weeks of acclimation, mice were given one of the following antibiotics for one week: amoxicillin, ciprofloxacin, or vancomycin. Antibiotic treatment was followed by one of the following recovery treatments: natural recovery (NR); *Bifidobacterium bifidum* JCM1254 as a probiotic (PR); and fecal transplant (FT). The recovery treatment was followed by 7 days of no treatments to allow the mice to recover. Each 3-week cycle was repeated three times during this 9-week experiment. Mice in the control were provided with water alone throughout the experiment.

Quantification of Total Bacterial Load Using Quantitative PCR

After genomic DNA extraction, we quantified the total bacterial load by measuring the number of copies of the 16S ribosomal RNA (16S rRNA) gene by quantitative PCR (qPCR) performed with a Thermal Cycler Dice Real-Time System (TaKaRa Bio., Kyoto, Japan). Each reaction mixture had a total volume of 15 μL and contained the following: 7.5 μL of TB Green® Premix Ex Taq™ II (TaKaRa Bio, Kyoto, Japan), 0.6 μL of each forward (5′-ACTCCTACGGGAGGCAGCAGT-3′) and reverse (5′-ATTACCGCGGCTGCTGGC-3′) primers, 1 μL of extracted DNA (diluted to 5 ng/μL), and 5.3 μL of water. The cycling conditions included an initial denaturation of 10 min at 95°C followed by 40 cycles of 95°C for 30 s and 68°C for 1 min. We used known concentrations of genomic DNA extracted from *Bacteroides thetaiotamicron* for reference curves for DNA quantification.

Microbiome Analysis

Sequencing of the V3–V4 region of the 16S rRNA gene was performed with an Illumina MiSeq platform (Illumina, Inc., San Diego, CA, United States) as described previously (Odamaki et al., 2019). After removing sequences consistent with data from phiX reads from the raw Illumina paired-end reads, the sequences were analyzed using the QIIME2 software package version 2017.10[1]. After trimming of the 3′ region of the forward and the reverse reads (30 and 90 bases, respectively), the paired-end reads were joined, and potential chimeric sequences were removed using DADA2 (Callahan et al., 2016). Taxonomical classification was performed using a Naive Bayes classifier trained on the Greengenes 13.8 16S rRNA reference set with a 99% threshold of OTU full-length sequences. When possible, species were determined by Blastn analysis of the representative OTU sequences, for which the NCBI rRNA database was used.

Quantification of Inflammation-Related Gene Expression Using Reverse-Transcription qPCR

Intestinal tissue samples were place in 2 mL plastic tubes with one stainless steel bead and approximately 200 mg of 0.1 mm zirconia beads. Samples were homogenized by vigorous shaking for 20 min at 1500 rpm using the Shake Master NEO (Bio Medical Science, Tokyo, Japan). Following RNA extraction using NucleoSpin® RNA (TaKaRa Bio., Kyoto, Japan) according to the manufacturer's instructions, cDNA was synthesized from 500 ng of total RNA by reverse transcription (RT) using PrimeScript II 1st strand cDNA Synthesis Kit (TaKaRa Bio., Kyoto, Japan).To measure the expression of inflammation-related genes in the intestinal tissue, RT-qPCR was carried out with a Thermal Cycler Dice Real-Time System (TaKaRa Bio). Each RT-qPCR reaction contained the following: 7.5 μL of TB Green® Premix Ex Taq™ II (TaKaRa Bio., Kyoto, Japan), 0.6 μL of each forward and reverse primers, 1 μL of the appropriately diluted cDNA solution, and 5.9 μL of water. The specificity of all primers was confirmed by analyzing the melting curves after the PCR was run. The cycling conditions were as follows: 95°C for 30 s, followed by 40 cycles of 95°C for 5 s, 60°C for 30 s, and a dissociation phase with 95°C for 15 s, 60°C for 30 s, and 95°C for 15 s. Standard curves were created for respective genes using the PCR-amplified fragments as templates. The primers were designed using Primer3 Plus software[2], and the primer sets are listed in **Supplementary Table 1**.

[1]https://qiime2.org/

[2]http://www.bioinformatics.nl/cgi-bin/primer3plus/primer3plus.cgi

Diversity/Similarity Metrics and Statistical Analysis

Statistical analyses were performed using R ver. 3.6.0[3]. Species richness (α diversity) of the samples was estimated by the number of OTUs in each microbial profile using the Shannon Index (Shannon and Weaver, 1949) and the Chao1 Index. We used Two-Way Repeated Measures ANOVA (rm-ANOVA) with Tukey's HSD *post hoc* test to determine the effect of each treatment over time. To determine the recovery of microbial communities, we quantified the magnitude of the microbial shift by comparing the microbiome profiles at baseline (Week 0) with profiles from other time points using the Bray-Curtis Dissimilarity Index. We further analyzed community structure using principal components analysis (PCA) and exploratory factor analysis. To determine the statistical differences in cecum weight and expression of inflammation-related genes, we used a One-Way ANOVA with *post hoc* Dunnett's test. We also performed Pearson's correlation analysis to identify specific taxa that were positively or negatively associated with cecum weight and expression of inflammation-related genes.

RESULTS AND DISCUSSION

The goal of this study was to assess the efficacy of the probiotic strain, *Bifidobacterium bifidum* JCM 1254, in the recovery period after the repeated antibiotic disturbance. Using mouse models, we administered three different antibiotics with varying bacterial targets and spectrum of activity. A subsequent recovery treatment consisted of *B. bifidum* supplementation or fecal transplants from healthy donor mice (age-matched mice from the control group). The key findings of this study are as follows: (1) the response of the gut microbiome varies significantly with the type of disturbance; (2) *B. bifidum* is most effective when antibiotic disturbance increases proinflammatory species; (3) probiotic supplementation does not restore the diversity of the gut microbiome to baseline levels but can contribute to the recovery of host health. Our results provide insight into how disturbance ecology affects the gut microbial community and its response to recovery treatments.

Vancomycin Significantly Alters the Gut Microbiome and Increases Proinflammatory Species

We first compared the effect on the structure of the gut microbiome of repeated antibiotic exposure, testing vancomycin, ciprofloxacin, and amoxicillin (see **Table 1** for spectrum and mode of action). To do so, we administered each antibiotic in drinking water for 7 days, allowed for 14 days of natural recovery, and repeated this process three times (Natural Recovery; **Figure 1**). Although statistically insignificant, the percent body weight increase had a tendency to be greater for all antibiotics compared to control (**Supplementary Figures 1A–C**). We then analyzed the fecal microbiome by meta-16S rRNA sequencing. For all antibiotic types, we did not see a significant variation in bacterial load over time (**Supplementary Figures 1D–F**). This is possibly because we collected fecal samples after seven days of antibiotic administration, which allowed the taxa unaffected by the antibiotics to proliferate during that time. Similar trends with vancomycin (Cheng et al., 2017) and amoxicillin (Cabral et al., 2019) have also been previously reported.

However, clear differences between antibiotics were seen when we compared α-diversity using the Shannon Index (evenness; **Figure 2A**) and the Chao1 Index (species richness; **Figure 2B**). The results of Two-Way rm-ANOVA show that the type of antibiotic differentially affected α-diversity (**Supplementary Table 2**). For ciprofloxacin, antibiotic administration had no significant effect on α-diversity over time, even though ciprofloxacin has been shown to significantly alter the gut microbiome in human subjects (Dethlefsen and Relman, 2011). This may be because we utilized murine models, in which ciprofloxacin is shown to have a limited effect on the community structure of the gut microbiome in some studies (Schubert et al., 2015). Furthermore, ciprofloxacin is considered to have limited activity against anaerobic microbes (Goldstein and Citron, 1988). For amoxicillin, α-diversity was significantly reduced in terms of both evenness (>34% reduction) and species richness (>60% reduction) after the first antibiotic disturbance event, but recovered to control levels within two weeks. While this pattern continued after the second and third antibiotic disturbance events for species richness, evenness was not significantly affected after the first disturbance event, as amoxicillin is a β-lactam antibiotic that affects both Gram-positive and -negative bacteria. Of the three antibiotics, vancomycin had the strongest effect on α-diversity. The first antibiotic disturbance significantly reduced evenness (>52% reduction) and richness (>81% reduction), both of which did not recover throughout the experiment.

In addition to α-diversity, we assessed recovery by quantifying the magnitude of the microbial shift from baseline (Week 0) using the Bray-Curtis Index of Dissimilarity (**Figure 2C**), and the results of Two-Way rm-ANOVA show that the differences in the antibiotic type significantly affected the microbial communities during recovery (**Supplementary Table 3**). For this study, we considered communities that returned to baseline community structures based on this index as "recovered." For both ciprofloxacin and amoxicillin, dissimilarity increased with each antibiotic disturbance event, and gradually decreased over the following two weeks. Examination at the phylum level showed that each antibiotic disturbance event increased the relative abundance of Proteobacteria (12%, ciprofloxacin; 20%, amoxicillin), which then decreased over time (**Figure 2D**). Although some level of recovery was observed, the microbial communities did not return to baseline levels throughout the experiment, which is consistent with previous studies that report that repeated antibiotic use leads to incomplete recovery (Dethlefsen and Relman, 2011). With vancomycin, the microbial communities displayed patterns consistent with α-diversity, and community dissimilarity remained high throughout the experiment after the first antibiotic disturbance. At the phylum level, the relative abundance of Proteobacteria

[3]www.r-project.org

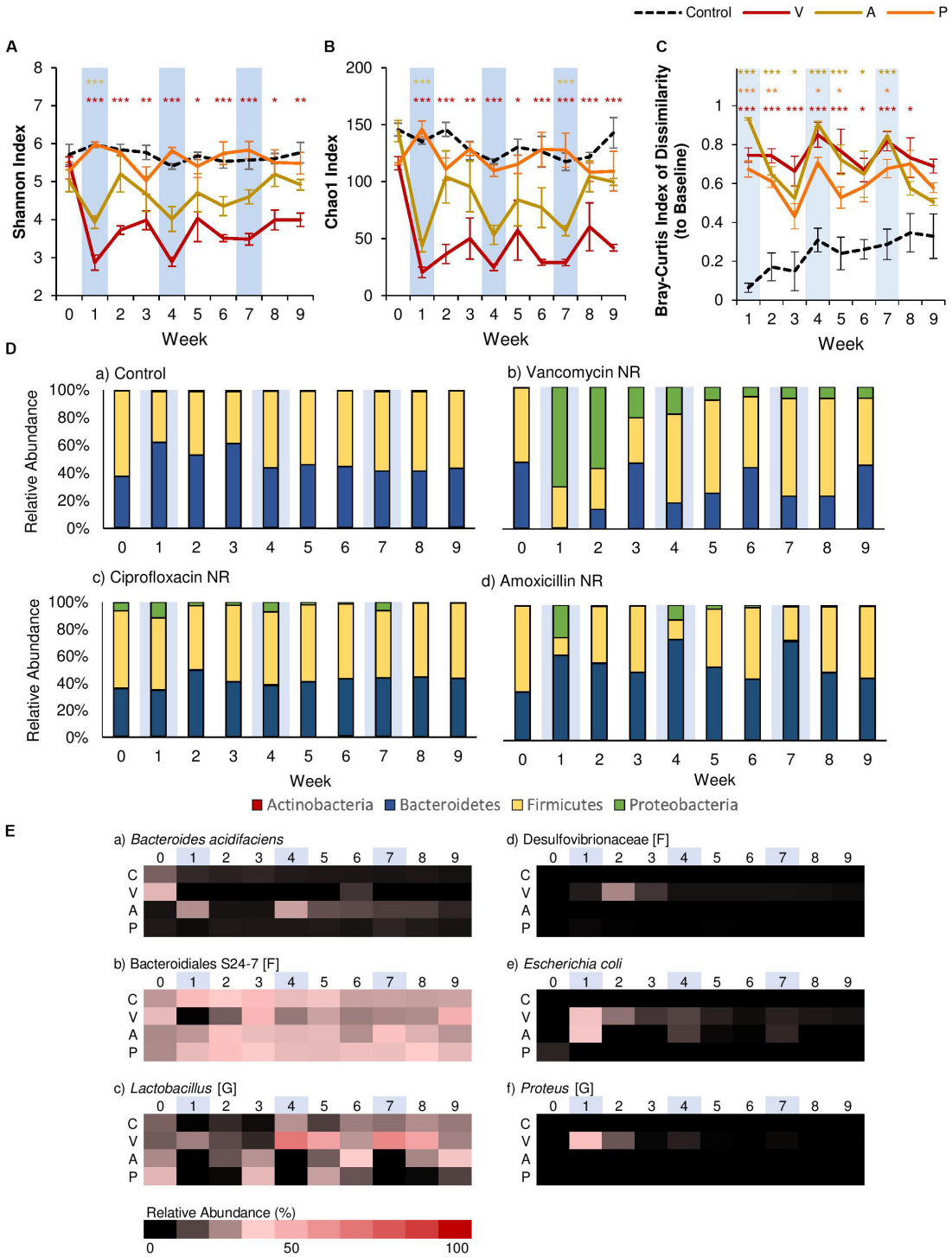

FIGURE 2 | Comparison of the effects of vancomycin, ciprofloxacin, and amoxicillin on the gut microbiome. Each antibiotic was administered for 7 days every 3 weeks, and changes to the fecal microbiome over time were observed by meta-16S rRNA sequencing. Alpha diversity measured by **(A)** Shannon Index and **(B)** Chao1 Index for each treatment over time ± standard error. **(C)** Bray-Curtis Index of Dissimilarity vs baseline for each treatment over time ± standard error. The Bray-Curtis Index was used to quantify the amount of microbial shift from the first day of the experiment (baseline) for each individual. Colored asterisks indicate significance vs control for NR, PR, and FT groups based on Two-Way rm-ANOVA and Tukey's HSD *post hoc* test (*$p < 0.05$, **$p < 0.01$, ***$p < 0.001$). Data for the control samples are indicated as the black dotted line. Natural recovery data for vancomycin is in red, amoxicillin in yellow, and ciprofloxacin in orange. **(D)** The microbial community at each time point at the phylum level for **(a)** control, **(b)** vancomycin, **(c)** ciprofloxacin, and **(d)** amoxicillin. **(E)** Heat map of taxa that significantly changed after antibiotic administration. Significant taxa were identified using factor analysis (factor loading >0.2). The lowest taxonomic rank for which information was available is indicated in square brackets (F: family, G: genus). Weeks shaded in blue indicate weeks in which antibiotics were administered.

increased significantly after the first antibiotic disturbance event (70%). Although this increase was diminished after the second (19%) and third (8%) antibiotic disturbance events, the presence of Proteobacteria was persistent throughout the experiment (**Figure 2D**). For all antibiotics, the increase in Proteobacteria was less pronounced with repeated disturbances. Further examination with principal components analysis (PCA) based on the microbial community composition corroborated these observations. For vancomycin- and amoxicillin-treated groups, PCA revealed that communities after the first antibiotic administration formed a separate cluster (**Supplementary Figures 2A,B**). The subsequent second and third antibiotic treatments for vancomycin and amoxicillin clustered closer to the control communities, lending further evidence to the fact that the gut microbiome retains the memory of past disturbance events (Dethlefsen and Relman, 2011). For ciprofloxacin-treated groups, however, the different treatments did not create clear clusters (**Supplementary Figure 2C**).

Further examination using exploratory factor analysis showed that the increase in Proteobacteria can be attributed to *Escherichia coli* for all antibiotics (**Figure 2E**, **Supplementary Figure 3** and **Supplementary Table 4**). However, for vancomycin, there were also increases in proinflammatory species associated with dysbiosis. For example, after the first antibiotic disturbance event, we noted an increase in *Proteus* (34.7%, relative abundance; **Figure 2E**, **Supplementary Figure 3**), a genus associated with the onset of colitis (Shin et al., 2015). There was also an increase in the abundance of Desulfovibrionaceae (**Figure 2E**, **Supplementary Figure 3**), a family of sulfate-reducing bacteria often associated with high-fat diets (Clarke et al., 2012) during Week 2 (a 350-fold increase compared to baseline). In disturbance ecology, the type of disturbance is a critical factor that determines which specific members of the community are selected for over the course of time (Relman, 2012), and our results indicate that gut microbiome responses vary significantly by antibiotic type, with vancomycin having the most detrimental effects. Previous studies have shown that vancomycin is a particularly potent antibiotic that significantly reduces gut microbiome diversity (Vrieze et al., 2014) and causes intestinal dysbiosis (Cheng et al., 2017). Therefore, we focused on vancomycin and how different treatments (fecal transplants or probiotic administration) could contribute to the recovery of the gut microbial community in the following sections.

Fecal Transplants Restore Gut Microbiome Diversity

Past studies have indicated that fecal transplants contribute to relatively rapid recovery after antibiotic-induced dysbiosis (Ekmekciu et al., 2017; Suez et al., 2018). After each vancomycin administration, we administered fecal transplants from healthy, age-matched control mice for seven days. As expected, the fecal transplants produced a significant effect on both α-diversity metrics, as well as community dissimilarity (**Supplementary Tables 5**, **6**). α-Diversity was reduced after the first antibiotic disturbance event but completely recovered to control levels within two weeks of fecal transplants, and this pattern was observed for the subsequent disturbance events as well (**Figures 3A,B**). A similar pattern was observed for community dissimilarity, where each antibiotic administration increased dissimilarity, but fecal transplants restored community structures to baseline levels within two weeks (**Figure 3C**). Examination of community membership revealed that, compared to the natural recovery groups (V), fecal transplants were effective in reducing the Proteobacteria populations that had increased with each vancomycin administration (**Figure 3D**). While Proteobacteria populations persisted in the natural recovery groups (relative abundance >8%), Proteobacteria were nearly undetectable within two weeks after fecal transplants (relative abundance <1%), and the increase in inflammatory taxa such as *Proteus* was also suppressed (**Figure 3E**). Our results are consistent with previous studies, which have shown that fecal transplants are effective in correcting dysbiosis and reducing inflammation. Furthermore, a recent study by Burrello et al. (2018) demonstrated that fecal transplants promote recovery by stimulating immune cells to produce IL-10 and that the beneficial effects of fecal transplants seem to be correlated with the persistence of protective taxa such as Lactobacillaceae, Bifidobacteriaceae, Erysipelotrichaceae, Ruminococcacceae, and Bacteroidales S24-7.

Bifidobacterium bifidum Does Not Restore Diversity but Reduces Intestinal Inflammation

In addition to fecal transplants, probiotic supplementation with species like *Bifidobacterium* in the gut has been linked to a variety of positive effects, such as reduced incidences of diarrhea in infants (Hotta et al., 1987), improvement in immune functions (Mohan et al., 2008), anti-obesity effects (Kondo et al., 2010; Stenman et al., 2014; Moya-Pérez et al., 2015), and recovery after antibiotic disturbance (Grazul et al., 2016; Ekmekciu et al., 2017). However, how effective probiotics are in restoring the disturbed gut microbial community after antibiotics remains a topic of debate (Suez et al., 2019). In our study, to assess the efficacy of probiotics in recovery after vancomycin administration, we administered *Bifidobacterium bifidum* JCM 1254 to mice via oral gavage for 7 days. Our results indicate that probiotic administration seemed to have little effect on recovery. Like the natural recovery groups, α-diversity did not return to baseline levels after the first antibiotic disturbance event (**Figures 3A,B**), and community dissimilarity remained high (**Figure 3C**). Similarly, Suez et al. (2018) also reported that a probiotic blend including *Lactobacillus, Bifidobacterium, Lactococcus,* and *Streptococcus* genera did not promote recovery after antibiotic-induced dysbiosis. These results suggest that species commonly called "probiotics" may be insufficient for community recovery.

Our exploratory factor analysis showed that the relative abundance of *Lactobacillus* species, *Proteus* species, *E. coli*, and Bacteroidales S24–7 contributed significantly to community structure (**Supplementary Table 7**). Although α-diversity did not recover, the first *B. bifidum* supplementation caused a

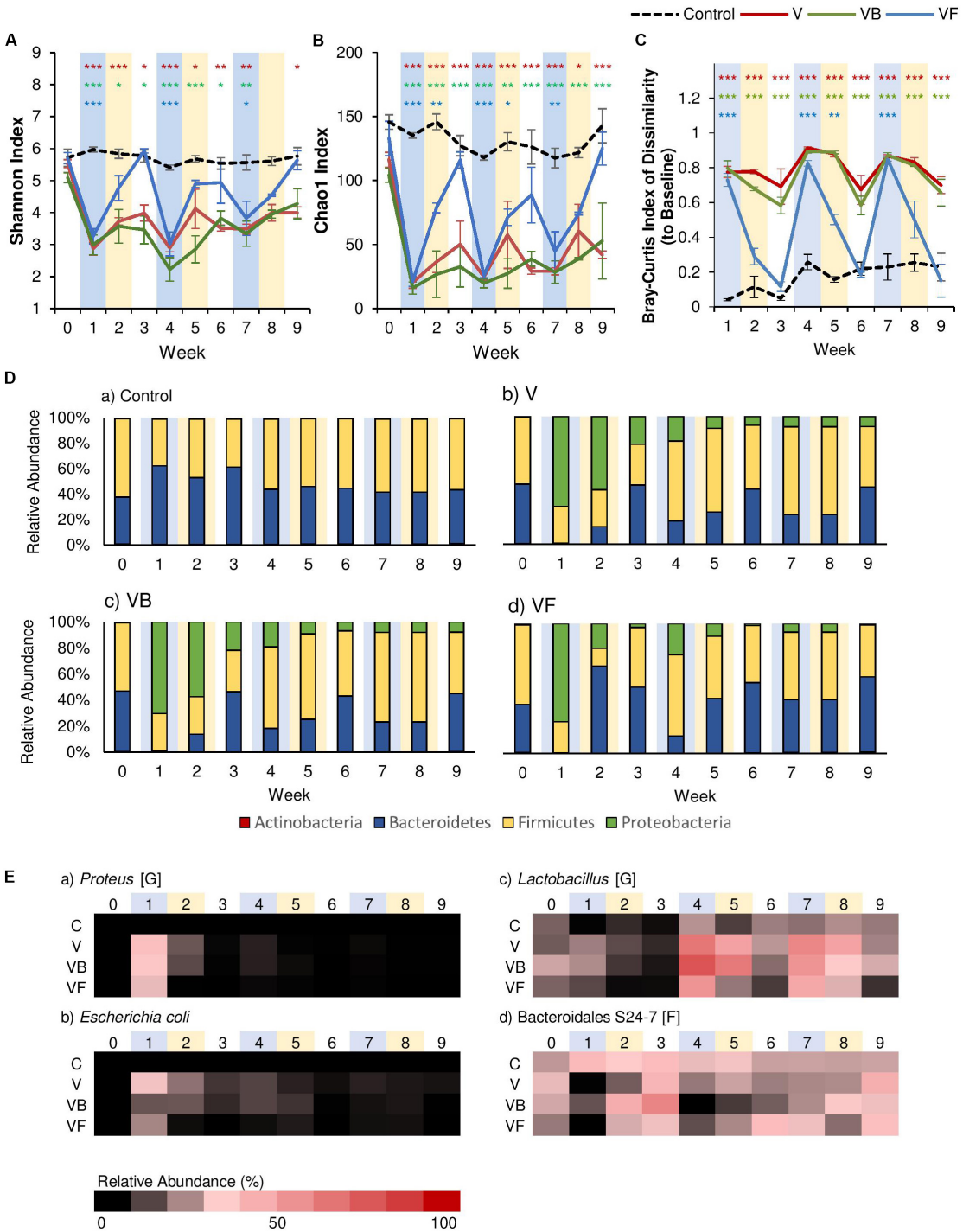

FIGURE 3 | The effect of recovery treatments on the gut microbiome after vancomycin. Vancomycin administration was followed by either natural recovery (NR), *Bifidobacterium bifidum* (PR), or fecal transplants (FT), and changes to the gut microbiome were observed over time. Alpha diversity measured by **(A)** Shannon Index and **(B)** Chao1 Index for each treatment over time ± standard error. **(C)** Bray-Curtis Index of Dissimilarity vs baseline for each treatment over time ± standard error. The Bray-Curtis Index was used to quantify the amount of microbial shift from the first day of the experiment (baseline) for each individual. Colored asterisks indicate significance vs control for NR, PR, and FT groups based on Two-Way rm-ANOVA and Tukey's HSD *post hoc* test (*$p < 0.05$, **$p < 0.01$, ***$p < 0.001$). Data for the control samples are indicated as the black dotted line, with NR (V) groups in red, PR (VB) groups in green, and FT (VF) groups in blue. **(D)** The microbial community at each time point at the phylum level for **(a)** control, **(b)** V, **(c)** VB, and **(d)** VF. **(E)** Heat map of taxa that significantly changed after antibiotic administration. Significant taxa were identified using factor analysis (factor loading >0.4). The lowest taxonomic rank for which information was available is indicated in square brackets (F: family, G: genus). Weeks shaded in blue indicate weeks in which antibiotics were administered, and weeks shaded in yellow indicate weeks in which a recovery treatment (natural recovery, probiotics, or fecal transplants) were administered.

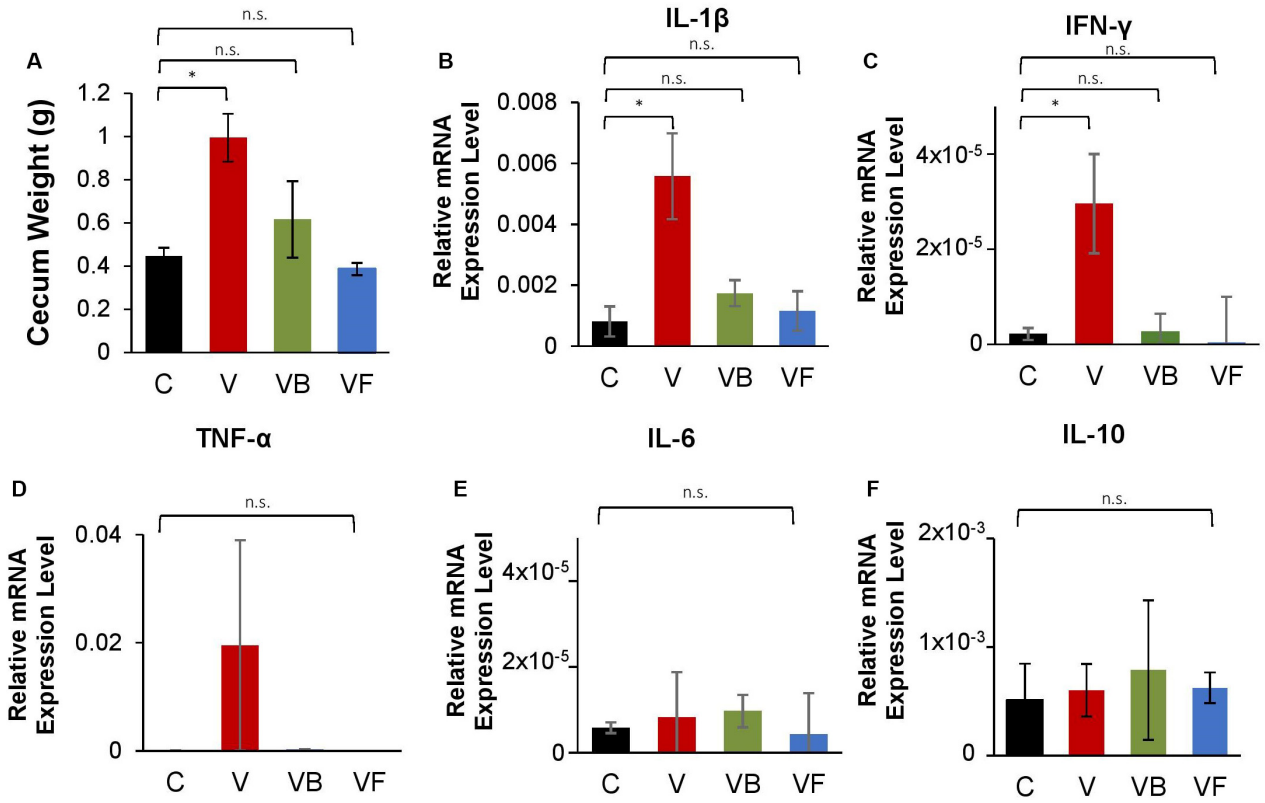

FIGURE 4 | Changes in cecum size and expression of inflammation-related genes in vancomycin-treated mice. At the end of the experiment, we measured cecum weight and measured the mRNA expression levels of inflammation-related genes in the large intestine for vancomycin-treated mice (C: control, V: vancomycin + natural recovery, VB: vancomycin + *B. bifidum*, VF: vancomycin + fecal transplant from control mice). **(A)** Cecum weight, relative mRNA expression of genes encoding **(B)** IL-β, **(C)** TNF-α, **(D)** INF-γ, **(E)** IL-6, and **(F)** IL-10 for vancomycin-treated mice, using *Actb* as a reference gene. Error bars indicate standard error, and significance was determined by One-Way ANOVA and Dunnett's test. (*$p < 0.05$, **$p < 0.01$, ***$p < 0.001$).

two-fold increase in the relative abundance of Bacteroidales S24–7 (**Figure 3E**), a family of fermenters often associated with a healthy microbiome in mice that produce short-chain fatty acids (SCFA) and vitamin B (Evans et al., 2014; Rooks et al., 2014; Ormerod et al., 2016). While not as effective as fecal transplants, probiotics were also able to suppress the increase of Proteobacteria, such as *E. coli* and *Proteus* populations (**Figure 3E**). Previous studies have also reported the reduction of Proteobacteria after *Bifidobacterium* supplementation. For example, the administration of *Bifidobacterium longum* decreased the relative abundance of Proteobacteria and reduced the expression of the gene encoding TNF-α in mice (Lee et al., 2019), and *B. infantis* supplementation decreased γ-Proteobacteria in infants (Underwood et al., 2013).

Furthermore, we observed that recovery treatments had a significant effect on cecum size (One-Way ANOVA: $F(3,12) = 5.513$, $p < 0.05$; **Figure 4A**). While mice in the natural recovery group (V) had a significantly larger cecum compared to the control (*post hoc* Dunnett's test: $p < 0.05$), the difference was insignificant for groups given *B. bifidum* (VB) and fecal transplants (VF), suggesting that cecal enlargement was corrected by *B. bifidum* administration and fecal transplants. A previous study has also reported an enlargement in the cecum of antibiotic-treated mice, possibly because of a decrease in intestinal motility (Puhl et al., 2012). Cecal enlargement may also have been caused by the increase of pro-inflammatory species. Further analysis with Pearson's correlation analysis revealed that there were strong positive correlations between cecum weight and the abundance of inflammatory taxa such as *Proteus* ($r = 0.91$, $p < 0.001$), and *E. coli* ($r = 0.84$, $p < 0.001$). Cecum weight and the expression of genes encoding IL-1β also showed a significant positive correlation ($r = 0.70$, $p < 0.05$).

Additionally, our RT-qPCR results indicate that the expression of genes encoding proinflammatory cytokines (IL-1β and INF-γ) was significantly increased in the natural recovery groups (**Figures 4B,C**), while expression was suppressed by probiotic administration and fecal transplants. Verma et al. (2019) recently identified *B. bifidum* cell surface polysaccharides as a factor that suppresses inflammation in the gut. Another possible anti-inflammatory mechanism may be modulated by indole-3-lactic acid (ILA) produced by *Bifidobacterium* species. ILA is an aromatic lactic acid and a metabolite of aromatic amino acids such as tryptophan, and serves as a ligand for the aryl hydrocarbon receptor (AhR) that regulates intestinal homeostasis. Meng et al. (2019) found

that ILA produced by *B. infantis* had anti-inflammatory effects on infant enterocytes *in vitro*, and this metabolite is also reported to be produced by *B. bifidum* (Sakurai et al., 2019). A recent study by Laursen et al. (2020) has shown that *Bifidobacterium* species possess a specific enzyme that convert aromatic pyruvates, precursors of aromatic amino acids, into aromatic lactic acids. Given these results, we hypothesize that *B. bifidum* supplementation suppresses the increase of proinflammatory species and ultimately reduces gut inflammation.

We also examined the expression of genes encoding TNF-α, IL-6, and IL-10, but did not find any significant differences between treatments (**Figures 4D–F**), suggesting that antibiotic-induced dysbiosis leads to the induction of specific inflammatory cytokines. Furthermore, we repeated this experiment for amoxicillin- and ciprofloxacin-treated mice, testing administered fecal transplants and *B. bifidum*. However, the effects of neither fecal transplants nor probiotics differed significantly from NR groups for α-diversity and community structure (**Supplementary Figures 4**, **5**), and no cecum enlargement was observed, even for antibiotic-treated groups (**Supplementary Figures 6A, 7A**). Furthermore, probiotics did not reduce the expression of inflammation-related genes after antibiotic administration. As neither amoxicillin nor ciprofloxacin caused a bloom in pro-inflammatory species (**Supplementary Figures 4B–F, 5B–F**), we hypothesize that in the absence of inflammatory species, the effect of fecal transplants and probiotic supplementation is negligible.

Increase in *Lactobacillus* Abundance Potentially Delays Gut Microbiome Recovery

One common event we observed for all antibiotics was the expansion of *Lactobacillus*, particularly for vancomycin-treated groups (**Figure 3E**). We also observed that the increase was especially noticeable after the second antibiotic administration, which led us to believe that it may be due to the superior capability of *Lactobacillus* to tolerate disturbances. Past studies have shown *Lactobacillus* species to have a high level of vancomycin resistance (Gueimonde et al., 2013), as well as a relatively high tolerance to low pH (Corcoran et al., 2005; O'May et al., 2005). Furthermore, Suez et al. (2018) found that *Lactobacillus* was a microbiome-inhibitory species. Although unconfirmed in this study, it is possible that the increased relative abundance of *Lactobacillus* may have contributed to the inhibited recovery from antibiotic administration (Suez et al., 2018).

Limitations

One of the limitations of this study is that we utilized a human-derived *Bifidobacterium* strain in murine models. Even in the human gut microbiome, the inability of probiotics to colonize the gut is a longstanding issue (Suez et al., 2019), but the lack of colonization was particularly evident in our study. Although we collected samples within 24 h of *B. bifidum* administration, its detection was limited in our 16S metagenomic analysis. Furthermore, we did not administer any prebiotics, possibly making colonization by *B. bifidum* in the gut even more difficult to achieve. A recent study by Cabral et al. (2019) has shown that the addition of fiber protected gut microbes from antibiotics, suggesting that the carbohydrates consumed in the diet alter the gut microbiome's response to disturbances. Therefore, to develop more efficient probiotic therapies, future studies ought to consider the type of diet and prebiotics that are co-administered with antibiotics and probiotics.

Conclusion

Despite these limitations, our study provides insight into how the gut microbiome responds to repeated disturbances and subsequent recovery treatments. In clinical settings, antibiotics are prescribed both frequently and repeatedly. A study based in the United Kingdom found that approximately 30% of patients are prescribed antibiotics at least once year (Shallcross et al., 2017). Although a different class of antibiotics is often re-prescribed with repeated use, results of our study elucidated how the repeated use of different types of antibiotics affects the response of the gut microbiome to recovery treatments. The type of disturbance (i.e., affected species, frequency, magnitude, and duration) is a key factor in community structuring, and its effect should be considered when examining the gut microbial community. The disturbance type determines which specific taxa and functions within the gut microbiome are selected for Relman (2012); moreover, we found that it also affects how the gut microbiome responds to the addition of probiotics. We found that probiotics were effective in reducing gut inflammation without recovering gut microbiome diversity. Additionally, our study showed that probiotics were most effective when antibiotic disturbance caused an increase in proinflammatory species. The results of the study could be applied to clinical settings, where predicting the response of the gut microbiome to different recovery treatments after dysbiosis would offer potential benefits.

DATA AVAILABILITY STATEMENT

The datasets generated for this study can be found in the EBI Metagenomics, under Accession Number PRJEB36500 (https://www.ebi.ac.uk/ena/browser/text-search?query=PRJEB36500).

ETHICS STATEMENT

The animal study was reviewed and approved by Kyoto University Animal Experimentation Committee.

AUTHOR CONTRIBUTIONS

MO conceived the project. MO and AG designed the study and performed mouse experiments. HT performed the quantification of inflammation-related genes. TO and J-ZX contributed to the metagenome dataset analysis. MO analyzed the data, performed statistical analyses, and wrote and drafted the manuscript.

All authors discussed the data and contributed to the completion of the final manuscript. TaK and ToK edited the manuscript. TaK supervised the study.

FUNDING

This study was supported in part by Grants-in-Aid for JSPS Research Fellows (19J14598 to MO and 17J08530 to AG) and JSPS-KAKENHI (19K15732 to AG and 18H02126 to TaK).

ACKNOWLEDGMENTS

We thank Dr. James A. Hejna for proofreading the manuscript and providing valuable feedback.

SUPPLEMENTARY MATERIAL

The Supplementary Material for this article can be found online at: https://www.frontiersin.org/articles/10.3389/fmicb.2020.01349/full#supplementary-material

REFERENCES

Alang, N., and Kelly, C. R. (2015). Weight gain after fecal microbiota transplantation. *Open Forum Infect. Dis.* 2, 1–2. doi: 10.1093/ofid/ofv004

Arifin, W. N., and Zahiruddin, W. M. (2017). Sample size calculation in animal studies using resource equation approach. *Malaysian J. Med. Sci.* 24, 101–105. doi: 10.21315/mjms2017.24.5.11

Baxter Healthcare (2007). *Vancomycin Hydrochloride (Vancomycin Hydrochloride) Injection, Solution*. 1–14. Available online at: https://www.accessdata.fda.gov/drugsatfda_docs/label/2007/050671s010lbl.pdf (accessed September 14, 2007)

Bayer HealthCare (2017). *Cipro (Ciprofloxacin) Package Insert*. 1–53. Available online at: https://www.accessdata.fda.gov/drugsatfda_docs/label/2016/019537s086lbl.pdf (accessed June 1, 2018).

Burrello, C., Garavaglia, F., Cribiù, F. M., Ercoli, G., Lopez, G., Troisi, J., et al. (2018). Therapeutic faecal microbiota transplantation controls intestinal inflammation through IL10 secretion by immune cells. *Nat. Commun.* 9:5184. doi: 10.1038/s41467-018-07359-8

Cabral, D. J., Penumutchu, S., Reinhart, E. M., Zhang, C., Korry, B. J., Wurster, J. I., et al. (2019). Microbial metabolism modulates antibiotic susceptibility within the murine Gut microbiome. *Cell Metab.* 30, 800–823e7. doi: 10.1016/j.cmet.2019.08.020

Callahan, B. J., Mcmurdie, P. J., Rosen, M. J., Han, A. W., Johnson, A. J., and Holmes, S. P. (2016). DADA2: high-resolution sample inference from illumina amplicon data. *Nat. Methods* 13, 581–583. doi: 10.1038/nmeth.3869.DADA2

Cheng, R. Y., Li, M., Li, S. S., He, M., Yu, X. H., Shi, L., et al. (2017). Vancomycin and ceftriaxone can damage intestinal microbiota and affect the development of the intestinal tract and immune system to different degrees in neonatal mice. *Pathog. Dis.* 75, 1–9. doi: 10.1093/femspd/ftx104

Cho, I., Yamanishi, S., Cox, L., Methé, B. A., Zavadil, J., Li, K., et al. (2012). Antibiotics in early life alter the murine colonic microbiome and adiposity. *Nature* 488, 621–626. doi: 10.1038/nature11400

Clarke, S. F., Murphy, E. F., Nilaweera, K., Ross, P. R., Shanahan, F., Cotter, P. W., et al. (2012). The gut microbiota and its relationship to diet and obesity:new insights. *Gut Microbes* 3, 1–17. doi: 10.4161/gmic.20168

Corcoran, B. M., Stanton, C., Fitzgerald, G. F., and Ross, R. P. (2005). Survival of probiotic lactobacilli in acidic environments is enhanced. *Appl. Environ. Microbiol.* 71, 3060–3067. doi: 10.1128/AEM.71.6.3060

David, L. A., Maurice, C. F., Carmody, R. N., Gootenberg, D. B., Button, J. E., Wolfe, B. E., et al. (2014). Diet rapidly and reproducibly alters the human gut microbiome. *Nature* 505, 559–563. doi: 10.1038/nature12820.Diet

Dethlefsen, L., and Relman, D. A. (2011). Incomplete recovery and individualized responses of the human distal gut microbiota to repeated antibiotic perturbation. *Proc. Natl. Acad. Sci. U.S.A.* 108, 4554–4561. doi: 10.1073/pnas.1000087107

Ekmekciu, I., von Klitzing, E., Fiebiger, U., Neumann, C., Bacher, P., Scheffold, A., et al. (2017). The probiotic compound VSL#3 modulates mucosal, peripheral, and systemic immunity following murine broad-spectrum antibiotic treatment. *Front. Cell. Infect. Microbiol.* 7:167. doi: 10.3389/fcimb.2017.00167

Elseviers, M. M., Van Camp, Y., Nayaert, S., Duré, K., Annemans, L., Tanghe, A., et al. (2015). Prevalence and management of antibiotic associated diarrhea in general hospitals. *BMC Infect. Dis.* 15:129. doi: 10.1186/s12879-015-0869-0

Evans, C. C., LePard, K. J., Kwak, J. W., Stancukas, M. C., Laskowski, S., Dougherty, J., et al. (2014). Exercise prevents weight gain and alters the gut microbiota in a mouse model of high fat diet-induced obesity. *PLoS One* 9:e92193. doi: 10.1371/journal.pone.0092193

Faith, J. J., Guruge, J. L., Charbonneau, M., Subramanian, S., Seedorf, H., Goodman, A. L., et al. (2013). The long-term stability of the human gut microbiota. *Science* 341:1237439. doi: 10.1126/science.1237439

Gerber, J. S., Bryan, M., Ross, R. K., Daymont, C., Parks, E. P., Localio, A. R., et al. (2016). Antibiotic exposure during the first 6 months of life and weight gain during childhood. *JAMA J. Am. Med. Assoc.* 315, 1258–1265. doi: 10.1001/jama.2016.2395

GlaxoSmithKline (2006). *Amoxil (Amoxicillin Capsules, Tablets, Chewable Tablets, and Powder for Oral Suspension)*, 4–21. Available online at: https://www.accessdata.fda.gov/drugsatfda_docs/label/2008/050760s11,050761s11,050754s12,050542s25lbl.pdf (accessed June 1, 2018).

Global Market Insights (2016). *Probiotics Market Size to Exceed USD 64 Billion by 2023*. Global Market Insights Inc. Available online at: https://www.prnewswire.com/news-releases/probiotics-market-size-to-exceed-usd-64-billion-by-2023-global-market-insights-inc-578769201.html (accessed May 10, 2016).

Goldenberg, S. D., Batra, R., Beales, I., Digby-Bell, J. L., Irving, P. M., Kellingray, L., et al. (2018). Comparison of different strategies for providing fecal microbiota transplantation to treat patients with recurrent clostridium difficile infection in two english hospitals: a review. *Infect. Dis. Ther.* 7, 71–86. doi: 10.1007/s40121-018-0189-y

Goldstein, E. J. C., and Citron, D. M. (1988). Comparative activities of cefuroxime, amoxicillin-clavulanic acid, ciprofloxacin, enoxacin, and ofloxacin against aerobic and anaerobic bacteria isolated from bite wounds. *Antimicrob. Agents Chemother.* 32, 1143–1148. doi: 10.1128/AAC.32.8.1143

Gotoh, A., Katoh, T., Sakanaka, M., Ling, Y., Yamada, C., Asakuma, S., et al. (2018). Sharing of human milk oligosaccharides degradants within bifidobacterial communities in faecal cultures supplemented with *Bifidobacterium bifidum*. *Sci. Rep.* 8, 1–14. doi: 10.1038/s41598-018-32080-3

Grazul, H., Kanda, L. L., and Gondek, D. (2016). Impact of probiotic supplements on microbiome diversity following antibiotic treatment of mice. *Gut Microbes* 7, 101–114. doi: 10.1080/19490976.2016.1138197

Gueimonde, M., Sánchez, B., de los Reyes-Gavilán, C. G., and Margolles, A. (2013). Antibiotic resistance in probiotic bacteria. *Front. Microbiol.* 4:202. doi: 10.3389/fmicb.2013.00202

He, C., Cheng, D., Peng, C., Li, Y., Zhu, Y., and Lu, N. (2018). High-fat diet induces dysbiosis of gastric microbiota prior to gut microbiota in association with metabolic disorders in mice. *Front. Microbiol.* 9:639. doi: 10.3389/fmicb.2018.00639

Hogenauer, C., Hammer, H. F., Krejs, G. J., and Reisinger, E. C. (1998). Mechanisms and management of antibiotic–associated diarrhea. *Clin. Infect. Dis.* 27, 702–710. doi: 10.1086/514958

Hotta, M., Sato, Y., Iwata, S., Yamashita, N., Sunakawa, K., Oikawa, T., et al. (1987). Clinical effects of *Bifidobacterium* preparations on pediatric intractable diarrhea. *Keio J. Med.* 36, 298–314. doi: 10.2302/kjm.36.298

Jernberg, C., Löfmark, S., Edlund, C., and Jansson, J. K. (2007). Long-term ecological impacts of antibiotic administration on the human intestinal microbiota. *ISME J.* 1, 56–66. doi: 10.1038/ismej.2007.3

Katoh, T., Ojima, M. N., Sakanaka, M., Ashida, H., Gotoh, A., and Katayama, T. (2020). Enzymatic adaptation of *Bifidobacterium bifidum* to host glycans, viewed from glycoside hydrolyases and carbohydrate-binding modules. *Microorganisms* 8, 1–18.

Kau, A. L., Ahern, P. P., Griffin, N. W., Goodman, A. L., and Gordon, J. I. (2011). Human nutrition, the gut microbiome and the immune system. *Nature* 474, 327–336. doi: 10.1038/nature10213

Kondo, S., Xiao, J. Z., Satoh, T., Odamaki, T., Takahashi, S., Sugahara, H., et al. (2010). Antiobesity effects of *Bifidobacterium breve* Strain B-3 supplementation in a mouse model with high-fat diet-Induced obesity. *Biosci. Biotechnol. Biochem.* 74, 1656–1661. doi: 10.1271/bbb.100267

Korpela, K., Salonen, A., Virta, L. J., Kumpu, M., Kekkonen, R. A., and De Vos, W. M. (2016). *Lactobacillus rhamnosus* GG intake modifies preschool children's intestinal microbiota, alleviates penicillin-associated changes, and reduces antibiotic use. *PLoS One* 11:e0154012. doi: 10.1371/journal.pone.0154012

Kostic, A. D., Gevers, D., Siljander, H., Vatanen, T., Hyötyläinen, T., Hämäläinen, A. M., et al. (2015). The dynamics of the human infant gut microbiome in development and in progression toward type 1 diabetes. *Cell Host Microbe* 17, 260–273. doi: 10.1016/j.chom.2015.01.001

Laursen, M. F., Sakanaka, M., von Burg, N., Andersen, D., Mörbe, U., Rivollier, A., et al. (2020). Breastmilk-promoted bifidobacteria produce aromatic lactic acids in the infant gut. *bioRxiv* [Preprint]. doi: 10.1101/2020.01.22.914994

Lee, H. J., Lee, K. E., Kim, J. K., and Kim, D. H. (2019). Suppression of gut dysbiosis by *Bifidobacterium longum* alleviates cognitive decline in 5XFAD transgenic and aged mice. *Sci. Rep.* 9, 1–12. doi: 10.1038/s41598-019-48342-7

Levy, S. B., and Marshall, B. (2004). Antibacterial resistance worldwide: causes, challenges and responses. *Nat. Med.* 10, S122–S129. doi: 10.1038/nm1145

Ley, R. E., Backhed, F., Turnbaugh, P., Lozupone, C. A., Knight, R. D., and Gordon, J. I. (2005). Obesity alters gut microbial ecology. *Proc. Natl. Acad. Sci. U.S.A.* 102, 11070–11075. doi: 10.1073/pnas.0504978102

MacPherson, C. W., Mathieu, O., Tremblay, J., Champagne, J., Nantel, A., Girard, S. A., et al. (2018). Gut bacterial microbiota and its resistome rapidly recover to basal state levels after short-term amoxicillin-clavulanic acid treatment in healthy adults. *Sci. Rep.* 8, 1–14. doi: 10.1038/s41598-018-29229-5

Meng, D., Sommella, E., Salviati, E., Campiglia, P., Ganguli, K., Djebali, K., et al. (2020). Indole-3-lactic acid, a metabolite of tryptophan, secreted by *Bifidobacterium longum* subspecies *infantis* is anti-inflammatory in the immature intestine. *Pediatr. Res.* doi: 10.1038/s41390-019-0740-x

Mohan, R., Koebnick, C., Schildt, J., Mueller, M., Radke, M., and Blaut, M. (2008). Effects of *Bifidobacterium lactis* Bb12 supplementation on body weight, fecal pH, acetate, lactate, calprotectin, and IgA in preterm infants. *Pediatr. Res.* 64, 418–422. doi: 10.1203/pdr.0b013e318181b7fa

Moya-Pérez, A., Neef, A., and Sanz, Y. (2015). *Bifidobacterium pseudocatenulatum* CECT 7765 reduces obesity-associated inflammation by restoring the lymphocyte-macrophage balance and gut microbiota structure in high-fat diet-fed mice. *PLoS One* 10:e0126976. doi: 10.1371/journal.pone.0126976

Odamaki, T., Bottacini, F., Mitsuyama, E., Yoshida, K., Kato, K., Xiao, J. Z., et al. (2019). Impact of a bathing tradition on shared gut microbe among Japanese families. *Sci. Rep.* 9, 1–8. doi: 10.1038/s41598-019-40938-3

O'May, G. A., Reynolds, N., Smith, A. R., Kennedy, A., and Macfarlane, G. T. (2005). Effect of pH and antibiotics on microbial overgrowth in the stomachs and duodena of patients undergoing percutaneous endoscopic gastrostomy feeding. *J. Clin. Microbiol.* 43, 3059–3065. doi: 10.1128/JCM.43.7.3059-3065.2005

Ormerod, K. L., Wood, D. L. A., Lachner, N., Gellatly, S. L., Daly, J. N., Parsons, J. D., et al. (2016). Genomic characterization of the uncultured Bacteroidales family S24-7 inhabiting the guts of homeothermic animals. *Microbiome* 4, 1–17. doi: 10.1186/s40168-016-0181-2

Petersen, C., and Round, J. L. (2014). Defining dysbiosis and its influence on host immunity and disease. *Cell. Microbiol.* 16, 1024–1033. doi: 10.1111/cmi.12308

Puhl, N. J., Uwiera, R. R. E., Jay Yanke, L., Brent Selinger, L., and Douglas Inglis, G. (2012). Antibiotics conspicuously affect community profiles and richness, but not the density of bacterial cells associated with mucosa in the large and small intestines of mice. *Anaerobe* 18, 67–75. doi: 10.1016/j.anaerobe.2011.12.007

Qin, J., Li, Y., Cai, Z., Li, S., Zhu, J., Zhang, F., et al. (2012). A metagenome-wide association study of gut microbiota in type 2 diabetes. *Nature* 490, 55–60. doi: 10.1038/nature11450

Relman, D. A. (2012). The human microbiome: ecosystem resilience and health. *Nutr. Rev.* 70, 1–12. doi: 10.1111/j.1753-4887.2012.00489.x.The

Rooks, M. G., Veiga, P., Wardwell-Scott, L. H., Tickle, T., Segata, N., Michaud, M., et al. (2014). Gut microbiome composition and function in experimental colitis during active disease and treatment-induced remission. *ISME J.* 8, 1403–1417. doi: 10.1038/ismej.2014.3

Round, J. L., and Mazmanian, S. K. (2009). The gut microbiota shapes intestinal immune responses during health and disease. *Nat. Rev. Immunol.* 9, 313–323. doi: 10.1038/nri2515

Rowland, I., Gibson, G., Heinken, A., Scott, K., Swann, J., Thiele, I., et al. (2018). Gut microbiota functions: metabolism of nutrients and other food components. *Eur. J. Nutr.* 57, 1–24. doi: 10.1007/s00394-017-1445-8

Sakanaka, M., Hansen, M. E., Gotoh, A., Katoh, T., Yoshida, K., Odamaki, T., et al. (2019). Evolutionary adaptation in fucosyllactose uptake systems supports bifidobacteria-infant symbiosis. *Sci. Adv.* 5:eaaw7696. doi: 10.1126/sciadv.aaw7696

Sakurai, T., Odamaki, T., and Xiao, J. Z. (2019). Production of indole-3-lactic acid by *Bifidobacterium* strains isolated fromhuman infants. *Microorganisms* 7:340. doi: 10.3390/microorganisms7090340

Schubert, A. M., Sinani, H., and Schloss, P. D. (2015). Antibiotic-induced alterations of the murine gut microbiota and subsequent effects on colonization resistance against *Clostridium* difficile. *mBio* 6, 1–10. doi: 10.1128/mBio.00974-15

Shahinas, D., Silverman, M., Sittler, T., Chiu, C., Kim, P., Allen-Vercoe, E., et al. (2012). Toward an understanding of changes in diversity associated with fecal microbiome transplantation based on 16S rRNA gene deep sequencing dea. *mBio* 3, 1–10. doi: 10.1128/mBio.00338-12.Editor

Shallcross, L., Beckley, N., Rait, G., Hayward, A., and Petersen, I. (2017). Antibiotic prescribing frequency amongst patients in primary care: a cohort study using electronic health records. *J. Antimicrob. Chemother.* 72, 1818–1824. doi: 10.1093/jac/dkx048

Shannon, C. E., and Weaver, W. (1949). The mathematical theory of communication. *Math. Theory Commun.* 27:117. doi: 10.2307/3611062

Shin, N. R., Whon, T. W., and Bae, J. W. (2015). *Proteobacteria*: microbial signature of dysbiosis in gut microbiota. *Trends Biotechnol.* 33, 496–503. doi: 10.1016/j.tibtech.2015.06.011

Stenman, L. K., Waget, A., Garret, C., Klopp, P., Burcelin, R., and Lahtinen, S. (2014). Potential probiotic *Bifidobacterium animalis* ssp. lactis 420 prevents weight gain and glucose intolerance in diet-induced obese mice. *Benef. Microbes* 5, 437–445. doi: 10.3920/BM2014.0014

Stokholm, J., Blaser, M. J., Thorsen, J., Rasmussen, M. A., Waage, J., Vinding, R. K., et al. (2018). Maturation of the gut microbiome and risk of asthma in childhood. *Nat. Commun.* 9, 1–10. doi: 10.1038/s41467-017-02573-2

Suez, J., Zmora, N., Segal, E., and Elinav, E. (2019). The pros, cons, and many unknowns of probiotics. *Nat. Med.* 25, 716–729. doi: 10.1038/s41591-019-0439-x

Suez, J., Zmora, N., Zilberman-Schapira, G., Mor, U., Dori-Bachash, M., Bashiardes, S., et al. (2018). Post-antibiotic gut mucosal microbiome reconstitution is impaired by probiotics and improved by autologous FMT. *Cell* 174, 1406–1423. doi: 10.1016/j.cell.2018.08.047

Thaiss, C. A., Zeevi, D., Levy, M., Zilberman-Schapira, G., Suez, J., Tengeler, A. C., et al. (2014). Transkingdom control of microbiota diurnal oscillations promotes metabolic homeostasis. *Cell* 159, 514–529. doi: 10.1016/j.cell.2014.09.048

Theriot, C. M., Koenigsknecht, M. J., Carlson, P. E. C. Jr., Hatton, G. E., Nelson, A. M., Li, B., et al. (2014). Antibiotic-induced shifts in the mouse gut microbiome and metabolome increase susceptibility to Clostridium difficile infection. *Nat. Commun.* 5:3114. doi: 10.1038/ncomms4114.Antibiotic-induced

U.S. Food and Drug Administration (2019). *Important Safety Alert Regarding Use of Fecal Microbiota for Transplantation and Risk of Serious Adverse Reactions Due to Transmission of Multi-Drug Resistant Organisms*. Available online at: https://www.fda.gov/vaccines-blood-biologics/safety-availability-biologics/important-safety-alert-regarding-use-fecal-microbiota-transplantation-and-risk-serious-adverse (accessed July 1, 2019).

Underwood, M. A., Kalanetra, K. M., Bokulich, N. A., Lewis, Z. T., Mirmiran, M., Tancredi, D. J., et al. (2013). A comparison of two probiotic strains of bifidobacteria in preterm infants. *J. Pediatr.* 163, 1585–1591. doi: 10.1016/j.jpeds.2013.07.017

Verma, R., Lee, C., and Jeun, E. J. (2019). Cell surface polysaccharides of *Bifidobacterium bifidum* induce the generation of Foxp3 + regulatory T cells. *Sci. Immunol.* 103, 3–4. doi: 10.1097/TP.0000000000002550A

Vrieze, A., Out, C., Fuentes, S., Jonker, L., Reuling, I., Kootte, R. S., et al. (2014). Impact of oral vancomycin on gut microbiota, bile acid metabolism, and insulin sensitivity. *J. Hepatol.* 60, 824–831. doi: 10.1016/j.jhep.2013.11.034

Wiström, J., Norrby, S. R., Myhre, E. B., Eriksson, S., Granström, G., Lagergren, L., et al. (2001). Frequency of antibiotic-associated diarrhoea in 2462 antibiotic-treated hospitalized patients: a prospective study. *J. Antimicrob. Chemother.* 47, 43–50. doi: 10.1093/jac/47.1.43

Yatsunenko, T., Rey, F. E., Manary, M. J., Trehan, I., Dominguez-Bello, M. G., Contreras, M., et al. (2012). Human gut microbiome viewed across age and geography. *Nature* 486, 222–227. doi: 10.1038/nature11053

Conflict of Interest: J-ZX and TO were employed by Morinaga Milk Industry Co., Ltd.

The remaining authors declare that the research was conducted in the absence of any commercial or financial relationships that could be construed as a potential conflict of interest.

frontiers in Microbiology

REVIEW
published: 08 September 2020
doi: 10.3389/fmicb.2020.575072

Microbiota and Cancer: The Emerging Beneficial Role of Bifidobacteria in Cancer Immunotherapy

*Giulia Longhi[1], Douwe van Sinderen[2], Marco Ventura[1,3] and Francesca Turroni[1,3]**

[1] Laboratory of Probiogenomics, Department of Chemistry, Life Sciences, and Environmental Sustainability, University of Parma, Parma, Italy, [2] Alimentary Pharmabotic Centre (APC) Microbiome Institute and School of Microbiology, Bioscience Institute, National University of Ireland, Cork, Ireland, [3] Microbiome Research Hub, University of Parma, Parma, Italy

Many intestinal bacteria are believed to be involved in various inflammatory and immune processes that influence tumor etiology because of their metabolic properties and their ability to alter the microbiota homeostasis. Although many functions of the microbiota are still unclear, there is compelling experimental evidence showing that the intestinal microbiota is able to modulate carcinogenesis and the response to anticancer therapies, both in the intestinal tract and other body sites. Among the wide variety of gut-colonizing microorganisms, various species belonging to the *Bifidobacterium* genus are believed to elicit beneficial effects on human physiology and on the host-immune system. Recent findings, based on preclinical mouse models and on human clinical trials, have demonstrated the impact of gut commensals including bifidobacteria on the efficacy of tumor-targeting immunotherapy. Although the underlying molecular mechanisms remain obscure, bifidobacteria and other microorganisms have become a promising aid to immunotherapeutic procedures that are currently applied to treat cancer. The present review focuses on strategies to recruit the microbiome in order to enhance anticancer responses and develop therapies aimed at fighting the onset and progression of malignancies.

Keywords: microbiota, cancer, *Bifidobacterium*, microbial biomarker, probiotics

OPEN ACCESS

Edited by:
Zhongtang Yu,
The Ohio State University,
United States

Reviewed by:
Jose Munoz,
Northumbria University,
United Kingdom
Valerio Rossini,
University College Cork, Ireland
Shin Yoshimoto,
Morinaga Milk Industry Co., Ltd.,
Japan

****Correspondence:***
Francesca Turroni
francesca.turroni@unipr.it;
francesca.turroni@gmail.com

Specialty section:
This article was submitted to Microbial Symbioses, a section of the journal Frontiers in Microbiology

Received: *23 June 2020*
Accepted: *17 August 2020*
Published: *08 September 2020*

Citation:
Longhi G, van Sinderen D, Ventura M and Turroni F (2020) Microbiota and Cancer: The Emerging Beneficial Role of Bifidobacteria in Cancer Immunotherapy. Front. Microbiol. 11:575072. doi: 10.3389/fmicb.2020.575072

GENERAL FEATURES OF THE GUT MICROBIOTA

The definition of microbiome and microbiota is rather complex and often these two terms are used interchangeably. The microbiota represents the entire population of microorganisms colonizing a specific ecological niche, whereas the microbiome encompasses the full genetic complement of an entire microbiota (Ursell et al., 2012b). In recent years, many studies have focused on the analysis of the bacterial composition that inhabits various sites of the human body. In particular, the Human Microbiome Project (HMP), based on the concept that we are organisms made up of a large number of human and bacterial cells, aims to define the microbiome that consists and/or influences our metabolism, our physiology and any predispositions to diseases (Turnbaugh et al., 2007). The currently employed molecular techniques applied to the microbiota analysis, including the recently emerged metagenomic technology, are based on culture-independent methods. Their application have been made possible due to the advancement of next-generation sequencing methods (NGS),

allowing the compositional evaluation of bacterial populations and the discovery of essentially the entire genetic blueprint of microbial communities (i.e., microbiota and microbiome analysis) (Mancabelli et al., 2020).

The human microbiota comprises trillions of symbiotic microbial cells, present in different areas of the body. The majority of these are located in the intestine where they are involved in various functions including nutrient assimilation, vitamin synthesis, bile acid/salt and sterol metabolism, immune stimulation, and maintenance of intestinal homeostasis. Given the variety and importance of such functions, the intestinal microbiota operates as a separate organ of the human and animal superorganism (Brestoff and Artis, 2013; Guinane and Cotter, 2013; Molinero et al., 2019; Illiano et al., 2020).

The differences in bacterial composition in each microbial habitat are due to different environmental conditions such as pH, oxygen levels/redox state, availability of nutrients, humidity and temperature. All these environmental features allow various populations to thrive and exert different activities, while interacting with the (human) host environment (Ursell et al., 2012b).

The composition of the human intestinal microbiota is very complex and includes bacteria, archaea, fungi and viruses that have adapted to live on the mucous surface of the intestine or in its lumen (Nuriel-Ohayon et al., 2016), developing immediately after birth and varying between different gut locations, between individuals and over time. Until today, it has been assumed that the neonatal gut intestine was a sterile niche up until birth (Putignani et al., 2014), though various scientific reports have questioned this notion, claiming that bacteria are present in the gut before birth (Nuriel-Ohayon et al., 2016). However, a growing number of scientific publications have argued against such a possibility and most evidence currently favors the idea of a sterile placenta (Lauder et al., 2016). The period immediately following birth is deemed to be crucial for the appropriate development of the gut microbiota (Turroni et al., 2020). Vaginal delivery and breastfeeding are the main defining factors that favor efficient and correct microbial colonization events of the neonatal gastrointestinal tract (Milani et al., 2017a). Among the first colonizers of the infant gut microbiota are bifidobacteria (Turroni et al., 2012), rapidly populating the infant gut within the first weeks following birth. This remarkable phenomenon of gut colonization is believed to be at least partially dependent on the bifidogenic activities of specific mother milk-derived oligosaccharides, commonly referred to as human milk oligosaccharides (HMOs) (Turroni et al., 2019). Recent studies have shown that the bifidobacteria present in the mother's gut microbiota strongly correlates with that of her baby, indicative of vertical transmission of bacteria from mother to baby (Rautava et al., 2012; Nuriel-Ohayon et al., 2016).

The transition to complementary feeding, and therefore the introduction of solid foods, favors the differentiation of the intestinal microbiota and increases microorganisms belonging to the families of *Lachnospiraceae*, *Ruminococcaceae*, *Eubacteriaceae*, *Rikenellaceae*, and *Sutterellaceae* (Laursen et al., 2016). During subsequent years, the microbiota develops to form its adult state and tends to maintain this homeostasis (Underhill and Iliev, 2014), which means that the microbiota composition of a healthy adult gut is stable (Rodriguez et al., 2015). The intestinal bacterial profile in adulthood displays a high level of inter-individual variability, being influenced by a wide range of factors such as health status, dietary habits, use of antibiotics or other drugs, age, genetics, ethnicity and geography (Ursell et al., 2012b; Yatsunenko et al., 2012). The main bacterial phyla of the human gut microbiota encompass members of the *Firmicutes*, *Bacteroidetes*, *Actinobacteria*, *Proteobacteria*, *Tenericutes*, and *Fusobacteria*. Notably, the gut microbiota of adults are dominated by Firmicutes and Bacteroidetes, which together make up 90% of the human gut microbiota (Rajilic-Stojanovic et al., 2007). The adult gut microbiota composition is radically different from that of the infant's intestine, in which Actinobacteria, and in particular bifidobacteria, are commonly the most numerous microorganisms (Turroni et al., 2012). In addition, the adult microbiota has proven to be more complex than that of infants in terms of the total number of bacteria and microbial diversity (Eckburg et al., 2005). The microbiota composition changes with aging and becomes less complex in terms of number of species and relative abundance in the elderly population (Claesson et al., 2011). Throughout life, diet influences bacterial colonization and persistence in the intestine, thus shaping the gut microbiota composition (Fuentes and de Vos, 2016). In this context, butyrogenic bacteria such as members of the genus *Clostridium* cluster XIVa, responsible of butyrate production, are more abundant in the fecal microbiota of omnivores than in the vegetarian microbiota, including humans. However, in response to a Western-based diet, which is characterized by the presence of low fiber levels and high fat intake, the bacteria responsible for fiber degradation, such as *Prevotella*, *Succinivibrio*, *Treponema*, and *Bifidobacterium*, are reduced in abundance. Conversely, a diet mainly based on meat causes an increase of bile-tolerant bacteria (e.g., *Alistipes*, *Bilophila*) to the detriment of the microorganisms involved in the metabolism of plant polysaccharides (*Firmicutes*) (Milani et al., 2016).

Gut microbiota plays a key role in maintaining and supporting human health. Any deviation from its "normal" composition, a condition for which the generic term dysbiosis was coined (Tamboli et al., 2004), is believed to herald the onset or the worsening of certain diseases, including autoimmunity, colorectal cancer, metabolic diseases, and bacterial infections (Prakash et al., 2011). Indeed, recent work has indicated that altered microbial communities and intestinal barrier impairment are associated with the development of a number of chronic inflammatory disorders, including inflammatory bowel disease (IBD), celiac disease, multiple sclerosis, rheumatoid arthritis, psoriasis, type 2 diabetes, allergic diseases, cardiovascular, and neurodegenerative diseases (Yu, 2018), some of which may directly or indirectly lead to cancer (Stidham and Higgins, 2018).

THE ROLE OF MICROBIOTA IN CARCINOGENESIS

Through their metabolic activities, intestinal bacteria are believed to influence various inflammatory and immune

processes that are implicated in tumor etiology, such as in colorectal cancer (CRC) (Kinross et al., 2011; Clemente et al., 2012). CRC is one of the major causes of mortality in developing countries (Jemal et al., 2011). Even though it is well-established that a healthy environment and lifestyle reduce the risk of carcinogenesis, it is still extremely difficult to identify the triggering factor(s) of cancer in individuals, due to its multifactorial etiology (Hanahan and Weinberg, 2011). Currently, the incidence of cancer is still increasing, possibly and in part due to cancer-associated lifestyle choices such as smoking, "westernized" diet and physical inactivity. However, increased exposure to known carcinogens or suspected carcinogens may also be a contributing factor (Torre et al., 2015). Cancer may therefore result from the impact of various genetic factors acting in concert with a range of environmental and life-style associated insults (Garrett, 2015). Studies involving germ-free animals, i.e., animals without a resident intestinal microbiota, have provided compelling evidence for tumor-promoting effects of the microbial composition in spontaneous, as well as genetically or carcinogen-induced tumorigenesis in various organs (Schwabe and Jobin, 2013). Germ-free mice exhibit severe defects in their immunity system, with a near-absent mucous layer and altered IgA secretion (Gopalakrishnan et al., 2018a). Similarly, depletion of the intestinal bacterial microbiota in mice by means of antibiotic treatment, reduces the development of cancer in the liver and in the colon (Dapito et al., 2012; Yoshimoto et al., 2013). It has been suggested that common microbial inhabitants of the human gut, such as *Escherichia coli*, which normally coexist harmoniously with their mammalian host and promote intestinal homeostasis, may sometimes facilitate colorectal carcinogenesis (Cuevas-Ramos et al., 2010). Indeed, some virulent *E. coli* strains with acquired pathogenicity islands encoding for a multi-enzymatic machinery for the production of a peptide-polyketide hybrid genotoxin named colibactin, can colonize the human gastrointestinal tract and cause gut diseases (Sun and Kato, 2016). These particular *E. coli* strains are more commonly present in the mucosa of CRC and IBD patients and they induce double-strand DNA breaks, mutations and chromosomal rearrangements. They also modulate the tumor microenvironment favoring the emergence of senescent cells, which may affect tumor promotion and cancer progression via the secretion of growth factors (Dalmasso et al., 2014).

In addition, a recent report has demonstrated that intestinal bacteria belonging to the class of Gammaproteobacteria can influence the efficacy of cancer therapies by metabolizing the chemotherapeutic drug gemcitabine into its inactive form, commonly used to treat pancreatic ductal adenocarcinoma (PDAC) (Geller et al., 2017). Moreover, thanks to the current knowledge on the role of gut microbes in gastrointestinal carcinoma development, novel approaches targeting the gut microbiota represent a promising way to prevent cancer or at least to delay cancer cell proliferation (Brennan and Garrett, 2016). Therefore, the gastrointestinal microbiota appears to play opposing roles in both preventing and promoting carcinogenesis.

One of the main activities of the colonic intestinal microbiota is to acquire energy by fermenting dietary elements (e.g., polysaccharides) that are not metabolized by host enzymes or by the microorganisms residing in the upper gastrointestinal tract (GIT) (Rowland et al., 2018). Many of such indigestible carbohydrates, resistant to human digestion, enter the colon where they are metabolized by resident microbiota into short chain fatty acids (SCFAs) such as butyrate, propionate and acetate, which are in turn absorbed by the intestinal epithelial cells (IECs) through passive diffusion (Pryde et al., 2002). SCFAs, and in particular butyrate, represent the primary energy source for IECs and play an important role in maintaining the integrity of the associated epithelial layer (Lauder et al., 2016).

Furthermore, butyrate is a plausible candidate for tumor suppression and prevention because it inhibits cell proliferation and induces cell differentiation or apoptosis when added to tumor-derived cell lines (Hamer et al., 2008; Fung et al., 2012). In addition, some lactic acid bacteria (LAB) have been proposed to confer benefits to the host by influencing metabolic, immunological and protective functions in the colon (Marteau et al., 2001). In animal models, treatment with certain LAB was shown to prevent carcinogen-induced pre-neoplastic lesions or tumors (Wollowski et al., 2001). Besides, it has also been demonstrated that particular LAB species are involved in the detoxification of certain carcinogens such as polycyclic aromatic hydrocarbons (PAH) and heterocyclic aromatic amines (Knasmuller et al., 2001; Hope et al., 2005). PAH may also damage DNA of colonocytes (Diggs et al., 2011). However, the mechanism by which these bacteria achieve inactivation of carcinogens remains unclear; it may be that certain gut commensals catalyze detoxification reactions and/or produce metabolites that cause carcinogen detoxification (Rafter, 2003).

Furthermore, gut microorganisms that lack the ability to produce butyric acid may influence the growth of butyrogenic microorganisms by synthetizing metabolites that are specifically utilized by these bacteria. In this respect, bifidobacteria synthesize various organic acids, such as acetic acid that can be used as a metabolic precursor for butyric acid biosynthesis by butyrogenic microorganisms such as *Faecalibacterium prausnitzii* and *Eubacterium rectale* (Waddington et al., 2010).

As mentioned above, bacteria belonging to the *Clostridium* genus, despite exerting physiologically important effects on the colonic epithelium and on the host metabolism of omnivores, are known to convert bile acids into secondary products such as deoxycholic acid (DCA), which is a known carcinogen (Knasmuller et al., 2001; Staley et al., 2017). This finding shows how intestinal microorganism sometimes play a key role in the activation and detoxification of various classes of carcinogens, thereby influencing cancer risk for individuals (Hambly et al., 1997).

Many tumor-promoting effects of the microbiota, not only in colorectal cancer but also in other cancer types, are caused by altered host-microbiota interactions and dysbiosis. The microbiological imbalance, caused by the failure of some control mechanisms like barrier defects, immune defects and loss of

eubiosis, may cause a modification of intercellular tight junctions (Llopis et al., 2009), in turn causing effective penetration of antigens responsible for the activation of gut associated lymphoid tissue (GALT) with consequent tissue damage (Arseneau and Cominelli, 2009). These combined factors enhance the chances of pathogenic bacteria to encourage carcinogenesis under particular conditions. In this context, infection with *Helicobacter pylori*, which is classified as a carcinogenic microorganism by the International Agency for Research on Cancer (IARC), may lead to the sequential development of gastritis, gastric ulcer, atrophy and finally gastric cancer (Fox and Wang, 2007). However, gastric cancer is also promoted by the presence of a complex microbiota. This phenomenon was identified in murine models treated with *H. pylori*, which developed fewer tumors than their pathogen-free counterparts. This is probably due to the ability of *H. pylori* to provoke gastric atrophy and hypochlorhydria, which causes the stomach being susceptible to bacterial overgrowth, and subsequently increased bacterial conversion of dietary nitrates into carcinogens (Lofgren et al., 2011).

Besides, dysbiosis is regarded as one of the highest risk factors of chronic inflammation through immune system activation (Fujimura et al., 2010). Rudolf Virchow first suggested the connection between inflammation and cancer in 1863, when he observed the presence of leukocytes within tumor tissues and hypothesized that the presence of these cells mirrored the origin of the tumors in sites characterized by chronic inflammation (Virchow, 1989). IBDs, including Crohn's disease (CD), are genetically linked to a phenotype characterized by a significant reduction of the microbiota complexity, an increased abundance of *Enterobacteriaceae*, *Pasteurellaceae*, *Fusobacteriaceae*, *Neisseriaceae*, *Veillonellaceae*, and *Gemellaceae*, and decreased abundance of *Bifidobacteriaceae*, *Erysipelotrichaceae*, *Clostridiales*, and *Bacteroidales* (Gevers et al., 2014). *Faecalibacterium prausnitzii*, which represents about 5% of the intestinal microbiota in healthy adults, is also a widely recognized microbial marker associated with IBD (Martin et al., 2017). Low levels of *F. prausnitzii* in fecal and mucosal samples have been shown to be predictive of both incidence and recurrence of IBD (Sokol et al., 2008, 2009). This is mainly due to the critical role played by this bacterium in maintaining intestinal homeostasis and health through regulation of the metabolic activity of colonocytes (Scheppach, 1994) and the integrity of the mucous layer (Wrzosek et al., 2013).

It is well-established that individuals with IBD have a higher risk of developing gastrointestinal cancer, with risk level corresponding to the duration and severity of mucosal inflammation (Hope et al., 2005). The increased risk of cancer in IBD patients may be associated with the chronic cellular proliferation required to repair damage to the epithelial monolayer caused by constant inflammation. In chronic inflammation, cytokines secreted by immune cells stimulate the pathways that are also connected to cancer proliferation (Morgillo et al., 2018). For example, tumor necrosis factor-alpha (TNF-α) and interleukin 6 (IL-6), the main cytokines released during chronic inflammation, are known to stimulate proliferation of cancer cells, their survival and their dissemination.

CANCER AND NOVEL MICROBIAL MARKERS

As described above, there is accumulating scientific evidence that certain members of the microbiota are implicated in tumor development. One bacterium that has recently attracted the interest of the scientific community based on studies of the microbiome of colorectal cancer is *Fusobacterium nucleatum* (Mima et al., 2016). This microorganism belongs to the Fusobacteria phylum, which are Gram-negative, non-spore-forming, typically non-motile anaerobes with a tapered rod shape (Brennan and Garrett, 2019). Among those species colonizing humans, *F. nucleatum* is the most abundant in the oral cavity and a common member of the oral microbiota, playing integral and important roles in biofilm development, contributing to both periodontal health and disease (Kolenbrander et al., 2010). Due to its elongated shape and adhesin production, it acts as a bridge-organism by connecting microorganisms and cells (Kaplan et al., 2009; Wu et al., 2015). *F. nucleatum* possesses a mutualistic relationship with other members of the oral microbiota, and its interactions with human tissues range from neutral to pathological interactions. In the particular case of periodontitis, *F. nucleatum* increases the infectivity of other pathogenic oral microorganisms, thereby underpinning this disease (Brennan and Garrett, 2019). In particular, *F. nucleatum* may induce expression of the β-defensin 2 peptide and certain pro-inflammatory cytokines (Krisanaprakornkit et al., 2000; Brennan and Garrett, 2019) as well as increase the invasive potential of *Porphyromonas gingivalis* (Taxman et al., 2012), suggesting that during periodontitis these bacteria act cooperatively to evade the immune system and develop an inflammatory-permissive environment.

Indeed, studies have shown that *F. nucleatum* is involved not only in oral inflammation such as periodontitis (Krisanaprakornkit et al., 2000), but also in brain abscesses (Kai et al., 2008), pericarditis (Han et al., 2003), Lemierre syndrome (Weeks et al., 2010), and in acute appendicitis (Swidsinski et al., 2011). The microbiome analyses of colorectal carcinomas reveal a significant enrichment of *Fusobacterium* species, in particular phylotypes more similar to *F. nucleatum*, *Fusobacterium mortiferum* and *Fusobacterium necrophorum*. The enrichment of the fusobacterial load in cancer is confirmed by histological analysis on tumor tissues when compared to adjacent tissues and by the DNA of *F. nucleatum* found in the CRC metastases (Kostic et al., 2012). Moreover, it has been demonstrated that patients with CRC possess identical strains of *F. nucleatum* in their CRC and saliva specimens. Although the relationship between these bacteria and CRC is not well-understood, this finding does suggest that *F. nucleatum* strains associated with CRC may have originated from the oral cavity (Komiya et al., 2019). High abundances of these bacteria are also found at the level of adenomas, epithelial neoplastic lesions that can become malignant and be precursors of most

colorectal cancers. In fact, in patients with early CRC (Yachida et al., 2019) *F. nucleatum* increases in abundance during the very early stages of carcinogenesis, thus suggesting that it could be involved in the tumor onset and progression (Kostic et al., 2013). Its abundance in colorectal instead of adjacent tissues may be caused by the strong adhesive and invasive abilities of fusobacteria toward colonic epithelial cells due to the *FadA* surface protein (*Fusobacterium* adhesin A), which interacts with E-cadherin to mediate changes in β-catenin and other signaling pathways, thereby inducing inflammatory changes and contributing to carcinogenesis (Han et al., 2000; Strauss et al., 2011; Rubinstein et al., 2013). The presence of *F. nucleatum* cells plays an important role also on the binding between Gal-GalNAc and Fap2, becoming overexpressed in CRC (Abed et al., 2016). The high numerical presence of fusobacteria at the tumor site may also be derived from the growth advantage that fusobacteria provide to the tumor by eliciting myeloid immune cell responses that promote tumor growth. Fusobacteria elicit a metabolic advantage to tumor cells in a competitive tumor environment. Like non-saccharolytic bacteria and in contrast to *Enterobacteriaceae*, fusobacteria, which can metabolize glucose and amino acids, will not compete for glucose in a tumor microenvironment as they can use amino acids and peptides as nutrient sources, thereby supporting tumor metabolism (Vander et al., 2009). *F. nucleatum* strains can by means of a rudimentary electron transport chain establish a respiratory-like metabolism (Kapatral et al., 2002) allowing them to persist and slowly replicate in the hypoxic tumor microenvironment. Due to its ability to express adhesive molecules, *F. nucleatum* is able to form biofilms that enhance oxygen tolerance (Gursoy et al., 2010). A previous study has shown that the administration of *F. nucleatum* in ApcMin/+ mice, which carry a point mutation in the Adenomatous Polyposis Coli (APC) gene on a single allele, accelerates the progression and carcinogenesis, provokes infiltration of specific myeloid cells into the tumor and creates a pro-inflammatory environment through the induction of the NF-κB pathway (Kostic et al., 2013). This suggests that the tumorigenic effects of fusobacteria operate downstream of the loss of the APC tumor suppressor and the consequent intestinal dysplasia that occurs in ApcMin/+ mice. Moreover, this may explain why increased abundance of *F. nucleatum* occurs already during the first phase of adenoma, as the APC mutation is among the first molecular alterations that arise in the epithelium while it is in transition to become adenoma (Kostic et al., 2013). However, early somatic mutations that can lead to loss of tight junction, cellular contacts, polarity and mucus layer in the gut, may promote infiltration and enrichment of *Fusobacterium* spp.

Furthermore, *F. nucleatum* may function as a predictive marker of tumor recurrence because its numbers are increased in CRC patients who show post-chemotherapy relapse (Sun et al., 2019). It was therefore assumed that it may induce chemoresistance by blocking chemotherapy-induced apoptosis and activating pathway for autophagy by inducing upregulation of multiple autophagy signaling elements (pULK1, ULK1, and ATG7) (Yu et al., 2017).

The Fusobacteriales order also includes the *Leptotrichiaceae* family, whose *Leptotrichia* spp. appears to be predominantly present in CRC tissues (Warren et al., 2013). *Leptotrichia* spp. are Gram-negative facultative anaerobes, commensal members of the oral microbiome and subgingival plaque, but they can also be present in the gut, urogenital system, and female genital tract (Eribe et al., 2004). Isolated from several periodontal lesions, abscesses and systemic infections, they are opportunistic pathogens (Manson et al., 2014). In fact, previous studies describe the occurrence of *Leptotrichia buccalis*-mediated bacteremia in patients with neutropenia and progressive malignancy, though its incidence in serious bacteremic infections remains comparatively low (Reig et al., 1985; Weinberger et al., 1991).

Due to its microbial co-aggregation ability, *Fusobacterium* is found together not only with *Leptotrichia* but also with *Campylobacter* spp., which are all anaerobic bacteria that commonly colonize the same niche in the oral cavity. Co-occurrence of *Fusobacterium* and *Campylobacter* spp. is observed in CRC patients with a prevalence of *Campylobacter* spp. in CRC lesions compared with adjacent healthy tissues (Warren et al., 2013). Some genotoxins produced by enteric pathogenic species such as *Salmonella*, *Escherichia*, and *Campylobacter* have a synergistic effect on carcinogenesis (Guerra et al., 2011; Bezine et al., 2014). *Campylobacter jejuni* is a well-characterized human pathogen and one of the main causes of acute gastroenteritis and colitis (Brauner et al., 2010). A specific cytolethal distending toxin (CDT), produced by *C. jejuni* and composed of three subunits, plays a key role in carcinogenesis. In particular, one specific subunit (CdtB) is implicated in promoting carcinogenesis, since mutation of the corresponding gene in *C. jejuni* causes reduction of both tumor cells and neoplastic progression. This subunit, which can induce extensive DNA damage in host cells and in turn provoke cell apoptosis, is known to stimulate tumor proliferation (He et al., 2019). The above mentioned CDT activities have previously been associated with carcinogenesis in studies reporting high level of *cdt* mutant strains present both in biopsies of CRC patients and in hepatocarcinogenesis and intestinal tumorigenesis in mice (Ge et al., 2007; Buc et al., 2013; Ge et al., 2017).

However, the precise role played by *Fusobacterium, Leptotrichia*, and *Campylobacter* in the etiology of carcinogenesis is still not fully understood and requires further study.

NEW DIAGNOSTIC APPROACHES USING MICROBIAL MARKERS

A lot of effort has been devoted to identifying microbes that can be employed as biological markers for CRC. At the same time, research endeavors have also focused on the most appropriate technique to detect such microbes. The most frequently used method is a test performed on the sera of CRC patients, allowing the detection of cell-free DNA (cfDNA) corresponding to DNA fragments originating from tumor cells. These fragments can be further examined for mutations and genomic abnormalities, providing both diagnostic and prognostic biomarkers (Tan et al., 2016). So far, different diagnostic tests, being useful for the detection of CRC but having low specificity and sensitivity, are performed on fecal occult blood. Additionally, the detection of

mutated DNA in stool is a promising technique (Dhaliwal et al., 2015). Detection of IgA and IgG antibodies against some of these potential microbial biomarkers may also represent a future diagnostic tool (Wang et al., 2016).

Various recent studies involving large patient cohorts have focused on the characterization of the microbiome of colorectal adenomas and on cancer, aimed at assessing the presence of *F. nucleatum* in stool and tissue samples of patients, who had received a positive CRC diagnosis (Kostic et al., 2012; McCoy et al., 2013; Peng et al., 2018).

Diagnostic tests designed to determine the presence of biomarkers are very useful not only for diagnosis, but also for assessing the patient's prognosis and for developing therapies aimed at combating the onset and progression of tumors. However, there are ongoing debates on the use of *F. nucleatum* as a reliable CRC biomarker. Not only the method for microbial detection is important in this context, but also the predictive accuracy of microbial biomarker(s) using larger population-scale studies that also take into account the differences due to ethnicity and geography (Brennan and Garrett, 2019).

As *F. nucleatum* appears to influence myeloid cell tumor infiltration, the phenotype of T cells and the cytotoxic activity of NK cells has received significant scientific attention (Routy et al., 2018). Furthermore, the high abundance of *F. nucleatum* in tissues and fecal samples of cancer patients who show relapse after having undergone chemotherapy is indicative of the impact of this bacterium on chemotherapy resistance. This potential biomarker activates the process of autophagy and compromises chemotherapy-mediated cancer cell death (Yu et al., 2017). These findings have resulted in a therapy that is directed to specifically target *F. nucleatum*, before or concomitant with the administration of chemotherapy. Most *F. nucleatum* isolates are sensitive to antibiotics such as erythromycin, other macrolides (Riordan, 2007), metronidazole (Bullman et al., 2017) and numerous β-lactam based antibiotics with the exception of penicillin (Nyfors et al., 2003). Additionally, epidemiological and clinical data suggest that non-steroidal anti-inflammatory drugs (NSAIDs) such as aspirin may be effective as a primary and secondary preventive measure in CRC (Chan et al., 2012). However, it may be more advantageous to use narrow-spectrum antibiotics specific for *F. nucleatum* and targeting tumor tissue in order to protect the anaerobic bacteria that play a crucial role in improving the response to chemotherapy and immunotherapy (Brennan and Garrett, 2019).

Currently, cancer treatment strategies are increasingly focusing on immunotherapy and chemoprevention. The former one, including the use of COX-2 inhibitors and selective EP2 antagonists, plays a significant role in counteracting *F. nucleatum*-associated CRC (Shang and Liu, 2018). EP2 enhances the expression of NF-κB-targeted proinflammatory genes induced by TNF-α in neutrophils, promoting colon tumorigenesis by means of expanding inflammation and creating a tumor microenvironment. Selective EP2 antagonists are promising drugs for the chemoprevention of *F. nucleatum*-associated CRC (Ma et al., 2015). COX-2 is considered an inhibitor of antigen-specific tumor immunotherapy. Therefore, COX-2 inhibitors reduce the risk of CRC by inhibiting inflammatory pathways, and the use of such inhibitors may therefore be important to enhance efficacy of immune-based therapy in CRC patients (Gobel et al., 2014). Immunotherapy may also represent an effective strategy to prevent *F. nucleatum*-positive CRC. The interaction between Fap2 and TIGIT receptor protects tumors against immune cell attack and inhibits antitumor immunity (Gur et al., 2015).

The reduction of *Fusobacterium* populations in the oral cavity, where they are most abundant, or in the gastrointestinal tract may work to delay or prevent tumor progression for patients at increased risk of CRC (Kostic et al., 2013). For this reason, *F. nucleatum* has been the target of vaccine and/or antimicrobial therapies. The formulation of a possible vaccine has already been tested to fight the problem of halitosis. This vaccine targets FomA, which is a protein of the outer membrane expressed by certain strains of *F. nucleatum* and necessary for bacterial co-aggregation and its associated pathogenicity. Inhibition of co-aggregation by inactivation of *F. nucleatum* FomA will prevent the progress of oral infections (Liu et al., 2010). Another option to reduce *F. nucleatum* abundance could be a replacement therapy of the microbial ecosystem aimed at modifying host and tumor microbiota through the use of consortia of engineered microorganisms or selected cocktails of human-derived isolates (Petrof et al., 2013).

IMMUNOTHERAPY AS A NEW FRONTIER IN THE FIGHT AGAINST CANCER

Cancer remains a major cause of mortality and many of the therapies that have been used so far to fight it are very often ineffective and bring high degree of toxicity (Puzanov et al., 2017). Until recently, cancer was routinely treated through surgical, chemotherapy and/or radiotherapy approaches (Yu W.D. et al., 2019). However, the high level of toxicity and the high incidence of cancer recurrence always make these therapies desirable or effective. A new frontier in cancer therapy is represented by immunotherapy (Yang, 2015), which holds a lot of promise in terms of therapeutic success and allows tumor targeting in a much more specific way than other currently applied therapies. In addition, immunotherapy offers the advantage of immune system memory against malignant cells to achieve a durable cure with minimal toxicity (Helmy et al., 2013). Two forms of immunotherapy are currently recognized: (i) "passive" immunotherapy that includes agents such as cytokines, antibodies and transferred immune cells that target the tumor directly, and (ii) "active" immunotherapy that mobilizes the immune system to eliminate the tumor (through vaccination) (Finn, 2012).

The antibody-mediated approach is a well-established, specific immunotherapy for cancer in clinical practice (Finn, 2012). Monoclonal antibodies for therapeutic purposes have been designed to bind with high affinity to specific cell surface molecules on cancer cells to direct the immune system toward the elimination of malignant cells (Shepard et al., 2017).

Perhaps the most intriguing class of antibody therapeutics currently being developed for cancer includes the one designed to activate anti-tumor therapeutic immunity, encompassing the immune checkpoint blockade (ICB). Immune checkpoint therapy targets regulatory pathways in T cells by removing their inhibitory signals, thereby enabling tumor-reactive T cells to overcome regulatory mechanisms and to mount an effective antitumor response (Sharma and Allison, 2015). Since many of these antibodies are activated by ligand-receptor interaction, the immune checkpoints can be readily blocked by antibodies or modulated by recombinant forms of ligands or receptors (Routy et al., 2018). The two most actively studied are cytotoxic T-lymphocyte-associated antigen 4 (CTLA-4) and programmed cell death protein 1 (PD-1), which are both inhibitory receptors, regulating immune responses at different levels and by different mechanisms (Pardoll, 2012). In 2011, CTLA-4 became the first validated target of ICB in the treatment of patients with melanoma, and in spite of the beneficial effects, this therapy is accompanied by various toxic effects that can sometimes lead to autoimmune issues (Prieto et al., 2012; Schachter et al., 2017).

In the same manner, different antibodies that disrupt the interaction between PD-1 and its ligands have been approved for therapeutic purposes. PD-L1 together with PD-L2 are binding and functional partners of PD-1, expressed on the surface of many organ cells and in various tissues (Freeman et al., 2000; Latchman et al., 2001) playing a dominant role in the suppression of T cell responses, especially in the tumor microenvironment (Zou and Chen, 2008), thereby preventing effector immune cells from killing cancer cells (Azuma et al., 2008). Recent studies have shown how anti-PD-1 outperforms anti-CTLA-4 therapy in efficacy, survival and adverse events (Schachter et al., 2017).

A novel way to fight cancer employs genetic engineering of the immune effector cells in order to modify their functions. Following the interest given to the first successful treatments with chimeric antigen receptor (CAR) T-cell in B-cell acute lymphoblastic leukemia (Maude et al., 2018), high level expectations have been created which will require detailed investigations (Kochenderfer et al., 2010; Kalos et al., 2011). CAR T-cells are produced by transducing a genetically engineered CAR fusion protein by means of a retrovirus or lentivirus into autologous T-cells (Sermer and Brentjens, 2019).

However, ICB and CAR T-cell therapies are not universally effective due to the genetic instability of tumors which may lead to cessation of the expression of antigens targeted by T cells or which may eliminate the mechanisms that present them (Bronte and Mocellin, 2009).

BACTERIA ELICITING BENEFICIAL EFFECTS TOWARD CANCER TARGETED BY IMMUNOTHERAPIES

ICB has revolutionized the therapeutic approach in immunogenic cancers like melanoma (Vetizou et al., 2015) and renal cell carcinoma (RCC) (Motzer et al., 2015) as well as malignancy considered non-immunogenic like non-small cell lung cancers (NSCLC) (Borghaei et al., 2015; Carbone et al., 2017) or mismatch-repair-deficient colorectal cancer (Le et al., 2015).

Various studies have indicated that microbiota composition impacts on the efficacy of ICB therapies. The use of antibiotics to induce intestinal dysbiosis in preclinical mouse models has underlined the contribution of certain commensal bacteria such as *Bacteroides fragilis* (Vetizou et al., 2015) and *Bifidobacterium* (Sivan et al., 2015). Mice treated with broad-spectrum antibiotics or germ-free (GF) mice that lack some bacterial species, in particular *Bacteroides*, are resistant to CTLA-4 blockade therapy. The response to the inhibition of CTLA-4 is regained with the oral administration of *Ba. fragilis*. Recolonization of the intestinal microbiota by *Ba. fragilis* consequently causes T-cell helper (TH1) responses to increase in the lymph nodes closest to the tumor, thereby improving the efficacy of the CTLA-4 blockade. A similar significant response is observed in cases of fecal transplantation of *Bacteroides* species in GF mice (**Figure 1**; Vetizou et al., 2015). In parallel, another trial compared the antitumor cytotoxic T lymphocytes (CTLs) responses in mice purchased from two different facilities differing in their commensal microbes. Indeed, Jackson Laboratory (JAX) mice but not Taconic Farms (TAC) mice, may be colonized by commensal microbes that facilitate antitumor immunity. Of note, *Bifidobacterium* was found to be particularly abundant in the colon of JAX mice that exhibited reduced growth of melanomas and improved CTL-mediated immune-surveillance. The presence of *Bifidobacterium* was shown to be positively associated with antitumor T cell responses, indicating that certain species of this genus, identified as *Bifidobacterium breve*, *Bifidobacterium longum* and *Bifidobacterium adolescentis*, elicit beneficial antitumor immune effects (Sivan et al., 2015).

In addition, the selective transfer of *B. breve* or *B. longum* into mice that typically are devoid of these species was sufficient to reduce melanoma natural growth and restore anti-melanoma specific T cell responses. As a result, the frequency of tumor-specific CTLs residing in melanoma lesions increased in mice carrying *B. breve* or *B. longum* cells, on respect of germ-free mice or mice without bifidobacteria in the gut (**Figure 1**; Sivan et al., 2015). The use of bioluminescent imaging (BLI) allows the detection of certain bacterial species, including species of bifidobacteria, following administration in tumor-bearing mice (Cronin et al., 2012). Preclinical therapeutic studies had already demonstrated the ability of different bacterial strains to migrate to the tumor site (Grillot-Courvalin et al., 1998). Once administered, bifidobacteria can survive in the hypoxic tumor environment due to the nutrient-rich environment created by cell death in necrotic regions. This finding demonstrates the potential for non-pathogenic bacteria as vectors for cancer therapy in order to deliver therapeutic or diagnostic agents (Cronin et al., 2012).

The specific mechanism by which bifidobacteria or other commensal bacteria stimulate antitumor immune responses remains to be elucidated. However, it has been shown that these bacteria stimulate the maturation of dendritic cells that, like antigen-presenting cells (APC), play a role in activating T-cells. CTLA-4 is a homolog of APCs' receptor that binds with higher affinity and downregulates T-cell activation. Anti-CTLA-4 monoclonal antibodies block this interaction favoring

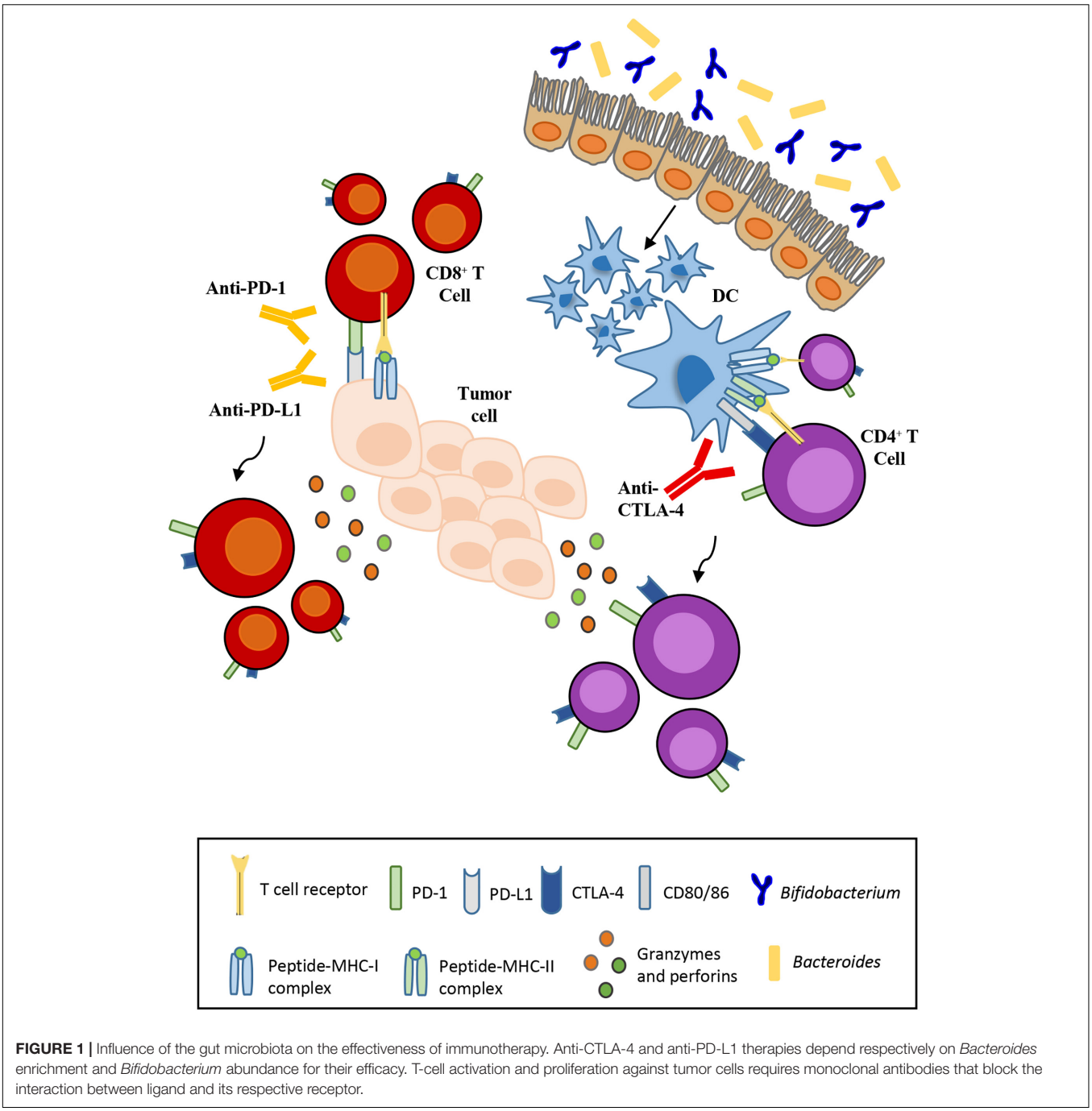

FIGURE 1 | Influence of the gut microbiota on the effectiveness of immunotherapy. Anti-CTLA-4 and anti-PD-L1 therapies depend respectively on *Bacteroides* enrichment and *Bifidobacterium* abundance for their efficacy. T-cell activation and proliferation against tumor cells requires monoclonal antibodies that block the interaction between ligand and its respective receptor.

T-cell activation and proliferation (Krummel and Allison, 1995). In contrast, PD-1 has two ligands, i.e., PD-L1 and PD-L2, where PD-L1 is expressed by cancer cells and tumor-infiltrating macrophages, while PD-L2 is expressed by APCs (Francisco et al., 2010). The interaction of PD-L1 with PD-1 may induce T cell suppression. PD-1 blockade by monoclonal antibodies restores the function of T-lymphocytes.

The translational relevance of these findings to humans was then shown in other studies that clearly demonstrated the significant contribution of different commensals in the positive response to immunotherapy treatment against different types of cancer; *Akkermansia muciniphila* on NSCLC or RCC patients, and *Fecalibacterium* spp. or *Bifidobacterium* spp. on melanoma patients (Gopalakrishnan et al., 2018b; Matson et al., 2018; Routy et al., 2018).

Recently, the impact of antibiotics (ATB) use in patients with different types of cancer (lung, renal, urothelial) who were treated with PD-1/PDL-1 inhibitors was investigated (Routy et al., 2018). As observed in murine-based trials, patients treated with ATB show reduced survival regardless of the type of tumor and a

general reduction in the anti-PD-1/PD-L1 therapeutic responses. From the analysis and comparison of the microbiota obtained from fecal samples of the immunotherapy responding (R) and non-responding (NR) subjects (according to the best clinical response as assessed by Response Evaluation Criteria in Solid Tumors), differences were particularly noted in the abundance of *A. muciniphila*, which was more present in R patients and positively associated with an increase of more than 3 months of tumor-free survival (Routy et al., 2018). An increased abundance of other commensals such as *Ruminococcus* spp., *Alistipes* spp. and *Eubacterium* spp., was also observed, while *B. adolescentis*, *B. longum*, and *Parabacteroides distasonis* were underrepresented (Matson et al., 2018). To test the effective correlation between *A. muciniphila* and the response to PD-1/PDL-1 inhibitors, a recolonization of ATB-treated mice reared in specific pathogen-free (SPF) conditions (or alternatively GF animals) by fecal microbiota transplantation (FMT) was performed using patient stool by oral gavage of feces harvested at diagnosis from different NSCLC patients, R and NR. This *in vivo* test corroborated the clinical data according to which mice receiving FMT from R, therefore with marked presence of *A. muciniphila*, demonstrated a better response to immuno-oncological therapies (Routy et al., 2018) and a significant reduction in tumor size with a greater accumulation of immune cells at the level of the cancerous microenvironment. Indeed, the release of IL-12 cytokines, which support the role of T lymphocytes, in response to the significant presence of *A. muciniphila* (Sivan et al., 2015), seems to have increased. However, the precise immunomodulatory mechanism still remains unclear (Collado et al., 2007). Moreover, the clinical significance of the gut microbiota as a novel biomarker of immune checkpoint inhibitor (ICI) response needs to be validated in prospective studies.

Evaluation of the gut microbiota composition of patients with cutaneous melanoma treated with anti-PD-1 confirmed a marked presence of Clostridiales and Ruminococcaceae bacteria, especially *Faecalibacterium* in the intestine of R patients, while in NR patients *Bacteroides thetaiotaomicron*, *E. coli*, and *Anaerotruncus colihominis* are more abundant (Gopalakrishnan et al., 2018b). High abundance of *Faecalibacterium* was positively correlated with a significantly prolonged progression-free survival, in line with recently published data (Chaput et al., 2017). It is worth mentioning that these dissimilar microbial compositions observed in different studies may be due to the use of different models or analytical methodologies, for example the use of mice as opposed to human beings. In the latter case, as already mentioned, age, diet and geographical position also influence the intestinal bacterial composition. In addition, the specific anticancer drug used in the immunotherapy approach and the different type of malignant tumor are likely to have a key effect on the microbial diversity found.

BIFIDOBACTERIAL IMMUNOMODULATORY EFFECTS

As discussed above, modification of the gut microbiota appears to provide a novel way to improve the efficacy and reduce the side effects of current anticancer therapeutic approaches (Villeger et al., 2019). Many strategies are considered to enhance the effectiveness of cancer treatment, such as modulation of the intestinal microbiota, which is currently receiving a lot of scientific attention (Bashiardes et al., 2017; Helmink et al., 2019). The use of microorganisms known as probiotics, i.e., microbes which, when administered in adequate amounts, confer health benefits to the host, is becoming an important research field (Gibson et al., 2017). There are several beneficial effects of probiotics on host health, from blocking pathogenic bacteria to promoting intestinal epithelial cell survival, but the most important is the modulation of the immune system (Yan and Polk, 2011). Bifidobacteria are among those bacteria that are currently widely used as probiotics and that are capable of interacting with the immune system (Villeger et al., 2019). A growing number of studies have highlighted bifidobacteria as commensal organisms capable of stimulating and modulating specific pathways, through which they influence the host immune responses, both innate and adaptive (Palmer et al., 2007; Arboleya et al., 2016; Hidalgo-Cantabrana et al., 2017; Pickard et al., 2017; Ruiz et al., 2017; Alessandri et al., 2019). In fact, various strains of *Bifidobacterium* individually or in combination with other strains have been evaluated as probiotics for different diseases and some of these have shown quite promising results in alleviating the symptoms of IBD, IBS, diarrhoa and allergy (Tojo et al., 2014). However, the molecular mechanisms underlying the interaction between bifidobacteria and the host immune system are not yet fully understood.

First described in 1899, bifidobacteria are Gram-positive, anaerobic, non-motile, non-sporulating, saccharolytic, and bifid-shaped microorganisms with a high G + C DNA content (Ventura et al., 2007). Beyond their carbohydrate metabolism functions (Milani et al., 2015), bifidobacteria are widely exploited by food and pharmaceutical companies as health-promoting microorganisms (Linares et al., 2017). The molecular mechanisms, by which these bacteria colonize the intestine, adhere to the host's intestinal epithelium and elicit a positive effect on the immune response, represent a current and active research topic. There are some extracellular structures, secreted enzymes and bioactive metabolites that have been implicated to play a fundamental role in the interaction of bifidobacteria with their hosts (Turroni et al., 2013; McCarville et al., 2017; Alessandri et al., 2019; O'Connell Motherway et al., 2019). In the following section, some salient details of these extracellular structures identified in bifidobacteria are discussed.

Exopolysaccharides

The cell envelope of a wide range of bacteria is covered by one or more glycan layers known as capsular polysaccharides (CPS) or exopolysaccharides (EPS). From a research point of view EPS producers have received substantial interest as these extracellular polymers have been reported to play a specific role in host-microbe interactions and human health by promoting adhesion to the intestinal mucosa, as well as by modulating the intestinal microbiota composition, and conferring selective advantage to bacteria through protection

to adverse conditions such as presence of bile salts or pH insults (Fanning et al., 2012a). For example, *Bifidobacterium animalis* subsp. *lactis* has developed strategies to tolerate physiological bile salt concentrations by synthetizing EPS, probably as a mechanism of protection against toxic compound (Ruas-Madiedo et al., 2009).

Some of these microbial biopolymers are also receiving renewed interest due to their involvement in promoting human health (Ruas-Madiedo et al., 2009; Ferrario et al., 2016). In this context, an *in vitro* experiment was carried out to evaluate the level of stimulation of the pro and anti-inflammatory cytokines following contact with the EPS extracted from different bifidobacterial species. This study revealed that the differentiation of T cells is strongly influenced by the physical-chemical features of the particular EPS used. Two different *B. adolescentis* strains (IF1-03 and IF1-11) not only stimulate the production of anti-inflammatory cytokines but also contribute to the reduction of the area of ulceration and thickening of the intestinal wall (Yu R. et al., 2019). In addition, a recent *in vivo* study reported that a *Bifidobacterium bifidum* strain due to the presence of a cell surface-associated β-glucan/galactan (CSGG) can induce the generation of $Foxp3^+$ regulatory T cell, eliciting a strong suppressive activity toward experimental colitis (Verma et al., 2018).

This finding suggests that a positive correlation exists between the composition, structure and size of a given EPS polymer and the corresponding elicited immune response (Salazar et al., 2014). Similar results were obtained in other *in vitro* studies, which were confirmed by *in vivo* trials (Hidalgo-Cantabrana et al., 2014; Yu R. et al., 2019). In this context, it has been demonstrated that the EPS-producing *B. breve* UCC2003 strain evokes lower expression of proinflammatory cytokines interferon alpha (IFN-α), TNF-α, and IL-12 in splenocytes isolated from naïve mice and this finding suggests that the EPS layer plays a crucial role in the persistence of this strain in the host intestine, reducing the risk of immune clearance against this microbial strain (Fanning et al., 2012a). Notably, the genome of *B. breve* UCC2003 has been shown to encompass two putative EPS-encoding clusters. One cluster (*epsRhm*) was found to include genes that are putatively responsible for rhamnose biosynthesis, whereas the second cluster (*eps*) presents two adjacent oppositely oriented genes (*eps*1 and *eps*2), encodes regulatory components, glycosyltransferases and export functions (Fanning et al., 2012b). According to previous studies, *B. breve* UCC2003 EPS, metabolized by members of the infant microbiota, promotes the health status of infants (Pungel et al., 2020) and downregulates apoptotic responses to protect epithelial cells under imposed inflammatory conditions (Hughes et al., 2017), supporting the notion that EPS-mediated immune response is influenced by the physicochemical nature of these polymers.

Pili/Fimbriae

Pili or fimbriae are proteinaceous extracellular appendages produced by many bacteria, that protrude from the bacterial cell surface and that can be involved in microbe-host interactions promoting adhesion to the intestinal epithelium or facilitating aggregation with other bacterial cells (Scott and Zahner, 2006; Kline et al., 2010; Foroni et al., 2011). Two different types of pili have been described in bifidobacteria, i.e., sortase-dependent pili, and the type IVb pili, both of which are also known as tight adherence pili (Tad pili) (O'Connell Motherway et al., 2011; Milani et al., 2017b). Bifidobacterial sortase-dependent pili are not only responsible for adhesion and interaction with the host, but also are involved in the microbe-microbe interactions and in stimulation/modulation of the host immune system. Indeed, a case study focused on *B. bifidum* PRL2010 demonstrated that sortase-dependent pili have a crucial role in promoting aggregation between bacterial cells of a heterogeneous population, increasing the colonization of host intestinal mucosa (Turroni et al., 2014). Similarly, a related study highlighted that sortase-dependent pili produced by *B. bifidum* PRL2010 activated various signals in macrophages by locally inducing high levels of the cytokine TNF-α, yet reducing the expression of other pro-inflammatory cytokines, such as IL-12, associated with systemic response (Turroni et al., 2013). Apparently, this facilitates cross-talk between this bifidobacterial strain and host immune cells without causing a detrimental inflammatory cascade response.

The other bifidobacterial pilus type, the Tad pilus, that has been characterized in detail in the model organism *B. breve* UCC2003 (O'Connell Motherway et al., 2011, 2019; Milani et al., 2017b), has been shown to promote the maturation of epithelial cells, stimulating growth of their immature intestinal mucosa and contributing to host mucosal homeostasis (O'Connell Motherway et al., 2019). However, this is still a hypothesis that has not been proven yet in humans though demonstrated in murine models.

Serpins

Serpins (Serine protease inhibitors) are prokaryotic and eukaryotic enzymes, synthetized by particular members of the bifidobacterial intestinal community and involved in the regulation of various protease-mediated processes (Potempa et al., 1994; Turroni et al., 2010). The production of serpins is not widespread in bifidobacteria, in fact it has been identified only in few species like *B. breve*, *B. longum* subsp. *longum*, *B. longum* subsp. *infantis*, *B. longum* subsp. *suis*, *Bifidobacterium cuniculi*, *Bifidobacterium scardovii*, and *Bifidobacterium dentium* (Turroni et al., 2010). Notably, the expression of serpin-encoding genes is induced in response of the presence of a specific two-component regulatory system (Alvarez-Martin et al., 2012). Bacterial infection or intestinal tissue damage typical of inflammatory bowel diseases and ulcerative colitis are the main factors by which serine proteases may be released. Beyond eliciting anti-inflammatory activity through the prevention of negative effects of high levels of human serine proteases, serpins may assist bifidobacteria to protect themselves against host-derived proteases and survive in a competitive environment (Turroni et al., 2010; Kainulainen et al., 2013). Recently the anti-inflammatory efficacy of these enzymes has been demonstrated in the prevention of gluten-related immunopathology, of which effects of are significantly alleviated due to the ability of serpin to modulate the immune system, to maintain barrier

function and to inhibit elastases released during inflammation (McCarville et al., 2017).

Besides pili, EPS and serpins, there are other bifidobacterial-associated extracellular proteins affecting the host immune system. A specific *B. bifidum* strain is able to produce two type of extracellular molecules such as BopA and TagA. The latter is a protein located on the outer bacterial surface that acts like a peptidoglycan lytic enzyme causing the activation or the proliferation of dendritic cells and the induction of IL-2 (Guglielmetti et al., 2014). BopA is a surface-associated protein not only able to stimulate production of IL-8 but also to enhance adhesion of bifidobacteria to epithelial cells through the high hydrophobicity of this lipoprotein (Guglielmetti et al., 2008; Kainulainen et al., 2013).

Finally, bifidobacterial metabolism influences intestinal immune homeostasis and inflammatory response through microbe-microbe cross-feeding activities (Alessandri et al., 2019). Bifidobacterial metabolism of non-digestible carbohydrates leads to the production of acetate and lactate, which in turn can be converted by secondary degraders into butyrate, thereby resulting in a so-called butyrogenic effect (O'Callaghan and van Sinderen, 2016). Various studies have reported on the mutual beneficial effects of co-cultivation of *Bifidobacterium* strains with butyrate producers in the presence of diet-derived sugars and host-derived glycans promoting growth yield of both strains (Rios-Covian et al., 2015; Riviere et al., 2015; Schwab et al., 2017; Bunesova et al., 2018). Moreover, bifidobacteria, unlike other enteric microorganisms such as *Bacteroides*, display a limited hydrolytic capacity toward xylan (Ejby et al., 2013). In fact, bifidobacteria are not able to grow on xylan on their own, nevertheless they manage to grow on this substrate when co-cultivated with *Bacteroides ovatus*. This phenomenon is due to the extracellular activity of *Ba. ovatus* that degrades xylan chains, allowing an efficient uptake of the produced xylo-oligosaccharides by a dedicated ABC transporter encoded by various bifidobacterial species (Rogowski et al., 2015).

BACTERIAL THERAPY SUPPORTING IMMUNOTHERAPIES

The complexity of the gut microbiota plays a key role in the response to the ICI. Therefore, the benefit of the treatments are reduced in those patients who have taken antibiotics and thus display an intestinal microbiota of reduced diversity (Villeger et al., 2019). Moreover, patients responding to the therapy have a different microbiota, in species composition and diversity, compared to patients that do not respond to immunotherapy (Routy et al., 2018). As mentioned above, accumulating evidence suggests that modulation of the gut microbiota affects the host responses to various forms of cancer therapy, most notably immunotherapies (Robertson et al., 2017). Several methods are currently being studied including the use of prebiotics, probiotics and fecal microbiota transplantation. The notion of using microbial components or their products in anti-cancer therapy dates back to 1891 when Coley used killed *Streptococcus pyogenes* in combination with a second killed organism now known as *Serratia marcescens* in the treatment of bone sarcoma (McCarthy, 2006). 16S ribosomal RNA (rRNA)-based sequencing of gene amplicons and shotgun metagenomics analyses of stool samples allow the identification of particular bacteria that are more abundant in responding vs. non-responding patients (Matson et al., 2018; Elkrief et al., 2019). Moreover, researchers have identified a consortium of human-associated bacterial strains acting together to induce interferon-γ-producing CD8 T cells in order to confer resistance to certain bacterial infections, such as *Listeria monocytogenes*, while also being effective in inhibiting tumor growth in conjunction with ICIs (Tanoue et al., 2019). These findings reinforce the notion that the gut microbiota can be considered as a therapeutic target in the treatment of various diseases through manipulation of host physiological functions, which may be associated with less risk when compared to other biotherapeutic approaches (Tanoue et al., 2019). Data supporting the important role for improved immunotherapeutic efficacy have been obtained by transferring fecal bacteria from responsive patients into GF or antibiotic-treated SPF mice, which has been inoculated with tumors and treated with mAbs to CTLA-4 or PD-1/PD-L1 (Vetizou et al., 2015). However, there are several critical parameters to consider for this approach. For example, fecal material should be sourced from a healthy individual who has been screened in order to eliminate the risk of inadvertently transmitting infections that could cause inflammation-induced carcinogenesis or formation of dysplasia or polyps (Wong et al., 2017; Chen et al., 2019; Fessler et al., 2019). FMT is a biological drug recognized by the U.S. Food and Drug Administration, though its safety remains a controversial issue because of the unidentified composition and pathogenicity of fecal bacteria that might be transmitted (Chen et al., 2019).

Another means of intervention may be modulation of the autochthonous commensal microbial community via prebiotics or dietary changes to favor colonization and expansion of selected beneficial bacteria (Zitvogel et al., 2018). A prebiotic is defined as a selectively fermented ingredient that allows specific changes, both in the composition and/or activity in the gastrointestinal microbiota that confers benefits upon host well-being and health (Roberfroid, 2007). For example it has been shown that they could favor the proliferation of beneficial bacterial species that are already present in the host, such as *Faecalibacterium*, *Eubacterium*, and *Roseburia* spp. These taxa are also able to produce organic acids (i.e., produce acetate, propionate and butyrate), that are known to play a role in preventing cancer and may have both local and systemic biological effects; in particular butyrate, a preferred energy source of colonocytes (Ambalam et al., 2016). Even probiotics may possess anticancer effects at different stages of carcinogenesis, being attributable to the binding of mutagens or carcinogens, with subsequent biotransformation into less toxic metabolites (Raman et al., 2013). *In vivo* studies have provided evidence that administration of probiotics has significant protective effects against CRC by reducing aberrant crypt foci (ACF), producing SCFA, down-regulating pro-inflammatory cytokines, inhibiting pathogens and cancer-causing microbes, and by immune-stimulation and reduction of pro-carcinogenic enzymatic activities (O'Mahony et al., 2001; Bertkova et al., 2010; Pithva et al., 2015). In this

context, fermented products are known to be an important source of both nutrients and microorganisms. Microbial metabolites and live microorganisms are considered to have positive effects on host health and in this context there is robust evidence that the intake of fermented foods significantly decreases cancer risk, bladder cancer, CRC and esophageal cancer risk. In contrast, the intake of fermented foods is inversely correlated with prostate cancer, renal cancer and ovarian cancer risks (Zhang et al., 2019). The precise mechanisms involved have not yet been described and further studies should be done to confirm such preliminary yet exciting results. Recently, research has revealed the critical role played by CD47, which is a widely expressed protein present on the surface of many cancer cells triggering a deleterious signal to the macrophages inviting them not to attack (Advani et al., 2018). Experiments have shown that tumor-bearing mice, which are normally respondent to anti-CD47 treatments, failed to obtain benefits from therapy when intestinal bacteria were destroyed by taking a cocktail of antibiotics. In contrast, mice that did not respond to immunotherapy were shown to benefit from cancer treatments when they were receiving a mixture of *Bifidobacterium* species consisting of *B. bifidum*, *B. longum*, *Bifidobacterium animalis* subsp. *lactis*, and *B. breve*, which migrate to and integrate cancer cells where they interact with the immune system of the host stimulating an immune signaling pathway called interferon gene stimulation (STING). Essentially, this represents a process that translates into an abundant activation of the immune cells, which allows enhancement of the anti-CD47 therapy by increasing its ability to destroy cancer cells (Shi et al., 2020).

Bacterial therapy protocols are being developed in cancer treatment, based on previous success of studies describing cancer patients entering remission after a bacterial treatment (Enck, 1991). Bacterial therapies are based upon the ability of the microbial cell to selectively interact with and kill cancer cells *in situ* and stimulate a strong anti-cancer immune response (Forbes et al., 2018). Preclinical studies have shown that these therapies retard tumor growth and increase survival (Dang et al., 2001; Ganai et al., 2009). A prime example of a cancer therapy protocol is based on attenuated microbial cells in the treatment of superficial bladder cancer with the *Bacillus* Calmette-Guerin (BCG) vaccine. This therapy likely stimulates the non-specific immune responses against the tumor and represents the only anti-cancer bacterial therapy that is currently considered as an established standard of care (Kamat et al., 2015). Bacterial therapies work mainly by direct oncolysis mediated by the secretion of exotoxins or competition for nutrients (Middlebrook and Dorland, 1984), but, intracellular bacteria can kill the host's cancer cells by inducing apoptosis or uncontrolled proliferation causing the outbreak of infected cancer cells (Uchugonova et al., 2015). Currently, bacterial therapy is commonly used in cases of metastatic disease for specific targeting of cancerous cells and tissues. For this purpose many active bacteria were designed to colonize only the tumor microenvironment (Kasinskas and Forbes, 2007; Zhang et al., 2014) and to induce cell death specifically in cancer by oncolytic function (St Jean et al., 2014). In addition, designed immune-sensitizing bacteria induce responses to cancer-specific antigens directly (Wood and Paterson, 2014) or indirectly by spreading the epitope (Seavey et al., 2009).

CONCLUSION

There is a growing number of studies demonstrating that intestinal microbiota can be linked to positive effects in clinical outcomes of cancer therapy. Modulation of the gut microbiota is one of the ways to counteract cancer, improving responsiveness to anti-cancer therapies, in particular immunotherapies. Bifidobacteria, which are commonly used as probiotics for their health-promoting features, have been shown to improve tumor control to the same degree as immune checkpoint blockade therapy, with combination treatment nearly abolishing tumor outgrowth. However, despite their well-established role in stimulating human health, the precise mechanisms by which bifidobacteria solicit beneficial effects in fighting cancer are far from being fully understood. The importance of this emerging beneficial role in terms of early diagnosis and the effectiveness of therapies is remarkable. Knowing that the composition of the microbiota is predictive for the presence or absence of disease may guide the development of novel, less invasive tests, and may subsequently lead to the development of personalized treatments.

AUTHOR CONTRIBUTIONS

GL: writing – original draft preparation. DS, MV, and FT: writing – review, editing, and conceptualization. All authors contributed to the article and approved the submitted version.

FUNDING

This work received support from the EU Joint Programming Initiative – A Healthy Diet for a Healthy Life (JPI HDHL, http://www.healthydietforhealthylife.eu/) to DS [in conjunction with Science Foundation Ireland (SFI), Grant No. 15/JP-HDHL/3280]. DS was a member of APC Microbiome Ireland, funded by Science Foundation Ireland through the Irish Government's National Development Plan (Grant Nos. SFI/12/RC/2273-P1 and SFI/12/RC/2273-P2). The study was supported by the Fondazione Cariparma, under TeachInParma Project (DS). The authors declare that this study received funding from GenProbio srl. The funder was not involved in the study design, collection, analysis, interpretation of data, the writing of this article or the decision to submit it for publication.

ACKNOWLEDGMENTS

We thank GenProbio srl for financial support of the Laboratory of Probiogenomics.

REFERENCES

Abed, J., Emgard, J. E., Zamir, G., Faroja, M., Almogy, G., and Grenov, A. (2016). Fap2 mediates *Fusobacterium nucleatum* colorectal adenocarcinoma enrichment by binding to tumor-expressed gal-GalNAc. *Cell Host Microbe* 20, 215–225. doi: 10.1016/j.chom.2016.07.006

Advani, R., Flinn, I., Popplewell, L., Forero, A., Bartlett, N. L., and Ghosh, N. (2018). CD47 blockade by Hu5F9-G4 and rituximab in non-hodgkin's lymphoma. *N. Engl. J. Med.* 379, 1711–1721. doi: 10.1056/NEJMoa1807315

Alessandri, G., Ossiprandi, M. C., MacSharry, J., van Sinderen, D., and Ventura, M. (2019). Bifidobacterial dialogue with its human host and consequent modulation of the immune system. *Front. Immunol.* 10:2348. doi: 10.3389/fimmu.2019.02348

Alvarez-Martin, P., O'Connell Motherway, M., Turroni, F., Foroni, E., Ventura, M., and van Sinderen, D. (2012). A two-component regulatory system controls autoregulated serpin expression in Bifidobacterium breve UCC2003. *Appl. Environ. Microbiol.* 78, 7032–7041. doi: 10.1128/AEM.01776-12

Ambalam, P., Raman, M., Purama, R. K., and Doble, M. (2016). Probiotics, prebiotics and colorectal cancer prevention. *Best Pract. Res. Clin. Gastroenterol.* 30, 119–131. doi: 10.1016/j.bpg.2016.02.009

Arboleya, S., Watkins, C., Stanton, C., and Ross, R. P. (2016). Gut bifidobacteria populations in human health and aging. *Front. Microbiol.* 7:1204. doi: 10.3389/fmicb.2016.01204

Arseneau, K. O., and Cominelli, F. (2009). Leukocytapheresis in ulcerative colitis: a possible alternative to biological therapy? *Dig. Liver Dis.* 41, 551–552. doi: 10.1016/j.dld.2009.05.014

Azuma, T., Yao, S., Zhu, G., Flies, A. S., Flies, S. J., and Chen, L. (2008). B7-H1 is a ubiquitous antiapoptotic receptor on cancer cells. *Blood* 111, 3635–3643. doi: 10.1182/blood-2007-11-123141

Bashiardes, S., Tuganbaev, T., Federici, S., and Elinav, E. (2017). The microbiome in anti-cancer therapy. *Semin. Immunol.* 32, 74–81. doi: 10.1016/j.smim.2017.04.001

Bertkova, I., Hijova, E., Chmelarova, A., Mojzisova, G., Petrasova, D., and Strojny, L. (2010). The effect of probiotic microorganisms and bioactive compounds on chemically induced carcinogenesis in rats. *Neoplasma* 57, 422–428. doi: 10.4149/neo_2010_05_422

Bezine, E., Vignard, J., and Mirey, G. (2014). The cytolethal distending toxin effects on Mammalian cells: a DNA damage perspective. *Cells* 3, 592–615. doi: 10.3390/cells3020592

Borghaei, H., Paz-Ares, L., Horn, L., Spigel, D. R., Steins, M., and Ready, N. E. (2015). Nivolumab versus docetaxel in advanced nonsquamous non-small-cell lung cancer. *N. Engl. J. Med.* 373, 1627–1639. doi: 10.1056/NEJMoa1507643

Brauner, A., Brandt, L., Frisan, T., Thelestam, M., and Ekbom, A. (2010). Is there a risk of cancer development after Campylobacter infection? *Scand. J. Gastroenterol.* 45, 893–897. doi: 10.3109/00365521003734133

Brennan, C. A., and Garrett, W. S. (2016). Gut microbiota, inflammation, and colorectal cancer. *Annu. Rev. Microbiol.* 70, 395–411. doi: 10.1146/annurev-micro-102215-095513

Brennan, C. A., and Garrett, W. S. (2019). *Fusobacterium nucleatum* – symbiont, opportunist and oncobacterium. *Nat. Rev. Microbiol.* 17, 156–166. doi: 10.1038/s41579-018-0129-6

Brestoff, J. R., and Artis, D. (2013). Commensal bacteria at the interface of host metabolism and the immune system. *Nat. Immunol.* 14, 676–684. doi: 10.1038/ni.2640

Bronte, V., and Mocellin, S. (2009). Suppressive influences in the immune response to cancer. *J. Immunother.* 32, 1–11. doi: 10.1097/CJI.0b013e3181837276

Buc, E., Dubois, D., Sauvanet, P., Raisch, J., Delmas, J., and Darfeuille-Michaud, A. (2013). High prevalence of mucosa-associated E coli producing cyclomodulin and genotoxin in colon cancer. *PLoS ONE* 8:e56964. doi: 10.1371/journal.pone.0056964

Bullman, S., Pedamallu, C. S., Sicinska, E., Clancy, T. E., Zhang, X., and Cai, D. (2017). Analysis of *Fusobacterium* persistence and antibiotic response in colorectal cancer. *Science* 358, 1443–1448. doi: 10.1126/science.aal5240

Bunesova, V., Lacroix, C., and Schwab, C. (2018). Mucin cross-feeding of infant *Bifidobacteria* and *Eubacterium hallii*. *Microb. Ecol.* 75, 228–238. doi: 10.1007/s00248-017-1037-4

Carbone, D. P., Reck, M., Paz-Ares, L., Creelan, B., Horn, L., and Steins, M. (2017). First-line nivolumab in stage IV or recurrent non-small-cell lung cancer. *N. Engl. J. Med.* 376, 2415–2426. doi: 10.1056/NEJMoa1613493

Chan, A. T., Arber, N., Burn, J., Chia, W. K., Elwood, P., and Hull, M. A. (2012). Aspirin in the chemoprevention of colorectal neoplasia: an overview. *Cancer Prev. Res. (Phila)* 5, 164–178. doi: 10.1158/1940-6207.CAPR-11-0391

Chaput, N., Lepage, P., Coutzac, C., Soularue, E., Le Roux, K., and Monot, C. (2017). Baseline gut microbiota predicts clinical response and colitis in metastatic melanoma patients treated with ipilimumab. *Ann. Oncol.* 28, 1368–1379. doi: 10.1093/annonc/mdx108

Chen, D., Wu, J., Jin, D., Wang, B., and Cao, H. (2019). Fecal microbiota transplantation in cancer management: current status and perspectives. *Int. J. Cancer* 145, 2021–2031. doi: 10.1002/ijc.32003

Claesson, M. J., Cusack O'Sullivan, S. O., Greene-Diniz, R., de Weerd, H., Flannery, E., Marchesi, J. R., et al. (2011). Composition, variability, and temporal stability of the intestinal microbiota of the elderly. *Proc. Natl. Acad. Sci. U.S.A.* 108(Suppl. 1), 4586–4591. doi: 10.1073/pnas.1000097107

Clemente, J. C., Ursell, L. K., Parfrey, L. W., and Knight, R. (2012). The impact of the gut microbiota on human health: an integrative view. *Cell* 148, 1258–1270. doi: 10.1016/j.cell.2012.01.035

Collado, M. C., Derrien, M., Isolauri, E., de Vos, W. M., and Salminen, S. (2007). Intestinal integrity and Akkermansia muciniphila, a mucin-degrading member of the intestinal microbiota present in infants, adults, and the elderly. *Appl. Environ. Microbiol.* 73, 7767–7770. doi: 10.1128/AEM.01477-07

Cronin, M., Akin, A. R., Collins, S. A., Meganck, J., Kim, J. B., and Baban, C. K. (2012). High resolution in vivo bioluminescent imaging for the study of bacterial tumour targeting. *PLoS ONE* 7:e30940. doi: 10.1371/journal.pone.0030940

Cuevas-Ramos, G., Petit, C. R., Marcq, I., Boury, M., Oswald, E., and Nougayrede, J. P. (2010). *Escherichia coli* induces DNA damage in vivo and triggers genomic instability in mammalian cells. *Proc. Natl. Acad. Sci. U.S.A.* 107, 11537–11542. doi: 10.1073/pnas.1001261107

Dalmasso, G., Cougnoux, A., Delmas, J., Darfeuille-Michaud, A., and Bonnet, R. (2014). The bacterial genotoxin colibactin promotes colon tumor growth by modifying the tumor microenvironment. *Gut Microbes* 5, 675–680. doi: 10.4161/19490976.2014.969989

Dang, L. H., Bettegowda, C., Huso, D. L., Kinzler, K. W., and Vogelstein, B. (2001). Combination bacteriolytic therapy for the treatment of experimental tumors. *Proc. Natl. Acad. Sci. U.S.A.* 98, 15155–15160. doi: 10.1073/pnas.251543698

Dapito, D. H., Mencin, A., Gwak, G. Y., Pradere, J. P., Jang, M. K., and Mederacke, I. (2012). Promotion of hepatocellular carcinoma by the intestinal microbiota and TLR4. *Cancer Cell* 21, 504–516. doi: 10.1016/j.ccr.2012.02.007

Dhaliwal, A., Vlachostergios, P. J., Oikonomou, K. G., and Moshenyat, Y. (2015). Fecal DNA testing for colorectal cancer screening: molecular targets and perspectives. *World J. Gastrointest. Oncol.* 7, 178–183. doi: 10.4251/wjgo.v7.i10.178

Diggs, D. L., Huderson, A. C., Harris, K. L., Myers, J. N., Banks, L. D., Rekhadevi, P. V., et al. (2011). Polycyclic aromatic hydrocarbons and digestive tract cancers: a perspective. *J. Environ. Sci. Health C Environ. Carcinog Ecotoxicol. Rev.* 29, 324–357. doi: 10.1080/10590501.2011.629974

Eckburg, P. B., Bik, E. M., Bernstein, C. N., Purdom, E., Dethlefsen, L., Sargent, M., et al. (2005). Diversity of the human intestinal microbial flora. *Science* 308, 1635–1638. doi: 10.1126/science.1110591

Ejby, M., Fredslund, F., Vujicic-Zagar, A., Svensson, B., Slotboom, D. J., and Abou, M. (2013). Hachem: structural basis for arabinoxylo-oligosaccharide capture by the probiotic Bifidobacterium animalis subsp. *lactis Bl*-04. *Mol. Microbiol.* 90, 1100–1112. doi: 10.1111/mmi.12419

Elkrief, A., Derosa, L., Zitvogel, L., Kroemer, G., and Routy, B. (2019). The intimate relationship between gut microbiota and cancer immunotherapy. *Gut Microbes* 10, 424–428. doi: 10.1080/19490976.2018.1527167

Enck, R. E. (1991). Understanding tolerance, physical dependence and addiction in the use of opioid analgesics. *Am. J. Hosp. Palliat Care* 8, 9–11. doi: 10.1177/104990919100800102

Eribe, E. R. K., Paster, B. J., Caugant, D. A., Dewhirst, F. E., Stromberg, V. K., Lacy, G. H., et al. (2004). Genetic diversity of Leptotrichia and description of *Leptotrichia goodfellowii* sp. *nov. Leptotrichia hofstadii* sp. nov., *Leptotrichia*

shahii sp. nov. and *Leptotrichia wadei* sp. nov. *Int. J. Syst. Evol. Microbiol.* 54(Pt 2), 583–592. doi: 10.1099/ijs.0.02819-0

Fanning, S., Hall, L. J., Cronin, M., Zomer, A., MacSharry, J., and Goulding, D. (2012a). Bifidobacterial surface-exopolysaccharide facilitates commensal-host interaction through immune modulation and pathogen protection. *Proc. Natl. Acad. Sci. U.S.A.* 109, 2108–2113. doi: 10.1073/pnas.1115621109

Fanning, S., Hall, L. J., and van Sinderen, D. (2012b). Bifidobacterium breve UCC2003 surface exopolysaccharide production is a beneficial trait mediating commensal-host interaction through immune modulation and pathogen protection. *Gut Microbes* 3, 420–425. doi: 10.4161/gmic.20630

Ferrario, C., Milani, C., Mancabelli, L., Lugli, G. A., Duranti, S., and Mangifesta, M. (2016). Modulation of the eps-ome transcription of bifidobacteria through simulation of human intestinal environment. *FEMS Microbiol Ecol* 92:fiw056. doi: 10.1093/femsec/fiw056

Fessler, J., Matson, V., and Gajewski, T. F. (2019). Exploring the emerging role of the microbiome in cancer immunotherapy. *J Immunother. Cancer* 7:108. doi: 10.1186/s40425-019-0574-4

Finn, O. J. (2012). Immuno-oncology: understanding the function and dysfunction of the immune system in cancer. *Ann. Oncol.* 23(Suppl. 8), viii6–viii9. doi: 10.1093/annonc/mds256

Forbes, N. S., Coffin, R. S., Deng, L., Evgin, L., Fiering, S., and Giacalone, M. (2018). White paper on microbial anti-cancer therapy and prevention. *J. Immunother. Cancer* 6:78. doi: 10.1186/s40425-018-0381-3

Foroni, E., Serafini, F., Amidani, D., Turroni, F., He, F., and Bottacini, F. (2011). Genetic analysis and morphological identification of pilus-like structures in members of the genus Bifidobacterium. *Microb. Cell Fact* 10(Suppl. 1), S16. doi: 10.1186/1475-2859-10-S1-S16

Fox, J. G., and Wang, T. C. (2007). Inflammation, atrophy, and gastric cancer. *J. Clin. Invest.* 117, 60–69. doi: 10.1172/JCI30111

Francisco, L. M., Sage, P. T., and Sharpe, A. H. (2010). The PD-1 pathway in tolerance and autoimmunity. *Immunol. Rev.* 236, 219–242. doi: 10.1111/j.1600-065X.2010.00923.x

Freeman, G. J., Long, A. J., Iwai, Y., Bourque, K., Chernova, T., and Nishimura, H. (2000). Engagement of the PD-1 immunoinhibitory receptor by a novel B7 family member leads to negative regulation of lymphocyte activation. *J. Exp. Med.* 192, 1027–1034. doi: 10.1084/jem.192.7.1027

Fuentes, S., and de Vos, W. M. (2016). How to manipulate the microbiota: fecal microbiota transplantation. *Adv. Exp. Med. Biol.* 902, 143–153. doi: 10.1007/978-3-319-31248-4_10

Fujimura, K. E., Slusher, N. A., Cabana, M. D., and Lynch, S. V. (2010). Role of the gut microbiota in defining human health. *Expert Rev. Anti Infect. Ther.* 8, 435–454. doi: 10.1586/eri.10.14

Fung, K. Y., Cosgrove, L., Lockett, T., Head, R., and Topping, D. L. (2012). A review of the potential mechanisms for the lowering of colorectal oncogenesis by butyrate. *Br. J. Nutr.* 108, 820–831. doi: 10.1017/S0007114512001948

Ganai, S., Arenas, R. B., and Forbes, N. S. (2009). Tumour-targeted delivery of TRAIL using *Salmonella* typhimurium enhances breast cancer survival in mice. *Br. J. Cancer* 101, 1683–1691. doi: 10.1038/sj.bjc.6605403

Garrett, W. S. (2015). Cancer and the microbiota. *Science* 348, 80–86. doi: 10.1126/science.aaa4972

Ge, Z., Feng, Y., Ge, L., Parry, N., Muthupalani, S., and Fox, J. G. (2017). *Helicobacter* hepaticus cytolethal distending toxin promotes intestinal carcinogenesis in 129Rag2-deficient mice. *Cell Microbiol.* 19. doi: 10.1111/cmi.12728

Ge, Z., Rogers, A. B., Feng, Y., Lee, A., Xu, S., Taylor, N. S., et al. (2007). Bacterial cytolethal distending toxin promotes the development of dysplasia in a model of microbially induced hepatocarcinogenesis. *Cell Microbiol.* 9, 2070–2080. doi: 10.1111/j.1462-5822.2007.00939.x

Geller, L. T., Barzily-Rokni, M., Danino, T., Jonas, O. H., Shental, N., and Nejman, D. (2017). Potential role of intratumor bacteria in mediating tumor resistance to the chemotherapeutic drug gemcitabine. *Science* 357, 1156–1160. doi: 10.1126/science.aah5043

Gevers, D., Kugathasan, S., Denson, L. A., Van Treuren, W., and Ren, B. (2014). The treatment-naive microbiome in new-onset Crohn's disease. *Cell Host Microbe* 15, 382–392. doi: 10.1016/j.chom.2014.02.005

Gibson, G. R., Hutkins, R., Sanders, M. E., Prescott, S. L., Reimer, R. A., and Salminen, S. J. (2017). Expert consensus document: the international scientific association for probiotics and prebiotics (ISAPP) consensus statement on the definition and scope of prebiotics. *Nat. Rev. Gastroenterol. Hepatol.* 14, 491–502. doi: 10.1038/nrgastro.2017.75

Gobel, C., Breitenbuecher, F., Kalkavan, H., Hahnel, P. S., Kasper, S., and Hoffarth, S. (2014). Functional expression cloning identifies COX-2 as a suppressor of antigen-specific cancer immunity. *Cell Death Dis.* 5:e1568. doi: 10.1038/cddis.2014.531

Gopalakrishnan, V., Helmink, B. A., Spencer, C. N., Reuben, A., and Wargo, J. A. (2018a). The influence of the gut microbiome on cancer, immunity, and cancer immunotherapy. *Cancer Cell* 33, 570–580. doi: 10.1016/j.ccell.2018.03.015

Gopalakrishnan, V., Spencer, C. N., Nezi, L., Reuben, A., Andrews, M. C., and Karpinets, T. V. (2018b). Gut microbiome modulates response to anti-PD-1 immunotherapy in melanoma patients. *Science* 359, 97–103. doi: 10.1126/science.aan4236

Grillot-Courvalin, C., Goussard, S., Huetz, F., Ojcius, D. M., and Courvalin, P. (1998). Functional gene transfer from intracellular bacteria to mammalian cells. *Nat. Biotechnol.* 16, 862–866. doi: 10.1038/nbt0998-862

Guerra, L., Cortes-Bratti, X., Guidi, R., and Frisan, T. (2011). The biology of the cytolethal distending toxins. *Toxins (Basel)* 3, 172–190. doi: 10.3390/toxins3030172

Guglielmetti, S., Tamagnini, I., Mora, D., Minuzzo, M., Scarafoni, A., Arioli, S., et al. (2008). Implication of an outer surface lipoprotein in adhesion of Bifidobacterium bifidum to Caco-2 cells. *Appl. Environ. Microbiol.* 74, 4695–4702. doi: 10.1128/AEM.00124-08

Guglielmetti, S., Zanoni, I., Balzaretti, S., Miriani, M., Taverniti, V., and De Noni, I. (2014). Murein lytic enzyme TgaA of Bifidobacterium bifidum MIMBb75 modulates dendritic cell maturation through its cysteine- and histidine-dependent amidohydrolase/peptidase (CHAP) amidase domain. *Appl. Environ. Microbiol.* 80, 5170–5177. doi: 10.1128/AEM.00761-14

Guinane, C. M., and Cotter, P. D. (2013). Role of the gut microbiota in health and chronic gastrointestinal disease: understanding a hidden metabolic organ. *Therap. Adv. Gastroenterol.* 6, 295–308. doi: 10.1177/1756283X13482996

Gur, C., Ibrahim, Y., Isaacson, B., Yamin, R., Abed, J., and Gamliel, M. (2015). Binding of the Fap2 protein of *Fusobacterium nucleatum* to human inhibitory receptor TIGIT protects tumors from immune cell attack. *Immunity* 42, 344–355. doi: 10.1016/j.immuni.2015.01.010

Gursoy, U. K., Pollanen, M., Kononen, E., and Uitto, V. J. (2010). Biofilm formation enhances the oxygen tolerance and invasiveness of *Fusobacterium nucleatum* in an oral mucosa culture model. *J. Periodontol.* 81, 1084–1091. doi: 10.1902/jop.2010.090664

Hambly, R. J., Rumney, C. J., Fletcher, J. M., Rijken, P. J., and Rowland, I. R. (1997). Effects of high- and low-risk diets on gut microflora-associated biomarkers of colon cancer in human flora-associated rats. *Nutr. Cancer* 27, 250–255. doi: 10.1080/01635589709514534

Hamer, H. M., Jonkers, D., Venema, K., Vanhoutvin, S., Troost, F. J., and Brummer, R. J. (2008). Review article: the role of butyrate on colonic function. *Aliment. Pharmacol. Ther.* 27, 104–119. doi: 10.1111/j.1365-2036.2007.03562.x

Han, X. Y., Weinberg, J. S., Prabhu, S. S., Hassenbusch, S. J., Fuller, G. N., Tarrand, J. J., et al. (2003). Fusobacterial brain abscess: a review of five cases and an analysis of possible pathogenesis. *J. Neurosurg.* 99, 693–700. doi: 10.3171/jns.2003.99.4.0693

Han, Y. W., Shi, W., Huang, G. T., Park, N. H., Kuramitsu, H., et al. (2000). Interactions between periodontal bacteria and human oral epithelial cells: *Fusobacterium nucleatum* adheres to and invades epithelial cells. *Infect. Immun.* 68, 3140–3146. doi: 10.1128/iai.68.6.3140-3146.2000

Hanahan, D., and Weinberg, R. A. (2011). Hallmarks of cancer: the next generation. *Cell* 144, 646–674. doi: 10.1016/j.cell.2011.02.013

He, Z., Gharaibeh, R. Z., Newsome, R. C., Pope, J. L., Dougherty, M. W., and Tomkovich, S. (2019). Campylobacter jejuni promotes colorectal tumorigenesis through the action of cytolethal distending toxin. *Gut* 68, 289–300. doi: 10.1136/gutjnl-2018-317200

Helmink, B. A., Khan, M. A. W., Hermann, A., Gopalakrishnan, V., and Wargo, J. A. (2019). The microbiome, cancer, and cancer therapy. *Nat. Med.* 25, 377–388. doi: 10.1038/s41591-019-0377-7

Helmy, K. Y., Patel, S. A., Nahas, G. R., and Rameshwar, P. (2013). Cancer immunotherapy: accomplishments to date and future promise. *Ther. Deliv.* 4, 1307–1320. doi: 10.4155/tde.13.88

Hidalgo-Cantabrana, C., Delgado, S., Ruiz, L., Ruas-Madiedo, P., Sanchez, B., and Margolles, A. (2017). Bifidobacteria and their health-promoting effects. *Microbiol. Spectr.* 5. doi: 10.1128/microbiolspec.BAD-0010-2016

Hidalgo-Cantabrana, C., Nikolic, M., Lopez, P., Suarez, A., Miljkovic, M., and Kojic, M. (2014). Exopolysaccharide-producing *Bifidobacterium animalis* subsp. lactis strains and their polymers elicit different responses on immune cells from blood and gut associated lymphoid tissue. *Anaerobe* 26, 24–30. doi: 10.1016/j.anaerobe.2014.01.003

Hope, M. E., Hold, G. L., Kain, R., and El-Omar, E. M. (2005). Sporadic colorectal cancer–role of the commensal microbiota. *FEMS Microbiol. Lett.* 244, 1–7. doi: 10.1016/j.femsle.2005.01.029

Hughes, K. R., Harnisch, L. C., Alcon-Giner, C., Mitra, S., Wright, C. J., and Ketskemety, J. (2017). Bifidobacterium breve reduces apoptotic epithelial cell shedding in an exopolysaccharide and MyD88-dependent manner. *Open Biol.* 7:160155. doi: 10.1098/rsob.160155

Illiano, P., Brambilla, R., and Parolini, C. (2020). The mutual interplay of gut microbiota, diet and human disease. *FEBS J.* 287, 833–855. doi: 10.1111/febs.15217

Jemal, A., Bray, F., Center, M. M., Ferlay, J., Ward, E., and Forman, D. (2011). Global cancer statistics. *CA Cancer J. Clin.* 61, 69–90. doi: 10.3322/caac.20107

Kai, A., Cooke, F., Antoun, N., Siddharthan, C., and Sule, O. (2008). A rare presentation of ventriculitis and brain abscess caused by *Fusobacterium nucleatum*. *J. Med. Microbiol.* 57(Pt 5), 668–671. doi: 10.1099/jmm.0.47710-0

Kainulainen, V., Reunanen, J., Hiippala, K., Guglielmetti, S., Vesterlund, S., Palva, A., et al. (2013). BopA does not have a major role in the adhesion of Bifidobacterium bifidum to intestinal epithelial cells, extracellular matrix proteins, and mucus. *Appl. Environ. Microbiol.* 79, 6989–6997. doi: 10.1128/AEM.01993-13

Kalos, M., Levine, B. L., Porter, D. L., Katz, S., Grupp, S. A., Bagg, A., et al. (2011). T cells with chimeric antigen receptors have potent antitumor effects and can establish memory in patients with advanced leukemia. *Sci. Transl. Med.* 3:95ra73. doi: 10.1126/scitranslmed.3002842

Kamat, A. M., Flaig, T. W., Grossman, H. B., Konety, B., Lamm, D., and O'Donnell, M. A. (2015). Expert consensus document: consensus statement on best practice management regarding the use of intravesical immunotherapy with BCG for bladder cancer. *Nat. Rev. Urol.* 12, 225–235. doi: 10.1038/nrurol.2015.58

Kapatral, V., Anderson, I., Ivanova, N., Reznik, G., Los, T., and Lykidis, A. (2002). Genome sequence and analysis of the oral bacterium *Fusobacterium nucleatum* strain ATCC 25586. *J. Bacteriol.* 184, 2005–2018. doi: 10.1128/jb.184.7.2005-2018.2002

Kaplan, C. W., Lux, R., Haake, S. K., and Shi, W. (2009). The *Fusobacterium nucleatum* outer membrane protein RadD is an arginine-inhibitable adhesin required for inter-species adherence and the structured architecture of multispecies biofilm. *Mol. Microbiol.* 71, 35–47. doi: 10.1111/j.1365-2958.2008.06503.x

Kasinskas, R. W., and Forbes, N. S. (2007). *Salmonella* typhimurium lacking ribose chemoreceptors localize in tumor quiescence and induce apoptosis. *Cancer Res.* 67, 3201–3209. doi: 10.1158/0008-5472.CAN-06-2618

Kinross, J. M., Darzi, A. W., and Nicholson, J. K. (2011). Gut microbiome-host interactions in health and disease. *Genome Med.* 3:14. doi: 10.1186/gm228

Kline, K. A., Dodson, K. W., Caparon, M. G., and Hultgren, S. J. (2010). A tale of two pili: assembly and function of pili in bacteria. *Trends Microbiol.* 18, 224–232. doi: 10.1016/j.tim.2010.03.002

Knasmuller, S., Steinkellner, H., Hirschl, A. M., Rabot, S., Nobis, E. C., and Kassie, F. (2001). Impact of bacteria in dairy products and of the intestinal microflora on the genotoxic and carcinogenic effects of heterocyclic aromatic amines. *Mutat. Res.* 480–481, 129–138. doi: 10.1016/s0027-5107(01)00176-2

Kochenderfer, J. N., Wilson, W. H., Janik, J. E., Dudley, M. E., Stetler-Stevenson, M., and Feldman, S. A. (2010). Eradication of B-lineage cells and regression of lymphoma in a patient treated with autologous T cells genetically engineered to recognize CD19. *Blood* 116, 4099–4102. doi: 10.1182/blood-2010-04-281931

Kolenbrander, P. E., Palmer, R. J. Jr., Periasamy, S., and Jakubovics, N. S. (2010). Oral multispecies biofilm development and the key role of cell-cell distance. *Nat. Rev. Microbiol.* 8, 471–480. doi: 10.1038/nrmicro2381

Komiya, Y., Shimomura, Y., Higurashi, T., Sugi, Y., Arimoto, J., and Umezawa, S. (2019). Patients with colorectal cancer have identical strains of *Fusobacterium nucleatum* in their colorectal cancer and oral cavity. *Gut* 68, 1335–1337. doi: 10.1136/gutjnl-2018-316661

Kostic, A. D., Chun, E., Robertson, L., Glickman, J. N., Gallini, C. A., and Michaud, M. (2013). *Fusobacterium nucleatum* potentiates intestinal tumorigenesis and modulates the tumor-immune microenvironment. *Cell Host Microbe* 14, 207–215. doi: 10.1016/j.chom.2013.07.007

Kostic, A. D., Gevers, D., Pedamallu, C. S., Michaud, M., Duke, F., and Earl, A. M. (2012). Genomic analysis identifies association of *Fusobacterium* with colorectal carcinoma. *Genome Res.* 22, 292–298. doi: 10.1101/gr.126573.111

Krisanaprakornkit, S., Kimball, J. R., Weinberg, A., Darveau, R. P., Bainbridge, B. W., and Dale, B. A. (2000). Inducible expression of human beta-defensin 2 by *Fusobacterium nucleatum* in oral epithelial cells: multiple signaling pathways and role of commensal bacteria in innate immunity and the epithelial barrier. *Infect. Immun.* 68, 2907–2915. doi: 10.1128/iai.68.5.2907-2915.2000

Krummel, M. F., and Allison, J. P. (1995). CD28 and CTLA-4 have opposing effects on the response of T cells to stimulation. *J. Exp. Med.* 182, 459–465. doi: 10.1084/jem.182.2.459

Latchman, Y., Wood, C. R., Chernova, T., Chaudhary, D., Borde, M., and Chernova, I. (2001). PD-L2 is a second ligand for PD-1 and inhibits T cell activation. *Nat. Immunol.* 2, 261–268. doi: 10.1038/85330

Lauder, A. P., Roche, A. M., Sherrill-Mix, S., Bailey, A., Laughlin, A. L., and Bittinger, K. (2016). Comparison of placenta samples with contamination controls does not provide evidence for a distinct placenta microbiota. *Microbiome* 4:29. doi: 10.1186/s40168-016-0172-3

Laursen, M. F., Andersen, L. B., Michaelsen, K. F., Molgaard, C., Trolle, E., Bahl, M. I., et al. (2016). Infant gut microbiota development is driven by transition to family foods independent of maternal obesity. *mSphere* 1:e69-15. doi: 10.1128/mSphere.00069-15

Le, D. T., Uram, J. N., Wang, H., Bartlett, B. R., Kemberling, H., and Eyring, A. D. (2015). PD-1 blockade in tumors with mismatch-repair deficiency. *N. Engl. J. Med.* 372, 2509–2520. doi: 10.1056/NEJMoa1500596

Linares, D. M., Gomez, C., Renes, E., Fresno, J. M., Tornadijo, M. E., Ross, R. P., et al. (2017). Lactic acid bacteria and bifidobacteria with potential to design natural biofunctional health-promoting dairy foods. *Front. Microbiol.* 8:846. doi: 10.3389/fmicb.2017.00846

Liu, P. F., Shi, W., Zhu, W., Smith, J. W., Hsieh, S. L., Gallo, R. L., et al. (2010). Vaccination targeting surface FomA of *Fusobacterium nucleatum* against bacterial co-aggregation: implication for treatment of periodontal infection and halitosis. *Vaccine* 28, 3496–3505. doi: 10.1016/j.vaccine.2010.02.047

Llopis, M., Antolin, M., Carol, M., Borruel, N., Casellas, F., and Martinez, C. (2009). Lactobacillus casei downregulates commensals' inflammatory signals in Crohn's disease mucosa. *Inflamm. Bowel Dis.* 15, 275–283. doi: 10.1002/ibd.20736

Lofgren, J. L., Whary, M. T., Ge, Z., Muthupalani, S., Taylor, N. S., and Mobley, M. (2011). Lack of commensal flora in *Helicobacter* pylori-infected INS-GAS mice reduces gastritis and delays intraepithelial neoplasia. *Gastroenterology* 140, 210–220. doi: 10.1053/j.gastro.2010.09.048

Ma, X., Aoki, T., Tsuruyama, T., and Narumiya, S. (2015). Definition of prostaglandin E2-EP2 signals in the colon tumor microenvironment that amplify inflammation and tumor growth. *Cancer Res.* 75, 2822–2832. doi: 10.1158/0008-5472.CAN-15-0125

Mancabelli, L., Milani, C., Lugli, G. A., Fontana, F., Turroni, F., van Sinderen, D., et al. (2020). The impact of primer design on amplicon-based metagenomic profiling accuracy: detailed insights into bifidobacterial community structure. *Microorganisms* 8:131. doi: 10.3390/microorganisms8010131

Manson, A., McGuire Cochrane, K., Griggs, A. D., Haas, B. J., Abeel, T., and Zeng, Q. (2014). Evolution of invasion in a diverse set of *Fusobacterium* species. *mBio* 5:e01864. doi: 10.1128/mBio.01864-14

Marteau, P. R., de Vrese, M., Cellier, C. J., and Schrezenmeir, J. (2001). Protection from gastrointestinal diseases with the use of probiotics. *Am. J. Clin. Nutr.* 73(2 Suppl.), 430S–436S. doi: 10.1093/ajcn/73.2.430s

Martin, R., Miquel, S., Benevides, L., Bridonneau, C., Robert, V., and Hudault, S. (2017). Functional characterization of novel *Faecalibacterium prausnitzii* strains isolated from healthy volunteers: a step forward in the use of prausnitzii, F., as a next-generation probiotic. *Front. Microbiol.* 8:1226. doi: 10.3389/fmicb.2017.01226

Matson, V., Fessler, J., Bao, R., Chongsuwat, T., Zha, Y., Alegre, M. L., et al. (2018). The commensal microbiome is associated with anti-PD-1 efficacy in metastatic melanoma patients. *Science* 359, 104–108. doi: 10.1126/science.aao3290

Maude, S. L., Laetsch, T. W., Buechner, J., Rives, S., Boyer, M., Bittencourt, H., et al. (2018). Tisagenlecleucel in children and young adults with B-cell lymphoblastic leukemia. *N. Engl. J. Med.* 378, 439–448. doi: 10.1056/NEJMoa1709866

McCarthy, E. F. (2006). The toxins of william coley, B., and the treatment of bone and soft-tissue sarcomas. *Iowa Orthop. J.* 26, 154–158.

McCarville, J. L., Dong, J., Caminero, A., Bermudez-Brito, M., Jury, J., and Murray, J. A. (2017). A commensal *Bifidobacterium longum* strain prevents gluten-related immunopathology in mice through expression of a serine protease inhibitor. *Appl. Environ. Microbiol.* 83:e1323-17. doi: 10.1128/AEM.01323-17

McCoy, A. N., Araujo-Perez, F., Azcarate-Peril, A., Yeh, J. J., Sandler, R. S., and Keku, T. O. (2013). Fusobacterium is associated with colorectal adenomas. *PLoS ONE* 8:e53653. doi: 10.1371/journal.pone.0053653

Middlebrook, J. L., and Dorland, R. B. (1984). Bacterial toxins: cellular mechanisms of action. *Microbiol. Rev.* 48, 199–221.

Milani, C., Duranti, S., Bottacini, F., Casey, E., Turroni, F., and Mahony, J. (2017a). The first microbial colonizers of the human gut: composition, activities, and health implications of the infant gut microbiota. *Microbiol. Mol. Biol. Rev.* 81:e36-17. doi: 10.1128/MMBR.00036-17

Milani, C., Mangifesta, M., Mancabelli, L., Lugli, G. A., Mancino, W., Viappiani, A., et al. (2017b). The sortase-dependent fimbriome of the genus bifidobacterium: extracellular structures with potential to modulate microbe-host dialogue. *Appl. Environ. Microbiol.* 83:e1295-17. doi: 10.1128/AEM.01295-17

Milani, C., Ferrario, C., Turroni, F., Duranti, S., Mangifesta, M., van Sinderen, D., et al. (2016). The human gut microbiota and its interactive connections to diet. *J. Hum. Nutr. Diet.* 29, 539–546. doi: 10.1111/jhn.12371

Milani, C., Lugli, G. A., Duranti, S., Turroni, F., Mancabelli, L., and Ferrario, C. (2015). Bifidobacteria exhibit social behavior through carbohydrate resource sharing in the gut. *Sci. Rep.* 5:15782. doi: 10.1038/srep15782

Mima, K., Nishihara, R., Qian, Z. R., Cao, Y., Sukawa, Y., and Nowak, J. A. (2016). *Fusobacterium nucleatum* in colorectal carcinoma tissue and patient prognosis. *Gut* 65, 1973–1980. doi: 10.1136/gutjnl-2015-310101

Molinero, N., Ruiz, L., Sanchez, B., Margolles, A., and Delgado, S. (2019). Intestinal bacteria interplay with bile and cholesterol metabolism: implications on host physiology. *Front. Physiol.* 10:185. doi: 10.3389/fphys.2019.00185

Morgillo, F., Dallio, M., Della Corte, C. M., Gravina, A. G., Viscardi, G., and Loguercio, C. (2018). Carcinogenesis as a result of multiple inflammatory and oxidative hits: a comprehensive review from tumor microenvironment to gut microbiota. *Neoplasia* 20, 721–733. doi: 10.1016/j.neo.2018.05.002

Motzer, R. J., Escudier, B., McDermott, D. F., George, S., Hammers, H. J., and Srinivas, S. (2015). Nivolumab versus everolimus in advanced renal-cell carcinoma. *N. Engl. J. Med.* 373, 1803–1813. doi: 10.1056/NEJMoa1510665

Nuriel-Ohayon, M., Neuman, H., and Koren, O. (2016). Microbial changes during pregnancy, birth, and infancy. *Front. Microbiol.* 7:1031. doi: 10.3389/fmicb.2016.01031

Nyfors, S., Kononen, E., Syrjanen, R., Komulainen, E., and Jousimies-Somer, H. (2003). Emergence of penicillin resistance among *Fusobacterium nucleatum* populations of commensal oral flora during early childhood. *J. Antimicrob. Chemother.* 51, 107–112. doi: 10.1093/jac/dkg022

O'Callaghan, A., and van Sinderen, D. (2016). Bifidobacteria and their role as members of the human gut microbiota. *Front. Microbiol.* 7:925. doi: 10.3389/fmicb.2016.00925

O'Connell Motherway, M., Houston, A., O'Callaghan, G., Reunanen, J., O'Brien, F. O., and Driscoll, T. (2019). A bifidobacterial pilus-associated protein promotes colonic epithelial proliferation. *Mol. Microbiol.* 111, 287–301. doi: 10.1111/mmi.14155

O'Connell Motherway, M., Zomer, A., Leahy, S. C., Reunanen, J., Bottacini, F., and Claesson, M. J. (2011). Functional genome analysis of *Bifidobacterium breve* UCC2003 reveals type IVb tight adherence (Tad) pili as an essential and conserved host-colonization factor. *Proc. Natl. Acad. Sci. U.S.A.* 108, 11217–11222. doi: 10.1073/pnas.1105380108

O'Mahony, L., Feeney, M., O'Halloran, S., Murphy, L., Kiely, B., and Fitzgibbon, J. (2001). Probiotic impact on microbial flora, inflammation and tumour development in IL-10 knockout mice. *Aliment. Pharmacol. Ther.* 15, 1219–1225. doi: 10.1046/j.1365-2036.2001.01027.x

Palmer, C., Bik, E. M., DiGiulio, D. B., Relman, D. A., and Brown, P. O. (2007). Development of the human infant intestinal microbiota. *PLoS Biol.* 5:e177. doi: 10.1371/journal.pbio.0050177

Pardoll, D. M. (2012). The blockade of immune checkpoints in cancer immunotherapy. *Nat. Rev. Cancer* 12, 252–264. doi: 10.1038/nrc3239

Peng, B. J., Cao, C. Y., Li, W., Zhou, Y. J., Zhang, Y., and Nie, Y. Q. (2018). Diagnostic performance of intestinal *Fusobacterium nucleatum* in colorectal cancer: a meta-analysis. *Chin. Med. J. (Engl.)* 131, 1349–1356. doi: 10.4103/0366-6999.232814

Petrof, E. O., Claud, E. C., Gloor, G. B., and Allen-Vercoe, E. (2013). Microbial ecosystems therapeutics: a new paradigm in medicine? *Benef. Microbes* 4, 53–65. doi: 10.3920/BM2012.0039

Pickard, J. M., Zeng, M. Y., Caruso, R., and Nunez, G. (2017). Gut microbiota: role in pathogen colonization, immune responses, and inflammatory disease. *Immunol. Rev.* 279, 70–89. doi: 10.1111/imr.12567

Pithva, S. P., Ambalam, P. S., Ramoliya, J. M., Dave, J. M., and Vyas, B. R. (2015). Antigenotoxic and antimutagenic activities of probiotic *Lactobacillus rhamnosus* Vc against N-methyl-N'-Nitro-N-nitrosoguanidine. *Nutr. Cancer* 67, 1142–1150. doi: 10.1080/01635581.2015.1073751

Potempa, J., Korzus, E., and Travis, J. (1994). The serpin superfamily of proteinase inhibitors: structure, function, and regulation. *J. Biol. Chem.* 269, 15957–15960.

Prakash, S., Rodes, L., Coussa-Charley, M., and Tomaro-Duchesneau, C. (2011). Gut microbiota: next frontier in understanding human health and development of biotherapeutics. *Biologics* 5, 71–86. doi: 10.2147/BTT.S19099

Prieto, P. A., Yang, J. C., Sherry, R. M., Hughes, M. S., Kammula, U. S., and White, D. E. (2012). CTLA-4 blockade with ipilimumab: long-term follow-up of 177 patients with metastatic melanoma. *Clin. Cancer Res.* 18, 2039–2047. doi: 10.1158/1078-0432.CCR-11-1823

Pryde, S. E., Duncan, S. H., Hold, G. L., Stewart, C. S., and Flint, H. J. (2002). The microbiology of butyrate formation in the human colon. *FEMS Microbiol. Lett.* 217, 133–139. doi: 10.1111/j.1574-6968.2002.tb11467.x

Pungel, D., Treveil, A., Dalby, M. J., Caim, S., Colquhoun, I. J., and Booth, C. (2020). *Bifidobacterium breve* UCC2003 exopolysaccharide modulates the early life microbiota by acting as a potential dietary substrate. *Nutrients* 12:948. doi: 10.3390/nu12040948

Putignani, L., Del Chierico, F., Petrucca, A., Vernocchi, P., and Dallapiccola, B. (2014). The human gut microbiota: a dynamic interplay with the host from birth to senescence settled during childhood. *Pediatr. Res.* 76, 2–10. doi: 10.1038/pr.2014.49

Puzanov, I., Diab, A., Abdallah, K., Bingham, C. O. III, Brogdon, C., and Dadu, R. (2017). for Immunotherapy of cancer toxicity management working: managing toxicities associated with immune checkpoint inhibitors: consensus recommendations from the society for immunotherapy of cancer (SITC) toxicity management working group. *J. Immunother. Cancer* 5:95. doi: 10.1186/s40425-017-0300-z

Rafter, J. (2003). Probiotics and colon cancer. *Best Pract. Res. Clin. Gastroenterol.* 17, 849–859. doi: 10.1016/S1521-6918(03)00056-8

Rajilic-Stojanovic, M., Smidt, H., and de Vos, W. M. (2007). Diversity of the human gastrointestinal tract microbiota revisited. *Environ. Microbiol.* 9, 2125–2136. doi: 10.1111/j.1462-2920.2007.01369.x

Raman, M., Ambalam, P., Kondepudi, K. K., Pithva, S., Kothari, C., and Patel, A. T. (2013). Potential of probiotics, prebiotics and synbiotics for management of colorectal cancer. *Gut. Microbes* 4, 181–192. doi: 10.4161/gmic.23919

Rautava, S., Luoto, R., Salminen, S., and Isolauri, E. (2012). Microbial contact during pregnancy, intestinal colonization and human disease. *Nat. Rev. Gastroenterol. Hepatol.* 9, 565–576. doi: 10.1038/nrgastro.2012.144

Reig, M., Baquero, F., Garcia-Campello, M., and Loza, E. (1985). *Leptotrichia buccalis* bacteremia in neutropenic children. *J. Clin. Microbiol.* 22, 320–321.

Riordan, T. (2007). Human infection with *Fusobacterium necrophorum* (Necrobacillosis), with a focus on Lemierre's syndrome. *Clin. Microbiol. Rev.* 20, 622–659. doi: 10.1128/CMR.00011-07

Rios-Covian, D., Gueimonde, M., Duncan, S. H., Flint, H. J., and de los Reyes-Gavilan, C. G. (2015). Enhanced butyrate formation by cross-feeding between *Faecalibacterium prausnitzii* and *Bifidobacterium adolescentis*. *FEMS Microbiol. Lett.* 362:fnv176. doi: 10.1093/femsle/fnv176

Riviere, A., Gagnon, M., Weckx, S., Roy, D., and De Vuyst, L. (2015). Mutual cross-feeding interactions between *Bifidobacterium longum* subsp. longum *NCC*2705 and *Eubacterium rectale* ATCC 33656 explain the bifidogenic and butyrogenic effects of arabinoxylan oligosaccharides. *Appl. Environ. Microbiol.* 81, 7767–7781. doi: 10.1128/AEM.02089-15

Roberfroid, M. (2007). Prebiotics: the concept revisited. *J. Nutr.* 137(3 Suppl. 2), 830S–837S. doi: 10.1093/jn/137.3.830S

Robertson, A. G., Kim, J., Al-Ahmadie, H., Bellmunt, J., Guo, G., and Cherniack, A. D. (2017). Comprehensive molecular characterization of muscle-invasive bladder cancer. *Cell* 171, 540–556.e25. doi: 10.1016/j.cell.2017.09.007

Rodriguez, J. M., Murphy, K., Stanton, C., Ross, R. P., Kober, O. I., and Juge, N. (2015). The composition of the gut microbiota throughout life, with an emphasis on early life. *Microb. Ecol. Health Dis.* 26:26050. doi: 10.3402/mehd.v26.26050

Rogowski, A., Briggs, J. A., Mortimer, J. C., Tryfona, T., Terrapon, N., and Lowe, E. C. (2015). Glycan complexity dictates microbial resource allocation in the large intestine. *Nat. Commun.* 6:7481. doi: 10.1038/ncomms8481

Routy, B., Le Chatelier, E., Derosa, L., Duong, C. P. M., Alou, M. T., and Daillere, R. (2018). Gut microbiome influences efficacy of PD-1-based immunotherapy against epithelial tumors. *Science* 359, 91–97. doi: 10.1126/science.aan3706

Rowland, I., Gibson, G., Heinken, A., Scott, K., Swann, J., Thiele, I., et al. (2018). Gut microbiota functions: metabolism of nutrients and other food components. *Eur. J. Nutr.* 57, 1–24. doi: 10.1007/s00394-017-1445-8

Ruas-Madiedo, P., Gueimonde, M., Arigoni, F., de los Reyes-Gavilan, C. G., and Margolles, A. (2009). Bile affects the synthesis of exopolysaccharides by *Bifidobacterium animalis*. *Appl. Environ. Microbiol.* 75, 1204–1207. doi: 10.1128/AEM.00908-08

Rubinstein, M. R., Wang, X., Liu, W., Hao, Y., Cai, G., and Han, Y. W. (2013). *Fusobacterium nucleatum* promotes colorectal carcinogenesis by modulating E-cadherin/beta-catenin signaling via its FadA adhesin. *Cell Host Microbe* 14, 195–206. doi: 10.1016/j.chom.2013.07.012

Ruiz, L., Delgado, S., Ruas-Madiedo, P., Sanchez, B., and Margolles, A. (2017). Bifidobacteria and their molecular communication with the immune system. *Front. Microbiol.* 8:2345. doi: 10.3389/fmicb.2017.02345

Salazar, N., Lopez, P., Garrido, P., Moran, J., Cabello, E., and Gueimonde, M. (2014). Immune modulating capability of two exopolysaccharide-producing *Bifidobacterium* strains in a wistar rat model. *Biomed. Res. Int.* 2014:106290. doi: 10.1155/2014/106290

Schachter, J., Ribas, A., Long, G. V., Arance, A., Grob, J. J., and Mortier, L. (2017). Pembrolizumab versus ipilimumab for advanced melanoma: final overall survival results of a multicentre, randomised, open-label phase 3 study (KEYNOTE-006). *Lancet* 390, 1853–1862. doi: 10.1016/S0140-6736(17)31601-X

Scheppach, W. (1994). Effects of short chain fatty acids on gut morphology and function. *Gut* 35(1 Suppl.), S35–S38. doi: 10.1136/gut.35.1_suppl.s35

Schwab, C., Ruscheweyh, H. J., Bunesova, V., Pham, V. T., Beerenwinkel, N., and Lacroix, C. (2017). Trophic interactions of infant bifidobacteria and *Eubacterium hallii* during L-fucose and fucosyllactose degradation. *Front. Microbiol.* 8:95. doi: 10.3389/fmicb.2017.00095

Schwabe, R. F., and Jobin, C. (2013). The microbiome and cancer. *Nat. Rev. Cancer* 13, 800–812. doi: 10.1038/nrc3610

Scott, J. R., and Zahner, D. (2006). Pili with strong attachments: gram-positive bacteria do it differently. *Mol. Microbiol.* 62, 320–330. doi: 10.1111/j.1365-2958.2006.05279.x

Seavey, M. M., Maciag, P. C., Al-Rawi, N., Sewell, D., and Paterson, Y. (2009). An anti-vascular endothelial growth factor receptor 2/fetal liver kinase-1 Listeria monocytogenes anti-angiogenesis cancer vaccine for the treatment of primary and metastatic Her-2/neu+ breast tumors in a mouse model. *J. Immunol.* 182, 5537–5546. doi: 10.4049/jimmunol.0803742

Sermer, D., and Brentjens, R. (2019). CAR T-cell therapy: full speed ahead. *Hematol. Oncol.* 37(Suppl. 1), 95–100. doi: 10.1002/hon.2591

Shang, F. M., and Liu, H. L. (2018). *Fusobacterium nucleatum* and colorectal cancer: a review. *World J. Gastrointest. Oncol.* 10, 71–81. doi: 10.4251/wjgo.v10.i3.71

Sharma, P., and Allison, J. P. (2015). The future of immune checkpoint therapy. *Science* 348, 56–61. doi: 10.1126/science.aaa8172

Shepard, H. M., Phillips, G. L., Thanos, C. D., and Feldmann, M. (2017). Developments in therapy with monoclonal antibodies and related proteins. *Clin. Med. (Lond.)* 17, 220–232. doi: 10.7861/clinmedicine.17-3-220

Shi, Y., Zheng, W., Yang, K., Harris, K. G., Ni, K., and Xue, L. (2020). Intratumoral accumulation of gut microbiota facilitates CD47-based immunotherapy via STING signaling. *J. Exp. Med.* 217:e20192282. doi: 10.1084/jem.20192282

Sivan, A., Corrales, L., Hubert, N., Williams, J. B., Aquino-Michaels, K., and Earley, Z. M. (2015). Commensal *Bifidobacterium* promotes antitumor immunity and facilitates anti-PD-L1 efficacy. *Science* 350, 1084–1089. doi: 10.1126/science.aac4255

Sokol, H., Pigneur, B., Watterlot, L., Lakhdari, O., Bermudez-Humaran, L. G., and Gratadoux, J. J. (2008). *Faecalibacterium prausnitzii* is an anti-inflammatory commensal bacterium identified by gut microbiota analysis of Crohn disease patients. *Proc. Natl. Acad. Sci. U.S.A.* 105, 16731–16736. doi: 10.1073/pnas.0804812105

Sokol, H., Seksik, P., Furet, J. P., Firmesse, O., Nion-Larmurier, I., and Beaugerie, L. (2009). Low counts of *Faecalibacterium prausnitzii* in colitis microbiota. *Inflamm. Bowel Dis.* 15, 1183–1189. doi: 10.1002/ibd.20903

St Jean, A. T., Swofford, C. A., Panteli, J. T., Brentzel, Z. J., and Forbes, N. S. (2014). Bacterial delivery of *Staphylococcus aureus* alpha-hemolysin causes regression and necrosis in murine tumors. *Mol. Ther.* 22, 1266–1274. doi: 10.1038/mt.2014.36

Staley, C., Weingarden, A. R., Khoruts, A., and Sadowsky, M. J. (2017). Interaction of gut microbiota with bile acid metabolism and its influence on disease states. *Appl. Microbiol. Biotechnol.* 101, 47–64. doi: 10.1007/s00253-016-8006-6

Stidham, R. W., and Higgins, P. D. R. (2018). Colorectal cancer in inflammatory bowel disease. *Clin. Colon Rectal. Surg.* 31, 168–178. doi: 10.1055/s-0037-1602237

Strauss, J., Kaplan, G. G., Beck, P. L., Rioux, K., Panaccione, R., and Devinney, R. (2011). Invasive potential of gut mucosa-derived *Fusobacterium nucleatum* positively correlates with IBD status of the host. *Inflamm. Bowel Dis.* 17, 1971–1978. doi: 10.1002/ibd.21606

Sun, C. H., Li, B. B., Wang, B., Zhao, J., Zhang, X. Y., and Li, T. T. (2019). The role of *Fusobacterium nucleatum* in colorectal cancer: from carcinogenesis to clinical management. *Chronic Dis. Transl. Med.* 5, 178–187. doi: 10.1016/j.cdtm.2019.09.001

Sun, J., and Kato, I. (2016). Gut microbiota, inflammation and colorectal cancer. *Genes Dis.* 3, 130–143. doi: 10.1016/j.gendis.2016.03.004

Swidsinski, A., Dorffel, Y., Loening-Baucke, V., Theissig, F., Ruckert, J. C., and Ismail, M. (2011). Acute appendicitis is characterised by local invasion with *Fusobacterium nucleatum/necrophorum*. *Gut* 60, 34–40. doi: 10.1136/gut.2009.191320

Tamboli, C. P., Neut, C., Desreumaux, P., and Colombel, J. F. (2004). Dysbiosis in inflammatory bowel disease. *Gut* 53, 1–4. doi: 10.1136/gut.53.1.1

Tan, C. R., Zhou, L., and El-Deiry, W. S. (2016). Circulating tumor cells versus circulating tumor DNA in colorectal cancer: pros and cons. *Curr. Colorectal Cancer Rep.* 12, 151–161. doi: 10.1007/s11888-016-0320-y

Tanoue, T., Morita, S., Plichta, D. R., Skelly, A. N., Suda, W., and Sugiura, Y. (2019). A defined commensal consortium elicits CD8 T cells and anti-cancer immunity. *Nature* 565, 600–605. doi: 10.1038/s41586-019-0878-z

Taxman, D. J., Swanson, K. V., Broglie, P. M., Wen, H., Holley-Guthrie, E., and Huang, M. T. (2012). Porphyromonas gingivalis mediates inflammasome repression in polymicrobial cultures through a novel mechanism involving reduced endocytosis. *J. Biol. Chem.* 287, 32791–32799. doi: 10.1074/jbc.M112.401737

Tojo, R., Suarez, A., Clemente, M. G., de los Reyes-Gavilan, C. G., Margolles, A., and Gueimonde, M. (2014). Intestinal microbiota in health and disease: role of bifidobacteria in gut homeostasis. *World J. Gastroenterol.* 20, 15163–15176. doi: 10.3748/wjg.v20.i41.15163

Torre, L. A., Bray, F., Siegel, R. L., Ferlay, J., Lortet-Tieulent, J., and Jemal, A. (2015). Global cancer statistics, 2012. *CA Cancer J. Clin.* 65, 87–108. doi: 10.3322/caac.21262

Turnbaugh, P. J., Ley, R. E., Hamady, M., Fraser-Liggett, C. M., Knight, R., and Gordon, J. I. (2007). The human microbiome project. *Nature* 449, 804–810. doi: 10.1038/nature06244

Turroni, F., Duranti, S., Milani, C., Lugli, G. A., van Sinderen, D., and Ventura, M. (2019). *Bifidobacterium bifidum*: a key member of the early human gut microbiota. *Microorganisms* 7:544. doi: 10.3390/microorganisms7110544

Turroni, F., Foroni, E., O'Connell Motherway, M., Bottacini, F., Giubellini, V., and Zomer, A. (2010). Characterization of the serpin-encoding gene of *Bifidobacterium breve* 210 B. *Appl. Environ. Microbiol.* 76, 3206–3219. doi: 10.1128/AEM.02938-09

Turroni, F., Milani, C., Duranti, S., Lugli, G. A., Bernasconi, S., and Margolles, A. (2020). The infant gut microbiome as a microbial organ influencing host well-being. *Ital. J. Pediatr.* 46:16. doi: 10.1186/s13052-020-0781-0

Turroni, F., Peano, C., Pass, D. A., Foroni, E., Severgnini, M., and Claesson, M. J. (2012). Diversity of bifidobacteria within the infant gut microbiota. *PLoS ONE* 7:e36957. doi: 10.1371/journal.pone.0036957

Turroni, F., Serafini, F., Foroni, E., Duranti, S., O'Connell Motherway, M., and Taverniti, V. (2013). Role of sortase-dependent pili of *Bifidobacterium bifidum* PRL2010 in modulating bacterium-host interactions. *Proc. Natl. Acad. Sci. U.S.A.* 110, 11151–11156. doi: 10.1073/pnas.1303897110

Turroni, F., Serafini, F., Mangifesta, M., Arioli, S., Mora, D., van Sinderen, D., et al. (2014). Expression of sortase-dependent pili of Bifidobacterium bifidum PRL2010 in response to environmental gut conditions. *FEMS Microbiol. Lett.* 357, 23–33. doi: 10.1111/1574-6968.12509

Uchugonova, A., Zhang, Y., Salz, R., Liu, F., Suetsugu, A., and Zhang, L. (2015). Imaging the different mechanisms of prostate cancer cell-killing by tumor-targeting *Salmonella* typhimurium A1-R. *Anticancer Res.* 35, 5225–5229.

Underhill, D. M., and Iliev, I. D. (2014). The mycobiota: interactions between commensal fungi and the host immune system. *Nat. Rev. Immunol.* 14, 405–416. doi: 10.1038/nri3684

Ursell, L. K., Clemente, J. C., Rideout, J. R., Gevers, D., Caporaso, J. G., and Knight, R. (2012a). The interpersonal and intrapersonal diversity of human-associated microbiota in key body sites. *J. Allergy Clin. Immunol.* 129, 1204–1208. doi: 10.1016/j.jaci.2012.03.010

Ursell, L. K., Metcalf, J. L., Parfrey, L. W., and Knight, R. (2012b). Defining the human microbiome. *Nutr. Rev.* 70(Suppl. 1), S38–S44. doi: 10.1111/j.1753-4887.2012.00493.x

Vander, M. G., Heiden Cantley, L. C., and Thompson, C. B. (2009). Understanding the Warburg effect: the metabolic requirements of cell proliferation. *Science* 324, 1029–1033. doi: 10.1126/science.1160809

Ventura, M., Canchaya, C., Tauch, A., Chandra, G., Fitzgerald, G. F., and Chater, K. F. (2007). Genomics of *Actinobacteria*: tracing the evolutionary history of an ancient phylum. *Microbiol. Mol. Biol. Rev.* 71, 495–548. doi: 10.1128/MMBR.00005-07

Verma, R., Lee, C., Jeun, E. J., Yi, J., Kim, K. S., and Ghosh, A. (2018). Cell surface polysaccharides of Bifidobacterium bifidum induce the generation of Foxp3(+) regulatory T cells. *Sci. Immunol.* 3:eaat6975. doi: 10.1126/sciimmunol.aat6975

Vetizou, M., Pitt, J. M., Daillere, R., Lepage, P., Waldschmitt, N., and Flament, C. (2015). Anticancer immunotherapy by CTLA-4 blockade relies on the gut microbiota. *Science* 350, 1079–1084. doi: 10.1126/science.aad1329

Villeger, R., Lopes, A., Carrier, G., Veziant, J., Billard, E., and Barnich, N. (2019). Intestinal microbiota: a novel target to improve anti-tumor treatment? *Int. J. Mol. Sci.* 20:4584. doi: 10.3390/ijms20184584

Virchow, R. (1989). Cellular pathology. As based upon physiological and pathological histology. Lecture XVI–Atheromatous affection of arteries. 1858. *Nutr. Rev.* 47, 23–25. doi: 10.1111/j.1753-4887.1989.tb02747.x

Waddington, L., Cyr, T., Hefford, M., Hansen, L. T., and Kalmokoff, M. (2010). Understanding the acid tolerance response of bifidobacteria. *J. Appl. Microbiol.* 108, 1408–1420. doi: 10.1111/j.1365-2672.2009.04540.x

Wang, H. F., Li, L. F., Guo, S. H., Zeng, Q. Y., Ning, F., Liu, W. L., et al. (2016). Evaluation of antibody level against *Fusobacterium nucleatum* in the serological diagnosis of colorectal cancer. *Sci. Rep.* 6:33440. doi: 10.1038/srep33440

Warren, R. L., Freeman, D. J., Pleasance, S., Watson, P., Moore, R. A., and Cochrane, K. (2013). Co-occurrence of anaerobic bacteria in colorectal carcinomas. *Microbiome* 1:16. doi: 10.1186/2049-2618-1-16

Weeks, D. F., Katz, D. S., Saxon, P., and Kubal, W. S. (2010). Lemierre syndrome: report of five new cases and literature review. *Emerg. Radiol.* 17, 323–328. doi: 10.1007/s10140-010-0858-y

Weinberger, M., Wu, T., Rubin, M., Gill, V. J., and Pizzo, P. A. (1991). *Leptotrichia buccalis* bacteremia in patients with cancer: report of four cases and review. *Rev. Infect. Dis.* 13, 201–206. doi: 10.1093/clinids/13.2.201

Wollowski, I., Rechkemmer, G., and Pool-Zobel, B. L. (2001). Protective role of probiotics and prebiotics in colon cancer. *Am. J. Clin. Nutr.* 73(2 Suppl.), 451S–455S. doi: 10.1093/ajcn/73.2.451s

Wong, S. H., Zhao, L., Zhang, X., Nakatsu, G., Han, J., and Xu, W. (2017). Gavage of fecal samples from patients with colorectal cancer promotes intestinal carcinogenesis in germ-free and conventional mice. *Gastroenterology* 153, 1621–1633.e6. doi: 10.1053/j.gastro.2017.08.022

Wood, L. M., and Paterson, Y. (2014). Attenuated *Listeria monocytogenes*: a powerful and versatile vector for the future of tumor immunotherapy. *Front. Cell Infect. Microbiol.* 4:51. doi: 10.3389/fcimb.2014.00051

Wrzosek, L., Miquel, S., Noordine, M. L., Bouet, S., Joncquel, M., and Chevalier-Curt, J. (2013). *Bacteroides thetaiotaomicron* and Faecalibacterium prausnitzii influence the production of mucus glycans and the development of goblet cells in the colonic epithelium of a gnotobiotic model rodent. *BMC Biol.* 11:61. doi: 10.1186/1741-7007-11-61

Wu, T., Cen, L., Kaplan, C., Zhou, X., Lux, R., Shi, W., et al. (2015). Cellular components mediating coadherence of *Candida albicans* and *Fusobacterium nucleatum*. *J. Dent. Res.* 94, 1432–1438. doi: 10.1177/0022034515593706

Yachida, S., Mizutani, S., Shiroma, H., Shiba, S., Nakajima, T., and Sakamoto, T. (2019). Metagenomic and metabolomic analyses reveal distinct stage-specific phenotypes of the gut microbiota in colorectal cancer. *Nat. Med.* 25, 968–976. doi: 10.1038/s41591-019-0458-7

Yan, F., and Polk, D. B. (2011). Probiotics and immune health. *Curr. Opin. Gastroenterol.* 27, 496–501. doi: 10.1097/MOG.0b013e32834baa4d

Yang, Y. (2015). Cancer immunotherapy: harnessing the immune system to battle cancer. *J. Clin. Invest.* 125, 3335–3337. doi: 10.1172/JCI83871

Yatsunenko, T., Rey, F. E., Manary, M. J., Trehan, I., Dominguez-Bello, M. G., and Contreras, M. (2012). Human gut microbiome viewed across age and geography. *Nature* 486, 222–227. doi: 10.1038/nature11053

Yoshimoto, S., Loo, T. M., Atarashi, K., Kanda, H., Sato, S., and Oyadomari, S. (2013). Obesity-induced gut microbial metabolite promotes liver cancer through senescence secretome. *Nature* 499, 97–101. doi: 10.1038/nature12347

Yu, L. C. (2018). Microbiota dysbiosis and barrier dysfunction in inflammatory bowel disease and colorectal cancers: exploring a common ground hypothesis. *J. Biomed. Sci.* 25:79. doi: 10.1186/s12929-018-0483-8

Yu, R., Zuo, F., Ma, H., and Chen, S. (2019). Exopolysaccharide-producing bifidobacterium adolescentis strains with similar adhesion property induce differential regulation of inflammatory immune response in Treg/Th17 axis of DSS-colitis mice. *Nutrients* 11:782. doi: 10.3390/nu11040782

Yu, T., Guo, F., Yu, Y., Sun, T., Ma, D., and Han, J. (2017). *Fusobacterium nucleatum* promotes chemoresistance to colorectal cancer by modulating autophagy. *Cell* 170, 548–563.e16. doi: 10.1016/j.cell.2017.07.008

Yu, W. D., Sun, G., Li, J., Xu, J., and Wang, X. (2019). Mechanisms and therapeutic potentials of cancer immunotherapy in combination with radiotherapy and/or chemotherapy. *Cancer Lett.* 452, 66–70. doi: 10.1016/j.canlet.2019.02.048

Zhang, K., Dai, H., Liang, W., Zhang, L., and Deng, Z. (2019). Fermented dairy foods intake and risk of cancer. *Int. J. Cancer* 144, 2099–2108. doi: 10.1002/ijc.31959

Zhang, M., Swofford, C. A., and Forbes, N. S. (2014). Lipid A controls the robustness of intratumoral accumulation of attenuated *Salmonella* in mice. *Int. J. Cancer* 135, 647–657. doi: 10.1002/ijc.28700

Zitvogel, L., Ma, Y., Raoult, D., Kroemer, G., and Gajewski, T. F. (2018). The microbiome in cancer immunotherapy: diagnostic tools and therapeutic strategies. *Science* 359, 1366–1370. doi: 10.1126/science.aar6918

Zou, W., and Chen, L. (2008). Inhibitory B7-family molecules in the tumour microenvironment. *Nat. Rev. Immunol.* 8, 467–477. doi: 10.1038/nri2326

Conflict of Interest: The authors declare that the research was conducted in the absence of any commercial or financial relationships that could be construed as a potential conflict of interest.

The reviewer VR declared a shared affiliation, with no collaboration, with one of the authors, DS, to the handling editor at the time of review.

frontiers in Microbiology

ORIGINAL RESEARCH
published: 15 September 2020
doi: 10.3389/fmicb.2020.573335

Riboflavin Biosynthesis and Overproduction by a Derivative of the Human Gut Commensal *Bifidobacterium longum* subsp. *infantis* ATCC 15697

Ana Solopova[1†], Francesca Bottacini[1†], Elena Venturi degli Esposti[2†], Alberto Amaretti[2,3], Stefano Raimondi[2], Maddalena Rossi[2,3] and Douwe van Sinderen[1,4*]*

[1] APC Microbiome Ireland, University College Cork, Cork, Ireland, [2] Department of Chemistry, University of Modena and Reggio Emilia, Modena, Italy, [3] BIOGEST-SITEIA, University of Modena and Reggio Emilia, Modena, Italy, [4] School of Microbiology, University College Cork, Cork, Ireland

OPEN ACCESS

Edited by:
Paloma López,
Margarita Salas Center for Biological Research (CSIC), Spain

Reviewed by:
Pasquale Russo,
University of Foggia, Italy
Patricia Ruas-Madiedo,
Institute of Dairy Products of Asturias (IPLA), Spain

***Correspondence:**
Maddalena Rossi
maddalena.rossi@unimore.it
Douwe van Sinderen
d.vansinderen@ucc.ie

[†] These authors have contributed equally to this work

Specialty section:
This article was submitted to Food Microbiology, a section of the journal Frontiers in Microbiology

Received: 16 June 2020
Accepted: 17 August 2020
Published: 15 September 2020

Citation:
Solopova A, Bottacini F, Venturi degli Esposti E, Amaretti A, Raimondi S, Rossi M and van Sinderen D (2020) Riboflavin Biosynthesis and Overproduction by a Derivative of the Human Gut Commensal Bifidobacterium longum subsp. infantis ATCC 15697. Front. Microbiol. 11:573335. doi: 10.3389/fmicb.2020.573335

Riboflavin or vitamin B_2 is the precursor of the essential coenzymes flavin mononucleotide (FMN) and flavin adenine dinucleotide (FAD). Despite increased interest in microbial synthesis of this water-soluble vitamin, the metabolic pathway for riboflavin biosynthesis has been characterized in just a handful of bacteria. Here, comparative genome analysis identified the genes involved in the *de novo* biosynthetic pathway of riboflavin in certain bifidobacterial species, including the human gut commensal *Bifidobacterium longum* subsp. *infantis* (*B. infantis*) ATCC 15697. Using comparative genomics and phylogenomic analysis, we investigated the evolutionary acquisition route of the riboflavin biosynthesis or *rib* gene cluster in *Bifidobacterium* and the distribution of riboflavin biosynthesis-associated genes across the genus. Using *B. infantis* ATCC 15697 as model organism for this pathway, we isolated spontaneous riboflavin overproducers, which had lost transcriptional regulation of the genes required for riboflavin biosynthesis. Among them, one mutant was shown to allow riboflavin release into the medium to a concentration of 60.8 ng mL^{-1}. This mutant increased vitamin B_2 concentration in a fecal fermentation system, thus providing promising data for application of this isolate as a functional food ingredient.

Keywords: probiotic, vitamin B_2, gut commensal, vitamin biosynthesis, health benefit

INTRODUCTION

Riboflavin (i.e., vitamin B_2) is a precursor of flavin mononucleotide (FMN) and flavin adenine dinucleotide (FAD), cofactors acting as essential electron carriers in redox reactions of cell metabolism (LeBlanc et al., 2011). Besides playing an important role in a range of biochemical reactions, riboflavin serves as a signaling molecule in bacterial quorum sensing and bacterium-plant interactions, while intermediates of the riboflavin biosynthesis pathway are also involved in host-microbe signaling (Rajamani et al., 2008; Corbett et al., 2014; Dakora et al., 2015). Only plants, fungi, and various eubacteria encode the complete enzymatic machinery for *de novo* riboflavin

biosynthesis (Bacher et al., 2000; Fischer et al., 2004). Humans need to regularly obtain this vitamin through their diet as they are unable to synthesize or store it. For this reason, riboflavin is an ingredient in various fortified foods and multivitamin supplements. Absorption of riboflavin occurs in the small and large intestine through specific carriers (Thakur et al., 2017). The recommended daily allowance for riboflavin increases with age, reaching up to 1.1 and 1.3 mg in adult women and men, respectively, and is the highest (1.6 mg) in lactating mothers (Institute of Medicine, 1998).

Riboflavin had been produced by chemical means until commercially competitive microbial processes were developed to facilitate large-scale production. Biotechnological processes with various microbial cell factories such as *Bacillus subtilis*, *Candida flareri,* and especially, *Ashbya gossypii*, represent typical examples of white biotechnology (Stahmann et al., 2000; Ledesma-Amaro et al., 2015). In recent years, vitamin production by lactic acid bacteria (LAB) and bifidobacteria has received increased attention. These organisms are widely exploited by the food and pharmaceutical industries as starters for fermented products and/or as probiotic supplements aiming to improve human health. Utilization of vitamin-producing bacteria in food manufacturing has the obvious advantage of achieving *in situ* food fortification, which represents a non-artificial and economically viable strategy (Thakur et al., 2016). Vitamin-producing probiotic strains that may colonize, at least transiently, the human intestine, have the advantage of providing the host with a continuous supply of this micronutrient. Certain members of the genus *Bifidobacterium* have previously been proposed to supply vitamins, but, unlike folate, riboflavin-producing bifidobacteria have so far not been assessed (Pompei et al., 2007a,b; D'Aimmo et al., 2012; Sugahara et al., 2015). Notably, among bifidobacteria the presence of a complete riboflavin biosynthesis pathway and associated cluster has so far only been reported in *B. longum* subsp. *infantis* (Sela et al., 2008; Kwak et al., 2016).

Bacteria synthesize FMN and FAD according to the pathway outlined in **Figure 1**, starting from one molecule of guanosine-5′-triphosphate (GTP) and two molecules of ribulose-5-phosphate (Vitreschak et al., 2002; Fischer et al., 2004). The RibAB, RibD, RibE and RibH riboflavin biosynthetic enzymes are encoded by the *rib* operon, while the genes encoding RibCF and RibU, the latter a transporter for the uptake of pre-formed riboflavin, are typically located elsewhere on the chromosome (Vitreschak et al., 2002; Burgess et al., 2006a; Thakur et al., 2016). The first step of riboflavin biosynthesis is catalyzed by the enzyme GTP cyclohydrolase/dihydroxy-2-butanone-phosphate synthase (RibAB), which is responsible for the formation of formate and 3,4-dihydroxy-2-butanone 4-phosphate (DHBP) from D-ribulose 5-phosphate and 2,5-diamino-6-beta-ribosyl-4(3H)-pyrimidinone 5'-phosphate (DARP) from GTP, which are precursors of the aromatic ring of riboflavin. A reductase/deaminase (RibD) catalyzes the subsequent reduction of the ribose side chain in DARP to produce 5-amino-6-(5-phospho-D-ribitylamino)uracil. The last two steps of the pathway are then completed by a lumazine synthase (RibH) and a riboflavin synthase (RibE). The obtained riboflavin is then converted by phosphorylation into FMN and FAD by a reaction catalyzed by a riboflavin kinase/FAD synthase (RibCF; **Figures 1A,B**). In Firmicutes and in Actinobacteria, *de novo* biosynthesis is regulated through a feedback mechanism involving transcriptional attenuation via an FMN-sensing mRNA riboswitch (Mironov et al., 2002; Vitreschak et al., 2002). If present, FMN is bound with high affinity by the 5'-untranslated region (5'-UTR) of the nascent transcript of the *rib* operon, which serves as the FMN-binding aptamer. The binding causes the transcript to switch to its anti-antiterminator structure, allowing a termination hairpin to form thereby prematurely ending *rib* operon transcription (Kil et al., 1992; Mironov et al., 2002; Vitreschak et al., 2002).

Roseoflavin is an antibacterial compound and a structural analog of riboflavin, produced by *Streptomyces davawensis* (Mack et al., 1998; Ott et al., 2009). This antimetabolite binds to the active site of FAD synthetase and flavokinase yielding inactive complexes of roseoflavin mononucleotide (RoFMN) and roseoflavin adenine dinucleotide (RoFAD), thereby inhibiting major cellular reactions. Additionally, RoFMN mimics FMN in the riboswitch regulation and suppresses *de novo* vitamin production (Mack et al., 1998; Ott et al., 2009; Ludwig et al., 2018). Isolation of spontaneous roseoflavin-resistant mutants is a reliable method to obtain riboflavin-overproducing strains of various species, since increased vitamin production counteracts roseoflavin toxicity by competitive binding to FAD synthetase (Matsui et al., 1982). This approach, which does not involve deliberate genetic engineering and may thus be acceptable for food applications, has generated various riboflavin-producing mutants that can be exploited to produce riboflavin-enriched foods employing LAB and propionibacteria (e.g., *Lactococcus lactis*, *Lactobacillus plantarum*, *Lactobacillus fermentum*, *Propionibacterium freudenreichii*; Burgess et al., 2004, 2006b; LeBlanc et al., 2005, 2006; Capozzi et al., 2011; Russo et al., 2014; Juarez Del Valle et al., 2016; Mohedano et al., 2019; Yepez et al., 2019; Ge et al., 2020).

The biosynthetic pathway for riboflavin had previously been predicted for some bifidobacterial strains, such as the type strain *Bifidobacterium longum* subsp. *infantis* ATCC 15697 (hereinafter referred to as *B. infantis* ATCC 15697; Kwak et al., 2016). However, riboflavin-(over)producing strains have never been described and little is known about biosynthesis and regulation of this vitamin in bifidobacteria. In the present study, the presence of the riboflavin and FMN/FAD biosynthetic pathway was assessed in all annotated *Bifidobacterium* genomes. Spontaneous roseoflavin-resistant mutants of *B. infantis* ATCC 15697 were obtained and were shown to constitutively produce riboflavin, which was released in the growth medium. Promising evidence for or a potential application in the probiotic industry was obtained in a fecal fermentation system, in which the strain was shown to increase the overall riboflavin concentration.

MATERIALS AND METHODS

Comparative Bioinformatic Analysis

Protein coding sequences derived from a total of 662 representative strains from 83 bifidobacterial (sub)species were retrieved from the NCBI Reference Sequence collection

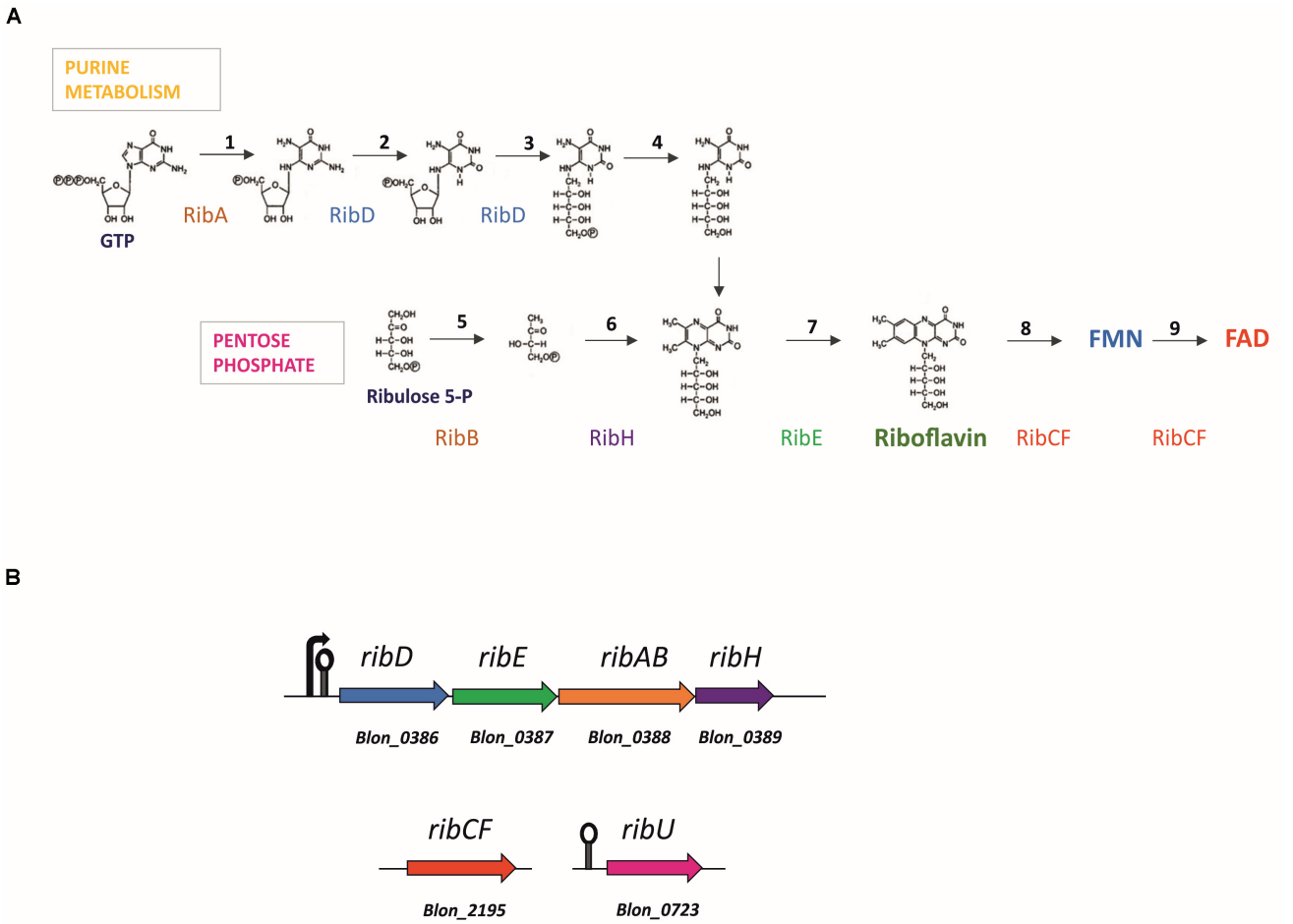

FIGURE 1 | Flavin adenine dinucleotide (FAD) biosynthesis and corresponding gene loci predicted in the genome of *Bifidobacterium longum*. **(A)** General bacterial pathway of FAD biosynthesis. Stoichiometrically, the formation of riboflavin requires one equivalent of GTP and two equivalents of ribulose 5-phosphate. Reactions are catalyzed by enzymes: RibAB (1, 5), bifunctional GTP cyclohydrolase II [EC:3.5.4.25]/(3,4-dihydroxy-2-butanone 4-phosphate synthase [EC:4.1.99.12]; RibD (2, 3), bifunctional diaminohydroxyphosphoribosylaminopyrimidine deaminase [EC:3.5.4.26]/5-amino-6-(5-phosphoribosylamino)uracil reductase [EC:1.1.1.193]; unknown enzyme (4), 5-amino-6-(5-phospho-D-ribitylamino)uracil phosphatase [EC:3.1.3.104]; RibH (6), 6,7-dimethyl-8-ribityllumazine synthase [EC:2.5.1.78]; RibE (7) riboflavin synthase [EC:2.5.1.9]; RibCF (8, 9), bifunctional riboflavin kinase [EC:2.7.1.26]/FAD synthetase [EC:2.7.7.2]; Based on Bacher et al., 2000; **(B)** Gene loci encoding for the riboflavin synthesis enzymes in *Bifidobacterium infantis* ATCC 15697. Arrow marks the promoter, lollipop marks the FMN riboswitch upstream the *rib* cluster and *ribU* gene.

Refseq[1] database and constituted the input for the comparative analysis. The occurrence and distribution of the riboflavin biosynthesis genes Blon_386–389 and Blon_2195 across *Bifidobacterium* was performed using BLASTP alignments (Altschul et al., 1990) against a database build from the open reading frames (ORFs) collection of each bifidobacterial species. Proteins homologous to any of the riboflavin-associated gene products from *B. infantis* across the *Bifidobacterium* genus were identified using cut-off values of 40% of similarity across 70% of protein length and an *e*-value of < 0.0001 for significance. The result of the alignments was represented as a heatmap using the "heatmaply" package implemented in the statistical software R[2] and using a two-way hierarchical clustering with a color gradient expressing the degree of sequence similarity across bifidobacterial species, which were also classified by the origin of isolation. A homologous cluster was defined as present across bifidobacterial genomes when the four genes constituting the *ribDEABH* cluster were found co-located within the same genomic region with an average similarity above 40% at protein level.

Prediction of the FMN riboswitch in *B. infantis* and *Bifidobacterium* was performed using Infernal tool v1.1.3 implemented in Bioconda environment[3] and the alignment of the FMN riboswitch was performed using Muscle

[1]ftp://ftp.ncbi.nlm.nih.gov/genomes/refseq/bacteria

[2]https://www.r-project.org/about.html

[3]https://github.com/bioconda

alignment tool v3.8.31 (Edgar, 2004) and visualized using https://alignmentviewer.org/.

Chemicals and Media

All chemicals were purchased from (Sigma-Aldrich, St. Louis MO, United States) unless otherwise stated.

Bifidobacteria were routinely cultured anaerobically in Lactobacilli de Man, Rogosa and Sharpe (MRS) Broth (BD Difco, Sparks, MD, United States) containing 0.5 g L^{-1} cysteine HCl.

Riboflavin production in pure *Bifidobacterium* cultures was tested in riboflavin-free semi-synthetic medium mSM7. Based on SM7 medium (Pompei et al., 2007a) with modifications, mSM7 is composed assembling three sterile solutions: (A) 10 × carbohydrate solution (sterilized by autoclaving at 121°C for 20 min); (B) 10 × vitamin solution (pyridoxine, 2 mg L^{-1}; nicotinic acid, 2 mg L^{-1}; thiamine, 2 mg L^{-1}; calcium pantothenate, 1 mg L^{-1}; p-aminobenzoic acid, 0.05 mg L^{-1}; biotin, 0.05 mg L^{-1}; ascorbic acid, 1 mg L^{-1}; adenine sulfate, 20 mg L^{-1}; xanthine, 40 mg L^{-1}; vitamin B_{12}, 0.7 mg L^{-1}; folate, 0.5 mg L^{-1}; sterilized by filtration); (C) 1.25 × basal solution (Difco™ Casamino Acids, vitamin assay BD, Franklin Lakes, NJ, United States), 10 g L^{-1}; sodium acetate, 10 g L^{-1}; $(NH_4)_2SO_4$, 5 g L^{-1}; urea, 2 g L^{-1}; $MgSO_4 \cdot 7\ H_2O$, 0.2 g L^{-1}; $FeSO_4 \cdot 7\ H_2O$, 0.01 g L^{-1}; $MnSO_4 \cdot 7\ H_2O$, 0.007 g L^{-1}; NaCl, 0.01 g L^{-1}; Tween 80, 1 g L^{-1}; cysteine, 0.5 g L^{-1}; autoclaved for 30 min at 110°C after adjusting the pH to 7.0. Batch fermentations were carried out in mSM7 supplemented with glucose, lactose, fructo-oligosaccharides (FOS) [P95, degree of polymerization (DP) 2–8, Beneo-Orafti, Mannheim, Germany], galacto-oligosaccharides (GOS, DP 3–9, Vivinal, FrieslandCampina, Amersfoort, Netherlands), xylooligosaccharides (XOS, DP 2–6, FrieslandCampina), or inulin (HP, DP > 23, Beneo-Orafti), to achieve the final concentration of 10 g L^{-1}.

Isolation of Roseoflavin-Resistant Mutants

The approach taken to isolate roseoflavin resistant mutants is summarized in **Supplementary Figure S1**. *B. infantis* ATCC 15697 was cultured overnight in 5 mL of mMRSlac [i.e., modified De Man et al. (1960) and Sharpe medium made from first principles and supplemented with 1% lactose instead of glucose]. Cells were collected by centrifugation (6,000 × *g* for 10 min), washed twice with 5 mL of sterile H_2O, and resuspended in 10 mL of mSM7lac (1% lactose). The culture was allowed to grow for 5 h under anaerobic conditions. Aliquots of 100 μL of cell suspension were spread onto agar plates of mSM7lac supplemented with 0, 25, or 50 μg mL^{-1} roseoflavin and incubated anaerobically at 37°C for 48 h. Following isolation of roseoflavin-resistant derivatives, the promoter and the 5'-UTR regions of the *rib* operon of a number of such derivatives were PCR amplified (using primers 5' TTCTCCGATACGGGCGATTG 3' and 5' TTCGTGGCATCGACCGACAG 3') and the obtained products were subjected to Sanger sequencing (Eurofins Genomics, Germany). The obtained sequences were aligned using Muscle (Edgar, 2004) and the alignment visualized using Alignmentviewer[4].

Cultivation Conditions

The wild-type (WT) of the type strain *B. infantis* ATCC 15697 and selected roseoflavin-resistant derivatives were subcultured in mSM7 supplemented with glucose (mSM7glucose) and were then incubated anaerobically at 37°C for 48 h. Growth and production of intracellular and extracellular riboflavin were assayed in liquid cultures of mSM7 supplemented with glucose, lactose, FOS, GOS, XOS, or inulin. Cultures were propagated three times in the same medium before measuring riboflavin concentration in the supernatants or in the cell extracts. Growth was determined by measuring the final optical density at 600 nm (OD_{600}).

Controlled-pH batch cultivation was carried out in triplicate in laboratory-scale bioreactors (500 mL Mini Bio, Applikon Biotechnology, Delft, the Netherlands) containing 0.3 L of mSM7 supplemented with lactose (mSM7lac). Bioreactor was inoculated (10% v/v) with exponential phase pre-cultures grown in the same medium. The culture was kept at 37°C under CO_2 atmosphere and stirred at 250 rpm. The pH was continuously measured (Mettler Toledo InPro 3030/325) and kept at 5.5, the optimal pH value for bifidobacteria (Amaretti et al., 2007), by automatic titration with 1 M NaOH. Samples were periodically collected for analysis of carbohydrates, fermentation products, and growth.

Carbohydrates and fermentation products were analyzed in the supernatants using an HPLC apparatus with refractive index detector (1200 System, Agilent Technologies, Waldbronn, Germany). Elution was carried out with 0.6 mL/min of 0.005 M H_2SO_4 through an ion exclusion column (Aminex HPX-87 H, Bio-Rad Laboratories, Inc., Hercules, CA, United States) maintained at 60°C.

Riboflavin Assay

Riboflavin concentration was assayed in cell extracts and culture supernatants. 50 mL of the culture was centrifuged at 9.000 × *g* for 10 min at 4°C. The supernatant was filtered through a 0.22 μm filter and frozen at -20°C. The biomass was washed with the same volume of 0.1 M Na-phosphate buffer pH 7.0. The pellet was resuspended in the buffer (1/10 of the initial volume of the culture), and the suspension was frozen at -20°C. The thawed biomass was passed through the One Shot Cell Disrupter (Constant Systems, Ltd., Daventry, United Kingdom) at 40 KPsi. The cell extract, obtained by centrifugation of the sample at 13.000 × *g*, 15 min, 4°C was maintained at -20°C.

Riboflavin concentration was quantified using a microbiological bioassay with *Lactobacillus casei* subsp. *rhamnosus* ATCC 7469 as test organism, based on Woodson et al. (1946). Growth of the test organism was measured in 5 mL of Riboflavin Assay Medium (BD, Flanklin Lakes, NJ, United States) supplemented with 5 mL of properly diluted sample and compared with a calibration curve in the range of 0–300 ng mL^{-1}, according to the protocol described by the medium manufacturer. Microbiological assay measurements were replicated at least six times.

[4]https://alignmentviewer.org

Real-Time Quantitative qRT-PCR

Differential expression of *rib* genes was confirmed by real-time quantitative RT-PCR (qRT-PCR). *B. longum* subsp. *infantis* ATCC 15697 (WT) and its spontaneous mutant ROS25 were grown in mSM7lac supplemented or not with 20 ng mL^{-1} riboflavin until mid-exponential growth phase (OD_{600nm} 0.45–0.7). Cells were harvested by centrifugation at 6.000 × *g* for 10 min at 4°C and the pellet was immediately frozen at -80°C. For RNA isolation, cells were resuspended in 0.5 mL of TE buffer (10 mM Tris-HCl, 1 mM EDTA, pH 8.0), transferred to a 2 mL screw cap tube. 0.5 g of glass beads (∼100 μm in diameter), 50 μL of 10 % sodium dodecyl sulfate (SDS; Sigma-Aldrich, Saint Louis, MO, United States), and 500 μL of premixed phenol:chloroform:isoamyl alcohol (25:24:1) were added to the thawed cells in the screw cap tube. Cells were disrupted using three cycles of 60 s of bead-beating with a 1 min interval on ice. The cell lysate was cleared by 10 min centrifugation at 10.000 × *g*, at 4°C. The upper phase was extracted with 500 μL of chloroform:isoamyl alcohol (24:1). The two phases were separated by centrifugation (10 min, 10.000 × *g*, 4°C) and total RNA was isolated from the aqueous phase using the High Pure RNA Isolation Kit (Roche Molecular Systems, Inc., Pleasanton, CA, United States), according to the manufacturer's instructions. Total RNA was treated with DNase I RNAse-free (Roche Molecular Systems, Inc.) according to manufacturer's instructions. cDNA synthesis was performed using total RNA as a template and Transcriptor Reverse Transcription Kit (Roche Molecular Systems, Inc.) according to manufacturer's instructions. qRT-PCR experiments were carried out using SYBR Green MasterMix (Thermo Fisher Scientific, Waltham, MA, United States) using cDNA samples as a template. Primers to amplify *ribD* and two housekeeping genes were designed using the Universal ProbeLibrary Assay Design Center (Roche Molecular Systems, Inc.). The *groEL* and *gyrA* genes were used as housekeeping genes with a presumed constitutive level of transcription to correct for variability in the initial amount of total RNA. All qRT-PCRs were performed in triplicate by means of a LightCycler 480 system (Roche Molecular Systems, Inc.) instrument using 384-well plates. Thermal cycling conditions were as recommended by the manufacturer (Roche Molecular Systems, Inc.). The $2^{-\Delta\Delta CT}$ method was used to calculate relative changes in gene transcription determined from qRT-PCR experiments. Relative transcription levels of targeted genes from WT and ROS25 were compared using the Student's *t*-test and were considered significantly upregulated when a *p*-value of < 0.05 was obtained.

RNA Isolation and Sequencing

B. longum subsp. *infantis* ATCC 15697 (WT) and its spontaneous mutant ROS25 were grown in mSM7lac until mid-exponential growth phase (OD_{600nm} of 0.7, to obtain a sufficient RNA yield) for RNA-seq experiments performed in duplicate. Cells were then harvested by centrifugation and the obtained pellets were frozen and stored at -80°C. For RNA extraction, total RNA of each of the cultures was mixed with 800 μl of QIAzoL Lysis Reagent (Qiagen, Venlo, Netherlands) in a sterile tube containing glass beads (Merck, Darmstadt, Germany). Cells were lysed by alternating 2 min of stirring the Precellys 24 homogenizer (Bertin instruments, Montigny-le-Bretonneux, France) with 2 min of static cooling; this step was repeated three times. The sample was centrifuged at 12,000 × *g* for 15 min and the upper phase was recovered. The RNA was purified using the RNAesy Mini Kit (Qiagen), following the manufacturer's protocol. RNA concentration and purity were evaluated by a Picodrop microliter spectrophotometer (Victory Scientific, Cambridge, United Kingdom). Before RNA sequencing, 2.5 μg of total RNA was treated to remove the ribosomal RNA by the Ribo-Zero Magnetic Kit (Illumina, Inc., San Diego, CA, United States), followed by purification of the rRNA-depleted sample by ethanol precipitation. RNA was processed according to the manufacturer's protocol. The yield of rRNA depletion was confirmed by a Tape station 2200 (Agilent Technologies, Santa Clara, CA, United States). A whole transcriptome library was constructed using the TruSeq Stranded RNA LT Kit (Illumina, Inc.) and samples were loaded into a NextSeq High Output v2 Kit Chemicals 150 cycles (Illumina), according to the technical support guidelines.

RNA-Seq Analysis

Following sequencing, the reads were depleted of adapters, quality filtered (with overall quality, quality window and length filters) and aligned to the *B. infantis* ATCC 15697 reference genome (genomic features model GTF file[5]) through bowtie2 aligner[6]. The alignment SAM files were further processed using Samtools to obtain BAM files necessary to obtain matrices with read counts per gene (normalized by gene length). Differential gene expression (DGE) analysis was performed using the R statistical platform and the DESeq2 package available as part of the Bioconductor release (v.3.9). As a pre-processing step, rows with zero counts (unmapped genes) were discarded from the count matrices. Differential expression analysis was performed on the count matrices using the DESeq function in DESeq2. Genes with an FDR-adjusted *p*-value of < 0.05 and a log2-fold change of > 3 were considered significantly upregulated.

Determination of β-Galactosidase Activity and Protein Concentration in the Supernatant

β-galactosidase activity and total protein concentration were determined in the supernatant of ROS25 and WT cultures grown for 6 h in mSM7lac, obtained from three independent experiments. β-galactosidase activity assay was performed with *o*-nitrophenyl-β-D-galactopyranoside (*o*NPG). The pH of the supernatant was corrected to 7.0 with a NaOH 3 M solution. One mL of the sample was incubated at 37°C for 3 min after the addition of 0.2 mL of 4 mg mL^{-1} *o*NPG. The reaction was

[5]https://bacteria.ensembl.org

[6]http://bowtie-bio.sourceforge.net/bowtie2/index.shtml

stopped by adding 0.5 mL of 1 M Na_2CO_3. The absorbance of the sample was read at 420 nm. One unit of β-galactosidase was defined as the amount of enzyme required to release 1 μmol of nitrophenol per minute under the assay conditions. The activity was normalized to the OD_{600} units of the culture.

To quantify protein levels in the supernatant, the culture was centrifuged at 9,000 × *g* for 10 min at 4°C. The volume of supernatant corresponding to two units of OD_{600} of the culture was transferred to a 2 mL tube and was mixed with the same volume of 20% (w/v) trichloroacetic acid. The sample was vortexed, incubated for 1 h in ice, then centrifuged at 13,000 × *g* for 10 min at 0°C. The pellet was washed with 300 μl cold acetone. After gently mixing of the suspension by inversion, the sample was centrifuged at 13,000 × *g* for 10 min at 0°C, and the pellet was allowed to dry for 30 min at room temperature. The sample was resuspended in 20 μl of Laemmli Loading buffer (Bio-Rad Laboratories, Inc., Hercules, CA, United States) and supplemented of 2 μl NaOH 1 M. Proteins were separated by SDS-PAGE using a 5% stacking and 10% resolving gels. Coomassie brilliant blue-stained gels were scanned in transmissive mode using a white light source with the GS-800 Calibrated Densitometer (Bio-Rad Laboratories, Inc.). Taking into account that the proteins of each run derived from the same amount of biomass, the total protein levels of the supernatants were presented as percentage of the highest value obtained in the data set. In the permeability assays, means of WT and ROS25 were compared with Student's *t*-test and were considered significantly different when a *p*-value of < 0.05 was obtained.

Fecal Cultures

Fresh fecal samples were obtained from 10 healthy volunteers (five men and five women, aged 25–50 years), who had provided written informed consent according to the experimental protocol with ref. no. 968/2019/SPER/UNIMO-RIBOBIF and approved by the local research ethics committee (Comitato Etico dell'Area Vasta Emilia Nord, Italy). Feces were homogenized with 3 mm sterile borosilicate glass beads in mSM7 medium supplemented with 10 % GOS (mSM7GOS), in an anaerobic cabinet (Concept Plus, Ruskinn Technology, Ltd., Bridgend, United Kingdom), under an 85% N_2, 10% CO_2, and 5% H_2 atmosphere. Analysis of riboflavin content in feces was carried out on dilutions of the fresh 10 % slurry.

Two sets of fermentation experiments were run in parallel: (A) fecal cultures inoculated with the fecal slurry pasteurized for 10 min at 80°C; (B) fecal cultures inoculated with a viable microbiota. Fifty mL of mSM7GOS were supplemented with 5 mL of 10% fecal slurry (pasteurized or not) and with 2.5 mL of ROS25 or WT suspension (2.5 mL of mSM7GOS in the control). The inocula of ROS25 and WT were prepared by centrifuging a 24 h culture in mSM7GOS at 6,000 × *g* for 10 min at 4°C, and resuspending the pellet in 1/10 of the volume of the same medium. Riboflavin content was analyzed after inoculation, and after 16 and 24 h of incubation at 37°C in anaerobic conditions. Two-way analysis of variance (ANOVA), followed by Tukey's *post hoc* test, was used to evaluate differences between carbon sources and strains (WT and ROS25) in pure culture experiments and between time points and groups (control, WT, an ROS25) in fecal cultures. Differences were considered significant when a *p*-value of < 0.05 was obtained.

RESULTS

Identification of Riboflavin Biosynthesis Genes in *Bifidobacterium* Genomes

The riboflavin and FMN/FAD biosynthetic pathway was reconstructed in annotated *Bifidobacterium* genomes available in the Kyoto Encyclopedia of Genes and Genomes (KEGG) database. All genes necessary for *de novo* riboflavin biosynthesis were found in the genome of *B. infantis* ATCC 15697 (**Figure 1B**), as previously reported by Kwak et al. (2016). The set of genes includes a complete *rib* operon (*ribD*, *ribE*, *ribAB,* and *ribH* homologues, corresponding to locus tags Blon_0386 to Blon_0389) encoding the enzymes for riboflavin biosynthesis from GTP and ribulose-5-phosphate, and an unconnected *ribCF* (Blon_2195) homologue encoding a bifunctional riboflavin kinase/FMN adenylyltransferase, responsible for the conversion of riboflavin into FMN and FAD (**Figures 1A,B**). The genome also harbors a *ribU* homologue (Blon_0723), predicted to encode a transporter for the uptake of pre-formed riboflavin located at a genomic position that is unconnected to that of the *rib* operon or *ribCF* (**Figure 1B**).

The protein sequences deduced from the *rib* genes of *B. infantis* ATCC 15697 were utilized as query in a search aimed at identifying homologues in an ORF dataset that was extracted from 662 genomes, being representative of 83 bifidobacterial (sub)species. Our combined BLASTP and MCL clustering analysis revealed that *de novo* riboflavin biosynthesis appears to be a rather uncommon feature among members of the genus *Bifidobacterium*, since homologues of the complete *rib* operon were identified in just 16 out of 83 bifidobacterial species, most of which (14 out of 16) had been isolated from primates (**Figure 2A**). In contrast, homologues of *ribCF* and *ribU* are conserved across all members of the genus, occurring as single copy genes in all investigated species (**Figure 2A**). This indicates a general ability of bifidobacteria to rely on the provision of pre-formed, extracellular vitamin B_2 to ensure a constant FAD/FMN supply. Notably, homologues of the *ribCF* and *ribU* genes from *B. infantis* have been identified as essential genes in *Bifidobacterium breve* UCC2003 using a combination of Tn5 transposon library and TraDIS sequencing (Ruiz et al., 2017), supporting their crucial involvement in specific housekeeping functions in the *Bifidobacterium* genus. Inspection of the phylogenetic trend of the two housekeeping genes *rpoB* and *groEL*, and that of the riboflavin-associated genes *ribCF* and *ribU* substantiated that the latter had followed the same evolutionary course of other housekeeping functions of this genus, indicating that the uptake and utilization/conversion of riboflavin represents a core feature of *Bifidobacterium* that had already been incorporated in the genomes of its ancestors (**Figure 2B**). In support of this notion, homologues of the *ribCF* gene harbored by bifidobacterial species isolated from insects presented the lowest similarity compared to species from other

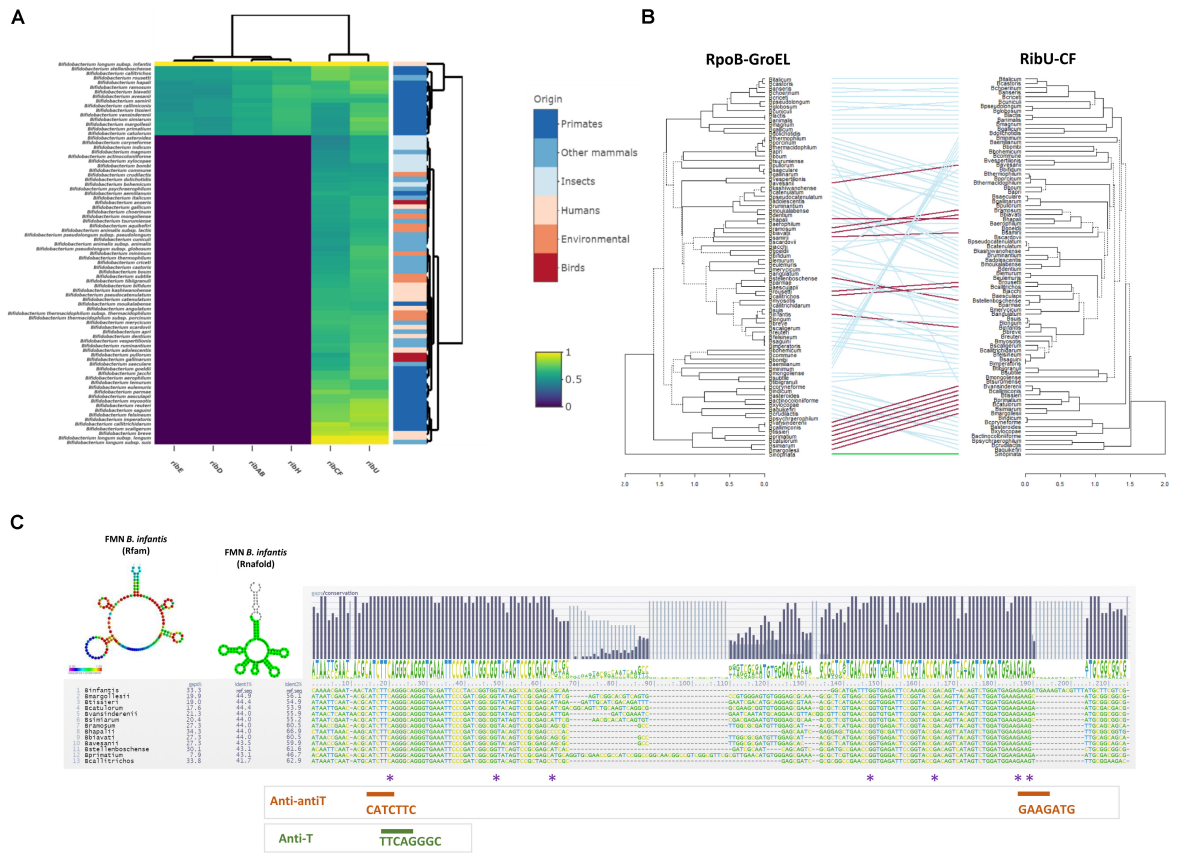

FIGURE 2 | Comparative analysis of riboflavin biosynthesis in *Bifidobacterium*. **(A)** Comparative heatmap representing the distribution of riboflavin-associated genes from *Bifidobacterium infantis* ATCC 15697 across the *Bifidobacterium* genus. Color gradients indicate the percentage of identity in BLASTP alignments of open reading frames (ORFs) derived from bifidobacterial genomes grouped by origin of isolation; **(B)** Entanglement trees obtained from the concatenation of *rpoB, groEL* vs. *ribU, ribCF* genes across the genus *Bifidobacterium*. The two Neighbor Joining (NJ) trees were built using the MEGA package (statistical validation of 100 bootstrap replicates) and visualized using the "Dendextend" package in R v3.6.2. Connecting lines are color coded based on the presence (red) or absence (blue) of a *rib* cluster. The outgroup is indicated in green. **(C)** Sequence alignment of FMN region in *B. infantis* and 13 bifidobacterial strains containing a complete *rib* cluster. Sequence conservation is indicated with a logo for the consensus. Colored asterisks indicate mutations in FMN riboswitch region upstream of the *rib* cluster identified in ROS-resistant isolates. Prediction of the FMN folding was based on Rfam aligment (bases color-coded based on sequence conservation to the Rfam model RF00050) and was predicted by Rnafold. The obtained structures were obtained using the Infernal and Rnafold predictions in https://structrnafinder.integrativebioinformatics.me/ (Arias-Carrasco et al., 2018).

ecological niches (40–50% of identity across 70% of sequence length; **Figure 2A**). As bifidobacterial isolates from insects have been identified as being most related to the ancestor of the genus *Bifidobacterium* (Milani et al., 2014), the ability to synthesize riboflavin seems a genetic feature that was not originally present in this genus. Instead, this property must have been more recently acquired by certain bifidobacterial species, likely in an ecological context of riboflavin deficiency.

A PSI-BLAST analysis against the *nr* database was performed using the amino acid sequence of the riboflavin synthase (RibE) as a query. Approximately 90 different taxa encoding RibE above 50% identity (across 100% of sequence length) were identified. Phylogenetic inference revealed that the *rib* clusters found in the 15 non-human associated bifidobacteria (**Figure 2A**) are related and form a separate clade when compared to the *rib* cluster present in *B. infantis* (**Supplementary Figure S2**). Phylogenetic relationship analysis suggests that *B. infantis* acquired and retained, or lost the primate-associated *rib* cluster and then reacquired a *rib* cluster via a separate horizontal transfer event (**Supplementary Figure S2**), perhaps facilitated by another intestinal bacterium, which could have been either a gut commensal or pathogen such as *Streptococcus* or *Clostridium*.

In order to verify our findings and test the functionality of the *rib* cluster we focused on the human-gut commensal *B. longum* subsp. *infantis* ATCC 15697, which was predicted to encode the complete *de novo* riboflavin biosynthesis pathway.

FMN Riboswitch Comparison Across *Bifidobacterium*

To investigate the presence and sequence conservation of the FMN riboswitch, a sequence of 500 bp in the 5'-UTR upstream of *ribD* was extracted from the *Bifidobacterium* spp. genomes bearing the complete *rib* operon. The structural elements responsible for the presumed FMN riboswitch, comprised of

the antiterminator (AntiT, 5' -TTCAGGGC-3') which promotes *rib* transcription and two anti-antiterminators (Anti-antiT: 5'-CATCTTC-3' and 5'-GAAGATG-3') which pair in the presence of FMN/FAD and cause premature transcriptional termination (Winkler et al., 2002), were detected in all 5'-UTRs. Aligning the FMN riboswitch sequences of various bifidobacteria revealed that Anti-T and Anti-antiT are located in a conserved region (**Figure 2C**), suggesting that the FMN riboswitch is functional and regulates *rib* operon transcription. An FMN riboswitch was also identified in the 5'-untranslated region (5'-UTR) of the *ribU* uptake system, indicating that riboflavin synthesis and uptake are both controlled by the level of flavin cofactors and vitamin in the environment.

Riboflavin Production in *B. longum* subsp. *infantis* ATCC 15697 and Characterization of Roseoflavin-Resistant Mutants

To verify the predicted ability of *B. infantis* ATCC 15697 to produce riboflavin, it was cultured in a semi-synthetic medium lacking riboflavin (mSM7lac), allowing growth only if the *de novo* biosynthetic pathway for this vitamin was functional. The strain grew abundantly (final OD_{600nm} = 3.0) and produced the vitamin, albeit at a low level (less than 0.2 ng mL^{-1} in a cell extract after 48 h of incubation), without any detectable release of riboflavin in the medium.

To obtain spontaneous mutants with improved riboflavin production, *B. infantis* ATCC 15697 was exposed to 25 and 50 μg mL^{-1} roseoflavin on mSM7lac plates. Roseoflavin-resistant colonies were obtained at a similar mutational frequency (3.4×10^{-7}) with either of the two concentrations of this antimetabolite. A selection of seven roseoflavin-resistant isolates, hereinafter identified with a ROS designation (**Table 1**), was assayed for vitamin B_2 production. All ROS mutants exhibited an increased riboflavin production level of at least one magnitude when compared with the WT. The concentration of vitamin released in the supernatant by the mutants ranged from 2.5 to 35 ng mL^{-1} (**Table 1**).

The promoter and the 5'UTR regions of the *rib* operons of the seven assessed ROS mutants were sequenced, to identify the mutations likely responsible for the increase in riboflavin production. The mutants all harbored single point mutations at distinct positions of the putative FMN riboswitch (**Figure 2C** and **Table 1**). The identified point mutations were either G → A or C → T transitions. Three mutants acquired mutations in one of the two anti-antiterminator regions (**Figure 2C** and **Table 1**). The highest riboflavin production was observed in mutant ROS25, which was shown to carry a G → A transition in the anti-antiterminator region of the riboswitch (**Table 1**).

TABLE 1 | Mutations identified in flavin mononucleotide (FMN) riboswitch of roseoflavin-resistant mutants and extracellular riboflavin.

Mutant	Position in FMN Riboswitch	Base Wild-Type (WT)	Base mutant	Riboflavin concentration (ng mL^{-1})
ROS20	6	C	T	18
ROS21	41	C	T	2.5
ROS22	31	G	A	6.5
ROS23	102	G	A	16
ROS25	105	G	A	35
ROS26	81	G	A	4.5
ROS29	64	G	A	8
WT	–	–	–	< 0.2

Average values are shown (n = 3).

Riboswitch Disruption and Global Gene Expression Changes in Spontaneous Mutant ROS25

In order to assess the effect of the point mutation in the FMN riboswitch region of ROS25, the transcription level of *ribD* (i.e., the first gene of the *rib* operon) was compared between the WT and strain ROS25 during the mid-exponential growth phase in mSM7lac (**Figure 3**). When riboflavin was not available in the medium, transcription of *ribD* was 15-fold higher in ROS25 than in WT (p-value < 0.05). Addition of 20 ng mL^{-1} riboflavin to the culture resulted in reduced *ribD* transcription in WT (p-value < 0.05), but did not exert a feedback repressive effect in ROS25, where the response of the riboswitch was lost and the *rib* operon was shown to be constitutively expressed.

To assess the global transcriptional effect of the mutation in the riboswitch that caused riboflavin overproduction in ROS25, an RNA-seq experiment was performed on WT and ROS25 cultures growing in mSM7lac without riboflavin supplementation (**Supplementary Table S1**). The genes of the *rib* cluster were the most differentially expressed between WT and ROS25. Transcription levels of this cluster in ROS25 were 18-fold

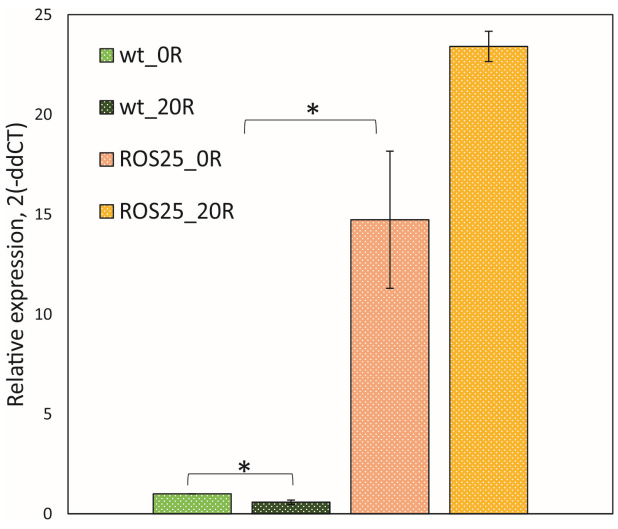

FIGURE 3 | Roseoflavin-resistant isolates. Relative expression of *ribD* in wild-type (WT) and ROS25 cells grown to the mid-exponential growth phase in mSM7lac with 0 or 20 ng mL^{-1} riboflavin measured by qRT-PCR. *indicate statistically significant differences between ROS25 and WT samples (p-value < 0.05).

higher than its counterpart in WT. Furthermore, various ABC transporters and sugar permeases were highly expressed in ROS25, suggesting a more active sugar metabolism in the mutant than in WT. Genes encoding glycosyltransferases involved in cell wall metabolism and extracellular polysaccharide biosynthesis were also upregulated in ROS25 (**Supplementary Table S1**). Besides the point mutation in the FMN riboswitch, additional genetic changes may be present in the genome of ROS25, which may explain the above transcriptional differences. Transcription of *ribC* was similar in both strains, while the genes encoding FAD-dependent proteins appear to be downregulated in ROS25 (p-value < 0.05; **Supplementary Table S1**).

Effect of Carbon Sources on Riboflavin Production

To assess the effect of different carbon sources on riboflavin production, the intracellular and extracellular production of the vitamin was determined in batch cultures of WT and ROS25 grown in mSM7 containing glucose, lactose, raffinose, GOS, XOS, FOS or inulin as the sole carbon source. Both WT and ROS25 grew well with all the carbon sources except XOS (**Figure 4**). The growth yield was similar with glucose, lactose, raffinose, FOS, and GOS ($P > 0.05$), but lower with inulin (p-value < 0.05). Notably, the lowest biomass yield was obtained on inulin, presumably due to the presence of long chains that are not

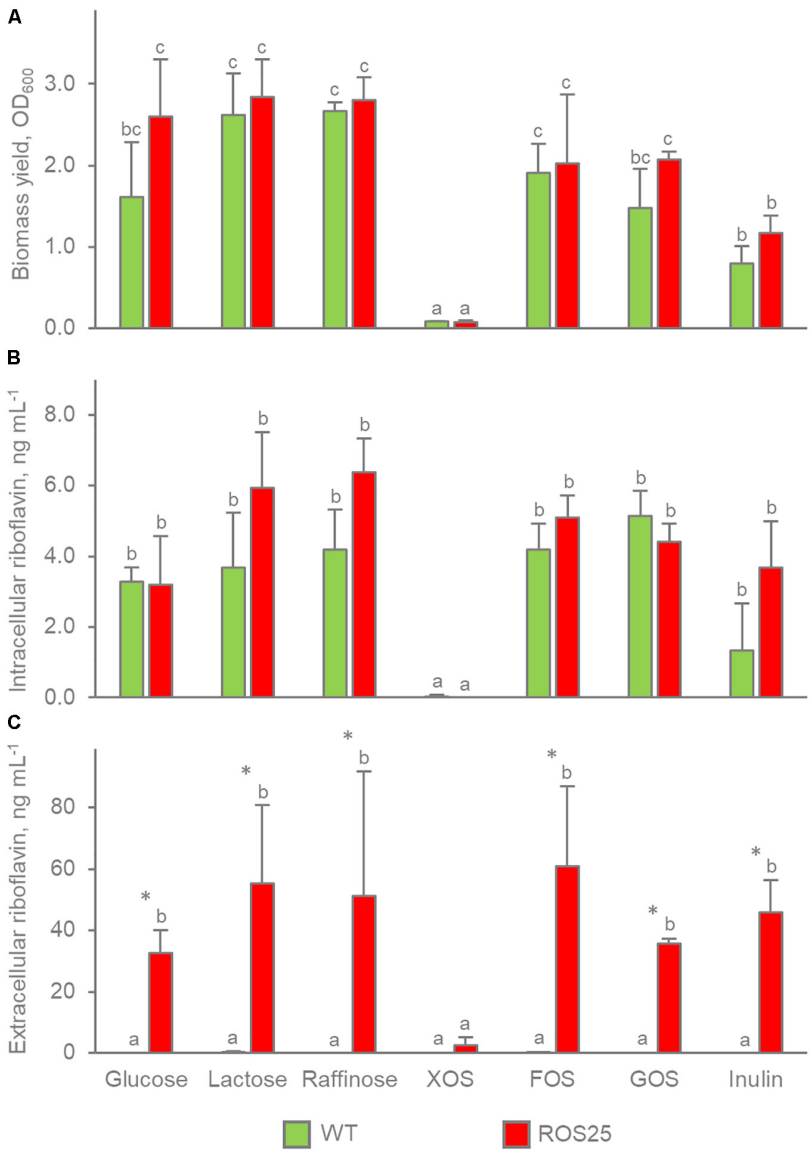

FIGURE 4 | Growth yield (OD_{600nm}) and riboflavin production in batch cultures of ROS25 and wild-type (WT) grown in mSM7 media containing varying carbohydrate sources (1%). **(A)** OD_{600nm}; **(B)** intracellular riboflavin ng mL^{-1} of culture; **(C)** extracellular riboflavin ng mL^{-1} of supernatant. Values are means ± SD, $n = 3$. * indicates statistically significant differences between ROS25 and WT samples ($P < 0.05$); lowercase letters indicate statistical significant differences for the same strains on the diverse carbon sources between (p-value < 0.05).

metabolized by *B. longum* subsp. *infantis*, as reported previously (Kim et al., 2013).

Except for XOS, where poor growth resulted in negligible amounts of vitamin B_2 production, the carbon source did not affect the concentration of riboflavin accumulated within the cells or released in the supernatant by both WT and ROS25 cultures (p-value > 0.05). WT and ROS25 presented a similar concentration of intracellular riboflavin regardless of the carbon source (p-value > 0.05). In contrast, the difference between WT and ROS25 was significant with respect to the concentration of vitamin released in the medium (p-value < 0.05). The supernatants obtained from WT cultures typically contained < 0.2 ng mL^{-1} riboflavin, while those corresponding to ROS25 reached up to 60.8 ng mL^{-1} for a culture grown on FOS as the carbon source.

Riboflavin Production and Release by ROS25

The kinetics of growth and associated riboflavin production was studied during pH-controlled batch fermentations of ROS25 in mSM7lac (**Figure 5**). Following a short lag phase, the culture rapidly grew and entered the stationary phase after 15 h, when lactose and the monosaccharides generated by its hydrolysis got exhausted. Accumulation of acetic and lactic acids originating from carbohydrate fermentation was observed concomitant with growth (**Figure 5**), while riboflavin was released in the medium throughout growth as well, reaching the highest concentration (65.3 μg L^{-1}) when the culture entered into the stationary phase, then slightly declined. The highest rate of vitamin production (13.9 ng mL^{-1} h^{-1}) was observed after 6 h of growth when the specific growth rate was also at its highest level (0.31 h^{-1}).

The extracellular concentrations of riboflavin, β-galactosidase, and total protein content were compared with those obtained for WT in order to assess if riboflavin was released in the supernatant by ROS25 due to cell lysis. After 6 h of growth in mSM7lac, WT and ROS25 cultures presented the same turbidity, but the latter had a significantly higher level of extracellular riboflavin, β-galactosidase, and total protein content (**Figure 6**). These data indicate higher cell wall permeability or partial lysis of ROS25 compared to a similarly grown WT.

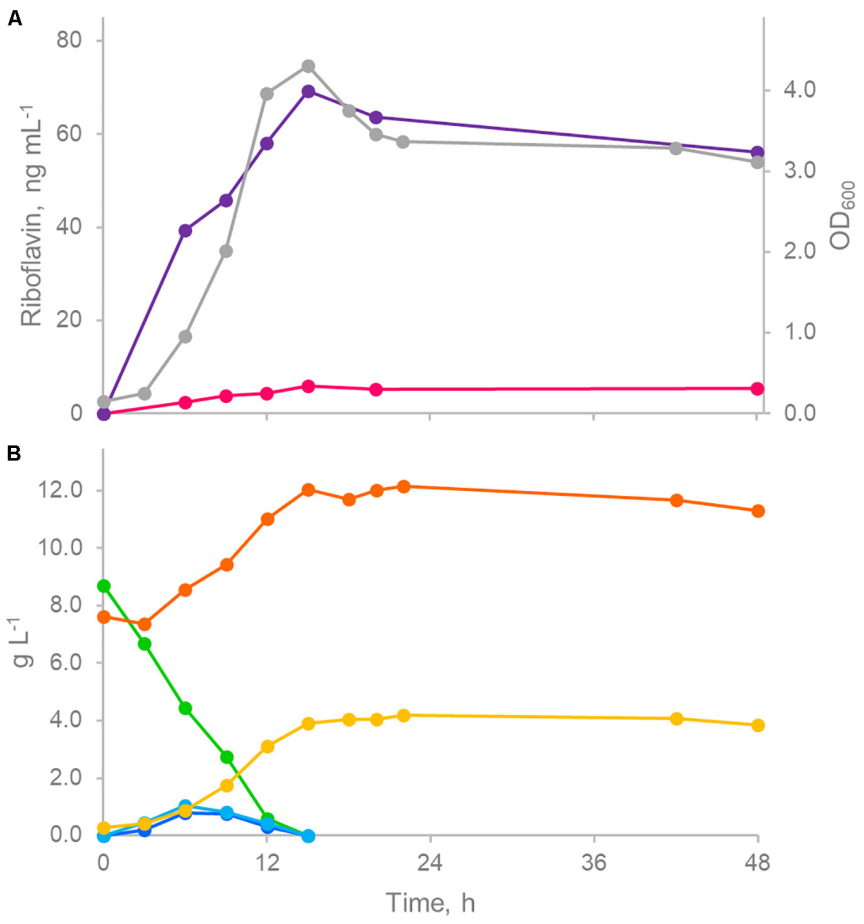

FIGURE 5 | Controlled pH batch fermentation of ROS25 in mSM7lac. **(A)** Time course of biomass (gray) and riboflavin production (intracellular, fuchsia; extracellular, purple). **(B)** Time course of sugars (lactose, green; galactose, light blue; glucose, blue) and fermentation products (acetic acid, orange; lactic acid, green). The figure represents one representative experiment of the triplicate.

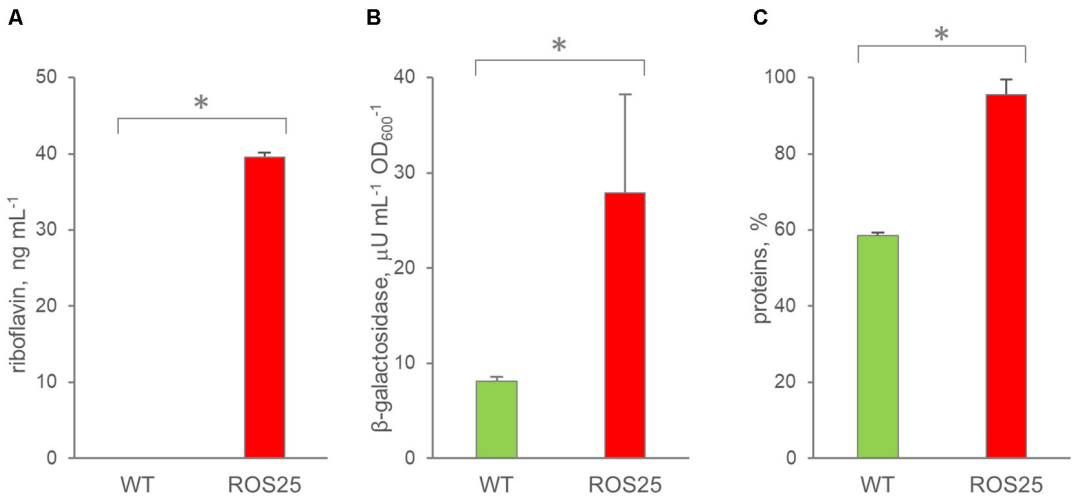

FIGURE 6 | Permeability of wild-type (WT) and ROS25 cultures grown for 6 h in mSM7lac. Dosage of **(A)** extracellular riboflavin; **(B)** β-galactosidase, **(C)** proteins in the supernatant. Values are means ± SD, $n = 3$. * indicates statistically significant differences between ROS25 and WT samples (p-value < 0.05).

Production of Riboflavin in Fecal Cultures Supplemented With WT and ROS25

To assess whether consumption of ROS25 as probiotic would result in *in situ* riboflavin production which could benefit the host, the mutant was employed in fecal fermentations. Fresh feces of 10 healthy adults presented a riboflavin concentration ranging between 80.7 and 728.2 ng g^{-1}, with a mean of 298.4 and a median of 251.5 ng g^{-1} (**Supplementary Figure S3**). The six samples with the lowest concentration were selected to prepare fecal cultures and inoculated (1:100 w/v) in mSM7GOS medium. Changes in riboflavin concentration were determined following inoculation with 10^6 cfu mL^{-1} of ROS25, when compared to inoculation of the same level of WT and to control cultures that were not supplemented with bifidobacteria. To discriminate between riboflavin originating from the bifidobacterial supplement and that from other fecal bacteria, a parallel set of fermentations was carried out, where the fecal inoculum was heat treated prior to bifidobacterial inoculation.

With each fecal sample, heat treatment of feces and subsequent supplementation with ROS25 yielded the biggest change in riboflavin concentration after 16 or 24 h of incubation (**Figure 7B**), with a mean value of 61.2 ng mL^{-1}. Under the same conditions, the cultures inoculated with WT yielded a mean of 7.9 ng mL^{-1}, significantly lower than ROS25 and similar to the control.

All cultures inoculated with viable fecal bacteria accumulated riboflavin during the first 16 h of the process (p-value < 0.05), irrespective of bifidobacterial supplementation. This indicated that other members of microbiota are producing riboflavin as well. Following 16 and 24 h of incubation, riboflavin concentration was the highest in the cultures supplemented with ROS25 and the lowest in those supplemented with WT (p-value < 0.05). Nonetheless, values were widely dispersed within groups, thus the difference between ROS25, WT and the control groups was not significant.

DISCUSSION

Bifidobacteria are widely used as probiotics for their recognized health benefits and the ability to synthesize important biomolecules, e.g., vitamins, exopolysaccharides, short-chain fatty acids, etc. (Bottacini et al., 2017). The *de novo* synthesis of riboflavin represents a relatively uncommon feature in bifidobacterial genomes, being mainly found in representative species isolated from primates and just in one human gut commensal, *B. infantis*. Presumably, riboflavin synthesis is not crucial for survival of auxotrophic bifidobacterial species as other members of gut microbiota release this vitamin (Sharma et al., 2019). Even if the host diet does not supply a sufficient amount of riboflavin for every member of the gut microbiome, vitamin sharing allows successful colonization of the gut by bifidobacteria. For this reason, riboflavin overproducers holding probiotic attributes could be potential candidates for *in situ* production of the vitamin, once these strains reach the host intestine (Arena et al., 2014). Considering the extensive application of bifidobacteria in the food and pharmaceutical fields, coupled with consumer demand for healthier foods, the use of food-grade microorganisms as *in situ* vitamin delivery systems represents an attractive alternative to food fortification (LeBlanc et al., 2013, 2020; Steinert et al., 2016).

In the current study we performed an extensive comparative genome analysis of members of the genus *Bifidobacterium*, which allowed the identification of the genes required for uptake and metabolism of riboflavin (*ribU* and *ribCF*), both of which represent housekeeping and essential gene functions. A *de novo* biosynthetic pathway of this vitamin was previously predicted to be present in *B. infantis*, however, our comparative study identified for the first time a complete *rib* cluster

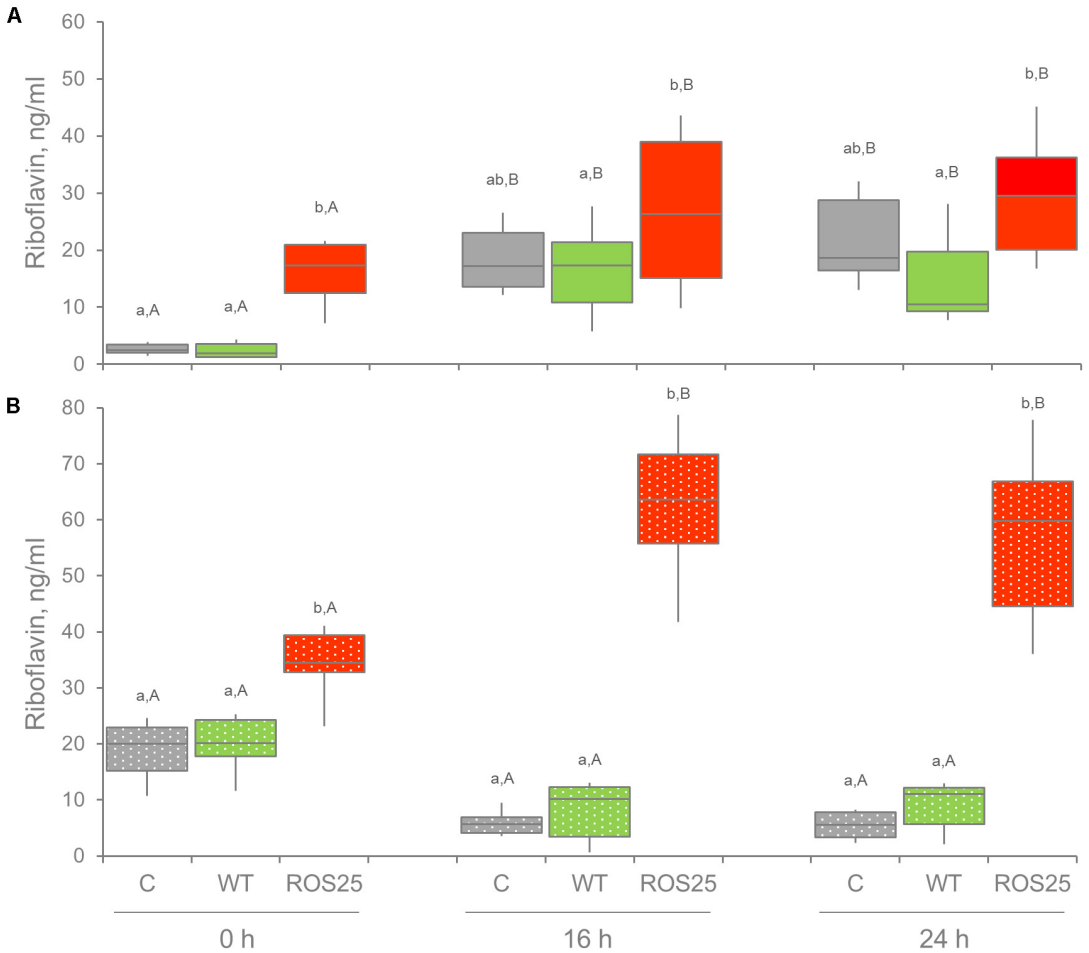

FIGURE 7 | Extracellular riboflavin in fecal cultures. Riboflavin concentration was determined in the supernatant of fecal cultures at 0, 16, and 24 h of incubation in the absence of supplements (C) and in presence of riboflavin producing bifidobacteria [wild-type (WT) and ROS25]. **(A)** Fecal cultures with alive microbiota; **(B)** fecal cultures with pasteurized gut microbiota. Lower letters indicate statistically significant differences at the same time point among C, WT, and ROS25 cultures (p-value < 0.05); upper case letters indicate statistically significant differences for the same culture at various time points (p-value < 0.05).

(*ribDEABH*) in several bifidobacterial representative taxa, among which *B. infantis* is the only human commensal, thus making this species particularly relevant for the development of probiotic riboflavin overproducers. Our comparative genomics and phylogenomic analysis suggests that the acquisition of the *rib* cluster by *B. infantis* was the result of a horizontal transfer event, which is different from that observed in other non-human residential bifidobacteria, and likely originating from *Streptococcus* or *Clostridium*.

It is worth mentioning that *B. infantis* represents an unusual bifidobacterial strain with a "selfish" strategy of gut colonization characterized by efficient consumption of available carbohydrates (e.g., Human Milk Oligosaccharides structures or HMOs), thus making the saccharolytic metabolism of this species particularly demanding in terms of redox cofactors (e.g., FAD). For this reason, the acquisition of the *rib* cluster by *B. infantis* may have represented an important additional supply of riboflavin and FAD in support of its metabolism and strategy of gut colonization. *B. infantis* was specifically isolated from an infant gut, thus riboflavin synthesis could be a specific adaptation to the infant gut or diet (Sela et al., 2008).

The toxic riboflavin analog roseoflavin was used to isolate spontaneous roseoflavin-resistant mutants that upon further analysis exhibit riboflavin overexpression. All mutations that had occurred in the *rib* operon promoter were mapped in conserved regions of the predicted FMN riboswitch sequence located in the promoter region of the riboflavin biosynthesis cluster. Analysis of the spontaneous mutant ROS25, which was to shown to exhibit the highest production of riboflavin among the assessed mutants, indicated that a G → A transition in the anti-antiterminator region had caused deregulation of the FMN riboswitch. As a result of this deregulation, the riboflavin biosynthesis became constitutive in *B. infantis* ROS25, with an excess of this vitamin diffusing into the growth medium. Curiously, no deletions or insertions were found in the FMN riboswitch region, which is in contrast to observations made for *L. lactis* and *L. plantarum* (Burgess et al., 2004; Ge et al., 2020). Transitions are the most frequent

type of point mutations occurring in bacteria, being induced by spontaneous tautomeric shifts (i.e., transient changes to an alternative form of a nucleobase molecule) which lead to base mispairing during replication (Griffiths et al., 2000). Apparently, high riboflavin production does not pose a constricting metabolic burden on a cell when grown under favorable laboratory conditions.

Despite the fact that superior analytical methods can be employed to provide a more reliable riboflavin quantification (e.g., HPLC and fluorescence; Mohedano et al., 2019), our screenings based on an established microbiological assay clearly demonstrate riboflavin overproduction in ROS25 and other obtained roseoflavin-resistant derivatives when compared to the WT strain ATCC 15697).

The mechanism by which riboflavin was released by ROS25 remains unclear. Comparison of permeability of exponential-growth cultures of WT and ROS25 indicated a more permeable cell envelope in ROS25 when compared to WT that, however, did not affect biomass yields and robustness of the culture. The mechanism underlying augmented permeability deserves deeper investigation, as it was not evident from RNAseq analysis.

Even though fecal cultures are artifacts that do not reflect the *in vivo* situation, where many factors affect the balance between vitamin production and consumption, including absorption by the host, the vitamin overproducing derivative ROS25 increased riboflavin level in both pasteurized and unpasteurized fecal cultures. Thus, this strain deserves to be challenged in a study *in vivo*, to find whether it can be successfully utilized as a probiotic vitamin "factory" improving the vitamin status of the host. Since no genetic engineering techniques were used to modify this strain, ROS25 and similar strains could be readily used to replace the standard probiotic strain in food formulations and would supply their host with the required vitamin intake. According to our results, the strain increased riboflavin level in both pasteurized and unpasteurized fecal cultures. Sharing of B-group vitamins has been suggested to promote stability in gut microbial communities (Sharma et al., 2019).

Besides the direct benefit to the host, such riboflavin production in the gut could help to stabilize bifidobacterial species that are auxotrophic for this vitamin. In fact, recent studies have explored the possibility of using vitamins (e.g., riboflavin, niacin) as prebiotics in order to stimulate a selected population of beneficial gut microbiota (Steinert et al., 2016; Fangmann et al., 2018).

DATA AVAILABILITY STATEMENT

The datasets presented in this study can be found in online repositories. The names of the repository/repositories and accession number(s) can be found in the article/**Supplementary Material**. RNA sequencing raw data are available from the Sequence Read Archive (SRA) database under the SRA accession PRJNA639329.

AUTHOR CONTRIBUTIONS

FB and DvS conceived the study. FB, AS, AA, SR, and MR designed the experiments. EE, AS, AA, and SR carried out the experiments. FB, AS, DvS, AA, SR, and MR analyzed the data. FB, AS, DvS, AA, SR, and MR wrote the manuscript. All authors discussed the results and commented on the manuscript.

FUNDING

The authors AS and FB were supported by Science Foundation Ireland (SFI; Grant numbers SFI/12/RC/2273-P1 and SFI/12/RC/2273-P2) to DvS. AS was recipient of IRC Postdoctoral fellowship (GOIPD/2019/353) and FB was a recipient of a FEMS Research Grant (FEMS-RG-2016-0103) and FEMS/ESCMID Award. AA, SR, and MR were supported by FFABR 2017, Fondo per il Finanziamento delle Attività Base di Ricerca, funded by MIUR (Ministero dell'Istruzione, dell'Università e della Ricerca).

SUPPLEMENTARY MATERIAL

The Supplementary Material for this article can be found online at: https://www.frontiersin.org/articles/10.3389/fmicb.2020.573335/full#supplementary-material

REFERENCES

Altschul, S. F., Gish, W., Miller, W., Myers, E. W., and Lipman, D. J. (1990). Basic local alignment search tool. *J. Mol. Biol.* 215, 403–410. doi: 10.1016/S0022-2836(05)80360-2

Amaretti, A., Bernardi, T., Tamburini, E., Zanoni, S., Lomma, M., Matteuzzi, D., et al. (2007). Kinetics and metabolism of *Bifidobacterium adolescentis* MB 239 growing on glucose, galactose, lactose, and galactooligosaccharides. *Appl. Environ. Microbiol.* 73, 3637–3644. doi: 10.1128/AEM.02914-06

Arena, M. P., Russo, P., Capozzi, V., Lopez, P., Fiocco, D., and Spano, G. (2014). Probiotic abilities of riboflavin-overproducing *Lactobacillus* strains: a novel promising application of probiotics. *Appl. Environ. Microbiol.* 98, 7569–7581. doi: 10.1007/s00253-014-5837-x

Arias-Carrasco, R., Vásquez-Morán, Y., Nakaya, H. I., and Maracaja-Coutinho, V. (2018). StructRNAfinder: an automated pipeline and web server for RNA families prediction. *BMC Bioinformatics* 19:55. doi: 10.1186/s12859-018-2052-2

Bacher, A., Eberhardt, S., Fischer, M., Kis, K., and Richter, G. (2000). Biosynthesis of vitamin b2 (riboflavin). *Annu. Rev. Nutr.* 20, 153–167. doi: 10.1146/annurev.nutr.20.1.153

Bottacini, F., van Sinderen, D., and Ventura, M. (2017). Omics of bifidobacteria: research and insights into their health-promoting activities. *Biochem. J.* 474, 4137–4152. doi: 10.1042/BCJ20160756

Burgess, C., O'Connell-Motherway, M., Sybesma, W., Hugenholtz, J., and van Sinderen, D. (2004). Riboflavin production in *Lactococcus lactis*: potential for in situ production of vitamin-enriched foods. *Appl. Environ. Microbiol.* 70, 5769–5777. doi: 10.1128/AEM.70.10.5769-5777.2004

Burgess, C. M., Slotboom, D. J., Geertsma, E. R., Duurkens, R. H., Poolman, B., and van Sinderen, D. (2006a). The riboflavin transporter RibU in *Lactococcus lactis*: molecular characterization of gene expression and the transport mechanism. *J. Bacteriol.* 188, 2752–2760. doi: 10.1128/JB.188.8.2752-2760.2006

Burgess, C. M., Smid, E. J., Rutten, G., and van Sinderen, D. (2006b). A general method for selection of riboflavin-overproducing food grade micro-organisms. *Microb. Cell Fact* 5:24. doi: 10.1186/1475-2859-5-24

Capozzi, V., Menga, V., Digesu, A. M., De Vita, P., van Sinderen, D., Cattivelli, L., et al. (2011). Biotechnological production of vitamin B2-enriched bread and pasta. *J. Agric. Food Chem.* 59, 8013–8020. doi: 10.1021/jf201519h

Corbett, A. J., Eckle, S. B., Birkinshaw, R. W., Liu, L., Patel, O., Mahony, J., et al. (2014). T-cell activation by transitory neo-antigens derived from distinct microbial pathways. *Nature* 509, 361–365. doi: 10.1038/nature13160

D'Aimmo, M. R., Mattarelli, P., Biavati, B., Carlsson, N. G., and Andlid, T. (2012). The potential of bifidobacteria as a source of natural folate. *J. Appl. Microbiol.* 112, 975–984. doi: 10.1111/j.1365-2672.2012.05261.x

Dakora, F. D., Matiru, V. N., and Kanu, A. S. (2015). Rhizosphere ecology of lumichrome and riboflavin, two bacterial signal molecules eliciting developmental changes in plants. *Front. Plant Sci.* 6:700. doi: 10.3389/fpls.2015.00700

De Man, J. C., Rogosa, M., and Sharpe, M. E. (1960). A medium for the cultivation of *Lactobacilli*. *J. Appl. Bacteriol.* 23, 130–135. doi: 10.1111/j.1365-2672.1960.tb00188.x

Edgar, R. C. (2004). MUSCLE: multiple sequence alignment with high accuracy and high throughput. *Nucleic Acids Res.* 32, 1792–1797. doi: 10.1093/nar/gkh340

Fangmann, D., Theismann, E. M., Turk, K., Schulte, D. M., Relling, I., Hartmann, K., et al. (2018). Targeted microbiome intervention by microencapsulated delayed-release niacin beneficially affects insulin sensitivity in humans. *Diabetes Care* 41, 398–405. doi: 10.2337/dc17-1967

Fischer, M., Romisch, W., Saller, S., Illarionov, B., Richter, G., Rohdich, F., et al. (2004). Evolution of vitamin B2 biosynthesis: structural and functional similarity between pyrimidine deaminases of eubacterial and plant origin. *J. Biol. Chem.* 279, 36299–36308. doi: 10.1074/jbc.M404406200

Ge, Y. Y., Zhang, J. R., Corke, H., and Gan, R. Y. (2020). Screening and spontaneous mutation of pickle-derived lactobacillus plantarum with overproduction of riboflavin, related mechanism, and food application. *Foods* 9:88. doi: 10.3390/foods9010088

Griffiths, A. J. F., Miller, J. H., Suzuki, D. T., Lewontin, R. C., and Gelbart, W. M. (2000). *An Introduction to Genetic Analysis*, 7th Edn, New York, NY: W. H. Freeman.

Institute of Medicine (1998). *Dietary Reference Intakes for Thiamin, Riboflavin, Niacin, Vitamin B6, Folate, Vitamin B12, Pantothenic Acid, Biotin, and Choline*. Washington, DC: The National Academies Press. doi: 10.17226/6015

Juarez Del Valle, M., Laino, J. E., de Moreno de LeBlanc, A., Savoy, de Giori, G., and LeBlanc, J. G. (2016). Soyamilk fermented with riboflavin-producing *Lactobacillus plantarum* CRL 2130 reverts and prevents ariboflavinosis in murine models. *Br. J. Nutr.* 116, 1229–1235. doi: 10.1017/S0007114516003378

Kil, Y. V., Mironov, V. N., Gorishin, I., Kreneva, R. A., and Perumov, D. A. (1992). Riboflavin operon of *Bacillus subtilis*: unusual symmetric arrangement of the regulatory region. *Mol. Gen. Genet.* 233, 483–486. doi: 10.1007/bf00265448

Kim, J. H., An, H. J., Garrido, D., German, J. B., Lebrilla, C. B., and Mills, D. A. (2013). Proteomic analysis of *Bifidobacterium longum* subsp. infantis reveals the metabolic insight on consumption of prebiotics and host glycans. *PLoS One* 8:e57535. doi: 10.1371/journal.pone.0057535

Kwak, M. J., Kwon, S. K., Yoon, J. K., Song, J. Y., Seo, J. G., Chung, M. J., et al. (2016). Evolutionary architecture of the infant-adapted group of *Bifidobacterium* species associated with the probiotic function. *Syst. Appl. Microbiol.* 39, 429–439. doi: 10.1016/j.syapm.2016.07.004

LeBlanc, J. G., Burgess, C., Sesma, F., Savoy de Giori, G., and van Sinderen, D. (2005). Ingestion of milk fermented by genetically modified *Lactococcus lactis* improves the riboflavin status of deficient rats. *J. Dairy Sci.* 88, 3435–3442. doi: 10.3168/jds.s0022-0302(05)73027-7

LeBlanc, J. G., Laino, J. E., del Valle, M. J., Vannini, V., van Sinderen, D., Taranto, M. P., et al. (2011). B-group vitamin production by lactic acid bacteria–current knowledge and potential applications. *J. Appl. Microbiol.* 111, 1297–1309. doi: 10.1111/j.1365-2672.2011.05157.x

LeBlanc, J. G., Levit, R., Savoy de Giori, G., and de Moreno de LeBlanc, A. (2020). Application of vitamin-producing lactic acid bacteria to treat intestinal inflammatory diseases. *Appl. Microbiol. Biotechnol.* 104, 3331–3337. doi: 10.1007/s00253-020-10487-10481

LeBlanc, J. G., Milani, C., de Giori, G. S., Sesma, F., van Sinderen, D., and Ventura, M. (2013). Bacteria as vitamin suppliers to their host: a gut microbiota perspective. *Curr. Opin. Biotechnol.* 24, 160–168. doi: 10.1016/j.copbio.2012.08.005

LeBlanc, J. G., Rutten, G., Bruinenberg, P., Sesma, F., de Giori, G. S., and Smid, E. J. (2006). A novel dairy product fermented with *Propionibacterium freudenreichii* improves the riboflavin status of deficient rats. *Nutrition* 22, 645–651. doi: 10.1016/j.nut.2006.01.002

Ledesma-Amaro, R., Serrano-Amatriain, C., Jimenez, A., and Revuelta, J. L. (2015). Metabolic engineering of riboflavin production in *Ashbya gossypii* through pathway optimization. *Microb. Cell Fact* 14:163. doi: 10.1186/s12934-015-0354-x

Ludwig, P., Sevin, D. C., Busche, T., Kalinowski, J., Bourdeaux, F., Grininger, M., et al. (2018). Characterization of the small flavin-binding dodecin in the roseoflavin producer *Streptomyces davawensis*. *Microbiology* 164, 908–919. doi: 10.1099/mic.0.000662

Mack, M., van Loon, A. P., and Hohmann, H. P. (1998). Regulation of riboflavin biosynthesis in *Bacillus subtilis* is affected by the activity of the flavokinase/flavin adenine dinucleotide synthetase encoded by ribC. *J. Bacteriol.* 180, 950–955. doi: 10.1128/jb.180.4.950-955.1998

Matsui, K., Hsiu-Chuan, W., Takako, H., Hirokazu, M., Sabu, K., Kunihiro, S., et al. (1982). Riboflavin production by roseoflavin-resistant strains of some bacteria. *Agric. Biol. Chem.* 46, 2003–2008. doi: 10.1080/00021369.1982.10865390

Milani, C., Lugli, G. A., Duranti, S., Turroni, F., Bottacini, F., Mangifesta, M., et al. (2014). Genomic encyclopedia of type strains of the genus *Bifidobacterium*. *Appl. Environ. Microbiol.* 80, 6290–6302. doi: 10.1128/AEM.02308-14

Mironov, A. S., Gusarov, I., Rafikov, R., Lopez, L. E., Shatalin, K., Kreneva, R. A., et al. (2002). Sensing small molecules by nascent RNA: a mechanism to control transcription in bacteria. *Cell* 111, 747–756. doi: 10.1016/s0092-8674(02)01134-1130

Mohedano, M. L., Hernandez-Recio, S., Yepez, A., Requena, T., Martinez-Cuesta, M. C., Pelaez, C., et al. (2019). Real-time detection of riboflavin production by *Lactobacillus plantarum* strains and tracking of their gastrointestinal survival and functionality *in vitro* and *in vivo* using mCherry labeling. *Front. Microbiol.* 10:1748. doi: 10.3389/fmicb.2019.01748

Ott, E., Stolz, J., Lehmann, M., and Mack, M. (2009). The RFN riboswitch of *Bacillus subtilis* is a target for the antibiotic roseoflavin produced by *Streptomyces davawensis*. *RNA Biol.* 6, 276–280. doi: 10.4161/rna.6.3.8342

Pompei, A., Cordisco, L., Amaretti, A., Zanoni, S., Matteuzzi, D., and Rossi, M. (2007a). Folate production by bifidobacteria as a potential probiotic property. *Appl. Environ. Microbiol.* 73, 179–185. doi: 10.1128/AEM.01763-06

Pompei, A., Cordisco, L., Amaretti, A., Zanoni, S., Raimondi, S., Matteuzzi, D., et al. (2007b). Administration of folate-producing bifidobacteria enhances folate status in Wistar rats. *J. Nutr.* 137, 2742–2746. doi: 10.1093/jn/137.12.2742

Rajamani, S., Bauer, W. D., Robinson, J. B., Farrow, J. M. III, Pesci, E. C., Teplitski, M., et al. (2008). The vitamin riboflavin and its derivative lumichrome activate the LasR bacterial quorum-sensing receptor. *Mol. Plant Microb. Interact.* 21, 1184–1192. doi: 10.1094/MPMI-21-9-1184

Ruiz, L., Bottacini, F., Boinett, C. J., Cain, A. K., O'Connell-Motherway, M., Lawley, T. D., et al. (2017). The essential genomic landscape of the commensal *Bifidobacterium breve* UCC2003. *Sci. Rep.* 7:5648. doi: 10.1038/s41598-017-05795-y

Russo, P., Capozzi, V., Arena, M. P., Spadaccino, G., Duenas, M. T., Lopez, P., et al. (2014). Riboflavin-overproducing strains of *Lactobacillus fermentum* for riboflavin-enriched bread. *Appl. Microbiol. Biotechnol.* 98, 3691–3700. doi: 10.1007/s00253-013-5484-7

Sela, D. A., Chapman, J., Adeuya, A., Kim, J. H., Chen, F., Whitehead, T. R., et al. (2008). The genome sequence of *Bifidobacterium longum* subsp. infantis reveals adaptations for milk utilization within the infant microbiome. *Proc. Natl. Acad. Sci. U.S.A.* 105, 18964–18969. doi: 10.1073/pnas.0809584105

Sharma, V., Rodionov, D. A., Leyn, S. A., Tran, D., Iablokov, S. N., Ding, H., et al. (2019). B-vitamin sharing promotes stability of gut microbial communities. *Front. Microbiol.* 10:1485. doi: 10.3389/fmicb.2019.01485

Stahmann, K. P., Revuelta, J. L., and Seulberger, H. (2000). Three biotechnical processes using *Ashbya gossypii*, *Candida famata*, or *Bacillus subtilis* compete with chemical riboflavin production. *Appl. Microbiol. Biotechnol.* 53, 509–516. doi: 10.1007/s002530051649

Steinert, R. E., Sadaghian Sadabad, M., Harmsen, H. J., and Weber, P. (2016). The prebiotic concept and human health: a changing landscape with riboflavin as a novel prebiotic candidate? *Eur. J. Clin. Nutr.* 70:1461. doi: 10.1038/ejcn.2016.141

Sugahara, H., Odamaki, T., Hashikura, N., Abe, F., and Xiao, J. Z. (2015). Differences in folate production by bifidobacteria of different origins. *Biosci. Microbiota Food Health* 34, 87–93. doi: 10.12938/bmfh.2015-003

Thakur, K., Tomar, S. K., and De, S. (2016). Lactic acid bacteria as a cell factory for riboflavin production. *Microb. Biotechnol.* 9, 441–451. doi: 10.1111/1751-7915.12335

Thakur, K., Tomar, S. K., Singh, A. K., Mandal, S., and Arora, S. (2017). Riboflavin and health: a review of recent human research. *Crit. Rev. Food Sci. Nutr.* 57, 3650–3660. doi: 10.1080/10408398.2016.1145104

Vitreschak, A. G., Rodionov, D. A., Mironov, A. A., and Gelfand, M. S. (2002). Regulation of riboflavin biosynthesis and transport genes in bacteria by transcriptional and translational attenuation. *Nucleic Acids Res.* 30, 3141–3151. doi: 10.1093/nar/gkf433

Winkler, W. C., Cohen-Chalamish, S., and Breaker, R. R. (2002). An mRNA structure that controls gene expression by binding FMN. *Proc. Natl. Acad. Sci. U.S.A.* 99, 15908–15913. doi: 10.1073/pnas.212628899

Woodson, H. W., Kirch, E. R., and Bergeim, O. (1946). A study of the microbiological assay of riboflavin. *J. Am. Pharm. Assoc. Am. Pharm. Assoc.* 35, 253–255. doi: 10.1002/jps.3030350806

Yepez, A., Russo, P., Spano, G., Khomenko, I., Biasioli, F., Capozzi, V., et al. (2019). In situ riboflavin fortification of different kefir-like cereal-based beverages using selected Andean LAB strains. *Food Microbiol.* 77, 61–68. doi: 10.1016/j.fm.2018.08.008

Conflict of Interest: The authors declare that the research was conducted in the absence of any commercial or financial relationships that could be construed as a potential conflict of interest.

frontiers in Microbiology

ORIGINAL RESEARCH
published: 19 November 2020
doi: 10.3389/fmicb.2020.599555

Two-Stage Interpretation of Changes in TEER of Intestinal Epithelial Layers Protected by Adhering Bifidobacteria During *E. coli* Challenges

*Lu Yuan, Henny C. van der Mei, Henk J. Busscher and Brandon W. Peterson**

Department of Biomedical Engineering, University Medical Center Groningen, University of Groningen, Groningen, Netherlands

Mechanisms of gastrointestinal protection by probiotic bacteria against infection involve amongst others, modulation of intestinal epithelial barrier function. Trans-epithelial electrical resistance (TEER) is widely used to evaluate cellular barrier functions. Here, we developed a two-stage interpretative model of the time-dependence of the TEER of epithelial layers grown in a transwell during *Escherichia coli* challenges in the absence or presence of adhering bifidobacteria. *E. coli* adhesion in absence or presence of adhering bifidobacteria was enumerated using selective plating. After 4–8 h, *E. coli* challenges increased TEER to a maximum due to bacterial adhesion and increased expression of a tight-junction protein [zonula occludens-1 (ZO-1)], concurrent with a less dense layer structure, that is indicative of mild epithelial layer damage. Before the occurrence of a TEER-maximum, decreases in electrical conductance (i.e., the reciprocal TEER) did not relate with para-cellular dextran-permeability, but after occurrence of a TEER-maximum, dextran-permeability and conductance increased linearly, indicative of more severe epithelial layer damage. Within 24 h after the occurrence of a TEER maximum, TEER decreased to below the level of unchallenged epithelial layers demonstrating microscopically observable holes and apoptosis. Under probiotic protection by adhering bifidobacteria, TEER-maxima were delayed or decreased in magnitude due to later transition from mild to severe damage, but similar linear relations between conductance and dextran permeability were observed as in absence of adhering bifidobacteria. Based on the time-dependence of the TEER and the relation between conductance and dextran-permeability, it is proposed that bacterial adhesion to epithelial layers first causes mild damage, followed by more severe damage after the occurrence of a TEER-maximum. The mild damage caused by *E. coli* prior to the occurrence of TEER maxima was reversible upon antibiotic treatment, but the severe damage after occurrence of TEER maxima could not be reverted by antibiotic treatment. Thus, single-time TEER is interpretable in two ways, depending whether increasing to or decreasing from its maximum. Adhering bifidobacteria elongate the time-window available for antibiotic treatment to repair initial pathogen damage to intestinal epithelial layers.

Keywords: TEER, probiotics, intestinal microflora, tight-junctions, barrier integrity, real-time monitoring

OPEN ACCESS

Edited by:
Lorena Ruiz,
Institute of Dairy Products of Asturias (IPLA), Spain

Reviewed by:
Esther Orozco,
Center for Research and Advanced Studies of the National Polytechnic Institute of Mexico (CINVESTAV), Mexico
Atte Von Wright,
University of Eastern Finland, Finland

****Correspondence:***
Brandon W. Peterson
b.w.peterson@umcg.nl

Specialty section:
This article was submitted to Food Microbiology, a section of the journal Frontiers in Microbiology

Received: *27 August 2020*
Accepted: *26 October 2020*
Published: *19 November 2020*

Citation:
Yuan L, van der Mei HC, Busscher HJ and Peterson BW (2020) Two-Stage Interpretation of Changes in TEER of Intestinal Epithelial Layers Protected by Adhering Bifidobacteria During E. coli Challenges. Front. Microbiol. 11:599555. doi: 10.3389/fmicb.2020.599555

INTRODUCTION

Trans-epithelial electrical resistance (TEER) measurements constitute a simple, non-invasive method to monitor the barrier integrity of epithelial or endothelial cell layers (Chen et al., 2015). The electrical resistances comprised in an epithelial or endothelial cell layer involve most notably the resistances of the apical and basolateral cell membranes and the intra-cellular fluid (the trans-cellular pathway) in series. These serial resistances operate in parallel with the resistance of the extra-cellular fluid contained in the tight-junctions (Suzuki et al., 2017) between cells (the para-cellular pathway) (Benson et al., 2013; Odijk et al., 2015). Since tight-junctions not only contain extra-cellular fluid but also a variety of tight-junction proteins acting as a bridge between neighboring cells, electrical current flows equally through the trans-cellular and the para-cellular pathway (Krug et al., 2009). TEER therewith reflects the integrity of the cell layer and its barrier function (Butt et al., 1990; Lippmann et al., 2012; Béduneau et al., 2014; Van der Helm et al., 2016). For non-invasive measurements of the integrity of mono-culture cell layer, TEER measurements constitute the "gold standard" (Maherally et al., 2018).

The barrier function of tight-junctions regulates host nutrition and waste removal (Groschwitz and Hogan, 2009), maintenance of homeostasis (Gareau et al., 2010) and protection of the host against pathogen invasion, such as by *Escherichia coli* that can cause severe intestinal infection (LeBlanc, 2003). At the same time, human intestinal epithelial layers are colonized by a large number of commensal bacteria, offering protection against pathogen colonization and invasion. In case the delicate balance of the gut microflora is disrupted and pathogens start to colonize, disease results (Ouwehand et al., 2016). The increasing development of antibiotic resistance amongst many pathogens makes eradication of intestinal pathogens using antibiotics more and more difficult, while indiscriminate use of antibiotics may not only kill pathogens but also the commensal intestinal microflora (Ouwehand et al., 2016; Wypych and Marsland, 2018).

Probiotics are defined by the World Health Organization as "live microorganisms that, when administered in adequate amounts, confer a health benefit on the host" (Hill et al., 2014). Probiotic bacteria are applied more and more for complementing the commensal microflora and the promotion of a healthy intestinal microflora. Probiotics operate through a variety of mechanisms including competitive inhibition of pathogen adhesion, pathogen displacement, production of bioactive metabolites, such as bacteriocins and biosurfactants, and modulation of epithelial barrier function (Ohland and MacNaughton, 2010; Reid et al., 2011). TEER has been frequently used to evaluate pathogen challenges and probiotic protection of intestinal epithelial layers. Whereas pathogenic *E. coli* or *Clostridium perfringens* have been commonly described to decrease TEER and expression of tight-junction proteins, such as claudin, occludin or zonula occludens-1 (ZO-1), a key tight-junction associated protein (Shinoda et al., 2016; Bhat et al., 2019), probiotic lactobacilli are known to increase TEER concurrent with increased expression of tight-junction proteins (Anderson et al., 2010; Corridoni et al., 2012; Barnett et al., 2018). Even in a heat-killed state, lactobacilli prevented intestinal epithelial layers against cytokine disruption, as concluded from TEER measurements (Zeng et al., 2016). Most studies on TEER and probiotic bacteria involve lactobacilli. Frequently however, the monitoring of TEER is stopped when probiotic protection is at its maximum (Anderson et al., 2010) and not pursued beyond. Also, bifidobacteria are known to exert probiotic effects, and lipopolysaccharide (LPS)-induced decreases in TEER could be prevented by bifidobacteria (Ling et al., 2016). There are, to our knowledge, only a few studies which demonstrate protective effects of probiotic bacteria with respect to intestinal epithelial integrity through TEER measurements in the simultaneous presence of pathogens, but most of these pertain to lactobacilli adhering on intestinal epithelial layers challenged by *E. coli* (Michail and Abernathy, 2002) or *Salmonella* (Fajdiga et al., 2006; Lépine et al., 2018). Experiments involving simultaneous probiotic and pathogen presence are clearly preferable, since, e.g., production and release of biosurfactants by probiotic strains, may interfere with pathogen colonization (Reid et al., 2011).

This study aims to propose a two-stage interpretative model of increasing and decreasing TEER of intestinal epithelial layers during a pathogenic *E. coli* challenge in the absence and presence of adhering probiotic bifidobacteria or the adsorbed biosurfactants they produce. To this end, we evaluated the TEER and dextran permeability of intestinal epithelial layers as a function of time during *E. coli* challenges. *E. coli* challenges were applied in the absence or presence of different adhering bifidobacterial strains or prior to and after adsorption of biosurfactants produced by the bifidobacteria used. In addition, the numbers of *E. coli* adhering to the intestinal epithelial cells were determined in the absence and presence of adhering bifidobacteria. Experiments were carried out *in vitro* in a transwell system using different co-cultures of intestinal epithelial layers and bacteria. Intestinal epithelial cell layers were imaged after cytoskeleton staining using confocal laser scanning microscopy (CLSM). Tight-junction associated protein staining was done to visualize ZO-1, while Annexin V-FITC staining was applied to observe apoptosis, employing fluorescence microscopy.

MATERIALS AND METHODS

Bacterial Culturing and Harvesting

Bifidobacterium breve ATCC 15700, *Bifidobacterium longum* ATCC 15707, and *Bifidobacterium infantis* ATCC 15697 are all commensals of the human intestines and were purchased from American Type Culture Collection, while *E. coli* Hu 734 is a human clinical isolate. Bifidobacteria were streaked on RC (Reinforced Clostridial, Becton Dickinson, United States) agar plates from frozen stock and grown under anaerobic conditions (85% N_2, 5% CO_2, 10% H_2) at 37°C for 48 h. *E. coli* was streaked on a blood agar plate and incubated at 37°C for 24 h. *E. coli* colonies grew on blood agar in absence of a clear- or greenish-colored zone around them, indicating absence of hemolytic activity of the strain (Buxton, 2005). Subsequently, one colony was transferred to RCM (Reinforced Clostridial Medium) broth

for the bifidobacteria and to lysogeny broth (LB, Sigma-Aldrich, United States) for *E. coli*. Strains were cultured for 24 h after which bacteria were transferred (1:20) to fresh culture medium and grown for 18 h under the appropriate conditions. Bacteria were harvested by centrifugation for 5 min at 10,000 *g* and 10°C, washed twice with sterile PBS (phosphate buffered saline; 5 mM K_2HPO_4, 5 mM KH_2PO_4, 0.15 M NaCl, pH 7.0), and re-suspended in PBS for further use. Bacterial concentrations were determined by enumeration in a Bürker-Türk counting chamber, after which suspensions were diluted to concentrations required in an experiment.

Inhibition of *E. coli* Growth by Bifidobacteria

In order to evaluate possible inhibitory effects of bifidobacteria on *E. coli* growth, a zone of inhibition assay was used. Briefly, a cotton swab was immersed in 10^5 mL^{-1} *E. coli* suspension and spread on an RC agar plate. Then, a 10 μL droplet of 10^9 mL^{-1} *B. breve*, *B. longum* or *B. infantis* suspension was added on an agar plate inoculated with *E. coli*. After anaerobic incubation at 37°C for 48 h, diameters of the inhibition zone around a droplet with suspended bifidobacteria were measured in three different directions and averaged.

Biosurfactant Release by Bifidobacteria

Biosurfactant production and release of the three probiotic bifidobacterial strains was quantitated using axisymmetric-drop-shape-analysis-by-profile (ADSA-P) (Van der Vegt et al., 1991; Kwok et al., 1994). Briefly, a 100 μL droplet of a bifidobacterial suspension (5×10^9 mL^{-1} in PBS) was put on a hydrophobic glass coverslip (Paul Marienfeld GmbH & Co. KG, Germany), and placed in a humidified enclosed chamber (Velraeds et al., 1996). The shape of the droplet was recorded as a function of time up to 2 h at room temperature. Biosurfactant release lowers the liquid surface tension and therewith causes time-dependent flattening of the droplet (**Supplementary Movies 1 and 2**). Assuming an axisymmetric drop shape, the surface tension of the suspension was calculated from the Laplace equation of capillarity

$$\Delta P = \gamma \left(\frac{1}{R_1} + \frac{1}{R_2} \right) \quad (1)$$

which, γ is the liquid surface tension, R_1 and R_2 are the two principal radii of curvature of the droplet, and ΔP is the pressure difference across the interface. Bifidobacteria were considered to be biosurfactant releasing when the surface tension of the bacterial suspension droplet decreased by more than 8 mJ m^{-2} after 2 h (Van der Vegt et al., 1991).

Biosurfactants released by each of the different bifidobacterial strains were collected after culturing in RCM for 24 h, followed by 1:20 transfer into 200 mL RCM for 18 h (Chander et al., 2012). Spent culture medium was centrifuged at 10,000 *g* at 4°C for 20 min and the supernatant collected. The pH of supernatant was adjusted to 2 with 6 M hydrochloric acid and kept at 4°C overnight to precipitate lipids and proteins. Finally, supernatant was centrifuged again at 10,000 *g* at 4°C for 20 min, and the precipitate collected and dissolved in 10 mL PBS (pH 7.0) to a concentration of 11 mg mL^{-1} for further experiments. For control, freshly prepared RCM, not used for bacterial growth, was subjected to the same procedure.

Intestinal Epithelial Cell Culturing and Harvesting

Caco-2 BBe cells (ATCC CRL-2102) are commonly used as a model of the human intestinal epithelial cells and were obtained from the American Type Culture Collection. Cells were grown in Dulbecco's Modified Eagle Medium containing 4.5 g L^{-1} glucose (DMEM-HG, Gibco, United States) and 10% (vol/vol) fetal bovine serum (FBS, Gibco, United States) in 5% CO_2 humidified incubator at 37°C. Cells were passaged after 80% confluency was achieved. Three milliliters EDTA-Trypsin (2.5 g L^{-1}, Gibco, United States) was used for detaching cells in a T-75 flask at 37°C for 5 min. After detachment, DMEM-HG with 10% FBS was added for trypsin neutralization. Cells were collected by centrifugation at 800 *g* for 5 min. The cellular pellet was re-suspended and diluted in fresh culture medium at a concentration of 10^4 mL^{-1} or 2×10^5 mL^{-1} depending on the further experiment involved, as enumerated with an automated cell counter equipped with a 60 μm sensor (Merck Millipore, United States).

Co-culture Experiments of Caco-2 BBe Layers With Bacteria and TEER Measurements

Caco-2 BBe cells were grown on 0.4 μm pore size poly(ethylene terephthalate) transwell inserts with a 1.13 cm^2 membrane (Greiner Bio-One, Austria) from cells suspended in full culture medium (2×10^5 cells mL^{-1}, 0.5 mL) and the medium was refreshed every 2 days. From day 10 on, the integrity of the cellular monolayer was monitored from its TEER as measured using a Millicell® ERS-2 meter (Millipore, United States). A stable TEER $\geq$ 400 Ω cm^2, characteristic for intestinal epithelial layers grown in a transwell, was usually reached within 10–14 days. When the TEER was above 400 Ω cm^2, the epithelial layer was exposed to 0.1 mL of bifidobacteria suspended in PBS (5×10^6 mL^{-1}) for 4 h to allow their adhesion, after which 0.1 mL of *E. coli* suspension in PBS was added at different concentrations (10^2 mL^{-1}, 10^4 mL^{-1}, 10^6 mL^{-1}). Next cells and bacteria were grown for 24 h at 37°C in a humidified incubator with 5% CO_2 in co-culture medium. Co-culture medium was designed to allow optimal growth of Caco-2 BBe cells and bifidobacteria (**Supplementary Figure 1**). Caco-2 BBe cell layers in absence or presence of adhering bifidobacteria and/or *E. coli* challenges were used as controls. In a separate series of experiments, bifidobacterial biosurfactants dissolved in PBS were adsorbed to the Caco-2 BBe cell layer for 1 h prior to initiating an *E. coli* challenge.

TEER was measured as a function of time on three different locations of an epithelial layer and calculated using

$$\mathrm{TEER}_{\mathrm{layer}} = \{R_{\mathrm{measured}} - R_{\mathrm{membrane}}\} \times \text{membrane area} \quad (2)$$

which, $\mathrm{TEER}_{\mathrm{layer}}$ (Ω cm^2) is the TEER of an epithelial layer after subtraction of the TEER of the membrane without a cellular layer,

$R_{measured}$ (Ω) is the resistance measured of the membrane with a cellular layer and $R_{membrane}$ is the resistance of the membrane measured in absence of a cellular layer.

Adhesion of *E. coli* on Epithelial Cell Layers in Presence or Absence of Adhering Bifidobacteria or Adsorbed Biosurfactants

To evaluate whether bifidobacteria or isolated biosurfactants reduced the adhesion of *E. coli* on epithelial cell layer, cell layers with stable TEER $\geq$ 400 Ω cm^2 were exposed to bifidobacteria (10^6 mL^{-1}) for 4 h or isolated biosurfactant (11 mg mL^{-1}) for 1 h at 37°C, prior to exposure to *E. coli* (10^6 mL^{-1}). *E. coli* adhesion was measured 2 h after initiating the challenge (before the TEER maximum) and at the TEER maximum (4 h after challenge initiation). To this end, cell layers were washed five times with PBS and sonicated with 0.5 mL^{-1} PBS for 15 s to detach cells with adhering bacteria from the membrane. A serial dilution series was prepared in PBS and plated on LB agar plates and incubated at 37°C under aerobic conditions for 24 h in order to enumerate the number of colony forming *E. coli* units per cm^2 (CFU/cm^2) cell layer.

Fluorescence Microscopy

Imaging of Epithelial Cell Layers

For the visualization of the Caco-2 BBe cytoskeleton, cells were fixed with 3.7% (wt/vol) paraformaldehyde and permeabilized with 0.5% (vol/vol) Triton X-100. Subsequently, cells were stained with Phalloidin-FITC (Sigma-Aldrich, United States, 495 nm excitation/520 nm emission) and 4′,6-diamidino-2-phenylindole dihydrochloride (DAPI; Sigma-Aldrich, United States, 364 nm excitation/454 nm emission) to visualize F-actin and nuclei, respectively. Cells were imaged using CLSM with 63× magnification objective lens and 0.5 μm depth per stack (Leica SP2, Germany). Fiji Software (Schindelin et al., 2012) was used to analyze the CLSM images. Images were taken of epithelial cell layers prior to and during *E. coli* challenges at 10^4 mL^{-1} for 4, 8, and 24 h.

Visualization of Tight-Junction Associated Proteins

To visualize the effects of *E. coli* and bifidobacteria on tight-junction proteins in epithelial layers, cells were treated as described above, but after permeabilization cells were exposed to 5% BSA in PBS for 1 h at room temperature to block non-specific adsorption, washed once with PBS containing 0.1% Triton X-100 (PBST) for 5 min, and subsequently labeled with primary antibody rabbit-anti-human ZO-1 (1:200, #40-2300, Invitrogen) at 4°C overnight. Next, cells were washed twice with PBST for 5 min, and labeled with secondary antibody Rhodamine Red-X Donkey anti-Rabbit (1:100, #711-295-152, Jackson Immunolab, excitation 570 nm/emission 590 nm) for 1 h. Finally, cells were washed with PBST and PBS, each for 5 min and ZO-1 visualized employing fluorescence microscopy with the green laser (Leica DM4000, Germany).

Apoptosis Staining

To evaluate apoptosis in cellular layers upon *E. coli* challenges, cells were stained with Annexin V-FITC (Thermo Fisher Scientific, United States) which targets phosphatidylserine molecules translocated from the inner face of the plasma membrane to the cell surface, i.e., a sign of early apoptosis (Chen et al., 2008). To this end, cell layers were washed once with PBS, followed by washing with Annexin V-binding buffer and subsequently labeled with Annexin V-FITC (1:40, excitation 488 nm/emission 520 nm) at room temperature for 10 min. Then, cells were washed again with the binding buffer and additionally stained at room temperature for 5 min with propidium iodine (20 μg mL^{-1}, excitation 535 nm/emission 617 nm) to confirm apoptosis signs (Chen et al., 2008) employing fluorescence microscopy. Propidium iodine is a nucleus stain, only entering membrane damaged cells. For comparison, cell layers were purposely brought in an apoptotic state by exposure to 60°C for 20 min prior to imaging.

Dextran Permeability Measurements

The para-cellular permeabilities of the intestinal epithelial cell layers prior to and during *E. coli* challenges in absence or presence of probiotics were determined by measuring the transport of 4 or 10 kDa fluorescein isothiocyanate (FITC)-labeled dextran (FD4 or FD10S; Sigma-Aldrich, St. Louis, MO, United States) across the cell layer over time (Hubatsch et al., 2007). Free FITC in the FITC-dextran purchased, had been removed by multiple precipitations in ethanol yielding stable solutions, that were free of FITC not bound to dextran (De Belder and Granath, 1973). Dextrans were dissolved in DMEM-HG medium (5 mg mL^{-1}) and 100 μL of a dextran solution was added to the apical surface of Caco-2 BBe cells in the transwell insert. 100 μL aliquots were taken from the DMEM-HG medium underneath the membrane after different time intervals during *E. coli* challenges up to 24 h, while replenishing with the same amount of fresh medium. Fluorescence intensities of the aliquots were measured using a fluorescence microplate reader (485 nm excitation/520 nm emission). FITC-labeled dextran transport across the cell layers was quantified using a calibration curve of fluorescence intensity as a function of FITC-labeled dextran concentration (**Supplementary Figure 2**).

The apparent para-cellular permeability coefficient (P_{app}) was calculated according to Artursson and Karlsson (1991)

$$P_{\mathrm{app}} = \left(\frac{\Delta Q}{\Delta t}\right) \times \left(\frac{1}{(A\ x\ C_0)}\right) \tag{3}$$

which, ΔQ is the FITC-labeled dextran mass (g) transported through the cell layer within a time period Δt (min), A is the membrane surface area (cm^2) and C_0 is the initial concentration (g mL^{-1}) of FITC-labeled dextran above the apical cell surface of the epithelial cells grown on the transwell membrane.

Statistical Analysis

All experiments were conducted in triplicate, and the results are represented as means ± standard error of

the mean (SEM). Student's *t*-test were used for two groups comparison and one- or two-way ANOVA were performed, followed with Tukey or Dunnett multiple comparison using GraphPad Prism 7.00. Significance was adapted at $p < 0.05$.

RESULTS

Inhibition of *E. coli* Growth by Bifidobacteria

Escherichia coli growth was inhibited by *B. breve* ATCC 15700, *B. longum* ATCC 15707, and *B. infantis* ATCC 15697 as determined by zone of inhibition measurements. *B. breve* and *B. longum* exhibited significantly larger zones ($p < 0.05$, one-way ANOVA) of inhibition against *E. coli* than *B. infantis* (**Figure 1**).

Biosurfactant Production by Bifidobacteria

The surface tensions of *B. breve*, *B. longum*, and *B. infantis* suspensions in PBS at t equals 0 amounted 67.6 ± 3.6 mJ m^{-2} and decreased by more than 8 mJ m^{-2} within 2 h, regardless of the strain involved (**Figure 2**). Considering a decrease in surface tension of more than 8 mJ m^{-2} as indicative of biosurfactant release (Van der Vegt et al., 1991), all three bifidobacterial strains can be regarded as biosurfactant releasing strains. Surface tensions of solutions of biosurfactants isolated from *B. breve, B. longum,* and *B. infantis* (11 mg mL^{-1}) amounted 53.3 ± 0.7 mJ m^{-2}, 52.1 ± 1.3 mJ m^{-2}, and 54.7 ± 2.9 mJ m^{-2}, respectively. The components isolated from fresh RCM culture medium had a higher surface tension of 61.5 ± 0.7 mJ m^{-2} than the biosurfactant solutions and suspensions of bifidobacteria after 2 h release of biosurfactants.

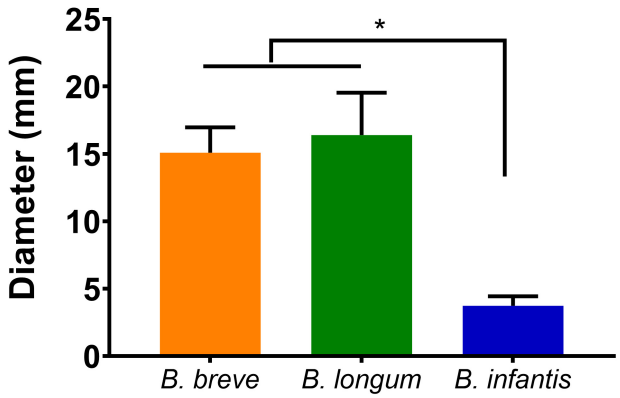

FIGURE 1 | Diameter of the inhibition zones around droplets with suspended bifidobacteria: *B. breve* ATCC 15700, *B. longum* ATCC 15707, and *B. infantis* ATCC 15697 on *E. coli* Hu 734 covered agar plates. Error bars represent standard errors of the mean over three experiments with separately grown bacteria. *indicates statistical significant differences (one-way ANOVA followed with Tukey for multi-comparison, $p < 0.05$).

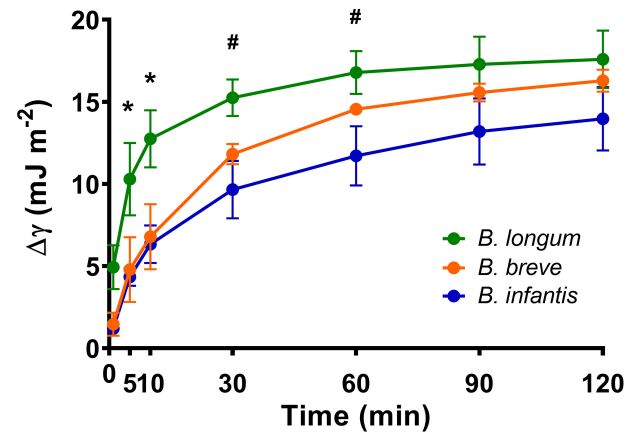

FIGURE 2 | Surface tension decreases ($\Delta\gamma_{lv}$) of *B. breve* ATCC 15700, *B. longum* ATCC 15707, and *B. infantis* ATCC 15697 suspensions as function of time, as an indication of biosurfactant production and release. Initial surface tensions of the bacterial suspensions in PBS amounted 67.6 ± 3.6 (mJ m^{-2}). Error bars represent standard errors of the mean over three experiments with separately grown bacteria. *indicates statistically significant differences ($p < 0.05$) between *B. longum* and both other strains, #indicates statistically significant differences ($p < 0.05$) between *B. longum* and *B. infantis*.

Time-Dependence of the TEER of Epithelial Cell Layers Co-cultured With Bacteria

Trans-epithelial electrical resistance of Caco-2 BBe cell layers as a function of time during an *E. coli* Hu 734 challenge in absence and presence of adhering bifidobacteria are presented in **Figure 3**, while quantitative features of the time-dependence of TEER are compiled in **Table 1**. Caco-2 BBe cell layers in absence of adhering probiotic bacteria or pathogen challenges, demonstrated a stable TEER of around 613 ± 78 Ω cm^2. During challenging the epithelial layer with *E. coli*, TEER increased over time to reach a maximal value after 4–8 h (**Figure 3A** and **Table 1**). The TEER maximum occurred earliest at the highest *E. coli* challenge concentration (10^6 mL^1). For the two lower *E. coli* concentrations, the TEER maximum occurred later while resistance increased with *E. coli* concentrations up to 10^4 mL^{-1}. However, for all *E. coli* challenge concentrations, the TEER of the layer was reduced to around 100 Ω cm^2 or less after 24 h of challenge (see **Table 1**), with the strongest decrease occurring at the highest *E. coli* challenge concentration (10^6 mL^{-1}). The presence of adhering probiotic *B. breve* in absence of an *E. coli* challenge on the cellular layers also yielded a TEER maximum similar as during an *E. coli* challenge, but this maximum occurred generally later and was relatively low (**Figure 3B**). A reduction in 24 h TEER as observed during an *E. coli* challenge was also seen, but only for adhering *B. breve* and not for *B. longum* and *B. infantis* (see **Table 1**).

The presence of adhering bifidobacteria affected the effects of pathogenic *E. coli* challenge in two ways, depending on the probiotic strain involved (**Figure 3B** and **Table 1**): (1) it delayed the development of a TEER maximum due to the *E. coli* challenge,

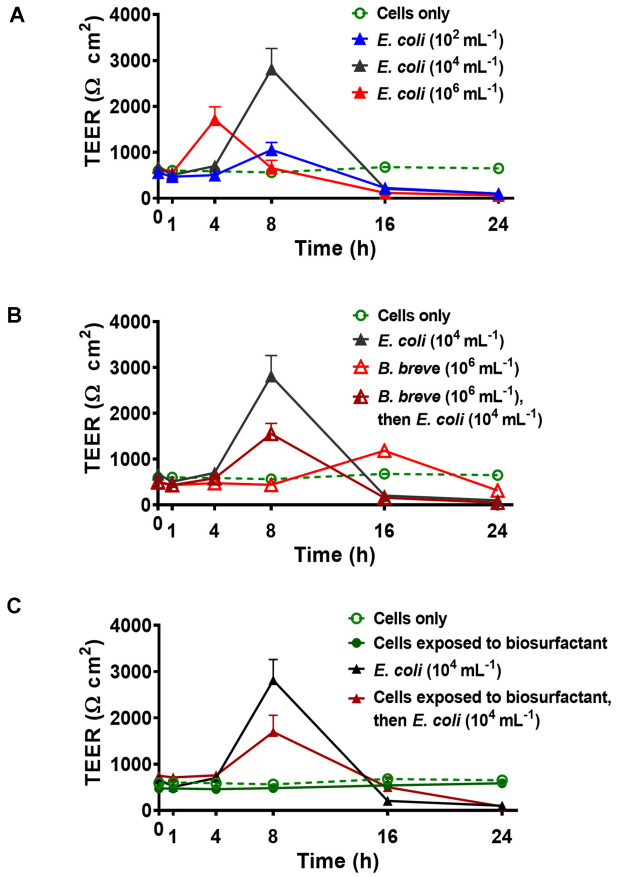

FIGURE 3 | Examples of the TEER of Caco-2 BBe cell layers as a function of time upon challenging with *E. coli* Hu 734 in the absence and presence of adhering bifidobacteria or adsorbed biosurfactants. Time zero corresponds with the initiation of the *E. coli* challenge. Error bars represent standard errors of the mean over three experiments with separately grown bacteria. **(A)** TEER of Caco-2 BBe cell layers during challenges with *E. coli* at different concentrations in suspension. **(B)** TEER of Caco-2 BBe cell layers with adhering *B. breve* (4 h) and subsequently challenged with *E. coli*. **(C)** TEER of Caco-2 BBe cell layers during challenges with *E. coli* prior to and after adsorption (1 h) of *B. breve* biosurfactants, including the TEER of epithelial layers with adsorbed biosurfactants in the absence of an *E. coli* challenge.

and/or (2) it reduced the value of the TEER maximum. However, adhering bifidobacteria could not prevent the reduction in TEER after 24 h exposure to an *E. coli* challenge (**Table 1**).

Trans-epithelial electrical resistance of epithelial layers exposed to biosurfactant solutions did not increase over time, and by consequence the TEER values did not show a maximum over the experimental period (**Figure 3C** and **Table 1**). Additionally, the 24 h TEER value was similar as of an unchallenged epithelial layer (**Table 1**). During an *E. coli* challenge, epithelial layers with adsorbed biosurfactants demonstrated a similarly low TEER maximum when challenged with *E. coli* in the presence of adhering bifidobacteria (**Figure 3C** and **Table 1**). Like adhering bifidobacteria, adsorbed biosurfactants could not prevent a TEER decrease to below the level of untreated cell layers after a 24 h challenge with *E. coli* (**Table 1**).

Adhesion of *E. coli* on the Epithelial Cell Layers

The number of adhering of *E. coli* per unit area on the epithelial cell layers increased significantly ($p < 0.05$) over time toward the occurrence of the TEER maximum, regardless of the absence or presence of adhering bifidobacteria or the adsorbed biosurfactants they produce (**Figure 4**). Protection of the cell layers by adhering bifidobacteria against *E. coli* adhesion can be seen both 2 and 4 h after initiating *E. coli* adhesion. Probiotic adhesion caused greater reductions in *E. coli* adhesion than adsorbed biosurfactants, although this was not statistically significant.

Visualization of Cell Layers Prior to and After an *E. coli* Challenge

F-actin and nucleus staining of epithelial cell layers showed a dense network of cells (**Figures 5A,E**), held together by clearly visible tight-junction proteins (**Figure 5I**). During an *E. coli* challenge, the number of cells and cytoskeleton (**Figures 5B,F**), as well as tight-junction proteins connecting neighboring cells (**Figure 5J**), remained roughly similar as before challenge in the first 4 h. At the TEER maximum, the layer structure was less dense (**Figure 5C**) than before an *E. coli* challenge, as can be seen from both the F-actin (**Figure 5C**) and nucleus images (**Figure 5G**). Thus, at the TEER maximum, mild damage to the epithelial layer had developed. At the same time, tight-junction proteins were still present outlining the circumference of all cells, but with a more "fuzzy" red-fluorescence rim than in cell layers in absence of an *E. coli* challenge (compare **Figure 5K** and **Figure 5I**). This likely indicates scattered increased expression of tight-junction protein ZO-1. After 24 h of challenge, i.e., well after the TEER maximum occurred, large black holes were visible (**Figure 5D**), with a decreased number of nuclei (**Figure 5H**). Furthermore, tight-junction proteins were no longer fully outlining the circumference of each cell (**Figure 5L**), illustrating severe damage to the integrity of the epithelial cell layer. Apoptotic cells were only observed after 24 h *E. coli* challenges (**Figure 5P**) and not for shorter challenge times prior to the TEER maximum (**Figures 5N,O**), indicating that apoptosis only occurred after the TEER maximum.

Para-Cellular Permeability by Dextran

Mass transport of 4 and 10 kDa dextran increased linearly over time through intestinal epithelial layers in the absence of an *E. coli* challenge or probiotic protection (**Supplementary Figure 4**). Permeabilities calculated from the FITC-dextran transport upon *E. coli* challenges are presented in **Figure 6** as a function of the conductance, i.e., the reciprocal TEER, indicative of ion transport through the cell layers. In absence of an *E. coli* challenge, 4 kDa dextran demonstrated slightly (1.5×) but significantly ($p < 0.01$, *t*-test) higher permeabilities than 10 kDa dextran. Permeabilities were relatively stable up to 8–12 h under *E. coli* challenges (**Figures 6A,B**) while electrical conductance was decreasing due to bacterial adhesion. After a minimum in conductance, i.e., the maximum in TEER, dextran permeability increased linearly with conductance, suggesting that

TABLE 1 | Summary of the time-dependence of trans-epithelial electrical resistances of Caco-2 BBe layers, challenged by different concentrations of pathogenic *E. coli* Hu 734 in the absence or presence of adhering probiotic bifidobacteria or adsorbed biosurfactants (see **Figure 3** for examples).

E. coli concentration (mL^{-1})		Time to maximum (h)	Maximal TEER (Ω cm^2)	24 h TEER (Ω cm^2)
No adhering probiotic bacteria/no adsorbed biosurfactants				
0		No maximum	No maximum	613 ± 78
10^2		8	1055 ± 160	101 ± 31[a]
10^4		8	2814 ± 449	101 ± 6[a]
10^6		4	1713 ± 280	62 ± 9[a]
Adhering *B. breve* ATCC 15700				
0		16	1183 ± 26[b]	316 ± 63[a]
10^2		16	729 ± 493	83 ± 11a
10^4		8	1551 ± 230[b]	50 ± 4[a]
10^6		4	1229 ± 241	60 ± 13[a]
Adhering *B. longum* ATCC 15707				
0		No maximum	No maximum	661 ± 34
10^2		8	620 ± 71	57 ± 22[a]
10^4		8	1742 ± 232[b]	56 ± 5[a]
10^6		8	1380 ± 122	64 ± 20[a]
Adhering *B. infantis* ATCC 15697				
0		No maximum	No maximum	749 ± 136
10^2		8	764 ± 138	49 ± 11[a]
10^4		8	1405 ± 145[b]	77 ± 11[a]
10^6		8	1220 ± 261	67 ± 16[a]
Adsorbed biosurfactants only				
0	*B. breve*	No maximum	No maximum	584 ± 41
	B. longum	No maximum	No maximum	628 ± 21
	B. infantis	No maximum	No maximum	656 ± 4
10^4	*B. breve*	8	1695 ± 362[b]	82 ± 10[a]
	B. longum	8	1583 ± 36[b]	80 ± 3[a]
	B. infantis	8	1998 ± 138[b]	81 ± 7[a]

All data are expressed as means ± standard error of the mean over three different experiments with separately grown cellular layers and bacteria.[a]Significant differences in TEER at $p < 0.05$ with respect to cellular layers grown in the absence of adhering probiotic bacteria and E. coli challenges.[b]Statistically significant differences between the absence and presence of adhering probiotic bacteria at corresponding E. coli concentrations.

transported ions use the same para-cellular pathway through an intestinal epithelial layer as dextran, irrespective of its molecular weight. Thus barrier damage has become more severe. In line with the data in **Table 1**, epithelial layers challenged with a higher (10^6 mL^{-1}) concentration of *E. coli* (**Figures 6C,D**) demonstrated a minimum conductance after a shorter exposure time (i.e., 6 h) followed by a linear trajectory at longer exposure times. Under probiotic protection, similar relations between permeability and conductance were observed (**Figures 6E,F**) as in absence of adhering bifidobacteria, but with a delayed occurrence of the transition from mild to more severe epithelial layer damage, characterized by the on-set of linearity between conductance and permeability.

DISCUSSION

Intestinal epithelial layers were challenged by *E. coli* in the absence or presence of different adhering bifidobacterial strains. Unchallenged intestinal epithelial cell layers grown in a transwell had a TEER value of 613 Ω cm^2, in agreement with literature data on Caco-2 cell layers (Odijk et al., 2015) and considered representative of intestinal barrier integrity.

Escherichia coli challenges led to an increase in TEER within 4–8 h and resistance depended on the *E. coli* challenge concentration and the number *E. coli* adhering to the epithelial cell layers (**Table 1** and **Figure 4**). The increase in TEER to a maximal resistance upon pathogen challenges is due to a combination of factors. Firstly, the number of bacteria adhering to the epithelial cell layer increases, yielding an additional resistance to the TEER of the cell layer, while also adhering pathogens can down regulate cellular ion transporters, contributing to a higher TEER (Turner et al., 2000; Gill et al., 2007; Hodges et al., 2008; Das et al., 2018). Secondly, during the period of increasing TEER, a clear "fuzzy" red-fluorescence rim indicative of ZO-1 expression developed around epithelial cells in the layer upon pathogen challenge (**Figures 5I–L**). Such a "fuzzy" coat was less clearly observed in absence of an *E. coli* challenge, which may imply scattered, increased expression of the tight-junction protein ZO-1 of cells under pathogen challenge. This is in line with the known stimulation of integrin-expression in mammalian cells by low level pathogen challenges to allow them to adhere more intimately to surfaces

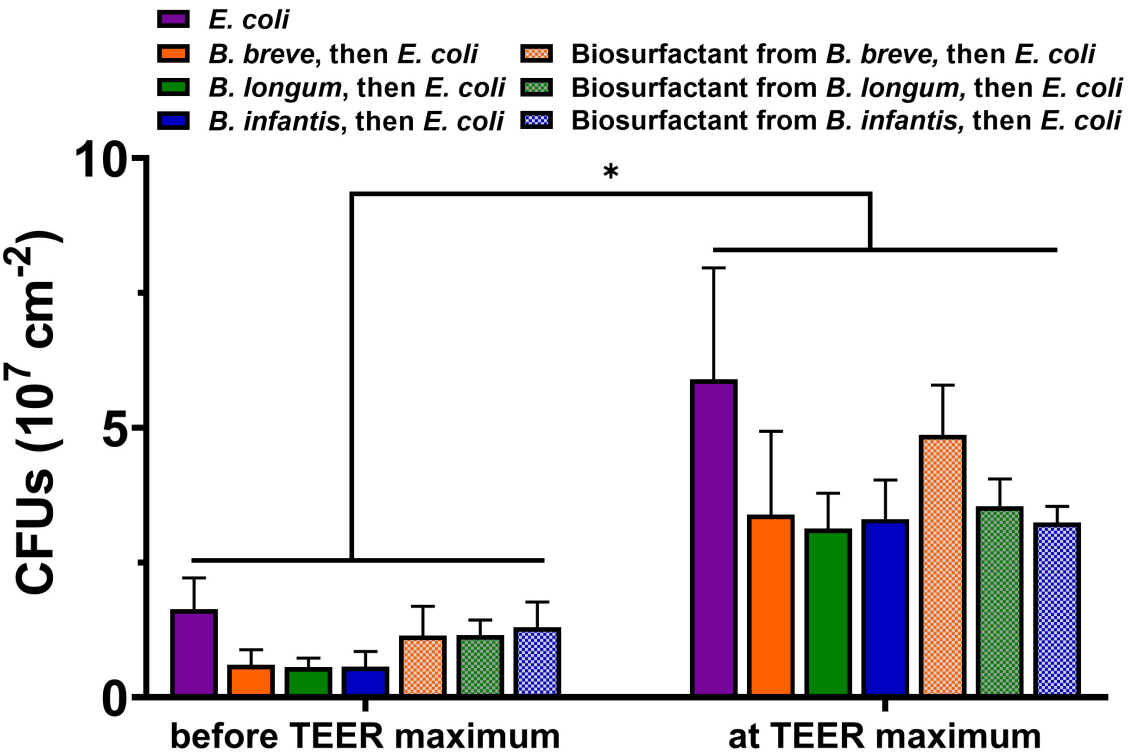

FIGURE 4 | Adhesion of *E. coli* Hu 734 on intestinal epithelial cell layers in the absence or presence of adhering *B. breve* ATCC 15700, *B. longum* ATCC 15707, *B. infantis* ATCC 15697 or their adsorbed biosurfactants. *E. coli* adhesion was enumerated 2 h after initiating *E. coli* adhesion (before the TEER maximum occurred) and at the TEER maximum (4 h after initiating *E. coli* adhesion). PBS was used as a control. Error bars represent standard errors of the mean over three experiments with separately grown cellular layers and bacteria. *indicates statistically significant difference in CFUs before the occurrence of TEER maximum and at the TEER maximum.

(Kim et al., 2009; Engels-Deutsch et al., 2011; Yue et al., 2015). Microscopically, the cell layer became less densely structured, although no indication of apoptotic processes was seen (**Figure 5**). During the time period that TEER increased to a maximal value, a clear relation between transport of ions (i.e., conductance) and changing dextran permeability was lacking (**Figure 6**). Collectively, this suggests that the increase in TEER toward its maximum is a result of bacterial adhesion to the epithelial cell layer, increased expression of tight-junction proteins, most notably ZO-1 and mild damage to the epithelial layer. Importantly, the damage to epithelial layers occurring prior to the TEER maximum is reversible upon antibiotic treatment (see **Supplementary Figure 5**).

Once TEER had reached a maximum upon an *E. coli* challenge, it decreased to below the level of an unchallenged epithelial layer, concurrent with microscopically observable severe damage, including holes in the epithelial layer and apoptosis due to bacterial toxins (Turner et al., 2000; Gill et al., 2007; Hodges et al., 2008; Das et al., 2018). This damage also widened up the tight-junctions and caused cell dissociation, providing a low resistance para-cellular pathway for electrical current after the occurrence of the TEER maximum, characteristic of what has been dubbed as "leaky" epithelial (Troeger et al., 2007b). The linear relation between conductance and dextran permeability supports bacterial widening of tight-junctions, not only allowing increased transport of ions but also of dextran. Pathogenic bacteria possess a wide array of mechanisms that can either affect the epithelial cytoskeleton (de Souza Santos and Orth, 2015) or even fully breakdown tight-junctions and epithelial cell layers due to secretion of toxins (Turner et al., 2000; Gill et al., 2007; Hodges et al., 2008; Franco and Shuman, 2012; Das et al., 2018), in line with the course of TEER and the relation between conductance and dextran permeability over time observed here. Severely damaged epithelial layers at or after the occurrence of the TEER maximum could not be reverted upon antibiotic treatment (see also **Supplementary Figure 5**).

Adhesion of *B. breve* in absence of *E. coli* challenges led to a delayed and far lower TEER maximum than observed during an *E. coli* challenge, occurring only after 16 h. Adhesion of *B. longum* and *B. infantis* did not lead to a TEER maximum. Absence of a TEER maximum in case of adhering probiotic bacteria may have two reasons: (1) since permanent instillation of probiotic bacteria in the gut is usually troublesome (Williams, 2010; Zmora et al., 2018), this attests to their low adhesiveness (Zmora et al., 2018); (2) the "healthy" character of probiotic bacteria may be accompanied by an inability to stimulate integrin-expression in the epithelial layer to the same extent as a pathogen might do (Wang et al., 2006; Parolin et al., 2018). In addition, 24 h adhesion of the probiotic strains did not result in a strong decrease in TEER to below the level of an unchallenged epithelial

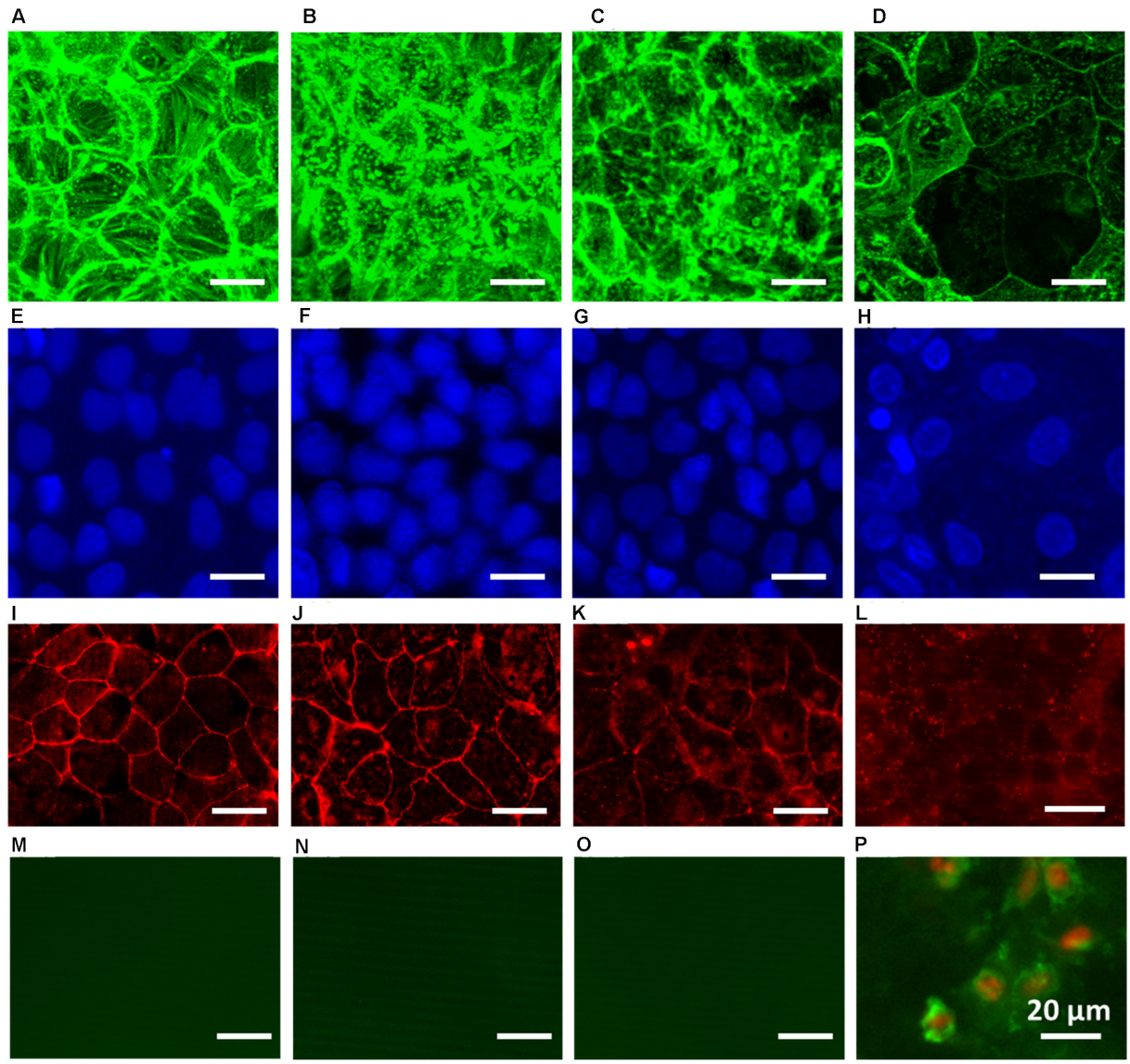

FIGURE 5 | Overlayer images of confocal stacks of Caco-2 BBe cell layers showing green-fluorescent cytoskeleton **(A–D)** and blue-fluorescent nuclei **(E–H)**, fluorescence images of red-fluorescent ZO-1 tight-junction proteins **(I–L)** and apoptosis of green-fluorescent membrane-damaged cells with red-fluorescent nuclei **(M–P)**. For comparison, a fluorescent image of apoptotic cells is shown in **Supplementary Figure 3**. **(A,E,I,M)** 24 h Caco-2 BBe cell layers grown in the absence of an *E. coli* challenge. **(B,F,J,N)** Caco-2 BBe cell layers in the presence of an *E. coli* (10^4 mL^{-1}) challenge before the occurrence of the TEER maximum, i.e., at 4 h. **(C,G,K,O)** Caco-2 BBe cell layers grown in the presence of an *E. coli* (10^4 mL^{-1}) challenge at the TEER maximum, i.e., at 8 h. **(D,H,L,P)** Caco-2 BBe cell layers grown in the presence of an *E. coli* (10^4 mL^{-1}) challenge after the occurrence of the TEER maximum, i.e., after 24 h.

layer as caused by a pathogenic *E. coli* strain (*B. breve* did cause a small but significant decrease in 24 h TEER, but not to the low level observed for *E. coli* only). Other probiotic strains than bifidobacteria have been found before to maintain or enhance epithelial barrier integrity, i.e., maintaining a stable or increased TEER, during short co-culture times (Ramos et al., 2013), while pathogenic strains more readily damaged barrier integrity of epithelial layers (Hasan et al., 2018). Adsorbed biosurfactant protected epithelial layers according to a similar TEER response as observed when bifidobacteria were adhering on the epithelial layers during *E. coli* challenges. This confirms the crucial role of biosurfactants in probiotic action (Rivardo et al., 2009; Sharma and Saharan, 2014). In the present study, it will likely reflect the ability of adsorbed biosurfactants to protect a surface against pathogen adhesion (see also **Figure 4**; Velraeds et al., 1996, 1997, 1998, 2000; Busscher et al., 1997;

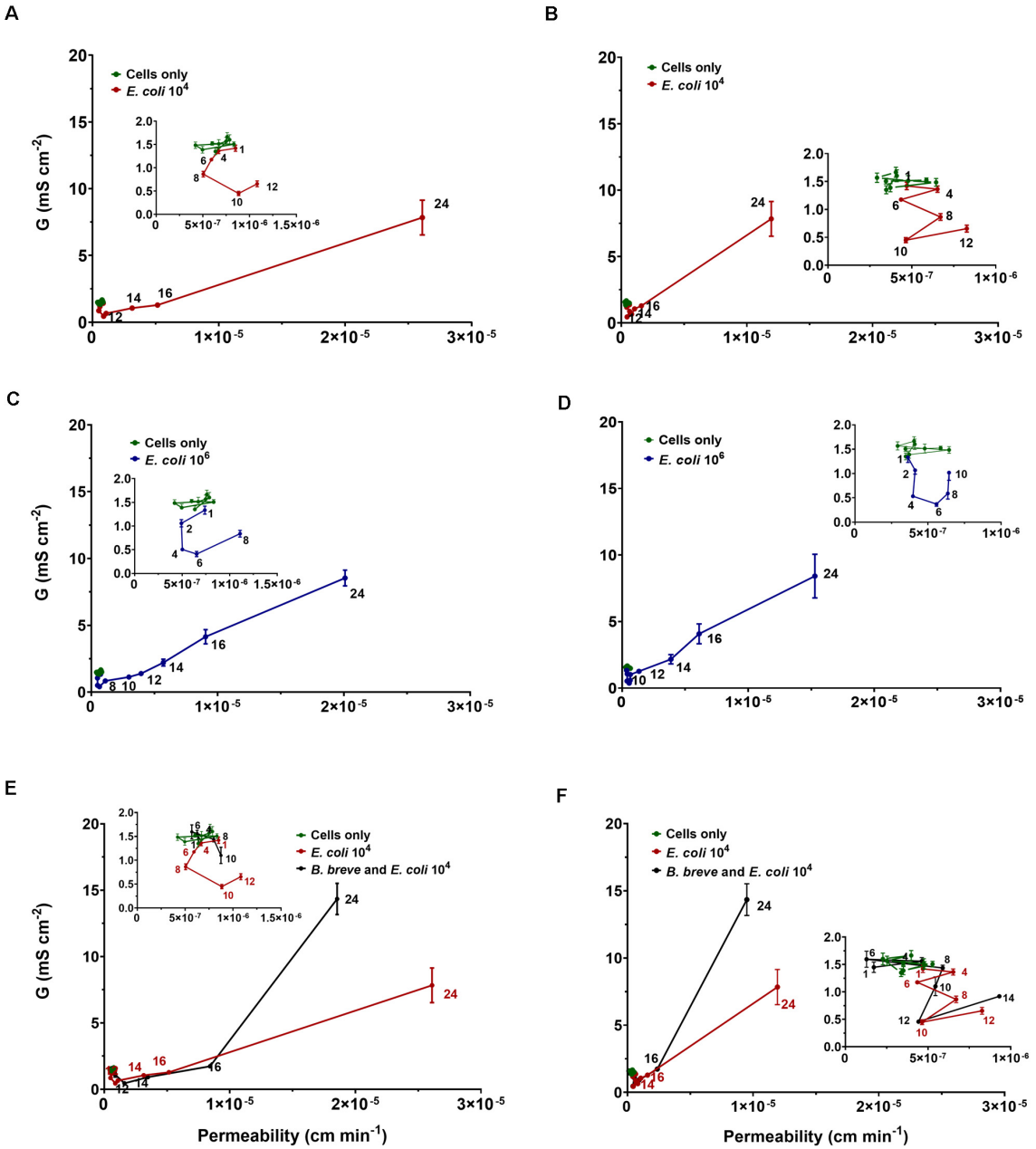

FIGURE 6 | The conductance G (reciprocal TEER) of Caco-2 BBe cell layers at different times after initiating an *E. coli* challenge in the absence and presence of *B. breve* ATCC 15700 (10^6 mL^{-1}) as a function of their permeability. The insets detail conductance as a function of permeability prior to the onset of linearity. **(A)** Conductance of epithelial cell layers as a function of permeability for 4 kDa FITC-labeled dextran at an *E. coli* challenge of (10^4 mL^{-1}). **(B)** Same as panel a, now for 10 kDa FITC-labeled dextran. **(C)** Conductance of epithelial cell layers as a function of permeability for 4 kDa FITC-labeled dextran at an *E. coli* challenge of (10^6 mL^{-1}). **(D)** Same as panel c, now for 10 kDa FITC-labeled dextran. **(E)** Conductance of epithelial cell layers as a function of permeability for 4 kDa FITC-labeled dextran at *E. coli* challenge (10^4 mL^{-1}) in absence and presence of *B. breve* (10^6 mL^{-1}). **(F)** Same as panel e, now for 10 kDa FITC-labeled dextran. Error bars represent standard errors of the mean over three experiments with separately grown cellular layers and bacteria.

Van Hoogmoed et al., 2004; Rivardo et al., 2009). Also in a TEER-based study, bioactive metabolites ("cell-free supernatant") of *Bifidobacterium lactis* protected Caco-2 epithelial junctions against *E. coli* (Putaala et al., 2008), which is in line with protection offered by adsorbed biosurfactants in this study. However, the study of Putaala et al. (2008) was done with bioactive metabolites that were not identified as possessing biosurfactants. The time-dependent changes observed in the TEER of intestinal epithelial layers during probiotic protection and pathogen challenge can be interpreted on the basis of a two-stage damage model to the cell layer (**Figure 7**). In the model, adhering bacteria are assumed to initially increase TEER

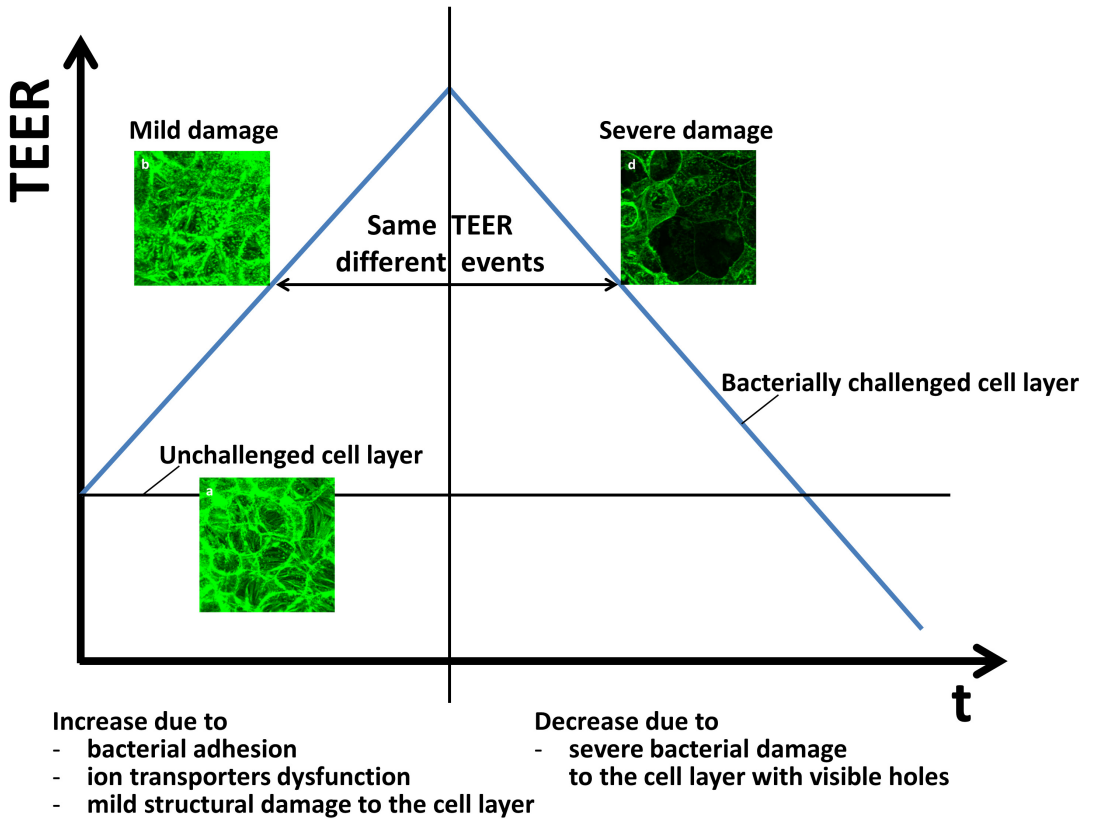

FIGURE 7 | Two-stage damage model to the intestinal epithelial layers during probiotic protection and pathogen challenge. Error bars represent standard errors of the mean over three experiments with separately grown bacteria and cells.

due to their adhesion to the cellular layer directly providing an additional resistance, stimulation of tight-junction protein expression and dysfunctioning of cellular ions transporters. At the same time, bacterial toxins cause mild damage to the epithelial layer. Mild damage is characterized by a less dense structure of the cell layer, in absence of a relation between ion transport, i.e., conductance and dextran permeability.

After longer exposure times, marked by the appearance of a TEER maximum, pathogen challenges cause more severe damage to the cell layer, including apoptosis, widening of tight-junctions and creation of holes that taken together decreases the TEER to below the TEER of an unchallenged epithelial layer. In this severe damage stage, transport of ions (conductance) and dextran (permeability) are linearly related. Probiotic bifidobacteria did not demonstrate this course of events and moreover, all bifidobacterial strains in our study reduced the negative impact of a pathogenic *E. coli* strain on epithelial barrier function, as evidence by a delayed appearance of the second damage stage to the epithelial layer. Therefore, this two-stage damage model provides a more extensive way to explain biological events in an epithelial cell layer during simultaneous probiotic protection and pathogen challenge (**Figure 7**). Adhesion of probiotic bacteria protects epithelial layers against damage by adhering pathogenic *E. coli* is reflected by a delayed occurrence of a lower TEER maximum. However, eventually upon long-term exposure, both probiotic bacteria and pathogenic bacteria may cause damage to the epithelial barrier integrity, as evidenced by a strongly reduced TEER. This is a common observation *in vitro*, both for probiotic bacteria (Kim et al., 2012) as well as for pathogenic strains (Hasan et al., 2018). This may reflect that overdosing of probiotics as a daily intake should be avoided and may lead to diarrhea (Boyle et al., 2006; Williams, 2010). However, the relatively short time period over which both probiotic and pathogenic bacteria cause damage to the epithelial barrier integrity *in vitro* is not reflecting the *in vivo* situation adequately (Deng et al., 2018). *In vivo*, cellular turnover, which is not included in our *in vitro* model employed, will delay the occurrence of these complications.

Our two-stage interpretation of changes in TEER of intestinal epithelial layers, will extend to other pathogens than *E. coli*, including protozoa (Li et al., 1994; Troeger et al., 2007a) and also encompassing the *in vivo* situation (Alaish et al., 2013), for which similar decreases in TEER (Deng et al., 2018; Malago et al., 2003) and increased dextran permeabilities (Alaish et al., 2013) have been described. However, due to difference in virulence between pathogens and the complexity of the *in vivo* situation, the time-frame of the different stages distinguished on the basis of changes TEER may be different. In murine models for example, apoptosis due to a *Clostridium difficile* pathogen challenge occurred already within 2 h (Deng et al., 2018).

Concluding, for proper interpretation of TEER readings and description of the status of cell layers, single-time point reading of TEER is clearly insufficient to describe changes in the epithelial layer and tight-junctions. Events prior to and after the appearance of a maximal TEER are distinctly different, depending whether measured when TEER is increasing toward its maximum or decreasing from it. Moreover, antibiotic treatment could not revert the severe damage to epithelial layers after the occurrence of a TEER maximum. Since probiotic protection delays or inhibits the formation of the TEER maximum depending on the probiotic strain used, probiotics thus elongates the time-window for effective antibiotic treatment of infected intestinal epithelium.

DATA AVAILABILITY STATEMENT

The raw data supporting the conclusions of this article will be made available by the authors, without undue reservation.

AUTHOR CONTRIBUTIONS

LY carried out the experiments under the daily supervision of BP. All authors designed the experiments, analyzed the data, and contributed to manuscript preparation.

FUNDING

This work was funded by the University Medical Center Groningen, Groningen, Netherlands.

SUPPLEMENTARY MATERIAL

The Supplementary Material for this article can be found online at: https://www.frontiersin.org/articles/10.3389/fmicb.2020.599555/full#supplementary-material

REFERENCES

Alaish, S. M., Smith, A. D., Timmons, J., Greenspon, J., Eyvazzadeh, D., Murphy, E., et al. (2013). Gut microbiota, tight junction protein expression, intestinal resistance, bacterial translocation and mortality following cholestasis depend on the genetic background of the host. *Gut Microbiota* 4, 292–305. doi: 10.4161/gmic.24706

Anderson, R. C., Cookson, A. L., McNabb, W. C., Park, Z., McCann, M. J., Kelly, W. J., et al. (2010). *Lactobacillus plantarum* MB452 enhances the function of the intestinal barrier by increasing the expression levels of genes involved in tight junction formation. *BMC Microbiol.* 10:316. doi: 10.1186/1471-2180-10-316

Artursson, P., and Karlsson, J. (1991). Correlation between oral drug absorption in humans and apparent drug permeability coefficients in human intestinal epithelial (Caco-2) cells. *Biochem. Biophys. Res. Commun.* 175, 880–885. doi: 10.1016/0006-291X(91)91647-U

Barnett, A. M., Roy, N. C., Cookson, A. L., and Mcnabb, W. C. (2018). Metabolism of caprine milk carbohydrates by probiotic bacteria and Caco-2: HT29–MTX epithelial co-cultures and their impact on intestinal barrier integrity. *Nutrients* 10:949. doi: 10.3390/nu10070949

Béduneau, A., Tempesta, C., Fimbel, S., Pellequer, Y., Jannin, V., Demarne, F., et al. (2014). A tunable Caco-2/HT29-MTX co-culture model mimicking variable permeabilities of the human intestine obtained by an original seeding procedure. *Eur. J. Pharm. Biopharm.* 87, 290–298. doi: 10.1016/j.ejpb.2014.03.017

Benson, K., Cramer, S., and Galla, H. J. (2013). Impedance-based cell monitoring: barrier properties and beyond. *Fluids Barriers CNS* 10:5. doi: 10.1186/2045-8118-10-5

Bhat, M. I., Sowmya, K., Kapila, S., and Kapila, R. (2019). *Escherichia coli* K12: an evolving opportunistic commensal gut microbe distorts barrier integrity in human intestinal cells. *Microb. Pathog.* 133:103545. doi: 10.1016/j.micpath.2019.103545

Boyle, R. J., Robins-Browne, R. M., and Tang, M. L. K. (2006). Probiotic use in clinical practice: what are the risks? *Am. J. Clin. Nutr* 83, 1256–1264. doi: 10.1093/ajcn/83.6.1256

Busscher, H. J., Van Hoogmoed, C. G., Geertsema-Doornbusch, G. I., Van der Kuijl-Booij, M., and Van der Mei, H. C. (1997). Streptococcus thermophilus and its biosurfactants inhibit adhesion by *Candida* spp. *on silicone rubber*. *Appl. Environ. Microbiol.* 63, 3810–3817. doi: 10.1128/aem.63.10.3810-3817.1997

Butt, B. Y. A. M., Jones, H. C., and Abbott, N. J. (1990). Electrical resistance across the blood-brain barrier in anaesthetized rats: a developmental study. *J. Physiol.* 429, 47–62. doi: 10.1113/jphysiol.1990.sp018243

Buxton, R. (2005). *Blood Agar Plates and Hemolysis Protocols. American Society for Microbiology*. Available online at: https://www.asm.org/getattachment/7ec0de2b-bb16-4f6e-ba07-2aea25a43e76/protocol-2885.pdf (accessed March 23, 2020).

Chander, C. R. S., Lohitnath, T., Kumar, D. J. M., and Kalaichelvan, P. T. (2012). Production and characterization of biosurfactant from *Bacillus subtilis* MTCC441 and its evaluation to use as bioemulsifier for food bio-preservative. *Adv. Appl. Sci. Res.* 3, 1827–1831.

Chen, S., Cheng, A. C., Wang, M. S., and Peng, X. (2008). Detection of apoptosis induced by new type gosling viral enteritis virus *in vitro* through fluorescein annexin V-FITC/PI double labeling. *World J. Gastroentero.* 14, 2174–2178. doi: 10.3748/wjg.14.2174

Chen, S., Einspanier, R., and Schoen, J. (2015). Transepithelial electrical resistance (TEER): a functional parameter to monitor the quality of oviduct epithelial cells cultured on filter supports. *Histochem. Cell Biol.* 144, 509–515. doi: 10.1007/s00418-015-1351-1

Corridoni, D., Pastorelli, L., Mattioli, B., Locovei, S., Ishikawa, D., Arseneau, K. O., et al. (2012). Probiotic bacteria regulate intestinal epithelial permeability in experimental ileitis by a TNF-dependent mechanism. *PLoS One* 7:e42067. doi: 10.1371/journal.pone.0042067

Das, S., Jayaratne, R., and Barrett, K. E. (2018). The role of ion transporters in the pathophysiology of infectious diarrhea. *Cell Mol. Gastroenterol. Hepatol.* 6, 33–45. doi: 10.1016/j.jcmgh.2018.02.009

De Belder, A. N., and Granath, K. (1973). Preparation and properties of fluorescein-labelled dextrans. *Carbohydr. Res.* 30, 375–378. doi: 10.1016/S0008-6215(00)81824-8

de Souza Santos, M., and Orth, K. (2015). Subversion of the cytoskeleton by intracellular bacteria: lessons from *Listeria. Salmonella and Vibrio*. *Cell. Microbiol.* 17, 164–173. doi: 10.1111/cmi.12399

Deng, H., Yang, S., Zhang, Y., Qian, K., Zhang, Z., Liu, Y., et al. (2018). *Bacteroides fragilis* prevents *Clostridium difficile* infection in a mouse model by restoring gut barrier and microbiome regulation. *Front. Microbiol.* 9:2976. doi: 10.3389/fmicb.2018.02976

Engels-Deutsch, M., Rizk, S., and Haïkel, Y. (2011). *Streptococcus mutans* antigen I/II binds to α5β1 integrins via its A-domain and increases β1 integrins expression on periodontal ligament fibroblast cells. *Arch. Oral Biol.* 56, 22–28. doi: 10.1016/j.archoralbio.2010.08.010

Fajdiga, S., Koninkx, J. F. J. G., Tooten, P. C. J., and Marinšek-Logar, R. (2006). Interference of *Salmonella enteritidis* and *Lactobacillus* spp. *with IL*-8 levels and transepithelial electrical resistance of enterocyte-like Caco-2 cells. *Folia Microbiol.* 51, 268–272. doi: 10.1007/BF02931810

Franco, I. S., and Shuman, H. A. (2012). A pathogen's journey in the host cell: bridges between actin and traffic. *Bioarchitecture* 2, 38–42. doi: 10.4161/bioa.20422

Gareau, M. G., Sherman, P. M., and Walker, W. A. (2010). Probiotics and the gut microbiota in intestinal health and disease. *Nat. Rev. Gastroenterol. Hepatol.* 7, 503–514. doi: 10.1038/nrgastro.2010.117

Gill, R. K., Hecht, G., Dudeja, P. K., Clayburgh, D. R., Saksena, S., and Zaheer, A. (2007). Mechanism underlying inhibition of intestinal apical Cl-/OH- exchange

following infection with enteropathogenic E . *coli*. *J. Clin. Invest.* 117, 428–437. doi: 10.1172/JCI29625

Groschwitz, K. R., and Hogan, S. P. (2009). Intestinal barrier function: molecular regulation and disease pathogenesis. *J. Allergy Clin. Immunol.* 124, 3–20. doi: 10.1016/j.jaci.2009.05.038

Hasan, S., Sebo, P., and Osicka, R. (2018). A guide to polarized airway epithelial models for studies of host–pathogen interactions. *FEBS J.* 285, 4343–4358. doi: 10.1111/febs.14582

Hill, C., Guarner, F., Reid, G., Gibson, G. R., Merenstein, D. J., Pot, B., et al. (2014). Expert consensus document: the international scientific association for probiotics and prebiotics consensus statement on the scope and appropriate use of the term probiotic. *Nat. Rev. Gastroenterol. Hepatol.* 11, 506–514. doi: 10.1038/nrgastro.2014.66

Hodges, K., Alto, N. M., Ramaswamy, K., Dudeja, P. K., and Hecht, G. (2008). The enteropathogenic *Escherichia coli* effector protein EspF decreases sodium hydrogen exchanger 3 activity. *Cell Microbiol.* 10, 1735–1745. doi: 10.1111/j.1462-5822.2008.01163.x

Hubatsch, I., Ragnarsson, E. G. E., and Artursson, P. (2007). Determination of drug permeability and prediction of drug absorption in Caco-2 monolayers. *Nat. Protoc.* 2, 2111–2119. doi: 10.1038/nprot.2007.303

Kim, H. J., Huh, D., Hamilton, G., and Ingber, D. E. (2012). Human gut-on-a-chip inhabited by microbial flora that experiences intestinal peristalsis-like motions and flow. *Lab Chip* 12, 2165–2174. doi: 10.1039/c2lc40074j

Kim, M., Ogawa, M., Fujita, Y., Yoshikawa, Y., Nagai, T., Koyama, T., et al. (2009). Bacteria hijack integrin-linked kinase to stabilize focal adhesions and block cell detachment. *Nature* 459, 578–582. doi: 10.1038/nature07952

Krug, S. M., Fromm, M., and Günzel, D. (2009). Two-path impedance spectroscopy for measuring paracellular and transcellular epithelial resistance. *Biophys. J.* 97, 2202–2211. doi: 10.1016/j.bpj.2009.08.003

Kwok, D. Y., Vollhardt, D., Miller, R., Li, D., and Neumann, A. W. (1994). Axisymmetric drop shape analysis as a film balance. *Colloids Surf. A Physicochem. Eng. Asp.* 88, 51–58. doi: 10.1016/0927-7757(94)80085-5

LeBlanc, J. J. (2003). Implication of virulence factors in *Escherichia coli* O157:H7 pathogenesis. *Crit. Rev. Microbiol.* 29, 277–296. doi: 10.1080/713608014

Lépine, A. F. P., De Wit, N., Oosterink, E., Wichers, H., Mes, J., and De Vos, P. (2018). *Lactobacillus acidophilus* attenuates *Salmonella*-induced stress of epithelial cells by modulating tight-junction genes and cytokine responses. *Front. Microbiol.* 9:1439. doi: 10.3389/fmicb.2018.01439

Li, E., Stenson, W. F., Kunz-Jenkins, C., Swanson, P. E., Duncan, R., and Stanley, S. L. (1994). *Entamoeba histolytica* interactions with polarized human intestinal Caco-2 epithelial cells. *Infect. Immun.* 62, 5112–5119. doi: 10.1128/iai.62.11.5112-5119.1994

Ling, X., Linglong, P., Weixia, D., and Hong, W. (2016). Protective effects of bifidobacterium on intestinal barrier function in LPS-induced enterocyte barrier injury of Caco-2 monolayers and in a rat NEC model. *PLoS One* 11:e0161635. doi: 10.1371/journal.pone.0161635

Lippmann, E. S., Azarin, S. M., Kay, J. E., Nessler, R. A., Wilson, H. K., Al-Ahmad, A., et al. (2012). Derivation of blood-brain barrier endothelial cells from human pluripotent stem cells. *Nat. Biotechnol.* 30, 783–791. doi: 10.1038/nbt.2247

Maherally, Z., Fillmore, H. L., Tan, S. L., Tan, S. F., Jassam, S. A., Quack, F. I., et al. (2018). Real-time acquisition of transendothelial electrical resistance in an all-human, *in vitro*, 3-dimensional, blood–brain barrier model exemplifies tight-junction integrity. *FASEB J.* 32, 168–182. doi: 10.1096/fj.201700162R

Malago, J. J., Koninkx, J. F. J. G., Ovelgönne, H. H., Asten, F. J. A. M., Van Swennenhuis, J. F., and Van Dijk, J. E. (2003). Expression levels of heat shock proteins in enterocyte-like Caco-2 cells after exposure to *Salmonella enteritidis*. *Cell Stress Chaperones* 8, 194–203. doi: 10.1379/1466-1268(2003)008<0194:elohsp>2.0.co;2

Michail, S., and Abernathy, F. (2002). *Lactobacillus plantarum* reduces the in vitro secretory response of intestinal epithelial cells to enteropathogenic *Escherichia coli* infection. *J. Pediatr. Gastr. Nutr.* 35, 350–355. doi: 10.1097/01.mpg.0000025389.13337.3f

Odijk, M., Van der Meer, A. D., Levner, D., Kim, H. J., Van der Helm, M. W., Segerink, L. I., et al. (2015). Measuring direct current trans-epithelial electrical resistance in organ-on-a-chip microsystems. *Lab Chip* 15, 745–752. doi: 10.1039/c4lc01219d

Ohland, C. L., and MacNaughton, W. K. (2010). Probiotic bacteria and intestinal epithelial barrier function. *Am. J. Physiol.* 298, G807–G819. doi: 10.1152/ajpgi.00243.2009

Ouwehand, A. C., Forssten, S., Hibberd, A. A., Lyra, A., and Stahl, B. (2016). Probiotic approach to prevent antibiotic resistance. *Ann. Med.* 48, 246–255. doi: 10.3109/07853890.2016.1161232

Parolin, C., Frisco, G., Foschi, C., Giordani, B., Salvo, M., Vitali, B., et al. (2018). *Lactobacillus crispatus* BC5 interferes with *Chlamydia trachomatis* infectivity through integrin modulation in cervical cells. *Front. Microbiol.* 9:2630. doi: 10.3389/fmicb.2018.02630

Putaala, H., Salusjärvi, T., Nordström, M., Saarinen, M., Ouwehand, A. C., Hansen, E. B., et al. (2008). Effect of four probiotic strains and *Escherichia coli* O157:H7 on tight junction integrity and cyclo-oxygenase expression. *Res. Microbiol.* 159, 692–698. doi: 10.1016/j.resmic.2008.08.002

Ramos, C. L., Thorsen, L., Schwan, R. F., and Jespersen, L. (2013). Strain-specific probiotics properties of *Lactobacillus fermentum*, *Lactobacillus plantarum* and *Lactobacillus brevis* isolates from Brazilian food products. *Food Microbiol.* 36, 22–29. doi: 10.1016/j.fm.2013.03.010

Reid, G., Younes, J. A., Van der Mei, H. C., Gloor, G. B., Knight, R., and Busscher, H. J. (2011). Microbiota restoration: natural and supplemented recovery of human microbial communities. *Nat. Rev. Microbiol.* 9, 27–38. doi: 10.1038/nrmicro2473

Rivardo, F., Turner, R. J., Allegrone, G., Ceri, H., and Martinotti, M. G. (2009). Anti-adhesion activity of two biosurfactants produced by *Bacillus* spp. *prevents biofilm formation of human bacterial pathogens*. *Appl. Microbiol. Biotechnol.* 83, 541–553. doi: 10.1007/s00253-009-1987-7

Schindelin, J., Arganda-Carreras, I., Frise, E., Kaynig, V., Longair, M., Pietzsch, T., et al. (2012). Fiji: an open-source platform for biological-image analysis. *Nat. Methods* 9, 676–682. doi: 10.1038/nmeth.2019

Sharma, D., and Saharan, B. S. (2014). Simultaneous production of biosurfactants and bacteriocins by probiotic *Lactobacillus casei* MRTL3. *Int. J. Microbiol.* 2014:698713. doi: 10.1155/2014/698713

Shinoda, T., Shinya, N., Ito, K., Ohsawa, N., Terada, T., Hirata, K., et al. (2016). Structural basis for disruption of claudin assembly in tight junctions by an enterotoxin. *Sci. Rep.* 6:33632. doi: 10.1038/srep33632

Suzuki, H., Tani, K., and Fujiyoshi, Y. (2017). Crystal structures of claudins: insights into their intermolecular interactions. *Ann. N.Y. Acad. Sci.* 1397, 25–34. doi: 10.1111/nyas.13371

Troeger, H., Epple, H.-J., Schneider, T., Wahnschaffe, U., Ullrich, R., Burchard, G.-D., et al. (2007a). Effect of chronic *Giardia lamblia* infection on epithelial transport and barrier function in human duodenum. *Gut* 56, 328–335. doi: 10.1136/gut.2006.100198

Troeger, H., Richter, J. F., Beutin, L., Günzel, D., Dobrindt, U., Epple, H.-J., et al. (2007b). *Escherichia coli* α-haemolysin induces focal leaks in colonic epithelium: a novel mechanism of bacterial translocation. *Cell. Microbiol.* 9, 2530–2540. doi: 10.1111/j.1462-5822.2007.00978.x

Turner, J. R., Black, E. D., Ward, J., Tse, C.-M., Uchwat, F. A., Alli, H. A., et al. (2000). Transepithelial resistance can be regulated by the intestinal brush-border Na+/ H+ exchanger NHE3. *Am. J. Physiol. Cell Physiol.* 279, C1918–C1924.

Van der Helm, M. W., Odijk, M., Frimat, J. P., Van der Meer, A. D., Eijkel, J. C. T., Van den Berg, A., et al. (2016). Direct quantification of transendothelial electrical resistance in organs-on-chips. *Biosens. Bioelectron.* 85, 924–929. doi: 10.1016/j.bios.2016.06.014

Van der Vegt, W., Van der Mei, H. C., Noordmans, J., and Busscher, H. J. (1991). Assessment of bacterial biosurfactant production through axisymmetric drop shape analysis by profile. *Appl. Microbiol. Biotechnol.* 35, 766–770. doi: 10.1007/BF00169892

Van Hoogmoed, C. G., Van der Mei, H. C., and Busscher, H. J. (2004). The influence of biosurfactants released by *S. mitis BMS on the adhesion of pioneer strains and cariogenic bacteria*. *Biofouling* 20, 261–267. doi: 10.1080/08927010400027050

Velraeds, M. M. C., Van de Belt-Gritter, B., Busscher, H. J., Reid, G., and Van der Mei, H. C. (2000). Inhibition of uropathogenic biofilm growth on silicone rubber in human urine by lactobacilli - A teleologic approach. *World J. Urol.* 18, 422–426. doi: 10.1007/PL00007084

Velraeds, M. M. C., Van de Belt-Gritter, B., Van der Mei, H. C., Reid, G., and Busscher, H. J. (1998). Interference in initial adhesion of uropathogenic bacteria and yeasts to silicone rubber by a *Lactobacillus acidophilus*

biosurfactant. *J. Med. Microbiol.* 47, 1081–1085. doi: 10.1099/00222615-47-12-1081

Velraeds, M. M. C., Van der Mei, H. C., Reid, G., and Busscher, H. J. (1996). Inhibition of initial adhesion of uropathogenic *Enterococcus faecalis* by biosurfactants from *Lactobacillus* isolates. *Appl. Environ. Microbiol.* 62, 1958–1963. doi: 10.1128/aem.62.6.1958-1963.1996

Velraeds, M. M. C., Van der Mei, H. C., Reid, G., and Busscher, H. J. (1997). Inhibition of initial adhesion of uropathogenic *Enterococcus faecalis* to solid substrata by an adsorbed biosurfactant layer from *Lactobacillus acidophilus*. *Urology* 49, 790–794. doi: 10.1016/S0090-4295(97)00065-4

Wang, B., Yurecko, R. S., Dedhar, S., and Cleary, P. P. (2006). Integrin-linked kinase is an essential link between integrins and uptake of bacterial pathogens by epithelial cells. *Cell. Microbiol.* 8, 257–266. doi: 10.1111/j.1462-5822.2005.00618.x

Williams, N. T. (2010). Clinical review: probiotics. *Am. J. Health. Syst. Pharm.* 67, 449–458. doi: 10.2146/ajhp090168

Wypych, T. P., and Marsland, B. J. (2018). Antibiotics as instigators of microbial dysbiosis: implications for asthma and allergy. *Trends Immunol.* 39, 697–711. doi: 10.1016/j.it.2018.02.008

Yue, C., Van der Mei, H. C., Kuijer, R., Busscher, H. J., and Rochford, E. T. J. (2015). Mechanism of cell integration on biomaterial implant surfaces in the presence of bacterial contamination. *J. Biomed. Mater. Res. A* 103, 3590–3598. doi: 10.1002/jbm.a.35502

Zeng, J., Jiang, J., Zhu, W., and Chu, Y. (2016). Heat-killed yogurt-containing lactic acid bacteria prevent cytokine-induced barrier disruption in human intestinal Caco-2 cells. *Ann. Microbiol.* 66, 171–178. doi: 10.1007/s13213-015-1093-2

Zmora, N., Zilberman-Schapira, G., Suez, J., Mor, U., Dori-Bachash, M., Bashiardes, S., et al. (2018). Personalized gut mucosal colonization resistance to empiric probiotics is associated with unique host and microbiome features. *Cell* 174, 1388–1405. doi: 10.1016/j.cell.2018.08.041

Conflict of Interest: HB is director of a consulting company SASA BV.

The remaining authors declare that the research was conducted in the absence of any commercial or financial relationships that could be construed as a potential conflict of interest. Opinions and assertions contained herein are those of the authors and are not construed as necessarily representing views of the funding organization or their respective employer(s).

frontiers in Microbiology

REVIEW
published: 04 February 2021
doi: 10.3389/fmicb.2021.609418

Plant Glycan Metabolism by Bifidobacteria

Sandra M. Kelly[1], Jose Munoz-Munoz[2] and Douwe van Sinderen[1]**

[1] School of Microbiology and APC Microbiome Ireland, University College Cork, Cork, Ireland, [2] Microbial Enzymology Group, Department of Applied Sciences, Northumbria University, Newcastle upon Tyne, United Kingdom

Members of the genus *Bifidobacterium*, of which the majority have been isolated as gut commensals, are Gram-positive, non-motile, saccharolytic, non-sporulating, anaerobic bacteria. Many bifidobacterial strains are considered probiotic and therefore are thought to bestow health benefits upon their host. Bifidobacteria are highly abundant among the gut microbiota of healthy, full term, breast-fed infants, yet the relative average abundance of bifidobacteria tends to decrease as the human host ages. Because of the inverse correlation between bifidobacterial abundance/prevalence and health, there has been an increasing interest in maintaining, increasing or restoring bifidobacterial populations in the infant, adult and elderly gut. In order to colonize and persist in the gastrointestinal environment, bifidobacteria must be able to metabolise complex dietary and/or host-derived carbohydrates, and be resistant to various environmental challenges of the gut. This is not only important for the autochthonous bifidobacterial species colonising the gut, but also for allochthonous bifidobacteria provided as probiotic supplements in functional foods. For example, *Bifidobacterium longum* subsp. *longum* is a taxon associated with the metabolism of plant-derived poly/oligosaccharides in the adult diet, being capable of metabolising hemicellulose and various pectin-associated glycans. Many of these plant glycans are believed to stimulate the metabolism and growth of specific bifidobacterial species and are for this reason classified as prebiotics. In this review, bifidobacterial carbohydrate metabolism, with a focus on plant poly-/oligosaccharide degradation and uptake, as well as its associated regulation, will be discussed.

Keywords: bifidobacteria, plant glycans, plant oligosaccharides, fiber, glycosyl hydrolase, CAZy enzymes, carbohydrate metabolism

OPEN ACCESS

Edited by:
Michael Gänzle,
University of Alberta, Canada

Reviewed by:
David Andrew Mills,
University of California System, United States
Christian U. Riedel,
University of Ulm, Germany

****Correspondence:***
Sandra M. Kelly
115224042@umail.ucc.ie
Douwe van Sinderen
d.vansinderen@ucc.ie

Specialty section:
This article was submitted to Food Microbiology, a section of the journal Frontiers in Microbiology

Received: *28 September 2020*
Accepted: *04 January 2021*
Published: *04 February 2021*

Citation:
Kelly SM, Munoz-Munoz J and van Sinderen D (2021) Plant Glycan Metabolism by Bifidobacteria. Front. Microbiol. 12:609418. doi: 10.3389/fmicb.2021.609418

INTRODUCTION

Bifidobacteria are gut commensals and members of the Actinobacteria phylum harbouring genomes with a relatively high G + C content (considered approximately 50% or higher) (Ventura et al., 2007). They have been isolated from the gastrointestinal tract (GIT) of many mammalian species, including humans, as well as of insects and birds (Milani et al., 2016). Certain bifidobacterial strains or species, such as *Bifidobacterium longum* subsp. *longum*, are considered probiotic and are associated with various health benefits to the host, such as pathogen protection, including production of acetate to protect against enteropathogenic infection (Fukuda et al., 2011), sequestration of iron at the detriment of gut pathogens (Vazquez-Gutierrez et al., 2016), competing for epithelial binding sites with pathogens (Vazquez-Gutierrez et al., 2016), immune modulation through exopolysaccharide

production (EPS) (Schiavi et al., 2016), alleviation of Irritable Bowel Syndrome (IBS) symptoms when supplied as a probiotic (Whorwell et al., 2006), and reducing the risk of contracting rotaviral diarrhea (Munoz et al., 2011). Bifidobacteria are known to metabolize a large number of glycans found in the gut environment. These glycans are metabolized through a unique pathway for carbohydrate fermentation which is termed the fructose-6-phosphoketolase (F6PK) pathway or 'Bifid Shunt' (de Vries and Stouthamer, 1967), which together with their distinctively high G + C content, above 50%, justified their taxonomic classification as a separate genus unrelated to lactic acid bacteria. The first bifidobacterial genome sequence, i.e., that of *B. longum* subsp. *longum* NCC2705, was published in 2002 (Schell et al., 2002), and its genome annotation reported a large number of genes dedicated to carbohydrate metabolism.

Bifidobacteria are highly prevalent in the infant gut and in particular the stool of breast-fed infants exhibit a significantly higher bifidobacterial abundance compared to their non-breast-fed counterparts (Bäckhed et al., 2015; Stewart et al., 2018). Human breast milk has been shown to contain viable bifidobacterial and is rich in so-called human milk oligosaccharides (HMOs) (Martín et al., 2009; Soto et al., 2014), which are highly specific growth substrates for particular bifidobacteria (Arboleya et al., 2011; James et al., 2016). It has also been found that the cessation of breast feeding and introduction to solid foods, referred to as weaning, is thought to induce changes to a more adult-like microbiome in infants (Bäckhed et al., 2015; Stewart et al., 2018). The relative abundance of bifidobacteria has been shown to decrease following weaning, and from adolescence into adulthood, with a further decline when their hosts become elderly (Hill et al., 2010; Odamaki et al., 2016).

Furthermore, the bifidobacterial species that are present in the human gut may vary depending on host age. One study reported that the *B. longum* subsp. *longum* taxon is associated with both the adult and infant gut, whilst *Bifidobacterium breve* is more frequently associated with the infant gut (Kato et al., 2017). In contrast, another study reported that *B. longum* subsp. *longum* and *B. breve* were associated with both the adult and infant gut (Turroni et al., 2009, 2012a; Odamaki et al., 2018). *Bifidobacterium dentium* has been found to be in higher abundance in the elderly gut although its natural niche is believed to be the oral cavity (Ouwehand et al., 2008). The type of sample taken for microbiota analysis, for instance colonic mucosal sample or stool sample, may determine which bifidobacterial species is more likely to be identified. However; another reason to explain why particular species of bifidobacteria are more prevalent and/or abundant in the infant or adult gut may be that they are specialized to metabolize specific dietary carbohydrates. For example, *B. breve* and *Bifidobacterium kashiwanohense* are generally capable of metabolising (certain) HMOs (Bunesova et al., 2016; James et al., 2016), whilst *B. longum* subsp. *longum* is specialized in the metabolism of particular plant glycans found in the adult diet (Schell et al., 2002; Riviere et al., 2018). *B. longum* subsp. *longum* strains have also been shown to encode members of glycosyl hydrolase (GH) families associated with the utilization of plant-derived carbohydrates (i.e., GH43, GH10, and GH5), reflecting their adaptation to plant glycan metabolism (Arboleya et al., 2018; Blanco et al., 2020).

A detailed understanding of carbohydrate metabolism of a particular bifidobacterial species and/or strains may offer opportunities to increase its abundance in the adult gut by dietary means. One way to positively modulate the gut microbiota is by the supplementation of so-called prebiotics, where a prebiotic is defined as 'a substrate that is selectively utilized by host microorganisms conferring a health benefit' (Gibson et al., 2017). Prebiotics that specifically stimulate bifidobacterial growth are termed 'bifidogenic' (Gibson and Roberfroid, 1995; Gibson et al., 1995). Knowledge on which plant carbohydrates can be metabolized by a bifidobacterial species/strain may therefore offer an opportunity to increase the abundance of bifidobacteria in the adult gut. For instance, *Bifidbacterium longum* subsp. *infantis* is associated with the infant gut, and is specialized in HMO metabolism, whilst *B. longum* subsp. *longum*, associated with both the infant and adult gut, can metabolize plant-derived oligosaccharides (O'Callaghan et al., 2015; Odamaki et al., 2018). This review will in particular focus on current knowledge regarding bifidobacterial plant-derived poly/oligosaccharide metabolism.

THE PLANT GLYCANS PRESENT IN THE GUT

Dietary fibers/glycans are found in the plant cell wall (**Figure 1**; Koropatkin et al., 2012) and are common components in cereals (Broekaert et al., 2011; Shewry and Hey, 2015), fruit (van Laere et al., 2000; Posé et al., 2018), vegetables (Jonker et al., 2020; Klaassen and Trindade, 2020) and red grapes (Apolinar-Valiente et al., 2013), thus being a typical constituent of the human diet. Dietary fibers/glycans are metabolized by the gut microbiota in the large intestine (Flint et al., 2012). In contrast, meta-transcriptomic data from the microbiota in the small intestine shows, that phosphotransferase systems for simple sugars such as fructose, glucose and sucrose are utilized for carbohydrate metabolism suggesting that the small intestine microbiota utilize simpler sugars and not dietary fibers/glycans (Zoetendal et al., 2012). Some examples of dietary glycans are fructo-oligosaccharides (FOS), β-glucan, inulin, pectin, arabinoxylan, xylan, arabinan and starch (Holscher, 2017). Dietary fibers represent polymeric carbohydrates, including lignin, consisting of ten or more monomeric subunits that cannot be hydrolysed by enzymes found in the upper part of the human gastrointestinal tract (such as lactases, amylases and sucrases) (Alimentarius, 2010). Plant carbohydrate polymers with a size less than 10 monomeric subunits, but between a degree of polymerisation (DP) of 3 and 9, may in certain jurisdictions also be classified as dietary fibers (Alimentarius, 2010). Glycan is a much broader term that refers to a wide variety of carbohydrates (polymers and oligosaccharides). Glycans of dietary origin are generally indigestible to the human host, yet may be metabolized by the gut microbiota, and may include carbohydrates with less than 10 monomeric units that have been generated by the gut microbiota following dietary fiber degradation (Koropatkin et al., 2012).

The plant cell wall consists of a matrix comprized of cellulose fibrils, hemicellulose, pectin and lignin (Flint et al., 2012). Hemicelluloses are polysaccharides with β-1,4-linked backbones

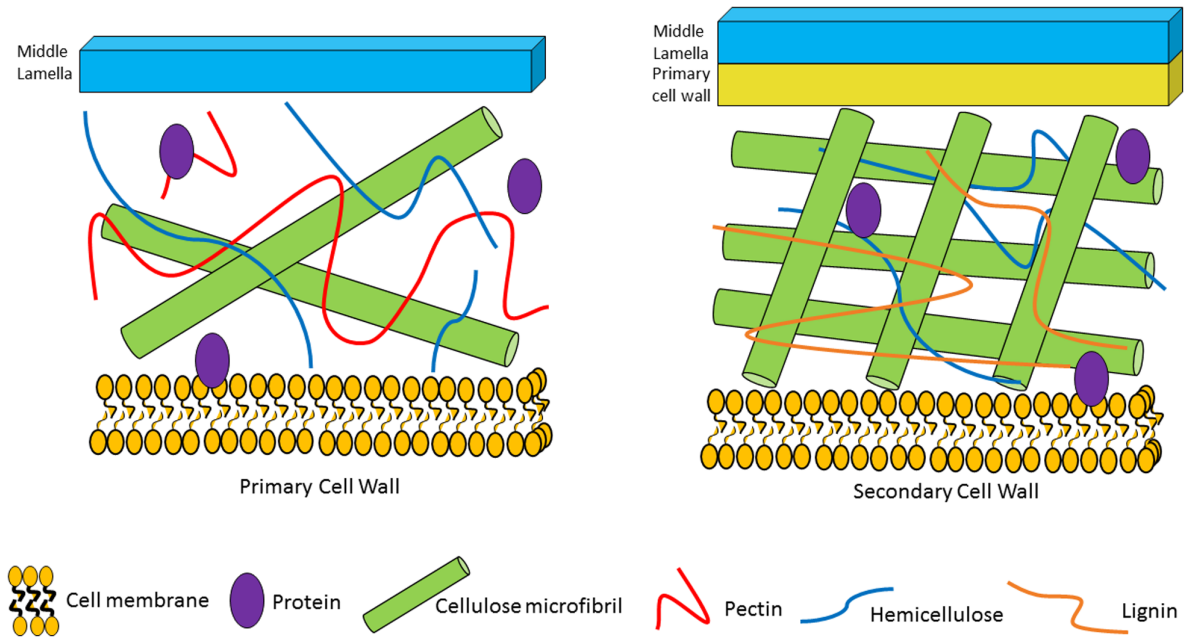

FIGURE 1 | Plant cell wall composition and associated plant glycans/fibers. The primary cell wall is located outside of the plant plasma cell membrane. It is composed of cellulose microfibrils, hemicellulose and pectin. The secondary cell wall is located between the primary cell wall and the plasma cell wall. It consists of cellulose microfibrils, hemicellulose and lignin.

of xylose, mannose or glucose, to form (arabino)xylan (AX), mannan, and xyloglucan or β-glucan, respectively (**Figure 2**; Scheller and Ulvskov, 2010; Flint et al., 2012). In this review we focus on AX and arabinoxylo-oligosaccahrides (AXOS) metabolism. Lignin is predominantly composed of polymerised phenolic compounds such as hydroxycinnamic acids (HCA) (Struijs et al., 2008; Scheller and Ulvskov, 2010). Pectin is composed of various, highly variable polysaccharides including homogalacturonan (HG), xylogalacturonan, apiogalacturonan, rhamnogalacturonan I (RGI) and rhamnogalacturonan II (RGII) (**Figure 3**; Harholt et al., 2010). These pectic polysaccharides all contain an α-1,4-linked galacturonic acid backbone (Mohnen, 2008). HG is the simplest pectic polysaccharide, consisting of unsubstituted α-1,4-linked galacturonic acid moieties, whilst RGI is associated with an α-1,4-linked, D-galacturonic acid and rhamnose-containing backbone which can be substituted by other polymers such as galactan, arabinogalactan and arabinan (Anderson, 2015). RGII is the most complex chain, with a HG backbone that can be substituted with over twenty different glycosyl linkages and five different side chains (O'Neill et al., 2007). Both hemicellulose and pectic carbohydrates may also be decorated with HCAs such as ferulic acid or chlorogenic acid (Agger et al., 2010).

It is important to note that it is unlikely that in the gut bifidobacteria can metabolize these large, mostly insoluble complex plant polysaccharides on their own; however, they may be able to utilize specific components and/or side chains of these glycans. Alternatively, it is possible that these plant-derived polysaccharides arrive in the large intestine undigested, where they are degraded by particular, so-called keystone species. Examples of such keystone species include *Bacteroides cellulosilyticus, Bacteroides caccae*, and *Dysgonomonas gadei*, which for example are capable of the degradation of type II arabinogalactan due to their extracellular endo-β-1,3-galactanase activity (Cartmell et al., 2018). This extracellular degradation allows the release of soluble oligosaccharides, such as arabino-oligosaccharides (AOS), AXOS, and galacto-oligosaccharides which may then become available as metabolic 'cross-feeding' substrates for other gut commensals, such as bifidobacteria. For example, *B. breve* UCC2003 can cross-feed on certain galacto-oligosaccharides released from larch wood arabinogalactan by *Ba. cellulosilyticus* (Munoz et al., 2020). Therefore, the current definition of a prebiotic does not include glycans, such as intact pectin or xylan, which may stimulate growth of a broad range of species in the GIT (Gibson et al., 2017). Knowledge on carbohydrate metabolism of bifidobacteria can therefore be exploited to develop prebiotics and/or 'synbiotics' [a combination of a probiotic organism and a corresponding prebiotic that selectively stimulates growth of the administered probiotic, and therefore its associated beneficial effect(s)] (van Zanten et al., 2012; Kearney and Gibbons, 2018; Swanson et al., 2020).

THE BIFID SHUNT – A UNIQUE CARBOHYDRATE METABOLIC PATHWAY

As mentioned above, bifidobacteria possess a unique pathway for carbohydrate assimilation which is termed the F6PK pathway (de Vries and Stouthamer, 1967, 1968). This complex pathway, with its key enzyme fructose-6-phosphoketolase, is very

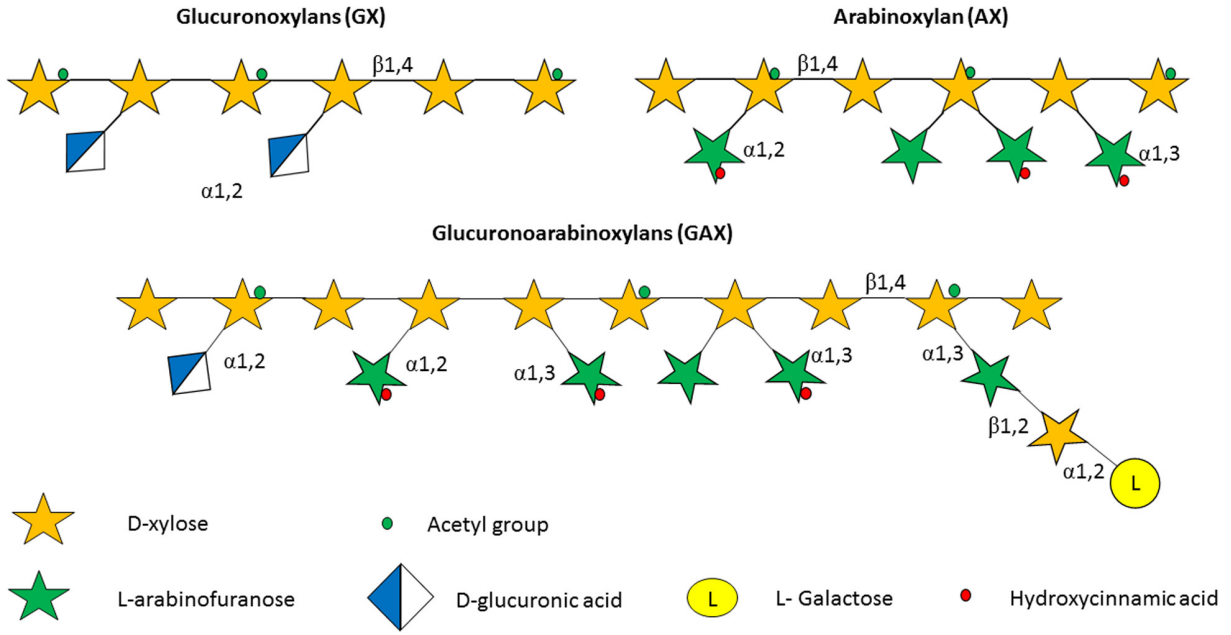

FIGURE 2 | Structure of some of the hemicelluloses found in the plant cell wall. Hemicelluloses consist of a xylan backbone composed of β-1,4-linked D-xylose moieties, some of which may be substituted with an acetyl group. In glucoronoxylan (GX) the xylan backbone is substituted with D-glucuronic acid, while in the case of arabinoxylan (AX) the carbohydrate decorations consist of α-1,2-linked and/or α-1,3-linked arabinofuranose moieties. Finally, the glycan backbone of glucoronoarabinoxylan (GAX) possesses arabinose substitutions as in AX, in addition to D-glucuronic acid decorations that are α-1,2-linked to the xylan backbone, as well as D-xylose and L-galactose moieties that are β-1,2 linked and α-1,2-linked, respectively, to the arabinose substitutions.

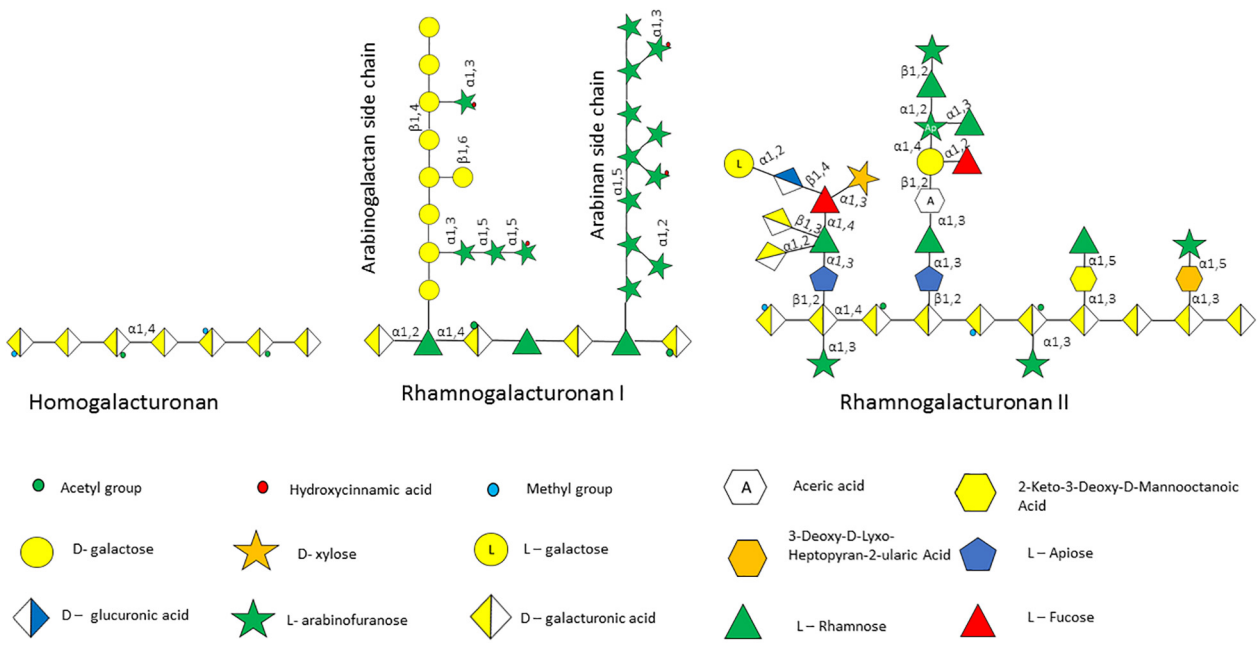

FIGURE 3 | Pectin polysaccharides associated with the plant cell wall. Pectin is made up of several polysaccharides including homogalacturonan, rhamnogalacturonan I and rhamnogalacturonan II, the structure of which is schematically depicted.

distinct from the homofermentative (Embden-Meyerhof-Parnas) or heterofermentative (phosphoketolase or pentose phosphate) glycolytic pathways (Macfarlane and Macfarlane, 2003; Mayo and van Sinderen, 2010) and is exclusively found in the *Bifidobacteriaceae* family and members of the *Coriobacteriales* order (Palframan et al., 2003; Killer et al., 2010; Gupta et al.,

2017). The F6PK pathway can assimilate both hexose and pentose sugars by fermentation into lactate and acetate (Egan and Van Sinderen, 2018), with a theoretical yield of 1.5 mol acetate and 1 mol of lactate for every mol of glucose consumed (de Vries and Stouthamer, 1967; Wolin et al., 1998), or a 1:1 ratio of lactate and acetate in the case of pentose sugar fermentation (Palframan et al., 2003). Hexose sugars are fed into the F6PK pathway as fructose-6-phosphate whilst pentose sugars can enter the pathway as ribulose-5-phosphate or xylulose-5-phosphate (Egan and Van Sinderen, 2018). However, the actual ratio of acetate to lactate produced depends on various factors including the individual strain, pH and growth rate, which in turn differs depending on the carbohydrate substrate utilized (Palframan et al., 2003; Watson et al., 2013; McLaughlin et al., 2015). The short chain fatty acid (SCFA) acetate, when produced by *B. longum* subsp. *longum* from fructose fermentation, has been shown to generate anti-inflammatory effects and/or to block epithelial apoptosis in a murine model, thereby preventing translocation of the Shiga toxin produced by *Escherichia coli* O157:H7 into the bloodstream, and in this way providing protection against this gut pathogen (Fukuda et al., 2011). In addition, lactate, an organic acid (but not a SCFA), has also been shown to have a direct effect on enterocyte proliferation and contributes to hyperproliferation of enterocytes after starvation in a mouse model thus supporting intestinal barrier integrity (Okada et al., 2013). The F6PK pathway theoretically produces 2.5 molecules of ATP per 1 metabolized glucose molecule, which is higher than the energy yield of homofermentation by lactobacilli species at 2 molecules of ATP per 1 molecule of glucose metabolized (Palframan et al., 2003).

BIFIDOBACTERIAL CARBOHYDRATE IMPORT

Bifidobacteria are capable of metabolizing a diverse range of mono-, di-, and oligo-saccharides found in the GIT environment, which they mainly import into their cytoplasm by means of so-called ABC-type (ATP-binding cassette) transporters or major facilitator superfamily (MFS) transport systems, such as proton symporters and proton-motive force-driven permeases (Schell et al., 2002; Pokusaeva et al., 2011a). Furthermore, most bifidobacterial species encode Phosphoenol Pyruvate-Phosphotransferase Systems (PEP-PTSs) (Maze et al., 2007; Turroni et al., 2012b). However, ABC-type transporters generally are the most commonly employed systems to internalize carbohydrates in bifidobacteria. For example, *B. longum* subsp. *longum* NCC2705 is predicted to encode 13 ABC type transporters, 3 MFS transporters, 1 PTS system, 1 glycoside pentoside cation symporter family transporter (GPH) and 1 major intrinsic protein family (MIP) transporter (Parche et al., 2007). Similarly, *Bifidobacterium longum* subsp. *infantis* ATCC15697 is predicted to encode 13 ABC transporter systems (Sela et al., 2008). However, there are exceptions; as a representative of its species *Bifidobacterium bifidum* PRL2010 preferentially utilizes PEP-PTS systems to import carbohydrates, most likely because this strain degrades complex carbohydrates extracellularly, thereby releasing mostly monosaccharides, explaining why PRL2010 encodes just two ABC-type transporters and four PEP-PTS systems (Turroni et al., 2012b). ABC-type transporters hydrolyse ATP in order to import their substrate, such as a carbohydrate, against a chemical gradient (Wilkens, 2015). An ABC-type transport system typically consists of two transmembrane-associated proteins, which act as permeases to translocate the substrate across the membrane and two ATP-binding proteins that provide the energy required for transport (Rees et al., 2009). The so-called substrate binding protein (SBP) binds a specific carbohydrate monomer or oligosaccharide (or very related substrates) and brings the substrate to the permease to be imported (Rees et al., 2009). This can affect the growth rate of a strain; for instance, the SBP of an ABC-type transporter specified by *Bifidobacterium animalis* subsp. *lactis* B1-04 binds preferentially to β-1,6-galactobiose over β-1,4-galactobiose, and this may in part contribute to faster growth of this strain on the former substrate (Theilmann et al., 2019). The heavy reliance on carbohydrate-specific ABC-type transporters by bifidobacteria for internalization of their carbon and energy sources may reflect the need for members of this genus to be versatile in metabolizing a diverse range of carbohydrates, including various plant-derived oligosaccharides present in the gut environment (Schneider, 2001; Chandravanshi et al., 2019), rather than relying on PEP-PTSs, which are mainly restricted to monosaccharide utilization (Deutscher et al., 2006). For example, an ABC-type transporter was found to confer the ability of *B. animalis* subsp. *lactis* B1-04 to metabolize the tri-saccharide raffinose (and related oligosaccharides) and this strain was able to outcompete *Bacteroides ovatus* when both strains are co-cultured on raffinose (Ejby et al., 2016).

ENZYMATIC DEGRADATION OF PLANT-OLIGOSACCHARIDES BY BIFIDOBACTERIA

A relatively high percentage, 13.7%, of the overall *Bifidobacterium* pan-genome is dedicated to carbohydrate metabolism (Milani et al., 2014, 2016), and a similar percentage, 13.23 and 12.5%, when representative genomes of *B. breve* and *B. longum* subsp. *longum*, respectively, are scrutinized (Bottacini et al., 2014; O'Callaghan et al., 2015). However, just 5.5% of the *Bifidobacterium* core genome (i.e., genus-wide conserved genes) is dedicated to carbohydrate metabolic pathways suggesting that in order to survive in the GIT environment the acquisition of carbohydrate metabolic genes in the accessory genome is important (Milani et al., 2014). This is not surprising considering the wide diversity of carbohydrates that bifidobacteria may encounter in the GIT environment. Bifidobacteria, like other members of the gut microbiota, possess 'Carbohydrate Active Enzymes' (CAZymes), such as GHs that break the glycosidic bonds between carbohydrate moieties and covalent linkages between carbohydrates and non-carbohydrate moieties. Carbohydrate esterases (CE) cleave the ester bound between a HCA and a carbohydrate residue, and thereby may provide

access to other GHs to hydrolyse plant-derived oligosaccharides (Kelly et al., 2018).

The process of hydrolysis by GHs can occur by two distinct routes, either (i) by means of a single displacement mechanism which takes place in a single step and which results in the inversion of the anomeric centre, or (ii) by a double displacement mechanism involving two catalytic steps resulting in the retention of the anomeric center following hydrolysis (Davies and Henrissat, 1995; Withers, 2001). Hydrolysis of a glycosidic linkage between two monosaccharides is usually mediated by two catalytic carboxylic residues in the corresponding GH, one being a proton donor represented by an acid, while the other acting as a proton acceptor and represented by a base, activating a water molecule that acts as a nucleophile, in the inverting enzyme (van den Broek et al., 2008). However, in the retaining configuration, one carboxylic residue acts as an acid/base and another as nucleophile (**Figure 4**; Davies and Henrissat, 1995).

In the first step of the double displacement mechanism one residue protonates the glycosidic oxygen leading to the hydrolysis of the glycolytic bond and the formation of an oxocarbenium ion-like transition state. A glycosyl-enzyme intermediate is then formed by the other residue (nucleophile) attacking the anomeric center of the sugar. In the second step of the reaction, termed deglycosylation, the basic residue deprotonates a water molecule which in turn attacks the glycosyl-enzyme intermediate to cause hydrolysis of the glycosyl-enzyme intermediate (**Figure 4**; Withers, 2001; van den Broek et al., 2008). CAZymes can either degrade oligo- or polysaccharides at the end of the molecule, most commonly from the non-reducing end, or in between individual saccharidic moieties, representing hydrolytic abilities that are referred to as exo or endo activity, respectively (Mangas-Sánchez and Adlercreutz, 2015). The remainder of this review will focus on bifidobacterial GHs and CEs involved in the degradation of a selected number of plant-derived poly- and oligo-saccharides.

XYLAN AND XYLO-OLIGOSACCAHRIDES (XOS)

Bifidobacteria are capable of growth on several plant-derived poly/oligo-saccharides and their derived monomers (Watson et al., 2013; McLaughlin et al., 2015). Specifically, the *B. longum* subsp. *longum* and *Bifidobacterium adolescentis* taxa seem to be particularly well adapted to plant-based carbohydrate utilisation (O'Callaghan et al., 2015). Hemicelluloses include carbohydrates that generally possess a β-1,4-linked backbone, for example xylan, which is composed of β-1,4-linked D-xylose moieties (Scheller and Ulvskov, 2010). Furthermore, this xylan backbone can be decorated or substituted with L- or D-arabinose, xylose, galactose and D-glucuronic acid (Ndeh and Gilbert, 2018). Based on the nature of these substituents xylan is further categorized into AX, glucuronoxylans (GX) and glucuronoarabinoxylans (GAX) (Rogowski et al., 2015). AX from corn may also contain α-1,2-linked galactose to arabinose side chains (Appeldoorn et al., 2010; Pollet et al., 2012; **Figure 5**).

It should be noted that the xylan backbone typically requires removal of its substitutions before it can be degraded, a process that may involve multiple enzymatic activities. Xylanases or endo-1,4-β-xylanases (EC 3.2.1.8, GH5, GH8, GH10, GH11, GH30, GH51, and GH98) are endo-acting enzymes that randomly hydrolyse the internal β-1,4 bond between D-xylose residues within a xylan polymer to produce XOS (with a degree of polymerisation ranging between two and nine) (**Figure 5A**; Collins et al., 2005). Currently, no bifidobacterial strain/species is known to be able to grow on the polymeric, insoluble xylan backbone. Therefore, it is likely that in the GIT species such as *Ba. ovatus*, *Bacteroides xylanisolvens* or *Bacteroides intestinalis* degrade the xylan backbone into soluble XOS, which then becomes available for other species to utilize (Zhang et al., 2014; Despres et al., 2016; Wang et al., 2016). Particular bifidobacterial species, e.g., *B. longum* subsp. *longum* and *B. adolescentis*, are able to metabolize xylan-derived XOS (Falck et al., 2013; Arboleya et al., 2018) and several enzymes have been implicated in the degradation of this oligomeric substrate by bifidobacteria. β- D-xylosidases (EC 3.2.1.7, GH1, GH2, GH3, GH43, GH51, GH52, GH54, GH116, and GH120) are exo-enzymes which can hydrolyse XOS starting at the non-reducing xylose residue. For instance, a β-1,4 xylosidase (EC 3.2.1.37) (GH51) from *B. breve* K-110 was shown to elicit activity against *p*-Nitrophenyl (*p*Np) β-D-xylopyranoside, yet exhibits very limited activity against xylan (Shin et al., 2003). Furthermore, *B. adolescentis* LMG10502 encodes two β-xylosidases: XylB (GH120) which hydrolyses XOS but not xylobiose, and XylC (GH43), which hydrolyses xylobiose (Lagaert et al., 2011; **Figure 5B**). In addition, the GH8 RexA or reducing-end, xylose-releasing exo-oligoxylanase enzyme (EC 3.2.1.156) (Valenzuela et al., 2016) from *B. adolescentis* LMG10502 was shown to elicit limited activity against xylan, no activity against xylobiose or *p*Np-β-D-xylopyranoside, though was shown to exhibit activity against XOS with a DP of 3 and above (**Figure 5C**; Lagaert et al., 2007).

Transcriptional and proteome analysis of *B. animalis* subsp. *lactis* BB-12 grown on XOS revealed expression of a number of xylanases, β-xylosidases and ABC transporters (Lagaert et al., 2007). Bifidobacterial species/strains that are able to utilize XOS, such as *B. longum* subsp. *longum* and *B. adolescentis*, usually metabolize XOS only up to a DP of six, i.e. xylohexose due to size limitations of the corresponding XOS transport system (Wang et al., 2010; Amaretti et al., 2013). It must be noted that generally bifidobacterial CAZymes act intracellularly, although extracellular hydrolysis of XOS by an apparently extracellular bifidobacterial β-1,4 xylosidase has been reported for *B. adolescentis* (Amaretti et al., 2013).

AX, AXOS, ARABINAN, ARABINOGALACTAN, AND CORN GAX

The xylose residues in xylan and XOS can be mono-substituted with L-arabinose at the C(O)2 or C(O)3 positions or di-substituted with L-arabinose at both C(O)2 and C(O)3 positions, while these arabinose substitutions can either be α-1,2-linked or α-1,3-linked (**Figure 2**; Scheller and Ulvskov, 2010; De Vuyst et al., 2014). Only a limited number of bifidobacterial species/strains, e.g., *B. longum* subsp. *longum*, are able to

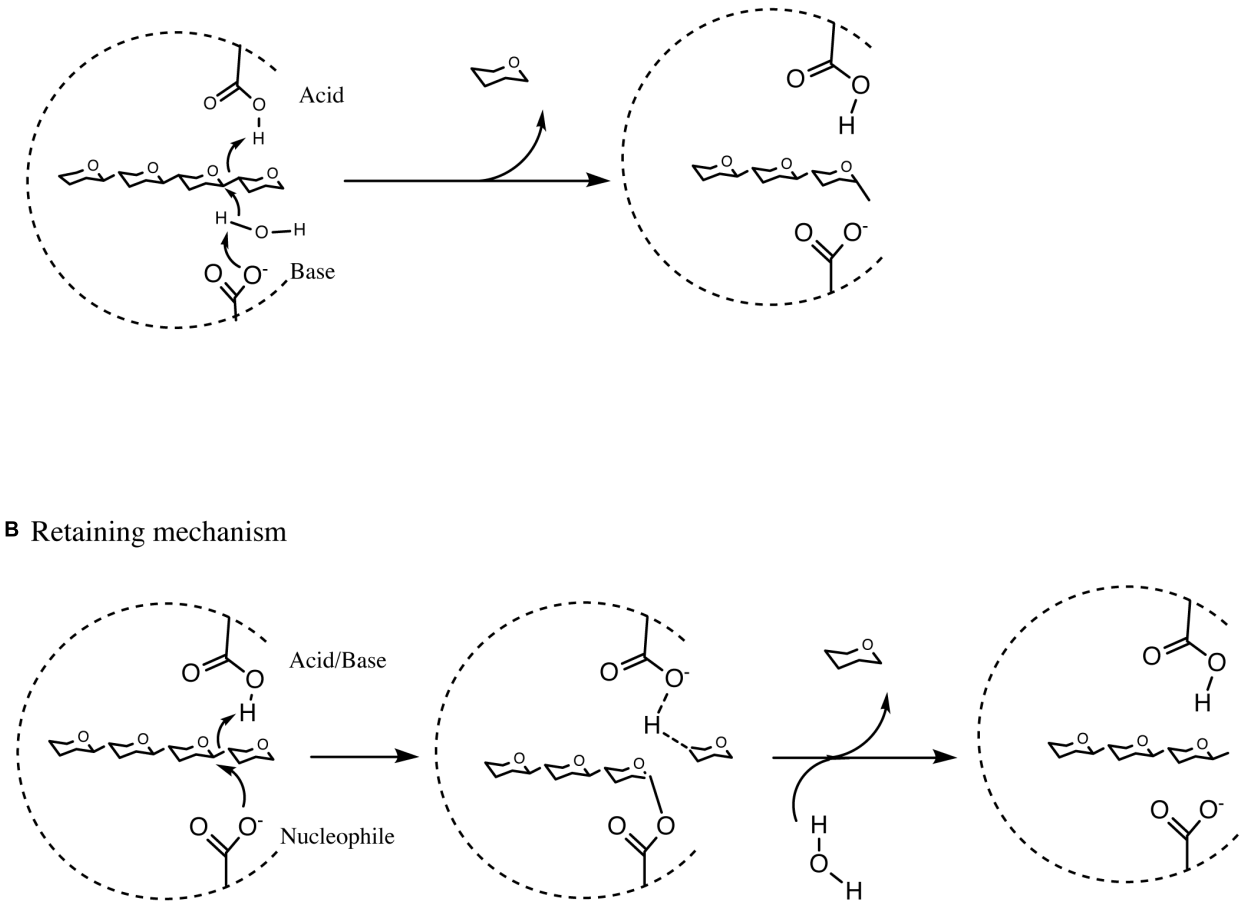

FIGURE 4 | Summary of Inverting hydrolysis, retaining hydrolysis and transglycosylation. **(A)** Summary of inverting single displacement mechanism. **(B)** Summary of retaining double displacement mechanism. See text for details of the reactions.

metabolize such AX and AXOS glycans (O'Callaghan et al., 2015; Riviere et al., 2015; Truchado et al., 2015). Depending on the particular bifidobacterial species/strain different components of AX or AXOS are utilized. One study classified bifidobacterial species/strains into five clusters based on the particular AX, AXOS, or XOS components a given strain could metabolize: cluster I, metabolism of monosaccharides arabinose and xylose, but no metabolism of XOS or arabinose substituents; cluster II, metabolism of mono- or di-substituted arabinose, yet no utilization of the XOS backbone; cluster III, utilization of the XOS backbone but no utilization of arabinose substituents; cluster IV, utilization of both arabinose substituents and XOS, up to xylotetraose of AXOS; cluster V, utilization of AXOS including up to xylohexose XOS chains (Riviere et al., 2014). Therefore, the presence of AX, AXOS, and XOS in the GIT supports growth of various bifidobacterial species/strains either directly or indirectly through possible cross-feeding activities (De Vuyst et al., 2014). In this sense, *Ba. ovatus* has been shown to support growth of *B. adolescentis* when they interact on simple xylans, such as wheat AX and birch GX (Rogowski et al., 2015). However, *Ba. ovatus* cannot cross-feed with *Bifidobacterium* sp. when they use complex dietary xylans, such as corn AX. The reason for this inability is that *Bifidobacterium* sp. lack the catalytic apparatus needed to metabolize the oligosaccharides released from complex dietary xylans by *Ba. ovatus*. This is consistent with the fact that *B. adolescentis* is unable to metabolize corn AX, even if it is pretreated with the GHs located on the surface of *Ba. ovatus* (Rogowski et al., 2015).

Pectin is composed of multiple complex glycans that can be utilized by the gut microbiota (Ndeh et al., 2017; Luis et al., 2018). Probably because of its complexity there are currently no known bifidobacterial species that are able to directly metabolize pectin (**Figure 3**). It is therefore presumed that other gut commensals such as *Bacteroides thetaiotaomicron* degrade these large polymers extracellularly and that certain bifidobacterial species can then scavenge the released mono- and oligosaccharides, as shown previously by co-cultivation of *B. longum* subsp. *longum* with *Ba. thetaiotaomicron* in the presence of arabinogalactan (Degnan and Macfarlane, 1995). *B. breve* UCC2003 can cross-feed on β-1,3 galacto-di/trisaccharides

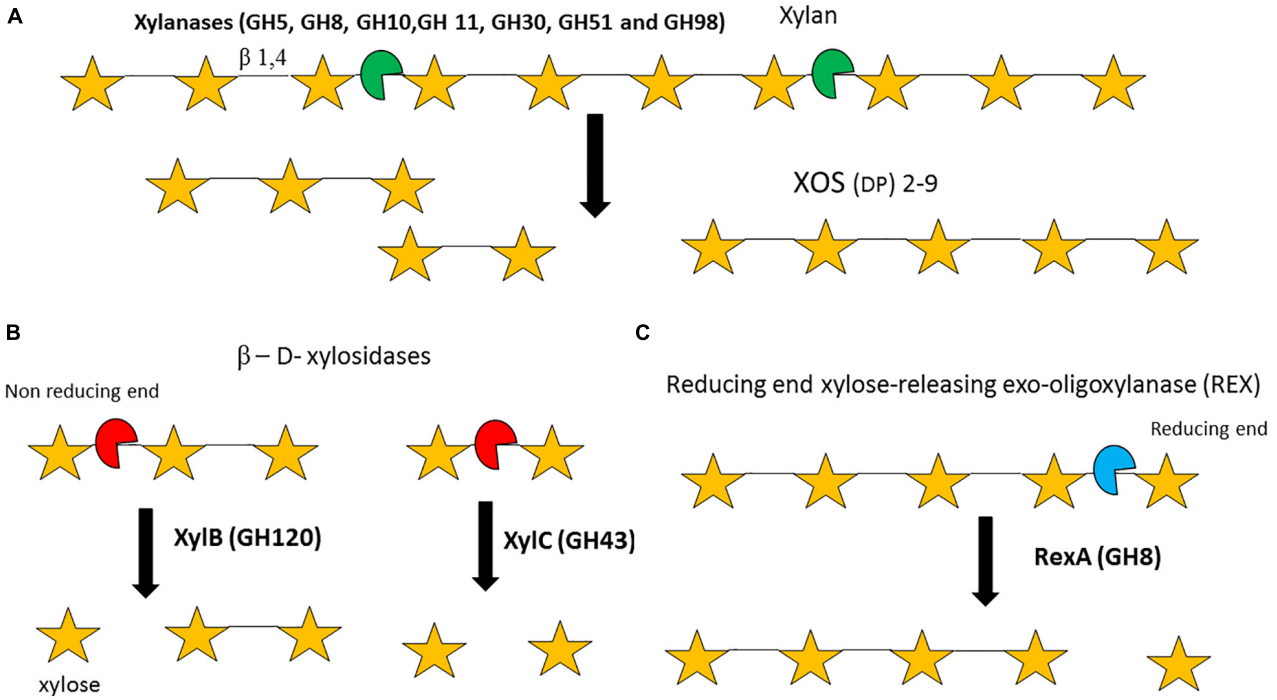

FIGURE 5 | Enzymatic degradation of xylan and xylo-oligosacharides (XOS). Degradation of the xylan backbone to XOS by endo-xylanases **(A)**. Degradation of XOS by β-D-xylosidases **(B)**. Degradation of XOS by a 'Reducing end xylose releasing exo-oligoxylanase **(C)**. DP = degree of polymerization. Enzyme names are indicated in bold. See text for details.

released from larchwood arabinogalactan by *Ba. cellulosilyticus* (Munoz et al., 2020). *B. longum* subsp. *longum* strains have been shown to grow on the pectic components arabinan and arabinogalactan (O'Connell Motherway et al., 2011; Komeno et al., 2019). Arabinan consists of an α-1,5-linked L-arabinose backbone that can be mono- or di-substituted with either α-1,2-linked and/or α-1,3-linked L-arabinose (Mohnen, 2008). Type I arabinogalactan is usually linked to other pectin-associated glycans, whereas type II arabinogalactan is O-linked to a protein backbone. Both arabinogalactan types are key components of the plant cell wall (Seifert and Roberts, 2007; Sakamoto and Ishimaru, 2013). Type I arabinogalactan is composed of a β-1,4-linked D-galactose backbone substituted by α-1,5-linked L-arabinose, while type II arabinogalactan is composed of a β-1,3-linked D-galactose backbone that can be substituted with α-1,3-linked arabinose and α-1,6-linked galactose side chains with further decorations with other minor monosaccharide components, such as rhamnose, (methyl)glucuronic acid, xylose or fucose (Mohnen, 2008; Sakamoto and Ishimaru, 2013; Cartmell et al., 2018).

α-L-arabinofuranosidases (EC 3.2.1.55, GH1, GH2, GH3, GH5, GH39, GH43, GH51, GH54, and GH62) are exo-acting enzymes that can cleave arabinose moieties from the polymeric backbone of xylan, XOS, galactan or arabinan/AOS (Margolles and de los Reyes-Gavilan, 2003; Lagaert et al., 2014). Arabinofuranosidases typically remove mono-substituted α-1,2 linked and/or α-1,3 linked arabinose from their particular substrate backbone (van den Broek et al., 2005; Bourgois et al., 2007), although certain arabinofuranosidases are specialized in removing arabinose from a di-substituted substrate (van den Broek et al., 2005; Cartmell et al., 2011). The ability to degrade AXOS has been shown to be species/strain dependent and certain bifidobacterial species/strains are only able to metabolize the arabinose substitutions on XOS (Riviere et al., 2014). An α-arabinofuranosidase (GH51) produced by *B. longum* subsp. *longum* has been shown to release arabinose from AX (Margolles and de los Reyes-Gavilan, 2003), while AbfA (GH43) from *B. adolescentis* was shown to remove arabinose residues from the C(O)2 and C(O)3 positions of mono-substituted xylose, and AbfB (GH51) and AXHd3 (GH43) were demonstrated to release arabinose residues from the C(O)3 of disubstituted xylose residues (van den Broek et al., 2005; Lagaert et al., 2010). L-arabinofuranosidases can also act as exo-enzymes on AOS present in arabinan or arabinogalactan. For example, an α-L-arabinofuranosidase (GH1) from *B. adolescentis* was shown to possess exo-activity on α-1,5-linked AOS (DP 2-5) (Suzuki et al., 2013). Similarly, the *B. longum* subsp. *longum* AraFC (GH43) was shown to be capable of removing α-1,2-linked and α-1,3-linked arabinose side chains of AX and arabinan, yet AraFD (GH43) was shown to exhibit hydrolytic activity towards α-1,5-linked arabinan (Komeno et al., 2019). α-L-arabinofuranosidases can also release arabinose side chains from galactose residues in arabinogalacatan; BlArafA (GH43), an α-arabinofuranosidase produced by *B. longum* subsp. *longum*, can release α-1,3-linked arabinose from β-1,6-galacto-oligosaccharides (Fujita et al., 2019). Endo-α-arabinases (EC 3.2.1.99) hydrolyse the

α-1,5-linkage within the arabinan backbone (Arnal et al., 2015) and it is likely that arabinofuranosidases must first remove the L-arabinose substituents before the backbone can be effectively cleaved. Currently, no endo-arabinases have been described in bifidobacteria. β-L-arabinofuranosidases (EC 3.2.1.185, GH127, GH142, and GH146) remove β-linked arabinose substitutions from plant-oligosaccharides; β-linkages are less common and found on extensins (proteoglycans that are abundant in carrots) type II arabinogalactan, RGI and RGII (from pectin polysaccharides) linked to plant cell wall proteins (Lansky et al., 2014; Ndeh et al., 2017; Luis et al., 2018). In *B. longum* subsp. *longum*, β-arabinofuranosidases HypBA1 (GH127) and HypBA2 (GH121) release arabinose from β-1,2-linked arabinosaccharides (DP 2-3) linked to hyproxyline (Fujita et al., 2011, 2014b). Several bifidobacterial α-L-arabinofuranosidases and β-L-arabinofuranosidases have been reported in literature and their salient features are summarized in **Table 1**.

Various enzymes are required to degrade plant-derived galactan. Exo-acting β-1,3-galactanases (EC 3.2.1.145, GH43 subfamily 24) cleave the β-1,3-D-galactose backbone of type II arabinogalactan even in the presence of β-1,6-D galactose side chains through a by-pass mechanism (Ichinose et al., 2006; Cartmell et al., 2018). Exo-acting β-1,4-galactanases (no designated EC number) cleave terminal β-1,4-linked galactose bonds (Sakamoto and Ishimaru, 2013). An exo-β-1,3 galactanase (GH43 subfamily 24), (Bl1,3Gal) isolated from *B. longum* subsp. *longum* was shown to hydrolyse β-1,3-linked galacto-oligosaccharides (DP between 2 and 5) and de-arabinosylated larchwood arabinogalactan (Fujita et al., 2014a). This Bl1,3Gal enzyme is unusual as it exhibits a higher activity for β-1,3-galactan when the latter substrate is substituted with β-1,6-side chains, apparently recognizing these side chains as a specificity determinant in the active site. Similarly, BgaA (GH2) of *B. breve* UCC2003 was shown to cleave β-1,3-linked galactobiose/triose (**Figure 6A**) (Munoz et al., 2020). An exo-β-1,6-galactobiohydrolase (Bl1,6-Gal, GH30) from the same species was shown to degrade β-1,6-linked galactose (DP between 2 and 4) and β-1,6-galactan, but was not able to degrade arabinose substituted substrates (Fujita et al., 2019; **Figure 6B**). Furthermore, depending on the linkage type of the galactan backbone degradation may involve endo-acting β-1,3-galactanases (EC 3.2.1.181, GH30) (Sakamoto and Ishimaru, 2013), β-1,4 galactanases (EC 3.2.1.89, GH53) (Zavaleta and Eyzaguirre, 2016) or β-1,6-galactanases (EC 3.2.1.164, GH30) (Sakamoto and Ishimaru, 2013).

In *B. longum* subsp. *longum*, an extracellular endo-acting β-galactanase, designated GalA, was found to be capable of cleaving β-1,4 and β-1,3-galactan linkages (Hinz et al., 2005; **Figure 6C**). The extracellular GalA (GH52) homolog in *B. breve* UCC2003, which is present in certain strains of this species, was found to elicit hydrolytic activity towards galactan, thereby releasing galacto-oligosaccharides (O'Connell Motherway et al., 2011). GalA is encoded by a galactan utilization cluster in both *B. breve* UCC2003 and *B. longum* subsp. *longum* strains, and in addition specifies an ABC type transporter, and GalG (GH42), a β-galactosidase (O'Connell Motherway et al., 2011, 2013). β-galactosidases (EC 3.2.1.23, GH1, GH2, GH35, GH39, GH42, GH59, GH147, and GH165) hydrolyse linkages between a galactose moiety and another sugar moiety and several β-galactosidases have been identified in *B. bifidum*, *B. longum* subsp. *longum*, *B. longum* subsp. *infantis* and *B. breve*, being able to hydrolyse β-1,3, β-1,4 or β-1,6 linkages in galacto-oligosaccahrides and HMO substrates (Goulas et al., 2007; Godoy et al., 2016; James et al., 2016; Sotoya et al., 2017; Ambrogi et al., 2019; **Figure 6D**).

Finally, the backbone or side chains of these plant-derived oligomers may also be substituted with HCAs. HCAs that are in free form are absorbed by the small intestine (Cremin et al., 2001), whereas HCAs that are linked to plant-derived polysaccharides are not readily absorbed in the small intestine and are therefore likely to reach the colon (Clifford, 2004). Many hemicelluloses and pectic plant polymers have HCAs attached by an ester bond to the (O)5 position of the sugar moiety (Saulnier and Thibault, 1999; Scheller and Ulvskov, 2010). HCA-specific esterases (EC 3.1.1.73, CE1 and CE6) catalyse the hydrolysis of the ester bond between a given HCA, for example ferulic acid and *p*-coumaric acid, and a sugar moiety (arabinose, galactose or xylose) on AX and pectin plant-oligomers (Wong, 2006). These HCA-specific esterases possess an alpha/beta hydrolase fold, a consensus motif (Gly-X-Ser-X-Gly) and a catalytic triad consisting of Ser-His-Asp residues (Bornscheuer, 2002). Bifidobacterial esterases active against HCAs have been described, including the CaeA esterase in *B. longum* subsp. *longum*, whose encoding gene is located within the same genetic locus as the genes encoding GH enzymes that are predicted to be involved in plant-oligosaccharide utilization (Raimondi et al., 2015; Fritsch et al., 2017; Kelly et al., 2018).

REGULATION OF CARBOHYDRATE METABOLISM IN BIFIDOBACTERIA

Carbon catabolite repression (CCR) refers to a global regulatory mechanism by which bacteria can preferentially metabolize the 'optimal' carbon source that has the greatest energy yield, amongst a mixture of carbon sources, and involves inhibition of the metabolic pathways of the less preferred carbon sources (Stülke and Hillen, 1999). This is important in the GIT environment where potentially multiple carbohydrate sources are present and the optimal carbon source must be consumed to increase chances of survival in the gut. There are many mechanisms of CCR and this can vary from species to species. For instance, CCR may involve transcriptional activation, transcriptional repression and/or translational regulation (Görke and Stülke, 2008). In the CCR paradigm, many bacteria, such as *Escherichia coli*, the 'optimal' substrate glucose is metabolized preferentially (Inada et al., 1996). Certain bacteria, e.g., *B. longum* subsp. *longum* and *Streptococcus thermophilus*, preferentially metabolize lactose over glucose (van den Bogaard et al., 2000; Kim et al., 2003; Parche et al., 2006). The preference of other sugars over glucose for metabolism is also termed reverse CCR (Görke

TABLE 1 | Summary of characterised bifidobacterial arabinofuranosidases.

Enzyme name/classification	Substrates	GH family	References	Species
AbfB	Arabinan, AX, arabinobiose - arabinopentose	GH51	Margolles and de los Reyes-Gavilan, 2003	*B. ll*
α-L-arabinofuranosidase				
BXA43	XOS (DP 2-4)	GH43	Viborg et al., 2013	*B. al*
β xylosidase/ α-L-arabinofuranosidase	*p*NP-α-L araf			
	*p*Np-β-D Xyl			
BAD0156	pNP-α-L araf	GH1	Suzuki et al., 2013	*B. a*
α-L-arabinofuranosidase	α-1,5 arabinosaccharides			
BlArafC	*p*NP-α-L araf	GH43	Komeno et al., 2019	*B. ll*
α-L-arabinofuranosidase	Arabinan			
	AX			
BlArafD	*p*NP-α-L araf	GH43	Komeno et al., 2019	*B. ll*
α-L-arabinofuranosidase	Arabinan			
BlArafA	*p*NP α L araf	GH43	Fujita et al., 2019	*B. ll*
α-L-arabinofuranosidase	α-1,3-Ara*f* Gal_3			
	Ara*f*-α-1,3-Ara*f*-α-OMe			
	Radish AG			
	Larch AG			
	Arabinan			
Blon_0625	*p*NP-α-L araf	GH3	Matsumoto et al., 2015	*B. li*
α-L-arabinofuranosidase				
HypBA2	β1,2-Arabinose hyproxyline	GH121	Fujita et al., 2011	*B. ll*
β-L-arabinofuranosidase				
	β1,2-linked arabinotriose - hyproxyline			
	Arabinan			
	Debranched Arabinan			
HyBA1	β 1,2-linked Arabinose – hyproxyline (DP 2 and 3)	GH127	Fujita et al., 2014b; Ito et al., 2014; Zhu et al., 2014	*B. ll*
β-L-arabinofuranosidase				
	Arabinobiose - ME			
AfuB-H1	*p*NP-α-L araf	GH51	Lee et al., 2011	*B. ll*
α-L-arabinofuranosidase				
AbfA	AX	GH43	Lagaert et al., 2010	*B. a*
α-L-arabinofuranosidase	AXOS			
	*p*NP-α-L araf			
	*p*NP-β-Xyl			
AbfB	AX,	GH43	Lagaert et al., 2010	*B. a*
α-L-arabinofuranosidase	AXOS			
	*p*NP-α-L araf			
	Arabinan			
AXH-d3	AX	GH43	van den Broek et al., 2005	*B. a*
	AXOS			
	Arabinan			
α-L- arabinofuranosidase	*p*NP-α-L araf	–	Shin et al., 2003	*B. b*
	Ginsenoside RC			

L araf, L-*arabinofuranose; D Xyl,* D-*xylopyranoside; ME, methyl group; Gal, galactose; OMe, O-linked methyl group; AG, arabinogalactan; AX, Arabinoxylan; AXOS, arabinoxylo-oligosaccharides; B. ll, Bifidobacterium longum subsp. longum; B. al, Bifidobacterium animalis subsp. lactis; B.b, Bifidobacterium breve; B. a, Bifidobacterium adolescentis; B. li, Bifidobacterium longum subsp. infantis.*

and Stülke, 2008). CCR-resembling regulation has previously been described in bifidobacteria. In particular, in *B. breve* UCC2003, a FOS utilization cluster inducible by growth on sucrose or Actilight, a commercial FOS prebiotic, was shown to be downregulated in the presence of glucose and/or fructose – sucrose mixes (Ryan et al., 2005). CCR may be important

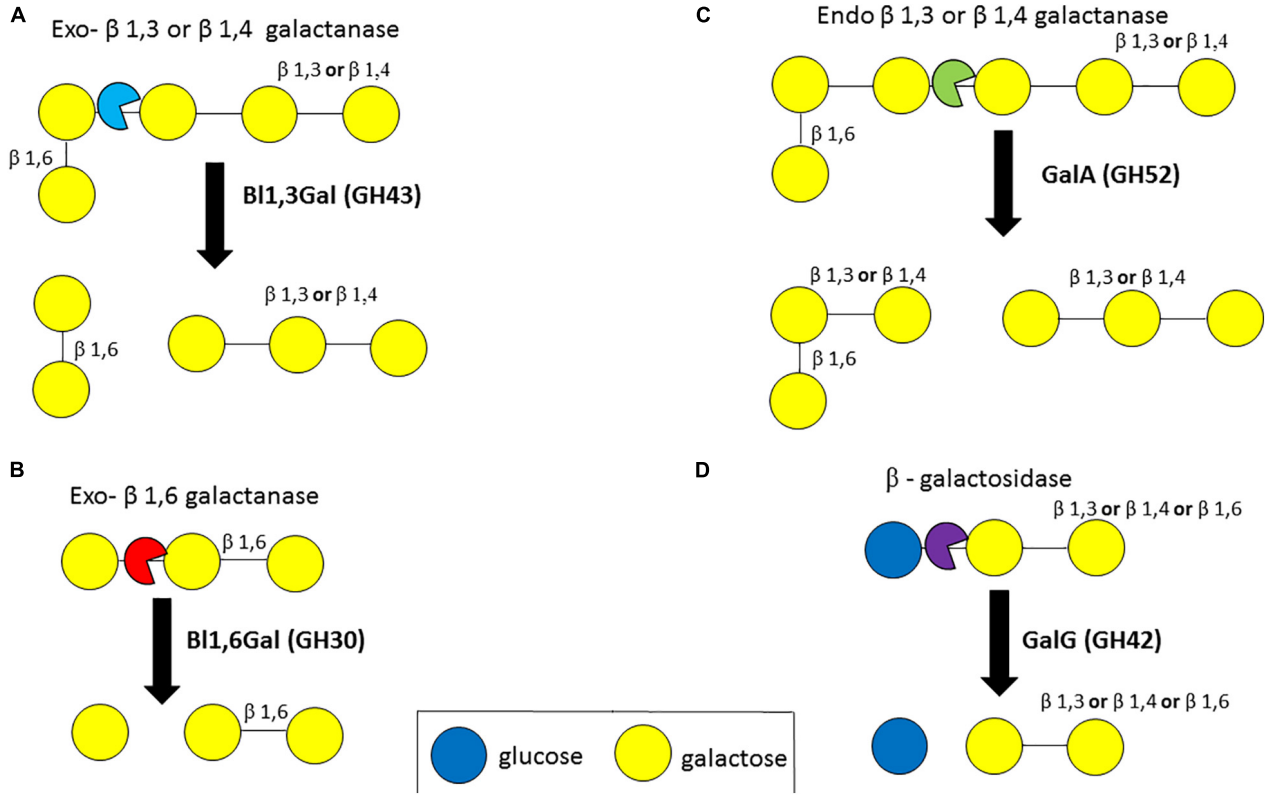

FIGURE 6 | Enzymatic degradation of galactan. Degradation of galactan by exo-β1,3- or β1,4-galactanases **(A)**. Degradation of galactan by exo-β1,6-galactanases **(B)**. Degradation of galactan by endo-β1,3- or β1,4-galactanases **(C)**. Degradation of a galactose-sugar moiety bond by β-galactosidases **(D)**. Enzyme names are indicated in bold. See text for details.

from an ecological perspective, as it may avoid species/strain competition for limited carbon sources in the gut environment (Brückner and Titgemeyer, 2002). However, CCR is not the only model to describe the regulation of carbohydrate metabolism in bacteria. Indeed, *B. breve* and *Corynebacterium glutamicum*, both members of the Actinobacteria phylum, have been shown to globally regulate their central metabolic flux and control co-metabolism of multiple sugars (Wendisch et al., 2000; Lanigan et al., 2019).

LacI-type transcriptional regulators are the most prevalent and abundant family of bifidobacterial TFs; in one study they were shown to account for 63% of all identified regulators encoded by ten bifidobacterial genomes (Khoroshkin et al., 2016). LacI-type transcriptional factors in bifidobacteria typically act as carbohydrate-specific transcriptional repressors and are therefore important allowing only appropriate expression of carbohydrate metabolism genes in the presence of the corresponding saccharidic substrate in the GIT environment. LacI-type transcription factors contain a so-called helix-turn-helix DNA binding domain at their N-terminus, a core domain to bind sugar ligands and a multimerization domain for the formation of dimers and/or tetramers (Lewis et al., 1996).

Bifidobacterial LacI-type transcriptional factors have been shown, *in silico* and *in vitro*, at a local level to control genes and/or operons involved in carbohydrate metabolism for various carbohydrates including HMOs (James et al., 2018), galactan (O'Connell Motherway et al., 2011), melezitose (O'Connell et al., 2014), AOS (Arzamasov et al., 2018), FOS (Ryan et al., 2005), ribose (Pokusaeva et al., 2010) and cellodextrin (Pokusaeva et al., 2011b). Nonetheless, other types of transcriptional regulation have been reported to be involved in transcriptional control of genes involved in carbohydrate metabolism. Examples are represented by a GntR-type transcription factor (TF) for sialic acid utilization (Egan et al., 2015), a so-called repressor open reading frame kinase (or ROK) TF for raffinose and stachyose metabolism (O'Connell et al., 2014), and a NagC/XylR-type repressor involved in sulfated sugar metabolism regulation (Egan et al., 2016). Therefore, LacI-type and other transcriptional regulator families play an important role in the regulation of bifidobacterial carbohydrate metabolism.

Central carbohydrate metabolism in bifidobacteria is represented by the 'Bifid Shunt', which is regulated by two LacI-type regulators, designated AraQ and MalR1 (Lanigan et al., 2019), employing a mechanism that is reminiscent to that reported for *C. glutamicum* (Wendisch et al., 2000). This mechanism of global carbohydrate regulation may be advantageous to bifidobacteria in the GIT environment by allowing these gut commensals to quickly and effectively respond to the various glycans that can be present in the GIT at any given time.

B. longum subsp. *longum*, AN INFANT AND ADULT ASSOCIATED BIFIDOBACTERIAL SPECIES

B. longum subsp. *longum* is a bifidobacterial species that is associated with both the infant and adult gut microbiota (Odamaki et al., 2018), while *B. longum* subsp. *infantis* is typically associated with the infant gut (Turroni et al., 2012a). As mentioned above a major factor that influences the bifidobacterial species composition in the infant or adult gut is the nature of the carbohydrates present in the diet, though other factors may also affect the ability of bifidobacteria to colonize and survive in the gut environment, as reviewed elsewhere (González-Rodríguez et al., 2013). In the infant gut and unaffected by host enzymes, HMOs are the main dietary glycans and these are mainly composed of hexose sugars; for example, most HMOs contain N-acetylglucosamine (GlcNac) and β1,3- or β1,4-linked lacto-N-biose (LNB, Galβ1,3GlcNac) residues with a terminal lactose at the reducing end (Smilowitz et al., 2014), and are frequently decorated with fucose or sialic acid (Bode and Jantscher-Krenn, 2012). *B. longum* subsp. *infantis* is able to metabolize a broad range of HMOs including those that are decorated with fucose and sialic acid (Sela et al., 2008; Zabel et al., 2019). This is due to *B. longum* subsp. *infantis* possessing a broad range of ABC transporters specialized to import HMOs which are then further processed by intracellular enzymes (Sela et al., 2008; Wong et al., 2020). In contrast, the ability of *B. longum* subsp. *longum* to metabolize HMOs is limited and generally this species can only metabolize LNB and LNT (Galβ1-3GlcNAcβ1-3Galβ1-4Glc), although some *B. longum* subsp. *longum* strains can utilize fucosylated HMOs (Garrido et al., 2016). *B. longum* subsp. *longum* strains that metabolize HMOs similarly encode ABC transporters for their uptake but can also encode extracellular enzymes to degrade HMOs including an extracellular lacto-*N*-biosidase that cleaves LNT into LNB and lactose (Yamada et al., 2017). *B. longum* subsp. *longum* therefore has both the capacity to metabolize HMOs from breast milk in the infant diet and plant-derived oligosaccharides present in the diet of adults. This may be why the *B. longum* subsp. *longum* species is found in both the infant and adult gut and is therefore an important bifidobacterial species that is part of the gut microbiota throughout the lifespan of the human host. This knowledge of HMO utilization and plant-derived glycan utilization therefore may be used to encourage an increase in the abundance in bifidobacteria after the weaning and hopefully prevent the decline in bifidobacteria as the human host ages.

CONCLUSION AND FUTURE PERSPECTIVES

The GIT environment is a dynamic, highly competitive and challenging ecological niche for bifidobacteria to colonize. To further complicate matters, the diet of the human host changes as we age, starting from breast milk in infancy to complex plant glycans in adulthood. Therefore, in order to survive the GIT environment bifidobacteria must be able to metabolize complex plant-oligosaccharide carbohydrates and most importantly choose the most metabolically efficient carbohydrate source if it is to compete with other microbial species in the GIT. Bifidobacteria represent a key genus among the gut microbiota and are present in the gut throughout life from infancy, adolescence, adulthood to old age. They are seen as a general indicator of health due to their purported probiotic properties. Therefore, as they decline with human host age it is important to understand how bifidobacterial species adapt and are able to metabolize plant-oligosaccharides more associated in the adult diet. This knowledge may allow the opportunity to increase the abundance of bifidobacteria in the adult and elderly human host potentially benefiting it with the probiotic effects attributed to bifidobacteria.

A key area in carbohydrate metabolism involves the question of how dependent bifidobacteria are on other microbial species (bacterial and/or fungal) to degrade complex insoluble plant glycans into oligosaccharidic substrates? Previously, it has been shown that growth of *Ba. cellulosilyticus* on arabinogalactan can support growth of *B. breve* by release of galacto-oligosaccharides (Munoz et al., 2020) demonstrating that cross-feeding occurs between species. Further investigations are needed to precisely assess the relationship between bifidobacteria and other species, in particular members of the *Bacteroides* genus. *Bacteroides* spp. are known for their ability to degrade complex plant glycans (Cartmell et al., 2018), and they are called 'messy eaters' that extracellularly degrade glycans releasing oligosaccharides for other GIT members, including bifidobacteria, to scavenge (Porter and Martens, 2016). More detailed studies are needed to understand these complex ecological interactions, which may then allow rational strategies to be exploited for the development of novel plant-derived oligosaccharide prebiotics.

Another area related to this research topic includes the role of HCA metabolism by bifidobacteria. Previously, esterases that cleave synthetic HCA substrates have been reported in bifidobacteria (Raimondi et al., 2015; Fritsch et al., 2017; Kelly et al., 2018). The gene encoding the CaeA esterase is located in a locus predicted to be involved in AOS metabolism (Arzamasov et al., 2018; Kelly et al., 2018). Removal of HCAs from plant-derived oligosaccharides is hypothesized to provide substrate access to GHs that might otherwise be sterically hindered by HCA substitutions. However, a lack of commercially available plant-derived oligosaccharide substrates retaining the HCA decorations remains a challenge to ascertain to what extent HCAs affect metabolism of complex plant-derived glycans. Furthermore, do released HCAs, which in *B. longum* subsp. *longum* happens intracellularly, provide any benefit to bifidobacteria? In other heterofermentative bacteria HCAs has been shown to act as external electron acceptors and their presence in growth media results in higher intracellular ATP levels (Filannino et al., 2014). HCAs also inhibit growth of certain gut pathogens, such as *Clostridium perfringens* (Lee et al., 2006), presumably due to membrane damage. However, how sensitive bifidobacteria are to the effects of HCAs is currently not studied.

Finally, different plant-oligosaccharides derived from hemicelluloses and pectin have highly complex structures, yet in

cases contain identical monomeric/oligomeric components and glycosidic linkages. Additionally, bifidobacterial genomes often contain multiple loci in different locations across the genome dedicated to the metabolism of dietary carbohydrates. It is likely that if bifidobacteria are provided with a buffet of plant-derived oligosaccharides to metabolize in the gut they must choose the most energetically favorable carbon source as they are competing for resources with other members of the microbiota. In future, more understanding of the bifidobacterial transcriptional regulation of plant derived oligosaccharides is needed and potentially this knowledge could lead to better understanding of the prebiotic plant-oligosaccharides preferentially utilized by bifidobacteria. This, however, requires that plant oligosaccharides are purified to a high quality, that the detailed structural (DP, covalent linkages and sidechain substitutions) information of these oligosaccharides is known and that sufficient amounts of oligosaccharides are purified to allow growth and transcriptional analyses. Currently, plant oligosaccharides are not widely available in large amounts at a reasonable costs, while characterizing oligosaccharides requires specialist techniques and expensive equipment such as mass-spectrometry, HPLC, HPAEC-PAD and NMR. Furthermore, following the acquisition of this information, animal models would need to be employed to assess the prebiotic/bifidogenic potential of a given oligosaccharide. In conclusion, the ability of bifidobacteria to utilize a variety of plant-derived oligosaccharides is an important characteristic of specific members of this genus to colonize and survive in the adult gut. Novel plant-glycan based prebiotics specific for bifidobacteria could be developed in the future, though this will require further research to fully understand plant-derived poly/oligosaccharide metabolic capabilities exerted by bifidobacteria.

AUTHOR CONTRIBUTIONS

SK, JM-M, and DS wrote and edited the manuscript. All authors contributed to the article and approved the submitted version.

FUNDING

SK and DS are members of the APC Microbiome Ireland which receives financial support from Science Foundation Ireland (SFI/12/RC/2273−P1 and SFI/12/RC/2273−P2) as part of the Irish Government's National Development Plan. JM-M received financial support from an internal grant from Northumbria University.

REFERENCES

Agger, J., Vikso-Nielsen, A., and Meyer, A. S. (2010). Enzymatic xylose release from pretreated corn bran arabinoxylan: differential effects of deacetylation and deferuloylation on insoluble and soluble substrate fractions. *J. Agric. Food Chem.* 58, 6141–6148. doi: 10.1021/jf100633f

Alimentarius, C. (2010). *Guidelines on Nutrition Labelling CAC/GL 2-1985 as Last Amended 2010. Joint FAO/WHO Food Standards Programme, Secretariat of the Codex Alimentarius Commission*. Rome: FAO.

Amaretti, A., Bernardi, T., Leonardi, A., Raimondi, S., Zanoni, S., and Rossi, M. (2013). Fermentation of xylo-oligosaccharides by *Bifidobacterium adolescentis* DSMZ 18350: kinetics, metabolism, and beta-xylosidase activities. *Appl. Microbiol. Biotechnol.* 97, 3109–3117. doi: 10.1007/s00253-012-4509-y

Ambrogi, V., Bottacini, F., O'Sullivan, J., O'Connell Motherway, M., Linqiu, C., Schoemaker, B., et al. (2019). Characterization of GH2 and GH42 β-galactosidases derived from bifidobacterial infant isolates. *AMB Express* 9, 9. doi: 10.1186/s13568-019-0735-3

Anderson, C. T. (2015). We be jammin': an update on pectin biosynthesis, trafficking and dynamics. *J. Exp. Bot.* 67, 495–502. doi: 10.1093/jxb/erv501

Apolinar-Valiente, R., Williams, P., Romero-Cascales, I., Gómez-Plaza, E., López-Roca, J. M., Ros-García, J. M., et al. (2013). Polysaccharide composition of Monastrell red wines from four different Spanish terroirs: effect of wine-making techniques. *J. Agric. Food Chem.* 61, 2538–2547. doi: 10.1021/jf304987m

Appeldoorn, M. M., Kabel, M. A., Van Eylen, D., Gruppen, H., and Schols, H. A. (2010). Characterization of Oligomeric Xylan structures from corn fiber resistant to pretreatment and simultaneous saccharification and fermentation. *J. Agric. Food Chem.* 58, 11294–11301. doi: 10.1021/jf102849x

Arboleya, S., Bottacini, F., O'Connell-Motherway, M., Ryan, C. A., Ross, R. P., van Sinderen, D., et al. (2018). Gene-trait matching across the *Bifidobacterium longum* pan-genome reveals considerable diversity in carbohydrate catabolism among human infant strains. *BMC Genomics* 19:33. doi: 10.1186/s12864-017-4388-9

Arboleya, S., Ruas-Madiedo, P., Margolles, A., Solis, G., Salminen, S., de Los Reyes-Gavilan, C. G., et al. (2011). Characterization and in vitro properties of potentially probiotic *Bifidobacterium* strains isolated from breast-milk. *Int. J. Food Microbiol.* 149, 28–36. doi: 10.1016/j.ijfoodmicro.2010.10.036

Arnal, G., Bastien, G., Monties, N., Abot, A., Anton Leberre, V., Bozonnet, S., et al. (2015). Investigating the function of an arabinan utilization locus isolated from a termite gut community. *Appl. Environ. Microbiol.* 81, 31–39. doi: 10.1128/aem.02257-14

Arzamasov, A. A., van Sinderen, D., and Rodionov, D. A. (2018). Comparative genomics reveals the regulatory complexity of bifidobacterial arabinose and arabino-oligosaccharide utilization. *Front. Microbiol.* 9:776. doi: 10.3389/fmicb.2018.00776

Bäckhed, F., Roswall, J., Peng, Y., Feng, Q., Jia, H., Kovatcheva-Datchary, P., et al. (2015). Dynamics and stabilization of the human gut microbiome during the first year of life. *Cell Host Microbe* 17, 690–703. doi: 10.1016/j.chom.2015.04.004

Blanco, G., Ruiz, L., Tamés, H., Ruas-Madiedo, P., Fdez-Riverola, F., Sánchez, B., et al. (2020). Revisiting the metabolic capabilities of *Bifidobacterium longum* susbp. longum and *Bifidobacterium longum* subsp. infantis from a glycoside hydrolase perspective. *Microorganisms* 8, 723. doi: 10.3390/microorganisms8050723

Bode, L., and Jantscher-Krenn, E. (2012). Structure-function relationships of human milk oligosaccharides. *Adv. Nutr.* 3, 383s–391s. doi: 10.3945/an.111.001404

Bornscheuer, U. T. (2002). Microbial carboxyl esterases: classification, properties and application in biocatalysis. *FEMS Microbiol. Rev.* 26, 73–81.

Bottacini, F., O'Connell Motherway, M., Kuczynski, J., O'Connell, K. J., Serafini, F., Duranti, S., et al. (2014). Comparative genomics of the *Bifidobacterium breve* taxon. *BMC Genomics* 15:170. doi: 10.1186/1471-2164-15-170

Bourgois, T. M., Van Craeyveld, V., Van Campenhout, S., Courtin, C. M., Delcour, J. A., Robben, J., et al. (2007). Recombinant expression and characterization of XynD from *Bacillus subtilis* subsp. *subtilis* ATCC 6051: a GH 43 arabinoxylan arabinofuranohydrolase. *Appl. Microbiol. Biotechnol.* 75, 1309–1317. doi: 10.1007/s00253-007-0956-2

Broekaert, W. F., Courtin, C. M., Verbeke, K., Van de Wiele, T., Verstraete, W., and Delcour, J. A. (2011). Prebiotic and other health-related effects of cereal-derived arabinoxylans, arabinoxylan-oligosaccharides, and xylooligosaccharides. *Crit. Rev. Food Sci. Nutr.* 51, 178–194. doi: 10.1080/10408390903004476

Brückner, R., and Titgemeyer, F. (2002). Carbon catabolite repression in bacteria: choice of the carbon source and autoregulatory limitation of sugar utilization. *FEMS Microbiol. Lett.* 209, 141–148. doi: 10.1111/j.1574-6968.2002.tb11123.x

Bunesova, V., Lacroix, C., and Schwab, C. (2016). Fucosyllactose and L-fucose utilization of infant *Bifidobacterium longum* and *Bifidobacterium kashiwanohense*. *BMC Microbiol.* 16:248. doi: 10.1186/s12866-016-0867-4

Cartmell, A., McKee, L. S., Peña, M. J., Larsbrink, J., Brumer, H., Kaneko, S., et al. (2011). The structure and function of an arabinan-specific alpha-1,2-arabinofuranosidase identified from screening the activities of bacterial GH43 glycoside hydrolases. *J. Biol. Chem.* 286, 15483–15495. doi: 10.1074/jbc.M110.215962

Cartmell, A., Muñoz-Muñoz, J., Briggs, J. A., Ndeh, D. A., Lowe, E. C., Baslé, A., et al. (2018). A surface endogalactanase in *Bacteroides thetaiotaomicron* confers keystone status for arabinogalactan degradation. *Nat. Microbiol.* 3, 1314–1326. doi: 10.1038/s41564-018-0258-8

Chandravanshi, M., Sharma, A., Dasgupta, P., Mandal, S. K., and Kanaujia, S. P. (2019). Identification and characterization of ABC transporters for carbohydrate uptake in *Thermus thermophilus* HB8. *Gene* 696, 135–148. doi: 10.1016/j.gene.2019.02.035

Clifford, M. N. (2004). Diet-derived phenols in plasma and tissues and their implications for health. *Planta Med.* 70, 1103–1114. doi: 10.1055/s-2004-835835

Collins, T., Gerday, C., and Feller, G. (2005). Xylanases, xylanase families and extremophilic xylanases. *FEMS Microbiol. Rev.* 29, 3–23. doi: 10.1016/j.femsre.2004.06.005

Cremin, P., Kasim-Karakas, S., and Waterhouse, A. L. (2001). LC/ES-MS detection of hydroxycinnamates in human plasma and urine. *J. Agric. Food Chem.* 49, 1747–1750. doi: 10.1021/jf000764y

Davies, G., and Henrissat, B. (1995). Structures and mechanisms of glycosyl hydrolases. *Structure* 3, 853–859. doi: 10.1016/s0969-2126(01)00220-9

de Vries, W., and Stouthamer, A. H. (1967). Pathway of glucose fermentation in relation to the taxonomy of bifidobacteria. *J. Bacteriol.* 93, 574–576.

de Vries, W., and Stouthamer, A. H. (1968). Fermentation of glucose, lactose, galactose, mannitol, and xylose by bifidobacteria. *J. Bacteriol.* 96, 472–478.

De Vuyst, L., Moens, F., Selak, M., Riviere, A., and Leroy, F. (2014). Summer Meeting 2013: growth and physiology of bifidobacteria. *J. Appl. Microbiol.* 116, 477–491. doi: 10.1111/jam.12415

Degnan, B. A., and Macfarlane, G. T. (1995). Arabinogalactan utilization in continuous cultures of *Bifidobacterium longum*: effect of co-culture with *Bacteroides* thetaiotaomicron. *Anaerobe* 1, 103–112. doi: 10.1006/anae.1995.1005

Despres, J., Forano, E., Lepercq, P., Comtet-Marre, S., Jubelin, G., Chambon, C., et al. (2016). Xylan degradation by the human gut *Bacteroides xylanisolvens* XB1AT involves two distinct gene clusters that are linked at the transcriptional level. *BMC Genomics* 17:326. doi: 10.1186/s12864-016-2680-8

Deutscher, J., Francke, C., and Postma, P. W. (2006). How phosphotransferase system-related protein phosphorylation regulates carbohydrate metabolism in bacteria. *Microbiol. Mol. Biol. Rev.* 70, 939–1031. doi: 10.1128/mmbr.00024-06

Egan, M., Jiang, H., O'Connell Motherway, M., Oscarson, S., and van Sinderen, D. (2016). Glycosulfatase-encoding gene cluster in *Bifidobacterium breve* UCC2003. *Appl Environ Microbiol* 82, 6611–6623. doi: 10.1128/aem.02022-16

Egan, M., O'Connell Motherway, M., and van Sinderen, D. (2015). A GntR-type transcriptional repressor controls sialic acid utilization in *Bifidobacterium breve* UCC2003. *FEMS Microbiol. Lett.* 362, 1–9. doi: 10.1093/femsle/fnu056

Egan, M., and Van Sinderen, D. (2018). "Chapter 8 – carbohydrate metabolism in Bifidobacteria," in *The Bifidobacteria and Related Organisms*, eds P. Mattarelli, B. Biavati, W. H. Holzapfel, and B. J. B. Wood, (Cambridge, MA: Academic Press), 145–164.

Ejby, M., Fredslund, F., Andersen, J. M., Vujicic Zagar, A., Henriksen, J. R., Andersen, T. L., et al. (2016). An ATP binding cassette transporter mediates the uptake of alpha-(1,6)-linked dietary oligosaccharides in *Bifidobacterium* and correlates with competitive growth on these substrates. *J. Biol. Chem.* 291, 20220–20231. doi: 10.1074/jbc.M116.746529

Falck, P., Precha-Atsawanan, S., Grey, C., Immerzeel, P., Stålbrand, H., Adlercreutz, P., et al. (2013). Xylooligosaccharides from hardwood and cereal Xylans produced by a thermostable Xylanase as carbon sources for *Lactobacillus brevis* and *Bifidobacterium adolescentis*. *J. Agric. Food Chem.* 61, 7333–7340. doi: 10.1021/jf401249g

Filannino, P., Gobbetti, M., De Angelis, M., and Di Cagno, R. (2014). Hydroxycinnamic acids used as external acceptors of electrons: an energetic advantage for strictly heterofermentative lactic acid bacteria. *Appl. Environ. Microbiol.* 80, 7574–7582. doi: 10.1128/aem.02413-14

Flint, H. J., Scott, K. P., Duncan, S. H., Louis, P., and Forano, E. (2012). Microbial degradation of complex carbohydrates in the gut. *Gut Microbes* 3, 289–306. doi: 10.4161/gmic.19897

Fritsch, C., Jansch, A., Ehrmann, M. A., Toelstede, S., and Vogel, R. F. (2017). Characterization of Cinnamoyl Esterases from Different Lactobacilli and Bifidobacteria. *Curr. Microbiol.* 74, 247–256. doi: 10.1007/s00284-016-1182-x

Fujita, K., Sakaguchi, T., Sakamoto, A., Shimokawa, M., and Kitahara, K. (2014a). *Bifidobacterium longum* subsp. *longum* Exo-beta-1,3-Galactanase, an enzyme for the degradation of type II arabinogalactan. *Appl. Environ. Microbiol.* 80, 4577–4584. doi: 10.1128/aem.00802-14

Fujita, K., Sakamoto, A., Kaneko, S., Kotake, T., Tsumuraya, Y., and Kitahara, K. (2019). Degradative enzymes for type II arabinogalactan side chains in *Bifidobacterium longum* subsp. *longum*. *Appl. Microbiol. Biotechnol.* 103, 1299–1310. doi: 10.1007/s00253-018-9566-4

Fujita, K., Sakamoto, S., Ono, Y., Wakao, M., Suda, Y., Kitahara, K., et al. (2011). Molecular cloning and characterization of a beta-L-arabinobiosidase in *Bifidobacterium longum* that belongs to a novel glycoside hydrolase family. *J. Biol. Chem.* 286, 5143–5150. doi: 10.1074/jbc.M110.190512

Fujita, K., Takashi, Y., Obuchi, E., Kitahara, K., and Suganuma, T. (2014b). Characterization of a novel β-L-arabinofuranosidase in *Bifidobacterium longum*: functional elucidation of a DUF1680 protein family member. *J. Biol. Chem.* 289, 5240–5249. doi: 10.1074/jbc.M113.528711

Fukuda, S., Toh, H., Hase, K., Oshima, K., Nakanishi, Y., Yoshimura, K., et al. (2011). Bifidobacteria can protect from enteropathogenic infection through production of acetate. *Nature* 469, 543–547. doi: 10.1038/nature09646

Garrido, D., Ruiz-Moyano, S., Kirmiz, N., Davis, J. C., Totten, S. M., Lemay, D. G., et al. (2016). A novel gene cluster allows preferential utilization of fucosylated milk oligosaccharides in *Bifidobacterium longum* subsp. *longum* SC596. *Sci. Rep.* 6, 35045. doi: 10.1038/srep35045

Gibson, G. R., Beatty, E. R., Wang, X., and Cummings, J. H. (1995). Selective stimulation of bifidobacteria in the human colon by oligofructose and inulin. *Gastroenterology* 108, 975–982. doi: 10.1016/0016-5085(95)90192-2

Gibson, G. R., Hutkins, R., Sanders, M. E., Prescott, S. L., Reimer, R. A., Salminen, S. J., et al. (2017). Expert consensus document: the international scientific association for probiotics and prebiotics (ISAPP) consensus statement on the definition and scope of prebiotics. *Nat. Rev. Gastroenterol. Hepatol.* 14, 491. doi: 10.1038/nrgastro.2017.75

Gibson, G. R., and Roberfroid, M. B. (1995). Dietary modulation of the human colonic microbiota: introducing the concept of prebiotics. *J.. Nutr.* 125, 1401–1412. doi: 10.1093/jn/125.6.1401

Godoy, A. S., Camilo, C. M., Kadowaki, M. A., Muniz, H. D. S., Espirito Santo, M., Murakami, M. T., et al. (2016). Crystal structure of β1→6-galactosidase from *Bifidobacterium bifidum* S17: trimeric architecture, molecular determinants of the enzymatic activity and its inhibition by α-galactose. *FEBS J.* 283, 4097–4112. doi: 10.1111/febs.13908

González-Rodríguez, I., Ruiz, L., Gueimonde, M., Margolles, A., and Sánchez, B. (2013). Factors involved in the colonization and survival of bifidobacteria in the gastrointestinal tract. *FEMS Microbiol. Lett.* 340, 1–10. doi: 10.1111/1574-6968.12056

Görke, B., and Stülke, J. (2008). Carbon catabolite repression in bacteria: many ways to make the most out of nutrients. *Nat. Rev. Microbiol.* 6, 613–624. doi: 10.1038/nrmicro1932

Goulas, T. K., Goulas, A. K., Tzortzis, G., and Gibson, G. R. (2007). Molecular cloning and comparative analysis of four beta-galactosidase genes from *Bifidobacterium bifidum* NCIMB41171. *Appl. Microbiol. Biotechnol.* 76, 1365–1372. doi: 10.1007/s00253-007-1099-1

Gupta, R. S., Nanda, A., and Khadka, B. (2017). Novel molecular, structural and evolutionary characteristics of the phosphoketolases from bifidobacteria and Coriobacteriales. *PLoS One* 12:e0172176. doi: 10.1371/journal.pone.0172176

Harholt, J., Suttangkakul, A., and Vibe Scheller, H. (2010). Biosynthesis of pectin. *Plant Physiol.* 153, 384–395. doi: 10.1104/pp.110.156588

Hill, J. E., Fernando, W. M., Zello, G. A., Tyler, R. T., Dahl, W. J., and Van Kessel, A. G. (2010). Improvement of the representation of bifidobacteria in fecal microbiota metagenomic libraries by application of the cpn60 universal primer cocktail. *Appl. Environ. Microbiol.* 76, 4550–4552. doi: 10.1128/aem.01510-09

Hinz, S. W., Pastink, M. I., van den Broek, L. A., Vincken, J. P., and Voragen, A. G. (2005). *Bifidobacterium longum* endogalactanase liberates galactotriose from type I galactans. *Appl. Environ. Microbiol.* 71, 5501–5510. doi: 10.1128/aem.71.9.5501-5510.2005

Holscher, H. D. (2017). Dietary fiber and prebiotics and the gastrointestinal microbiota. *Gut Microbes* 8, 172–184. doi: 10.1080/19490976.2017.1290756

Ichinose, H., Kuno, A., Kotake, T., Yoshida, M., Sakka, K., Hirabayashi, J., et al. (2006). Characterization of an exo-beta-1,3-galactanase from *Clostridium thermocellum*. *Appl. Environ. Microbiol.* 72, 3515–3523. doi: 10.1128/AEM.72.5.3515-3523.2006

Inada, T., Kimata, K., and Aiba, H. (1996). Mechanism responsible for glucose–lactose diauxie in *Escherichia coli*: challenge to the cAMP model. *Genes Cells* 1, 293–301. doi: 10.1046/j.1365-2443.1996.24025.x

Ito, T., Saikawa, K., Kim, S., Fujita, K., Ishiwata, A., Kaeothip, S., et al. (2014). Crystal structure of glycoside hydrolase family 127 β-l-arabinofuranosidase from *Bifidobacterium longum*. *Biochem. Biophys. Res. Commun.* 447, 32–37. doi: 10.1016/j.bbrc.2014.03.096

James, K., Motherway, M. O., Bottacini, F., and van Sinderen, D. (2016). *Bifidobacterium breve* UCC2003 metabolises the human milk oligosaccharides lacto-N-tetraose and lacto-N-neo-tetraose through overlapping, yet distinct pathways. *Sci. Rep.* 6, 38560. doi: 10.1038/srep38560

James, K., O'Connell Motherway, M., Penno, C., O'Brien, R. L., and van Sinderen, D. (2018). *Bifidobacterium breve* UCC2003 employs multiple transcriptional regulators to control metabolism of particular human milk oligosaccharides. *Appl. Environ. Microbiol.* 84, e02774-17. doi: 10.1128/AEM.02774-17

Jonker, D., Fowler, P., Albers, R., Tzoumaki, M. V., van Het Hof, K. H., and Aparicio-Vergara, M. (2020). Safety assessment of rhamnogalacturonan-enriched carrot pectin fraction: 90-Day oral toxicity study in rats and in vitro genotoxicity studies. *Food Chem. Toxicol.* 139, 111243. doi: 10.1016/j.fct.2020.111243

Kato, K., Odamaki, T., Mitsuyama, E., Sugahara, H., Xiao, J.-Z., and Osawa, R. (2017). Age-related changes in the composition of gut *Bifidobacterium* species. *Curr. Microbiol.* 74, 987–995. doi: 10.1007/s00284-017-1272-4

Kearney, S. M., and Gibbons, S. M. (2018). Designing synbiotics for improved human health. *Microb. Biotechnol.* 11, 141–144. doi: 10.1111/1751-7915.12885

Kelly, S. M., O'Callaghan, J., Kinsella, M., and van Sinderen, D. (2018). Characterisation of a hydroxycinnamic acid esterase from the *Bifidobacterium longum* subsp. *longum* Taxon. *Front. Microbiol.* 9:2690. doi: 10.3389/fmicb.2018.02690

Khoroshkin, M. S., Leyn, S. A., Van Sinderen, D., and Rodionov, D. A. (2016). Transcriptional regulation of carbohydrate utilization pathways in the *Bifidobacterium* genus. *Front. Microbiol.* 7:120. doi: 10.3389/fmicb.2016.00120

Killer, J., Kopeènı, J., Mrázek, J., Havlík, J., Koppová, I., Benada, O., et al. (2010). *Bombiscardovia coagulans* gen. nov., sp. nov., a new member of the family *Bifidobacteriaceae* isolated from the digestive tract of bumblebees. *Syst. Appl. Microbiol.* 33, 359–366. doi: 10.1016/j.syapm.2010.08.002

Kim, T.-B., Song, S.-H., Kang, S.-C., and Oh, D.-K. (2003). Quantitative comparison of lactose and glucose utilization in *Bifidobacterium longum* cultures. *Biotechnol. Progress* 19, 672–675. doi: 10.1021/bp0257426

Klaassen, M. T., and Trindade, L. M. (2020). RG-I galactan side-chains are involved in the regulation of the water-binding capacity of potato cell walls. *Carbohydr. Polym.* 227, 115353. doi: 10.1016/j.carbpol.2019.115353

Komeno, M., Hayamizu, H., Fujita, K., and Ashida, H. (2019). Two Novel alpha-l-Arabinofuranosidases from *Bifidobacterium longum* subsp. *longum* belonging to glycoside hydrolase family 43 cooperatively degrade Arabinan. *Appl. Environ. Microbiol.*. 85, e02582-18. doi: 10.1128/aem.02582-18

Koropatkin, N. M., Cameron, E. A., and Martens, E. C. (2012). How glycan metabolism shapes the human gut microbiota. *Nat. Rev. Microbiol.* 10, 323–335. doi: 10.1038/nrmicro2746

Lagaert, S., Pollet, A., Courtin, C. M., and Volckaert, G. (2014). β-Xylosidases and α-l-arabinofuranosidases: accessory enzymes for arabinoxylan degradation. *Biotechnol. Adv.* 32, 316–332. doi: 10.1016/j.biotechadv.2013.11.005

Lagaert, S., Pollet, A., Delcour, J. A., Lavigne, R., Courtin, C. M., and Volckaert, G. (2010). Substrate specificity of three recombinant α-l-arabinofuranosidases from *Bifidobacterium adolescentis* and their divergent action on arabinoxylan and arabinoxylan oligosaccharides. *Biochem. Biophys. Res. Commun.* 402, 644–650. doi: 10.1016/j.bbrc.2010.10.075

Lagaert, S., Pollet, A., Delcour, J. A., Lavigne, R., Courtin, C. M., and Volckaert, G. (2011). Characterization of two β-xylosidases from *Bifidobacterium adolescentis* and their contribution to the hydrolysis of prebiotic xylooligosaccharides. *Appl. Microbiol. Biotechnol.* 92, 1179–1185. doi: 10.1007/s00253-011-3396-y

Lagaert, S., Van Campenhout, S., Pollet, A., Bourgois, T. M., Delcour, J. A., Courtin, C. M., et al. (2007). Recombinant expression and characterization of a reducing-end Xylose-releasing Exo-oligoxylanase from *Bifidobacterium adolescentis*. *Appl. Environ. Microbiol.* 73, 5374–5377. doi: 10.1128/aem.00722-07

Lanigan, N., Kelly, E., Arzamasov, A. A., Stanton, C., Rodionov, D. A., and van Sinderen, D. (2019). Transcriptional control of central carbon metabolic flux in Bifidobacteria by two functionally similar, yet distinct LacI-type regulators. *Sci. Rep.* 9, 17851. doi: 10.1038/s41598-019-54229-4

Lansky, S., Salama, R., Dann, R., Shner, I., Manjasetty, B. A., Belrhali, H., et al. (2014). Cloning, purification and preliminary crystallographic analysis of Ara127N, a GH127 β-L-arabinofuranosidase from *Geobacillus stearothermophilus* T6. *Acta Crystallogr.* 70(Pt 8), 1038–1045. doi: 10.1107/S2053230X14012680

Lee, H. C., Jenner, A. M., Low, C. S., and Lee, Y. K. (2006). Effect of tea phenolics and their aromatic fecal bacterial metabolites on intestinal microbiota. *Res. Microbiol.* 157, 876–884. doi: 10.1016/j.resmic.2006.07.004

Lee, J. H., Hyun, Y. J., and Kim, D. H. (2011). Cloning and characterization of α-L-arabinofuranosidase and bifunctional α-L-arabinopyranosidase/β-D-galactopyranosidase from *Bifidobacterium longum* H-1. *J. Appl. Microbiol.* 111, 1097–1107. doi: 10.1111/j.1365-2672.2011.05128.x

Lewis, M., Chang, G., Horton, N. C., Kercher, M. A., Pace, H. C., Schumacher, M. A., et al. (1996). Crystal structure of the lactose operon represser and its complexes with DNA and inducer. *Science* 271, 1247–1254. doi: 10.1126/science.271.5253.1247

Luis, A. S., Briggs, J., Zhang, X., Farnell, B., Ndeh, D., Labourel, A., et al. (2018). Dietary pectic glycans are degraded by coordinated enzyme pathways in human colonic *Bacteroides*. *Nat. Microbiol.* 3, 210–219. doi: 10.1038/s41564-017-0079-1

Macfarlane, S., and Macfarlane, G. T. (2003). Regulation of short-chain fatty acid production. *Proc. Nutr. Soc.* 62, 67–72. doi: 10.1079/pns2002207

Mangas-Sánchez, J., and Adlercreutz, P. (2015). Enzymatic preparation of oligosaccharides by transglycosylation: a comparative study of glucosidases. *J. Mol. Catal. B Enzym.* 122, 51–55. doi: 10.1016/j.molcatb.2015.08.014

Margolles, A., and de los Reyes-Gavilan, C. G. (2003). Purification and functional characterization of a novel alpha-L-arabinofuranosidase from *Bifidobacterium longum* B667. *Appl. Environ. Microbiol.* 69, 5096–5103. doi: 10.1128/aem.69.9.5096-5103.2003

Martín, R., Jiménez, E., Heilig, H., Fernández, L., Marín, M. L., Zoetendal, E. G., et al. (2009). Isolation of Bifidobacteria from breast milk and assessment of the bifidobacterial population by PCR-denaturing gradient gel electrophoresis and quantitative real-time PCR. *Applied and Environ. Microbiol.* 75, 965–969. doi: 10.1128/aem.02063-08

Matsumoto, T., Shimada, S., Hata, Y., Tanaka, T., and Kondo, A. (2015). Multi-functional glycoside hydrolase: Blon_0625 from *Bifidobacterium longum* subsp. *infantis* ATCC 15697. *Enzyme Microb. Technol.* 68, 10–14. doi: 10.1016/j.enzmictec.2014.10.001

Mayo, B., and van Sinderen, D. (2010). *Bifidobacteria Genomics and Molecular Aspects*. Poole: Caister Academic Press.

Maze, A., O'Connell-Motherway, M., Fitzgerald, G. F., Deutscher, J., and van Sinderen, D. (2007). Identification and characterization of a fructose phosphotransferase system in *Bifidobacterium breve* UCC2003. *Appl. Environ. Microbiol.* 73, 545–553. doi: 10.1128/aem.01496-06

McLaughlin, H. P., Motherway, M. O., Lakshminarayanan, B., Stanton, C., Paul Ross, R., Brulc, J., et al. (2015). Carbohydrate catabolic diversity of bifidobacteria and lactobacilli of human origin. *Int. J. Food Microbiol.* 203, 109–121. doi: 10.1016/j.ijfoodmicro.2015.03.008

Milani, C., Lugli, G. A., Duranti, S., Turroni, F., Bottacini, F., Mangifesta, M., et al. (2014). Genomic encyclopedia of type strains of the genus *Bifidobacterium*. *Appl. Environ. Microbiol.* 80, 6290–6302. doi: 10.1128/aem.02308-14

Milani, C., Turroni, F., Duranti, S., Lugli, G. A., Mancabelli, L., Ferrario, C., et al. (2016). Genomics of the genus *Bifidobacterium* reveals species-specific adaptation to the glycan-rich gut environment. *Appl. Environ. Microbiol.* 82, 980–991. doi: 10.1128/aem.03500-15

Mohnen, D. (2008). Pectin structure and biosynthesis. *Curr. Opin. Plant Biol.* 11, 266–277. doi: 10.1016/j.pbi.2008.03.006

Munoz, J., James, K., Bottacini, F., and Van Sinderen, D. (2020). Biochemical analysis of cross-feeding behaviour between two common gut commensals when cultivated on plant-derived arabinogalactan. *Microb. Biotechnol.* 13, 1733–1747. doi: 10.1111/1751-7915.13577

Munoz, J. A., Chenoll, E., Casinos, B., Bataller, E., Ramon, D., Genoves, S., et al. (2011). Novel probiotic *Bifidobacterium longum* subsp. *infantis* CECT 7210 strain active against rotavirus infections. *Appl. Environ. Microbiol.* 77, 8775–8783. doi: 10.1128/aem.05548-11

Ndeh, D., and Gilbert, H. J. (2018). Biochemistry of complex glycan depolymerisation by the human gut microbiota. *FEMS Microbiol. Rev.* 42, 146–164. doi: 10.1093/femsre/fuy002

Ndeh, D., Rogowski, A., Cartmell, A., Luis, A. S., Baslé, A., Gray, J., et al. (2017). Complex pectin metabolism by gut bacteria reveals novel catalytic functions. *Nature* 544, 65–70. doi: 10.1038/nature21725

O'Callaghan, A., Bottacini, F., O'Connell Motherway, M., and van Sinderen, D. (2015). Pangenome analysis of *Bifidobacterium longum* and site-directed mutagenesis through by-pass of restriction-modification systems. *BMC Genomics* 16:832. doi: 10.1186/s12864-015-1968-4

O'Connell, K. J., Motherway, M. O. C., Liedtke, A., Fitzgerald, G. F., Paul Ross, R., Stanton, C., et al. (2014). Transcription of two adjacent carbohydrate utilization gene clusters in *Bifidobacterium breve* UCC2003 is controlled by LacI- and repressor open reading frame kinase (ROK)-type regulators. *Appl. Environ. Microbiol.* 80, 3604–3614. doi: 10.1128/AEM.00130-14

O'Connell Motherway, M., Fitzgerald, G. F., and van Sinderen, D. (2011). Metabolism of a plant derived galactose-containing polysaccharide by *Bifidobacterium breve* UCC2003. *Microb. Biotechnol.* 4, 403–416. doi: 10.1111/j.1751-7915.2010.00218.x

O'Connell Motherway, M., Kinsella, M., Fitzgerald, G. F., and van Sinderen, D. (2013). Transcriptional and functional characterization of genetic elements involved in galacto-oligosaccharide utilization by *Bifidobacterium breve* UCC2003. *Microb. Biotechnol.* 6, 67–79. doi: 10.1111/1751-7915.12011

Odamaki, T., Bottacini, F., Kato, K., Mitsuyama, E., Yoshida, K., Horigome, A., et al. (2018). Genomic diversity and distribution of *Bifidobacterium longum* subsp. *longum* across the human lifespan. *Sci. Rep.* 8, 85. doi: 10.1038/s41598-017-18391-x

Odamaki, T., Kato, K., Sugahara, H., Hashikura, N., Takahashi, S., Xiao, J. Z., et al. (2016). Age-related changes in gut microbiota composition from newborn to centenarian: a cross-sectional study. *BMC Microbiol.* 16:90. doi: 10.1186/s12866-016-0708-5

Okada, T., Fukuda, S., Hase, K., Nishiumi, S., Izumi, Y., Yoshida, M., et al. (2013). Microbiota-derived lactate accelerates colon epithelial cell turnover in starvation-refed mice. *Nat. Commun.* 4, 1654. doi: 10.1038/ncomms2668

O'Neill, E., Pozzi, C., Houston, P., Smyth, D., Humphreys, H., Robinson, D. A., et al. (2007). Association between methicillin susceptibility and biofilm regulation in *Staphylococcus aureus* isolates from device-related infections. *J. Clin. Microbiol.* 45, 1379–1388. doi: 10.1128/jcm.02280-06

Ouwehand, A. C., Bergsma, N., Parhiala, R., Lahtinen, S., Gueimonde, M., Finne-Soveri, H., et al. (2008). *Bifidobacterium microbiota* and parameters of immune function in elderly subjects. *Pathog. Dis.* 53, 18–25. doi: 10.1111/j.1574-695X.2008.00392.x

Palframan, R. J., Gibson, G. R., and Rastall, R. A. (2003). Carbohydrate preferences of *Bifidobacterium* species isolated from the human gut. *Curr. Issues Intest. Microbiol.* 4, 71–75.

Parche, S., Amon, J., Jankovic, I., Rezzonico, E., Beleut, M., Barutcu, H., et al. (2007). Sugar transport systems of *Bifidobacterium longum* NCC2705. *J. Mol. Microbiol. Biotechnol.* 12, 9–19. doi: 10.1159/000096455

Parche, S., Beleut, M., Rezzonico, E., Jacobs, D., Arigoni, F., Titgemeyer, F., et al. (2006). Lactose-over-glucose preference in *Bifidobacterium longum* NCC2705: glcP, encoding a glucose transporter, is subject to lactose repression. *J. Bacteriol.* 188, 1260–1265. doi: 10.1128/JB.188.4.1260-1265.2006

Pokusaeva, K., Fitzgerald, G. F., and van Sinderen, D. (2011a). Carbohydrate metabolism in Bifidobacteria. *Genes Nutr.* 6, 285–306. doi: 10.1007/s12263-010-0206-6

Pokusaeva, K., Neves, A. R., Zomer, A., O'Connell-Motherway, M., MacSharry, J., Curley, P., et al. (2010). Ribose utilization by the human commensal *Bifidobacterium breve* UCC2003. *Microb. Biotechnol.* 3, 311–323. doi: 10.1111/j.1751-7915.2009.00152.x

Pokusaeva, K., O'Connell-Motherway, M., Zomer, A., Macsharry, J., Fitzgerald, G. F., and van Sinderen, D. (2011b). Cellodextrin utilization by *Bifidobacterium breve* UCC2003. *Appl. Environ. Microbiol.* 77, 1681–1690. doi: 10.1128/AEM.01786-10

Pollet, A., Van Craeyveld, V., Van de Wiele, T., Verstraete, W., Delcour, J. A., and Courtin, C. M. (2012). In vitro fermentation of arabinoxylan oligosaccharides and low molecular mass arabinoxylans with different structural properties from wheat (*Triticum aestivum* L.) Bran and Psyllium (*Plantago ovata* Forsk) Seed Husk. *J. Agric. Food Chem.* 60, 946–954. doi: 10.1021/jf203820j

Porter, N. T., and Martens, E. C. (2016). Love thy neighbor: sharing and cooperativity in the gut microbiota. *Cell Host Microbe* 19, 745–746. doi: 10.1016/j.chom.2016.05.019

Posé, S., Marcus, S. E., and Knox, J. P. (2018). Differential metabolism of pectic galactan in tomato and strawberry fruit: detection of the LM26 branched galactan epitope in ripe strawberry fruit. *Physiol. Plant* 164, 95–105. doi: 10.1111/ppl.12748

Raimondi, S., Anighoro, A., Quartieri, A., Amaretti, A., Tomas-Barberan, F. A., Rastelli, G., et al. (2015). Role of bifidobacteria in the hydrolysis of chlorogenic acid. *Microbiologyopen* 4, 41–52. doi: 10.1002/mbo3.219

Rees, D. C., Johnson, E., and Lewinson, O. (2009). ABC transporters: the power to change. *Nat. Rev. Mol. Cell Biol.* 10, 218–227. doi: 10.1038/nrm2646

Riviere, A., Gagnon, M., Weckx, S., Roy, D., and De Vuyst, L. (2015). Mutual cross-feeding interactions between *Bifidobacterium longum* subsp. *longum* NCC2705 and Eubacterium rectale ATCC 33656 explain the bifidogenic and butyrogenic effects of arabinoxylan oligosaccharides. *Appl. Environ. Microbiol.* 81, 7767–7781. doi: 10.1128/aem.02089-15

Riviere, A., Moens, F., Selak, M., Maes, D., Weckx, S., and De Vuyst, L. (2014). The ability of bifidobacteria to degrade arabinoxylan oligosaccharide constituents and derived oligosaccharides is strain dependent. *Appl. Environ. Microbiol.* 80, 204–217. doi: 10.1128/aem.02853-13

Riviere, A., Selak, M., Geirnaert, A., Van den Abbeele, P., and De Vuyst, L. (2018). Complementary mechanisms for degradation of inulin-type fructans and Arabinoxylan oligosaccharides among Bifidobacterial strains suggest bacterial cooperation. *Appl. Environ. Microbiol.* 84, e02893-17. doi: 10.1128/aem.02893-17

Rogowski, A., Briggs, J. A., Mortimer, J. C., Tryfona, T., Terrapon, N., Lowe, E. C., et al. (2015). Glycan complexity dictates microbial resource allocation in the large intestine. *Nat. Commun.* 6, 7481. doi: 10.1038/ncomms8481

Ryan, S. M., Fitzgerald, G. F., and van Sinderen, D. (2005). Transcriptional regulation and characterization of a novel beta-fructofuranosidase-encoding gene from *Bifidobacterium breve* UCC2003. *Appl. Environ. Microbiol.* 71, 3475–3482. doi: 10.1128/AEM.71.7.3475-3482.2005

Sakamoto, T., and Ishimaru, M. (2013). Peculiarities and applications of galactanolytic enzymes that act on type I and II arabinogalactans. *Appl. Microbiol. Biotechnol.* 97, 5201–5213. doi: 10.1007/s00253-013-4946-2

Saulnier, L., and Thibault, J.-F. (1999). Ferulic acid and diferulic acids as components of sugar-beet pectins and maize bran heteroxylans. *J. Sci. Food Agric.* 79, 396–402. doi: 10.1002/(SICI)1097-0010(19990301)79:3<396::AID-JSFA262>3.0.CO;2-B

Schell, M. A., Karmirantzou, M., Snel, B., Vilanova, D., Berger, B., Pessi, G., et al. (2002). The genome sequence of *Bifidobacterium longum* reflects its adaptation to the human gastrointestinal tract. *Proc. Natl. Acad. Sci. U.S.A.* 99, 14422–14427. doi: 10.1073/pnas.212527599

Scheller, H. V., and Ulvskov, P. (2010). Hemicelluloses. *Annu. Rev. Plant Biol.* 61, 263–289. doi: 10.1146/annurev-arplant-042809-112315

Schiavi, E., Gleinser, M., Molloy, E., Groeger, D., Frei, R., Ferstl, R., et al. (2016). The surface-associated exopolysaccharide of *Bifidobacterium longum* 35624 plays an essential role in dampening host proinflammatory responses and repressing

local TH17 responses. *Appl. Environ. Microbiol.* 82, 7185–7196. doi: 10.1128/aem.02238-16

Schneider, E. (2001). ABC transporters catalyzing carbohydrate uptake. *Res. Microbiol.* 152, 303–310. doi: 10.1016/S0923-2508(01)01201-3

Seifert, G. J., and Roberts, K. (2007). The biology of arabinogalactan proteins. *Annu. Rev. Plant Biol.* 58, 137–161. doi: 10.1146/annurev.arplant.58.032806.103801

Sela, D. A., Chapman, J., Adeuya, A., Kim, J. H., Chen, F., Whitehead, T. R., et al. (2008). The genome sequence of *Bifidobacterium longum* subsp. *infantis* reveals adaptations for milk utilization within the infant microbiome. *Proc. Natl. Acad. Sci. U.S.A.* 105, 18964–18969. doi: 10.1073/pnas.0809584105

Shewry, P. R., and Hey, S. J. (2015). The contribution of wheat to human diet and health. *Food Energy Secur.* 4, 178–202. doi: 10.1002/fes3.64

Shin, H. Y., Lee, J. H., Lee, J. Y., Han, Y. O., Han, M. J., and Kim, D. H. (2003). Purification and characterization of ginsenoside Ra-hydrolyzing beta-D-xylosidase from *Bifidobacterium breve* K-110, a human intestinal anaerobic bacterium. *Biol. Pharm. Bull.* 26, 1170–1173. doi: 10.1248/bpb.26.1170

Smilowitz, J. T., Lebrilla, C. B., Mills, D. A., German, J. B., and Freeman, S. L. (2014). Breast milk oligosaccharides: structure-function relationships in the neonate. *Annu. Rev. Nutr.* 34, 143–169. doi: 10.1146/annurev-nutr-071813-105721

Soto, A., Martin, V., Jimenez, E., Mader, I., Rodriguez, J. M., and Fernandez, L. (2014). Lactobacilli and bifidobacteria in human breast milk: influence of antibiotherapy and other host and clinical factors. *J. Pediatr. Gastroenterol. Nutr.* 59, 78–88. doi: 10.1097/mpg.0000000000000347

Sotoya, H., Shigehisa, A., Hara, T., Matsumoto, H., Hatano, H., and Matsuki, T. (2017). Identification of genes involved in galactooligosaccharide utilization in *Bifidobacterium breve* strain YIT 4014T. *Microbiology* 163, 1420–1428. doi: 10.1099/mic.0.000517

Stewart, C. J., Ajami, N. J., O'Brien, J. L., Hutchinson, D. S., Smith, D. P., Wong, M. C., et al. (2018). Temporal development of the gut microbiome in early childhood from the TEDDY study. *Nature* 562, 583–588. doi: 10.1038/s41586-018-0617-x

Struijs, K., Vincken, J.-P., Verhoef, R., Voragen, A. G. J., and Gruppen, H. (2008). Hydroxycinnamic acids are ester-linked directly to glucosyl moieties within the lignan macromolecule from flaxseed hulls. *Phytochemistry* 69, 1250–1260. doi: 10.1016/j.phytochem.2007.11.010

Stülke, J., and Hillen, W. (1999). Carbon catabolite repression in bacteria. *Curr. Opin. Microbiol.* 2, 195–201. doi: 10.1016/S1369-5274(99)80034-4

Suzuki, H., Murakami, A., and Yoshida, K. (2013). Motif-guided identification of a glycoside hydrolase family 1 alpha-L-arabinofuranosidase in *Bifidobacterium adolescentis*. *Biosci. Biotechnol. Biochem.* 77, 1709–1714. doi: 10.1271/bbb.130279

Swanson, K. S., Gibson, G. R., Hutkins, R., Reimer, R. A., Reid, G., Verbeke, K., et al. (2020). The International scientific association for probiotics and prebiotics (ISAPP) consensus statement on the definition and scope of synbiotics. *Nat. Rev. Gastroenterol. Hepatol.* 17, 687–701. doi: 10.1038/s41575-020-0344-2

Theilmann, M. C., Fredslund, F., Svensson, B., Lo Leggio, L., and Abou Hachem, M. (2019). Substrate preference of an ABC importer corresponds to selective growth on beta-(1,6)-galactosides in *Bifidobacterium animalis* subsp. *lactis*. *J. Biol. Chem.* 294, 11701–11711. doi: 10.1074/jbc.RA119.008843

Truchado, P., Van den Abbeele, P., Riviere, A., Possemiers, S., De Vuyst, L., and Van de Wiele, T. (2015). *Bifidobacterium longum* D2 enhances microbial degradation of long-chain arabinoxylans in an in vitro model of the proximal colon. *Benef. Microbes* 6, 849–860. doi: 10.3920/bm2015.0023

Turroni, F., Foroni, E., Pizzetti, P., Giubellini, V., Ribbera, A., Merusi, P., et al. (2009). Exploring the diversity of the bifidobacterial population in the human intestinal tract. *Appl. Environ. Microbiol.* 75, 1534–1545. doi: 10.1128/aem.02216-08

Turroni, F., Peano, C., Pass, D. A., Foroni, E., Severgnini, M., Claesson, M. J., et al. (2012a). Diversity of bifidobacteria within the infant gut microbiota. *PLoS One* 7:e36957. doi: 10.1371/journal.pone.0036957

Turroni, F., Strati, F., Foroni, E., Serafini, F., Duranti, S., van Sinderen, D., et al. (2012b). Analysis of predicted carbohydrate transport systems encoded by *Bifidobacterium bifidum* PRL2010. *Appl. Environ. Microbiol.* 78, 5002–5012. doi: 10.1128/aem.00629-12

Valenzuela, S. V., Lopez, S., Biely, P., Sanz-Aparicio, J., and Pastor, F. I. (2016). The glycoside hydrolase family 8 reducing-End Xylose-releasing Exo-oligoxylanase Rex8A from *Paenibacillus barcinonensis* BP-23 is active on branched Xylooligosaccharides. *Appl. Environ. Microbiol.* 82, 5116–5124. doi: 10.1128/aem.01329-16

van den Bogaard, P. T., Kleerebezem, M., Kuipers, O. P., and de Vos, W. M. (2000). Control of lactose transport, beta-galactosidase activity, and glycolysis by CcpA in *Streptococcus thermophilus*: evidence for carbon catabolite repression by a non-phosphoenolpyruvate-dependent phosphotransferase system sugar. *J. Bacteriol.* 182, 5982–5989. doi: 10.1128/jb.182.21.5982-5989.2000

van den Broek, L. A., Hinz, S. W., Beldman, G., Vincken, J. P., and Voragen, A. G. (2008). *Bifidobacterium* carbohydrases-their role in breakdown and synthesis of (potential) prebiotics. *Mol. Nutr. Food Res.* 52, 146–163. doi: 10.1002/mnfr.200700121

van den Broek, L. A. M., Lloyd, R. M., Beldman, G., Verdoes, J. C., McCleary, B. V., and Voragen, A. G. J. (2005). Cloning and characterization of arabinoxylan arabinofuranohydrolase-D3 (AXHd3) from *Bifidobacterium adolescentis* DSM20083. *Appl. Microbiol. Biotechnol.* 67, 641–647. doi: 10.1007/s00253-004-1850-9

van Laere, K. M., Hartemink, R., Bosveld, M., Schols, H. A., and Voragen, A. G. (2000). Fermentation of plant cell wall derived polysaccharides and their corresponding oligosaccharides by intestinal bacteria. *J. Agric. Food Chem.* 48, 1644–1652. doi: 10.1021/jf990519i

van Zanten, G. C., Knudsen, A., Roytio, H., Forssten, S., Lawther, M., Blennow, A., et al. (2012). The effect of selected synbiotics on microbial composition and short-chain fatty acid production in a model system of the human colon. *PLoS One* 7:e47212. doi: 10.1371/journal.pone.0047212

Vazquez-Gutierrez, P., de Wouters, T., Werder, J., Chassard, C., and Lacroix, C. (2016). High iron-sequestrating Bifidobacteria inhibit enteropathogen growth and adhesion to intestinal epithelial cells in vitro. *Front. Microbiol.* 7:1480. doi: 10.3389/fmicb.2016.01480

Ventura, M., Canchaya, C., Tauch, A., Chandra, G., Fitzgerald, G. F., Chater, K. F., et al. (2007). Genomics of Actinobacteria: tracing the evolutionary history of an ancient phylum. *Microbiol. Mol. Biol. Rev.* 71, 495–548. doi: 10.1128/mmbr.00005-07

Viborg, A. H., Sorensen, K. I., Gilad, O., Steen-Jensen, D. B., Dilokpimol, A., Jacobsen, S., et al. (2013). Biochemical and kinetic characterisation of a novel xylooligosaccharide-upregulated GH43 beta-d-xylosidase/alpha-l-arabinofuranosidase (BXA43) from the probiotic *Bifidobacterium animalis* subsp. *lactis* BB-12. *AMB Express* 3, 56. doi: 10.1186/2191-0855-3-56

Wang, J., Sun, B., Cao, Y., and Wang, C. (2010). In vitro fermentation of xylooligosaccharides from wheat bran insoluble dietary fiber by Bifidobacteria. *Carbohydrate Polym.* 82, 419–423. doi: 10.1016/j.carbpol.2010.04.082

Wang, K., Pereira, G. V., Cavalcante, J. J., Zhang, M., Mackie, R., and Cann, I. (2016). *Bacteroides intestinalis* DSM 17393, a member of the human colonic microbiome, upregulates multiple endoxylanases during growth on xylan. *Sci. Rep.* 6, 34360. doi: 10.1038/srep34360

Watson, D., O'Connell Motherway, M., Schoterman, M. H., van Neerven, R. J., Nauta, A., and van Sinderen, D. (2013). Selective carbohydrate utilization by lactobacilli and bifidobacteria. *J. Appl. Microbiol.* 114, 1132–1146. doi: 10.1111/jam.12105

Wendisch, V. F., de Graaf, A. A., Sahm, H., and Eikmanns, B. J. (2000). Quantitative determination of metabolic fluxes during coutilization of two carbon sources: comparative analyses with *Corynebacterium glutamicum* during growth on acetate and/or glucose. *J. Bacteriol.* 182, 3088–3096. doi: 10.1128/jb.182.11.3088-3096.2000

Whorwell, P. J., Altringer, L., Morel, J., Bond, Y., Charbonneau, D., O'Mahony, L., et al. (2006). Efficacy of an encapsulated probiotic *Bifidobacterium infantis* 35624 in women with irritable bowel syndrome. *Am. J. Gastroenterol.* 101, 1581–1590. doi: 10.1111/j.1572-0241.2006.00734.x

Wilkens, S. (2015). Structure and mechanism of ABC transporters. *F1000Prime Rep.* 7, 14. doi: 10.12703/p7-14

Withers, S. G. (2001). Mechanisms of glycosyl transferases and hydrolases. *Carbohydrate Polym.* 44, 325–337. doi: 10.1016/S0144-8617(00)00249-6

Wolin, M. J., Zhang, Y., Bank, S., Yerry, S., and Miller, T. L. (1998). NMR detection of 13CH313COOH from 3-13C-glucose: a signature for *Bifidobacterium*

fermentation in the intestinal tract. *J.. Nutr.* 128, 91–96. doi: 10.1093/jn/128.1.91

Wong, C. B., Odamaki, T., and Xiao, J.-Z. (2020). Insights into the reason of Human-Residential Bifidobacteria (HRB) being the natural inhabitants of the human gut and their potential health-promoting benefits. *FEMS Microbiol. Rev.* 44, 369–385. doi: 10.1093/femsre/fuaa010

Wong, D. W. S. (2006). Feruloyl esterase. *Appl. Biochem. Biotechnol.* 133, 87–112.

Yamada, C., Gotoh, A., Sakanaka, M., Hattie, M., Stubbs, K. A., Katayama-Ikegami, A., et al. (2017). Molecular insight into evolution of symbiosis between breast-fed infants and a member of the human gut microbiome *Bifidobacterium longum*. *Cell Chem. Biol.* 24, 515–524.e5. doi: 10.1016/j.chembiol.2017.03.012

Zabel, B., Yde, C. C., Roos, P., Marcussen, J., Jensen, H. M., Salli, K., et al. (2019). Novel genes and metabolite trends in *Bifidobacterium longum* subsp. *infantis* Bi-26 metabolism of human milk oligosaccharide 2'-fucosyllactose. *Sci. Rep.* 9, 7983. doi: 10.1038/s41598-019-43780-9

Zavaleta, V., and Eyzaguirre, J. (2016). *Penicillium purpurogenum* produces a highly stable endo-β-(1,4)-galactanase. *Appl. Biochem. Biotechnol.* 180, 1313–1327. doi: 10.1007/s12010-016-2169-6

Zhang, M., Chekan, J. R., Dodd, D., Hong, P.-Y., Radlinski, L., Revindran, V., et al. (2014). Xylan utilization in human gut commensal bacteria is orchestrated by unique modular organization of polysaccharide-degrading enzymes. *Proc. Natl. Acad. Sci. U.S.A.* 111, E3708. doi: 10.1073/pnas.1406156111

Zhu, Z., He, M., Huang, C. H., Ko, T. P., Zeng, Y. F., Huang, Y. N., et al. (2014). Crystallization and preliminary X-ray diffraction analysis of a novel β-L-arabinofuranosidase (HypBA1) from *Bifidobacterium longum*. *Acta Crystallogr.* 70(Pt 5), 636–638. doi: 10.1107/S2053230X14001812

Zoetendal, E. G., Raes, J., van den Bogert, B., Arumugam, M., Booijink, C. C. G. M., Troost, F. J., et al. (2012). The human small intestinal microbiota is driven by rapid uptake and conversion of simple carbohydrates. *ISME J.* 6, 1415–1426. doi: 10.1038/ismej.2011.212

Conflict of Interest: The authors declare that the research was conducted in the absence of any commercial or financial relationships that could be construed as a potential conflict of interest.

frontiers in Microbiology

ORIGINAL RESEARCH
published: 08 March 2021
doi: 10.3389/fmicb.2021.625562

Characterization and Functional Test of Canine Probiotics

Hyun-Jun Jang[1], Seungwoo Son[2,3], Jung-Ae Kim[1,4], Min Young Jung[1], Yeon-jae Choi[1], Dae-Hyuk Kim[1,4,5], Hak Kyo Lee[2,3], Donghyun Shin[2,3] and Yangseon Kim[1]**

[1] Department of Research and Development, Center for Industrialization of Agricultural and Livestock Microorganisms, Jeongeup-si, South Korea, [2] Department of Agricultural Convergence Technology, Jeonbuk National University, Jeonju-si, South Korea, [3] The Animal Molecular Genetics & Breeding Center, Jeonbuk National University, Jeonju-si, South Korea, [4] Department of Bioactive Material Sciences, Jeonbuk National University, Jeonju-si, South Korea, [5] Department of Molecular Biology, Institute for Molecular Biology and Genetics, Jeonbuk National University, Jeonju-si, South Korea

Probiotics can modulate the composition of gut microbiota and benefit the host animal health in multiple ways. *Lactic acid bacteria* (LAB), mainly *Lactobacillus* and *Bifidobacterium* species, are well-known microbes with probiotic potential. In the present study, 88 microbial strains were isolated from canine feces and annotated. Among these, the four strains CACC517, 537, 558, and 566 were tested for probiotic characteristics, and their beneficial effects on hosts were evaluated both *in vitro* and *in vivo*; these strains exhibited antibiosis, antibiotic activity, acid and bile tolerance, and relative cell adhesion to the HT-29 monolayer cell line. Byproducts of these strains increased the viability and decreased oxidative stress in mouse and dog cell lines (RAW264.7 and DH82, respectively). Subsequently, when the probiotics were applied to the clinical trial, changes in microbial composition and relative abundance of bacterial strains were clearly observed in the experimental animals. Experimental groups before and after the application were obviously separated from PCA analysis of clinical results. Conclusively, these results could provide comprehensive understanding of the effects of probiotic strains (CACC517, 537, 558, and 566) and their industrial applications.

Keywords: canine, probiotics, Lactobacillus, Bifidobacterium, feed additives

OPEN ACCESS

Edited by:
Abelardo Margolles, Consejo Superior de Investigaciones Científicas (CSIC), Spain

Reviewed by:
Huaxi Yi, Ocean University of China, China
Neeta Agarwal, Indian Veterinary Research Institute (IVRI), India

***Correspondence:**
Donghyun Shin
sdh1214@gmail.com
Yangseon Kim
yangseon@cialm.or.kr

Specialty section:
This article was submitted to Food Microbiology, a section of the journal Frontiers in Microbiology

Received: *04 November 2020*
Accepted: *17 February 2021*
Published: *08 March 2021*

Citation:
Jang H-J, Son S, Kim J-A, Jung MY, Choi Y-j, Kim D-H, Lee HK, Shin D and Kim Y (2021) Characterization and Functional Test of Canine Probiotics. Front. Microbiol. 12:625562. doi: 10.3389/fmicb.2021.625562

INTRODUCTION

According to the 2001 definition by the World Health Organization (WHO), probiotics are live microorganisms that, when administered in adequate amounts, confer health benefits to the host (Hotel and Cordoba, 2001). Since Metchnikoff found and proposed the concept of probiotics for the first time more than a century ago (Podolsky, 2012), many different microorganisms have been considered as probiotics; these microorganisms are generally classified as lactobacilli, bifidobacteria, other lactic acid bacteria (LAB), and non-lactic acid bacteria (Holzapfel et al., 2001; Nagpal et al., 2012; Khalighi et al., 2016). In the interaction between host and probiotics, the mechanisms are generally categorized as act on competition between probiotics and pathogenic organisms for an adhesion site or a nutrient compound, synthesis of antimicrobial compounds by probiotics, and modulation of the host immune system. Collectively, these modes of action are considered when screening novel probiotic strains (Shokryazdan et al., 2017; Singh et al., 2018). The beneficial effects of probiotics during the interaction have been reported to contribute to intestinal health in hosts by regulating gut microbiota, stimulating and developing the immune system, activating and enhancing nutrient metabolism, and preventing and attenuating various diseases

such as digestive disorders, infectious diseases, cancer, and allergies (Michail et al., 2006; Yadav et al., 2008; Kumar et al., 2009, 2010, 2012; Manoj et al., 2009; Nagpal et al., 2012). The commercial potential of probiotics has been growing in a wide range of industrial fields, including food, feed, dairy, fermentation, and pharmaceuticals (Song et al., 2012; El Hage et al., 2017; Sharma and Im, 2018).

Dogs have been regarded as companion animals for thousands of years. Research on canine probiotics can be meaningful not only for dog health but also for human health, as there is interaction between dogs and their owners (Grzeskowiak et al., 2015). 16S rRNA sequencing revealed that various lactobacilli, including *L. acidophilus*, *L. fermentum*, *L. rhamnosus*, *L. salivarius*, *L. murinus*, *L. reuteri*, *L. animalis*, *L. sanfranciscensis*, and *L. paraplantarum*, were prevalent in all parts of the canine GIT (Beasley et al., 2006; Ritchie et al., 2008; Suchodolski et al., 2008; Tang et al., 2012; Silva et al., 2013). In addition, bifidobacteria of both animal- (*B. pseudolongum* and *B. animalis*) and human-origin (*B. catenulatum* and *B. bifidum*) have been found in canine feces (Kim and Adachi, 2007; Lamendella et al., 2008; Bunesova et al., 2012). However, functional studies of canine probiotics are rare. In this study, we isolated novel probiotics from dogs and characterized them both *in vitro* and *in vivo*. The findings of this study can contribute to the establishment of an integrated model for characterizing novel probiotics, and the characterized probiotics may have potential for use in industrial fields related to dogs.

MATERIALS AND METHODS

Animal Care

The Institutional Animal Care and Use Committee of the Institution approved all animal procedures (JBNU 2020-0139). All methods were performed in accordance with the relevant guidelines and regulations outlined in this protocol.

Isolation of Bacterial Strains From Canine Feces

Feces were collected from six dogs (mean ± SD age, 6.5 ± 2.65 months; the ratio of male to female, 2:1; body weight, 13.08 ± 8.53 kg). All dogs were privately owned and had indoor access. One gram of each fecal sample was processed by crushing and suspending in 10 mL physiological saline, followed by homogenization. For enumeration, a 10 times dilution series of each homogenate was prepared using sterile saline solution and 0.1 mL of the samples were spread on modified MRS (mMRS,de Man, Rogosa, and Sharpe with 0.05% cysteine-HCl agar), BS (Bifidobacterium Selective) agar plate then incubated in anaerobic atmosphere (5% hydrogen and 5% carbon dioxide, and 90% nitrogen) at 37°C for 48 h to obtain single colonies. Subsequently, each colony was sequenced using 16S rRNA gene sequencing method. The annotated 88 bacterial strains were screened by our standard screening procedures. From the screening, *Bifidobacterium longum* subsp. *longum* CACC517, *Pediococcus acidilactici* CACC537, *Lactobacillus plantarum* subsp. *plantarum* CACC558, and *Lactobacillus paracasei* subsp. *tolerans* CACC566 were selected for further analysis. As a reference strain, *Lactobacillus rhamnosus GG* ATCC53013 was obtained from Korean Collection for Type Cultures[1].

16S rRNA Gene Amplification and Sequencing

Briefly, 16S rRNA gene of the isolated bacterial strains were amplified using the universal primers 27F (5′-AGA GTT TGA TCC TGG CTC AG-3′) and 1492R (5′-GGT TAC CTT GTT ACG ACT T T-3′) (Lane, 1991). The PCR reaction was performed using a high-fidelity polymerase (AccuPrime Taq DNA Polymerase System, Invitrogen, Carlsbad, CA, United States) in a Biometra GmBH PCR machine (Göttingen, Germany), according to the manufacturer's instructions. The amplicons for 16S rRNA were sequenced using the primers 785F (5′-GGA TTA GAT ACC CTG GTA-3′) and 907R (5′-CCG TCA ATT CMT TTR AGT TT-3′).

Phylogenetic Analysis

Gene fragments were assembled using the SeqMan program (Lasergene software V7, DNASTAR, United States) and reference gene sequences were compared with gene sequences available in GenBank DNA databases[2] and Ribosomal Database Project (RDP) using BLAST (Altschul et al., 1990). Phylogenetic analysis of the 16S rRNA genes was performed using Molecular Evolutionary Genetic Analysis software, Version 7 (Kumar et al., 2016). Evolutionary relationships were constructed using the maximum likelihood method based on bootstrapping (Tamura and Nei, 1993).

Genome Sequencing, Annotation, and Comparison Genomics

DNA from each of the four strains was extracted using a DNeasy UltraClean microbial kit (Qiagen, Hilden, Germany) according to the manufacturer's instructions. Whole-genome shotgun sequencing of DNA samples of the four strains was carried out using PacBio SMRT sequencing technology. The recently described hierarchical genome assembly process (HGAP, v3.0) was applied to assemble the genomes of the four strains (Hong et al., 2009) and the final assemblies ranged from 2.0 Mb to 3.23 Mb in one contig (**Supplementary Figure 1** and **Table 1**). The genome sequence (ASM2650v1) of the reference strain (*Lactobacillus rhamnosus GG* ATCC53013) was acquired from NCBI GenBank and compared with the four strains isolated in this study. The genome sequences of the four strains were annotated using Prokka (v1.13) for genomic annotation (Seemann, 2014). The protein-coding sequences of the five strains were predicted and EggNOG (v2.0.1) annotation was carried out using EggNOG-mapper (Huerta-Cepas et al., 2015). The protein-coding sequences were predicted and categorized based on the COG database (v2.0) in Prokka results; the results are shown in **Table 1**. To evaluate the genetic relatedness among all 5 strains, including the reference strain, average nucleotide identity (ANI)

[1]https://kctc.kribb.re.kr/En/Kctc

[2]https://www.ncbi.nlm.nih.gov

TABLE 1 | Genome information of five used strains (Four stains form this study and One from NCBI).

Strains	ATCC53103	CACC517	CACC537	CACC558	CACC566
Genome size (bp)	3,010,111	2,281,664	2,035,984	3,250,114	3,123,521
GC (%)	46.7	59.8	42.0	44.6	46.3
CDS	2,832	1,835	1,897	3,030	2,984
tRNA	57	56	56	68	59
rRNA	15	12	15	16	15
Average nucleotide identity	–	64.46	66.20	65.80	77.47

was calculated using the JSpecies webserver (Richter et al., 2015). The nucleotide sequences of all five strains were first annotated using Prokka (Seemann, 2014) to obtain GFF formatted files, which were used to calculate the core genes. The core, accessory, and strain-specific genes were calculated using gene information from the Prokka result (**Figure 1B**).

Acid and Bile Salt Tolerance

To evaluate the tolerance of bacterial strains under low pH and high bile salt concentration, the stimulation of GIT was determined in the present study using a previously described procedure with modifications (Liong and Shah, 2005). For assessing the tolerance of microbial strains to acidic conditions, mMRS, BL (*Bifidobacterium* spp. culture medium) broth was adjusted to pH 2.5 (treatment) and 6.5 (control) using 1 M HCl. Next, overnight cultured isolates (approximately 1×10^7 CFU/mL) were added to each pH-adjusted medium and incubated for 2 h at 37°C (CACC517, 537, 558, and 566) without shaking, respectively. Bile tolerance of the strains was determined on the basis of growth in mMRS and BL broth with 0.3% and 1% oxgall (Difco, United States) for 2 h, using the same incubation temperatures and conditions described earlier for acid tolerance. All experiments were carried out under anaerobic conditions. After incubation, 10 × serial dilutions of the cultures were spread on agar plates, followed by 24 h of incubation at 37°C. Acid and bile tolerance were evaluated by enumeration of viable colonies, and each assay was performed in triplicate. In both cases, survival was calculated using the following formula (Kim et al., 2019):

$$Survivability\,(\%) = \frac{TreatmentCFU/ml}{ControlCFU/ml} \times 100$$

Antibacterial Analysis

Strains were evaluated for antibacterial activities against economically important enteropathogenic microorganisms, using a previously described disk diffusion method (Tagg and McGiven, 1971) with slight modifications. The following seven enteropathogenic bacteria were used as indicators of antibacterial activity: *Salmonella* Typhimurium NCCP 10438, *Salmonella* Enteritidis NCCP 14546, *Salmonella* Derby NCCP 12238, *Escherichia coli* K99 KCTC 2617, *Yersinia enterocolitica* NCCP 11129, *Yersinia pseudotuberculosis* NCCP 11125, and *Clostridium difficile* JCM1296. In brief, pathogenic strains were initially grown on appropriate media: *E. coli* was grown on Luria Bertani agar (LB), *Salmonella* spp. on Salmonella and Shigella agar (SSA), *and Yersinia* spp. on Brain Heart Infusion (BHI) agar at 30°C and 37°C for 20 h. Diffusion disks of 8 mm diameter were appropriately overlaid on the agar and 1×10^6 CFU/mL of the culture suspensions were dispensed onto the disks. The plates were incubated at 30°C and 37°C for 24 h and the diameters of the inhibition zones around each disk were measured (Kim et al., 2019).

Antibiotic Sensitivity

The sensitivities of the isolated microbial strains to a set of antibiotics were assessed using the E-test minimum inhibitory concentration (MIC) method (E-test bio Mẽrieux BIODISK, France) as previously described (Hummel et al., 2007), with some modifications. A total of 11 antibiotic strips impregnated with amoxicillin, ampicillin, clindamycin, gentamicin, kanamycin, metronidazole, tetracycline, vancomycin, and erythromycin at minimum inhibition concentrations (MIC) ranging from 0.016 to 256 μg/ml, and imipenem and trimethoprim-sulfamethoxazole at minimum inhibition concentrations (MIC) ranging from 0.016 to 32 μg/ml were used to test the target strains. Fresh samples of target strains were spread onto agar plates containing mMRS (CACC537,558 and 566), BS (CACC517) (Difco, United States), and the E-test strips were laid on the agar; the plates were incubated at 37°C for 24 h in anaerobic condition. To determine antibiotic sensitivity, the MIC was considered as the antibiotic concentration at which dense colonial growth intersected the strip. Tests were performed in triplicate for each strain for optimization (Amin et al., 2009; Kim et al., 2019).

Host Cell Adhesion Assay

The ability of microbial cells to adhere to the intestinal lining was determined using HT-29 colonic carcinoma cells derived from the human small intestine, according to a previous report with slight modifications (Kim et al., 2019). Monolayers of HT-29 cells were prepared in DMEM (Sigma, United States) supplemented with 10% fetal bovine solution (FBS) (Sigma, United States) in 24-well tissue plates (BD Biosciences, San Jose, CA, United States) at a concentration of 1×10^5 cells/well. To test the abilities of the strains for adhesion to host cells, HT-29 cells were incubated with 2×10^7 CFU/mL of a cultured strain for 2 h at 37°C with 5% CO_2. After incubation, the HT-29 cells were aspirated and washed three times with 1 × PBS to remove unbound microbial cells. Adherent cells were detached and appropriate dilution series were prepared, followed by enumeration of viable colonies on appropriate agar plates in triplicate.

Effectiveness Test for Host Cell Viability

Raw264.7 and DH82 cells were seeded at a density of 1×10^3 cells/well in separate 96 well plates and incubated for 24 h at 37°C with 5% CO_2. Cell viability was determined using the WST-1 Assay Kit (Enzo, United States). The bacterial strains were cultured for 20 h at 37°C and then adjusted the number of cells (approximately 1×10^8 CFU/mL). The bacterial culture was centrifuged at 8,000 rpm at 4°C for 10 min to obtain a supernatant. 10 μl of the supernatant

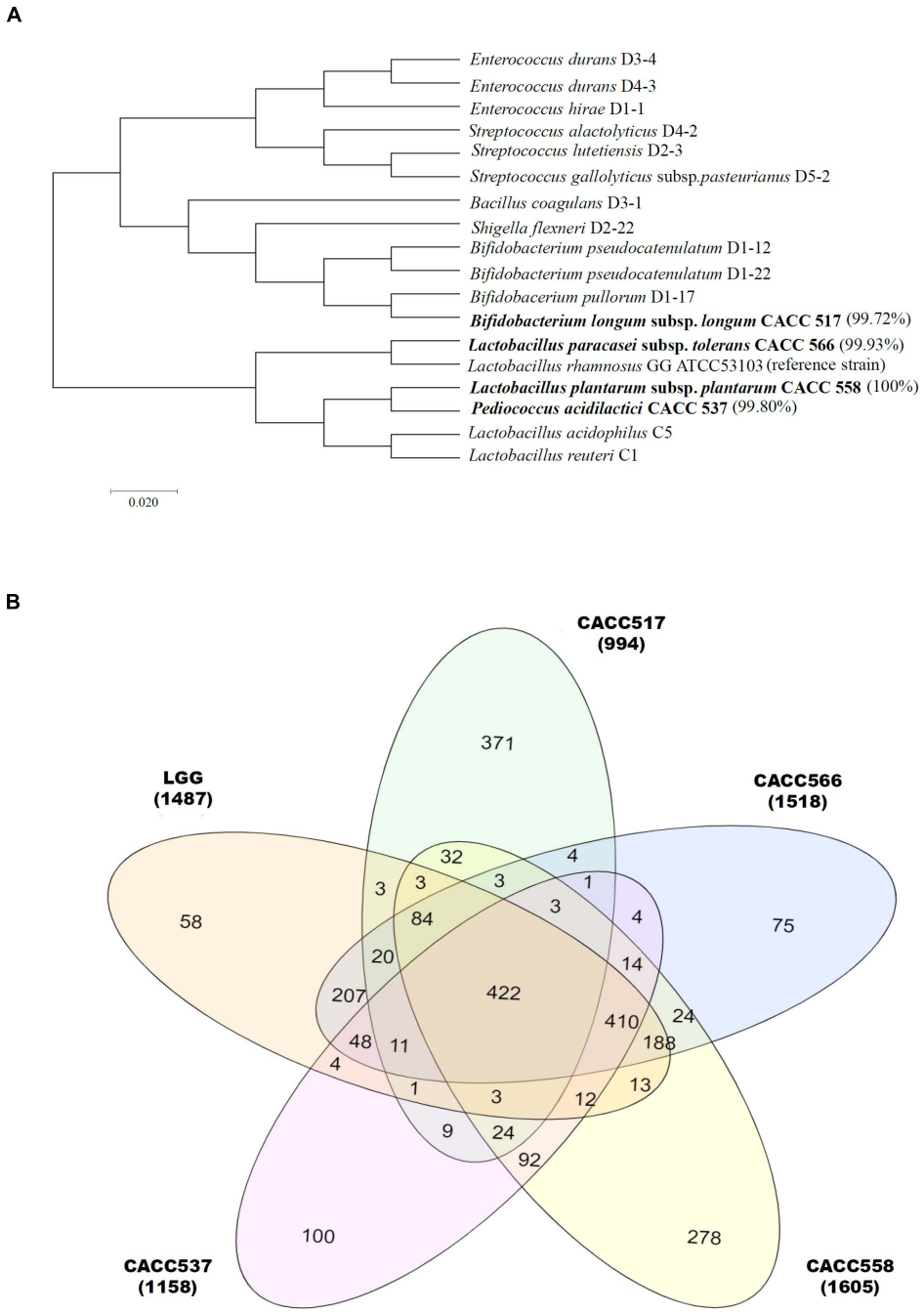

FIGURE 1 | Bacterial identification using 16S metagenomics approach. Eighty-eight bacterial strains were identified from dog feces. Molecular phylogenetic analysis showing their relationship, including CACC517, CACC537, CACC558, and CACC566, is displayed using the maximum-likelihood method (Ding and Shah, 2007; Guo et al., 2016). Bootstrap values of 500 replicates are shown at the tree nodes, as generated using MEGA 7. The scale bar corresponds to 0.02 units of the number of base substitutions per site **(A)**. Venn diagram plot represents three parts (core, accessory, and strain-specific) of the pan-genome. The center (422), overlapped (2∼4 times) and outer (non-overlapped) indicate the number of core, accessory and strain-specific genes respectively **(B)**.

was added to the cells and further incubated for 4 h at 37°C with 5% CO_2. The treated bacterial cells were diluted in a 10-fold dilution series. After that, the cells were incubated with 10 μl WST-1 reagent for 3 h before harvesting at the indicated time points. Absorbance was measured at both 450 nm and 650 nm (as a reference) using a UV-spectrophotometer (Tecan, Swiss) according to the manufacturer's instructions.

Test for Inhibitory Effect on Nitric Oxide Production (NO) in Host Cells

Measurement of NO production RAW264.7 and DH82 cells were seeded at a density of 1×10^3 cells/well in separate 96 well plates and incubated for 24 h at 37°C with 5% CO_2. The medium in each well was aspirated and replaced with fresh FBS-free DMEM. The bacterial strains were cultured for 20 h at 37°C and then adjusted the number of cells (approximately 1×10^8 CFU/mL). The bacterial culture was centrifuged at 8,000 rpm at 4°C for 10 min to obtain a supernatant. The treated supernatant was diluted in a 10-fold dilution series. Each diluent was adjusted to the volume of 100 μl with DMEN and incubated with host cells for 1 h at 37°C with 5% CO_2. After that in the incubated cells were treated with 500 ng/ml lipopolysaccharide (LPS) for 24 h at 37°C with 5% CO_2. The presence of nitrite in cell culture media was determined using the Griess Reagent System (Promega, Madison, WI, United States) according to the manufacturer's instructions. Briefly, 50 μl of cell culture medium with an equal volume of Griess reagent in a 96-well plate was incubated at room temperature for 10 min. Then, the absorbance was measured at 540 nm. The amount of nitrite in the media was calculated using the sodium nitrite ($NaNO_2$) standard curve.

Clinical Trial

This study used data from three Korean animal hospitals, and 37 dogs that were privately owned and had indoor access were recruited. Thirty-seven dogs (mean ± SD age, 62.95 ± 47.00 months; the ratio of male to female, 1.64:1; body weight, 5.73 ± 3.25 kg) were randomly grouped into four experimental groups (**Supplementary Table 2**). Each bacterial strain was cultured in mMRS and BL broth under anaerobic condition (5% hydrogen and 5% carbon dioxide, and 90% nitrogen) at 37°C for 48 h and then lyophilized. The probiotic products consisted of 5% fructo-oligosaccharide, 10% skim milk, 15% trehalose, 0.5% glycerin, 1% NaCl, and one of the following bacterial strains: CACC517, CACC537, CACC558, and CACC566. Each experimental group was administered 0.2 g probiotic product, including 10^8 bacteria, every day for 4 weeks. In detail, the powder of 0.2 g probiotic product was individually sealed in a medicine plastic bag. The powder was dissolved in 1 ml water and fed using a 1 ml syringe. No significant adverse symptoms were reported during the clinical trial. Blood and fecal samples were collected from the dogs before feeding the probiotic products and at 4 weeks after feeding the probiotic products. The blood samples were analyzed using complete blood count (CBC) and electrolyte tests according to standard protocols.

Microbial Community Analysis Using 16S rRNA Sequencing

DNA was isolated from the fecal samples, collected before and after the clinical trial in dogs, using Epi-center DNA isolation kits. We extracted approximately 900 ng of DNA from each sample. DNA quality was confirmed using a Bioanalyzer with an Agilent RNA 6000 Pico Kit (Agilent, Santa Clara, CA, United States). All samples from the reservoir were prepared using the 16S library preparation protocol and the Nextera XT DNA index kit (Illumina, San Diego, CA, United States) to target the V3-V4 variable regions of the 16S rRNA gene. We quantified the library by real-time PCR using a CFX96 real-time system (BioRad, Hercules, CA, United States). Before sequencing, all 54 samples passed a QC test. Samples were loaded onto a MiSeq reagent cartridge (Illumina) and then onto the instrument. Automated cluster generation was performed and a 300 bp single-end sequencing was performed. The resulting sequence reads were equally distributed across the samples. The Illumina MiSeq technology can generate up to 107 sequences in a single run (Kuczynski et al., 2012). Then, quantitative insights into microbial ecology (QIIME) then takes the instrument output and generates useful information about the community in each sample (Caporaso et al., 2010).

We divided the process into upstream and downstream stages. Sample identifier, barcode, and primer sequence information were required for the upstream stage of the QIIME workflow. This processing step combines sample demultiplexing, primer removal, and quality filtering. The first step in the upstream stage is the removal of the barcode sequence. During PCR amplification, some of the amplified sequences can be produced from multiple parent sequences, generating chimeric sequences. Therefore, we identified chimeric sequences in FASTA files from the GREENGENES database (DeSantis et al., 2006) and vsearch (Rognes et al., 2016). Then, we removed the identified chimera sequences from the FASTA files. The next step is clustering the preprocessed sequences into operational taxonomic units (OTUs), which in traditional taxonomy represent groups of organisms defined by intrinsic phenotypic similarity that constitute candidate taxa (Caporaso et al., 2010). For DNA sequence data, these clusters are formed based on sequence identity. In other words, sequences are clustered together if they are more similar than a user-defined identity threshold, presented as a percentage (s). This threshold level is traditionally set at 99% sequence similarity, conventionally assumed to represent bacterial species (Drancourt et al., 2000). An open-reference OTU picking process, in which reads were clustered against a reference sequence collection, was carried out and any read that did not hit the reference sequence collection was subsequently clustered *de novo* (Navas-Molina et al., 2013). PCA analysis was performed before and after probiotic treatment (**Figure 5B**). Multi-level taxonomic abundance was extracted using QIIME and Student's *t*-test (paired) was used to detect differentially abundant microbiota by comparing the relative abundance between samples collected before and after probiotics treatment (**Figure 5A** and **Table 4**). For the consideration of different reads generated, proportion of read count was used instead. We calculated species richness for a given number of individual samples with rarefaction curves using R package (BiodiversityR) (**Figure 6**).

Principal Component Analysis (PCA)

All values, including the results of CBC and electrolyte tests, were imported into SIMCA-P (version 14.1, Umetrics Inc., Kinnelon, NJ, United States) for multivariate statistical analysis to examine intrinsic variations in the data set. These data were scaled using

cantered unit variance scaling prior to the PCA. PCA score plots were used to interpret the intrinsic variation in the data.

Statistical Analysis

Statistical evaluation of the data was performed using analysis of variance with the general linear model for randomized complete block design. All treatments were performed in triplicate, and Tukey's HSD test was applied to define mean differences between specific treatments. The statistical significance ($P < 0.05$, $P < 0.01$, or $P < 0.001$) of the differences was determined. All analyses were conducted using JMP 14.3.0 (SAS Institute Inc. NC, United States).

RESULTS

Taxonomic Assignment and Probiotics Identification

In this study, over 36 species isolated from the feces of 6 dogs were identified using 16S RNA sequencing. A total of 88 bacterial strains were isolated and probiotic candidates were selected through prescreening (data not shown). Among these strains, four were further studied for probiotic characterization; these included *Bifidobacterium longum* subsp. *longum* CACC517, *Pediococcus acidilactici* CACC537, *Lactobacillus plantarum* subsp. *plantarum* CACC558, and *Lactobacillus paracasei* subsp. *tolerans* CACC566 (**Figure 1A**).

Probiotics Characterization

Genomic Structure and Genetic Feature

Whole genome sequences of the strains CACC517, CACC537, CACC558, and CACC566 were uploaded to NCBI with accession IDs PRJNA599536, PRJNA601629, PRJNA601672, and PRJNA601660, respectively. The total genome sizes of the four strains (CACC517, CACC537, CACC558, and CACC566) were 2.282 Mb, 2.036 Mb, 3.25 Mb, and 3,124 Mb, respectively (**Table 1** and **Supplementary Figure 1**). The G ++ C content of the genomes of these strains ranged from 42.0% to 59.8%. In addition, genome annotation using the eggNOG-mapper (Huerta-Cepas et al., 2015) revealed that the sequenced genomes consisted of 1,835 (CACC517), 1,897 (CACC537), 3,030 (CACC558), and 2,984 (CACC566) coding sequences. Carbohydrate transport and metabolism (G) (10.23%) and amino acid transport and metabolism (E) (9.44%) accounted for the largest proportion of protein coding categories in strain CACC517 (**Table 2**). The largest proportion of protein coding categories in CACC558 strains were Transcription (K) (9.7%) and Carbohydrate transport and metabolism (G) (8.29%). The largest proportion of protein coding categories in CACC566 and CACC537 were Carbohydrate transport and metabolism (G) (10.02%) and Transcription (K) (8.5%) (**Table 2**). Further, we performed core gene analysis of the five strains, including Lactobacillus Rhamnosus, based on the GFF file. The five strains contained 422 core genes, 1,217 accessory genes (511 genes: four strains shared genes, 314 genes: three strains shared genes, 392 genes: two strains shared genes), and 882 strain-specific genes (**Figure 1B**). Based on these results, we could expect different characteristics of the four strains sharing basic probiotic characteristics.

Acid and Bile Tolerance and Intestinal Adhesion Ability

When acid and bile tolerance were tested at pH 2.5 and 0.3% and 1% bile salts, respectively, CACC517, CACC537, CACC558, and CACC566 showed higher or equivalent survivability at 0.3% and 1% bile salts-treated conditions, but lower survivability at pH 2.5 compared to *Lactobacillus rhamnosus GG* ATCC53103 (LGG), the reference probiotic strain ($P < 0.001$) (**Figure 2A**). Assessment of the ability for adhesion to the intestinal lining, using the human colonic carcinoma cell line HT-29, revealed that CACC537, CACC558, and CACC566 exhibited superior or equivalent activity, whereas CACC517 showed slightly lower activity (61.7%) compared to LGG (76.3%) ($P < 0.05$ or $P < 0.001$) (**Figure 2B**). Thus, these results suggest that the bacterial strains are tolerant to bile salt environments but susceptible to acidic conditions, relative to the reference probiotic strain.

Antibacterial Activity and Antibiotic Sensitivity

The antibacterial activity test against various pathogenic bacteria revealed that all the strains showed antibacterial activity against *S. Typhimurium* NCCP 10438, *S. Enteritidis* NCCP 14546, *S. Derby* NCCP 12238, *E. coli* K99 KCTC 2617, and *Y. pseudotuberculosis* NCCP 11125. Additionally, CACC537 and CACC566 exhibited antibacterial activity against *Y. enterocolitica* NCCP 11129 while CACC517 exhibited antibacterial activity against *C. difficile* JCM1296. In particular, CACC558 exhibited antimicrobial activity against all the tested pathogenic bacteria (**Table 2**). Assessment of antibiotic sensitivity for commercial antibiotics demonstrated that all the tested strains were resistant to kanamycin and vancomycin, except CACC517. Additionally, CACC537 showed resistance to imipenem, while both CACC558 and CACC566 exhibited resistance to metronidazole and trimethoprim-sulfamethoxazole (**Table 3**). Therefore, we supposed that the strains have different spectra of antibacterial activities and antibiotic resistance.

In vitro and *in vivo* Host Responses to Probiotics

Enhancement of Host Cell Viability

To evaluate the enhancement of host cell viability by the byproducts of the probiotic bacterial strains (CACC517, CACC537, CACC558, and CACC566), the different culture media, in which the strains were separately cultured with different seeding densities, were added to murine macrophage cell line (RAW264.7) or canine macrophage cell line (DH82). The viability of the normally cultured host cells (RAW264.7 and DH82) was not significantly different from that of the negative control (medium only) (**Figure 3A**). In case of RAW264.7 cells, the culture media with seeding densities of 10^7, 10^6, and 10^5 CFU/mL of LGG exhibited increased viability compared to the negative control ($P < 0.05$, $P < 0.01$, *or* $P < 0.001$). All strains showed a superior or equivalent effect on the enhancement of

TABLE 2 | Antibacterial activity of the test strains against the indicator strains.

Strain	*Salmonella* Typhimurium NCCP 10438	*Salmonella* Enteritidis NCCP 14546	*Salmonella* Derby NCCP 12238	*E. coli* K99 KCTC 2617	*Yersinia enterocolitica* NCCP 11129	*Yersinia pseudotuberculosis* NCCP 11125	*Clostridium difficile* JCM1296
CACC517	++	+	+	+	–	+	+
CACC537	++	++	++	++	++	+++	–
CACC558	++	++	++	+	++	++	++
CACC566	++	++	+	++	+	+++	–

The inhibition zone (mm) around the paper disc containing the microbial cell-free supernatant was classified as ++, > 12–14 mm; +, > 11mm; w (weak), less than 9 mm; -, no inhibition zone.

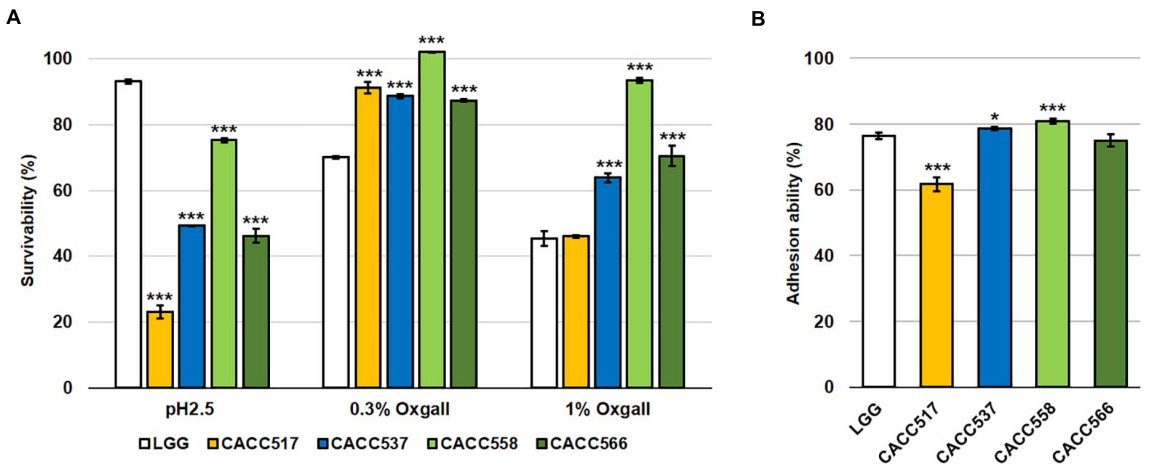

FIGURE 2 | Acid and bile tolerance, and intestinal adhesion activity. The survivability of the bacterial strain was tested after pH 2.5 or 0.3% and 1% bile salt treatments for 2 h **(A)** and their ability to adhere to the intestinal lining using the human colonic carcinoma cell line HT-29 **(B)**. A significant difference was determined compared to the reference strain (LGG, *Lactobacillus rhamnosus* GG ATCC53103). *$P < 0.05$; ***$P < 0.001$.

TABLE 3 | Minimum inhibitory concentrations (μg/ml) of antibiotics against the test strains.

Antibiotic	Antibiotic sensitivity			
	CACC517	CACC537	CACC558	CACC566
Amoxicillin	0.38	3	≥ 0.19	≥1.5
Ampicillin	0.25	2	≥ 0.094	≥1.5
Clindamycin	S	0.094	≥ 2	≥0.38
Erythromycin	0.032	48	≥ 1.5	≥0.25
Gentamicin	96	0.32	≥ 24	R
Imipenem	0.25	R	≥ 0.047	≥1.5
Kanamycin	R	R	R	R
Metronidazole	1	24	R	R
Tetracycline	0.38	R	≥ 16	≥1
Trimethoprim-sulfamethoxazole	4	0.75	R	R
Vancomycin	0.75	R	R	R

Quantitative antibiotic sensitivity is expressed as the minimum inhibitory concentration against the microbial strains and classified as R, resistant (≥32 and 256 μg/ml) or presented as values in bold (weakly tolerant) and regular font (sensitive to the antibiotic).

host cell viability compared to LGG ($P < 0.05$). However, culture medium with a seeding density of 10^8 CFU/mL of LGG decreased the viability of RAW264.7 compared to the negative control ($P < 0.05$) (upper part of **Figure 3A**). In case of DH82 cells, the culture media with seeding densities of 10^4, 10^3, 10^2, and 10 CFU/mL of LGG did not affect the viability. In addition, the culture medium with a seeding density of 10^4 CFU/mL of CACC517, CACC537, CACC558, and CACC566 did not affect the viability of DH82 cells. However, compared to LGG, the culture media of CACC537 and CACC558 increased cell viability under all seeding conditions. The culture media of CACC517 at seeding densities of 10^3 and 10^2 CFU/mL and CACC566 at a seeding density of 10^2 CFU/mL increased cell viability compared to LGG (lower part of **Figure 3A**). Therefore, we suggest that the byproducts of the bacterial strains can increase host cell viability.

Inhibition of Inflammatory Responses in Host Cells

To evaluate anti-inflammatory activities for host cells mediated by the byproducts of the bacterial strains (CACC517, CACC537, CACC558, and CACC566), host cells were stimulated by lipopolysaccharides (LPS). The culture media, in which the strains were separately cultured with different seeding densities, were added to stimulated RAW264.7 and DH82 cells. The levels of nitric oxide (NO) were measured using the Greiss assay. When LPS and bacterial culture media without any bacteria were simultaneously used to treat the host cells (LPS + media, negative control), the effect of LPS treatment was reduced, with higher NO

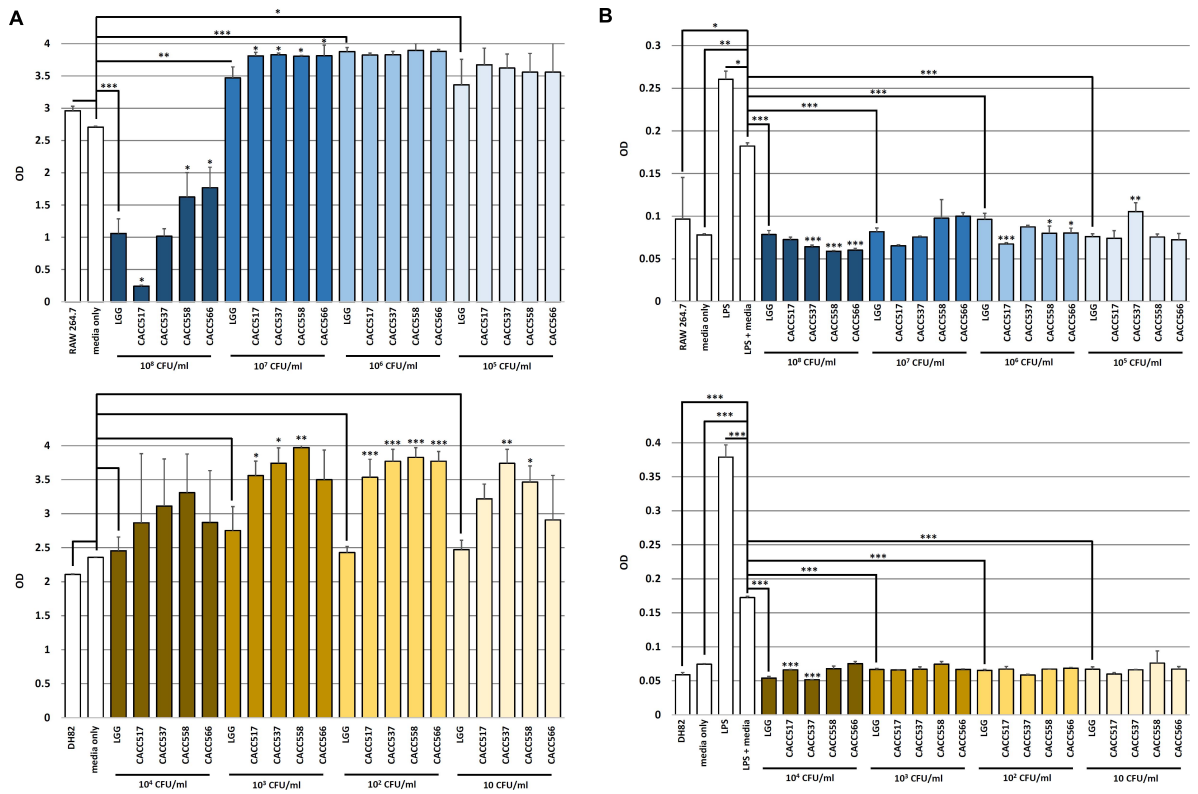

FIGURE 3 | Viability test and Inhibitory effect of nitric oxide (NO) production of host cells. The viability changes in RAW 264.7 (upper) and DH82 (lower) cells by the bacterial strains were determined using WST-1 assay. A significant difference between the reference strain (LGG, *Lactobacillus rhamnosus* GG ATCC53103) and negative control (bacterial media only) **(A)** was determined. The inhibitory effect of NO production in RAW 264.7 (upper) and DH82 (lower) cells by the bacterial strains were detected using Greiss assay. A significant difference between the reference strain (LGG, *Lactobacillus rhamnosus* GG ATCC53103) and the LPS-stimulated control including bacterial media only was determined **(B)**. Significant differences between each of CACC517, CACC537, CACC558, and CACC566 and the reference strain were determined. $^{*}P < 0.05$; $^{**}P < 0.01$; $^{***}P < 0.001$.

levels than the normally cultured cells (RAW264.7 and DH82) and the negative control ($P < 0.05$, $P < 0.01$, *or* $P < 0.001$) (**Figure 3B**). In case of RAW264.7 cells, culture media with all seeding density conditions of LGG decreased NO production compared to the negative control ($P < 0.001$). All strains, excluding CACC537 seeded at 10^5 CFU/mL, showed a superior or equivalent anti-inflammatory effect compared to LGG ($P < 0.05$, $P < 0.01$, *or* $P < 0.001$) (upper part of **Figure 3B**). In case of DH82 cells, culture media with all seeding density conditions of LGG decreased NO production compared to the negative control ($P < 0.001$). All strains, excluding CACC517 seeded at 10^4 CFU/mL, showed a superior or equivalent effect compared to LGG ($P < 0.001$) (lower part of **Figure 3B**). Therefore, we hypothesized that the byproducts of the bacterial strains can attenuate inflammatory responses and inhibit NO production.

Feeding Effects in Dogs

To evaluate the physiological effects of the bacterial strains in dogs, 10^8 CFU/ml of each bacterial strain (CACC517, CACC537, CACC558, and CACC566) was fed to dogs every day for 4 weeks. The blood of individual dogs was sampled before and after feeding. Subsequently, the blood samples were examined for complete blood count (CBC) and electrolyte tests. In total, 74 samples yielded 1645 values for 13 parameters of the CBC test and 10 parameters of the electrolyte test. The examined data were collectively integrated and analyzed using principal component analysis (PCA). The results of the PCA showed that individual dogs were clearly clustered by before and after bacterial feeding (**Figure 4A**). Moreover, the clusters were strain-specifically separated (**Figure 4B**). These results suggest that the bacterial strains can independently have a direct influence on the physiological status of dogs.

Gut Microbial Diversity Before and After Probiotics Treatment

16S rRNA gene sequencing was used to monitor changes in the microbial community in the fecal samples collected before and after feeding the bacterial strains (CACC517, CACC537, CACC558, and CACC566). The results of 16S rRNA sequencing revealed variability in the microbial composition and relative abundance at several levels in the fecal microbiota of dogs before and after probiotics treatment ($P < 0.1$) (**Table 4**). In the CACC517 treatment test, the relative abundance of Fusobacteria at the phylum level before and after probiotics

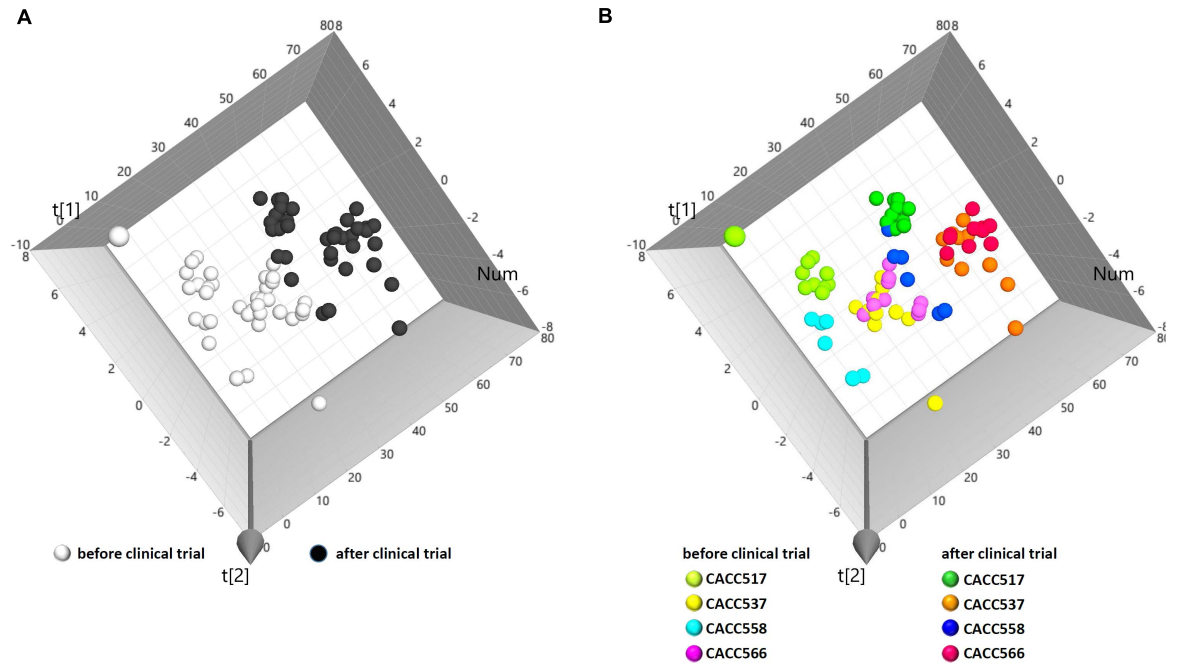

FIGURE 4 | Principal component analysis (PCA) of clinical data. From PCA (R^2X, 0.451; Q^2, 0.0698), individual data sets were labeled as before and after the overall clinical trial **(A)** or before and after the clinical trial of each bacterial strain **(B)**.

treatment was significantly different. Microbial taxonomy at the order level showed that the relative abundances of Erysipelotrichales and Fusobacteriales before and after probiotics treatment were significantly different, with *p*-values 0.036 and 0.079, respectively. The 16S rRNA sequencing results of the genera Clostridium and Fusobacterium before and after probiotics treatment were also significantly different. In the CACC537 treatment test, the relative abundance of Bacteroidetes at the phylum level, Bacteroidia at class level, Bacteroidales at order level, Bacteroidaceae at the family level, and Bacteroides at the genus level were significantly different. Microbial taxonomy at the genus level showed that the relative abundance of Bacteroides before and after probiotics treatment was significantly different. In the CACC558 treatment test, the relative abundance of Fusobacteria at the phylum level before and after probiotics treatment was significantly different. Microbial taxonomy at the order level showed that the relative abundance of Coriobacteriales, Erysipelotrichales, and Fusobacteriales before and after probiotics treatment were significantly different. The five families (Clostridiaceae, Coriobacteriaceae, Erysipelotrichaceae, Fusobacteriaceae, and Fusobacteriaceae) were significantly different before and after probiotics treatment (**Figure 5A** and **Table 4**).

Additionally, the 16S rRNA sequencing results of the genera Collinsella and Fusobacterium were significantly different before and after probiotics treatment. In the CACC537 treatment test, there were very few differentially abundant microbiota; only Porphyromonadaceae in the family and Bacteroides in genus were significantly different before and after the treatment. Additionally, we compared between the microbial composition and relative abundance at the genus level for each strain before and after probiotics treatment. In case of *Bifidobacterium*, which included the strain CACC517 and *Lactobacillus,* which includes CACC558, the mean relative abundance and variance decreased after probiotic treatment. Otherwise, the mean relative abundance and variance of *Lactobacillus,* including CACC566 and CACC537, increased after the treatment (**Table 4**).

Principal component analysis of all individual dogs showed that the PCA result was slightly different before and after probiotics treatments; however, it was not different among the strains CACC517, CACC537, CACC558, and CACC566 (**Figure 5B**). As shown in the rarefaction curve figure using all individuals, the number of OTUs was higher after probiotic treatment than before the treatment in CACC517 and CACC537 (**Figure 6**). However, we did not find a clear difference between before and after CACC566 treatment and diversity after CACC558 treatment. Based on this result, it can be seen that CACC517 and CACC537 altered the diversity of the intestinal microbial community.

DISCUSSION

In previous studies, bacteria of the canine gastrointestinal (GI) tract and feces were mainly categorized into five phyla: Firmicutes, Fusobacteria, Bacteroidetes, Proteobacteria, and Actinobacteria (Suchodolski et al., 2008; Honneffer et al., 2017; Coman et al., 2019). To screen functional probiotics in dog, we isolated the probiotic candidates CACC517, CACC537, CACC558, and CACC566 from canine feces and identified them

TABLE 4 | Differentially abundant microbiota before and after probiotics treatment.

Strain	Level	Microbe	Mean		*T*-test *P*-value (<0.1)
			Before	After	
CACC517 (*B. longum*)	Phylum	k__Bacteria; p__Fusobacteria	0.023	0.008	0.078
	Class	k__Bacteria; p__Firmicutes; c__Erysipelotrichi	0.038	0.089	0.036
	Class	k__Bacteria; p__Fusobacteria; c__Fusobacteriia	0.023	0.008	0.078
	Order	k__Bacteria; p__Firmicutes; c__Erysipelotrichi; o__Erysipelotrichales	0.038	0.089	0.036
	Order	k__Bacteria; p__Fusobacteria; c__Fusobacteriia; o__Fusobacteriales	0.023	0.008	0.079
	Family	k__Bacteria; p__Firmicutes; c__Erysipelotrichi; o__Erysipelotrichales; f__Erysipelotrichaceae	0.039	0.091	0.033
	Family	k__Bacteria; p__Fusobacteria; c__Fusobacteriia; o__Fusobacteriales; f__Fusobacteriaceae	0.023	0.009	0.075
	Genus	k__Bacteria; p__Firmicutes; c__Clostridia; o__Clostridiales; f__Clostridiaceae; g__Clostridium	0.001	0.020	0.079
	Genus	k__Bacteria; p__Fusobacteria; c__Fusobacteriia; o__Fusobacteriales; f__Fusobacteriaceae; g__Fusobacterium	0.023	0.009	0.076
CACC566 (*L. paracasei*)	Phylum	k__Bacteria; p__Bacteroidetes	0.100	0.229	0.023
	Class	k__Bacteria; p__Bacteroidetes; c__Bacteroidia	0.100	0.229	0.023
	Order	k__Bacteria; p__Bacteroidetes; c__Bacteroidia; o__Bacteroidales	0.100	0.229	0.023
	Family	k__Bacteria; p__Bacteroidetes; c__Bacteroidia; o__Bacteroidales; f__Bacteroidaceae	0.088	0.198	0.095
	Genus	k__Bacteria; p__Bacteroidetes; c__Bacteroidia; o__Bacteroidales; f__Bacteroidaceae; g__Bacteroides	0.088	0.200	0.096
CACC558 (*L. plantarum*)	Phylum	k__Bacteria; p__Fusobacteria	0.011	0.000	0.073
	Class	k__Bacteria; p__Firmicutes; c__Bacilli	0.130	0.232	0.085
	Class	k__Bacteria; p__Actinobacteria; c__Coriobacteriia	0.032	0.000	0.045
	Class	k__Bacteria; p__Firmicutes; c__Erysipelotrichi	0.049	0.014	0.033
	Class	k__Bacteria; p__Fusobacteria; c__Fusobacteriia	0.012	0.000	0.072
	Order	k__Bacteria; p__Actinobacteria; c__Coriobacteriia; o__Coriobacteriales	0.033	0.000	0.045
	Order	k__Bacteria; p__Firmicutes; c__Erysipelotrichi; o__Erysipelotrichales	0.049	0.015	0.034
	Order	k__Bacteria; p__Fusobacteria; c__Fusobacteriia; o__Fusobacteriales	0.012	0.000	0.072
	Order	k__Bacteria; p__Firmicutes; c__Bacilli; o__Lactobacillales	0.116	0.229	0.090
	Family	k__Bacteria; p__Firmicutes; c__Clostridia; o__Clostridiales; f__Clostridiaceae	0.179	0.061	0.072
	Family	k__Bacteria; p__Actinobacteria; c__Coriobacteriia; o__Coriobacteriales; f__Coriobacteriaceae	0.033	0.000	0.045
	Family	k__Bacteria; p__Firmicutes; c__Erysipelotrichi; o__Erysipelotrichales; f__Erysipelotrichaceae	0.049	0.015	0.034
	Family	k__Bacteria; p__Fusobacteria; c__Fusobacteriia; o__Fusobacteriales; f__Fusobacteriaceae	0.012	0.000	0.072
	Family	k__Bacteria; p__Firmicutes; c__Clostridia; o__Clostridiales; f__Veillonellaceae	0.004	0.000	0.023
	Genus	k__Bacteria; p__Actinobacteria; c__Coriobacteriia; o__Coriobacteriales; f__Coriobacteriaceae; g__Collinsella	0.027	0.000	0.083
	Genus	k__Bacteria; p__Fusobacteria; c__Fusobacteriia; o__Fusobacteriales; f__Fusobacteriaceae; g__Fusobacterium	0.012	0.000	0.070
CACC537 (*P. acidilactici*)	Family	k__Bacteria; p__Bacteroidetes; c__Bacteroidia; o__Bacteroidales; f__Porphyromonadaceae	0.003	0.001	0.096
	Genus	k__Bacteria; p__Bacteroidetes; c__Bacteroidia; o__Bacteroidales; f__Porphyromonadaceae; g__Parabacteroides	0.003	0.001	0.096

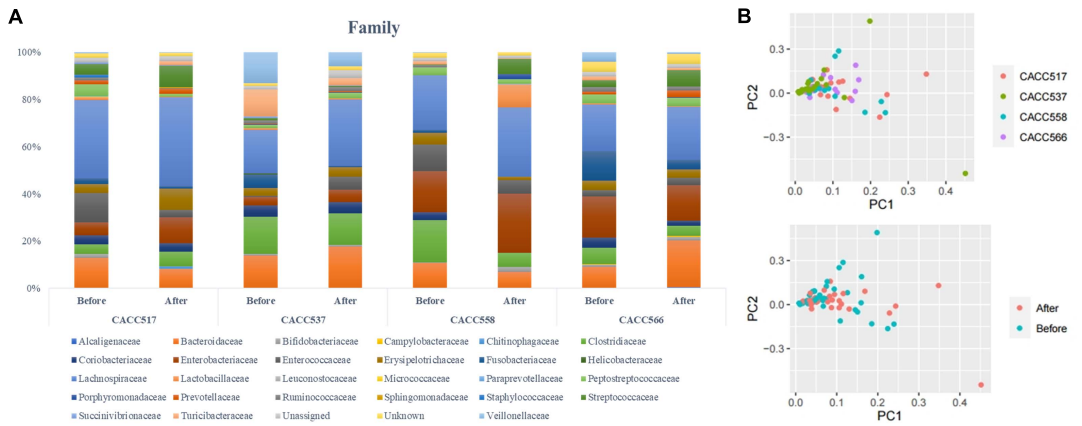

FIGURE 5 | Microbial community analysis using 16S rRNA sequencing. Multi-level taxonomic abundance was extracted using QIIME and Student's *t*-test (Paired) was used to detect differentially abundant microbiota by comparing relative abundance between the before and after probiotics treatment states **(A)** and PCA analysis of before and after probiotics treatment states was performed **(B)**.

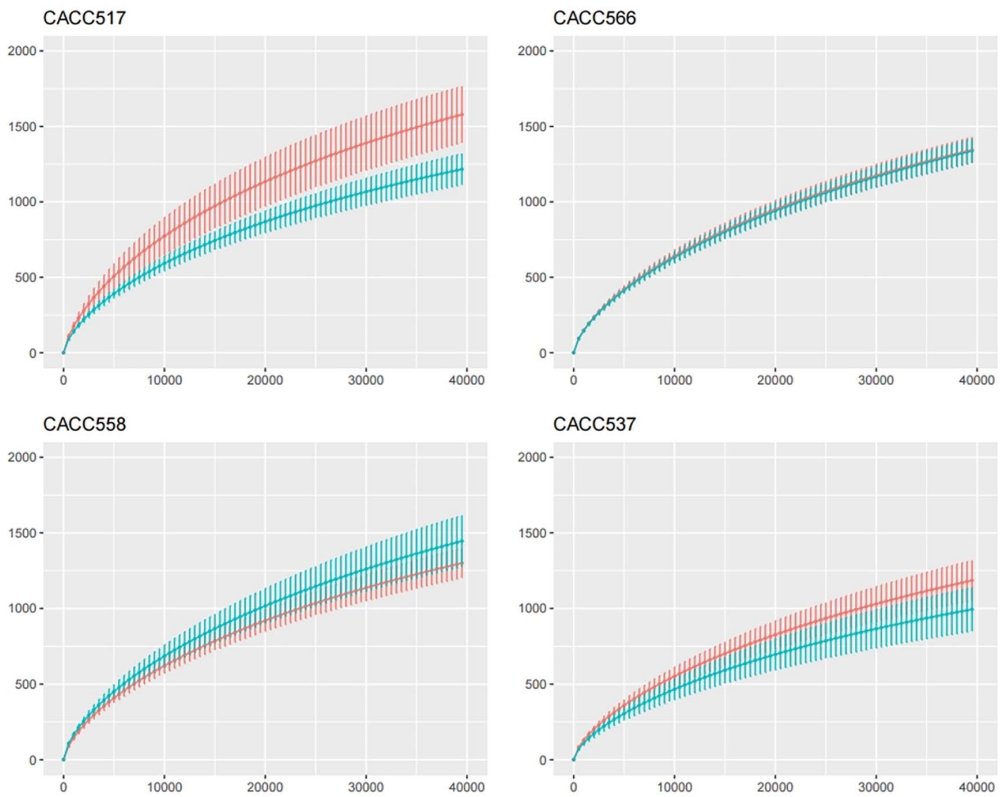

FIGURE 6 | Calculation of species richness for a given number of individual samples based on the construction of rarefaction curves using R package (BiodiversityR).

using 16s rRNA gene sequencing, which revealed that these candidates belonged to *Lactobacillus* species, *Bifidobacterium* species, and other lactic acid bacteria (LAB), which are considered as probiotics (Holzapfel et al., 2001).

To characterize the genomic information of these four strains, we compared the genomic information of them with LGG (LGG ATCC53103; genomic sequence version. ASM2650v1) and analyzed the genetic basis to identify the characteristics of each strain. The largest proportion of protein coding category in each of the four strains was Carbohydrate transport and metabolism (G). The results of this analysis indicated that the four strains from canine feces in this study were closely related to carbohydrate metabolism. In addition, this result was consistent with a study on changes in dog domestication (Caporaso et al.,

2010). Based on the results of EggNog analysis, we found that the categories with the largest variation in gene number were Transcription (K) and Amino acid transport and metabolism (E). Unlike wild wolves, which are carnivorous animals, present-day dogs have a more diverse diet, mainly including food containing starch, fat, and protein (Rowe et al., 1997). We inferred that changes in the domestication process of dogs caused changes in the gut microbiota of dogs. We identified many specific genes in the four strains and clearly correlated differences between the four strains and LGG. We further compared the correlation between *Lactobacillus rhamnosus* and LGG. The results indicated different effects of these four strains on the dog gut system.

The procedures for probiotic characterization have been well established. In terms of safety, functional and technological aspects, acid and bile salt tolerance, adherence to intestinal cells, and production of antimicrobial substances were evaluated using reference strains (Saarela et al., 2000). In our study, the bacterial strains were characterized as probiotics based on comparisons with LGG. LGG is a well-characterized probiotic isolated from the human intestinal tract (Silva et al., 1987) and has shown prominent survivability in the acidic condition and bile of stomach, as well as good adhesion to the human colonic carcinoma cell line HT-29 (Conway et al., 1987; Kim et al., 2019). Based on the comparison between the LGG and each of the isolated bacterial strains, CACC558 showed good bile salt tolerance, adherence to intestinal cells, and ability for inhibition of pathogenic bacteria. Thus, CACC558 can be considered a strong candidate for commercial probiotics.

Previous studies have reported the positive effects of LGG on host health, especially in the GI tract (Tao et al., 2006; Yan et al., 2007; Ciorba et al., 2012). In addition, LGG modulates the host immune system and attenuates LPS-induced inflammatory responses (Zhang et al., 2006; Lee et al., 2012; Fong et al., 2016). In our study, the bacterial strains (CACC517, CACC537, CACC558, and CACC566) showed improved or equivalent effects on host cell viability and inhibition of inflammatory responses compared to LGG, although elaborate optimization of treatment conditions was required in *in vitro* experiment. Interestingly, the bacterial strains exhibited overall superior effects compared to LGG in the canine macrophage cell line (DH82) than in the murine macrophage cell line (RAW264.7). Host preference for probiotics have been studied for their beneficial effects on the host by effectively balancing the microbial environment of the gut and enhancing nutrient digestibility, growth, and immune status (Ripamonti et al., 2011; Chiang et al., 2015; Cui et al., 2017; Dowarah et al., 2017, 2018; Abdou et al., 2018). However, direct comparative studies based on host differences are still limited. Thus, we propose that our results could provide evidence on the effectiveness of host-prefer probiotics, although it should be further studied to understand the specific interactions between a host and probiotic strains.

Currently, probiotic research is extending to a wide range of fields beyond intestinal health care, such as enhancement of immune response, maintenance of homeostasis, and even cancer prevention (Kumar et al., 2010; Kechagia et al., 2013). In this regard, analysis of blood, which is associated with overall host homeostasis and the immune system, can reflect the physiological changes of a subject due to probiotic effects. However, there is no conclusively single parameter to determine the physiological effects of probiotics in blood. Based on the clinical trial for the dogs that were privately owned and had indoor access, blood samples before and after treatments with the probiotics were analyzed by complete blood count (CBC) and electrolyte tests. From the analysis, lymphocyte or chloride was significantly increased after probiotics feeding ($P < 0.05$) (**Supplementary Figure 2**) and other blood components generally showed increased trends after treatment ($P < 0.5$) (**Supplementary Figure 3**). Lymphocyte number of white blood cell (WBC) reflects immunity and chloride (Cl) level is regarded as a supplementary factor if a healthy of the heart and kidneys are concerned (McClatchey, 2002; Rao et al., 2007). Thus, the increased levels can be considered as a positive clinical sign within normal ranges. Subsequently, we introduced the multicomponent analysis approach and collectively analyzed 23 blood-originated parameters (**Supplementary Table 3**). PCA showed that the treatment of each strain was obviously clustered between before and after the treatment suggesting an effect of probiotics treatment. Additionally, the individual dog showed relatively broad distribution within the group before treatment or the group after treatment. We supposed that the relatively broad distribution within a cluster reflects various environmental factors and physiological statuses of an individual dog.

The previous studies have reported the alteration of intestinal microbiota by probiotics treatment. For example, *Lactobacillus paracasei* DG intake increased the relative abundance of Proteobacteria and the Clostridiales genus Coprococcus while it decreased the Clostridiales genus Blautia, Anaerostipes, and Clostridium in human fecal microbiota compared to control group (Ferrario et al., 2014). The ingestion of fermented milk containing *Lactobacillus casei* Shirota elevated the numbers of Bifidobacterium and Lactobacillus while it reduced the number of *Clostridium difficile* in the fecal microbiota of the subjects than the placebo group (Nagata et al., 2016). The treatment of *Lactobacillus plantarum* JDFM LP11 increased the population of lactic acid bacteria in porcine feces (Shin et al., 2019). Recently, It suggested that a single probiotic strain that was appropriately chosen is equivalent or more effective than a multi-strain mixture (McFarland, 2020). In our study, analysis of the fecal samples revealed changes in the microbial composition and relative abundance before and after treatment with the probiotic strains. In case of CACC517 treatment, *Erysipelotrichaceae* at the family level significantly increased after probiotics treatment. A previous probiotic study showed that the relative abundance of *Erysipelotrichaceae* was lower in broilers supplemented with probiotics than in broilers supplemented with antibiotics (Neveling et al., 2017). Based on these results, we hypothesized that the composition of this family in gut microbiota could be controlled to replace antibiotics in the diet because members of the *Erysipelotrichaceae* family are closely linked to high immunogenicity and flourish (Neveling et al., 2017). *Fusobacterium* at the genus level was significantly decreased after probiotics treatment. A previous study reported that *Fusobacterium* may be associated with inflammatory bowel

disease (Gao et al., 2015). Therefore, it could be presumed that the reduction of *Fusobacterium* in normal cells by treatment with CACC517 could be helpful in preventing intestinal diseases. We identified significant differences in relative abundance of *Bacteroides* at the genus level before and after CACC566 treatment in dogs. In a previous human study, probiotics greatly enriched the relative abundance of beneficial bacteria *Bacteroides*. Previous studies have shown that the decrease in the abundance of *Bacteroides* is closely related to poor health. Moreover, butyrate produced by *Bacteroides* plays an important role in maintaining the intestinal health of the host, exerting immunity, and anti-tumor effects (Deng et al., 2020). In addition to these two stains, we confirmed important relative abundance of several microbial flora before and after CACC558 treatment in dogs. *Clostridiaceae* at the family level decreased after CACC558 treatment, and another study reported that *Clostridiaceae* was one of three key bacterial families related to the digestion of protein in dogs. Therefore, we believe that CACC558 treatment has a beneficial role in the digestion of protein in the dog gut. *Coriobacteriaceae* at the family level was significantly reduced after probiotic treatment in dogs, and a previous study reported that *Coriobacteriaceae* was more frequently detected in patients with Crohn's disease than in healthy subjects (Loh and Blaut, 2012). When dogs were treated with CACC558, the reduction in the abundance of *Coriobacteriaceae* was predicted to be helpful in preventing chronic inflammatory bowel diseases such as Crohn's disease. *Erysipelotrichaceae* at the family level significantly decreased after probiotic treatment in dogs. In the case of *Fusobacterium* at the genus level, this effect of CACC558 in dogs was the same as that of CACC517. The results of CACC517 treatment showed that *Fusobacterium* at the genus family level was significantly reduced after probiotic treatment in dogs. Interestingly, the effect of CACC558 treatment on *Erysipelotrichaceae* was the opposite of CACC517. We found that the four candidate strains had diverse effects in terms of extent and directions. We found that Parabacteroides at the genus level were significantly different before and after CACC537 treatment in dogs, and another previous study reported that this microorganism is closely associated with inflamed IBD mucosa (Zitomersky et al., 2013).

Collectively, we reported four novel canine probiotic strains and functional activities for the strains in *in vitro* experiment. We also found that the strains changed clinical parameters in blood and microbial abundance in feces under commercial probiotics feeding conditions. Therefore, our study could contribute to the feasibility of using these strains as probiotics in dogs.

DATA AVAILABILITY STATEMENT

The datasets presented in this study can be found in online repositories. The names of the repository/repositories and accession number(s) can be found in the article/**Supplementary Material**.

ETHICS STATEMENT

The animal study was reviewed and approved by the Institutional Animal Care and Use Committee of Jeonbuk National University. Written informed consent was obtained from the owners for the participation of their animals in this study.

AUTHOR CONTRIBUTIONS

DS and YK: conceptualization. H-JJ, DS, and YK: writing–original draft preparation. SS, J-AK, MJ, H-JJ, and Y-jC: methodology, investigation, and visualization. H-JJ, SS, and J-AK: formal analysis. D-HK: resources. SS, J-AK, MJ, H-JJ, D-HK and HL: writing–review and editing. All the authors approved the final version of the manuscript.

FUNDING

This research was supported by the Strategic Initiative for Microbiomes in Agriculture and Food grant No. 918002-4, Ministry of Agriculture, Food and Rural Affairs, South Korea.

ACKNOWLEDGMENTS

The authors especially thank Dr. Sung-Ho Lee of WooGene B&G Co., Ltd. for the comments and discussions about pet probiotics.

SUPPLEMENTARY MATERIAL

The Supplementary Material for this article can be found online at: https://www.frontiersin.org/articles/10.3389/fmicb.2021.625562/full#supplementary-material

Supplementary Figure 1 | Genomic structure of the bacterial strains.

Supplementary Figure 2 | The significant changes of blood components before and after the clinical trial.

Supplementary Figure 3 | The trends of blood components before and after the clinical trial.

Supplementary Table 1 | eggNOG-mapper results using five strains available complete genome sequences from NCBI and this study.

Supplementary Table 2 | Information on dogs for clinical trials.

Supplementary Table 3 | The results of the blood chemistry analysis for 37 dogs before and after the clinical trial.

REFERENCES

Abdou, A. M., Hedia, R. H., Omara, S. T., Mahmoud, M. A. E., Kandil, M. M., and Bakry, M. A. (2018). Interspecies comparison of probiotics isolated from different animals. *Vet. World* 11, 227–230. doi: 10.14202/vetworld.2018.227-230

Altschul, S. F., Gish, W., Miller, W., Myers, E. W., and Lipman, D. J. (1990). Basic local alignment search tool.

J. Mol. Biol. 215, 403–410. doi: 10.1016/S0022-2836(05)80360-2

Amin, M., Jorfi, M., Khosravi, A. D., Samarbafzadeh, A. R., and Farajzadeh Sheikh, A. (2009). Isolation and identification of *Lactobacillus casei* and *Lactobacillus plantarum* from Plants by PCR and detection of their antibacterial activity. *J. Biol. Sci.* 9, 810–814. doi: 10.3923/jbs.2009.810.814

Beasley, S. S., Manninen, T. J., and Saris, P. E. (2006). Lactic acid bacteria isolated from canine faeces. *J. Appl. Microbiol.* 101, 131–138. doi: 10.1111/j.1365-2672.2006.02884.x

Bunesova, V., Vlkova, E., Rada, V., Rockova, S., Svobodova, I., Jebavy, L., et al. (2012). *Bifidobacterium animalis* subsp. lactis strains isolated from dog faeces. *Vet. Microbiol.* 160, 501–505. doi: 10.1016/j.vetmic.2012.06.005

Caporaso, J. G., Kuczynski, J., Stombaugh, J., Bittinger, K., Bushman, F. D., Costello, E. K., et al. (2010). QIIME allows analysis of high-throughput community sequencing data. *Nat. Methods* 7, 335–336. doi10.1038/nmeth.f.303

Chiang, M. L., Chen, H. C., Chen, K. N., Lin, Y. C., Lin, Y. T., and Chen, M. J. (2015). Optimizing production of two potential probiotic Lactobacilli strains isolated from piglet feces as feed additives for weaned piglets. *Asian Aust. J. Anim. Sci.* 28, 1163–1170. doi: 10.5713/ajas.14.0780

Ciorba, M. A., Riehl, T. E., Rao, M. S., Moon, C., Ee, X., Nava, G. M., et al. (2012). *Lactobacillus* probiotic protects intestinal epithelium from radiation injury in a TLR-2/cyclo-oxygenase-2-dependent manner. *Gut* 61, 829–838. doi: 10.1136/gutjnl-2011-300367

Coman, M. M., Verdenelli, M. C., Cecchini, C., Bela, B., Gramenzi, A., Orpianesi, C., et al. (2019). Probiotic characterization of *Lactobacillus* isolates from canine faeces. *J. Appl. Microbiol.* 126, 1245–1256. doi: 10.1111/jam.14197

Conway, P. L., Gorbach, S. L., and Goldin, B. R. (1987). Survival of lactic acid bacteria in the human stomach and adhesion to intestinal cells. *J. Dairy Sci.* 70, 1–12. doi: 10.3168/jds.S0022-0302(87)79974-3

Cui, J., Xiao, M., Liu, M., Wang, Z., Liu, F., Guo, L., et al. (2017). Coupling metagenomics with cultivation to select host-specific probiotic microorganisms for subtropical aquaculture. *J. Appl. Microbiol.* 123, 1274–1285. doi: 10.1111/jam.13555

Deng, X., Tian, H., Yang, R., Han, Y., Wei, K., Zheng, C., et al. (2020). Oral probiotics alleviate intestinal dysbacteriosis for people receiving bowel preparation. *Front. Med. (Lausanne)* 7:73. doi: 10.3389/fmed.2020.00073

DeSantis, T. Z., Hugenholtz, P., Larsen, N., Rojas, M., Brodie, E. L., Keller, K., et al. (2006). Greengenes, a chimera-checked 16S rRNA gene database and workbench compatible with ARB. *Appl. Environ. Microbiol.* 72, 5069–5072. doi: 10.1128/AEM.03006-05

Ding, W. K., and Shah, N. P. (2007). Acid, bile, and heat tolerance of free and microencapsulated probiotic bacteria. *J. Food Sci.* 72, M446–M450. doi: 10.1111/j.1750-3841.2007.00565.x

Dowarah, R., Verma, A. K., Agarwal, N., Patel, B. H. M., and Singh, P. (2017). Effect of swine based probiotic on performance, diarrhoea scores, intestinal microbiota and gut health of grower-finisher crossbred pigs. *Livestock Sci.* 195, 74–79. doi: 10.1016/j.livsci.2016.11.006

Dowarah, R., Verma, A. K., Agarwal, N., Singh, P., and Singh, B. R. (2018). Selection and characterization of probiotic lactic acid bacteria and its impact on growth, nutrient digestibility, health and antioxidant status in weaned piglets. *PLoS One* 13:e0192978. doi: 10.1371/journal.pone.0192978

Drancourt, M., Bollet, C., Carlioz, A., Martelin, R., Gayral, J.-P., and Raoult, D. (2000). 16S ribosomal DNA sequence analysis of a large collection of environmental and clinical unidentifiable bacterial isolates. *J. Clin. Microbiol.* 38, 3623–3630. doi: 10.1128/JCM.38.10.3623-3630.2000

El Hage, R., Hernandez-Sanabria, E., and Van De Wiele, T. (2017). Emerging trends in "Smart Probiotics": functional consideration for the development of novel health and industrial applications. *Front. Microbiol.* 8:1889. doi: 10.3389/fmicb.2017.01889

Ferrario, C., Taverniti, V., Milani, C., Fiore, W., Laureati, M., De Noni, I., et al. (2014). Modulation of fecal Clostridiales bacteria and butyrate by probiotic intervention with Lactobacillus paracasei DG varies among healthy adults. *J. Nutr.* 144, 1787–1796. doi: 10.3945/jn.114.197723

Fong, F. L. Y., Kirjavainen, P. V., and El-Nezami, H. (2016). Immunomodulation of *Lactobacillus rhamnosus* GG (LGG)-derived soluble factors on antigen-presenting cells of healthy blood donors. *Sci. Rep.* 6:22845. doi: 10.1038/srep22845

Gao, Z., Guo, B., Gao, R., Zhu, Q., Wu, W., and Qin, H. (2015). Probiotics modify human intestinal mucosa-associated microbiota in patients with colorectal cancer. *Mol. Med. Rep.* 12, 6119–6127. doi: 10.3892/mmr.2015.4124

Grzeskowiak, L., Endo, A., Beasley, S., and Salminen, S. (2015). Microbiota and probiotics in canine and feline welfare. *Anaerobe* 34, 14–23. doi: 10.1016/j.anaerobe.2015.04.002

Guo, X., Chen, D. D., Peng, K. S., Cui, Z. W., Zhang, X. J., Li, S., et al. (2016). Identification and characterization of Bacillus subtilis from grass carp (*Ctenopharynodon idellus*) for use as probiotic additives in aquatic feed. *Fish Shellfish Immunol.* 52, 74–84. doi: 10.1016/j.fsi.2016.03.017

Holzapfel, W. H., Haberer, P., Geisen, R., Bjorkroth, J., and Schillinger, U. (2001). Taxonomy and important features of probiotic microorganisms in food and nutrition. *Am. J. Clin. Nutr.* 73, 365S–373S. doi: 10.1093/ajcn/73.2.365s

Hong, Z., Jiexin, W., Zhang, H., Zhigang, S., Yun, J., and Jianfeng, C. (2009). Facile preparation of danazol nanoparticles by high-gravity anti-solvent precipitation (HGAP) method. *Chin. J. Chem. Eng.* 17, 318–323. doi: 10.1016/S1004-9541(08)60210-4

Honneffer, J. B., Steiner, J. M., Lidbury, J. A., and Suchodolski, J. S. (2017). Variation of the microbiota and metabolome along the canine gastrointestinal tract. *Metabolomics* 13:26. doi: 10.1007/s11306-017-1165-3

Hotel, A. C. P., and Cordoba, A. (2001). Health and nutritional properties of probiotics in food including powder milk with live lactic acid bacteria. *Prevention* 5, 1–10.

Huerta-Cepas, J., Szklarczyk, D., Forslund, K., Cook, H., Heller, D., Walter, M. C., et al. (2015). eggNOG 4.5: a hierarchical orthology framework with improved functional annotations for eukaryotic, prokaryotic and viral sequences. *Nucleic Acids Res.* 44, D286–D293. doi: 10.1093/nar/gkv1248

Hummel, A. S., Hertel, C., Holzapfel, W. H., and Franz, C. M. (2007). Antibiotic resistances of starter and probiotic strains of lactic acid bacteria. *Appl. Environ. Microbiol.* 73, 730–739. doi: 10.1128/AEM.02105-06

Kechagia, M., Basoulis, D., Konstantopoulou, S., Dimitriadi, D., Gyftopoulou, K., Skarmoutsou, N., et al. (2013). Health benefits of probiotics: a review. *ISRN Nutr.* 2013:481651. doi: 10.5402/2013/481651

Khalighi, A., Behdani, R., and Kouhestani, S. (2016). Probiotics: a comprehensive review of their classification, mode of action and role in human nutrition. *Probiot. Prebiot. Hum. Nutr. Health* 10:63646. doi: 10.5772/63646

Kim, J. A., Bayo, J., Cha, J., Choi, Y. J., Jung, M. Y., Kim, D. H., et al. (2019). Investigating the probiotic characteristics of four microbial strains with potential application in feed industry. *PLoS One* 14:e0218922. doi: 10.1371/journal.pone.0218922

Kim, S. Y., and Adachi, Y. (2007). Biological and genetic classification of canine intestinal lactic acid bacteria and bifidobacteria. *Microbiol. Immunol.* 51, 919–928. doi: 10.1111/j.1348-0421.2007.tb03983.x

Kuczynski, J., Lauber, C. L., Walters, W. A., Parfrey, L. W., Clemente, J. C., Gevers, D., et al. (2012). Experimental and analytical tools for studying the human microbiome. *Nat. Rev. Genet.* 13, 47–58. doi: 10.1038/nrg3129

Kumar, M., Behare, P. V., Mohania, D., Arora, S., Kaur, A., and Nagpal, R. (2009). Health-promoting probiotic functional foods. *Focus Diet. Fibres* 20, 1–5.

Kumar, M., Kumar, A., Nagpal, R., Mohania, D., Behare, P., Verma, V., et al. (2010). Cancer-preventing attributes of probiotics: an update. *Int. J. Food Sci. Nutr.* 61, 473–496. doi: 10.3109/09637480903455971

Kumar, M., Verma, V., Nagpal, R., Kumar, A., Behare, P., Singh, B., et al. (2012). Anticarcinogenic effect of probiotic fermented milk and chlorophyllin on aflatoxin-B 1-induced liver carcinogenesis in rats. *Br. J. Nutr.* 107, 1006–1016. doi: 10.1017/S0007114511003953

Kumar, S., Stecher, G., and Tamura, K. (2016). MEGA7: molecular evolutionary genetics analysis version 7.0 for bigger datasets. *Mol. Biol. Evol.* 33, 1870–1874. doi: 10.1093/molbev/msw054

Lamendella, R., Santo Domingo, J. W., Kelty, C., and Oerther, D. B. (2008). Bifidobacteria in feces and environmental waters. *Appl. Environ. Microbiol.* 74, 575–584. doi: 10.1128/AEM.01221-07

Lane, D. (1991). "16S/23S rRNA sequencing," in *Nucleic Acid Techniques in Bacterial Systematics*, eds E. Stackebrandt and M. Goodfellow (New York, NY: John Wiley and Sons), 115–175.

Lee, S. K., Yang, K. M., Cheon, J. H., Kim, T. I., and Kim, W. H. (2012). [Anti-inflammatory mechanism of Lactobacillus rhamnosus GG in

lipopolysaccharide- stimulated HT-29 cell]. *Korean J. Gastroenterol.* 60, 86–93. doi: 10.4166/kjg.2012.60.2.86

Liong, M. T., and Shah, N. P. (2005). Acid and bile tolerance and cholesterol removal ability of lactobacilli strains. *J. Dairy Sci.* 88, 55–66. doi: 10.3168/jds.S0022-0302(05)72662-X

Loh, G., and Blaut, M. (2012). Role of commensal gut bacteria in inflammatory bowel diseases. *Gut Microbes* 3, 544–555. doi: 10.4161/gmic.22156

Manoj, K., Dheeraj, M., Devastotra, P., Behare, P., Ravinder, N., Ashok, K., et al. (2009). A probiotic fermented milk prepared by mixed culture reduces pathogen shedding and alleviates disease signs in rats challenged with pathogens. *Int. J. Probiot. Prebiot.* 4, 211–218.

McClatchey, K. D. (2002). *Clinical Laboratory Medicine*. Philadelphia, PA: Lippincott Williams & Wilkins.

McFarland, L. V. (2020). Efficacy of single-strain probiotics versus multi-strain mixtures: systematic review of strain and disease specificity. *Dig. Dis. Sci.* doi: 10.1007/s10620-020-06244-z [Epub ahead of print].

Michail, S., Sylvester, F., Fuchs, G., and Issenman, R. (2006). Clinical efficacy of probiotics: review of the evidence with focus on children. *J. Pediatr. Gastroenterol. Nutr.* 43, 550–557.

Nagata, S., Asahara, T., Wang, C., Suyama, Y., Chonan, O., Takano, K., et al. (2016). The effectiveness of *Lactobacillus* beverages in controlling infections among the residents of an aged care facility: a randomized placebo-controlled double-blind trial. *Ann. Nutr. Metab.* 68, 51–59. doi: 10.1159/000442305

Nagpal, R., Kumar, A., Kumar, M., Behare, P. V., Jain, S., and Yadav, H. (2012). Probiotics, their health benefits and applications for developing healthier foods: a review. *FEMS Microbiol. Lett.* 334, 1–15. doi: 10.1111/j.1574-6968.2012.02593.x

Navas-Molina, J. A., Peralta-Sánchez, J. M., González, A., Mcmurdie, P. J., Vázquez-Baeza, Y., Xu, Z., et al. (2013). Advancing our understanding of the human microbiome using QIIME. *Methods Enzymol.* 531, 371–444. doi: 10.1016/B978-0-12-407863-5.00019-8

Neveling, D. P., Van Emmenes, L., Ahire, J. J., Pieterse, E., Smith, C., and Dicks, L. M. T. (2017). Safety assessment of antibiotic and probiotic feed additives for *Gallus gallus* domesticus. *Sci. Rep.* 7:12767. doi: 10.1038/s41598-017-12866-7

Podolsky, S. H. (2012). Metchnikoff and the microbiome. *Lancet* 380, 1810–1811. doi: 10.1016/S0140-6736(12)62018-2

Rao, D., Le, T., and Bhushan, V. (2007). *First aid for the USMLE step 1 2008*. New York, NY: McGraw-Hill Medical.

Richter, M., Rosselló-Móra, R., Oliver Glöckner, F., and Peplies, J. (2015). JSpeciesWS: a web server for prokaryotic species circumscription based on pairwise genome comparison. *Bioinformatics* 32, 929–931. doi: 10.1093/bioinformatics/btv681

Ripamonti, B., Agazzi, A., Bersani, C., De Dea, P., Pecorini, C., Pirani, S., et al. (2011). Screening of species-specific lactic acid bacteria for veal calves multi-strain probiotic adjuncts. *Anaerobe* 17, 97–105. doi: 10.1016/j.anaerobe.2011.05.001

Ritchie, L. E., Steiner, J. M., and Suchodolski, J. S. (2008). Assessment of microbial diversity along the feline intestinal tract using 16S rRNA gene analysis. *FEMS Microbiol. Ecol.* 66, 590–598. doi: 10.1111/j.1574-6941.2008.00609.x

Rognes, T., Flouri, T., Nichols, B., Quince, C., and Mahé, F. (2016). VSEARCH: a versatile open source tool for metagenomics. *PeerJ* 4:e2584. doi: 10.7717/peerj.2584

Rowe, J., Choct, M., Brown, W., and Day, K. (1997). Variation in the carbohydrate composition of dog food. *Recent Adv. Anim. Nutr. Aust.* 1997:242.

Saarela, M., Mogensen, G., Fonden, R., Matto, J., and Mattila-Sandholm, T. (2000). Probiotic bacteria: safety, functional and technological properties. *J. Biotechnol.* 84, 197–215. doi: 10.1016/S0168-1656(00)00375-8

Seemann, T. (2014). Prokka: rapid prokaryotic genome annotation. *Bioinformatics* 30, 2068–2069. doi: 10.1093/bioinformatics/btu153

Sharma, G., and Im, S. H. (2018). Probiotics as a potential immunomodulating pharmabiotics in allergic diseases: current status and future prospects. *Allergy Asthma Immunol. Res.* 10, 575–590. doi: 10.4168/aair.2018.10.6.575

Shin, D., Chang, S. Y., Bogere, P., Won, K., Choi, J. Y., Choi, Y. J., et al. (2019). Beneficial roles of probiotics on the modulation of gut microbiota and immune response in pigs. *PLoS One* 14:e0220843. doi: 10.1371/journal.pone.0220843

Shokryazdan, P., Faseleh Jahromi, M., Liang, J. B., and Ho, Y. W. (2017). Probiotics: from isolation to application. *J. Am. Coll. Nutr.* 36, 666–676. doi: 10.1080/07315724.2017.1337529

Silva, B. C., Jung, L. R., Sandes, S. H., Alvim, L. B., Bomfim, M. R., Nicoli, J. R., et al. (2013). In vitro assessment of functional properties of lactic acid bacteria isolated from faecal microbiota of healthy dogs for potential use as probiotics. *Benef. Microbes* 4, 267–275. doi: 10.3920/BM2012.0048

Silva, M., Jacobus, N. V., Deneke, C., and Gorbach, S. L. (1987). Antimicrobial substance from a human Lactobacillus strain. *Antimicrob. Agents Chemother.* 31, 1231–1233. doi: 10.1128/AAC.31.8.1231

Singh, S., Bhatia, R., Singh, A., Singh, P., Kaur, R., Khare, P., et al. (2018). Probiotic attributes and prevention of LPS-induced pro-inflammatory stress in RAW264.7 macrophages and human intestinal epithelial cell line (Caco-2) by newly isolated Weissella cibaria strains. *Food Funct.* 9, 1254–1264. doi: 10.1039/C7FO00469A

Song, D., Ibrahim, S., and Hayek, S. (2012). Recent application of probiotics in food and agricultural science. *Probiotics* 10, 1–34.

Suchodolski, J. S., Camacho, J., and Steiner, J. M. (2008). Analysis of bacterial diversity in the canine duodenum, jejunum, ileum, and colon by comparative 16S rRNA gene analysis. *FEMS Microbiol. Ecol.* 66, 567–578. doi: 10.1111/j.1574-6941.2008.00521.x

Tagg, J. R., and McGiven, A. R. (1971). Assay system for bacteriocins. *Appl. Microbiol.* 21:943. doi: 10.1128/AM.21.5.943-943.1971

Tamura, K., and Nei, M. (1993). Estimation of the number of nucleotide substitutions in the control region of mitochondrial DNA in humans and chimpanzees. *Mol. Biol. Evol.* 10, 512–526.

Tang, Y., Manninen, T. J., and Saris, P. E. (2012). Dominance of *Lactobacillus acidophilus* in the facultative jejunal *Lactobacillus microbiota* of fistulated beagles. *Appl. Environ. Microbiol.* 78, 7156–7159. doi: 10.1128/AEM.01975-12

Tao, Y., Drabik, K. A., Waypa, T. S., Musch, M. W., Alverdy, J. C., Schneewind, O., et al. (2006). Soluble factors from Lactobacillus GG activate MAPKs and induce cytoprotective heat shock proteins in intestinal epithelial cells. *Am. J. Physiol. Cell Physiol.* 290, C1018–C1030. doi: 10.1152/ajpcell.00131.2005

Yadav, H., Jain, S., and Sinha, P. R. (2008). Oral administration of dahi containing probiotic *Lactobacillus acidophilus* and *Lactobacillus casei* delayed the progression of streptozotocin-induced diabetes in rats. *J. Dairy Res.* 75, 189–195. doi: 10.1017/S0022029908003129

Yan, F., Cao, H., Cover, T. L., Whitehead, R., Washington, M. K., and Polk, D. B. (2007). Soluble proteins produced by probiotic bacteria regulate intestinal epithelial cell survival and growth. *Gastroenterology* 132, 562–575. doi: 10.1053/j.gastro.2006.11.022

Zhang, L., Li, N., Des Robert, C., Fang, M., Liboni, K., Mcmahon, R., et al. (2006). *Lactobacillus rhamnosus* GG decreases lipopolysaccharide-induced systemic inflammation in a gastrostomy-fed infant rat model. *J. Pediatr. Gastroenterol. Nutr.* 42, 545–552. doi: 10.1097/01.mpg.0000221905.68781.4a

Zitomersky, N. L., Atkinson, B. J., Franklin, S. W., Mitchell, P. D., Snapper, S. B., Comstock, L. E., et al. (2013). Characterization of adherent bacteroidales from intestinal biopsies of children and young adults with inflammatory bowel disease. *PLoS One* 8:e63686. doi: 10.1371/journal.pone.0063686

Conflict of Interest: The authors declare that the research was conducted in the absence of any commercial or financial relationships that could be construed as a potential conflict of interest.

frontiers in Microbiology

ORIGINAL RESEARCH
published: 23 March 2021
doi: 10.3389/fmicb.2021.636822

Broad Purpose Vector for Site-Directed Insertional Mutagenesis in *Bifidobacterium breve*

Emily C. Hoedt[1,2†], Francesca Bottacini[2,3†], Nora Cash[2], Roger S. Bongers[4], Kees van Limpt[4], Kaouther Ben Amor[4], Jan Knol[4,5], John MacSharry[2,6,7] and Douwe van Sinderen[2,6*]*

[1] APC Microbiome Ireland, University College Cork, Cork, Ireland, [2] NHMRC Centre of Research Excellence in Digestive Health, School of Medicine and Public Health, The University of Newcastle, Callaghan, NSW, Australia, [3] Department of Biological Sciences, Munster Technological University, Cork, Ireland, [4] Danone Nutricia Research, Utrecht, Netherlands, [5] Laboratory of Microbiology, Wageningen University, Wageningen, Netherlands, [6] School of Microbiology, University College Cork, Cork, Ireland, [7] School of Medicine, University College Cork, Cork, Ireland

OPEN ACCESS

Edited by:
Riadh Hammami, University of Ottawa, Canada

Reviewed by:
Kaoru Nakasone, Kindai University, Japan
Haiyang Xia, Taizhou University, China

***Correspondence:**
Emily C. Hoedt
Emily.Hoedt@newcastle.edu.au
Douwe van Sinderen
d.vansinderen@ucc.ie

†These authors share first authorship

Specialty section:
This article was submitted to Food Microbiology, a section of the journal Frontiers in Microbiology

Received: *02 December 2020*
Accepted: *02 March 2021*
Published: *23 March 2021*

Citation:
Hoedt EC, Bottacini F, Cash N, Bongers RS, van Limpt K, Ben Amor K, Knol J, MacSharry J and van Sinderen D (2021) Broad Purpose Vector for Site-Directed Insertional Mutagenesis in Bifidobacterium breve. Front. Microbiol. 12:636822. doi: 10.3389/fmicb.2021.636822

Members of the genus *Bifidobacterium* are notoriously recalcitrant to genetic manipulation due to their extensive and variable repertoire of Restriction-Modification (R-M) systems. Non-replicating plasmids are currently employed to achieve insertional mutagenesis in *Bifidobacterium*. One of the limitations of using such insertion vectors is the presence within their sequence of various restriction sites, making them sensitive to the activity of endogenous restriction endonucleases encoded by the target strain. For this reason, vectors have been developed with the aim of methylating and protecting the vector using a methylase-positive *Escherichia coli* strain, in some cases containing a cloned bifidobacterial methylase. Here, we present a mutagenesis approach based on a modified and synthetically produced version of the suicide vector pORI28 (named pFREM28), where all known restriction sites targeted by *Bifidobacterium breve* R-M systems were removed by base substitution (thus preserving the codon usage). After validating the integrity of the erythromycin marker, the vector was successfully employed to target an α-galactosidase gene responsible for raffinose metabolism, an alcohol dehydrogenase gene responsible for mannitol utilization and a gene encoding a priming glycosyltransferase responsible for exopolysaccharides (EPS) production in *B. breve*. The advantage of using this modified approach is the reduction of the amount of time, effort and resources required to generate site-directed mutants in *B. breve* and a similar approach may be employed to target other (*bifido)bacterial* species.

Keywords: bifidobacteria, functional genomics, mutagenesis, DNA methylation, synthetic vector

INTRODUCTION

Bifidobacteria are common gut commensals that have been reported to elicit a number of beneficial effects on their host (Tojo et al., 2014; O'Callaghan and van Sinderen, 2016; Wong et al., 2019). These Gram-positive obligate anaerobes provide the host with nutrients through the breakdown of indigestible dietary carbohydrates (Turroni et al., 2018), have been shown to modulate the immune

system (O'Hara and Shanahan, 2007), alleviate symptoms in IBS (O'Mahony et al., 2005), and assist with pathogen exclusion (Lee and O'Sullivan, 2010). However, the precise mechanism of action for most of these attributes is still unclear. Site-directed gene disruption methods involving the use of non-replicating insertion plasmids [e.g., the insertion vector Ori^+ $RepA^-$ pORI28, originally developed for use in *Lactococcus lactis* (Law et al., 1995; Leenhouts et al., 1996)] are currently employed to understand the function of target genes. Notably, the lack of a replication (*repA*) gene within the pORI28 sequence requires the use of a $RepA^+$ helper strain to supply the RepA protein *in trans* to allow plasmid replication and maintenance (Law et al., 1995; Leenhouts et al., 1996). Members of *Bifidobacterium* are notoriously recalcitrant to genetic manipulation due to their thick cell wall, sensitivity to oxygen, and extensive and diverse Restriction-Modification (R-M) systems encoded within their genome sequence (Brancaccio et al., 2013; Bottacini et al., 2018b). As a result, one of the major limitations in using commonly available insertion vectors for targeted mutagenesis is the presence of various restriction sites, making them sensitive to the activity of endogenous restriction endonucleases encoded by the target strain (O'Connell Motherway et al., 2009; Bottacini et al., 2018b). Despite all of these difficulties, targeted mutants have been successfully made in a limited number of strains (Hirayama et al., 2012; Sakaguchi et al., 2012; Wei et al., 2012; Hidalgo-Cantabrana et al., 2015; O'Callaghan et al., 2015). For instance, a number of genes in *Bifidobacterium breve* UCC2003 have been knocked-out employing the insertion vector Ori^+ $RepA^-$ pORI19-tet (O'Connell Motherway et al., 2009), a derivative of the pORI28 system containing a tetracycline selection marker for *Bifidobacterium*. However, in order to facilitate the introduction of pORI19-tet into a target strain at sufficiently high frequency to allow gene disruption by homologous recombination an additional step of methylation of the vector is required. This methylation can be achieved in two ways: (i) the plasmid construct is introduced into a methylase positive *Escherichia coli* strain (e.g., the DAM^+ *E. coli* EC101) which may express a cloned methylase from an active R-M system present in the bifidobacterial target strain; (ii) the less frequently employed chemical methylation. This multi-step approach, despite being successfully applied previously, presents some practical hurdles and limitations: first of all the intermediate step of methylase cloning and methylation of the vector in *E. coli* is quite laborious and time consuming, secondly the system may not always be applicable in cases where target strains contain multiple active R-M systems or in cases where there is no information available on the R-M systems of the target strain.

There are three types of base modification within bifidobacteria and can be detected using a combination of PacBio SMRT and Illumina bisulfite sequencing (BS-seq) (Darst et al., 2010; Bottacini et al., 2018b), these consist of N6-methyladenine (m6A), N4-methylcytosine (m4C) and 5-methylcytosine (m5C). Previous work by O'Callaghan et al. (2015) showed how Pacbio sequencing and methylome analysis of two *B. longum* subsp. *longum* strains (NCIMB 8809 and CCUG 30698) has allowed the construction and synthesis of a tetracycline resistance gene (*tetW*), previously identified in *B. longum* H66 (Flórez et al., 2006), free of *Eco*RII restriction sites. The cloning of this bifidobacterial *tetW* gene into the Ori^+ $RepA^-$ pORI19 system coupled with the use of an *E. coli-Bifidobacterium* shuttle vector expressing a *B. longum* methyltransferase (MTase) from an active R-M system present in the target strain increased the accessibility for genetic manipulation (O'Callaghan et al., 2015). In a later study by Bottacini et al. (2018b), PacBio sequencing was used to compile a catalog of R-M systems encoded by *B. breve* strains. By employing a combination of PacBio sequencing (to predict m6A and m4C methylated bases) and bisulfite-treated Illumina sequencing (to detect m5C-methylated bases) the authors obtained a clear evaluation of the genetic barriers imposed by R-M systems within the *B. breve* species.

In the current study, we present an adapted method for bifidobacterial targeted mutagenesis based on a synthetically engineered derivative of pORI28 (henceforth referred to as pFREM28), from which all R-M motifs as previously identified in *B. breve* are removed and in which the original resistance marker is substituted with a bifidobacterial erythromycin resistance gene. The functionality of this system was validated for three distinct *B. breve* strains (UCC2003, NRBB01, and NRBB57), in which we successfully performed site-directed mutagenesis. The synthetic insertion vector pFREM28 represents a novel application of methylome data to circumvent the requirement of plasmid methylation for site-directed mutagenesis in *B. breve*. The pFREM28 vector requires no methylation before electroporation into the target strains, and its successful application implies that there is further potential for this approach to be applied for the design of custom-made synthetic plasmids to target other "genetically recalcitrant" *Bifidobacterium* species.

MATERIALS AND METHODS

Bacterial Strains and Routine Culture Conditions

Escherichia coli and bifidobacterial strains used in this study are detailed in **Table 3**. *E. coli* was routinely cultured in Luria Broth/agar (LB; 10 g/L tryptone, 5 g/L yeast extract, and 10 g/L sodium chloride, and where appropriate 20 g/L agar) aerobically at 37°C and broth cultures shaken at 180 rpm. Bifidobacterial cultures were routinely cultivated in Reinforced Clostridial Medium/Agar (RCM/A; Oxoid Ltd., United Kingdom). Where necessary, modified de-Man-Rogosa-Sharpe (mMRS) Medium was used of the following composition: 10 g/L Tryptone (Peptone from Casein), 2.5 g/L yeast extract, 3 g/L tryptose, 3 g/L potassium phosphate dibasic (K_2HPO_4), 3 g/L potassium phosphate monobasic (KH_2PO_4), 2 g/L tri-ammonium citrate, 0.2 g/L pyruvic acid (sodium pyruvate), 0.575 g/L magnesium sulfate heptahydrate ($MgSO_4.7H_2O$), 0.12 g/L manganese (II) sulfate tetrahydrate ($MnSO_4.4H_2O$), 0.034 g/L iron (II) sulfate heptahydrate ($FeSO_4.7H_2O$), 1 mL/L Tween80, broth supplemented with 0.05% L-cysteine-HCL. Bifidobacterial cultures were incubated at 37°C under anaerobic conditions in an anaerobic chamber (10% H_2, 10% CO_2, and 80% N_2). BioMérieux ETEST® (bioMérieux, France)

strips for chloramphenicol and erythromycin were used to assess minimum inhibitory concentrations (MIC) for each strain, bifidobacterial strains were on RCA plates incubated anaerobically for 24 h at 37°C and *E. coli* on LB agar. Where appropriate growth media contained chloramphenicol (Cm; 5 μg ml^{-1} applicable for all bifidobacterial strains described here), or erythromycin (Em; *E. coli* EC101 200 μg ml^{-1}, UCC2003 150 μg ml^{-1}, or 5 μg ml^{-1} for NRBB01/57), which were used for selection of *E. coli* or *B. breve* transformants.

In silico Design of pFREM28 Vector and Plasmid DNA Preparation

Restriction-Modification motifs for all current *B. breve* strains (including NRBB01, NRBB57, and UCC2003) had previously been identified (O'Connell Motherway et al., 2009; Bottacini et al., 2018b) using a combination of SMRT/bisulfite sequencing and comparative genome analysis (**Figure 2B**). Using an *in silico* method, the sequence of the suicide plasmid pORI28 was retrieved online[1] and used as a template, the native promoter and erythromycin resistance marker were replaced *in silico* with the sequence of an alternative Em^R marker capable of efficient expression in *B. breve* (locus_tag NRBB51_1114) (Bottacini et al., 2018a). Upstream of the coding sequence Em^R marker, a sequence of lactococcal P44 promoter (van der Vossen et al., 1987) was introduced *in silico*. All the sequence editing and removal of restriction sites were performed manually using the SnapGene v2.3[2] and Artemis (Carver et al., 2012) software tools before synthesis. Finally, BLASTP alignment was used to ensure the preservation of the sequence identity of the Em^R antibiotic selection marker (Bottacini et al., 2018b) after the introduced base substitutions. The resulting *in silico* constructed vector, which was designated pFREM28, was sent for synthesis using a commercial DNA synthesis provider (performed by BASECLEAR, Netherlands), and the obtained sequence was validated and delivered by this provider as a cloned fragment in the *E. coli* vector pUC57. Unique restriction sites (*Xba*I) were included at the left and right end of pFREM28 to allow for excision from pUC57 by restriction digestion. Following self-ligation and circularization of the obtained pFREM28 vector, the conditional replication functionality (**Figure 2A**) was confirmed using *E. coli* strain EC101, also demonstrating that the erythromycin MIC was > 256 μg/mL in this strain. Due to the medium/low copy number of this plasmid all subsequent plasmid work described is conducted using plasmid DNA extracted using GeneJET Plasmid Maxiprep Kit (Thermo Scientific) following the manufacturer's instructions coupled with an ethanol precipitation to concentrate the DNA.

Insertion Mutagenesis Plasmid Preparation

Targets for insertion mutagenesis were chosen and where applicable homologous regions were selected for amplification with Q5® High-Fidelity DNA Polymerase (BioLabs). Primers included restriction sites (**Table 2**), not present within the target gene, and allowed cloning of the insertion amplicon into the multiple cloning site of pFREM28. Restriction and ligation of the insertion amplicon and pFREM28 was completed following manufacturer's instructions and each clean-up step consisted of ethanol precipitation. Ligations were transformed into EC101 competent cells as described previously (Law et al., 1995) and plated on LB agar with 200 μg/mL erythromycin. Sequence validated clones were then recovered as described above.

Preparation of Electrocompetent Cells

Strains were cultivated overnight at 37°C in an anaerobic chamber (10% H_2, 10% CO_2, and 80% N_2) using either autoclaved or filter (0.2 μM) sterilized mMRS, supplemented with 0.05% L-cysteine·HCl. A selection of filter sterilized (0.2 μM) carbohydrates (glucose, lactose, fucose, Lacto-*N*-Neotetraose (LNnT) or lactose + fucose- 0.01 g/mL final) were tested to ascertain their impact on the transformation efficiency of each strain and as a result glucose was used to supplement mMRS for UCC2003 and NRBB57, while fucose + lactose was the carbohydrate combination used for NRBB01-associated transformations (0.01 g/mL final). Fresh 40 mL of mMRS was then inoculated with 5 mL of the overnight culture and 5 mL of select carbohydrates (0.01 g/mL final) and grown to an OD_{600} of 0.6. Cultures were then incubated on ice for 20 min and subsequently centrifuged (4,052 × *g*, 10 min at 4°C). Cell pellets were then washed twice with ice cold sucrose-citrate buffer (0.5 M sucrose and 1 mM ammonium citrate, pH 5.8) before resuspension in 200 μL of the same wash buffer. Electro-transformations (25 μF and 200 Ohms) with varied voltage (1,500, 1,750, 2,000, 2,250, and 2,500 V) were assessed (optimal: 25 μF, 200 Ohms, 2,500 V) with 50 μL of this suspension. Plasmids pNZ44 and pNZ123 (**Table 3**) were used in preliminarily tests at increasing concentrations (0.1, 0.2, 0.3, 0.5, 1, and 3 μg plasmid DNA) to determine the optimal concentration for maximal transformation efficiency of pFREM28 constructs (optimal: 3 μg). Electrotransformations were conducted using 2 mm electroporation cuvettes. After transformation, the cells were suspended in 1 mL of RCM and incubated anaerobically for 1 h at 37°C. Serial dilutions were plated on RCA containing erythromycin (5 μg/mL for NRBB01 and NRBB57, and 150 μg/mL for UCC2003) and plates were incubated anaerobically at 37°C for 48 h after which time the number of transformants were enumerated. Summary of the original and optimal transformation conditions are outlined in **Table 1**.

Phenotypic Screening of Insertional Mutants and Sequence Validation

Single colonies produced following mutagenesis were screened for disrupted phenotype by culturing in mMRS in the presence of control sugar (glucose) or the carbohydrate, of which the corresponding utilization cluster was targeted (raffinose or mannitol) and incubated anaerobically at 37°C. Wild type strains were also assessed for growth on each carbohydrate. Optical density (OD_{600nm}) was recorded after 24 h and results were

[1]https://www.addgene.org/71595

[2]https://www.snapgene.com

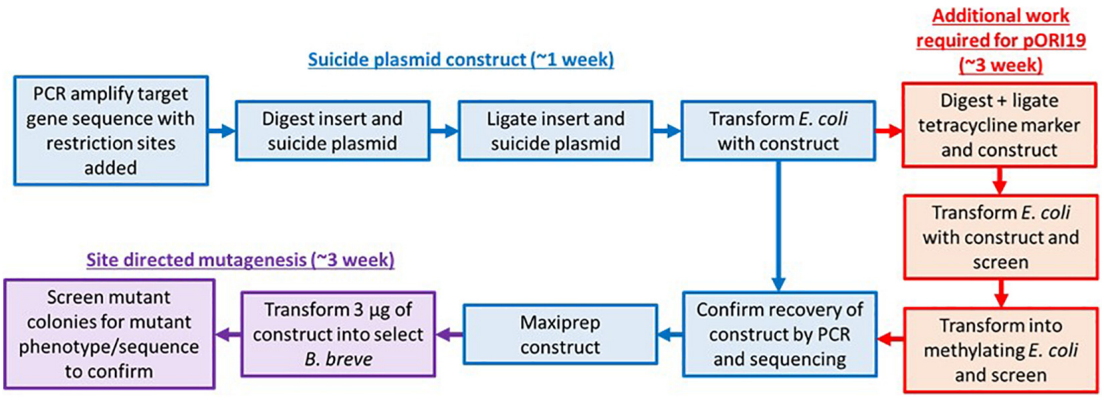

FIGURE 1 | Approaches for site-directed mutagenesis in bifidobacteria. Flow chart describing the original (inclusive of red pathway) and modified steps (exclusion of red pathway which can consist of either methylase cloning or vector methylation) required for performing site-directed mutagenesis in *Bifidobacterium*. The improved pFREM28 vector reduces labor and consumable cost as a step for methylation of the *E. coli-Bifidobacterium* shuttle vector is no longer required.

plotted using GraphPad v8.3.0. The gDNA was extracted using GenElute^{TM} Bacterial Genomic DNA Kit (Sigma) following manufacturer's instructions and quantified by Qubit^{TM} dsDNA BR Assay Kit (Invitrogen). PCR validation of each pFREM28 insertion was performed using bridging primers from within the insertion plasmid and upstream of each target region (**Table 2**). For the NRBB01 derivative carrying a mutation in the α-galactosidase-encoding gene, a high-quality draft genome was obtained by Illumina Miseq sequencing in order to confirm the expected gene disruption. Reads were assembled using Spades v3.14.0 with kmer lengths of 33, 55, 77, 99, and 127 and contigs were rearranged against the respective reference genome using Mauve v2.4.0. The insert was located using NCBI BLASTn and up to 10 Kb region containing the inserted pFREM28 was extracted from each mutant for further analysis. Open reading frames were predicted with Prodigal in anon mode (-p anon). Functions of protein coding sequences were annotated using BLAST (blastp v2.2.28+) against their respective reference genomes.

RESULTS AND DISCUSSION

Construction of pFREM28

The Ori^{+} RepA^{-} insertion vector pORI19-tet has been used to date for site-directed mutagenesis in strains of *B. breve*, including *B. breve* UCC2003, JCM 7017, and NCIMB 2258 (O'Connell et al., 2013a; Egan et al., 2014; Bottacini et al., 2018a). For a successful introduction of the vector into a target strain and subsequent integration into the bacterial chromosome by homologous recombination, a methylation step is required in order to protect the vector and cloned insert from the activity of R-M-associated restriction endonucleases in the target strain. Plasmid methylation has so far been achieved *via* the heterologous expression of selected methylases from the target strain into an *E. coli* host (**Figure 1** and **Supplementary Figure 1**), followed by the introduction of the mutagenesis vector in the methylase^{+} *E. coli* host prior to introduction into *B. breve* (O'Connell Motherway et al., 2009). In order to avoid the additional step of vector methylation and to provide a time-effective approach for gene disruption in *B. breve,* we designed an R-M-insensitive synthetic vector pFREM28 (**Figure 2A**) with the potential for broad application among various *B. breve* strains. This synthetic system was designed using the original pORI28 sequence as a template backbone (see text footnote 1) (Leenhouts et al., 1996), which was subsequently modified *in silico* before synthesis (**Figure 2A**). A total of 955 bp from the pORI28 vector was used as a backbone, including the ORI region and multiple cloning site. The first step in the design of the novel pFREM28 vector was the replacement of the original erythromycin selection marker in pORI28 with a marker that is suitable for expression in *Bifidobacterium*. In fact, the original erythromycin resistance marker in pORI28 appears to be poorly expressed in *Bifidobacterium*, thus causing unreliable selection. Due to the apparent insufficient expression of the erythromycin resistance gene, current protocols require the introduction of an additional bifidobacterial tetracycline resistance gene in pORI19-tet (a pORI28 derivative), a modification which has proven successful in gene disruption applications of *Bifidobacterium* (O'Connell Motherway et al., 2009; O'Callaghan et al., 2015). The antibiotic resistance marker selected for pFREM28 is a recently identified erythromycin resistance gene from *B. breve* NRBB51 (Bottacini et al., 2018a). The main advantage of using this novel marker is that it confers a high level of erythromycin resistance (up to 256 mg/ml) in *B. breve*, thus ensuring a reliable and clean selection (Bottacini et al., 2018a). The steps undertaken for the construction and optimization of pFREM28 vector are presented in **Figure 2**. Through *in silico* manipulation the sequence fragment of 929 bp containing the erythromycin resistance gene was extracted from the genome sequence of *B. breve* NRBB51 (locus_tag NRBB51_1114) and introduced to replace the original antibiotic marker in pORI28. In order to ensure a high level of expression of the antibiotic marker, further *in silico* edits were made and a 175 bp sequence containing the constitutive P44 promoter from *L. lactis* was obtained from the relevant

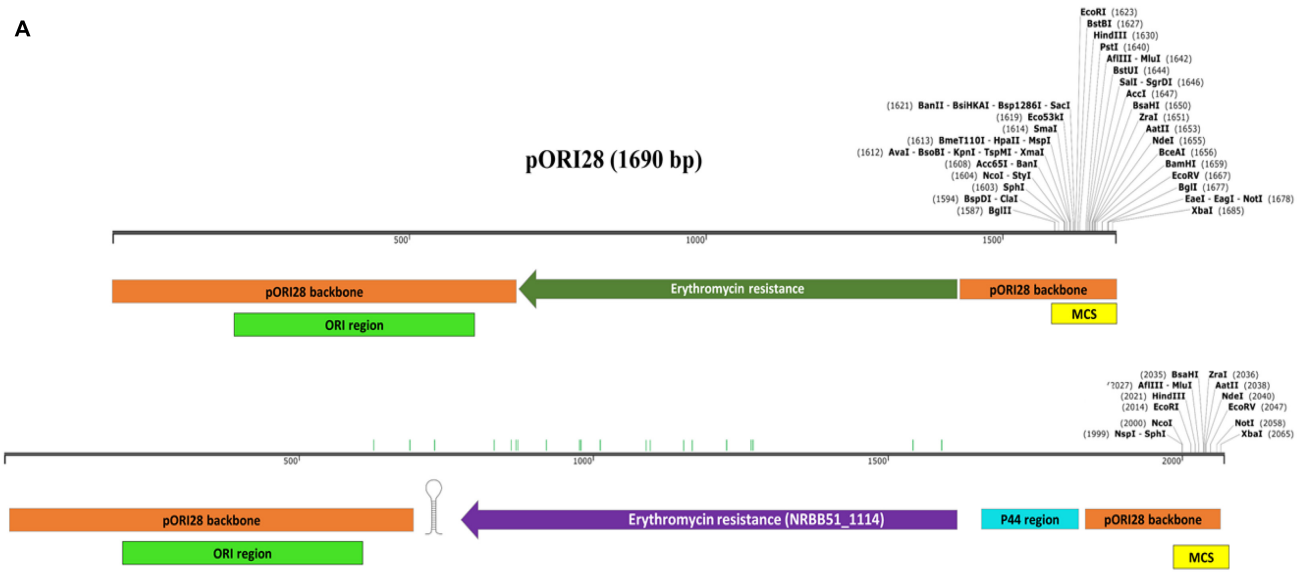

	R-M recognition sequence	pNZ44	pNZ123	pORI28	pFREM28 (unmodified)	pFREM28 (modified)
Type II	GATC	4	2	6	16	0
	RGATCY	0	2	4	6	0
	GGATC	0	1	2	5	0
	CCWGG	2	0	0	6	0
	GGCGCC	0	0	0	0	0
	TGGCCA	2	0	0	2	0
	GTCGAG	0	0	2	2	0
	CTGCAG	2	0	2	2	0
	RTCGAY	4	2	4	12	0
	CGGGAG	1	0	1	1	0
	GTCGAC	2	0	2	2	0
	GAGGAC	0	0	0	0	0
	GTRAAYG	1	1	1	0	0
	GGRCAG	1	1	0	2	0
	GGCGAG	0	0	0	1	0
Type I	GCANNNNNTGC	0	0	0	0	0
	CCAYNNNNGTC	0	0	0	0	0
	RAYCNNNNNCTG	0	2	4	0	0
	GACNNNNNNCATY	0	0	0	0	0
	CCANNNNNNNNTGG	0	0	0	0	0
	AGCNNNNNGTC	2	1	0	0	0
	GACNNNNNNRTTG	0	0	0	0	0
	GAGNNNNNRTTC	0	0	1	1	0
	RAYCNNNNNNTRCC	0	0	0	0	0

FIGURE 2 | Methylome-directed *in silico* construction of the pFREM28 insertion vector, starting from the pORI28 template. **(A)** Linear plasmid map of the pORI28 original template sequence compared to the newly constructed R-M insensitive vector pFREM28 (Em^R Ori + RepA-). The pFREM28 vector contains a different erythromycin resistance gene (locus tag: NRBB51_1114), with the P44 promoter region upstream and a transcriptional terminator downstream. The pORI28 backbone sequence used for the pFREM28 design is indicated in orange, while the ORI region is indicated in green and the multiple cloning site (MCS) in yellow. Green bars along the pFREM28 sequence indicate sites where restriction sites were eliminated. **(B)** Modified extract from Bottacini et al. (2018b) of a heatmap representing presence/absence of R-M motifs within *B. breve* strains. Motifs are grouped based on their assignment to Type I, Type II, and Type IIG R-M system and the type of modification (m6A, m4C, and m5C) is indicated. The number of target sites from the *B. breve* methylome Bottacini et al. (2018b) in plasmids pNZ44, pNZ123, pORI28, pFREM28 (before modification), and pFREM28 (after removal of RM sites) are also indicated. From the data presented it is possible to appreciate how the number of sites and the combination of R-M systems are variable across plasmids and *B. breve* strains.

publication (van der Vossen et al., 1987) and added to our vector design. The P44 promoter is capable of high expression in both *E. coli* and *Bifidobacterium* hosts and was positioned in our *in silico* construct upstream of the original ribosomal binding site (RBS; 5′-AGGAGC-3′) of the antibiotic marker (the promoter is 40 bp upstream the translational start of the Em^R gene). In order to ensure efficient transcriptional termination we decided to add to our *in silico* vector design a rho-independent terminator obtained from a previous transcriptomic study, where we predicted all rho-independent terminators in *B. breve* UCC2003 (Bottacini et al., 2017). The terminator sequence chosen for this purpose 5′-CCCCGACCCCAACCGGTCGGGGCTTCTTGCGTTG-3′ was extracted from the highly expressed *talA/B* operon in *B. breve* UCC2003 (Bottacini et al., 2017) and positioned downstream the Em^R gene in our vector sequence design. Finally, in order to make the construct insensitive to the endonuclease activity of known *B. breve* R-M systems, all motifs previously identified as a target sequence of such systems (Bottacini et al., 2018b) were manually removed *in silico* from the vector sequence. The

TABLE 1 | Original and optimal transformation conditions for UCC2003, NRBB01, and NRBB57.

Strain	COH	Media preparation	Aerobic vs. anaerobic	Amount plasmid DNA	Plasmid	Voltage	Transformation efficiency (transformants/μg DNA)
Original "standard" transformation parameters							
UCC2003	Glucose	Autoclaved	Aerobic	200 ng	pNZ44	2,000 V	$1.67 \times 10^3 \pm 2.33$
NRBB01	Glucose	Autoclaved	Aerobic	200 ng	pNZ44	2,000 V	$1.25 \times 10^3 \pm 1.37$
NRBB57	Glucose	Autoclaved	Aerobic	200 ng	pNZ44	2,000 V	$9.89 \times 10^2 \pm 6.34$
UCC2003	Glucose	Autoclaved	Aerobic	200 ng	pNZ123	2,000 V	$2.00 \times 10^7 \pm 2.11$
NRBB01	Glucose	Autoclaved	Aerobic	200 ng	pNZ123	2,000 V	$8 \times 10^6 \pm 5.65$
NRBB57	Glucose	Autoclaved	Aerobic	200 ng	pNZ123	2,000 V	$4.7 \times 10^5 \pm 5.24$
Optimal transformation parameters							
UCC2003	Glucose	Filtered	Aerobic	3 μg	pNZ44	2,500 V	$6.16 \times 10^3 \pm 4.37$
NRBB01	Fucose + lactose	Filtered	Aerobic	3 μg	pNZ44	2,500 V	$3.93 \times 10^3 \pm 0.51$
NRBB57	Glucose	Filtered	Aerobic	3 μg	pNZ44	2,500 V	$5.60 \times 10^4 \pm 1.59$
UCC2003	Glucose	Filtered	Aerobic	3 μg	pNZ123	2,500 V	$1.5 \times 10^7 \pm 1.40$
NRBB01	Fucose + lactose	Filtered	Aerobic	3 μg	pNZ123	2,500 V	$4.53 \times 10^7 \pm 4.33$
NRBB57	Glucose	Filtered	Aerobic	3 μg	pNZ123	2,500 V	$1.47 \times 10^7 \pm 0.90$

TABLE 2 | Primers used in this study.

Target gene	Primer sequence	Amplicon size (bp)
AG- Forward + *Eco*RI	gatcgaattcCGGCGAAGTAACGCTTGATG	546
AG- Reverse + *Hin*dIII	gatcaagcttCCGGATTGGTCAGG	
AD- Forward + *Eco*RI	gatcgaattcGTACCAGAAGGCGTTGGTCA	492
AD- Reverse + *Hin*dIII	gatcaagcttGAAACGCCCTTGATCTTGCC	
PGT— Forward + *Eco*RI	gatcgaattcCACCTACTTCTCCTCTACACC	463
PGT—Reverse + *Hin*dIII	gatcaagcttATCCAACGCTCGATAATAACC	
pFREM-MCS-F	ATAGCACGCCCGCATGCC	Target sequence insertion into pFREM28 insert confirmation.
pFREM-EmR-R	CCGTGTCCGTATGCAGAC	Genome integration confirmation, used with primers below.
AG-ins-com-F	ACCGTCATCCACCACGAATC	721
AD-ins-com-F	GGTCCAGAAGAATCCGGTGG	1,559
EPS-ins-com-F	GTCGGATCGTTGCGGAAATG	1,324

removal of restriction sites was achieved manually by single base substitutions *in silico*, where an alternative synonymous codon was always chosen to avoid any of the target motifs, thus preserving the amino acidic sequence encoded by the gene. A total number of 21 sites of the pFREM28 were thus modified (**Supplementary Table 1**). The vast majority of these modifications were located in the coding sequence of the erythromycin resistance marker. Notably, no modification was needed to be introduced in the ORI region of the plasmid (base position 210–610), thus not affecting any replication function of the vector. The modifications also necessitated the removal of a number of restriction sites of the multiple cloning site (MCS) region.

Following vector synthesis, the integrity and functionality of the selection marker was confirmed upon self-ligation, transformation and recovery of pFREM28 from the *E. coli* helper strain EC101. This strain, when harboring pFREM28, was shown to be resistant to erythromycin at a concentration of >256 μg/mL, in accord with what described previously in *B. breve* (Bottacini et al., 2018a).

Improved Transformation Efficiency

For testing purposes three *B. breve* strains (NRBB01, NRBB57, and UCC2003) were selected from our culture collection, which had previously been predicted to each contain distinct R-M systems (**Figure 2B**; O'Connell Motherway et al., 2009; Bottacini et al., 2018b). When standard transformation parameters and our routine plasmid pNZ44 were employed with these strains (McGrath et al., 2001), we achieved a transformation efficiency ranging from 10^2–10^3 transformants/μg DNA (**Table 1** and **Figure 3**). For successful mutagenesis, transformation efficiencies of at least 10^5 transformants/μg DNA are recommended (van Pijkeren and Britton, 2012; Zuo et al., 2019). Therefore, in order to improve the transformation efficiency of these strains before attempting targeted mutagenesis we assessed a range of parameters (various carbohydrates for growth, different media and medium preparation methods, changing electroporation voltage parameters, varying plasmid amount, and selecting a plasmid with a smaller number of known R-M motifs) during the preparation and electroporation of the *Bifidobacterium* cells. This fine-tuning of the transformation

TABLE 3 | Strains and plasmids used in this study.

Strain	Source	Accession	Study
E. coli EC101	*E. coli* JM101 with *repA* from pWV01 integrated in chromosome	VIBV01000001	Law et al. (1995)
B. breve UCC2003	Infant isolate, (Breast fed)	CP000303	Mayo et al. (2008)
B. breve NRBB01	Infant isolate—provided by Nutricia	CP021384	Bottacini et al. (2018b)
B. breve NRBB57	Infant isolate—provided by Nutricia	CP021389	Bottacini et al. (2018b)
Plasmid	**Relevant Properties**	**Accession**	**Study**
pNZ44	3 kb; *E. coli/Bifidobacterium* shuttle cloning vector containing constitutive P44 promoter from *L. lactis*; Cm^R	NA	McGrath et al. (2001)
pNZ123	2.5 kb; *E. coli/Bifidobacterium* shuttle cloning vector; Cm^R	NA	De Vos (1987), Platteeuw et al. (1994)
pFREM28	2 kb; *B. breve* R-M motif free suicide vector; Em^R	MT499887	This study

parameters was performed stepwise in order to increase the transformation efficiency to $\sim 10^7$ transformants/μg DNA (**Table 1** and **Figure 3**). Strains were grown overnight, and competent cells prepared employing various carbohydrates (glucose, LNnT, lactose, fucose or fucose + lactose), the strains exhibited varied transformation efficiency dependent on the different carbohydrate(s) supplied. The best results for UCC2003 and NRBB57 were observed when glucose was present and fucose + lactose for NRBB01. Secondly, the sterilization treatment of the mMRS medium was modified from autoclaving to filter sterilization (using a 0.22 μM filter), as this resulted in a noticeable increase of the transformation efficiency for NRBB01 and NRBB57 (10^4 and 10^5 transformants/μg DNA, respectively).

While certain *Bifidobacterium* species are reasonably aerotolerant with current protocols stating that competent cells can be prepared under aerobic conditions, before anaerobic incubation, we prepared competent cells under anaerobic and aerobic conditions to confirm the exact effect. Upon transformation and plating we did not notice any difference between aerobic or anaerobic prepared cells. However, we decided to proceed with cell preparation under aerobic conditions, as this offered a reduced risk of external contamination by working within a lamina flow hood. The number of R-M motifs present within a given sequence used for transformation are known to have a significant impact on the transformation efficiency (O'Connell Motherway et al., 2009; Bottacini et al., 2018b). We examined our routinely used pNZ44 for R-M motifs known to be present within our strains UCC2003, NRBB01 and NRBB57 (**Figure 2B**) and identified 19 motifs. To compare we selected the related plasmid pNZ123 (provided by NIZO (De Vos, 1987; Platteeuw et al., 1994) for electrotransformation which had only 12 motifs identified (**Figure 2B**) and found that indeed there was an increase for each of the strains when an alternative plasmid with fewer R-M motifs was selected. Using pNZ123 we next assayed increasing the amount of plasmid DNA (0.1, 0.2, 0.3, 0.5, 1, and 3 μg plasmid DNA) on the transformation efficiency, the highest amount of plasmid DNA improved the transformation efficiency ($\sim 10^6$ transformants/μg DNA for NRBB57). Finally, the voltage for electroporation was varied (1,500, 1,750, 2,000, 2,250, and 2,500 volts) from the original standard of 2,000 volts and as a result we observed an increase to 10^7 transformants/μg DNA for all strains when the voltage was increased to 2,500 volts.

While it became apparent that a number of factors are responsible for the transformation efficiency of our strains these were not all uniform. Comparison of the efficiencies achieved with both the "original" and "optimal" conditions (**Figure 2**) demonstrate that the modifications made had the most profound impact on NRBB57, for both plasmids used. While the other strains did also show improvement, this was marginal compared to NRBB57. Of note, for this strain we obtained the best transformation efficiency with the pNZ123 vector, despite the presence of two RAYC(N5)TGC motifs associated with a Type I RM system. This indicates that the restriction endonuclease of this system is only partially active. In general, we observed that the presence of R-M motifs had the most noticeable effect on the overall transformation efficiency and further justified our approach here to synthetically modify a "common" suicide vector to be free of R-M motifs to improve site-directed mutagenesis. As we did observe an improvement of transformation efficiency for our strains under the "optimal" conditions (**Table 1**) we determined that these parameters were ideal to proceed with targeted mutagenesis, described below, as we had exceeded the desired threshold of 10^5 transformants/μg DNA.

Methylase Free Site-Directed Mutagenesis

To assess the ability of pFREM28 to allow gene disruption we targeted two carbohydrate utilization pathways, in addition to a key exopolysaccharide/capsule (EPS) biosynthesis encoding gene previously described in *B. breve* (Fanning et al., 2012; O'Connell et al., 2013b; Bottacini et al., 2014). Our first target was an α-galactosidase gene which had previously been described as involved in the raffinose utilization in *B. breve* UCC2003 (O'Connell et al., 2013b), thus making this gene a suitable candidate to test our insertion system. The genome annotations for NRBB01 and NRRB57 also include a highly homologous α-galactosidase gene (percent identity > 98%, percent coverage 100%) free from any relevant restriction sites (see sites in **Figure 2B**), as such a 546 bp homologous region was selected and cloned into pFREM28, thus generating a single pFREM28(-AG)

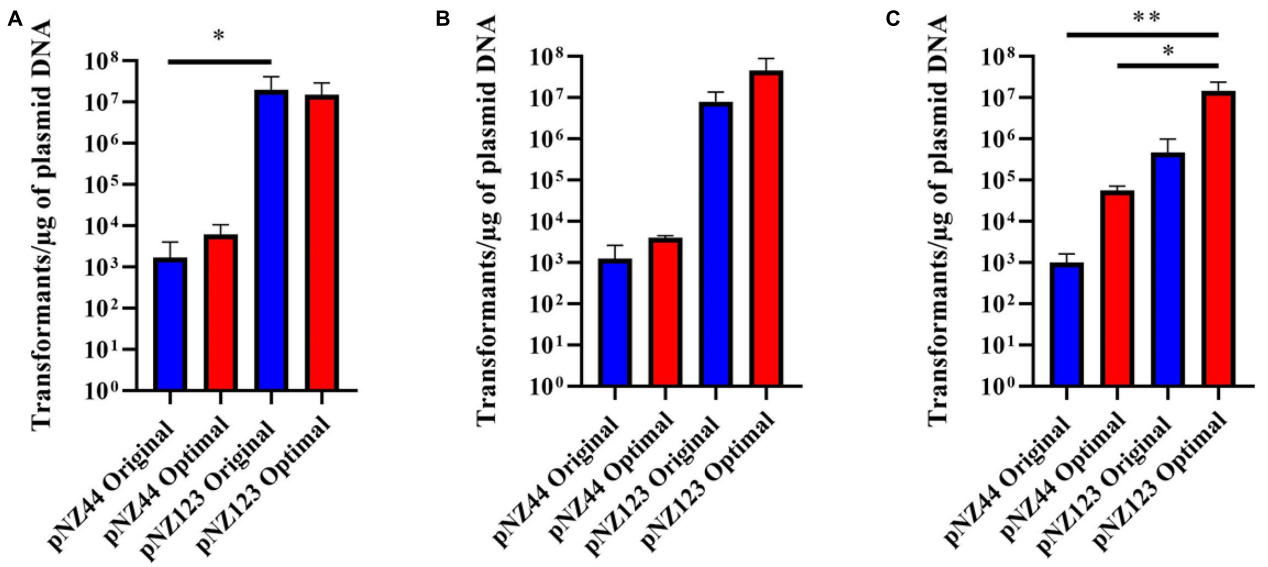

FIGURE 3 | Transformation efficiencies for *B. breve* strains **(A)** UCC2003, **(B)** NRBB01, and **(C)** NRBB57 when "original" (blue) or "optimal" (red) transformation conditions are used for either plasmid pNZ44 or pNZ123. Individual values represent the mean (±SD) produced from triplicate transformations and significance level (Unpaired *t*-test): **p*-value ≤ 0.05; ***p*-value ≤ 0.01. UCC2003 transformation efficiency is significantly higher when comparing pNZ44 to pNZ123 under original conditions. While NRBB01 efficiencies are not significantly different there is a marked increase when pNZ123 is employed. Significant improvements were observed for NRBB57 with pNZ44 under "original" and "optimal" conditions when compared to "optimal" pNZ123. In general, all strains demonstrate slight improvements in transformation efficiency when the "optimal" conditions were used, most notably for NRBB57.

construct to be tested in each strain. The subsequent introduction of pFREM28(-AG) in the three tested strains resulted in the successful generation of putative insertion mutants ($\sim 10^1$ Em^R transformants/µg DNA) in all three cases (**Figures 4A–C**), all mutants demonstrated an erythromycin MIC > 256 µg/mL. In each instance of mutant generation, we first screened the mutants *via* PCR to confirm the plasmid insertion (primers used upstream of the insert region and within pFREM28 are described in **Table 2** and **Figure 4A**). The mutants were then phenotypically assessed, validating their expected inability to utilize raffinose (**Figure 4B**), thus confirming that pFREM28 is capable of successful insertion into the target gene. As a final and definite confirmation of the site-specific integration event in the alpha-galactosidase-encoding gene, a single mutant (NRBB01-AG) was selected to be assessed by Illumina-mediated whole genome sequencing. The sequencing of the strains and subsequent assembly indeed authenticated the interruption of the alpha-galactosidase gene with the pFREM28-AG construct (**Figure 4C**).

An alcohol dehydrogenase (encoded by the gene with locus tag B7017_1848) has previously been described as correlating with growth on sorbitol/mannitol (Bottacini et al., 2014; Bottacini et al., 2018a) and the finding was confirmed by insertional mutagenesis in *B. breve* JCM 7017 (Bottacini et al., 2014). Also in this case homologous genes (percent identity and coverage 100%) were identified within NRBB01 and NRBB57 (NB the gene appears to be absent in UCC2003) (Bottacini et al., 2018a) and mutants were constructed targeting a 492 bp homologous region, free from any relevant restriction sites (see sites in **Figure 2**), within the alcohol-dehydrogenase gene for NRBB01 (NRBB01_1667) and NRBB57 (NRBB57_1926). Following transformation, several putative mutants were recovered ($\sim 10^1$ Em^R transformants/µg DNA) and validated using primers described in **Table 2** (**Supplementary Figure 2A**), for the two target strains and phenotypic screening confirmed the loss of mannitol utilization ability for NRBB01 and NRBB57 (**Supplementary Figure 2B**). As a final means of validation, mutants for each strain were selected for Illumina-mediated whole genome sequencing and each confirmed to have had the target alcohol dehydrogenase gene interrupted by pFREM28-AD (**Supplementary Figure 2C**), thus providing a second confirmation of the effectiveness of our synthetically designed pFREM28 insertion system.

Finally, we targeted the gene encoding the predicted priming undecaprenyl-phosphate galactosephosphotransferase, which had previously been identified in *B. breve* UCC2003 (locus tag Bbr_0430) as a key gene in the EPS biosynthetic pathway (Fanning et al., 2012). *B. breve* NRBB01 is phenotyped as an EPS-producer and contains an annotated priming undecaprenyl-phosphate galactosephosphotransferase (NRBB01_0373) which is 72% identical to that of UCC2003. Therefore, a 463 bp region of NRBB01_0373 was targeted for insertional mutagenesis [NB: NRBB57 is already EPS-negative, while UCC2003 has previously been mutated (Fanning et al., 2012)] free from any relevant restriction sites (see sites in **Figure 2**). Therefore, we designed a single construct for our validation of EPS biosynthesis in NRBB01 only. Em^R-resistant transformants were recovered following introduction of plasmid pFREM28-EPS into NRBB01 by electrotransformation and first validated through PCR (see **Table 2** and **Supplementary Figure 3A**). These putative EPS-negative NRBB01 derivatives were also shown to exhibit a clear

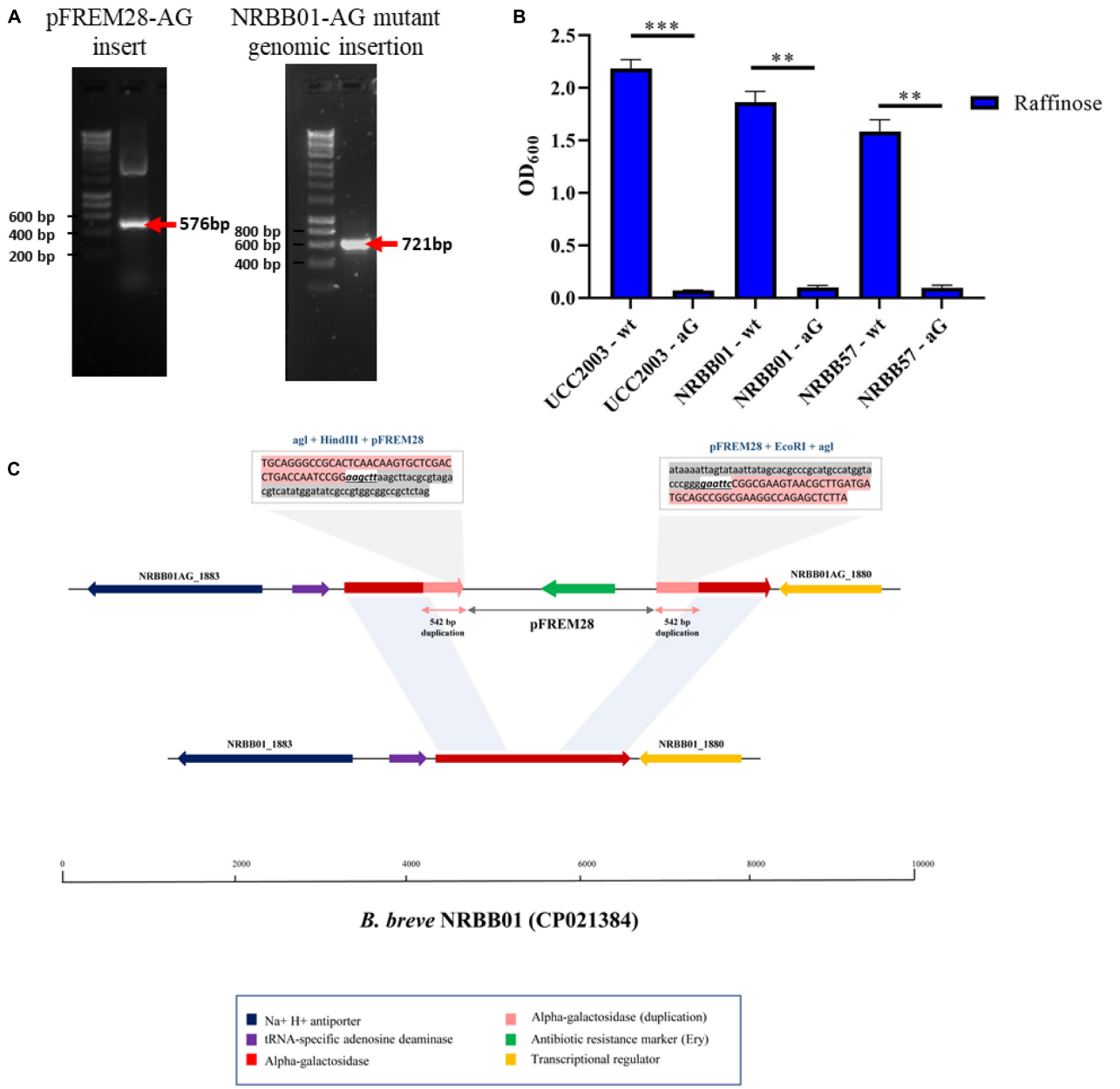

FIGURE 4 | Insertional mutagenesis of the alpha-galactosidase-encoding gene in *B. breve*. **(A)** PCR validation of 542 bp alpha-galactosidase-target gene sequence into pFREM28 and subsequent PCR validation of pFREM28-AG insert into the genome of our *B. breve* strains using primers described in **Table 2**. **(B)** Optical density (OD600) of *B. breve* strains UCC2003, NRBB01, and NRBB57 wild type and site-directed mutants targeting the alpha-galactosidase-encoding gene were grown for 24 h in the presence of raffinose. Individual values represent the mean (±SD) produced from duplicate cultures and significance level (Unpaired *t*-test): ns, not significant; **p*-value ≤ 0.05; ***p*-value ≤ 0.01; ****p*-value ≤ 0.001. **(C)** Sequence confirmation of the integration of the pFREM28-AG vector in the alpha-galactosidase gene of *B. breve* NRBB01. Locus map showing the comparison between *B. breve* NRBB01 wt harboring an intact alpha-galactosidase gene (gene ID NRBB01_1881) and the corresponding locus in the insertional mutant strain containing a disrupted gene. As result of the pFREM28-AG integration (gene ID NRBB01AG_1880 and NRBB01AG_1883) the two flanking regions of the integrant present a 542 bp duplication resulting from homologous recombination.

sedimentation phenotype in liquid growth media [indicative of a lack in EPS production (Fanning et al., 2012)] when compared to the wild type (**Supplementary Figure 3B**). Illumina-mediated whole genome sequencing once again confirmed our success at generating a site-directed mutant using pFREM28 (**Supplementary Figure 3C**).

CONCLUSION

Genetic manipulation of *Bifidobacterium* has been pursued for a number of years (Missich et al., 1994; Argnani et al., 1996) as a means to better understand their physiology and the mechanism of microbe-host interaction. However, due to the nature of

Bifidobacterium the introduction of foreign DNA is difficult and only seems to work for selected strains. Their sensitivity to oxygen, thick cell wall and, probably representing the biggest challenge, the diverse and variable R-M systems result in an average transformation efficiency $< 10^4$ transformants/μg of DNA (Argnani et al., 1996; Shkoporov et al., 2008; Fukiya et al., 2010; Alvarez-Martin et al., 2012) with a number being completely recalcitrant to transformation. As technology has improved so has our ability to transform various members of the *Bifidobacterium* genus, through the comprehensive predictions of R-M motifs through PacBio sequencing (O'Connell Motherway et al., 2014; Bottacini et al., 2018b) coupled with bisulfite sequencing to identify adenine and cytosine methylation (Darst et al., 2010), targeted methylation of plasmid DNA by chemical method (Yasui et al., 2009; Park et al., 2018), or vectors carrying methylation genes (O'Connell Motherway et al., 2009). Based on our observations, transformation efficiencies can vary from strain to strain in addition to the plasmid selected for transformation. In general, we obtained higher transformation efficiencies (up to 10^7) with the pNZ123 vector, which contains fewer restriction sites compared to pNZ44. This suggests that pNZ123 is less affected by the R-M barrier in the *B. breve* strains tested. We have also demonstrated here that other factors such as carbohydrate, media preparation, electroporation voltage, and amount of plasmid DNA or type of plasmid can have a significant impact on transformation efficiency.

Current standard lab practice for site-directed mutagenesis involves cloning of one or more parts of a targeted gene in a non-replicating vector that carries an antibiotic selection marker. Additionally, to protect insertional plasmids from R-M system degradation, the construct would need to be first passed through a methylase positive *E. coli* strain which expresses a cloned bifidobacterial methylase. Therefore, we aimed to redesign an insertional plasmid of broad application in *B. breve*, in order to reduce the work necessary to prepare an insertional plasmid before use (**Figure 1** and **Supplementary Figure 1**).

After validating the integrity of pFREM28 and the functionality of the erythromycin selection marker, the vector was successfully employed to target two separate carbohydrate pathways in three *B. breve* strains: UCC2003, NRBB01, and NRBB57 for the alpha-galactosidase gene, while NRBB01 and NRBB57 were manipulated for the alcohol dehydrogenase gene (as UCC2003 lacks of such gene). Finally, we targeted the EPS biosynthesis pathway (NRBB01 only) by inactivating a priming glycosyl transferase gene and observed a "dropping" phenotype typically associated with the lack of EPS production. The advantage of using this modified approach is the reduction of the amount of time and resources required to generate site-directed mutants in members of *B. breve* species without the need for cloning methyltransferases and methylation of the vector prior to transformation. It is worth noting that the removal of the Type I target sites constitutes another advantage of a methylase insensitive vector. According to the recently published *B. breve* R-M systems catalog (O'Connell Motherway et al., 2009; Bottacini et al., 2018b) many *B. breve* strains encode at least one Type I system, with some bifidobacterial strains possess multiple Type I and Type II systems. Methylation of the Type I target sites requires the cloning of not only a methyltransferase gene but also the associated specificity determinants, in order to achieve the desired methylation. Avoiding the cloning of multiple methyltransferases prior to performing insertional mutagenesis on a new strain constitutes another advantage in terms of saving time, resources and labor. Of course one has to take into consideration that the approach presented in the current manuscript has been exclusively applied to members of the *B. breve* species, but a similar approach may be developed for the generation of custom vectors to facilitate the genetic manipulation of even more challenging (bifido)bacterial species. The only foreseeable limitation would be the presence of R-M motifs within the region selected for insertion into pFREM28. If unavoidable a methylation step could be incorporated (as described above). Taken together, our study presents a successful application of the information derived from methylome analysis to extend functional genomics applications in *B. breve* and to provide the technical road map to target other members of *Bifidobacterium*, which have so far proven to be genetically inaccessible. Of course, further testing is required to evaluate the broader application of pFREM28 and similar vectors, including the possibility of employing longer fragments to increase recombination rate. Nevertheless, our study has shown that the design of strain- or species-specific custom vectors is a feasible option and opens the possibility of employing advanced synthetic biology applications to expand functional genomics in *Bifidobacterium*.

DATA AVAILABILITY STATEMENT

The datasets presented in this study can be found in online repositories. The sequences described in this study have been deposited in GenBank database under the following accession numbers: MT499887, MT978064, MT978066, MT978067, MT978065, and SRA raw data is available at PRJNA662028.

AUTHOR CONTRIBUTIONS

EH planned and performed the research and wrote the manuscript. FB performed the *in silico* design and analysis of the pFREM28 vector and assisted in manuscript writing. NC and RB performed research. KL, KA, JK, and JM planned and supervised research. DS planned and supervised research and performed manuscript editing. All authors contributed to the article and approved the submitted version.

FUNDING

This work was sponsored by Nutricia Research, Utrecht, Netherlands. Additionally, this publication has emanated from research supported in part by a grant from Science Foundation Ireland under Grant numbers (SFI/12/RC/2273-P1 and SFI/12/RC/2273-P2) for authors EH, FB, NC, JM, and DS. For the purpose of Open Access, the author has applied a CC BY public copyright licence to any Author Accepted Manuscript version arising from this submission. FB is the recipient of a FEMS Research Grant (FEMS-RG-2016-0103).

ACKNOWLEDGMENTS

The authors would like to sincerely thank Glycom A/S (Lyngby, Denmark) for the provision of purified HMO sample (LNnT) used in this study under their donation program.

SUPPLEMENTARY MATERIAL

The Supplementary Material for this article can be found online at: https://www.frontiersin.org/articles/10.3389/fmicb.2021.636822/full#supplementary-material

REFERENCES

Alvarez-Martin, P., O'Connell Motherway, M., Turroni, F., Foroni, E., Ventura, M., and van Sinderen, D. (2012). A two-component regulatory system controls autoregulated serpin expression in *Bifidobacterium breve* UCC2003. *Appl. Environ. Microbiol.* 78, 7032–7041. doi: 10.1128/aem.01776-12

Argnani, A., Leer, R. J., van Luijk, N., and Pouwels, P. H. (1996). A convenient and reproducible method to genetically transform bacteria of the genus *Bifidobacterium*. *Microbiology* 142(Pt 1), 109–114. doi: 10.1099/13500872-142-1-109

Bottacini, F., Morrissey, R., Esteban-Torres, M., James, K., van Breen, J., Dikareva, E., et al. (2018a). Comparative genomics and genotype-phenotype associations in *Bifidobacterium breve*. *Sci. Rep.* 8:10633. doi: 10.1038/s41598-018-28919-4

Bottacini, F., Morrissey, R., Roberts, R. J., James, K., van Breen, J., Egan, M., et al. (2018b). Comparative genome and methylome analysis reveals restriction/modification system diversity in the gut commensal *Bifidobacterium breve*. *Nucleic Acids Res.* 46, 1860–1877. doi: 10.1093/nar/gkx1289

Bottacini, F., O'Connell Motherway, M., Kuczynski, J., O'Connell, K. J., Serafini, F., Duranti, S., et al. (2014). Comparative genomics of the *Bifidobacterium breve* taxon. *BMC Genomics* 15:170. doi: 10.1186/1471-2164-15-170

Bottacini, F., Zomer, A., Milani, C., Ferrario, C., Lugli, G. A., Egan, M., et al. (2017). Global transcriptional landscape and promoter mapping of the gut commensal *Bifidobacterium breve* UCC2003. *BMC Genomics* 18:991. doi: 10.1186/s12864-017-4387-x

Brancaccio, V. F., Zhurina, D. S., and Riedel, C. U. (2013). Tough nuts to crack: site-directed mutagenesis of bifidobacteria remains a challenge. *Bioengineered* 4, 197–202. doi: 10.4161/bioe.23381

Carver, T., Harris, S. R., Berriman, M., Parkhill, J., and McQuillan, J. A. (2012). Artemis: an integrated platform for visualization and analysis of high-throughput sequence-based experimental data. *Bioinformatics* 28, 464–469. doi: 10.1093/bioinformatics/btr703

Darst, R. P., Pardo, C. E., Ai, L., Brown, K. D., and Kladde, M. P. (2010). Bisulfite sequencing of DNA. *Curr. Protoc. Mol. Biol.* Chapter 7, Unit–7.9.17. doi: 10.1002/0471142727.mb0709s91

De Vos, W. M. (1987). Gene cloning and expression in lactic streptococci. *FEMS Microbiol. Rev.* 3, 281–295. doi: 10.1111/j.1574-6968.1987.tb02466.x

Egan, M., Motherway, M. O. C., Kilcoyne, M., Kane, M., Joshi, L., Ventura, M., et al. (2014). Cross-feeding by *Bifidobacterium breve* UCC2003 during co-cultivation with *Bifidobacterium bifidum* PRL2010 in a mucin-based medium. *BMC Microbiol.* 14:282. doi: 10.1186/s12866-014-0282-7

Fanning, S., Hall, L. J., Cronin, M., Zomer, A., MacSharry, J., Goulding, D., et al. (2012). Bifidobacterial surface-exopolysaccharide facilitates commensal-host interaction through immune modulation and pathogen protection. *Proc. Natl. Acad. Sci. U.S.A.* 109, 2108–2113. doi: 10.1073/pnas.1115621109

Flórez, A. B., Ammor, M. S., Alvarez-Martín, P., Margolles, A., and Mayo, B. (2006). Molecular analysis of tet(W) gene-mediated tetracycline resistance in dominant intestinal *Bifidobacterium* species from healthy humans. *Appl. Environ. Microbiol.* 72, 7377–7379. doi: 10.1128/AEM.00486-06

Fukiya, S., Suzuki, T., Kano, Y., and Yokota, A. (2010). "Current status of *Bifidobacterium* gene manipulation technologies," in *Current Status of Bifidobacterium gene Manipulation Technologies*, eds K. Sonomoto and A. Yokota (Norfolk: Horizon Scientific Press), 33–51.

Hidalgo-Cantabrana, C., Sánchez, B., Álvarez-Martín, P., López, P., Martínez-Álvarez, N., Delley, M., et al. (2015). A single mutation in the gene responsible for the mucoid phenotype of *Bifidobacterium animalis* subsp. *lactis* confers surface and functional characteristics. *Appl. Environ. Microbiol.* 81, 7960–7968. doi: 10.1128/AEM.02095-15

Hirayama, Y., Sakanaka, M., Fukuma, H., Murayama, H., Kano, Y., Fukiya, S., et al. (2012). Development of a double-crossover markerless gene deletion system in *Bifidobacterium longum*: functional analysis of the alpha-galactosidase gene for raffinose assimilation. *Appl. Environ. Microbiol.* 78, 4984–4994. doi: 10.1128/aem.00588-12

Law, J., Buist, G., Haandrikman, A., Kok, J., Venema, G., and Leenhouts, K. (1995). A system to generate chromosomal mutations in *Lactococcus lactis* which allows fast analysis of targeted genes. *J. Bacteriol.* 177, 7011–7018. doi: 10.1128/jb.177.24.7011-7018.1995

Lee, J. H., and O'Sullivan, D. J. (2010). Genomic insights into bifidobacteria. *Microbiol. Mol. Biol. Rev.* 74, 378–416. doi: 10.1128/mmbr.00004-10

Leenhouts, K., Buist, G., Bolhuis, A., ten Berge, A., Kiel, J., Mierau, I., et al. (1996). A general system for generating unlabelled gene replacements in bacterial chromosomes. *Mol. Gen. Genet.* 253, 217–224. doi: 10.1007/s004380050315

Mayo, B., van Sinderen, D., and Ventura, M. (2008). Genome analysis of food grade lactic Acid-producing bacteria: from basics to applications. *Curr. Genomics* 9, 169–183. doi: 10.2174/138920208784340731

McGrath, S., Fitzgerald, G. F., and van Sinderen, D. (2001). Improvement and optimization of two engineered phage resistance mechanisms in *Lactococcus lactis*. *Appl. Environ. Microbiol.* 67, 608–616. doi: 10.1128/aem.67.2.608-616.2001

Missich, R., Sgorbati, B., and LeBlanc, D. J. (1994). Transformation of *Bifidobacterium longum* with pRM2, a constructed *Escherichia coli-B. longum* shuttle vector. *Plasmid* 32, 208–211. doi: 10.1006/plas.1994.1056

O'Callaghan, A., Bottacini, F., O'Connell Motherway, M., and van Sinderen, D. (2015). Pangenome analysis of *Bifidobacterium longum* and site-directed mutagenesis through by-pass of restriction-modification systems. *BMC Genomics* 16:832. doi: 10.1186/s12864-015-1968-4

O'Callaghan, A., and van Sinderen, D. (2016). Bifidobacteria and their role as members of the human gut microbiota. *Front. Microbiol.* 7:925. doi: 10.3389/fmicb.2016.00925

O'Connell, K. J., Motherway, M. O. C., Hennessey, A. A., Brodhun, F., Ross, R. P., Feussner, I., et al. (2013a). Identification and characterization of an oleate hydratase-encoding gene from *Bifidobacterium breve*. *Bioengineered* 4, 313–321. doi: 10.4161/bioe.24159

O'Connell, K. J., O'Connell Motherway, M., O'Callaghan, J., Fitzgerald, G. F., Ross, R. P., Ventura, M., et al. (2013b). Metabolism of four α-glycosidic linkage-containing oligosaccharides by *Bifidobacterium breve* UCC2003. *Appl. Environ. Microbiol.* 79, 6280–6292. doi: 10.1128/AEM.01775-13

O'Connell Motherway, M., O'Driscoll, J., Fitzgerald, G. F., and Van Sinderen, D. (2009). Overcoming the restriction barrier to plasmid transformation and targeted mutagenesis in *Bifidobacterium breve* UCC2003. *Microb. Biotechnol.* 2, 321–332. doi: 10.1111/j.1751-7915.2008.00071.x

O'Hara, A. M., and Shanahan, F. (2007). Mechanisms of action of probiotics in intestinal diseases. *Sci. World J.* 7, 31–46. doi: 10.1100/tsw.2007.26

O'Mahony, L., McCarthy, J., Kelly, P., Hurley, G., Luo, F., Chen, K., et al. (2005). *Lactobacillus* and *Bifidobacterium* in irritable bowel syndrome: symptom responses and relationship to cytokine profiles. *Gastroenterology* 128, 541–551. doi: 10.1053/j.gastro.2004.11.050

O'Connell Motherway, M., Watson, D., Bottacini, F., Clark, T. A., Roberts, R. J., Korlach, J., et al. (2014). Identification of restriction-modification systems of *Bifidobacterium animalis* subsp. *lactis* CNCM I-2494 by SMRT sequencing and associated methylome analysis. *PLoS One* 9:e94875. doi: 10.1371/journal.pone.0094875

Park, M. J., Park, M. S., and Ji, G. E. (2018). Improvement of electroporation-mediated transformation efficiency for a *Bifidobacterium* strain to a reproducibly high level. *J. Microbiol. Methods* 159, 112–119. doi: 10.1016/j.mimet.2018.11.019

Platteeuw, C., Simons, G., and de Vos, W. M. (1994). Use of the *Escherichia coli* beta-glucuronidase (*gusA*) gene as a reporter gene for analyzing promoters in lactic acid bacteria. *Appl. Environ. Microbiol.* 60:587. doi: 10.1128/aem.60.2.587-593.1994

Sakaguchi, K., He, J., Tani, S., Kano, Y., and Suzuki, T. (2012). A targeted gene knockout method using a newly constructed temperature-sensitive plasmid mediated homologous recombination in *Bifidobacterium longum*. *Appl. Microbiol. Biotechnol.* 95, 499–509. doi: 10.1007/s00253-012-4090-4

Shkoporov, A. N., Efimov, B. A., Khokhlova, E. V., Steele, J. L., Kafarskaia, L. I., and Smeianov, V. V. (2008). Characterization of plasmids from human infant *Bifidobacterium* strains: sequence analysis and construction of *E. coli-Bifidobacterium* shuttle vectors. *Plasmid* 60, 136–148. doi: 10.1016/j.plasmid.2008.06.005

Tojo, R., Suárez, A., Clemente, M. G., de los Reyes-Gavilán, C. G., Margolles, A., Gueimonde, M., et al. (2014). Intestinal microbiota in health and disease: role of bifidobacteria in gut homeostasis. *World J. Gastroenterol.* 20, 15163–15176. doi: 10.3748/wjg.v20.i41.15163

Turroni, F., Milani, C., Duranti, S., Ferrario, C., Lugli, G. A., Mancabelli, L., et al. (2018). Bifidobacteria and the infant gut: an example of co-evolution and natural selection. *Cell. Mol. Life Sci.* 75, 103–118. doi: 10.1007/s00018-017-2672-0

van der Vossen, J. M., van der Lelie, D., and Venema, G. (1987). Isolation and characterization of *Streptococcus cremoris* Wg2-specific promoters. *Appl. Environ. Microbiol.* 53, 2452–2457. doi: 10.1128/aem.53.10.2452-2457.1987

van Pijkeren, J.-P., and Britton, R. A. (2012). High efficiency recombineering in lactic acid bacteria. *Nucleic Acids Res.* 40:e76. doi: 10.1093/nar/gks147

Wei, X., Guo, Y., Shao, C., Sun, Z., Zhurina, D., Liu, D., et al. (2012). Fructose uptake in *Bifidobacterium longum* NCC2705 is mediated by an ATP-binding cassette transporter. *J. Biol. Chem.* 287, 357–367. doi: 10.1074/jbc.M111.266213

Wong, C. B., Odamaki, T., and Xiao, J.-z (2019). Beneficial effects of *Bifidobacterium longum* subsp. *longum* BB536 on human health: modulation of gut microbiome as the principal action. *J. Funct. Foods* 54, 506–519. doi: 10.1016/j.jff.2019.02.002

Yasui, K., Kano, Y., Tanaka, K., Watanabe, K., Shimizu-Kadota, M., Yoshikawa, H., et al. (2009). Improvement of bacterial transformation efficiency using plasmid artificial modification. *Nucleic Acids Res.* 37:e3. doi: 10.1093/nar/gkn884

Zuo, F., Zeng, Z., Hammarstrom, L., and Marcotte, H. (2019). Inducible plasmid self-destruction (IPSD) assisted genome engineering in *Lactobacilli* and *Bifidobacteria*. *ACS Synth. Biol.* 8, 1723–1729. doi: 10.1021/acssynbio.9b00114

Conflict of Interest: The authors declare that the research was conducted in the absence of any commercial or financial relationships that could be construed as a potential conflict of interest.

frontiers in Microbiology

ORIGINAL RESEARCH
published: 07 April 2021
doi: 10.3389/fmicb.2021.610080

Colonization of Supplemented *Bifidobacterium breve* M-16V in Low Birth Weight Infants and Its Effects on Their Gut Microbiota Weeks Post-administration

Ayako Horigome[1†], Ken Hisata[2†], Toshitaka Odamaki[1], Noriyuki Iwabuchi[3], Jin-zhong Xiao[1] and Toshiaki Shimizu[2]*

[1] Next Generation Science Institute, Morinaga Milk Industry Co., Ltd., Kanagawa, Japan, [2] Department of Pediatrics, Juntendo University Faculty of Medicine, Tokyo, Japan, [3] Food Ingredients and Technology Institute, Morinaga Milk Industry Co., Ltd., Kanagawa, Japan

The colonization and persistence of probiotics introduced into the adult human gut appears to be limited. It is uncertain, however, whether probiotics can successfully colonize the intestinal tracts of full-term and premature infants. In this study, we investigated the colonization and the effect of oral supplementation with *Bifidobacterium breve* M-16V on the gut microbiota of low birth weight (LBW) infants. A total of 22 LBW infants (12 infants in the M-16V group and 10 infants in the control group) were enrolled. *B. breve* M-16V was administrated to LBW infants in the M-16V group from birth until hospital discharge. Fecal samples were collected from each subject at weeks (3.7–9.3 weeks in the M-16V group and 2.1–6.1 weeks in the control group) after discharge. qPCR analysis showed that the administrated strain was detected in 83.3% of fecal samples in the M-16V group (at $\log_{10}$ 8.33 ± 0.99 cell numbers per gram of wet feces), suggesting that this strain colonized most of the infants beyond several weeks post-administration. Fecal microbiota analysis by 16S rRNA gene sequencing showed that the abundance of Actinobacteria was significantly higher ($P < 0.01$), whereas that of Proteobacteria was significantly lower ($P < 0.001$) in the M-16V group as compared with the control group. Notably, the levels of the administrated strain and indigenous *Bifidobacterium* bacteria were both significantly higher in the M-16V group than in the control group. Our findings suggest that oral administration of *B. breve* M-16V led to engraftment for at least several weeks post-administration and we observed a potential overall improvement in microbiota formation in the LBW infants' guts.

Keywords: low birth weight infants, gut microbiota, *Bifidobacterium breve* M-16V, probiotics, colonization

OPEN ACCESS

Edited by:
María Esteban-Torres, University College Cork, Ireland

Reviewed by:
Angelica Thomaz Vieira, Federal University of Minas Gerais, Brazil
Marie-Jose Butel, Université de Paris, France

***Correspondence:**
Ayako Horigome
a-horigome@morinagamilk.co.jp

† These authors have contributed equally to this work

Specialty section:
This article was submitted to Microbial Symbioses, a section of the journal Frontiers in Microbiology

Received: *25 September 2020*
Accepted: *17 March 2021*
Published: *07 April 2021*

Citation:
Horigome A, Hisata K, Odamaki T, Iwabuchi N, Xiao J-z and Shimizu T (2021) Colonization of Supplemented Bifidobacterium breve M-16V in Low Birth Weight Infants and Its Effects on Their Gut Microbiota Weeks Post-administration. Front. Microbiol. 12:610080. doi: 10.3389/fmicb.2021.610080

INTRODUCTION

The gut microbiota in infancy plays many important roles underpinning healthy development and thereby impacts future health. Recent studies have indicated that there is a link between infant gut dysbiosis and an increased risk of developing acute and long-term inflammatory diseases in later life such as asthma (Arrieta et al., 2015, 2018; Zimmermann et al., 2019), type 1 diabetes (Kostic et al., 2015) and obesity (Cox et al., 2014). Low birth weight (LBW) preterm infants have important

differences in the composition of their intestinal microbiota when compared with full-term infants (Henderickx et al., 2019). These differences are related to immaturely-developed guts and receiving antibiotic treatments, as well as the neonatal intensive care hospital environment itself, which limits a preterm infant's contact with commensal bacteria (Henderickx et al., 2019). The typical gut microbiota of preterm infants is characterized by the presence of potentially pathogenic bacteria commonly found in the hospital environment, such as *Klebsiella, Escherichia*, *Staphylococcus*, and *Enterococcus* (Patel et al., 2016; Stewart et al., 2016). Another characteristic is the low abundance of *Bifidobacterium* (Dalby and Hall, 2020), which is the most common genus in the normal infant gut and is thought to play pivotal roles in maintaining infant health (Leahy et al., 2005; Di Gioia et al., 2014). Combined with the underdeveloped gut and immune system in premature infants, gut dysbiosis increases their susceptibility to conditions such as sepsis and necrotizing enterocolitis (NEC) (Neu and Pammi, 2017), the latter of which is the most common and lethal gastrointestinal emergency for them. Therefore, early intervention to improve gut dysbiosis is essential for infants, especially premature ones.

Administration of probiotic *Bifidobacterium* strains is one potential approach for establishing normal gut microbiota in premature infants. Previous research studies have shown that supplementation with *Bifidobacterium* strains results in higher numbers of *Bifidobacterium* and the lower counts of *Enterobacteriaceae* in premature infants (Mohan et al., 2006; Ishizeki et al., 2013). *Bifidobacterium breve* M-16V is a probiotic strain originating from a healthy infant and has been incorporated into several products including infant formula (Wong et al., 2019). It has received GRAS status for foods including infant formula from the US Food and Drug Administration (GRAS No. 453–455). This strain has been shown to have gut microbiota modulating potential in infants and can protect against preterm- and infant-related diseases (Wong et al., 2019), although adequately powered, preferably cluster randomized controlled trials are needed to confirm these findings (Athalye-Jape et al., 2018). For example, a randomized, double-blind, placebo-controlled trial showed that *B. breve* M-16V supplementation for three weeks resulted in a significantly higher abundance of *B. breve* in the feces of preterm infants, unlike the placebo control group that had *B. breve* counts below the detection level (Patole et al., 2014). It was also reported that daily supplementation with *B. breve* M-16V decreased the incidence of NEC in very low birth weight neonates with a birth gestational age less than 34 weeks (Patole et al., 2016). The study was a retrospective cohort study involving 835 preterm neonates as historical controls and 920 preterm neonates receiving this strain. An experimental rat NEC model supported the preventive effect of *B. breve* M-16V administration on NEC and revealed that the mechanism involved modulation of Toll-like receptor expression and inflammatory response suppression (Satoh et al., 2016). To date, *B. breve* M-16V has been used to reduce the risk of preterm birth complications with LBW infants in more than 120 neonatal intensive care units (NICUs) in affiliated hospitals in Japan, Australia, New Zealand and Singapore (Umezaki et al., 2010; Patole et al., 2014, 2016; Athalye-Jape et al., 2018). As mentioned above, although live cells of *B. breve* M-16V have been confirmed to have effects on gut microbiota and infant health, little information exists about colonization of this strain in the gut and whether colonization following probiotic supplementation has a prolonged effect on gut microbiota.

Therefore, in the present study, we administered *B. breve* M-16V to LBW infants (gestation $\leq$ 37 weeks) admitted to NICU from birth to hospital discharge and followed up these patients for several weeks after discharge. We observed that *B. breve* M-16V colonized in the gut and contributed to a potential improvement of the gut microbiota composition in the LBW infants at least for several weeks post-administration.

MATERIALS AND METHODS

Subjects and Sample Collection

This study was reviewed and approved by the Ethics Committee of Juntendo University Hospital, Japan, and written informed parental consent was obtained. The outline of study schedule for each subject is shown in **Figure 1**. A total of 22 infants with gestational ages $\leq$37 weeks and birth weights <2,000 gram who were admitted to the NICU of the Juntendo University Urayasu Hospital (control group, n = 10) or the Juntendo University Hospital (M-16V group, n = 12) from March 2012 to February 2017 were enrolled. After birth, infants in the M-16V group were daily administrated a freeze-dried preparation of *B. breve* M-16V (dose, 1×10^9 CFU dissolved in 4 mL of sterile water) just before feeding. The probiotic administration was continued until hospital discharge. Infants in the control group were not administrated any probiotic supplement. At 2–9 weeks after hospital discharge, fresh fecal samples were collected from each subject's diaper to a tube. The fecal samples collected were stored below −18°C until delivery to the laboratory. Immediately upon receipt, the fecal samples were stored at −80°C until further analysis. Details of the study schedule for each subject is shown in **Supplementary Table 1**.

Fecal DNA Preparation and Microbiota Analysis

DNA was extracted from the fecal samples as previously described (Sugahara et al., 2015). Purified DNA was suspended in 2,000 μl of Tris-EDTA buffer (pH 8.0).

PCR amplification and DNA sequencing of the V3–V4 region of the bacterial 16S rRNA gene was performed on the Illumina MiSeq instrument (Illumina, San Diego, CA, United States) as previously described (Odamaki et al., 2016). After removing the sequences consistent with the data from the Genome Reference Consortium human build 38 (GRCh38) and the phiX reads from the raw Illumina paired-end reads, the sequences were analyzed using the QIIME2 software package (version 2017.10)[1]. Potential chimeric sequences were removed using DADA2 (Callahan et al., 2016), and 30 and 90 bases were trimmed from the 3′ region of the forward and the reverse reads, respectively. Taxonomical classification was performed using the Naive Bayes classifier

[1]https://qiime2.org/

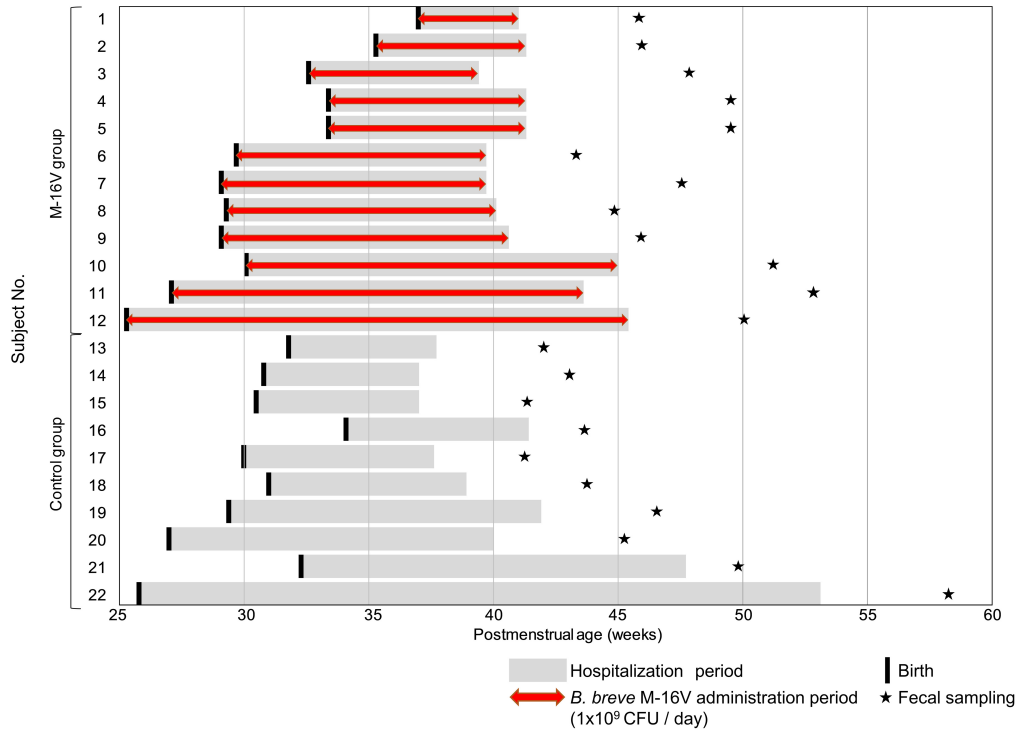

FIGURE 1 | Outline of study schedule for each subject across postmenstrual age.

trained on the Greengenes13.8 dataset with a 99% sequence similarity threshold for full-length Operational Taxonomic Units.

Quantitative PCR (qPCR)

The fecal DNAs as described above were applied for qPCR which was performed on the ABI PRISM 7500 Fast Real-Time PCR system (Thermo Fisher Scientific K.K., Uppsala, Sweden) with SYBR Premix Ex Taq (TaKaRa Bio, Shiga, Japan) to quantitate the *Bifidobacterium* species and strains. The primer sets used are shown in **Supplementary Table 2**. The primers specific for *Bifidobacterium longum*, *Bifidobacterium catenulatum,* and *Bifidobacterium adolescentis* groups have been described previously (Matsuki et al., 1998, 2004). The *B. breve* M-16V-specific primer set was designed using Primer 3 software (v.0.4.0) (Untergasser et al., 2012) after identifying unique regions in this strain by multiple sequences alignments of the complete genome sequences of *B. breve* M-16V and publically available genomes of *B. breve* strains. We confirmed the specificity of this specific primer set using other 37 *B. breve* strains in Morinaga Culture Collection.

PCR amplification was performed using the program previously described (Kato et al., 2017) with the exception of *B. breve* M-16V, whose detection consisted of an amplification program of one cycle at 95°C for 20 s, 40 cycles at 95°C for 3 s and 60°C for 30 s, and one final cycle at 95°C for 15 s. The following *Bifidobacterium* strains were used as the standards for species/strain-specific quantification: *B. breve* JCM1192^T, *B. longum* subsp. *longum* JCM1217^T, *Bifidobacterium bifidum* JCM1255^T, *Bifidobacterium pseudocatenulatum* JCM1200^T, *B. adolescentis* JCM1275^T, and *B. breve* M-16V.

Statistical Analysis

Statistical analyses were performed using EZR software ver. 1.50 (Kanda, 2013) or R software ver. 3.6.0. Intergroup differences were analyzed using the unpaired Student's *t*-test or Welch's *t*-test, and the Mann-Whitney *U*-test, for parametric and non-parametric data, respectively. Fisher's exact test or χ^2 test was conducted for categorical data. The cell number calculations for *Bifidobacterium* species or strains were substituted by $\log_{10}$ 6 per gram of wet feces for samples that fell below the detection limits. Differences in the gut microbiota profiles between the control and M-16V groups were analyzed by principal coordinate analysis (PCoA). A permutational multivariate analysis of variance (PERMANOVA) test for UniFrac distances was used for multivariate analysis to test the variation in microbiota composition explained by each factor. Associations between relative abundance of Actinobacteria or Proteobacteria and subject's characteristics were assessed by Spearman's rank correlation test. For all statements, $P < 0.05$ were considered to be statistically significant.

Data Availability

DNA sequences corresponding to the 16S rRNA gene data have been deposited in the DNA Data Bank of Japan (DDBJ) under accession number DRA010463.

RESULTS

General Characteristics of the Subjects

Altogether, 22 infants (10 in the control group and 12 in the M-16V group) were enrolled in this study. **Table 1** shows the characteristics of the subjects. There was no significant difference in the maternal features between the groups. As neonatal features, infants were matched for gender, gestational age and breast-feeding rate, and the hospitalization period/supplementation duration, postnatal age, and corrected age at the fecal sampling were comparable between the two groups. However, birth weight and discharge weight were significantly higher in the M-16V group than in the control group. The period from hospital discharge to fecal sampling was significantly longer in the M-16V group than in the control group.

TABLE 1 | Characteristics of the subjects.

	M-16V group (*n* = 12)	Control group (*n* = 10)	*P*-value
Maternal features			
Age (years)	34.0 ± 4.0	31.3 ± 3.3	0.100
C-section (*n*, %)	8 (66.7)	9 (90)	0.323
Antibiotics during labor (*n*, %)	10 (83.3)	9 (90)	1.000
GBS test (*n*, %)			
Positive	1 (8.3)	1 (10)	1.000
Negative	8 (66.7)	7 (70)	
Not done	3 (25)	2 (20)	
Neonatal features			
Gestational age (weeks)	31.0 ± 3.4	30.3 ± 2.4	0.613
Birth weight (g)	1350.5 ± 250.1	1096.3 ± 254.7	0.029*
Discharged weight (g)	3430.3 ± 926.1	2630.0 ± 451.1	0.017*
Male (*n*, %)	7 (58.3)	3 (30)	0.369
Chronic lung disease	1 (8.3)	1 (10)	1.000
Antibiotics exposure (*n*, %)	5 (41.7)	3 (30)	0.675
Treatment for PDA			
Clipping (*n*, %)	1 (8.3)	1 (10)	0.814
Indomethacin (*n*, %)	3 (25)	4 (40)	
Supplementation duration/hospitalization period (weeks)	10.6 ± 4.6	10.9 ± 6.6	0.887
Breast-feeding (%)†	54.2 ± 39.6	45.0 ± 23.0	0.526
Fecal sampling (weeks after discharge)	6.4 ± 1.9	4.3 ± 1.3	0.009**
Postnatal age at the fecal sampling (weeks)	17.0 ± 5.0	15.3 ± 6.8	0.509
Corrected age at the fecal sampling (weeks)	7.9 ± 2.8	5.5 ± 5.2	0.184

*Measured variable data are expressed as the mean ± SD. Intergroup differences were analyzed using the χ^2-test or Fisher's exact test for categorical data and the unpaired Student's t-test or Welch's t-test for measured variables.*P < 0.05; **P < 0.01.*

†*Percentage of breast milk among the total nutrition (breast milk + infant formula), as surveyed by questionnaire. GBS, Group B Streptococcus; PDA, patent ductus arteriosus.*

Effect of *B. breve* M-16V Administration on the Gut Microbiota of the Infants

To evaluate the effect of administering probiotics during early life on the composition of fecal microbiota, we collected fecal samples 3–9 weeks after their administration. No significant difference in the alpha diversity of the microbiota was observed between the groups (**Supplementary Table 3**). PCoA of the fecal microbiota based on the weighted UniFrac distance indicated that *B. breve* M-16V administration had an impact on the composition of the fecal microbiota (**Figure 2**). PERMANOVA testing revealed a significant difference in the gut microbiota profiles of the M-16V and control groups. As shown in **Table 2** and **Figure 3**, the dominant phylum identified in the M-16V group was Actinobacteria (74%), followed by Firmicutes (19.9%). In contrast, the gut microbiota from the control group showed a higher abundance of Proteobacteria (22.7%) than that of the M-16V group (3%). The relative abundance of Actinobacteria was significantly higher, whereas that of Proteobacteria was significantly lower in the M-16V group than in the control group. At the genus level, the relative abundances of *Bifidobacterium* and *Enterococcus* were significantly higher, whereas those of *Rothia*, *Lactococcus,* and *Klebsiella* were significantly lower in the M-16V group than in the control group.

TABLE 2 | Fecal microbiota composition.

	Median (IQRs) %		*P*-value
	M-16V group (*n* = 12)	Control group (*n* = 10)	
Phylum			
Actinobacteria	74.0 (61.9–79.8)	33.3 (3.0–64.9)	0.009**
Bacteroidetes	0.0 (0.0–0.3)	0.2 (0.1–0.3)	0.132
Firmicutes	19.9 (17.5–30.7)	31.9 (15.7–48.6)	0.628
Proteobacteria	3.0 (0.6–5.4)	22.7 (14–46.7)	0.000**
Genus			
Bifidobacterium	73.44 (60.96–78.87)	32.19 (2.56–64.28)	0.011*
*Clostridiaceae |g_*	0.08 (0.00–0.37)	0.30 (0.16–0.34)	0.366
Clostridiales |__|__	0.29 (0.04–0.89)	0.15 (0.05–0.25)	0.531
Clostridium	0.13 (0.00–0.64)	0.29 (0.00–0.75)	0.707
Enterococcus	11.60 (8.91–18.74)	1.90 (1.26–5.90)	0.011*
Escherichia	0.44 (0.00–2.99)	5.97 (0.63–9.91)	0.115
Klebsiella	0.22 (0.00–1.99)	7.22 (1.59–22.38)	0.015*
Lactobacillus	0.29 (0.08–1.03)	0.68 (0.35–0.91)	0.373
Lactococcus	0.00 (0.00–0.16)	0.19 (0.08–0.56)	0.044*
Parabacteroides	0.00 (0.00–0.13)	0.12 (0.07–0.20)	0.120
Rothia	0.02 (0.00–0.07)	0.24 (0.11–0.28)	0.017*
Staphylococcus	0.31 (0.08–0.59)	0.40 (0.04–1.36)	0.765
Streptococcus	2.57 (1.34–6.41)	7.61 (3.60–35.26)	0.050
Turicibacter	0.18 (0.05–0.43)	0.30 (0.15–0.40)	0.597
Veillonella	0.03 (0.00–0.18)	0.36 (0.00–0.84)	0.283

*Data are expressed as the medians (IQRs) of the taxa with a median relative abundance of >0.1% in at least one group. Intergroup differences were analyzed using the Mann-Whitney U-test. *P < 0.05; **P < 0.01. IQRs, interquartile range.*

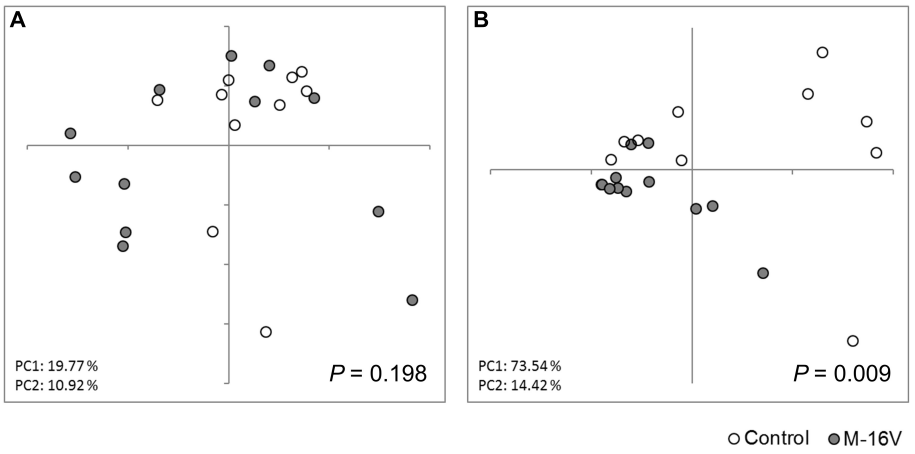

FIGURE 2 | Gut microbiota profiles by PCoA. **(A)** Unweighted and **(B)** weighted UniFrac PCoA of the fecal microbiota obtained from subjects in the control group (n = 10) and the M-16V group (n = 12). Intergroup differences were analyzed using PERMANOVA.

We investigated the influence of factors such as gestational age and birth/discharge weight on the intestinal microbiota. There were significant correlations between the relative abundance of Actinobacteria/Proteobacteria, which were the major differences between the two groups, and some factors including birth weight and others (**Supplementary Figures 1, 2**). In addition, we found that factors such as gestational age and birth/discharge weight contributed a small proportion of variance, and oral administration of *B. breve* M-16V was the only significant variable explaining variance in the infant microbiota composition, by the PERMANOVA multivariate analysis using a weighted UniFrac matrix (**Table 3**).

Quantitative PCR Detection of Bifidobacterium Species

Because the abundance difference in *Bifidobacterium* between the groups was the most remarkable, we investigated the bifidobacteria composition at the species level in addition to analyzing the *B. breve* M-16V abundance by qPCR. Notably, *B. breve* M-16V was detected in the fecal samples from all subjects in the M-16V group except for two infants (Subject Nos. 9 and 10 in **Figure 3**), suggesting that this strain colonized a subset of infants for at least several weeks after discontinuing the probiotics. The cell numbers for *Bifidobacterium* spp., *B. breve,* the *B. longum* group, and the *B. catenulatum* group were significantly higher in the M-16V group than in the control group (**Figure 4**).

DISCUSSION

Probiotics supplementation is a promising approach to improve dysbiosis and prevent gut microbiota-associated diseases in LBW infants. However, it is unclear whether the microbial components in probiotic treatments can persist in the gut during early life, although some studies indicated the potential for some probiotics (Frese et al., 2017; Alcon-Giner et al., 2020; Yousuf et al., 2020) as described below. This study found the colonization of *B. breve* M-16V in the intestinal tract of most LBW infants for at least several weeks following cessation of its administration as a probiotic. It has been reported that the persistence of introduced probiotics in the adult gut is limited. Most probiotic strains were only detectable for less than two weeks after the administration period despite their high detection rates in the gastrointestinal tract during probiotic treatment (Alander et al., 2001; Frese et al., 2012; Charbonneau et al., 2013). One notable study suggested a possible probiotic colonization in 30% of the adult subjects for up to 6 months after administration (Maldonado-Gómez et al., 2016). In contrast with adults, whose gut microbiota remains relatively stable (Faith et al., 2013), the composition of the gut microbiota in infants reportedly shows great shifts up to 2–4 years old when it reaches a more stable and mature composition (Voreades et al., 2014; Odamaki et al., 2016; Stewart et al., 2018). Furthermore, the microbiota composition is more immature and less stable in premature infants than full-term infants (Gritz and Bhandari, 2015; Henderickx et al., 2019). This instability of the gut microbiota in addition to the low abundance of *Bifidobacterium* potentially provided a niche opportunity for oral administration of bifidobacteria probiotic strains such as *B. breve* M-16V in LBW infants.

Another reason for the high colonization of *B. breve* M-16V might arise from the species-specific property. Bifidobacteria display a difference in their ecological adaptation among species and show genotypic and physiological differences related to their different residential origin. Bifidobacterial species of human origin are grouped as human-residential bifidobacteria (HRB) (Odamaki et al., 2015; Wong et al., 2018). Among HRB, *B. breve*, *B. longum* subsp. *infantis*, *B. longum* subsp. *longum*, and *B. bifidum*, which are prevalently isolated from the infant's intestine, are referred to as infant-type HRB. Unlike non-HRB such as *Bifidobacterium animalis* subsp. *lactis* and *Bifidobacterium thermophilum*, infant-type HRB have been reported to possess high ability to assimilate human milk

FIGURE 3 | Fecal microbiota composition of each subject. Relative abundance of each phylum (upper) and genus (lower) of microbiota of each subject. The four phyla and 15 genera indicated in **Table 2** were shown. In the middle of the figures, hospitalization period (that is, probiotic administration duration in the M-16V group), postnatal and corrected age at the fecal sampling scaled by red color were indicated. The darker the red color, the higher the value of administration duration/hospitalization period, postnatal age, and corrected age, respectively. Subject No. 1–12 were in the M-16V group, and subject No. 13–22 were in the control group.

oligosaccharides (HMOs) and undergo specific adaptation to the infant host (Wong et al., 2018). Indeed, Underwood et al. (2013) showed that *B. longum* subsp. *infantis* colonization was better than *B. animalis* subsp. *lactis* colonization in both formula-fed and human milk-fed premature infants. In human milk-fed infants, greater increases in fecal *Bifidobacterium* and decreases in γ-Proteobacteria followed the administration of *B. longum* subsp. *infantis* than that of *B. animalis* subsp. *lactis* (Underwood et al., 2013). Another study confirmed that *B. breve* or *B. longum* subsp. *infantis* were early colonizers apparently independent of early life-events, such as mode of delivery and type of feeding, while the colonization of *B. animalis* subsp. *lactis* was dependent solely on the type of feeding (Martin et al., 2016). The authors suggested that the frequent colonization by *B. animalis* subsp. *lactis* in infants exposed to formula feeding may result from the use of formula supplemented with probiotic strains belonging to this subspecies. These findings suggest that infant-type HRB are more effective colonizers of the infant gut. Consistent with this finding, it was shown the persistent colonization of probiotic strains of *B. longum*, *B. bifidum,* and *B. breve* up to 5 months after supplementation of commercially probiotics containing these *Bifidobacterium* strains and *Lactobacillus rhamnosus* strain in preterm infants (Yousuf et al., 2020). Another study also indicated that the administration of *B. longum* subsp. *infants* resulted in a colonization period of at least a month in the breast-fed infant gut (Frese et al., 2017). The authors postulated that the colonization of this strain was attributed to the ancient adaptations of *B. longum* subsp. *infantis* to HMOs; that is, the capacity to transport these substances into this bacterium's

TABLE 3 | Multivariate analysis using PERMANOVA to test the variation in microbiota composition explained by each factor.

Variable	R^2	*P*-value
Treatment (M-16V or Control)	0.238	0.009**
Gestational age (<30 or ≥ 30 weeks)	0.035	0.459
Birth weight (<1,200 or ≥1,200 g)	0.076	0.183
Discharge weight (<3,000 or ≥3,000 g)	0.036	0.444
Hospitalization period (<10 or ≥10 weeks)	0.029	0.527
Postnatal age at the fecal sampling (<16 or ≥ 16 weeks)	0.026	0.565
Corrected age at the fecal sampling (<7 or ≥7 weeks)	0.016	0.746
Fecal sampling (<5 or ≥5 weeks after discharge)	0.019	0.692
Residuals	0.524	
Total	1.000	

The PERMANOVA multivariate analysis was performed using a weighted UniFrac matrix.
***P < 0.01.*

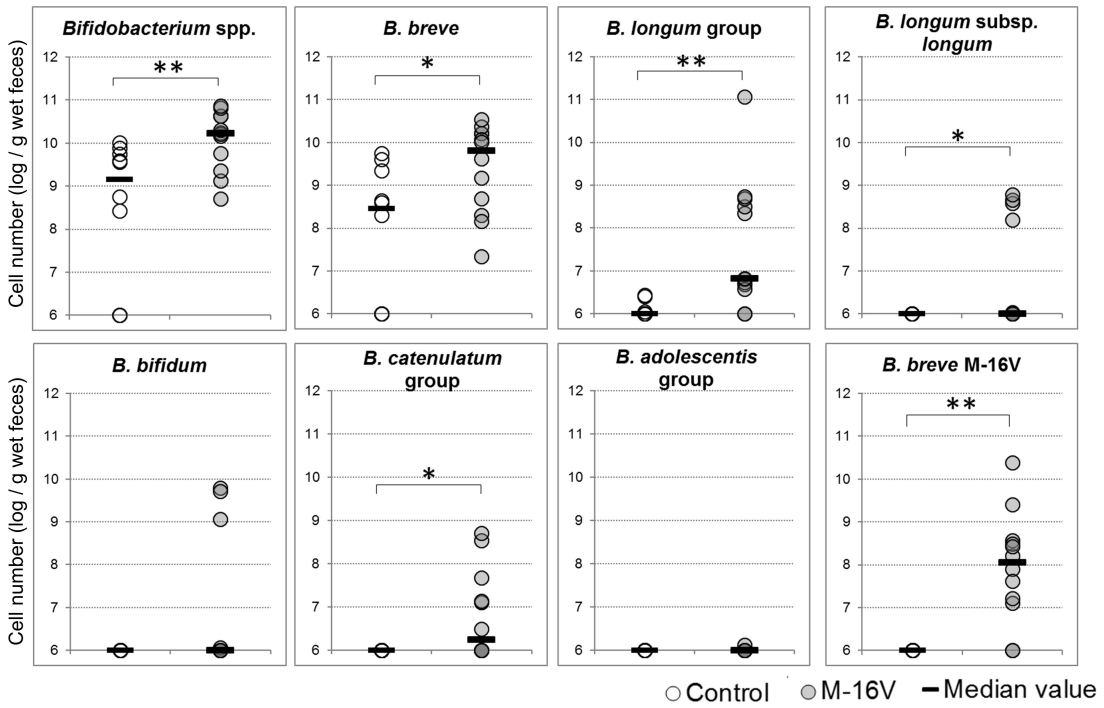

FIGURE 4 | Quantitative PCR detection of *Bifidobacterium* species and *B. breve* M-16V. Cell numbers were determined as the $\log_{10}$ of cells per gram wet weight in each fecal sample. The detection limit was below 10^6/g wet weight of feces. Intergroup differences were analyzed using the Mann-Whitney *U*-test. $^*P < 0.05$; $^{**}P < 0.01$.

cytoplasm and consume the full range of HMOs (Underwood et al., 2015). Through their study on probiotic supplementation of preterm infants (Alcon-Giner et al., 2020), suggested the ability of the probiotic *B. bifidum* strain to colonize the preterm infants' gut by showing its presence in two fecal samples collected at 41 and 50 days after supplementation. Noteworthy, genomic analysis of this strain showed the presence of genes involved in HMO utilization and mucin degradation which may aid the gut persistence (Alcon-Giner et al., 2020). In the present study, *B. breve* M-16V was detected in 83.3% of fecal samples from LBW infants in M-16V group at 3.7–9.3 weeks following its cessation of administration. Unfortunately, there were too few subjects to evaluate the influence of the infant feeding methods on the colonization of *B. breve* M-16V in this study; however, we noted that the two samples from the infants where *B. breve* M-16V was not detected were mixed-fed with breast milk and infant formula (data not shown). Further studies are needed to investigate the environmental factors that could affect the colonization of probiotics (e.g., whether or not the maternal genetic background related to HMO secretion or the feeding method affects colonization).

Recent studies have shown that the introduction of live microbes does not result in significant alterations of the fecal microbiota in healthy adults (Kim et al., 2013; Kristensen et al., 2016). Studies on infants are controversial with respect to this finding. Ishizeki et al. (2013) reported that the supplementation of single (*B. breve* M-16V) or multiple (*B. breve* M-16V, *B. longum* subsp. *infantis* M-63, and *B. longum* subsp. *longum* BB536) infant-type HRB strains to LBW infants resulted in the increase of the detection rate and number of *Bifidobacterium* in feces. Also, a study by Plummer et al. (2018) indicated that probiotic supplementation with *B. longum* subsp. *infantis* BB-02, *Streptococcus thermophilus* TH-4 and *B. animalis* subsp. *lactis* BB-12 from soon after birth increased the abundance of *Bifidobacterium* in the gut microbiota of very preterm infants during supplementation period. Furthermore, potential long-term contribution of probiotic strains on development of gut microbiota in preterm infants have been indicated by some researches (Alcon-Giner et al., 2020; Yousuf et al., 2020). On the other hand, a double-blind, randomized placebo-controlled intervention showed that intake of *Lactobacillus acidophilus* NCFM or *B. animalis* subsp. *lactis* Bi-07 to young children with atopic dermatitis for eight weeks did not affect the composition and diversity of the main bacterial populations in feces (Larsen et al., 2011). Similarly, no effect on the overall microbiota composition was observed when *Lactobacillus reuteri* DSM 17938 was administrated to breast-fed colicky infants for 21 days (Roos et al., 2013). We found that *B. breve* M-16V administration significantly impacted the overall microbiota composition beyond the non-administration period of 3.7–9.3 weeks. In the M-16V group, the relative abundance of Proteobacteria was significantly lower than in the control group. A sustained increase in Proteobacteria abundance is considered a signature of dysbiosis (Shin et al., 2015). Some reports have indicated an association between intestinal Proteobacteria and NEC in premature infants (Wang et al., 2009; Pammi et al.,

2017; Lindberg et al., 2020). Mirpuri et al. (2014) found that the IgA-dependent suppression of Proteobacteria in the infant gut was important for establishing a beneficial commensal population and reducing susceptibility to colonic injury and inflammation. At the genus level, the relative abundance of *Klebsiella*, which have been associated with neonatal bacterial infections (Podschun and Ullmann, 1998; Hornik et al., 2012) and NEC (Sim et al., 2015; Olm et al., 2019), were lower in the M-16V group than in the control group. Contrastingly, the relative abundance of *Bifidobacterium* was significantly higher in the M-16V group than in the control group. It has been reported that a higher abundance of *Bifidobacterium* in early infancy is associated with better immune system responses to vaccination, potentially enhancing immunological memory (Huda et al., 2019). Conversely, a lower abundance of *Bifidobacteriaceae*, which primarily includes the *Bifidobacterium* genus, is suggested to trigger the development of allergic sensitization, eczema, or asthma (Zimmermann et al., 2019).

Factors such as gestational age and birth weight have been reported to affect the developing gut microbiota in preterm neonates (Korpela et al., 2018; Henderickx et al., 2019; Alcon-Giner et al., 2020). Some factors including birth weight had significant correlations with the relative abundance of Actinobacteria/Proteobacteria. A part of these correlations might be due to the significant difference of the birth body weight between groups, and the close association among the birth weight, the gestational age, and the hospitalization period (**Supplementary Figure 3**). Our PERMANOVA multivariate analysis confirmed that the effect of the supplementation of *B. breve* M-16V on the gut microbiota was greater than that of other factors such as gestational age and birth weight.

Our qPCR analysis revealed that the cell numbers of the administrated strain and some of the indigenous bifidobacteria species were significantly higher in the M-16V group. It remains unclear as to why administering *B. breve* M-16V promoted the colonization of other bifidobacteria, but one possibility is that because acetic acid is the main metabolite it might suppress the growth of acid-sensitive bacteria such as Proteobacteria, thereby providing an appropriate environment for bifidobacteria growth. Overall, our findings suggest that *B. breve* M-16V administration can contribute to the establishment of a healthy gut microbiota composition in LBW infants.

There are several limitations in this study. First, this study is not a randomized controlled trial and included a small number of infants. Second, the birth weight and hospital discharge weight were significantly higher in the M-16V group than in the control group. Body weight is an important indicator of infant maturity and a key factor influencing the intestinal microbiota in neonates, that cannot be ignored especially in LBW infants. Third, the period from the discharge, that is, the cessation of probiotic administration in the M-16V group to the fecal sampling was significantly longer in the M-16V group than the control group, though the postnatal and the corrected age at sampling were not significantly different between the groups. Since the composition of the gut microbiota dramatically changes in the early life stage, the difference of the period from the hospital discharge to the fecal sampling could lead to the difference in the gut microbiota composition. However, it is assumed that the longer non-administration period in the M-16V group would not bring the overestimation of the colonization of *B. breve* M-16V in the infant's gut. Fourth, subjects in the two groups were from different hospitals, and the inclusion period lasted over 5 years. Such a long period might lead to change the hospital environment. The establishment of gut microbiota in very preterm infants is unstable and susceptible to the environment factors (Brooks et al., 2014) and the NICU practices (Rozé et al., 2020). Hence, a large-scale, double-blind, placebo-controlled study in the matched infants in the same facility with sequential fecal sampling from birth will be necessary to confirm the beneficial effects of *B. breve* M-16V that have been suggested in this study.

In conclusion, our results show that oral administration of *B. breve* M-16V leads to its colonization in the infant gut for at least several weeks after administration and potentially contributes to improved gut microbiota establishment. Further follow-up investigations will help to elucidate the durability of these effects through later childhood, and whether these effects carry implications for overall health later in life.

DATA AVAILABILITY STATEMENT

The datasets presented in this study can be found in online repositories. The names of the repository/repositories and accession number(s) can be found below: https://www.ddbj.nig.ac.jp/, DRA010463.

ETHICS STATEMENT

The studies involving human participants were reviewed and approved by the Ethics Committee of Juntendo University Hospital. Written informed consent to participate in this study was provided by the participants' legal guardian/next of kin.

AUTHOR CONTRIBUTIONS

J-ZX and TS conceived and designed the study. AH, NI, and KH performed the clinical trial and experiments. AH and TO analyzed the data and wrote the manuscript. TS supervised the overall study. All authors have read and approved the final manuscript.

ACKNOWLEDGMENTS

We thank Sachiko Takahashi, Eri Mitsuyama, and Nanami Hashikura for their technical support. We also thank Sandra Cheesman from Edanz Group (https://en-authorservices.edanzgroup.com/ac) for editing a draft of this manuscript.

SUPPLEMENTARY MATERIAL

The Supplementary Material for this article can be found online at: https://www.frontiersin.org/articles/10.3389/fmicb.2021.610080/full#supplementary-material

Supplementary Figure 1 | Relationship between Actinobacteria and subject's characteristics. Relationships between the relative abundance of Actinobacteria and the gestational age **(A)**, the birth weight **(B)**, the discharge weight **(C)**, the hospitalization/probiotic administration period **(D)**, the postnatal age at the fecal sampling **(E)**, the corrected age at the fecal sampling **(F)**, or the fecal sampling timing **(G)** in all subjects (black dashed line), the M-16V group (red circles and line), or the control group (blue circles and line). Associations were assessed by Spearman's rank correlation test. $^{*}P < 0.05$.

Supplementary Figure 2 | Relationship between Proteobacteria and subject's characteristics. Relationships between the relative abundance of Proteobacteria and the gestational age **(A)**, the birth weight **(B)**, the discharge weight **(C)**, the hospitalization/probiotic administration period **(D)**, the postnatal age at the fecal sampling **(E)**, the corrected age at the fecal sampling **(F)**, or the fecal sampling timing **(G)** in all subjects (black dashed line), the M-16V group (red circles and line), or the control group (blue circles and line). Associations were assessed by Spearman's rank correlation test. $^{*}P < 0.05$; $^{**}P < 0.01$.

Supplementary Figure 3 | Relationship between the birth weight, gestational age, and hospitalization. Relationships between the birth weight and gestational age **(A)**, the birth weight and the hospitalization period **(B)**, and the gestational age and the hospitalization period **(C)** in all subjects (black dashed line), the M-16V group (red circles and line), or the control group (blue circles and line). Associations were assessed by Spearman's rank correlation test. $^{*}P < 0.05$; $^{**}P < 0.01$.

Supplementary Table 1 | Study schedule for each subject.

Supplementary Table 2 | Quantitative PCR primer sets.

Supplementary Table 3 | Alpha-diversity of the gut microbiota.

REFERENCES

Alander, M., Mättö, J., Kneifel, W., Johansson, M., Kögler, B., Crittenden, R., et al. (2001). Effect of galacto-oligosaccharide supplementation on human faecal microflora and on survival and persistence of *Bifidobacterium lactis* Bb-12 in the gastrointestinal tract. *Int. Dairy J.* 11, 817–825. doi: 10.1016/S0958-6946(01)00100-5

Alcon-Giner, C., Dalby, M. J., Caim, S., Ketskemety, J., Shaw, A., Sim, K., et al. (2020). Microbiota supplementation with *Bifidobacterium* and *Lactobacillus* modifies the preterm infant gut microbiota and metabolome: an observational study. *Cell Rep. Med.* 1:100077. doi: 10.1016/j.xcrm.2020.100077

Arrieta, M. C., Arévalo, A., Stiemsma, L., Dimitriu, P., Chico, M. E., Loor, S., et al. (2018). Associations between infant fungal and bacterial dysbiosis and childhood atopic wheeze in a nonindustrialized setting. *J. Allergy Clin. Immunol.* 142, 424–434. doi: 10.1016/j.jaci.2017.08.041

Arrieta, M.-C., Stiemsma, L. T., Dimitriu, P. A., Thorson, L., Russell, S., Yurist-Doutsch, S., et al. (2015). Early infancy microbial and metabolic alterations affect risk of childhood asthma. *Sci. Transl. Med.* 7:307ra152. doi: 10.1126/scitranslmed.aab2271

Athalye-Jape, G., Rao, S., Simmer, K., and Patole, S. (2018). *Bifidobacterium breve* M-16V as a probiotic for preterm infants: a strain-specific systematic review. *J. Parenter. Enter. Nutr.* 42, 677–688. doi: 10.1177/0148607117722749

Brooks, B., Firek, B. A., Miller, C. S., Sharon, I., Thomas, B. C., Baker, R., et al. (2014). Microbes in the neonatal intensive care unit resemble those found in the gut of premature infants. *Microbiome* 2:1. doi: 10.1186/2049-2618-2-1

Callahan, B. J., McMurdie, P. J., Rosen, M. J., Han, A. W., Johnson, A. J. A., and Holmes, S. P. (2016). DADA2: high-resolution sample inference from Illumina amplicon data. *Nat. Methods* 13, 581–583. doi: 10.1038/nmeth.3869

Charbonneau, D., Gibb, R. D., and Quigley, E. M. M. (2013). Fecal excretion of *Bifidobacterium infantis* 35624 and changes in fecal microbiota after eight weeks of oral supplementation with encapsulated probiotic. *Gut Microbes* 4, 201–211. doi: 10.4161/gmic.24196

Cox, L. M., Yamanishi, S., Sohn, J., Alekseyenko, A. V., Leung, M., Cho, I., et al. (2014). Altering the intestinal microbiota during a critical developmental window has lasting metabolic consequences. *Cell* 158, 705–721. doi: 10.1016/j.cell.2014.05.052

Dalby, M. J., and Hall, L. J. (2020). Recent advances in understanding the neonatal microbiome. *F1000Research* 9:422. doi: 10.12688/f1000research.22355.1

Di Gioia, D., Aloisio, I., Mazzola, G., and Biavati, B. (2014). Bifidobacteria: their impact on gut microbiota composition and their applications as probiotics in infants. *Appl. Microbiol. Biotechnol.* 98, 563–577. doi: 10.1007/s00253-013-5405-9

Faith, J. J., Guruge, J. L., Charbonneau, M., Subramanian, S., Seedorf, H., Goodman, A. L., et al. (2013). The long-term stability of the human gut microbiota. *Science* 341:1237439. doi: 10.1126/science.1237439

Frese, S. A., Hutkins, R., and Walter, J. (2012). Comparison of the colonization ability of autochthonous and allochthonous strains of lactobacilli in the human gastrointestinal tract. *Adv. Microbiol.* 2, 399–409. doi: 10.4236/aim.2012.23051

Frese, S. A., Hutton, A. A., Contreras, L. N., Shaw, C. A., Palumbo, M. C., Casaburi, G., et al. (2017). Persistence of supplemented *Bifidobacterium longum* subsp. infantis EVC001 in breastfed infants. *mSphere* 2, e501–e517. doi: 10.1128/mSphere.00501-17

Gritz, E. C., and Bhandari, V. (2015). The human neonatal gut microbiome: a brief review. *Front. Pediatr.* 3:17. doi: 10.3389/fped.2015.00017

Henderickx, J. G. E., Zwittink, R. D., van Lingen, R. A., Knol, J., and Belzer, C. (2019). The preterm gut microbiota: an inconspicuous challenge in nutritional neonatal care. *Front. Cell. Infect. Microbiol.* 9:85. doi: 10.3389/fcimb.2019.00085

Hornik, C. P., Fort, P., Clark, R. H., Watt, K., Benjamin, D. K., Smith, P. B., et al. (2012). Early and late onset sepsis in very-low-birth-weight infants from a large group of neonatal intensive care units. *Early Hum. Dev.* 88, S69–S74. doi: 10.1016/S0378-3782(12)70019-1

Huda, M. N., Ahmad, S. M., Alam, M. J., Khanam, A., Kalanetra, K. M., Taft, D. H., et al. (2019). *Bifidobacterium* abundance in early infancy and vaccine response at 2 years of age. *Pediatrics* 143:e20181489. doi: 10.1542/peds.2018-1489

Ishizeki, S., Sugita, M., Takata, M., and Yaeshima, T. (2013). Effect of administration of bifidobacteria on intestinal microbiota in low-birth-weight infants and transition of administered bifidobacteria: a comparison between one-species and three-species administration. *Anaerobe* 23, 38–44. doi: 10.1016/j.anaerobe.2013.08.002

Kanda, Y. (2013). Investigation of the freely available easy-to-use software "EZR" for medical statistics. *Bone Marrow Transplant.* 48, 452–458. doi: 10.1038/bmt.2012.244

Kato, K., Odamaki, T., Mitsuyama, E., Sugahara, H., Xiao, J. Z., and Osawa, R. (2017). Age-related changes in the composition of gut *Bifidobacterium* species. *Curr. Microbiol.* 74, 987–995. doi: 10.1007/s00284-017-1272-4

Kim, S.-W., Suda, W., Kim, S., Oshima, K., Fukuda, S., Ohno, H., et al. (2013). Robustness of gut microbiota of healthy adults in response to probiotic intervention revealed by high-throughput pyrosequencing. *DNA Res.* 20, 241–253. doi: 10.1093/dnares/dst006

Korpela, K., Blakstad, E. W., Moltu, S. J., Strømmen, K., Nakstad, B., Rønnestad, A. E., et al. (2018). Intestinal microbiota development and gestational age in preterm neonates. *Sci. Rep.* 8:2453. doi: 10.1038/s41598-018-20827-x

Kostic, A. D., Gevers, D., Siljander, H., Vatanen, T., Peet, A., Tillmann, V., et al. (2015). The dynamics of the human infant gut microbiome in development and in progression towards type 1 diabetes. *Cell Host Microbe* 17, 260–273. doi: 10.1016/j.chom.2015.01.001

Kristensen, N. B., Bryrup, T., Allin, K. H., Nielsen, T., Hansen, T. H., and Pedersen, O. (2016). Alterations in fecal microbiota composition by probiotic supplementation in healthy adults: a systematic review of randomized controlled trials. *Genome Med.* 8:52. doi: 10.1186/s13073-016-0300-5

Larsen, N., Vogensen, F. K., Gøbel, R., Michaelsen, K. F., Abu Al-Soud, W., Sørensen, S. J., et al. (2011). Predominant genera of fecal microbiota in children with atopic dermatitis are not altered by intake of probiotic bacteria *Lactobacillus acidophilus* NCFM and *Bifidobacterium animalis* subsp. lactis Bi-07. *FEMS Microbiol. Ecol.* 75, 482–496. doi: 10.1111/j.1574-6941.2010.01024.x

Leahy, S. C., Higgins, D. G., Fitzgerald, G. F., and van Sinderen, D. (2005). Getting better with bifidobacteria. *J. Appl. Microbiol.* 98, 1303–1315. doi: 10.1111/j.1365-2672.2005.02600.x

Lindberg, T. P., Caimano, M. J., Hagadorn, J. I., Bennett, E. M., Maas, K., Brownell, E. A., et al. (2020). Preterm infant gut microbial patterns related to the development of necrotizing enterocolitis. *J. Matern. Neonatal Med.* 33, 349–358. doi: 10.1080/14767058.2018.1490719

Maldonado-Gómez, M. X., Martínez, I., Bottacini, F., O'Callaghan, A., Ventura, M., van Sinderen, D., et al. (2016). Stable engraftment of *Bifidobacterium longum* AH1206 in the human gut depends on individualized features of the resident microbiome. *Cell Host Microbe* 20, 515–526. doi: 10.1016/j.chom.2016.09.001

Martin, R., Makino, H., Yavuz, A. C., Ben-Amor, K., Roelofs, M., Ishikawa, E., et al. (2016). Early-life events, including mode of delivery and type of feeding, siblings and gender, shape the developing gut microbiota. *PLoS One* 11:e0158498. doi: 10.1371/journal.pone.0158498

Matsuki, T., Watanabe, K., Fujimoto, J., Kado, Y., Takada, T., Matsumoto, K., et al. (2004). Quantitative PCR with 16S rRNA-gene-targeted species-specific primers for analysis of human intestinal bifidobacteria. *Appl. Environ. Microbiol.* 70, 167–173. doi: 10.1128/aem.70.1.167

Matsuki, T., Watanabe, K., Tanaka, R., and Oyaizu, H. (1998). Rapid identification of human intestinal bifidobacteria by 16S rRNA-targeted species- and group-specific primers. *FEMS Microbiol. Lett.* 167, 113–121. doi: 10.1111/j.1574-6968.1998.tb13216.x

Mirpuri, J., Raetz, M., Sturge, C. R., Wilhelm, C. L., Benson, A., Savani, R. C., et al. (2014). *Proteobacteria*-specific IgA regulates maturation of the intestinal microbiota. *Gut Microbes* 5, 28–39. doi: 10.4161/gmic.26489

Mohan, R., Koebnick, C., Schildt, J., Schmidt, S., Mueller, M., Possner, M., et al. (2006). Effects of *Bifidobacterium lactis* Bb12 supplementation on intestinal microbiota of preterm infants: a double-blind, placebo-controlled, randomized study. *J. Clin. Microbiol.* 44, 4025–4031. doi: 10.1128/JCM.00767-06

Neu, J., and Pammi, M. (2017). Pathogenesis of NEC: impact of an altered intestinal microbiome. *Semin. Perinatol.* 41, 29–35. doi: 10.1053/j.semperi.2016.09.015

Odamaki, T., Horigome, A., Sugahara, H., Hashikura, N., Minami, J., Xiao, J., et al. (2015). Comparative genomics revealed genetic diversity and species/strain-level differences in carbohydrate metabolism of three probiotic bifidobacterial species. *Int. J. Genomics* 2015:567809. doi: 10.1155/2015/567809

Odamaki, T., Kato, K., Sugahara, H., Hashikura, N., Takahashi, S., Xiao, J., et al. (2016). Age-related changes in gut microbiota composition from newborn to centenarian: a cross-sectional study. *BMC Microbiol.* 16:90. doi: 10.1186/s12866-016-0708-5

Olm, M. R., Bhattacharya, N., Crits-Christoph, A., Firek, B. A., Baker, R., Song, Y. S., et al. (2019). Necrotizing enterocolitis is preceded by increased gut bacterial replication, *Klebsiella*, and fimbriae-encoding bacteria. *Sci. Adv.* 5:eaax5727. doi: 10.1126/sciadv.aax5727

Pammi, M., Cope, J., Tarr, P. I., Warner, B. B., Morrow, A. L., Mai, V., et al. (2017). Intestinal dysbiosis in preterm infants preceding necrotizing enterocolitis: a systematic review and meta-analysis. *Microbiome* 5:31. doi: 10.1186/s40168-017-0248-8

Patel, A. L., Mutlu, E. A., Sun, Y., Koenig, L., Green, S., Jakubowicz, A., et al. (2016). Longitudinal survey of microbiota in hospitalized preterm very-low-birth-weight infants. *J. Pediatr. Gastroenterol. Nutr.* 62, 292–303. doi: 10.1097/MPG.0000000000000913

Patole, S. K., Rao, S. C., Keil, A. D., Nathan, E. A., Doherty, D. A., and Simmer, K. N. (2016). Benefits of *Bifidobacterium breve* M-16V supplementation in preterm neonates - a retrospective cohort study. *PLoS One* 11:e0150775. doi: 10.1371/journal.pone.0150775

Patole, S., Keil, A., Chang, A., Nathan, E., Doherty, D., Simmer, K., et al. (2014). Effect of *Bifidobacterium breve* M-16V supplementation on fecal bifidobacteria in preterm neonates - a randomised double blind placebo controlled trial. *PLoS One* 9:e89511. doi: 10.1371/journal.pone.0089511

Plummer, E. L., Bulach, D. M., Murray, G. L., Jacobs, S. E., Tabrizi, S. N., Garland, S. M., et al. (2018). Gut microbiota of preterm infants supplemented with probiotics: sub-study of the ProPrems trial. *BMC Microbiol.* 18:184. doi: 10.1186/s12866-018-1326-1

Podschun, R., and Ullmann, U. (1998). *Klebsiella* spp. as nosocomial pathogens: epidemiology, taxonomy, typing methods, and pathogenicity factors. *Clin. Microbiol. Rev.* 11, 589–603.

Roos, S., Dicksved, J., Tarasco, V., Locatelli, E., Ricceri, F., Grandin, U., et al. (2013). 454 pyrosequencing analysis on faecal samples from a randomized DBPC trial of colicky infants treated with *Lactobacillus reuteri* DSM 17938. *PLoS One* 8:e56710. doi: 10.1371/journal.pone.0056710

Rozé, J.-C., Ancel, P.-Y., Marchand-Martin, L., Rousseau, C., Montassier, E., Monot, C., et al. (2020). Assessment of neonatal intensive care unit practices and preterm newborn gut microbiota and 2-year neurodevelopmental outcomes. *JAMA Netw. Open* 3:e2018119. doi: 10.1001/jamanetworkopen.2020.18119

Satoh, T., Izumi, H., Iwabuchi, N., Odamaki, T., Namba, K., Abe, F., et al. (2016). *Bifidobacterium breve* prevents necrotising enterocolitis by suppressing inflammatory responses in a preterm rat model. *Benef. Microbes* 7, 75–82. doi: 10.3920/BM2015.0035

Shin, N. R., Whon, T. W., and Bae, J. W. (2015). *Proteobacteria*: microbial signature of dysbiosis in gut microbiota. *Trends Biotechnol.* 33, 496–503. doi: 10.1016/j.tibtech.2015.06.011

Sim, K., Shaw, A. G., Randell, P., Cox, M. J., McClure, Z. E., Li, M.-S., et al. (2015). Dysbiosis anticipating necrotizing enterocolitis in very premature infants. *Clin. Infect. Dis.* 60, 389–397. doi: 10.1093/cid/ciu822

Stewart, C. J., Ajami, N. J., O'Brien, J. L., Hutchinson, D. S., Smith, D. P., Wong, M. C., et al. (2018). Temporal development of the gut microbiome in early childhood from the TEDDY study. *Nature* 562, 583–588. doi: 10.1038/s41586-018-0617-x

Stewart, C. J., Embleton, N. D., Marrs, E. C. L., Smith, D. P., Nelson, A., Abdulkadir, B., et al. (2016). Temporal bacterial and metabolic development of the preterm gut reveals specific signatures in health and disease. *Microbiome* 4:67. doi: 10.1186/s40168-016-0216-8

Sugahara, H., Odamaki, T., Hashikura, N., Abe, F., and Xiao, J. (2015). Differences in folate production by bifidobacteria of different origins. *Biosci. Microbiota Food Health* 34, 87–93. doi: 10.12938/bmfh.2015-003

Umezaki, H., Shinohara, K., Satoh, Y., Shoji, H., Satoh, H., Ohtsuka, Y., et al. (2010). Bifidobacteria prevents preterm infants from developing infection and sepsis. *Int. J. Probiotics Prebiotics* 5, 33–36.

Underwood, M. A., German, J. B., Lebrilla, C. B., and Mills, D. A. (2015). *Bifidobacterium longum* subspecies infantis: champion colonizer of the infant gut. *Pediatr. Res.* 77, 229–235. doi: 10.1038/pr.2014.156

Underwood, M. A., Kalanetra, K. M., Bokulich, N. A., Lewis, Z. T., Mirmiran, M., Tancredi, D. J., et al. (2013). A comparison of two probiotic strains of bifidobacteria in premature infants. *J. Pediatr.* 163, 1585–1591.e9. doi: 10.1016/j.jpeds.2013.07.017

Untergasser, A., Cutcutache, I., Koressaar, T., Ye, J., Faircloth, B. C., Remm, M., et al. (2012). Primer3–new capabilities and interfaces. *Nucleic Acids Res.* 40:e115. doi: 10.1093/nar/gks596

Voreades, N., Kozil, A., and Weir, T. L. (2014). Diet and the development of the human intestinal microbiome. *Front. Microbiol.* 5:494. doi: 10.3389/fmicb.2014.00494

Wang, Y., Hoenig, J. D., Malin, K. J., Qamar, S., Petrof, E. O., Sun, J., et al. (2009). 16S rRNA gene-based analysis of fecal microbiota from preterm infants with and without necrotizing enterocolitis. *ISME J.* 3, 944–954. doi: 10.1038/ismej.2009.37

Wong, C. B., Iwabuchi, N., and Xiao, J. Z. (2019). Exploring the science behind *Bifidobacterium breve* M-16V in infant health. *Nutrients* 11:1724. doi: 10.3390/nu11081724

Wong, C. B., Sugahara, H., Odamaki, T., and Xiao, J. Z. (2018). Different physiological properties of human-residential and non-human-residential bifidobacteria in human health. *Benef. Microbes* 9, 111–122. doi: 10.3920/BM2017.0031

Yousuf, E. I., Carvalho, M., Dizzell, S. E., Kim, S., Gunn, E., Twiss, J., et al. (2020). Persistence of suspected probiotic organisms in preterm infant gut microbiota weeks after probiotic supplementation in the NICU. *Front. Microbiol.* 11:574137. doi: 10.3389/fmicb.2020.574137

Zimmermann, P., Messina, N., Mohn, W. W., Finlay, B. B., and Curtis, N. (2019). Association between the intestinal microbiota and allergic sensitization, eczema, and asthma: a systematic review. *J. Allergy Clin. Immunol.* 143, 467–485. doi: 10.1016/j.jaci.2018.09.025

Conflict of Interest: AH, TO, NI, and J-ZX were employees of Morinaga Milk Industry Co., Ltd.

The remaining authors declare that the research was conducted in the absence of any commercial or financial relationships that could be construed as a potential conflict of interest.

frontiers in Microbiology

ORIGINAL RESEARCH
published: 03 May 2021
doi: 10.3389/fmicb.2021.662959

Infant-Associated Bifidobacterial β-Galactosidases and Their Ability to Synthesize Galacto-Oligosaccharides

*Valentina Ambrogi[1,2], Francesca Bottacini[1,3], John O'Callaghan[2], Eoghan Casey[1,2], Justin van Breen[1], Barry Schoemaker[4], Linqiu Cao[4], Bas Kuipers[4], Mary O'Connell Motherway[1], Margriet Schoterman[4] and Douwe van Sinderen[1,2]**

[1] APC Microbiome Ireland, University College Cork, Cork, Ireland, [2] School of Microbiology, University College Cork, Cork, Ireland, [3] Department of Biological Sciences, Munster Technological University, Cork, Ireland, [4] FrieslandCampina, Amersfoort, Netherlands

OPEN ACCESS

Edited by:
Alberto A. Iglesias, CONICET Coastline Agrobiotechnology Institute (IAL), Argentina

Reviewed by:
F. Javier Moreno, Institute of Food Science Research (CIAL), Spain
Victor Sebastian Blancato, CONICET Instituto de Biología Molecular y Celular de Rosario (IBR), Argentina

***Correspondence:**
Douwe van Sinderen
d.vansinderen@ucc.ie

Specialty section:
This article was submitted to Microbial Physiology and Metabolism, a section of the journal Frontiers in Microbiology

Received: *03 February 2021*
Accepted: *01 April 2021*
Published: *03 May 2021*

Citation:
Ambrogi V, Bottacini F, O'Callaghan J, Casey E, van Breen J, Schoemaker B, Cao L, Kuipers B, O'Connell Motherway M, Schoterman M and van Sinderen D (2021) Infant-Associated Bifidobacterial β-Galactosidases and Their Ability to Synthesize Galacto-Oligosaccharides. Front. Microbiol. 12:662959. doi: 10.3389/fmicb.2021.662959

Galacto-oligosaccharides (GOS) represent non-digestible glycans that are commercially produced by transgalactosylation of lactose, and that are widely used as functional food ingredients in prebiotic formulations, in particular in infant nutrition. GOS consumption has been reported to enhance growth of specific bacteria in the gut, in particular bifidobacteria, thereby supporting a balanced gut microbiota. In a previous study, we assessed the hydrolytic activity and substrate specificity of seventeen predicted β-galactosidases encoded by various species and strains of infant-associated bifidobacteria. In the current study, we further characterized seven out of these seventeen bifidobacterial β-galactosidases in terms of their kinetics, enzyme stability and oligomeric state. Accordingly, we established whether these β-galactosidases are capable of synthesizing GOS via enzymatic transgalactosylation employing lactose as the feed substrate. Our findings show that the seven selected enzymes all possess such transgalactosylation activity, though they appear to differ in their efficiency by which they perform this reaction. From chromatography analysis, it seems that these enzymes generate two distinct GOS mixtures: GOS with a relatively short or long degree of polymerization profile. These findings may be the stepping stone for further studies aimed at synthesizing new GOS variants with novel and/or enhanced prebiotic activities and potential for industrial applications.

Keywords: prebiotics, gut microbiota, microbiome, bifidogenic, galacto-oligosaccharides, infant, oligosaccharides, *Bifidobacterium*

INTRODUCTION

The human gut microbiota consists of a large number of microorganisms, some of which have shown to be positively associated with human host health and well-being (Edgar et al., 2011; Valdes et al., 2018). Among the various reported beneficial functions associated with a healthy gut microbiota are: homeostasis maintenance, protection against pathogens, harvesting nutrients and energy from our diet, and stimulation of the immune system (Lozupone et al., 2012). Changes in the human gut microbiota composition may occur at any age (Odamaki et al., 2016), and

are driven by various factors, such as environment (Rothschild et al., 2018), dietary habits (De Filippo et al., 2010), delivery mode, age, use of antibiotics (Langdon et al., 2016) and occurrence of disease (Wang, 2009; Valdes et al., 2018). For obvious reasons and fueled by microbiome research, recent decades have seen a remarkable increase in scientific and public interest in associations between diet, gut microbiota and human health. A considerable amount of scientific effort has been dedicated to the development of novel strategies aimed at maintaining a balanced microbiota. Among these are the supplementation of beneficial bacteria (probiotics), and/or the administration of mostly indigestible (i.e., by the host) dietary substances (referred to as prebiotics) to specifically stimulate the proliferation and/or metabolic activity of desired bacteria in the gut (Lozupone et al., 2012; Cheng et al., 2017). It has been shown that prebiotics can be used to influence the gut microbiota composition for the benefit of host health (Hutkins et al., 2016). Based on the definition recently proposed by the International Scientific Association for Probiotics and Prebiotics (ISAPP) consensus panel in 2017 (Gibson et al., 2017): a prebiotic is "a substrate that is selectively utilized by host micro-organisms conferring a health benefit." Galacto-oligosaccharides (GOS), together with inulin and fructo-oligosaccharides (FOS), were among the first recognized prebiotics, as they have been shown to promote growth of beneficial bacteria, in particular bifidobacteria and lactobacilli, in the human gut (Gibson and Roberfroid, 1995). Based on the ISAPP definition as mentioned above, several substrates have been exploited for their potential prebiotic activity, including inulin, inulin-type fructans or FOS and GOS (Macfarlane et al., 2008; Wilson and Whelan, 2017). Studies conducted in infants have shown that GOS increases the relative abundance of beneficial bacteria, such as bifidobacteria and lactobacilli, resulting in an intestinal microbiota composition that more closely resembles that of breast-fed infants (Fanaro et al., 2008; Giovannini et al., 2014; Sierra et al., 2015). In addition, a mixture of 90% short chain GOS (scGOS) and 10% long chain FOS (lcFOS) have shown to elicit similar effects on intestinal microbiota composition and associated metabolic profile (Boehm et al., 2002; Knol et al., 2005; Moro et al., 2005).

Primarily due to their demonstrated bifidogenicity, and supported by physicochemical stability and pleasant taste, GOS-containing products are extensively employed as functional ingredients in infant food formulations. Besides, GOS as an ingredient is also suitable for several other food applications such as beverages and bread products (Sako et al., 1999). In addition, the ability of GOS alone and as a mixture to promote particular skin conditions has attracted the interest of the cosmetic and pharmaceutical industry (Mori et al., 2016; Hong et al., 2017; Dall'Oglio et al., 2018; Suh et al., 2019). In order to render these potential applications commercially viable, reliable and large-scale GOS manufacturing technologies had to be developed. As a result, quite a substantial level of data is currently available in literature regarding GOS production (Tzortzis et al., 2005; Splechtna et al., 2006; Torres et al., 2010; Urrutia et al., 2013; Warmerdam et al., 2013; Martins et al., 2019).

Galacto-oligosaccharides are currently produced at an industrial scale using a transgalactosylation reaction catalyzed by a β-galactosidase enzyme where lactose is used as galactose donor and acceptor (Kim et al., 1997). The resulting GOS-containing product is an oligosaccharide mixture that is formed through a double-displacement reaction, which involves galactosylation and degalactosylation, and which can be enhanced by increasing the concentration of lactose (Brás et al., 2010). Among the commonly used sources of β-galactosidases (i.e., for industrial GOS synthesis) are those of fungal origin (Urrutia et al., 2013; Saqib et al., 2017). Bacterial enzymes have also been studied and employed for GOS production, including those derived from *Lactobacillus* species (Splechtna et al., 2006; Wichienchot et al., 2016), *Bacillus circulans* (Vivinal® GOS) (Torres et al., 2010), *Bifidobacterium* species (Laere et al., 2000; Han et al., 2014; Viborg et al., 2014) for the production of Bimuno GOS (Goulas and Tzortzis, 2007) and *Streptococcus thermophilus* in combination with *Aspergillus oryzae* (Chen and Gänzle, 2017). β-galactosidases typically belong to the glycosyl hydrolase families GH1, GH2, GH35 or GH42, and certain members of GH2 and GH42 have been exploited for GOS synthesis (Møller et al., 2001; Goulas et al., 2007; James et al., 2016).

In a previous study we characterized the hydrolytic activity and substrate specificity of a number of β-galactosidases encoded by various infant-associated bifidobacteria (Ambrogi et al., 2019). Following this preliminary characterization, a subset of seven bifidobacterial β-galactosidases was selected in the current report for further characterization in terms of their oligomeric state, enzyme stability and kinetics, as well as their suitability for GOS synthesis.

MATERIALS AND METHODS

Enzyme Preparation

Heterologous expression and purification of the seven bifidobacterial β-galactosidases assessed in this study (here designated as BgaA, BgaB, BgaC, BgaD, BgaE, BgaF, BgaG) (salient details of these enzymes can be found in **Table 1**) was carried out according to a previously described method (Ambrogi et al., 2019). Briefly, 2% of overnight cultures of *Lactococcus lactis* strains, each containing the expression plasmid pNZ8150 (Mierau and Kleerebezem, 2005) in which each of the seven His-tag-containing and β-galactosidase-encoding genes had been cloned (Ambrogi et al., 2019), were inoculated in 1.6 or 3.2 L of M17 broth (**Table 2**) supplemented with 0.5% glucose. Cultivation of *L. lactis* cultures was performed at 30°C until an Optical Density (OD_{600nm}) of 0.5 was reached, at which point target gene expression was induced by the addition of filter-sterilized cell free supernatant of the nisin-producing strain *L. lactis* NZ9700 (0.2% v/v) (de Ruyter et al., 1996). Following incubation at 30°C for 90 min, cells were harvested by centrifugation (8,000 × *g* for 10 min) and the obtained pellet was resuspended in lysis buffer (50 mM sodium phosphate buffer, pH 8; 300 mM NaCl; 10 mM imidazole). Cell disruption was performed by repeated bead beating (Mini BeadBeater-16, BioSpec, Bartlesville, OK, United States; three times for 1 min). Following this, debris was removed by centrifugation (10,000 × *g* for 30 min at 4°C) to produce a crude cell extract. Individual

TABLE 1 | Description of the enzymes employed.

Locus tag	Origin	GH family	Name	Accession number
Bbr_0010	*B. breve* UCC2003	GH2	BgaA	ABE94727.1
Bbr_0529	*B. breve* UCC2003	GH42	BgaB	ABE95226.1
B216_08266	*B. bifidum* LMG 13195	GH42	BgaC	EKE50024.1
B8809_0415	*B. longum* subsp. *longum* NCIMB 8809	GH42	BgaD	ALO72088.1
B8809_0611	*B. longum* subsp. *longum* NCIMB 8809	GH2	BgaE	ALO72284.1
B8809_1361	*B. longum* subsp. *longum* NCIMB 8809	GH2	BgaF	ALO73032.1
Blon_2016	*B. longum* subsp. *infantis* ATCC 15697	GH42	BgaG	ACJ53083.1

TABLE 2 | β-galactosidase purification characteristics.

Enzyme	Starting volume (L)	Concentration after Dialysis (mg/ml)	Volume after Dialysis (ml)	Enzyme yield (mg)	Approximate Purity (%)
BgaA	3.2	1.8	4	7.2	>95
BgaB	1.6	3.3	5	16.5	>95
BgaC	1.6	1.95	5	9.75	>95
BgaD	1.6	2.03	4	8.12	>95
BgaE	1.6	3.71	3	11.13	∼80
BgaF	3.2	1.6	4	6.4	∼80
BgaG	3.2	1.55	3	4.65	>95

His-tagged β-galactosidases were then purified from a given crude cell extract by Fast Protein Liquid Chromatography (FPLC, Akta pure) employing a 1 ml HisTrap^{TM} Hp column (GE Health Care). Elution was performed at a constant flow rate of 1.0 ml min^{-1} using the following two buffers 100 mM Tris–HCl + 150 mM NaCl, pH7 (buffer A), and 100 mM Tris–HCl + 150 mM NaCl + 250 mM Imidazole, pH7 (buffer B). The seven β-galactosidases were individually purified employing a standard linear elution gradient. The purity of the obtained enzymes was analyzed by SDS-polyacrylamide gel electrophoresis (SDS-PAGE), as described previously (Laemmli, 1970), on a 12.5% polyacrylamide (PAA) gel. SDS-PAGE gels were fixed and stained with Coomassie brilliant blue to identify fractions containing the purified protein and to assess purity. The elution fractions containing a given purified protein were selected, pooled and dialyzed against 40 mM sodium citrate buffer at pH 6.5 employing Centrifugal Filter Units with a 30 kDa cut-off (Merck Millipore Ltd.). Protein concentrations were determined by the Coomassie Brilliant blue method with the use of bovine serum albumin to generate a standard calibration curve (Ernst and Zor, 2010).

Absolute Mass Determination of β-Galactosidase Enzymes

Molecular weights of denatured protein monomers were estimated by SDS-PAGE and comparison to a Prestained Protein Marker reference (Broad Range (7–175 kDa); New England BioLabs, Hertfordshire, United Kingdom). These estimated molecular weights were compared to the calculated mass values based on the corresponding gene sequence (including the His-tag-encoding sequence) employing the ExPASy Bioinformatics Resource Portal (SIB Swiss Institute of Bioinformatics). In order to determine the absolute mass of the native form the enzymes, size exclusion chromatography was first carried out on an AKTA Pure HPLC system (GE Healthcare, Cork, Ireland) using a Superose 6 10/300 G/L column (GE Healthcare, Cork, Ireland) run in a buffer containing 50 mM Tris–HCl and 150 mM NaCl at pH 7.5 with a flow rate of 0.5 mL/min. Proteins were injected at a final concentration as listed in **Supplementary Table 1**. Detection was performed using OmniSec REVEAL, a dual-angle light-scattering apparatus and refractometer (RALS/LALS/RI) (Malvern Instruments, Malvern, United Kingdom). Absolute mass calculations were performed employing the OmniSec software (v10.4).

Assessment of β-Galactosidase Activity

β-galactosidase activity of the purified enzymes was quantified by using *o*-nitrophenyl-β-D-galactopyranoside (ONPG) or lactose as substrates. The ONPG-based assay was carried out at 40°C in 40 mM sodium acetate buffer (pH 6.5) as follows: 880 μl of citrate buffer was pre-heated for 5 min at 40°C, after which 20 μl of citrate buffer containing the purified enzyme was added (representing 10 μg of purified protein in the case of BgaA, BgaE, BgaF, and BgaG; 2.5 μg in the case of purified BgaB and BgaD; 1 μg in the case of purified BgaC). Then, 100 μl of substrate solution containing ONPG at each of the following concentrations was added: 0.83, 1.66, 3.32, 6.64, 9.96, 13.28, 33.20, and 66.39 mM. After 30 s of incubation at 40°C the reaction was terminated by the addition of 200 μl of 1 M Na_2CO_3. The release of *o*-nitrophenol (*o*NP) was measured spectrophotometrically at 420 nm.

When lactose was employed as a substrate, the enzymatic activity of the purified β-galactosidases was determined quantitatively using the D-glucose oxidase/peroxidase GOPOD assay kit (Megazyme, Bray, Ireland) according to a previously published protocol (Benjamins et al., 2014). For this assay, 5 ml of 12% lactose solution was pre-heated into a water bath at 40°C for 10 min, after which 1 ml of sample solution was added to

the reaction tube. Following 10 min incubation, the reaction was stopped by the addition of 1 ml of 1.5 M sodium hydroxide. The reaction mixture was cooled in ice water and 1 ml 1.5 M of HCl was added. The release of D-glucose from lactose was determined using the GOPOD method (Megazyme). One lactase unit (LU) was defined as the amount of enzyme that releases 1 μmol of D-glucose per minute (at the non-limiting lactose concentration used in this assay) at 40°C and pH 6.0, and individual enzyme activities were calculated employing the formula indicated below:

$$Lu/g = \frac{Gt - Gb}{0.18} \times 8 \times \frac{1}{10} \times \frac{1}{W} = \frac{(Gt - Gb)}{0.225 \times W}$$

Gt = Glucose concentration of the sample solution (mg/ml)
Gb = Glucose concentration of the blank (mg/ml)
0.18 = Amount of glucose, in mg, equivalent to 1 μmol
8 = Total volume of the reaction mixture (in ml)
10 = Reaction time of 10 min
W = Weight in grams of the enzyme in the sample solution

Enzyme stability over time at different storage conditions was evaluated by employing LU determination as follows. Enzymes were stored −20°C following purification and subsequent dialysis in the dialysis buffer [40 mM sodium citrate ($Na_3C_6H_5O_7$)] pH 6.5 with or without the addition of 20% glycerol. LU determination was performed at various time points: immediately after enzyme purification and dialysis, after one and 2 weeks, as well as after one, two and three months. In the case of proteins stored in dialysis buffer with glycerol, an additional time point at 4 months was also assessed. Statistical analysis was performed using one-way ANOVA, followed by Tukey's *post hoc* test. A *p*-value of less than 0.05 was considered significant.

Optimal Conditions for Lactose Hydrolysis

Optimal lactose hydrolysis conditions of the seven purified β-galactosidases were determined for each enzyme by first implementing the above described GOPOD method. Enzyme reactions were then terminated at various time points (*t*) set at 1, 3, and 10 min. In order to determine the optimum temperature for lactose hydrolysis, the assay was conducted at various temperatures (35, 40, 45, 50, 55, and 60°C). The assay was then performed at the determined optimal temperature at pH 5 and 6 in 0.1 M sodium acetate buffer ($C_2H_3NaO_2$) as well as pH 6, 7, and 8 in 0.1 M sodium phosphate buffer in order to assess the pH optimum of the enzyme reaction. Enzyme activity was expressed as LU/g for each temperature and pH condition using the formula indicated in the previous paragraph.

Enzyme Kinetics

Steady-state kinetic measurements were obtained using ONPG as a substrate, while enzyme reaction conditions were set at 40°C in 0.1 M sodium acetate buffer (pH 6.5) and with substrate concentrations ranging between 0.83 and 66.39 mM. One unit of β-galactosidase activity refers to the amount of enzyme required to release 1 μmol *o*NP (from the ONPG substrate) per minute at the applied temperature and pH conditions. The catalytic properties of the seven purified enzymes were determined according to the Michaelis-Menten kinetics model, where the maximum enzyme velocity (V_{max}) is extrapolated from the equation that calculates enzyme activity (Y) as a function of substrate concentration (X). The corresponding Km, which is calculated based on the concentration that causes V_{max} to halve, was determined according to the following equation:

$$Y = Et * kcat * X/(K_m + X)$$

Et represents the number of active sites present in the enzyme and kcat is the rate at which enzymes can convert substrate to product. All parameters were determined using Graph Pad Prism version 5 (Graphpad Software, United States).

Galacto-Oligosaccharide (GOS) Synthesis

Galacto-oligosaccharides synthesis assay was performed following a previously described method (Benjamins et al., 2014). The reaction was initiated following the addition of purified bifidobacterial β-galactosidase (to which water had been added to bring it to a total volume of 2 ml) to a lactose substrate slurry, consisting of 7.5 g lactose monohydrate (99% pure, Lactochem® Super Fine Powder, DMV-Fonterra Excipients GmbH & Co., Goch, Germany), corresponding to a final concentration of 48%, 5.1 g H_2O, 150 μl of 1 M citrate buffer (pH 7.0) and 75 μl of 1 M $MgCl_2$. The citrate buffer was employed to prevent acidification of the reaction and interference with enzyme activity for the duration of the experiment.

The enzyme dose used to initiate a given GOS reaction varied between 2.5 and 8 LU per gram of lactose, depending on the enzyme. The GOS synthesis reaction was performed at 50°C in a vessel (Wide neck clear GL50, VWR) under constant stirring for a period of 32–54 h.

Preliminary Compositional Analysis of GOS Preparations as Based on Glyco-Profiling by HPAEC-PAD

Preliminary compositional analysis of each obtained GOS mixture was determined by glyco-profile analysis employing a High Performance Anion Exchange Chromatography and pulsed amperometric detection (HPAEC-PAD; Dionex IC-3000 system; Thermo Scientific[1]). Separations were performed using a CarboPac PA1 (Thermo Scientific) analytical-anion exchange column (dimensions, 250 mm by 4 mm) with a CarboPac PA1 (Thermo Scientific) guard column (dimensions, 50 mm by 4 mm) and a detector (ED40) in the pulsed amperometric detection PAD mode (Dionex, Thermo Scientific). Qualitative analysis of the GOS Dionex profile was performed with an elution gradient according to a previously published method (Van Leeuwen et al., 2016) and the qualitative determination of the carbohydrate composition was performed by the use an elution gradient summarized in supplemental **Supplementary Table 3** at a constant flow rate of 1.0 ml min^{-1} at 30°C using the following eluents with programmed gradient for

[1]https://www.thermofisher.com/

the analysis: (A) 100 mmol NaOH, (B) 100 mmol NaOH, 500 mmol sodium acetate (NaAC), (C) 50 mmol NaAC and (D) Milli-Q water. The obtained chromatography profiles were analyzed employing CHROMELEON software Version 7 (Dionex, Thermo Scientific).

RESULTS AND DISCUSSION

Enzyme Preparation

The seven enzymes of interest were selected from a set of seventeen previously assessed GH2 and GH42 β-galactosidases encoded by various infant-derived bifidobacteria (Ambrogi et al., 2019). These seven enzymes (here named BgaA, BgaB, BgaC, BgaD, BgaE, BgaF, and BgaG; for salient features see **Table 1**) were selected based on their relatively broad substrate range and high catalytic activity toward lactose (Ambrogi et al., 2019).

Heterologous expression and purification of the seven selected proteins were performed according to a method reported in a previous study (Ambrogi et al., 2019). Of note, the purification protocol for these seven His6-tagged proteins was increased in scale using a starting volume of 3.2 L of enzyme-overexpressing bacterial culture (see section "Materials and Methods"). The final protein yields varied depending on the particular β-galactosidase purified: BgaG yield was the lowest at 4.65 mg, while BgaB produced the highest protein yield at 16.5 mg (**Table 2**). In all cases, the purification generated sufficient amounts of purified enzyme to perform further characterization and evaluation of transgalactosylase activity of these β-galactosidases. The purity of the obtained purified proteins was visually estimated to be higher than 95% for BgaA, BgaB, BgaC, BbgaD, and BgaG, while being around 80% for BgaE and BgaF due to some minor, non-specific protein bands visible in the corresponding SDS-PAGE gels (**Supplementary Figure 1**).

Optimization of Hydrolysis Conditions

In our previous study a qualitative assay of the seven selected enzymes (BgaA-G) established that these β-galactosidases were shown to exhibit variable substrate specificity, although they are all capable of hydrolyzing lactose (Ambrogi et al., 2019). In order to establish optimal lactose hydrolysis conditions the preferred temperature and pH for each of these seven enzymes were determined. These assays, which were conducted at a pH ranging between 6 and 8 and at various temperatures (between 35 and 60°C), showed that the seven purified β-galactosidases elicit optimal lactose hydrolysis activity at neutral conditions and a temperature range between 40 and 60°C (**Figure 1**; **Supplementary Table 3**), which is comparable to other described β-galactosidases (Osman et al., 2014). These results then served to assess the kinetic parameters of these enzymes as described in the paragraph below (which were conducted at a temperature of 40°C and pH 6.5).

Enzyme Characterization

In order to perform a kinetic assessment of the seven selected β-galactosidases, their hydrolytic activities toward ONPG and lactose were investigated. Assays for either substrate were conducted at 40°C in 0.1 M sodium acetate buffer (pH 6.5). As expected and in accordance to our previous findings (Ambrogi et al., 2019), all enzymes were shown to hydrolyze both ONPG and lactose. In the case of ONPG as a substrate, the steady-state kinetic constants were determined (V_{max}, K_m, K_{cat}, and K_{cat}/K_m) and the K_{cat} values were calculated based on V_{max} values obtained from non-linear regression (assuming the presence of a single active site) (**Table 3**). The K_m values were shown to be quite variable across the enzymes tested and ranged between 114.9 mM for BgaG (highest) and 5.178 mM for BgaF (lowest), thereby indicating that BgaG has the lowest affinity for ONPG. The enzyme velocity and the consequent catalytic efficiency (K_{cat}/K_m) values were highest for BgaB and BgaC under the conditions tested. The catalytic efficiency obtained was in line with a previous study, where the BbgII enzyme (which is a homolog of BgaB) was shown to exhibit a similar Kcat/Km value under comparable test conditions (Goulas et al., 2009). Of note, enzymes BgaB and BgaC represent β-galactosidases, homologs of which are widespread across infant-derived bifidobacteria (Ambrogi et al., 2019). In particular, BgaB (product of the gene Bbr_0529 in *B. breve* UCC2003) was previously described as required for the utilization of GOS and certain HMOs (O'Connell Motherway et al., 2013; James et al., 2016; Ambrogi et al., 2019). Of note, under the conditions tested, BgaG resulted in being the least efficient enzyme among the seven assessed β-galactosidases, while also exhibiting the lowest lactase activity (LU/g; **Supplementary Table 3**). Its homolog β-galIII in *B. longum* subsp. *infantis* HL96 (the two enzymes share 100% amino acid sequence identity) has previously been reported to possess a rather low lactose-associated hydrolytic rate (Hung et al., 2001), in agreement with our observation of low lactase activity (**Supplementary Table 3**). In order to investigate the stability of the seven enzymes when kept at a low temperature, changes in lactase activity of individual enzymes over time (up to 4 months) were assessed during enzyme storage at −20°C with or without the addition of 20% glycerol. Storage of the seven enzymes at −20°C resulted in a significant decrease activity after 1 month for BgaA and BgaE, while in the case of BgaD activity reduction was already clearly observed after 1 week storage at −20°C (**Supplementary Figure 2**). Conversely, BgaC activity appeared to gradually (and significantly) increase during the 3 months of testing, a phenomenon for which we do not have any plausible explanation. In contrast, BgaG lost all activity within 1 week (**Figure 2**, panel a, **Supplementary Figure 2A**). BgaB showed a significant difference only between the activity measured after purification and the activity at time point 2 weeks (**Figure 2**, panel a; **Supplementary Figure 2A**). In the case of BgaF no significant activity difference was observed between the first measurement and all subsequent time points assessed (**Figure 2**, panel a; **Supplementary Figure 2A**). Addition of 20% *v*/*v* glycerol to the enzyme preparations was shown to markedly enhance the stability of enzyme activity of some of the seven β-galactosidases (**Figure 2**, panel b). In particular, enzyme BgaG was shown to retain activity for the entire duration of the assay with no significant difference between the first measurement and all time points considered during the assay. BgaB, BgaC, and BgaD did not suffer from any significant activity decrease

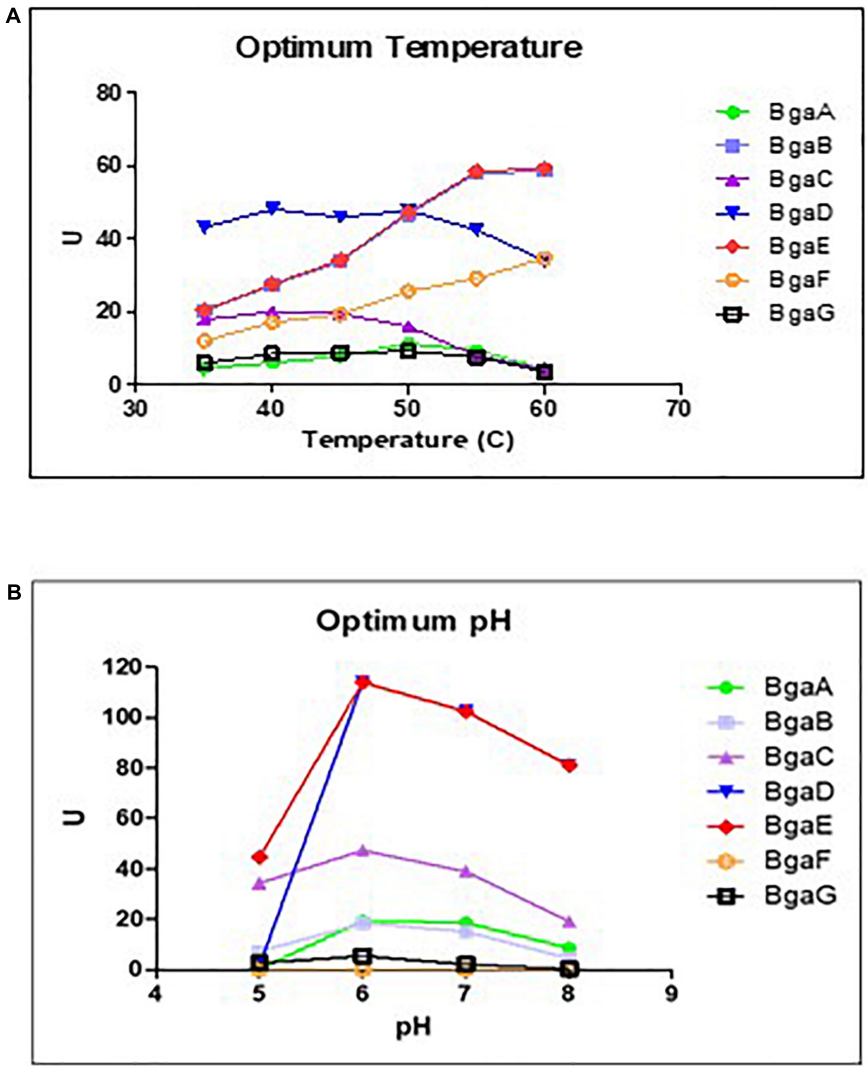

FIGURE 1 | Effects of pH and temperature on enzyme activity. Determination of optimum temperature **(A)** and the optimum of pH **(B)** on enzyme activity of the seven bifidobacterial β- galactosidases Data represent the rate extrapolated by plotting enzyme activity obtained from three independent experiments (mean). The experiments conducted to investigate the optimum temperature were performed at pH 6, while the experiments aimed to determined the optimum pH were performed at the best temperature obtained.

(**Figure 2**, panel b; **Supplementary Figure 2B**). Surprisingly, addition of glycerol for some unknown reason appeared to reduce BgaC activity, which then remained stable upon storage. For enzymes BgaA, BgaE and BgaF activity reduction was observed following one and 3 months of storage (**Figure 2**, panel b; **Supplementary Figure 2B**). In conclusion, the obtained results show that the addition of 20% *v*/*v* glycerol to the enzyme preparations substantially improves stability of at least some of the assessed enzymes.

Molecular Mass Determination

The seven investigated bifidobacterial β-galactosidases are all members of GH2 or GH42[2] families, and exhibit a rather broad substrate specificity (Ambrogi et al., 2019). In order to obtain a better understanding of the structural properties and oligomeric state of the seven bifidobacterial

TABLE 3 | Kinetic characterization of enzymes using ONPG as a substrate.

Enzyme	V_{max}	K_m	K_{cat}	K_{cat}/K_m
BgaA	105.7	10.8	1,227,000	1.14E + 05
BgaB	586.8	8.607	18,070,000	2.10E + 06
BgaC	512.4	38.26	39,960,000	1.04E + 06
BgaD	539	17	16,600,000	9.76E + 05
BgaE	42.46	11.12	484,058	4.35E + 04
BgaF	50.03	5.178	590,354	1.14E + 05
BgaG	177	114.9	1,310,000	1.14E + 04

[2]http://www.cazy.org/

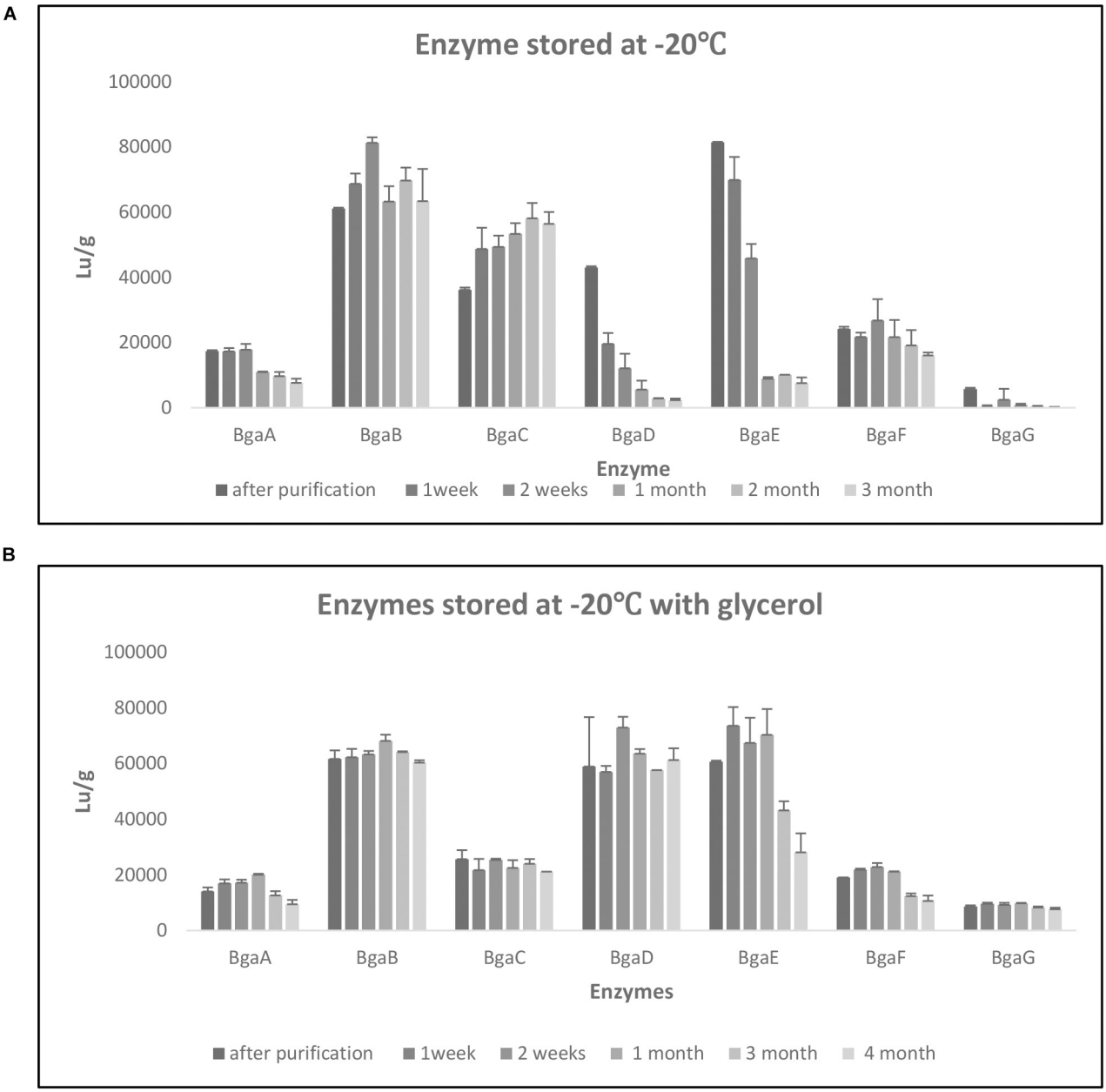

FIGURE 2 | Enzyme stability. Evaluation of enzyme stability under different storage conditions at –20°C for 3 months **(A)** and –20°C with glycerol for 4 months **(B)**. Data represent the mean of two independent experiments. The enzymatic activity was express in Lu/g as per Materials and Methods.

β-galactosidases, the absolute molecular mass of the native enzymes was experimentally determined by size exclusion chromatography coupled to a dual-angle light-scattering apparatus (see section "Materials and Methods"). Comparison between the predicted protein monomer sizes and the experimentally obtained molecular masses of the native enzymes showed that the native form of BgaA is a dimer, while those of BgaB, BgaC, BgaD, and BgaG appear to assemble as trimmers, and that the native state of BgaE is a tetramer (**Supplementary Table 1**).

Notably, BgaB, BgaC, and BgaG are proteins with sequence similarity above 70%, while it has previously been reported that Bga42A (which represents a homolog of BgaG) is also active as a trimer (Yoshida et al., 2012), being consistent with our observations (**Supplementary Table 1**). Also in agreement with our data is that β-gal I from *B. breve* DSM 20213, which is a homolog of BgaA (99% protein sequence similarity) has been reported to form an enzymatically active dimer (Arreola et al., 2014). In contrast, Bga2A of *B. longum* subsp. *infantis* ATCC15697 (a homolog of BgaE with 99% sequence

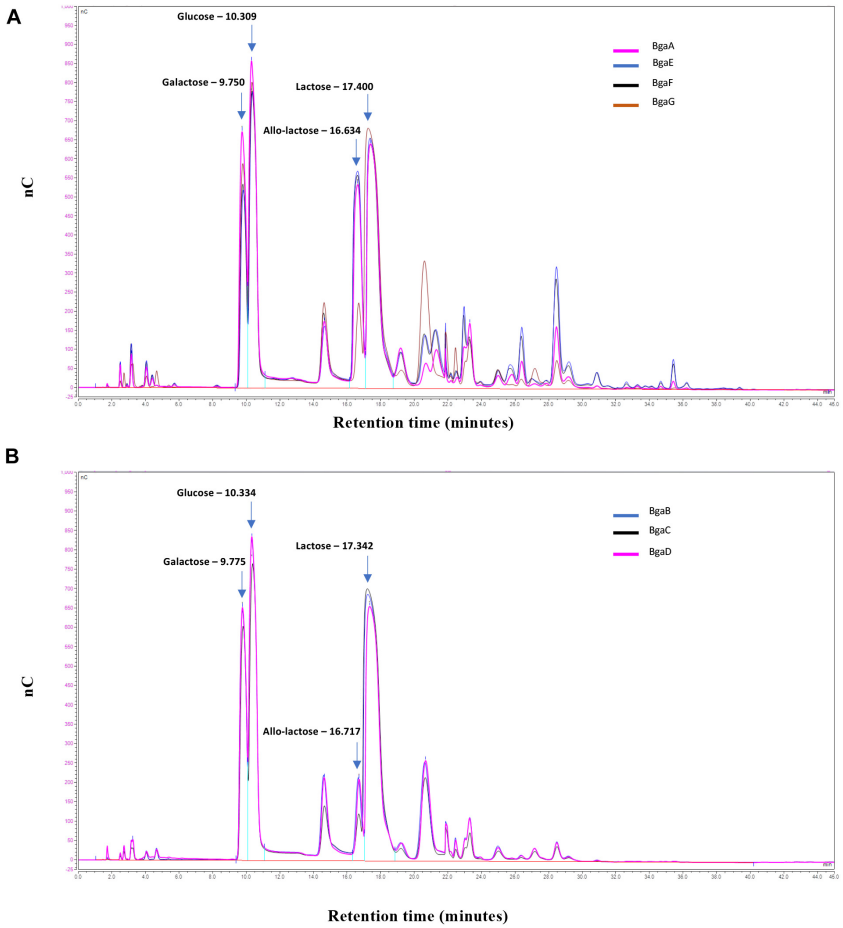

FIGURE 3 | GOS synthesis. HPAEC/PAD elution patterns of the oligosaccharides obtained by transgalactosylation activity of BgaE, BgaE, BgaF or BgaG **(A)** and BgaB, BgaC or BgaD **(B)** nC: nanoCoulomb (Quantitative currency measure proportional to the carbohydrate level).

similarity) has been reported to form an enzymatically active dimer (Yoshida et al., 2012). In conclusion, our analysis shows that the seven bifidobacterial β-galactosidases represent GH2 and GH42 family enzymes that are active in various oligomeric states.

GOS Synthesis

Transgalactosylation activity was assessed in order to determine if the seven bifidobacterial β-galactosidases are capable of GOS synthesis using lactose as the galactose acceptor and donor. Transgalactosylation occurs when β-galactosidase, following lactose hydrolysis, transfers the released galactose to another lactose unit as acceptor (instead of the hydroxyl group of water), thus resulting in the formation of oligosaccharides with a higher degree of polymerization (Kim et al., 1997). A GOS synthesis assay was performed at a temperature of 50°C with an starting lactose level of 50% (w/v) and employing an initial enzyme concentration of 4 LU per gram of lactose. Furthermore, enzyme levels corresponding to 2 LU or 4 LU per gram of lactose were added, respectively, after 15 and 22 h from the beginning of the reaction. The reactions were run over a period of 54 h. Based on the obtained results the enzymes BgaA, BgaD, BgaE, and BgaF were able to clarify the lactose slurry within the duration of the experiment. In contrast, BgaB, BgaC, and BgaG were shown to be unable to completely clarify the lactose slurry under the conditions tested, indicating that compared to BgaA, BgaD, BgaE, and BgaF, the BgaB, BgaC, and BgaG enzymes were apparently less efficient in lactose hydrolysis under the conditions used.

Samples of the transglycosylation reaction were taken at the end of the experiment, and the carbohydrate contents of the obtained reaction mixtures were evaluated by HPAEC-PAD (see section "Materials and Methods"). The generated chromatograms revealed that all seven enzymes are capable of transgalactosylation and that the reactions produce a mix of different mono- and oligosaccharides (**Figure 3**). Based on available carbohydrate standards, we identified galactose, glucose, allo-lactose and lactose (corresponding to peaks with retention times of 9.7, 10.3, 16.6, and 17.4 min, respectively), while also revealing a range of additional peaks that are presumed to represent various GOS with apparent different chain lengths and/or glycosidic linkages (**Figure 3**).

TABLE 4 | HPAEC quantitative analysis of obtained GOS mixtures.

	Galactose (%)	Glucose (%)	Allo-lactose (%)	Lactose (%)	Lactulose (%)	GOS (%)	GOS + Allo-lactose (%)
BgaA	11.7	18.2	8.0	50.9	1.5	9.7	17.7
BgaB	17.9	25.0	1.8	38.0	1.2	16.2	18.0
BgaC	14.9	19.5	0.8	50.5	1.3	12.9	13.7
BgaD	19.1	26.9	3.3	31.0	0.8	18.9	22.2
BgaE	8.2	20.6	18.8	16.6	0.6	35.2	54.0
BgaF	15.5	29.1	15.1	18.9	0.8	20.5	35.6
BgaG	4.8	8.4	4.3	70.8	1.9	9.9	14.2

It is worth noting that the transgalactosylation reactions involving BgaA, BgaE, BgaF, and BgaG produced what we identified as a GOS mixture with a relative long retention profile (here named group A), including peaks with a retention time of up to 40 min (**Figure 3**, panel a), possibly representing oligosaccharides with a relatively high degree of polymerization (DP). In contrast, BgaB, BgaC, and BgaD produced a GOS mixture with a relative short retention profile (designated here as group B) (**Figure 3**, panel b), possibly representing oligosaccharides with a relatively low DP. HPAEC quantitative analysis of the reaction mixtures indicated further differences between the seven enzymes with regards to their transgalactosylase activity. The obtained results confirmed that all seven enzymes tested were able to hydrolyze lactose, furthermore they were all shown to be capable of intra- (direct galactosyl transfer to D-glucose yields regioisomers of lactose) and inter- (transfer of galactose to acceptors other than water) molecular transgalactosylation, though at apparently varying efficiencies. For example, the highest efficiency of GOS production was obtained with BgaE with final GOS (including allo-lactose) levels of 54.0%, which was also associated with the lowest remaining lactose content at 16.6% (**Table 4**). A less efficient GOS production level was observed for BgaC and BgaG, with, respectively, 13.74 and 14.22% of final GOS (including allo-lactose), combined with higher levels of remaining lactose, respectively, corresponding to 50.52 and 70.81% (**Table 4**). The examples mentioned above suggest that, under the conditions used, BgaE is an enzyme suitable for lactose conversion into GOS. In contrast, under the same conditions, BgaG was not able to effectively convert lactose in to GOS through transgalactosylation, or even into glucose and galactose through hydrolysis. A reason for this difference may be that galactose acts as an inhibitor for the enzymatic reaction, as reported previously for several β-galactosidases (Jørgensen et al., 2001; Albayrak and Yang, 2002; Torres and Batista-Viera, 2012). Interestingly, enzymes belonging to group B and producing a short elution profile, are also members of the GH42 family, while enzymes from group A (with the exception of BgaG) that generate a longer elution profile are members of the GH2 family (**Table 1**). It is known that the structural conformation of the active site of a given β-galactosidase impacts on the transgalactosylation/hydrolysis ratio, thereby resulting in the production of chemically different GOS mixtures (Juers et al., 2012), being consistent with our observations. In addition, GH2 family enzymes are reported to utilize lactose as their primary or natural substrate (Husain, 2010; Rodriguez-Colinas et al., 2013), which is in line with our previous observations for BgaA, BgaE, and BgaF (which are all GH family two members) (Ambrogi et al., 2019) and with the observation that they represent the most active enzymes in our GOS synthesis assay (i.e., capable of clarifying the lactose slurry within the first 8 h from the start of the reaction). In contrast, members of GH42 family are more active toward various non-lactose substrates containing β-linked galactose moieties (Husain, 2010; Rodriguez-Colinas et al., 2013). Indeed, BgaB, BgaC, BgaD, and BgaG were previously reported to be highly active toward galactobioses (Galβ1-6Gal and Galβ1-4Gal) and β-D-galactotriose (Galβ1-4Galβ1-4Gal) (Ambrogi et al., 2019), where they also represent enzymes that appear to be less efficient in our GOS synthesis attempts.

Taken together, our findings clearly show that all seven tested bifidobacterial β-galactosidases are capable of producing GOS, but they differ significantly in terms of lactose-to-GOS conversion efficiency (resulting in high GOS and low lactose content in the final reaction product). From the preliminary chromatography analysis of produced GOS it seems that two distinct GOS mixtures are generated: GOS mixtures with short and long profiles. Further optimization of transgalactosylation conditions for each of the enzymes will be necessary in order to increase GOS content. In addition, further assessment will need to be performed in order to characterize the obtained GOS structures in more details, and to establish whether the GOS mixtures possess beneficial functions. Ultimately, this will allow selection of the most promising candidate(s) for future applications.

CONCLUSION

In the current study, seven β-galactosidases originating from infant-derived bifidobacteria were heterologously expressed and characterized in terms of their kinetics, storage stability, oligomeric state and suitability for GOS synthesis. Our analyses show that BgaG obtained from *B. longum* subsp. *infantis* is the enzyme with the lowest affinity for ONPG and lowest lactase activity, while BgaB and BgaC possess the highest velocity and catalytic efficiency among the seven β-galactosidases tested using ONPG as a substrate. Evaluation of enzyme stability during cold storage showed that the addition of glycerol allowed a substantially longer storage time without significantly affecting

hydrolytic activity. Furthermore, molecular mass determination by size exclusion chromatography established that the seven selected enzymes assume different oligomeric conformations in solution and assemble in either dimers, trimmers or tetramers, thus confirming the heterogeneity in bifidobacterial β-galactosidases.

Finally, all characterized enzymes were shown to possess transgalactosylation activity and are to varying extents capable of synthesizing GOS mixtures, some of which appear to be of distinct composition, although this will require further characterization. Based on our findings, it appears that BgaE represents the most efficient enzyme for GOS synthesis, at least under the conditions tested, thereby making this the most promising candidate from a GOS production perspective. Future research is needed to further characterize the generated GOS mixtures and to explore their ability to elicit functional benefits. Overall, this work highlights the potential of infant-derived bifidobacterial β-galactosidases to be exploited for the development of dietary GOS.

DATA AVAILABILITY STATEMENT

The original contributions presented in the study are included in the article/**Supplementary Material**, further inquiries can be directed to the corresponding author.

AUTHOR CONTRIBUTIONS

MS and DS conceived the study. VA, JO'C, MO'C, LC, and BK designed the experiments. VA, JB, EC, and BS carried out the experiments. VA and BS analyzed the data. VA, FB, JO'C, DS, MS, LC, BK, and BS wrote the manuscript. All authors discussed the results and commented on the manuscript.

FUNDING

This work was sponsored by FrieslandCampina. DS, VA, EC, FB, and MO'C are members of APC Microbiome Ireland, which is a research centre funded by the Science Foundation Ireland (SFI), through the Irish Government's National Development Plan. The authors and their work were supported by SFI (Grant SFI/12/RC/2273), FEMS Research Grant FEMS-RG-2016-0103, and HRB (Grant No. 513 PDTM/20011/9). The authors also thank Dr. Eric Benjamins for his support in performing this study.

SUPPLEMENTARY MATERIAL

The Supplementary Material for this article can be found online at: https://www.frontiersin.org/articles/10.3389/fmicb.2021.662959/full#supplementary-material

REFERENCES

Albayrak, N., and Yang, S. (2002). Production of Galacto-Oligosaccharides From Lactose by Aspergillus oryzae β -Galactosidase Immobilized on Cotton Cloth. *Biotechnol. Prog.* 77, 8–19. doi: 10.1021/bp010167b

Ambrogi, V., Bottacini, F., O'Sullivan, J., O'Connell Motherway, M., Linqiu, C., Schoemaker, et al. (2019). Characterization of GH2 and GH42 β-galactosidases derived from bifidobacterial infant isolates. *AMB Express* 9:9. doi: 10.1186/s13568-019-0735-3

Arreola, S. L., Intanon, M., Suljic, J., Kittl, R., Pham, N. H., Kosma, P., et al. (2014). Two β-galactosidases from the human isolate *Bifidobacterium breve* DSM 20213: Molecular cloning and expression, biochemical characterization and synthesis of galacto-oligosaccharides. *PLoS One* 9:e104056. doi: 10.1371/journal.pone.0104056

Benjamins, E., Boxem, L., KleinJan-Noeverman, J., and Broekhuis, T. A. (2014). Assessment of repetitive batch-wise synthesis of galacto-oligosaccharides from lactose slurry using immobilised β-galactosidase from *Bacillus circulans*. *Int. Dairy J.* 38, 160–168. doi: 10.1016/j.idairyj.2014.03.011

Boehm, G., Lidestri, M., Casetta, P., Jelinek, J., Negretti, F., Stahl, B., et al. (2002). Supplementation of a bovine milk formula with an oligosaccharide mixture increases counts of faecal bifidobacteria in preterm infants. *Arch. Dis. Child Fetal Neonatal Ed.* 86, F178–F181.

Brás, N. F., Fernandes, P. A., and Ramos, M. J. (2010). QM/MM Studies on the β-Galactosidase Catalytic Mechanism: Hydrolysis and Transglycosylation Reactions. *J. Chem. Theory Comput.* 6, 421–433. doi: 10.1021/ct900530f

Chen, X. Y., and Gänzle, M. G. (2017). Lactose and lactose-derived oligosaccharides: More than prebiotics? *Int. Dairy J.* 67, 61–72. doi: 10.1016/j.idairyj.2016.10.001

Cheng, W., Lu, J., Li, B., Lin, W., Zhang, Z., Wei, X., et al. (2017). Effect of Functional Oligosaccharides and Ordinary Dietary Fiber on Intestinal Microbiota Diversity. *Front. Microbiol.* 20:1750. doi: 10.3389/fmicb.2017

Dall'Oglio, F., Milani, M., and Micali, G. (2018). Effects of oral supplementation with FOS and GOS prebiotics in women with adult acne?: the " S. O. Sweet " study?: a proof-of-concept pilot trial. *Clin. Cosmet. Investig. Dermatol.* 11, 445–449. doi: 10.2147/CCID.S179627

De Filippo, C., Cavalieri, D., Di Paola, M., Ramazzotti, M., Poullet, J. B., Massart, S., et al. (2010). Impact of diet in shaping gut microbiota revealed by a comparative study in children from Europe and rural Africa. *Proc. Natl. Acad. Sci. U S A.* 107, 14691–14696. doi: 10.1073/pnas.1005963107

de Ruyter, P. G., Kuipers, O. P., and de Vos, W. M. (1996). Controlled gene expression systems for *Lactococcus lactis* with the food-grade inducer nisin. *Appl. Environ. Microbiol.* 62, 3662–3667. doi: 10.1128/AEM.62.10.3662-3667

Edgar, R. C., Haas, B. J., Clemente, J. C., Quince, C., and Knight, R. (2011). UCHIME improves sensitivity and speed of chimera detection. *Bioinformatics* 27, 2194–2200. doi: 10.1093/bioinformatics/btr381

Ernst, O., and Zor, T. (2010). Linearization of the bradford protein assay. *J. Vis. Exp.* 38:1918. doi: 10.3791/1918

Fanaro, S., Marten, B., Bagna, R., Vigi, V., Fabris, C., Peña-Quintana, L., et al. (2008). Galacto-oligosaccharides Are Bifidogenic and Safe at Weaning?: A Double-blind Randomized Multicenter Study. *J. Pediatr. Gastroenterol. Nutr.* 48, 82–88. doi: 10.1097/MPG.0b013e31817b6dd2

Gibson, G. R., and Roberfroid, M. (1995). Dietary Modulation of the Human Colonie Microbiota: Introducing the Concept of Prebiotics. *J. Nutr.* 125, 1401–1412. doi: 10.1093/jn/125.6.1401

Gibson, G. R., Hutkins, R., Sanders, M. E., Prescott, S. L., Reimer, R. A., Salminen, S. J., et al. (2017). Expert consensus document: The International Scientific Association for Probiotics and Prebiotics (ISAPP) consensus statement on the definition and scope of prebiotics. *Nat. Rev. Gastroenterol. Hepatol.* 14, 491–502. doi: 10.1038/nrgastro.2017.75

Giovannini, M., Verduci, E., Gregori, D., Ballali, S., Ghisleni, D., Riva, E., et al. (2014). Prebiotic Effect of an Infant Formula Supplemented with Galacto-Oligosaccharides?: Randomized Multicenter Trial. *J. Am. Coll. Nutr.* 33, 385–393. doi: 10.1080/07315724.2013.878232

Goulas, A. K., and Tzortzis, G. (2007). *Process for the production of oligosaccharides*. Watford: Saunders & Dolleymore.

Goulas, T., Goulas, A., Tzortzis, G., and Gibson, G. R. (2009). Comparative analysis of four beta-galactosidases from *Bifidobacterium bifidum* NCIMB41171: purification and biochemical characterisation. *Appl. Microbiol. Biotechnol.* 82, 1079–1088. doi: 10.1007/s00253-008-1795

Goulas, T. K., Goulas, A. K., Tzortzis, G., and Gibson, G. R. (2007). Molecular cloning and comparative analysis of four β-galactosidase genes from *Bifidobacterium* bifidum NCIMB41171. *Appl. Microbiol. Biotechnol.* 76, 1365–1372. doi: 10.1007/s00253-007-1099-1

Han, Y. R., Youn, S. Y., Ji, G. E., and Park, M. S. (2014). Production of α - and β - Galactosidases from *Bifidobacterium longum* subsp. *longum* RD47. *J. Microbiol. Biotechnol.* 24, 675–682. doi: 10.4014/jmb.1402.02037

Hong, Y. H., Chang, U. J., Kim, Y. S., Jung, E. Y., and Suh, H. J. (2017). Dietary galacto-oligosaccharides improve skin health: A randomized double blind clinical trial. *Asia Pac. J. Clin. Nutr.* 26, 613–618. doi: 10.6133/apjcn.052016.05

Hung, M., Xia, Z., and Hu, N. (2001). Molecular and biochemical analysis of two beta-galactosidases from *Bifidobacterium infantis* HL96. *Appl. Environ. Microbiol.* 67, 4256–4263. doi: 10.1128/aem.67.9.4256-4263.2001

Husain, Q. (2010). Beta galactosidases and their potential applications: a review. *Crit. Rev. Biotechnol.* 30, 41–62. doi: 10.3109/07388550903330497

Hutkins, R. W., Krumbeck, J. A., Bindels, L. B., Cani, P. D., Fahey, G., Goh, Y. J., et al. (2016). Prebiotics: Why definitions matter. *Curr. Opin. Biotechnol.* 37, 1–7. doi: 10.1016/j.copbio.2015.09.001

James, K., Motherway, M. O., Bottacini, F., and van Sinderen, D. (2016). *Bifidobacterium breve* UCC2003 metabolises the human milk oligosaccharides lacto-N-tetraose and lacto-N-neo-tetraose through overlapping, yet distinct pathways. *Sci. Rep.* 8:38560. doi: 10.1038/srep38560

Jørgensen, F., Hansen, O. C., and Stougaard, P. (2001). High-efficiency synthesis of oligosaccharides with a truncated β-galactosidase from *Bifidobacterium bifidum*. *Appl. Microbiol. Biotechnol.* 57, 647–652. doi: 10.1007/s00253-001-0845-z

Juers, D. H., Matthews, B. W., and Huber, R. E. (2012). LacZ β-galactosidase?: structure and function of an enzyme of historical and molecular biological importance. *Protein Sci.* 21, 1792–1807. doi: 10.1002/pro.2165

Kim, S. H., Lim, K. P., and Kim, H. S. (1997). Differences in the Hydrolysis of Lactose and Other Substrates by beta -D-Galactosidase from *Kluyveromyces lactis*. *J. Dairy Sci.* 80, 2264–2269. doi: 10.3168/jds.S0022-0302(97)76175-7

Knol, J., Scholtens, P., Kafka, C., Steenbakkers, J., Gro, S., Helm, K., et al. (2005). Colon Microflora in Infants Fed Formula with Galacto- and Fructo-Oligosaccharides?: More Like Breast-Fed Infants. *J. Pediatr. Gastroenterol. Nutr.* 40, 36–42. doi: 10.1097/00005176-200501000-00007

Laemmli, U. K. (1970). Cleavage of Structura l Proteins during the Assembly of the Head of Bacteriophage T4. *Nature* 227, 680–685. doi: 10.1038/227680a0

Laere, K. M. J., van, Abee, T., Schols, H. A., Beldman, G., and Voragen, A. G. J. (2000). Characterization of a Novel beta -Galactosidase from *Bifidobacterium adolescentis* DSM 20083 Active towards Transgalactooligosaccharides. *Appl. Environ. Microbiol.* 66, 1379–1384. doi: 10.1128/aem.66.4.1379-1384.2000

Langdon, A., Crook, N., and Dantas, G. (2016). The effects of antibiotics on the microbiome throughout development and alternative approaches for therapeutic modulation. *Genome. Med.* 8:39. doi: 10.1186/s13073-016-0294-z

Lozupone, C. A., Stombaugh, J. I., Gordon, J. I., Jansson, J. K., and Knight, R. (2012). Diversity, stability and resilience of the human gut microbiota. *Nature* 489, 220–230. doi: 10.1038/nature11550

Macfarlane, G. T., Steed, H., and Macfarlane, S. (2008). Bacterial metabolism and health-related effects of galacto-oligosaccharides and other prebiotics. *J. Appl. Microbiol.* 104, 305–344. doi: 10.1111/j.1365-2672.2007.03520

Martins, G. N., Ureta, M. M., Tymczyszyn, E. E., Castilho, P. C., and Gomez-Zavaglia, A. (2019). Technological Aspects of the Production of Fructo and Galacto-Oligosaccharides. Enzymatic Synthesis and Hydrolysis. *Front. Nutr.* 6:78. doi: 10.3389/fnut.2019.00078

Mierau, I., and Kleerebezem, M. (2005). 10 years of the nisin-controlled gene expression system (NICE) in *Lactococcus lactis*. *Appl. Microbiol. Biotechnol.* 68, 705–717. doi: 10.1007/s00253-005-0107-6

Møller, P. L., Jørgensen, F., Hansen, O., Madsen, S. M., and Stougaard, P. (2001). Intra- and extracellular beta-galactosidases from *Bifidobacterium bifidum* and *B. infantis*: molecular cloning, heterologous expression, and comparative characterization. *Appl. Environ. Microbiol.* 67, 2276–2283. doi: 10.1128/AEM.67.5.2276-2283.2001

Mori, N., Kano, M., Masuoka, N., Konno, T., Suzuki, Y., and Miyazaki, K. (2016). Effect of probiotic and prebiotic fermented milk on skin and intestinal conditions in healthy young female students. *Biosci. Microbiota Food Health* 35, 105–112. doi: 10.12938/bmfh.2015-022

Moro, G. E., Stahl, B., Fanaro, S., Jelinek, J., Bohem, G., and Coppa, G. V. (2005). Dietary prebiotic oligosaccharides are detectable in the faeces of formula-fed infants. *Acta Paediatr. Suppl.* 94, 27–30. doi: 10.1111/j.1651-2227.2005.tb02151.x

O'Connell Motherway, M., Kinsella, M., Fitzgerald, G. F., and Van Sinderen, D. (2013). Transcriptional and functional characterization of genetic elements involved in galacto-oligosaccharide utilization by *Bifidobacterium breve* UCC2003. *Microb. Biotechnol.* 6, 67–79. doi: 10.1111/1751-7915.12011

Odamaki, T., Kato, K., Sugahara, H., Hashikura, N., Takahashi, S., Xiao, J. Z., et al. (2016). Age-related changes in gut microbiota composition from newborn to centenarian: a cross-sectional study. *BMC Microbiol.* 16:90. doi: 10.1186/s12866-016-0708-5

Osman, A., Symeou, S., Trisse, V., Watson, K. A., Tzortzis, G., and Charalampopoulos, D. (2014). Synthesis of prebiotic galactooligosaccharides from lactose using bifidobacterial β-galactosidase (BbgIV) immobilised on DEAE-Cellulose, Q-Sepharose and amino-ethyl agarose. *Biochem. Eng. J.* 82, 188–199. doi: 10.1016/j.bej.2013.11.020

Rodriguez-Colinas, B., Kolida, S., Baran, M., Ballesteros, A. O., Rastall, R. A., and Plou, F. J. (2013). Analysis of fermentation selectivity of purified galacto-oligosaccharides by in vitro human faecal fermentation. *Appl. Microbiol. Biotechnol.* 97, 5743–5752. doi: 10.1007/s00253-013-4892-z

Rothschild, D., Weissbrod, O., Barkan, E., Kurilshikov, A., Korem, T., Zeevi, D., et al. (2018). Environment dominates over host genetics in shaping human gut microbiota. *Nature* 555, 210–215. doi: 10.1038/nature25973

Sako, T., Matsumoto, K., and Tanaka, R. (1999). Recent progress on research and applications of non-digestible galacto-oligosaccharides. *Int. Dairy J.* 9, 69–80. doi: 10.1016/S0958-6946(99)00046-1

Saqib, S., Akram, A., Ahsan, S., and Raazia, H. (2017). Sources of β -galactosidase and its applications in food industry. *Biotech* 7:79. doi: 10.1007/s13205-017-0645-5

Sierra, C., Bernal, M. J., Javier, B., Martinez, R., Dalmau, J., Ortuño, I., et al. (2015). Prebiotic effect during the first year of life in healthy infants fed formula containing GOS as the only prebiotic?: a multicentre, randomised, double-blind and placebo-controlled trial. *Eur. J. Nutr.* 54, 89–99. doi: 10.1007/s00394-014-0689-9

Splechtna, B., Nguyen, T. H., Steinböck, M., Kulbe, K. D., Lorenz, W., and Haltrich, D. (2006). Production of prebiotic galacto-oligosaccharides from lactose using β-galactosidases from *Lactobacillus reuteri*. *J. Agric. Food Chem.* 54, 4999–5006. doi: 10.1021/jf053127m

Suh, M. G., Hong, Y. H., Jung, E. Y., and Suh, H. J. (2019). Inhibitory effect of galactooligosaccharide on skin pigmentation. *Prev. Nutr. Food Sci.* 24, 321–326. doi: 10.3746/pnf.2019.24.3.321

Torres, D. P. M., Gonçalves, M., do, P. F., Teixeira, J. A., and Rodrigues, L. R. (2010). Galacto-Oligosaccharides: Production, properties, applications, and significance as prebiotics. *Compr. Rev. Food Sci. Food Saf.* 9, 438–454. doi: 10.1111/j.1541-4337.2010.00119.x

Torres, P., and Batista-Viera, F. (2012). Improved biocatalysts based on *Bacillus circulans* β-galactosidase immobilized onto epoxy-activated acrylic supports: Applications in whey processing. *J. Mol. Catal.* 83, 57–64. doi: 10.1016/j.molcatb.2012.07.004

Tzortzis, G., Goulas, A. K., and Gibson, G. R. (2005). Synthesis of prebiotic galactooligosaccharides using whole cells of a novel strain, Bifidobacterium bifidum NCIMB 41171. *Appl. Microbiol. Biotechnol.* 68, 412–416. doi: 10.1007/s00253-005-1919-0

Urrutia, P., Fernandez-arrojo, L., Ballesteros, A. O., Wilson, L., and Plou, F. J. (2013). Detailed Analysis of Galactooligosaccharides Synthesis with. *J. Agric. Food Chem.* 61, 1081–1087. doi: 10.1021/jf304354u

Valdes, A. M., Walter, J., Segal, E., and Spector, T. D. (2018). Role of the gut microbiota in nutrition and health. *BMJ* 361, 36–44. doi: 0.1136/bmj.k2179

Van Leeuwen, S. S., Kuipers, B. J. H., Dijkhuizen, L., and Kamerling, J. P. (2016). Comparative structural characterization of 7 commercial galacto-oligosaccharide (GOS) products. *Carbohydr. Res.* 425, 48–58. doi: 10.1016/j.carres.2016.03.006

Viborg, A. H., Fredslund, F., Katayama, T., Nielsen, S. K., Svensson, B., Kitaoka, M., et al. (2014). Aβ1-6/β1-3 galactosidase from *Bifidobacterium animalis* subsp. *lactis*Bl-04 gives insight into sub-specificities of β-galactoside catabolism within *Bifidobacterium*. *Mol. Microbiol.* 94, 1024–1040. doi: 10.1111/mmi.12815

Wang, B. (2009). Sialic Acid Is an Essential Nutrient for Brain Development and Cognition. *Annu. Rev. Nutr.* 29, 177–222. doi: 10.1146/annurev.nutr.28.061807.155515

Warmerdam, A., Paudel, E., Jia, W., Boom, R. M., and Janssen, A. E. M. (2013). Characterization of β-Galactosidase Isoforms from Bacillus circulans and Their Contribution to GOS Production. *Appl. Biochem. Biotechnol.* 170, 340–358. doi: 10.1007/s12010-013-0181-7

Wichienchot, S., Hemmaratchirakul, J., Jaturapiree, P., and Pruksasri, S. (2016). Evaluating prebiotic property of galactooligosaccharide produced by *Lactobacillus pentosus* var. *Plantarum* BFP32 in fecal batch culture. *Int. Food Res. J.* 23, 2241–2248.

Wilson, B., and Whelan, K. (2017). Prebiotic inulin-type fructans and galacto-oligosaccharides?: de fi nition, speci fi city, function, and application in gastrointestinal disorders. *J. Gastroenterol. Hepatol.* 32(Suppl. 1), 64–68. doi: 10.1111/jgh.13700

Yoshida, E., Sakurama, H., Kiyohara, M., Nakajima, M., Kitaoka, M., Ashida, H., et al. (2012). *Bifidobacterium longum* subsp. *infantis* uses two different β -galactosidases for selectively degrading type-1 and type-2 human milk oligosaccharides. *Glycobiology* 22, 361–368. doi: 10.1093/glycob/cwr116

Conflict of Interest: MS, BK, and LC are employees of FrieslandCampina.

The remaining authors declare that the research was conducted in the absence of any commercial or financial relationships that could be construed as a potential conflict of interest.

frontiers in Microbiology

ORIGINAL RESEARCH
published: 07 June 2021
doi: 10.3389/fmicb.2021.669442

Association and Occurrence of Bifidobacterial Phylotypes Between Breast Milk and Fecal Microbiomes in Mother–Infant Dyads During the First 2 Years of Life

Wenli Yan[1], Baolong Luo[1], Xuyao Zhang[1], Yongqing Ni[1] and Fengwei Tian[2]**

[1] School of Food Science and Technology, Shihezi University, Shihezi, China, [2] School of Food Science and Technology, Jiangnan University, Wuxi, China

OPEN ACCESS

Edited by:
Abelardo Margolles, Consejo Superior de Investigaciones Científicas, Spain

Reviewed by:
Stefano Raimondi, University of Modena and Reggio Emilia, Italy
Anders P. Hakansson, Lund University, Sweden

***Correspondence:**
Yongqing Ni
niyqlzu@sina.com
Fengwei Tian
fwtian@jiangnan.edu.cn

Specialty section:
This article was submitted to Microbial Symbioses, a section of the journal Frontiers in Microbiology

Received: *18 February 2021*
Accepted: *30 April 2021*
Published: *07 June 2021*

Citation:
Yan W, Luo B, Zhang X, Ni Y and Tian F (2021) Association and Occurrence of Bifidobacterial Phylotypes Between Breast Milk and Fecal Microbiomes in Mother–Infant Dyads During the First 2 Years of Life. Front. Microbiol. 12:669442. doi: 10.3389/fmicb.2021.669442

Breast milk acts as an intermediary for the transfer of functionally important commensal bacteria from mother to infant, especially for *Bifidobacterium* that can colonize the infant gut. However, the vast majority of rRNA amplicon-based studies reported the conspicuous intercohort and interindividual variation for the prevalence of *Bifidobacterium* in breast milk. In order to elucidate whether *Bifidobacterium* phylotypes persistently co-occured at the species or strain level in mother–breast milk–infant triads, we analyzed collectively the next-generation sequencing (NGS) datasets of bacterial 16S rRNA gene and the *Bifidobacterium*-specific *gro*EL gene from maternal feces, breast milk, and infant feces in a small yet very homogeneous cohort of 25 healthy Uyghur mother–infant pairs (lactation for 7–720 days) in Kashgar, Xinjiang, China. Overall, 16S rRNA gene analysis showed that microbiome in the newborn gut was closer to that of breast milk in the first 4 months of lactation, and subsequently showed an obvious trend of adulthood at 6–12 months. Based on the BLAST accurate taxonomic result of the representative sequences of all ASVs (amplicon sequencing variants), only three sets of ASVs could be clearly assigned into *Bifidobacterium* species, whereas the remaining eight sets of ASVs corresponded to four indefinite *Bifidobacterium* species group. By contrast, the *groEL* gene dataset was partitioned into 376 ASVs, at least belonging to 13 well-known *Bifidobacterium* species or subspecies, of which 15 ASVs, annotated to seven well-known *Bifidobacterium* species or subspecies, showed triadic synchronism in most 23 mother–infant pairs tested. However, several other rare bifidobacterial phylotypes, which were frequently encountered in animals, were found to display no correspondence of the presence between the three ecosystems of mother–infant pairs. Our test results were obviously to support the hypothesis that breast milk acts as an intermediary for the transfer of probiotic commensal bacteria from mother to infant, especially for endosymbiotic *Bifidobacterium* that can colonize

the infant gut. Some oxygen-insensitive exogenous *Bifidobacterium* phylotypes with a cosmopolitan lifestyle may be indirectly transferred to breast milk and the infant's intestinal tract through environmental contamination. Thus, the *gro*EL gene proved to be a very effective target for the depth resolution of *Bifidobacterium* community by high-throughput sequencing technologies.

Keywords: human breast milk, mother–infant dyads, microbiome, *Bifidobacterium*, association

INTRODUCTION

Breast milk is generally regarded as the best source of nutrients for healthy growth and development of infants (Bode, 2012; Ballard and Morrow, 2013). Over the past decade and a half, many studies have focused on the bacterial community of breast milk using both culture-dependent and culture-independent techniques. Culture-independent techniques, based on the amplicon analysis of 16S rRNA gene, revealed the presence of several hundred bacterial species from breast milk up to now, the most common genus of which includes *Staphylococcus*, *Streptococcus*, *Flavobacterium*, *Propionibacterium*, *Burkholderia*, *Rothia*, *Corynebacterium*, and *Lactobacillus*, commonly known as a core milk microbiota (Heikkila and Saris, 2003; Groenlund et al., 2007; Martin et al., 2007; Perez et al., 2007; Collado et al., 2009; Hunt et al., 2011; Fitzstevens et al., 2017).

The origins of the bacteria in breast milk are thought to include the maternal gut (via an entero-mammary pathway) and through bacterial exposure of the breast during nursing (skin microbiota and the oral cavity of the infant) (Mueller et al., 2015). Increasingly, accumulating evidence highlights that the maternal gut serves as the most relevant source of bacteria that are detectable in breast milk. With the consumption of breast milk, and the reduced oxygen/redox potential in the infant gut, the obligate anaerobic bacteria emerge in the infant gut, especially the *Bifidobacterium* species and *Bacteroides* species (Ferretti et al., 2018). In the skin microbiome of a healthy human, by contrast, a member of *Bifidobacterium* was not detected (Oh et al., 2016), and was reported occasionally in the oral cavity of infants and the vagina of their mothers (Sundin et al., 2017; Dzidic et al., 2018; Nyangahu and Jaspan, 2019). So, breast milk constitutes the main source of an array of potentially beneficial bacteria to the breastfed infant gut.

Previous studies showed that total bacteria concentration is lower in colostrum than in transitional and mature milk, with increasing levels of *Bifidobacterium* in breast milks over lactation time (Cabrera-Rubio et al., 2012; Khodayar-Pardo et al., 2014; Sakwinska et al., 2016). Indeed, in a previous study, no bifidobacteria were detected from colostrum, and *Bifidobacterium* strains were isolated only from breast milk samples obtained 7 days after birth or later. Again, despite the use of advanced next-generation sequencing (NGS) of 16S rRNA gene amplicon, presences of *Bifidobacterium* spp. were sporadically reported in a few colostrum samples or not at all. In contrast, the prevalence of bifidobacteria in transitional and mature milks was generally increased, but its relative abundance is only 0.1–1.3% or lower. More notably, *Bifidobacterium* populations were not also detected in a considerable proportion of transitional and mature milk samples, although an identical test method was applied to the same batch of samples (Hunt et al., 2011; Urbaniak et al., 2016; McGuire and McGuire, 2017; Murphy et al., 2017).

In general, bacterial loads of feces samples are five to seven orders of magnitude higher than in breast milk (Fernandez et al., 2013). From 1 to 6 months of age, members of the genus *Bifidobacterium* clearly dominate the infant gut microbiota, regardless of delivery mode, representing an average of 10–90% of the total infant gut microbiota (Turroni et al., 2012; Lim et al., 2016; Lundgren et al., 2018). However, a small proportion of infants have very low abundance or undetectable bifidobacteria as members of the fecal microbiota regardless of breast milk or formula feeding (Koenig et al., 2011; Yatsunenko et al., 2012; Subramanian et al., 2014).

While multiple studies have shown that specific *Bifidobacterium* strains in the maternal gut are transferred to the infant gut through breastfeeding (Makino et al., 2011, 2013; Milani et al., 2015; Duranti et al., 2017), the sources and ways of acquisition of these potential probiotic bacteria regarding establishing a sound intestinal microbiome for infants are poorly understood. As a whole, it is not clear how bifidobacterial community from the maternal gut or breast milk progressively transmits to the infant gut during the first 2 years of life, and whether there is the concordance of the presence of *Bifidobacterium* spp. between the three ecosystems, represented by maternal feces, breast milk, and neonatal feces.

Next-generation sequencing is a more sensitive and less biased analytical method than the culture-based method (Hunt et al., 2011; Jost et al., 2013; Ward et al., 2013). These methods generate tens of thousands of 16S rRNA gene sequences per DNA sample, but taxa present in very low abundance could still be missed (Meehan et al., 2018). In addition, 16S rRNA gene-based profiling of the human microbiota is strongly influenced by sample processing and the choice of PCR primers, leading to underrepresentation of bifidobacteria in 16S rRNA sequence dataset. Also, it is difficult to identify the members of *Bifidobacterium* at species level by 16S rRNA short variable region amplicon sequencing (Schloss and Westcott, 2011). All these reasons result in inconsistent detection of the proportional abundance of specific bacteria taxa of human microbiota, including *Bifidobacterium* spp. Particularly, breast milk samples are highly variable in bacterial load values. There are large individual differences over time between samples from the different mothers and, in some cases, even within individuals at different time points (Bode et al., 2014; Moossavi et al., 2019). Therefore, we are more interested in the

co-occurrence and combination of gut symbiotic *Bifidobacterium* phylotypes in mother–breast milk–infant triads than in their absolute content.

More recently, the *groEL* gene proved to be a very effective target for the identification and quantification of *Bifidobacterium* spp. through high-throughput sequencing technologies or qPCR (Junick and Blaut, 2012; Hu et al., 2017). In this study, a comparative analysis of feces and breast milk microbiota in a small, yet very homogeneous cohort of 25 healthy mother–infant pairs in Kashgar, northwest China (n = 25, infants' age from 7 days to 2 years), was presented, using high-throughput sequencing technologies of the 16S ribosomal RNA gene and *groEL* gene specific to the genus *Bifidobacterium*. Our research objective is to assess the association of bifidobacterial phylotypes between infant feces and their mothers' breast milk and maternal feces in mother–breast milk–infant triads, with the emphasis on the number and changes of *Bifidobacterium* phylotypes in the infant feces and breast milk.

TABLE 1 | Demographic characteristics of our cohort.

Characteristics and demographic data	Values or no. (%)
Infant gender	
Male	15 (60)
Female	10 (40)
Maternal BMI condition	
Normal (18.5–23.9)	16 (64)
Slightly fat (24.0–26.9)	4 (16)
Obesity (27–29.9)	3 (12)
Severe obesity (≥30)	1 (4)
Unknown	1 (4)
Infant age at specimen collection (days)	
7–180	8 (32)
206–365	8 (32)
366–720	9 (36)
Feeding patterns	
Exclusively	9 (36)
Partial feeding	16 (64)
Infant weight (kg)	7.58 ± 2.89*
Infant length (cm)	58.50 ± 9.63*
Infant age (days)	312.04 ± 191.71

**Mean ± SD.*

MATERIALS AND METHODS

Sample Collection

We collected breast milk and feces samples from mothers and their infants between 7 and 720 days after birth, during clinic or home study visits and recruited mother–infant pairs meeting the following criteria: (i) the Uighur people native to Kashgar, Xingjiang, (ii) vaginal delivery at full-term (≥37 week gestation), (iii) exclusive breastfeeding during the first 5 months and the lactation continuing until sampling, and (iv) no antibiotic/probiotic exposure of either the mother or the infant during pregnancy, intrapartum, or postnatally. All the participants were healthy and did not require hospitalization. They were included for microbiota analysis with standard collection protocol (Sakwinska et al., 2016). Nevertheless, our samples were collected from all the mother–infant pairs for only one time, and a longitudinal study was not carried out.

Demographic and clinical data were recorded in a specific case report form. All participants responded to a general questionnaire including socioeconomic, lifestyle aspects, and body mass index (BMI) of the mother. The case report recorded the number of gestational weeks at delivery, delivery method, feeding patterns, the gender, height, weight, and head circumference (for the newborn) of the infant. All demographic data of our cohort is summarized in **Table 1**, and this cohort has been reported in a previous study, which was focused on *Lactobacillus* (Zhang et al., 2020).

Standard sterile collection tubes were used to collect feces and breast milk (with the aid of a breast pump) samples. For breast milk, the first few drops (0.5–1 ml) were discarded, and the breast was thoroughly cleansed with chlorhexidine solution before manually collecting 3–5 ml of milk. Samples were immediately transported to the laboratory using portable refrigerators and ice packs. Each breast milk sample was divided into several 1-ml servings into sterile centrifuge tube and 500-mg feces sample were divided into a sterile centrifuge tube ready for DNA extraction and then were all frozen at −80°C in batches for processing and remained frozen until DNA extraction. All samples were collected and stored on the same day, and total bacterial DNA was extracted within 7 days of sampling as well as sequenced, to reduce the errors caused by the condition of storage, experiment, and sequencing.

DNA Extraction and High-Throughput Sequencing

For breast milk samples, TIANamp Blood DNA Kit (TIANGEN, Beijing, China) was utilized with some modifications, referring to Sakwinska et al. (2016) to extract bacteria DNA. One milliliter of breast milk was centrifuged at full speed (12,000 rpm) for 10 min at 4°C. The pellets were resuspended in 200 μl of Tris-EDTA buffer and treated with 10 μl of lysozyme (50 mg/ml) and 5 μl of DNase-free RNase (20 mg/ml) for 30 min at 37°C. Twenty-five milligrams of glass beads (10 μm) was added to the solution and treated with three bead-beating steps in a FastPrep instrument (MP Biomedicals, Irvine, CA, United States) at 5.5 movements per second for 1 min. After the instantaneous centrifugation, the supernatants were collected and treated with 20 μl of proteinase K for 20 min at 56°C. Two hundred microliters of GB buffer was added, and samples were incubated at 65°C for 10 min, and then 200 μl of ethanol was added. DNA was further purified using Spin Columns CB3 (TIANGEN) following the manufacturer's instructions. The feces samples were processed with the TIANamp DNA Stool Kit (TIANGEN, Beijing, China) according to the manufacturer's instructions. Extracted DNA was quantified using the nucleic acid quantifier (NanoDrop Technologies, Wilmington, DE, United States).

Sequencing Data Processing

For each sample, the V4–V5 region of the 16S rRNA gene and the *groEL* gene was amplified and sequenced according to the manufacturer's instructions (Illumina, San Diego, CA, United States) by Shanghai Personal Biotechnology Co., Ltd., Shanghai, China[1]. Primer pairs for *groEL* sequences (Bif-groEL-F: 5-TCC GAT TAC GAY CGY GAG AAG CT-3/Bif-groEL-R: 5-CSG CYT CGG TSG TCA GGA ACA G-3) belonging to the target *Bifidobacterium* and available in GenBank release 234.0 (Benson et al., 2011) were designed by the Jiangnan University (Hu et al., 2017).

Raw sequences were processed by using a pipeline combining USEARCH v10.0 (Edgar, 2010) and QIIME (Caporaso et al., 2010). High-quality reads, as selected using the default values in USEARCH, were binned into ASVs (amplicon sequence variants) according to the denoising (error correcting) Illumina amplicon reads using Unoise3 (Edgar, 2017), through an open-reference strategy. Taxonomic identification of ASVs for the V4–V5 region sequences was assigned using the Naive Bayes classifier of the Ribosomal Database Project (RDP) against Greengenes database (August 2013 release). Meanwhile the taxonomy of ASVs for the *groEL* sequences was performed through comparison with the Chaperonin Sequence Database[2] (Hill et al., 2004) and the National Center for Biotechnology Information (NCBI).

The diversity index was calculated by QIIME, and statistics and plot were performed using R software (version 4.0.2). Observed ASVs and Shannon index were analyzed as alpha rarefaction metrics. Weighted and unweighted UniFrac distances were computed as beta diversity, which was used for principal coordinate analyses (PCoA), and the function "adonis" of the *vegan* package of R software was utilized to test the significance of separation by permutational multivariate analysis of variance. *p*-values were corrected for multiple comparisons using the Benjamini–Hochberg method. $p < 0.05$ was considered statistically significant. The R function *hclust()* and package *ggtree* were utilized to cluster samples based on the Bray–Curtis similarity index using average linkage clustering and generate the dendrogram. Linear discriminant analysis (LDA) effect size (LEfSe) analysis was performed by R package *dplyr* and an open-reference strategy (Zhang et al., 2018). The bifidobacterial co-occurrence relationship of breast milk, infant feces, and maternal feces was determined based on the Spearman correlation coefficient and was visualized using the *AnnotationDBi* package.

RESULTS

Microbial Community Structures in Breast Milk

The extracted bacterial DNA was phylogenetically characterized by the 16S rRNA gene (V4–V5 regions) Illumina sequencing. A total of 1,620,470 high-quality reads were obtained. Reads were binned into 1,936 ASVs. The bacterial community was distinct between breast milk, maternal feces, and infant feces in both composition and diversity. In the breast milk and feces samples, the most abundant phylum was, respectively, *Proteobacteria* (average relative abundance: 46.5%) and *Firmicutes* (mothers: 60.2%, infants: 58.3%; **Figure 1A**). The two most frequently present families in the breast milk were *Enterobacteriaceae* (25.5%) and *Streptococcaceae* (19.3%). In the infant feces samples, *Streptococcaceae* (26.1%), *Lactobacillaceae* (16.3%), and *Enterobacteriaceae* (11.5%), were the three most dominant families. In the maternal feces, *Ruminococcaceae* (17.6%) and *Streptococcaceae* (9.2%) constituted the predominant families. *Pseudomonadaceae*, as a family consisting of mostly aerobic bacteria, has an average relative abundance (rel. ab.) in breast milk that was obviously higher (2.2%) than those in the feces (infants: 0.2%, mothers: 0.04%), whereas the average rel. ab. of *Ruminococcaceae*, as one of the most important anaerobic bacterial families, was lower in breast milk (<0.1%) than in feces (infants: 3.8%; mothers: 17.6%). The results of the adonis analysis based on Euclidean matrix calculated from microbial relative abundance at the family level (**Supplementary Table 1**) showed that the correlation between the microbial community structure (the family level) of breast milk and maternal BMI, feeding patterns, infants' age, gender, and weight status was not significant ($R^2 < 0.2$, $p > 0.05$); the microbial community structure of the maternal feces was only significantly correlated with the weight status ($R^2 = 0.23$, $p = 0.001$), while that of infants' feces was only significantly correlated with age (day; $R^2 = 0.13$, $p < 0.01$).

We next used LEfSe to perform differentially abundant analysis at different taxonomic levels (from phylum to genus) between samples from three ecosystems (maternal feces, infant feces, and breast milk). Only the ASVs with relative abundance more than 0.01% were selected for the more accurate analysis. LEfSe analysis identified 109 differentially abundant genera and 198 differentially predominant families in three ecosystems (**Supplementary Figure 1**). From the cladogram that represents differentially abundant taxonomic level from phylum to genus level, it was evident that the breast milk harbored significantly more indicator taxa. In order to further observe the relationship of microbial composition of infants' feces samples with that of samples from maternal feces and breast milk at different stages of lactation, we investigated the occurrence of biomarkers (LDA score > 3, $p < 0.001$) and dominant families in three ecosystems. Also, according to the results (**Figure 1B**), we found that feces microbiome of infants of younger age were more similar to breast milk microbiome (hierarchical clustering), which was represented by higher relative abundance of Enterobacteriaceae and *Citrobacter*, while the feces microbiome of infants with higher age were closer to those of mothers, mainly represented as higher relative abundance of *Prevotella* and *Catenibacterium*. It indicated that the temporal succession of the microbial community structure of the infants' gut is actually a process by which the microbial composition similar to breast milk microbiome tends to be similar to the maternal gut microbiome.

Next, FEAST, a microbial sources tracking tool (Shenhav et al., 2019), was used to calculate the microbial source proportion of 25 infants' feces, that from their mothers' feces, and breast milk at ASV level. We found that the feces microbiome of the majority of

[1]http://www.personalbio.cn/

[2]http://www.cpndb.ca

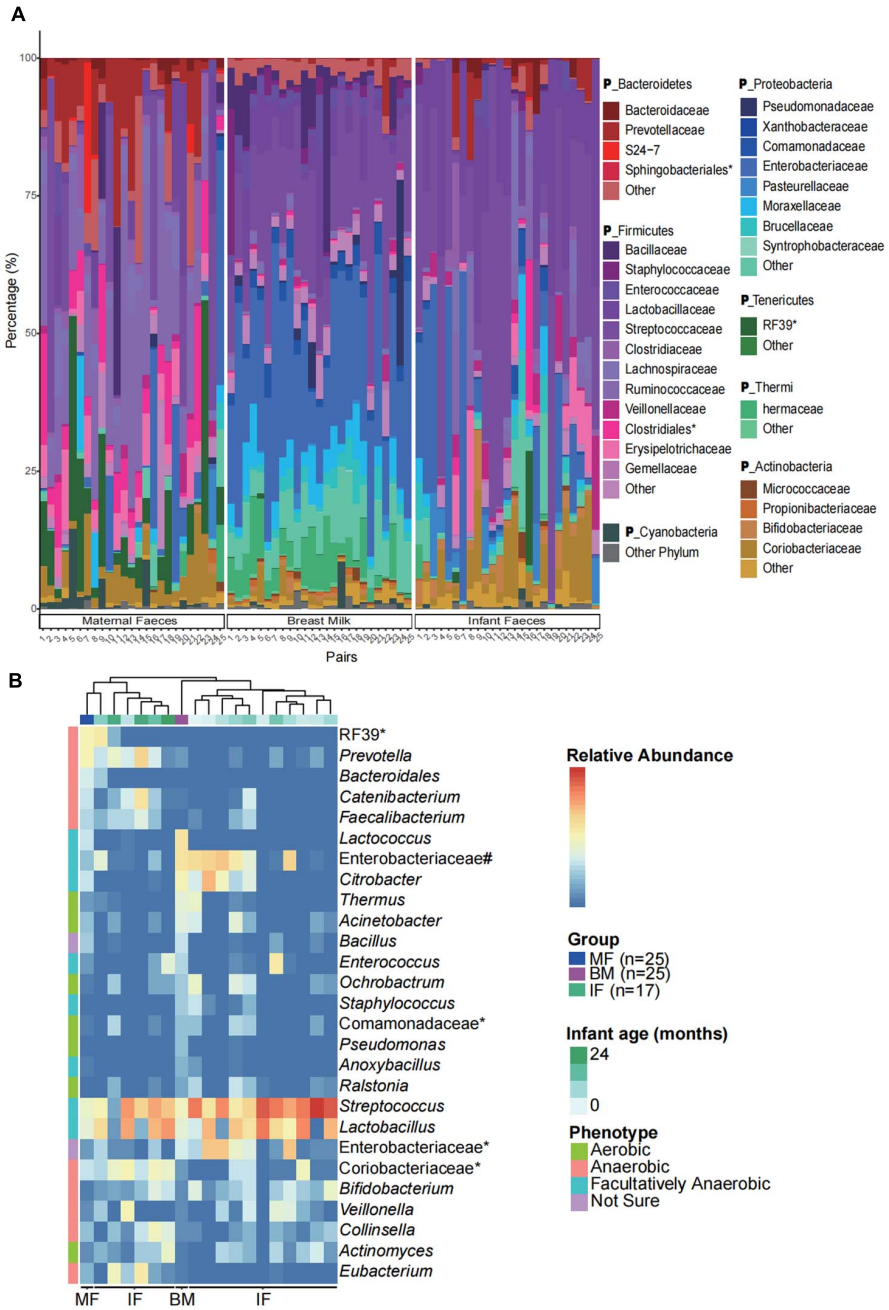

FIGURE 1 | Microbial community characteristics of the infant feces, maternal feces, and breast milk samples. **(A)** Community structure of the dominant bacteria in breast milk and feces samples of all infants and their mothers at the family level. IF, infant feces; MF, maternal feces; BM, breast milk. *The unclassified bacteria at the family level. The **P_** in taxonomy labels indicate that the level of taxonomy is phylum. **(B)** The relative abundance of the biomarkers (at the genus level) in feces samples of 17 infants aged 0, 1, 2, 3, 4, 5, 6, 7, 8, 9, 11,12,13, 15, 20, 21, and 24 months (only one infant feces sample per month) and in feces and breast milk samples of all mothers (n = 25). The groups are ordered by hierarchical clustering of Bray–Curtis dissimilarities. *The unclassified bacteria at the genus level. #Other genera of Enterobacteriaceae. The biologically interpretable phenotypes (oxygen tolerance) are predicted by algorithm BugBase.

infants (16/25) were more likely to be derived from their mothers' breast milk than from their mother's feces (**Figure 2**). The correlation between the ratio of source proportion of mother's faces and breast milk and infants' gender, weight status, and maternal obesity were not significant ($p > 0.05$; data not shown).

Intra- and Intergroup Diversity Analysis

A constrained principal coordinate analyses (CPCoA) based on the Bray–Curtis distance showed that the microbiota of breast milk, maternal feces, and infant feces, as expected, clustered separately, and the adonis test confirmed that the reported

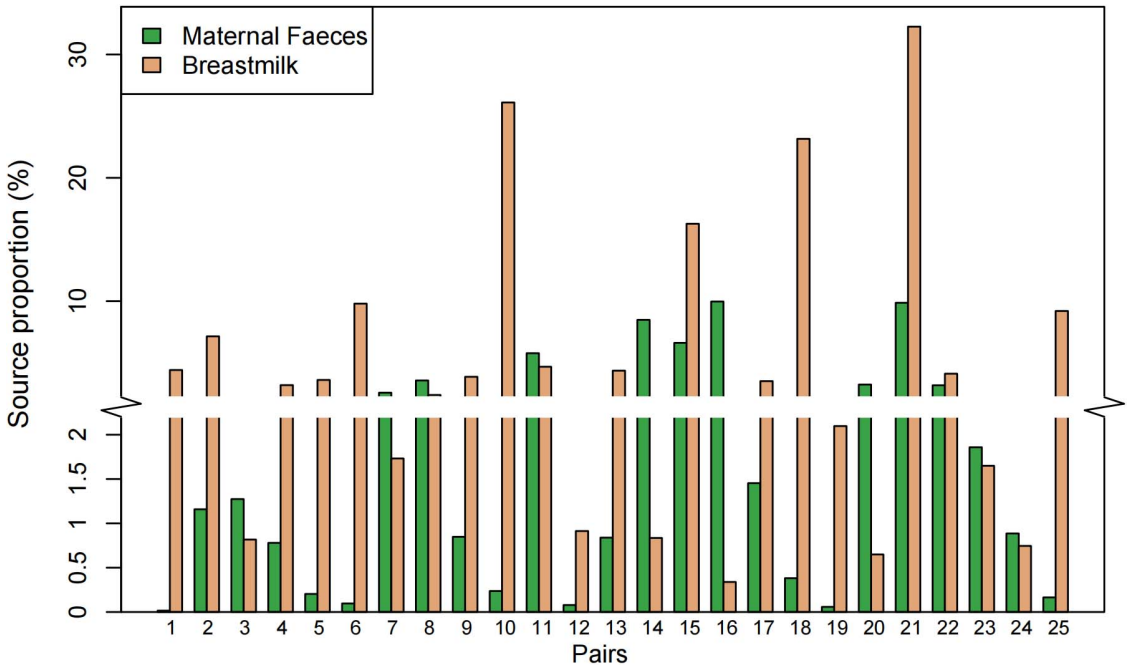

FIGURE 2 | Proportion of the microbial sources at amplicon sequencing variants (ASV) level in infant feces using the FEAST model. The *y*-axis truncation value is 2.1–2.9.

separation was significant (**Figure 3A**). The average microbiota profile obtained for breast milk was significantly more diverse (observed ASV index = 204 ± 109; **Figure 3B**) than both maternal and infant feces (176 ± 81 and 148 ± 118, respectively); interestingly, according to the unweighted UniFrac metric, the variability among breast milk samples was the lowest across all samples (0.30 ± 0.05; Kruskal–Wallis test $p < 0.0001$; **Figure 3C**). Meanwhile, the same result is presented in **Figure 3D**, which considers both phylogeny and relative abundance (α-diversity and β-diversity determined by Rao's diversity decomposition at the ASVs level) (Rao, 1984). In other words, the breast milk ecosystem of the 25 enrolled mothers was more complex and less heterogeneous among samples (in terms of bacterial species) than the fecal ecosystem, suggesting that the bacteria from other ecosystems, except the maternal gut, also could be transferred to breast milk.

Bacterial Groups With Statistical Differences

Bifidobaterium Profile Identified by 16S rRNA Gene Sequencing

It may be clear that seeding of early life microbiota with maternal microbes leaves a lasting imprint on the biology of infants. Considering the importance of *Bifidobacterium* as a health-promoting commensal of the gut microbiome in populations, it is necessary for us to delve deeply into the subdata of bifidobacteria in the whole dataset of mother and child pairs, rather than simply categorizing them into the "other" group in each sample as some reports have done. In the present study, in order to obtain more accurate taxonomic results at species level, the representative sequences of all 11 ASVs (which were identified as members of the *Bifidobaterium* genus) were extracted to homology search using NCBI BLAST[3]. Due to the limited resolving power of the 16S rRNA gene in the identification of different bacteria species, only three ASVs were clearly assigned into the *Bifidobacterium* species level: *Bifidobacterium adolescentis*, *B. pseudolongum*, and *B. bifidum*, respectively. The representative sequences of the remaining eight ASVs corresponded to four species groups (Query Coverage and Percent Identity were both 100%) of *Bifidobacterium* (each contains multiple closely related species recognized), namely, *B. breve/longum* (three ASVs), *B. pseudocatenulatum/kashiwanohense* (three ASVs), *B. adolescentis/faecale* (one ASV), and *B. angulatum/merycium* (one ASV). Overall, the average relative abundance of *Bifidobacterium* species groups varied depending on the types of samples, and their prevalence differed significantly among sample sets of three ecosystems. As shown in **Table 2**, the most predominant phylotype was the one belonging to the *B. breve/longum* group, the prevalence of which was 100% in infant feces. As expected, the average rel. ab of the *B. adolescentis* in maternal feces was higher than that in breast milk and infant feces, but its detection rate was only 72% in maternal feces, with seven maternal feces being negative. The *B. pseudocatenulatum/kashiwanohense* group was detected in approximately 80% of infant feces. The detection rate of *B. bifidum* in breast milk and infant feces was higher than in maternal feces. *B. pseudolongum* was detected in only four breast

[3]https://blast.ncbi.nlm.nih.gov/BlastAlign.cgi

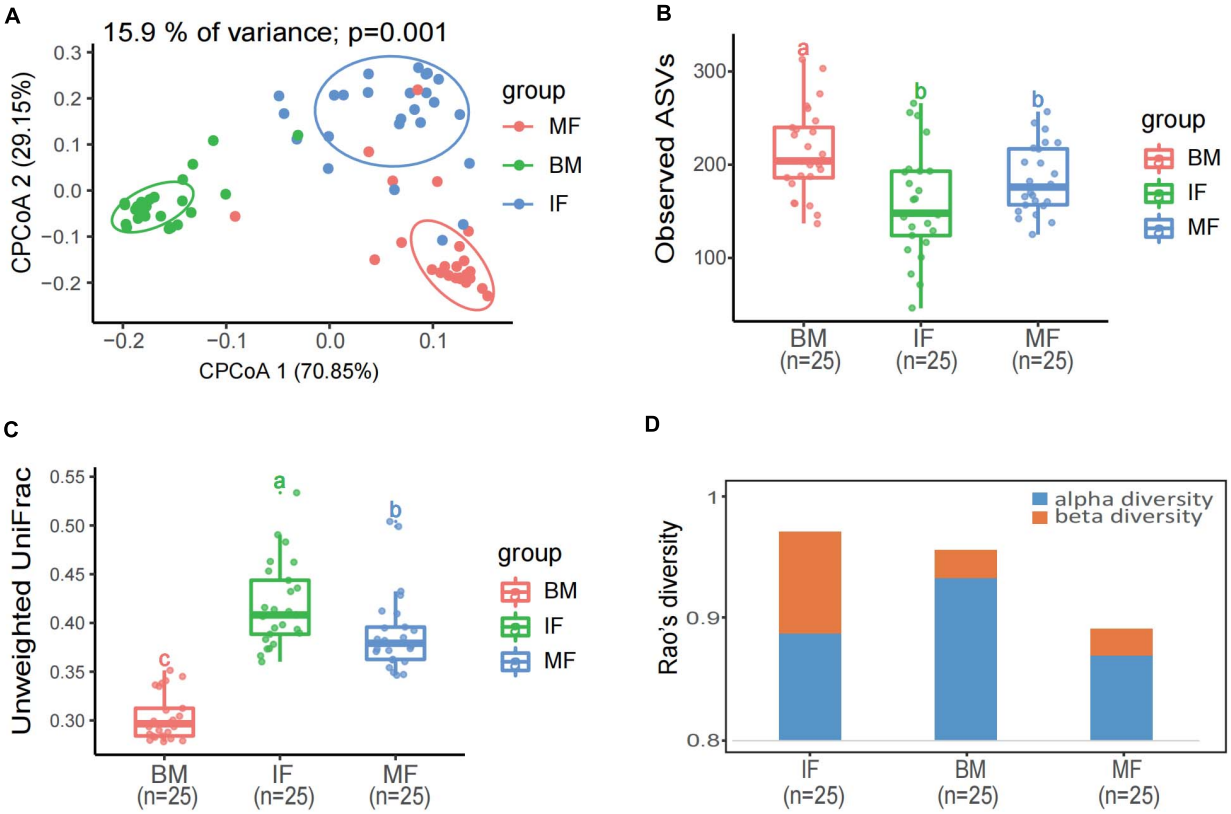

FIGURE 3 | Diversity analysis of bacterial communities in infant feces, maternal feces, and breast milk samples. **(A)** Constrained principal coordinate analysis plot of Bray–Curtis distances between samples including three groups (15.9% of variance, $p = 0.001$; $n = 75$). Ellipses represent a 95% confidence interval around the cluster centroid. IF, infant feces; MF, maternal feces; BM, breast milk. **(B)** Box plot of the observed ASV index and **(C)** intragroup unweighted UniFrac distances calculated for maternal feces group (red), breast milk group (green), and infant's feces group (blue) samples. Statistical analysis was performed using the permutational multivariate analysis of variance. **(D)** The α-diversity and β-diversity of three groups determined by Rao's diversity decomposition at the ASVs level, considering both phylogeny and relative abundance.

milk and undetected at any feces samples. Because the sequences that were annotated to match *Bifidobacterium* accounted for a very low proportion in the 16S rRNA gene datasets of all three types of samples, a limited number of ASVs were found to share among the three ecosystems.

Bifidobacterium Profile Identified by *gro*EL Gene Sequencing

In *gro*EL gene Illumina sequencing dataset, two samples (a maternal feces sample and an infant feces sample from a different mother–infant pair) with extremely low reads (<800) were removed. A total of 1,702,445 high-quality reads were obtained, and then were binned into ASVs (n = 376) according to the denoising (error correcting). As expected, the large majority of the recovered reads (90%) matched the DNA of the members of the genus *Bifidobacterium*. In order to accurately assess the association between maternal breast milk and fecal bifidobacterial community, our analysis was performed at the species level as much as possible. Consequently, multiple ASVs that hit the same nearest neighbor were identified as belonging to a specific species and/or subspecies regardless of the small sequence divergence. Taxonomic annotation showed that 376 ASVs were assigned to at least 13 members of *Bifidobacterium* that contain five well known subspecies, including *B. adolescentis* (counts of ASVs: 49), *B. angulatum* (34), *B. animalis* subsp. *animalis*

TABLE 2 | The relative abundance and detection rate of bifidobacteria group obtained by the National Center for Biotechnology Information (NCBI) comparison in the three ecosystems.

Taxa	Average relative abundance (detection rate) (%)		
	MF	BM	IF
Bifidobacterium bifidum	0.003 (12)	0.053 (64)	0.104 (60)
Bifidobacterium breve/longum	0.107 (56)	0.283 (96)	1.834 (100)
Bifidobacterium pseudocatenulatum/ kashiwanohense	0.028 (24)	0.011 (32)	0.358 (80)
Bifidobacterium adolescentis	0.031 (72)	0.019 (24)	0.017 (24)
Bifidobacterium adolescentis/faecale	0.057 (4)	0.054 (64)	0.003 (12)
Bifidobacterium pseudolongum	0 (0)	0.016 (16)	0 (0)
Bifidobacterium angulatum/merycium	0.002 (16)	0 (4)	0.004 (20)

(4), *B. animalis* ssp. *lactis* (4), *B. bifidum* (36), *B. breve* (16), *B. kashiwanohense* (85), *B. longum* ssp. *infantis* (58), *B. longum* ssp. *longum* (36), *B. pseudocatenulatum* (22), *B. pseudolongum* (8), *B. pseudolongum* ssp. *globosum* (6), and *B. ruminantium* (18). A neighbor-joining phylogenetic tree containing the representative sequences of all ASVs and closely related bifidobacterial taxon was constructed (**Supplementary Figure 2**).

The bifidobacterial community profiles presented in all samples among three ecosystems are shown in **Figure 4**, which showed noticeable differences between sample groups in the composition, relative abundance, and diversity. In infant feces samples, the bifidobacterial community structure (composition and abundance) were more similar to that in breast milk samples (**Figure 4A**). However, the beta diversity analysis exhibited diametrically opposed results. As was shown in the result of hierarchical clustering and PCoA based on the unweighted UniFrac distance (ignored the abundance of all phylotypes in each sample), the bifidobacterial flora in the infant feces is more similar to that in the maternal feces even if there were significant differences between the three ecosystems ($p < 0.001$) (**Figures 4B,C**). The result of PCoA based on weighted UniFrac distance indicated that *Bifidobacterium* microbiome of maternal feces samples was more distinctive compared with that of breast milk and infant feces (**Figure 4D**).

Analysis of proportion abundances and detection rates (presence/absence), based on the whole *groEL* gene amplicons (**Figure 5**), shows that the dominant bifidobacteria taxon in breast milk and infant fecal samples were *B. longum* ssp. *infantis* (the average rel. ab. Of 43.5 and 39.0% in breast milk and infant feces, respectively, of the *groEL* gene amplicons of the genus *Bifidobacterium*) and *B. kashiwanohense* (14.8% in breast milk and 29.1% in infant feces), followed by *B. breve* and *B. longum* ssp. *longum*. On the contrary, the fecal samples from the mothers were dominated by *B. adolescentis* and *B. angulatum*, accounting for 52.0 and 12.6%, respectively, of the *groEL* gene amplicons of the genus *Bifidobacterium*. In contrast to maternal feces samples, the average rel. ab. of these two bifidobacterial species were very low in breast milk (1.2 and 0.2%) and infant feces (1.7 and 1.3%). Intriguingly, *B. bifidum*, considered as one of the infant-type bifidobacteria, was more abundant in the feces samples of mothers than that of infants. Another special bifidobacteria was *B. ruminantium* with the highest detection rates (100%) and lower relative abundance (0.06%) in maternal feces. However, its mean relative abundance in breast milk (<0.001%) and infant feces (0.8%) was significantly decreased, and no *B. ruminantium* ASV was detected in quite a few samples, especially in breast milk samples (detection rates in breast milk and infant feces: 30.4 and 70.0%).

The Co-occurrence of *Bifidobacterium* Phylotype in Mother–Breast Milk–Infant Triads Based on *gro*EL Gene

To get a better view of the bifidobacterial co-occurrence and association between mother–infant pairs, the detection rates (presence/absence) and average rel. ab. of each *Bifidobacterium* phylotype and its corresponding ASVs in breast milk and feces samples were analyzed deeply in mother–breast milk–infant triads (23 pairs with three ecosystem data simultaneously). Of 13 *Bifidobacterium* phylotypes (species or subspecies), 7 phylotypes, namely, *B. adolescentis*, *B. kashiwanohense*, *B. longum* ssp. *infantis*, *B. bifidum*, *B. breve*, *B. longum* ssp. *longum*, and *B. pseudocatenulatum*, were identified to be universally distributed in more than 90% samples of three ecosystems, with the exception of *B. bifidum* whose prevalence in the maternal feces was 78%, implying that they are shared nearly by all 23 mother–infant pairs analyzed (**Table 3**). ASV with an average rel. ab. greater than 1% in any one ecosystem was defined as dominant ASV, and 50 dominant ASVs were obtained. Among these 50 dominant ASVs, the co-occurrence of different ASVs belonging to the same *Bifidobacterium* phylotype was not exactly the same in infant–milk–mother triads (**Figure 6**). In these dominant ASVs, 14 ASVs were annotated as *B. kashiwanohense*, and they could be clustered into three clusters by a phylogenetic tree. Among them, the cluster composed of ASV_26, ASV_43, ASV_71, and ASV_82 had lower detection rates in breast milk samples than in feces samples; on the contrary, the detection rate of ASV_21 in breast milk was higher. It is worth noting that there were nine dominant ASVs annotated as *B. adolescentis*, but only one ASV has a high co-occurrence rate in infant–milk–mother triads (21/23). Moreover, out of a total of 49 ASVs, assigned to *B. adolescentis*, 18 ASVs were detected only in maternal feces samples in more than half of mother–infant pairs (more than 11 pairs) (**Supplementary Table 2**). In contrast, of the eight dominant ASVs annotated as *B. longum* ssp. *infantis*, six ASVs were co-occurrence in more than half of the infant–milk–mother triads of mother–infant pairs. Moreover, *B. ruminantium* and *B. angulatum* presented in almost all maternal feces samples, but were absent in more than half of the breast milk samples. In 11 mother–infant pairs, *B. ruminantium* was concurrently detected in the feces samples of infants and their mothers, but was not detected in the corresponding breast milk samples. Interestingly, we found that among the dominant ASVs annotated as *B. ruminantium*, if they can be detected in the infant feces sample, they can also be detected in feces samples of their mothers. In addition, the detection frequency of *B. animalis* and *B. pseudolongum* in breast milk samples (100 and 91.3%) was significantly higher than that in the feces samples of mothers (30.4 and 21.7%) and infants (30.4 and 69.6%). In terms of the same mother–infant pair, the dominant ASV (ASV_11), annotated as *B. animalis* ssp. *Animalis*, was concurrently detected in infants' feces samples and their mothers' breast milk samples of 16 mother–infant dyads, but present only in the feces samples of the corresponding five mothers.

To investigate the concordance of microbial co-occurrence between the three ecosystems, we next assessed the correlations between ASVs, which were classified into eight common *Bifidobacterium* species (or subspecies) and rare groups. Approximately 87–122 ASVs (nodes) and 219–524 connections (edges) were retained in the co-occurrence networks across all ecosystems (**Figure 7**). The components and topographies of the networks of the breast milk group were significantly different from those of the feces sample groups, and the most remarkable difference was the connections of adult- to infant-type bifidobacteria. The topographies of the network

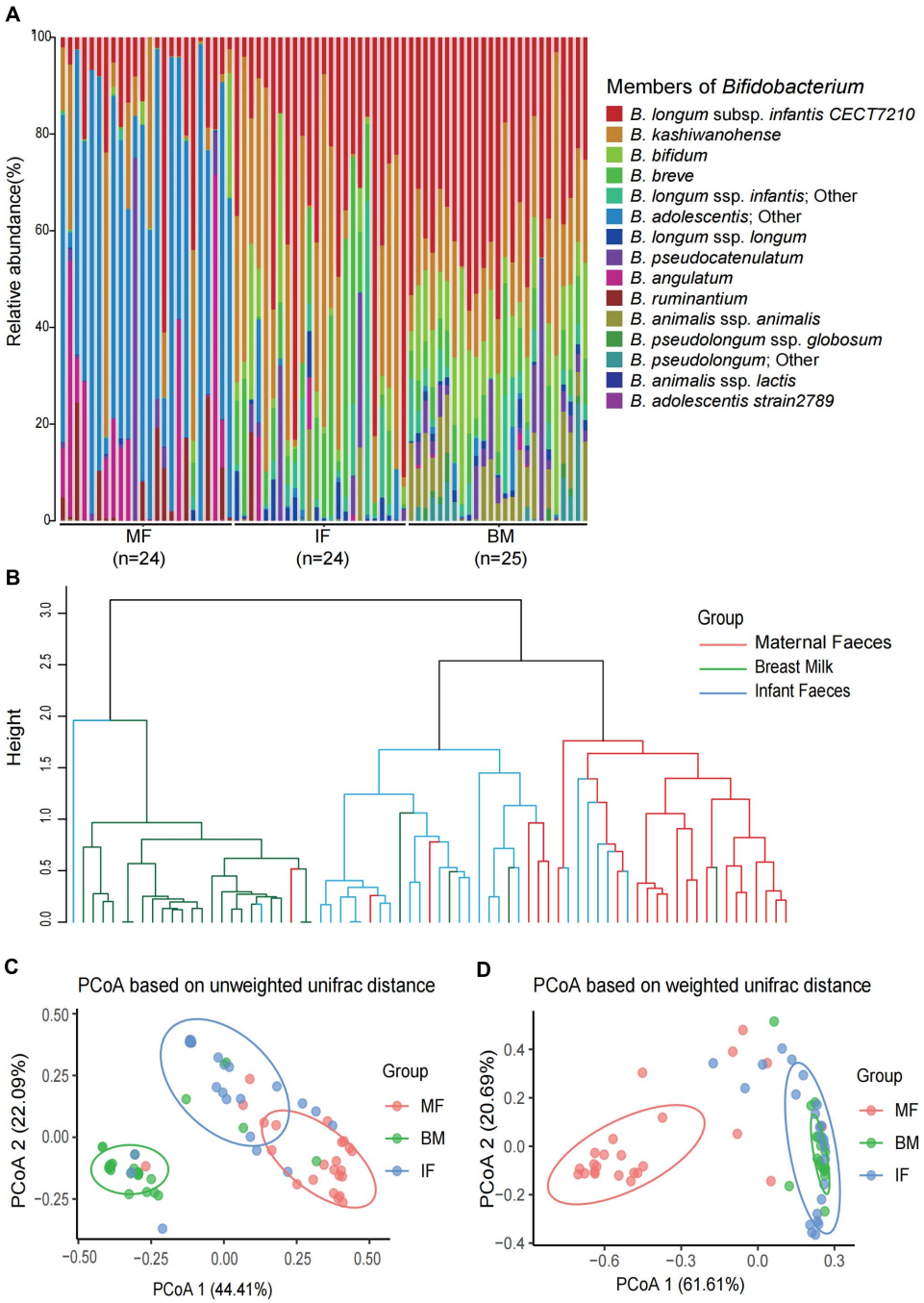

FIGURE 4 | The composition and diversity of *Bifidobacterium* phylotypes in each infant feces, maternal feces, and breast milk samples. **(A)** The composition of *Bifidobacterium* phylotypes in each infant feces, maternal feces, and breast milk samples. **(B)** The hierarchical clustering based on unweighted UniFrac distance among the three ecosystems samples. Principal coordinate analysis based on unweighted UniFrac distances **(C)** and weighted UniFrac distances **(D)** among the three ecosystems. Ellipses represent a 95% confidence interval around the cluster centroid. In both PCoAs, first and second principal components (PCoA1 and PCoA2) were plotted. The significant difference of each two groups in panels **(C,D)** was evaluated by permutational multivariate analysis of variance. All *p*-values of each two groups are less than 0.001.

of the breast milk group (**Figure 7A**) were relatively simple with a connection index of 0.059, compared with 0.062 and 0.071, respectively, for the infant feces (**Figure 7B**) and maternal feces groups (**Figure 7C**). The connections of adult-type bifidobacteria (*B. adolescentis* and *B. angulatum*) showed low frequencies of co-occurrence across breast milk samples with other bifidobateria, especially the so-called infant-type bifidobacterial species. For example, the ASVs annotated

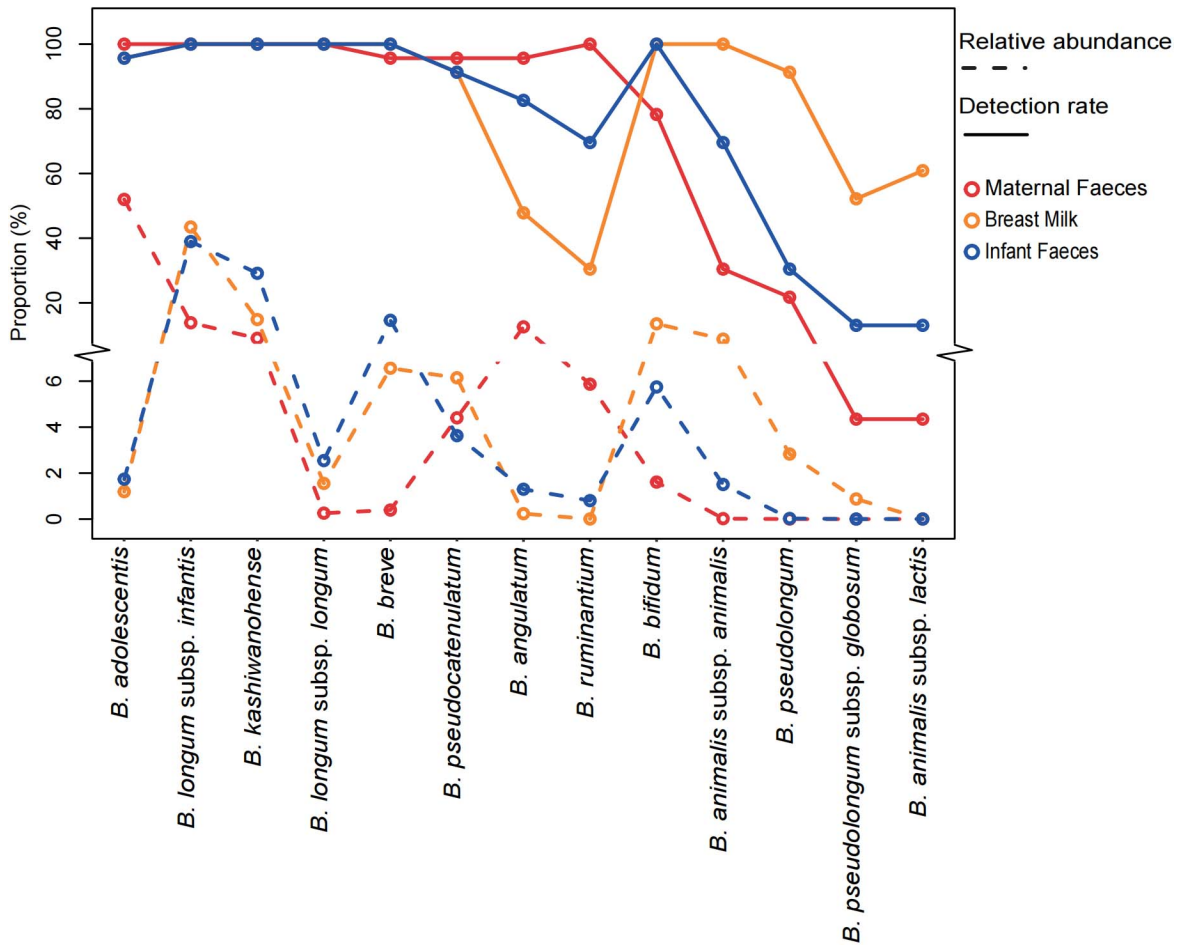

FIGURE 5 | The relative abundance and detection rate of 13 *Bifidobacterium* species or subspecies in the three systems of 23 mother–infant pairs. The y-axis truncation value is 6.1–8.9.

to *B. adolescentis* in the network of breast milk samples emerged as a separate cluster and had no co-occurrence with ASVs of other bifidobacteria (**Figure 7A**). In the network of infant fecal *Bifidobacterium* microbiota, a cluster with tight positive correlation was formed by typical infant-type bifidobacteria, *B. breve*, and *B. longum* ssp. *infantis*, along with *B. longum* ssp. *longum*, while adult-type bifidobacteria (*B. adolescentis* and *B. angulatum*) formed another cluster with *B. ruminantium* and a small number of ASVs annotated to *B. kashiwanohense*. It is noted especially that these two major clusters showed a significant negative correlation by multiple connections (**Figure 7B**). In the bifidobacterial co-occurrence network of maternal feces, one obvious characteristic is that there is significant negative correlation between one *B. adolescentis* ASV with the highest average relative abundance, and multiple ASVs belong to the *B. kashiwanohense* and *B. longum* ssp. *longum*. In addition, the vast majority of adult-type bifidobacterial ASVs (*B. adolescentis* and *B. angulatum*) had very few connections with other ASVs, although some *B. angulatum* ASVs were positively correlated with one *B. longum* ssp. *infantis* ASV (**Figure 7C**).

DISCUSSION

There is evidence that breast milk acts as an intermediary for the transfer of functionally important bacteria from mother to infant (Lyons et al., 2020). In particular, the interest in the gut symbiotic members of *Lactobacillus* and *Bifidobacterium* that can colonize the infant gut has grown significantly, mainly because their presence has been associated with a healthy microbiota (Arboleya et al., 2016; Ojo-Okunola et al., 2019). Breast milk is an important source of *Bifidobacterium* for the newborn gut (Oh et al., 2016). Due to the fact that total bacterial loads of breast milk are five to seven orders of magnitude lower than in feces samples (Fernandez et al., 2013), the amount of bifidobacteria in breast milk samples is very low compared with feces samples, especially the feces samples of infants. As a result, most studies based on culture techniques have reported very inconsistent results regarding the number and combination of *Bifidobacterium* phylotypes in breast milks within a specific population or across cohorts (Martin et al., 2009; Jost et al., 2013; Soto et al., 2014; Milani et al., 2015; Damaceno et al., 2017). However, most studies on vertical transmission of

TABLE 3 | The occurrence frequency of 13 *Bifidobacterium* species or subspecies in samples from 23 mother–infant pairs.

Taxa	Mother–infant pairs				
	MF and BM*	MF and IF*	BM and IF*	MF and BM and IF**	All not***
B. adolescentis	1	1	0	20	1
B. angulatum	0	8	2	10	0
Bifidobacterium ruminantium	4	11	0	4	0
B. pseudolongum ssp. *globosum*	0	1	1	0	9
B. pseudolongum	3	0	5	2	2
Bifidobacterium animalis ssp. *animalis*	2	0	11	5	0
B. pseudocatenulatum	1	1	1	19	0
B. breve	0	0	1	22	0
B. bifidum	0	0	5	18	0
B. kashiwanohense	0	0	0	23	0
B. longum ssp. *infantis*	0	0	0	23	0
B. longum ssp. *longum*	0	0	0	23	0
B. animalis ssp. *lactis*	0	2	2	0	8

**Can only be detected in two ecosystems simultaneously.*
***Can be detected in three ecosystems simultaneously.*
****Cannot be detected in any of three ecosystems.*

Bifidobacterium strains between the mother infant pair confirmed their co-occurrence among maternal intestine, breast milk, and the corresponding infant's intestine. Nevertheless, such potential vertical transmission and the co-occurrence of *Bifidobacterium* is still only partially understood.

In the current study, the microbial composition of the three ecosystems was remarkably different: the abundance of aerobic bacteria (such as Pseudomonadaceae) in breast milk and that of anaerobic bacteria (such as Ruminococcaceae) in the maternal gut was significantly higher than another two ecosystems. This observation could be explained by the different conditions of the resident communities in the three ecosystems for pH, oxygen levels, and nutrients availability as reported also in earlier studies (Chen et al., 2018). However, within the cohort as a whole, *Bifidobacterium* spp. were detected at low relative abundances (mean relative abundances of 0.23, 0.44, and 2.32%) in the samples of the three ecosystems (maternal feces, breast milk, and neonatal feces). Based on very accurate and painstaking analyses of 16S rRNA gene dataset, our results showed that except for one maternal feces sample where no reads assigned to *Bifidobacterium* was observed, the presence of 16S rRNA reads assigned to *Bifidobacterium* could be identified in all breast milk and other feces samples, but its relative abundance was as low as 0.004% in a few breast milk and 0.02% in a few infant feces samples (data not shown). Previous studies showed that total bacteria concentration is lower in colostrum than in transitional and mature milk, with increasing levels of *Bifidobacterium* in breast milk over lactation time (Cabrera-Rubio et al., 2012; Khodayar-Pardo et al., 2014). In fact, the presence of *Bifidobacterium* was sporadically reported in a few colostrum samples or not at all (Hunt et al., 2011; Boix-Amoros et al., 2016; Drago et al., 2017; Chen et al., 2018). In our other study, in only about 5.4% of colostrum samples were retrieved 16S rRNA ASVs corresponding to *Bifidobacterium*, with <0.05% mean relative abundance (data not shown).

According to the published literature, most studies using high-throughput sequencing of 16S rRNA gene amplicon have reported conspicuous intercohort variation regarding the prevalence and relative abundance of *Bifidobacterium* in microbiome of breast milks and the infant gut, when compared with the stability of the adult gut microbiome (Murphy et al., 2017; Lackey et al., 2019; Moossavi et al., 2019). In the present study, it is curious that the relative abundance of *Bifidobaterium* (2.32%) in the microbiome of the infant gut was much lower than that in similar studies by other research groups, who reported that bifidobacteria achieved large proportions of the gut microbiota in the first few months after birth, ranging from 10 to 90% (Turroni et al., 2012; Lim et al., 2016; Duranti et al., 2017; Lundgren et al., 2018). The high abundance of bifidobacteria in the gut of breastfeeding infants was explained by the fact that host-derived glycans, like gut mucins and breast milk oligosaccharides in breast milk as specific growth substrates fertilize bifidobacterial growth, especially *B. longum* subsp. *infantis*, *B. bifidum*, and *B. breve* containing specific gene clusters encoding enzymes that are capable of hydrolyzing HMOs (Aakko et al., 2017; Turroni et al., 2017; Lawson et al., 2020). Thus, further research is needed to determine the reason for such a low relative abundance of *Bifidobacterium* in the intestinal tract of infants across our cohort, especially the association with breast milk oligosaccharides and diet and lifestyle, and environmental factors. In fact, some previous studies similarly reported that a proportion of infants targeting other populations have very low abundance or undetectable bifidobacteria as members of the fecal microbiota regardless of breast milk or formula feeding (Tannock et al., 2013, 2016). Duranti et al. (2017) reported very large interindividual variations for the relative abundance of *Bifidobacterium* in infant gut microbiota, with an abundance as low as 0.05%. In adults, bifidobacteria have been reported to commonly make up 1–10% of the gut microbiota (Arboleya et al., 2016). In our cohort, *Bifidobacterium* spp. were detected at low proportions (0.23%) in maternal feces samples. In fact, it was surprising that the complete absence of bifidobacteria in the Hadza gut microbiota is reported (Schnorr et al., 2014).

Given that determining the bacterial species with partial 16S rRNA sequences has to be taken with care, the representative sequences of all 11 *Bifidobaterium* ASVs in the 16S rRNA gene dataset were NCBI BLAST homology searched in order to obtain more accurate taxonomic results. Our results showed that they were annotated to seven species or species groups, of which the most predominant phylotype was the *B. breve/longum* group in breast milk and infant gut, with the prevalence being 100%. Although the average rel. ab of the *B. adolescentis* in maternal gut was higher than that in breast milk and infant gut, its prevalence was only 72% in the maternal gut, with seven maternal gut samples being negative. By contrast, the relative abundance of *Bifidobaterium* in the breast milk microbiome is similar to what has been reported in other

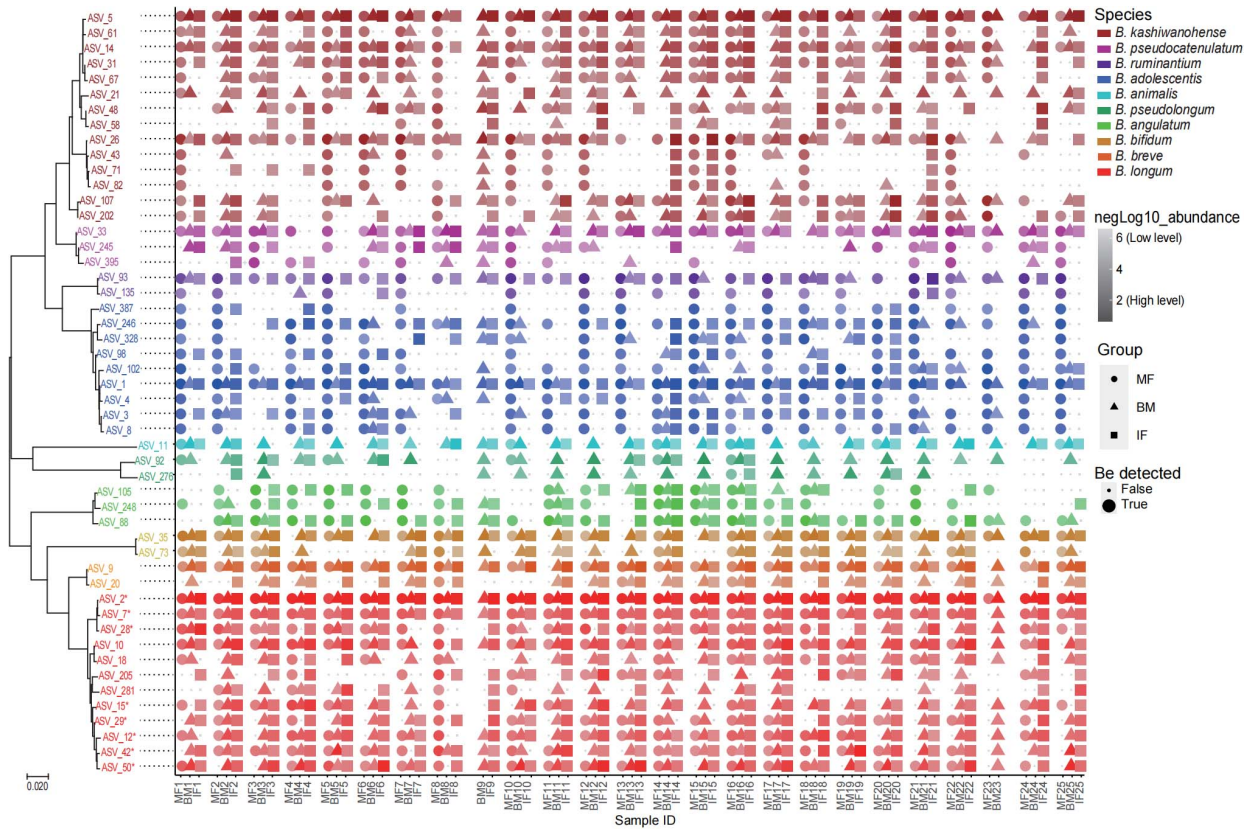

FIGURE 6 | Phylogenetic tree of the 50 dominant ASVs and their co-occurrence in samples from 25 mother–breast milk–infant triads. The color of the text in the tree represents different bifidobacteria species. The color gradient of symbols represents the level of logarithm of relative abundance (the darker the color, the higher the relative abundance), the shapes represent different ecosystems, and the size is the logical value of whether the ASV can be detected in the sample. **B. longum* subsp. *infantis*.

studies. For example, in a study that targeted HBM samples collected between 6 and 10 weeks postpartum from lactating South African women, the average relative abundances of the genus *Bifidobacterium* was about 1.0%, yet with 28% of breast milk samples being free of bifidobacteria (Ojo-Okunola et al., 2019). In another study (Moossavi et al., 2019), NGS data based on 16S rRNA gene sequencing of V4 hypervariable region revealed that only 39% of breast milk samples contained *Bifidobacterium*, with mean relative abundance of 0.25 ± 0.98%. A recent study (Kumar et al., 2016) investigated the influence of geographical location on breast mature milk microbiota of healthy mothers, and the genus *Bifidobacterium* was found only in samples from South African women and not from Finland, Spain, and Beijing, China. Furthermore, in a study of 145 American women at approximately 6 weeks postpartum, mean relative abundances of the genus *Bifidobacterium* was about 0.65%. However, the relative abundances of *Bifidobacterium* were significantly different between breast milk microbiome types (Lundgren et al., 2018). In addition, a previous study in Taiwan and mainland China similarly reported that *B. longum* was the predominant bifidobacterial species with mean relative abundance of 0.3%, but its prevalence was only 62.4% (Li et al., 2017). Some studies have not even reported the presence and relative abundance of *Bifidobacterium* in breast milk during the first months postpartum (Browne et al., 2019), while other studies reported that *Bifidobacterium* spp. were detected at low proportions in human breast milk samples, but their prevalence was not described (Boix-Amoros et al., 2016; Chen et al., 2018; Meehan et al., 2018).

As described in all studies mentioned above, most studies on breast milk microbiome using the NGS of specific 16S variable gene regions reported only their results at the taxonomic level of genus. Particularly, the pitfalls inherent to 16S subregions, such as V3–V5, including the limited discriminating power among sequences belonging to the phylum Actinobacteria and the underrepresentation of rare OTUs with low abundance, may lead to skewed estimates of bifidobacterial community (Ellegaard and Engel, 2016; Johnson et al., 2019). Consequently, the choice of PCR primers can lead to underrepresentation of bifidobacterial community in 16S rRNA sequencing dataset, concealing the number and diversity of species- and strain-level sequence variants (Sim et al., 2012; Alcon-Giner et al., 2017).

In addition to the above reasons, another possible explanation for the underrepresentation of *Bifidobacterium*, which is in the downstream data analysis methods, some rare bacterial genus with very low abundance, including *Bifidobacterium*, which

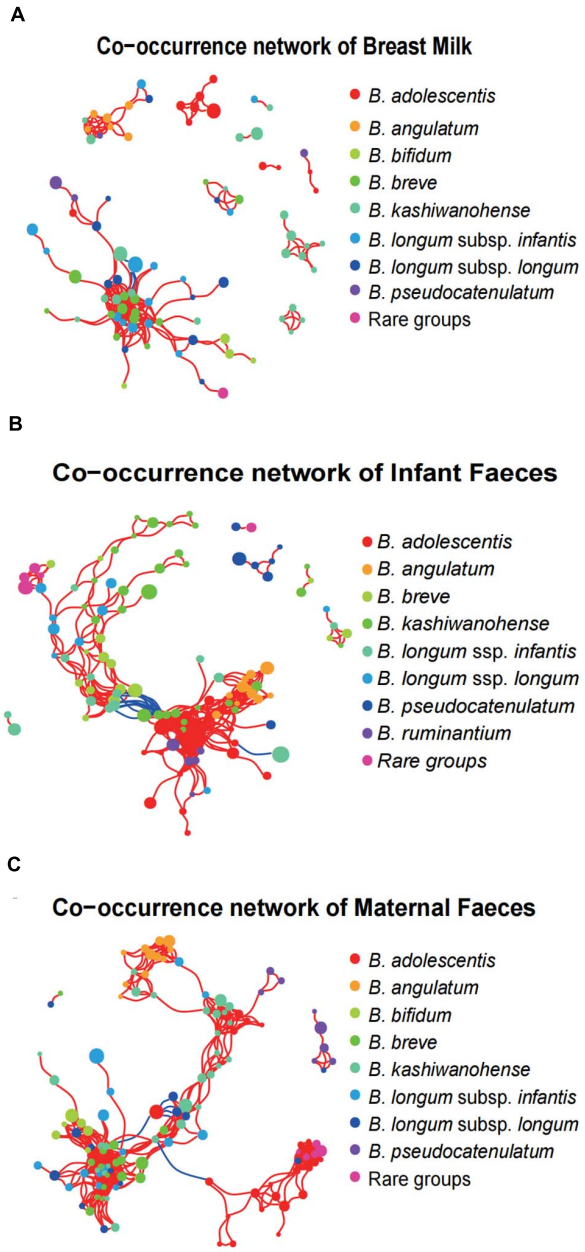

FIGURE 7 | Bifidobacterial co-occurrence networks in the three systems. Co-occurrence networks of *Bifidobacterium* phylotypes in breast milk **(A)**, infant feces **(B)**, and maternal feces **(C)**. Each node in the network indicates an ASV, and the color represents bifidobacterial phylotypes. Each co-occurring pair among bacterial populations has an absolute Spearman rank correlation above 0.7 [red line: positive correlation ($R > 0.70$); blue line: negative (blue) correlation ($R < -0.70$)] with an FDR-corrected significance level under 0.01.

might be categorized into the "other" group in each sample, cannot be ruled out (Meehan et al., 2018). Particularly at the ASV level, taxa exhibiting such a low relative abundance (reads less than 10) are often dismissed in data analysis of high throughput for microbial community and diversity analysis, thereby leading to inconsistent results regarding the occurrence of bifidobacteria in mother–infant pairs (Chen et al., 2018). All of the above situations may be the reasons why there are always portions of the same set of samples from each of multiple independent cohort studies showing *Bifidobacterium* negative, despite using the same method.

A very interesting phenomenon was that the publications that investigated the bacteria vertical transfer from mother to infant have not reported the vertical transfer of *B. longum* subsp. *infantis* to date. The most likely explanation of this finding is that, in contrast to *B. longum* subsp. *longum*, which can be detected in the intestinal tracts of both adults and infants, the *B. longum* subsp. *infantis*, as a typical infant-type bifidobacterial phylotype is difficult to capture because it is a very low abundance taxon in the adult gut, even using metagenomic methods (Ward et al., 2013; Zhang et al., 2015; Vatanen et al., 2019). For example, only 10% of Finnish infants harbored *Bifidobacterium longum* subsp. *infantis*, whereas Russian infants commonly maintained a probiotic *Bifidobacterium bifidum* strain in infancy (Vatanen et al., 2019). More recently, the *groEL* gene proved to be a very effective target for the identification and quantification of *Bifidobacterium* spp. through high-throughput sequencing technologies or qPCR (Junick and Blaut, 2012; Hu et al., 2017). In our study, according to the denoising, taxonomic annotation showed that 376 *Bifidobaterium* ASVs in the *groEL* gene dataset were assigned to at least 13 well-known *Bifidobacterium* species or subspecies. Of them, seven phylotypes, including *B. longum* subsp. *infantis*, were identified to be universally distributed in all 23 mother–infant pairs analyzed. More remarkably, the so-called infant-type *Bifidobacterium* phylotype, such as *B. bifidum*, *B. breve*, and *B. longum* subsp. *Infantis*, was found to be present in the gut of all mothers, while *B. adolescentis*, a typical adult-type bifidobacterial phylotype, was almost detected in all infant feces and breast milk samples. Therefore, in terms of the occurrence and ecological distribution of human-associated bifidobacterial species, there should not be a very strict infant vs. adult subdivision. Our test results were obviously to support the hypothesis that breast milk as a seeding mediator inoculated the infant gut microbiome, regardless of the infant-type *Bifidobacterium* phylotype and adult-type bifidobacterial phylotype (Turroni et al., 2017). Of interest, *Bifidobaterium* ASV data obtained by the *groEL* gene sequences revealed relatively high intrasubject variability in *B. longum*, including *B. longum* ssp. *infantis* (58 ASVs) and *B. longum* ssp. *longum* (36 ASVs), compared with other common *Bifidobacterium* species, *B. bifidum* (36 ASVs), or *B. breve* (16 ASVs), which was consistent with the results reported in a recent study on strain-specific functional adaptation in the human gut microbiome during early life (Vatanen et al., 2019). Notably, comparison of the *groEL* gene-based ASVs identified in the data sets indicated the presence of identical ASVs in different sample pairs, implying that these identical sequences correspond to very closely related strains that presented in non-corresponding mother–infant dyads. Different ASVs of *B. kashiwanohense* showed different co-occurrence relationships in breast milk and feces samples, which may be caused by the bias of different strains to different ecosystems (Vatanen et al., 2019). Despite

this genetic similarity, it can be determined that there may be great phenotypic variation between strains of the same species (homotypic strains) (Van Rossum et al., 2020). Further studies are needed to prove whether the phenotypic variation of strains in the mother-to-infant transmission process will be changed due to the ecosystem.

Moreover, there were very low relative proportion abundances of other six bifidobacterial taxa, whose prevalence (presence/absence) displayed both interindividual and sample set variations. According to the definition of microbial ecology, these *Bifidobacterium* phylotypes should belong to the rare taxa. However, thus far, little is known about the occurrence and the ecological relevance of rare *Bifidobacterium* phylotypes in human body environments. For example, in our cohort, rare *Bifidobacterium* phylotypes presented in the majority of maternal and infant gut, such as *B. ruminantium* and *B. angulatum*, with the highest detection rate (100%) and lower relative abundance (0.02%) in maternal gut, were not detected in quite a few breast milk samples. On the contrary, rare phylotypes like *B. animalis* and *B. pseudolongum*, showing almost 100% the detection frequency in breast milk samples, were absent in quite a few guts across all mother–infant pairs, especially in the mother gut. Among them, *B. animalis* ssp. *animalis* was concurrently detected in infants' gut and their mothers' breast milk of 16 mother–infant dyads, but presented only in the gut of the corresponding five mothers. In fact, *B. animalis* subsp. *lactis/animalis* and *B. pseudolongum*, which are frequently found in various animals, are scarcely encountered in the human intestinal tract, suggesting that they are not shared between mothers and their respective infant (Delcenserie et al., 2011; Lugli et al., 2019). Possibly, the probiotic endosymbiotic *Bifidobacterium* species are transmitted from mother to infant by direct vertical transmission during early life in most cases. However, another possibility that some oxygen-insensitive *Bifidobacterium* phylotypes with a cosmopolitan lifestyle (*B. animalis* and *B. adolescentis*) are indirectly transferred to breast milk and the infant's intestinal tract through environmental contamination cannot be ruled out (Bondue and Delcenserie, 2015). Coincidentally, a study from an Argentine population described *B. animalis* subsp. *lactis* strains that originated from 16 breast milk samples (Zacarias et al., 2011). Besides, analogous to our result, a recent study also reported the presence of *B. pseudolongum* in the breast milk (Chen et al., 2018). Furthermore, our investigations are under way to clarify the importance and generality of the latter transmission route.

It is already known that there is a mutualistic cross-feeding or resource-sharing phenomenon in the bifidobacteria community of breastfed infant gut (Turroni et al., 2017). In the present study, we employed network-based analyses to elucidate the association and co-occurrence between *Bifidobacterium* phylotypes present in each of the three ecosystems of mother–breast milk–infant triads at the species or strain level (ASV). Strikingly, as shown in the network of infant gut, the major cluster where typical infant-type bifidobacterial ASVs intertwined with each other showed a significant negative correlation with a major cluster structured by adult-type bifidobacteria ASVs through multiple connections, indicating the presence of co-exclusion association. This result seems not to be in accordance with the reports by Turroni and cooperator (Turroni et al., 2016), who found that a strain of *B. adolescentis* exhibited mutalisitic cross-feeding behaviors when cocultured with *B. bifidum*, *B. breve*, and *B. longum* subsp. *infantis* strain, respectively. However, in the network of breast milk, the ASVs of different bifidobacterial phylotypes, including adult types, emerged as a separate cluster and displayed weak correlation with each other, suggesting that such ecological relationships might represent the random associations of bifidobacterial species in the poorly competitive ecosystem of breast milk. At present, our investigations are under way to clarify the association between maternal breast milk and infant fecal bifidobacterial profiles at the different stages of lactation, to pay close attention to the combination and longitudinal changes of *Bifidobacterium* phylotypes (species or strain level) between different ethnic groups during early life.

CONCLUSION

By analyzing bacterial 16S rRNA gene datasets from the maternal stool, breast milk, and infant stool in a small yet very homogeneous cohort of 25 healthy Uyghur mother–infant pairs in Kashgar, Xinjiang, China, only three sets of ASVs could be clearly assigned into *B. adolescentis*, *B. pseudolongum*, and *B. bifidum*, respectively, whereas the remaining eight sets of ASVs corresponded to four *Bifidobacterium* species groups containing more than two closely related species. More remarkably, the *gro*EL gene proved to be a very effective mark gene for the depth resolution of *Bifidobacterium* community by high-throughput sequencing technology, allowing all *Bifidobaterium* ASVs to be assigned to at least 13 well-known *Bifidobacterium* species or subspecies. Among them, seven well-known *Bifidobacterium* phylotypes showed synchronism in 23 mother–infant pairs. However, several other rare bifidobacterial phylotypes, which were frequently encountered in animals, were found to display no correspondence of the presence between the three ecosystems of mother–infant pairs. Consequently, our test results were obviously to support the hypothesis that breast milk acts as an intermediary for the transfer of functionally important commensal bacteria from mother to infant, especially for endosymbiotic *Bifidobacterium* that can colonize the infant gut. In contrast, some oxygen-insensitive exogenous *Bifidobacterium* phylotypes with a cosmopolitan lifestyle may be indirectly transferred to breast milk and the infant's intestinal tract through environmental contamination. Furthermore, the so-called infant-type *Bifidobacterium* phylotype, was found to be present in the gut of all mothers, while adult-type bifidobacterial phylotypes were almost detected in all infant gut and breast milk samples, indicating that there should not be a very strict infant vs. adult subdivision in terms of the occurrence and ecological distribution of human-associated bifidobacterial species.

DATA AVAILABILITY STATEMENT

The datasets presented in this study can be found in online repositories. The names of the

repository/repositories and accession number(s) can be found below: www.ncbi.nlm.nih.gov/, BioProject ID PRJNA659245 and PRJNA702483.

ETHICS STATEMENT

The studies involving human participants were reviewed and approved by Ethics Committee of the First Affiliated Hospital, Shihezi University School of Medicine. Written informed consent to participate in this study was provided by the participants' legal guardian/next of kin.

AUTHOR CONTRIBUTIONS

YN and FT conceptualized the study and acquired the funding. WY and XZ conducted the experimental investigation. WY was in charge of the bioinformatics, statistics, figures, and wrote the original draft. YN wrote, reviewed, and edited the manuscript. BL collected the samples. All authors contributed to the article and approved the submitted version.

FUNDING

This work was supported by the joint key funds of the National Natural Science Foundation of China and the Autonomous Region Government of Xinjiang, China (grant no. U1903205).

SUPPLEMENTARY MATERIAL

The Supplementary Material for this article can be found online at: https://www.frontiersin.org/articles/10.3389/fmicb.2021.669442/full#supplementary-material

Supplementary Figure 1 | Differentially abundant bacterial taxa between maternal feces (MF), breast milk (BM) and infant feces (IF) samples. **(A)** LEfSe comparison of microbiota in feces and breast milk samples. The genera listed in green describe breast milk, genera listed in blue describe infant feces, and genera listed in red describe maternal feces samples. Significant bacterial genera were determined by Kruskal–Wallis test ($P < 0.05$) with LDA score greater than 3. **(B)** Cladogram representation of differentially abundant bacterial taxonomic group detected using LEfSe. Different colors indicate the group in which clade was most abundant.

Supplementary Figure 2 | Phylogenetic tree constructed based on the bifidobacterial ASV sequences. Outer circle color represents the phylogenetic strains.

REFERENCES

Aakko, J., Kumar, H., Rautava, S., Wise, A., Autran, C., Bode, L., et al. (2017). Human milk oligosaccharide categories define the microbiota composition in human colostrum. *Benef. Microbes* 8, 563–567. doi: 10.3920/bm2016.0185

Alcon-Giner, C., Caim, S., Mitra, S., Ketskemety, J., Wegmann, U., Wain, J., et al. (2017). Optimisation of 16S rRNA gut microbiota profiling of extremely low birth weight infants. *BMC Genomics* 18:841. doi: 10.1186/s12864-017-4229-x

Arboleya, S., Watkins, C., Stanton, C., and Ross, R. P. (2016). Gut bifidobacteria populations in human health and aging. *Front. Microbiol.* 7:1204. doi: 10.3389/fmicb.2016.01204

Ballard, O., and Morrow, A. L. (2013). Human milk composition nutrients and bioactive factors. *Pediatr. Clin. N. Am.* 60, 49–74. doi: 10.1016/j.pcl.2012.10.002

Benson, D. A., Karsch-Mizrachi, I., Lipman, D. J., Ostell, J., and Sayers, E. W. (2011). GenBank. *Nucleic Acids Res.* 39, D32–D37. doi: 10.1093/nar/gkq1079

Bode, L. (2012). Human milk oligosaccharides: every baby needs a sugar mama. *Glycobiology* 22, 1147–1162. doi: 10.1093/glycob/cws074

Bode, L., Mcguire, M., Rodriguez, J. M., Geddes, D. T., Hassiotou, F., Hartmann, P. E., et al. (2014). It's alive: microbes and cells in human milk and their potential benefits to mother and infant. *Adv. Nutr.* 5, 381–396. doi: 10.3945/an.114.006643

Boix-Amoros, A., Collado, M. C., and Mira, A. (2016). Relationship between milk microbiota, bacterial load, macronutrients, and human cells during lactation. *Front. Microbiol.* 7:492. doi: 10.5389/fmicb.7016.00492

Bondue, P., and Delcenserie, V. (2015). Genome of bifidobacteria and carbohydrate metabolism. *Korean J. Food Sci. An.* 35, 1–9. doi: 10.5851/kosfa.2015.35.1.1

Browne, P. D., Aparicio, M., Alba, C., Hechler, C., Beijers, R., Miguel Rodriguez, J., et al. (2019). Human milk microbiome and maternal postnatal psychosocial distress. *Front. Microbiol.* 10:2333. doi: 10.3389/fmicb.2019.02333

Cabrera-Rubio, R., Carmen Collado, M., Laitinen, K., Salminen, S., Isolauri, E., and Mira, A. (2012). The human milk microbiome changes over lactation and is shaped by maternal weight and mode of delivery. *Am. J. Clin. Nutr.* 96, 544–551. doi: 10.3945/ajcn.112.037382

Caporaso, J. G., Kuczynski, J., Stombaugh, J., Bittinger, K., Bushman, F. D., Costello, E. K., et al. (2010). QIIME allows analysis of high-throughput community sequencing data. *Nat. Methods* 7, 335–336. doi: 10.1038/nmeth.f.303

Chen, P.-W., Lin, Y.-L., and Huang, M.-S. (2018). Profiles of commensal and opportunistic bacteria in human milk from healthy donors in Taiwan. *J. Food Drug Anal.* 26, 1235–1244. doi: 10.1016/j.jfda.2018.03.004

Collado, M. C., Delgado, S., Maldonado, A., and Rodriguez, J. M. (2009). Assessment of the bacterial diversity of breast milk of healthy women by quantitative real-time PCR. *Lett. Appl. Microbiol.* 48, 523–528. doi: 10.1111/j.1472-765X.2009.02567.x

Damaceno, Q. S., Souza, J. P., Nicoli, J. R., Paula, R. L., Assis, G. B., Figueiredo, H. C., et al. (2017). Evaluation of potential probiotics isolated from human milk and colostrum. *Probiotics Antimicro.* 9, 371–379. doi: 10.1007/s12602-017-9270-9271

Delcenserie, V., Gavini, F., China, B., and Daube, G. (2011). Bifidobacterium pseudolongum are efficient indicators of animal fecal contamination in raw milk cheese industry. *BMC Microbiol.* 11:178. doi: 10.1186/1471-2180-11-178

Drago, L., Toscano, M., De Grandi, R., Grossi, E., Padovani, E. M., and Peroni, D. G. (2017). Microbiota network and mathematic microbe mutualism in colostrum and mature milk collected in two different geographic areas: Italy versus Burundi. *ISME J.* 11, 875–884. doi: 10.1038/ismej.2016.183

Duranti, S., Lugli, G. A., Mancabelli, L., Armanini, F., Turroni, F., James, K., et al. (2017). Maternal inheritance of bifidobacterial communities and bifidophages in infants through vertical transmission. *Microbiome* 5:66. doi: 10.1186/s40168-017-0282-286

Dzidic, M., Abrahamsson, T. R., Artacho, A., Collado, M. C., Mira, A., and Jenmalm, M. C. (2018). Oral microbiota maturation during the first 7 years of life in relation to allergy development. *Allergy* 73, 2000–2011. doi: 10.1111/all.13449

Edgar, R. C. (2010). Search and clustering orders of magnitude faster than BLAST. *Bioinformatics* 26, 2460–2461. doi: 10.1093/bioinformatics/btq461

Edgar, R. C. (2017). UNBIAS: an attempt to correct abundance bias in 16S sequencing, with limited success. *bioRxiv [preprint]* doi: 10.1101/124149

Ellegaard, K. M., and Engel, P. (2016). Beyond 16S rRNA community profiling: intra-species diversity in the gut microbiota. *Front. Microbiol.* 7:1475. doi: 10.3389/fmicb.2016.01475

Fernandez, L., Langa, S., Martin, V., Maldonado, A., Jimenez, E., Martin, R., et al. (2013). The human milk microbiota: origin and potential roles in health and disease. *Pharmacol. Res.* 69, 1–10. doi: 10.1016/j.phrs.2012.09.001

Ferretti, P., Pasolli, E., Tett, A., Asnicar, F., Gorfer, V., Fedi, S., et al. (2018). Mother-to-infant microbial transmission from different body sites shapes the

developing infant gut microbiome. *Cell Host Microbe* 24, 133–145. doi: 10.1016/j.chom.2018.06.005

Fitzstevens, J. L., Smith, K. C., Hagadorn, J. I., Caimano, M. J., Matson, A. P., and Brownell, E. A. (2017). Systematic review of the human milk microbiota. *Nutr. Clin. Pract.* 32, 354–364. doi: 10.1177/0884533616670150

Groenlund, M. M., Gueimonde, M., Laitinen, K., Kociubinski, G., Groenroos, T., Salminen, S., et al. (2007). Maternal breast-milk and intestinal bifidobacteria guide the compositional development of the Bifidobacterium microbiota in infants at risk of allergic disease. *Clin. Exp. Allergy* 37, 1764–1772. doi: 10.1111/j.1365-2222.2007.02849.x

Heikkila, M. P., and Saris, P. E. J. (2003). Inhibition of Staphylococcus aureus by the commensal bacteria of human milk. *J. Appl. Microbiol.* 95, 471–478. doi: 10.1046/j.1365-2672.2003.02002.x

Hill, J. E., Penny, S. L., Crowell, K. G., Goh, S. H., and Hemmingsen, S. M. (2004). cpnDB: a chaperonin sequence database. *Genome Res.* 14, 1669–1675. doi: 10.1101/gr.2649204

Hu, L. J., Lu, W. W., Wang, L. L., Pan, M. L., Zhang, H., Zhao, J. X., et al. (2017). Assessment of bifidobacterium species using groEL gene on the basis of illumina MiSeq high-throughput sequencing. *Genes* 8:336. doi: 10.3390/genes8110336

Hunt, K. M., Foster, J. A., Forney, L. J., Schuette, U. M. E., Beck, D. L., Abdo, Z., et al. (2011). Characterization of the diversity and temporal stability of bacterial communities in human milk. *PLoS One* 6:e21313. doi: 10.1371/journal.pone.0021313

Johnson, J. S., Spakowicz, D. J., Hong, B. Y., Petersen, L. M., Demkowicz, P., Chen, L., et al. (2019). Evaluation of 16S rRNA gene sequencing for species and strain-level microbiome analysis. *Nat. Commun.* 10:5029. doi: 10.1038/s41467-019-13036-13031

Jost, T., Lacroix, C., Braegger, C., and Chassard, C. (2013). Assessment of bacterial diversity in breast milk using culture-dependent and culture-independent approaches. *Br. J. Nutr.* 110, 1253–1262. doi: 10.1017/s0007114513000597

Junick, J., and Blaut, M. (2012). Quantification of human fecal bifidobacterium species by use of quantitative real-time PCR analysis targeting the groEL gene. *Appl. Environ. Microbiol.* 78, 2613–2622. doi: 10.1128/aem.07749-7711

Khodayar-Pardo, P., Mira-Pascual, L., Collado, M. C., and Martinez-Costa, C. (2014). Impact of lactation stage, gestational age and mode of delivery on breast milk microbiota. *J. Perinatol.* 34, 599–605. doi: 10.1038/jp.2014.47

Koenig, J. E., Spor, A., Scalfone, N., Fricker, A. D., Stombaugh, J., Knight, R., et al. (2011). Succession of microbial consortia in the developing infant gut microbiome. *Proc. Natl. Acad. Sci. U S A.* 108, 4578–4585. doi: 10.1073/pnas.1000081107

Kumar, H., Du Toit, E., Kulkarni, A., Aakko, J., Linderborg, K. M., Zhang, Y., et al. (2016). Distinct patterns in human milk microbiota and fatty acid profiles across specific geographic locations. *Front. Microbiol.* 7:1619. doi: 10.3389/fmicb.2016.01619

Lackey, K. A., Williams, J. E., Meehan, C. L., Zachek, J. A., Benda, E. D., Price, W. J., et al. (2019). What's normal? microbiomes in human milk and infant feces are related to each other but vary geographically: the inspire study. *Front. Nutr.* 6:45. doi: 10.3389/fnut.2019.00045

Lawson, M. A. E., O'neill, I. J., Kujawska, M., Javavdi, S. G., Wijeyesekera, A., Flegg, Z., et al. (2020). Breast milk-derived human milk oligosaccharides promote *Bifidobacterium* interactions within a single ecosystem. *ISME J.* 14, 635–648. doi: 10.1038/s41396-019-0553-552

Li, S.-W., Watanabe, K., Hsu, C.-C., Chao, S.-H., Yang, Z.-H., Lin, Y.-J., et al. (2017). Bacterial composition and diversity in breast milk samples from mothers living in Taiwan and Mainland China. *Front. Microbiol.* 8:965. doi: 10.3389/fmicb.2017.00965

Lim, E. S., Wang, D., and Holtz, L. R. (2016). The bacterial microbiome and virome milestones of infant development. *Trends Microbiol.* 24, 801–810. doi: 10.1016/j.tim.2016.06.001

Lugli, G. A., Duranti, S., Albert, K., Mancabelli, L., Napoli, S., Viappiani, A., et al. (2019). Unveiling genomic diversity among members of the species *Bifidobacterium pseudolongum*, a widely distributed gut commensal of the animal kingdom. *Appl. Environ. Microbiol.* 85:e03065. doi: 10.1128/aem.03065-3018

Lundgren, S. N., Madan, J. C., Emond, J. A., Morrison, H. G., Christensen, B. C., Karagas, M. R., et al. (2018). Maternal diet during pregnancy is related with the infant stool microbiome in a delivery mode-dependent manner. *Microbiome* 6:109. doi: 10.1186/s40168-018-0490-498

Lyons, K. E., Ryan, C. A., Dempsey, E. M., Ross, R. P., and Stanton, C. (2020). Breast milk, a source of beneficial microbes and associated benefits for infant health. *Nutrients* 12:1039. doi: 10.3390/nu12041039

Makino, H., Kushiro, A., Ishikawa, E., Kubota, H., Gawad, A., Sakai, T., et al. (2013). Mother-to-infant transmission of intestinal bifidobacterial strains has an impact on the early development of vaginally delivered infant's microbiota. *PLoS One* 8:e78831. doi: doi:10.1371/journal.pone.0078331

Makino, H., Kushiro, A., Ishikawa, E., Muylaert, D., Kubota, H., Sakai, T., et al. (2011). Transmission of intestinal Bifidobacterium longum subsp longum strains from mother to infant, determined by multilocus sequencing typing and amplified fragment length polymorphism. *Appl. Environ. Microbiol.* 77, 6788–6793. doi: 10.1128/aem.05346-5311

Martin, R., Heilig, G. H. J., Zoetendal, E. G., Smidt, H., and Rodriguez, J. M. (2007). Diversity of the *Lactobacillus* group in breast milk and vagina of healthy women and potential role in the colonization of the infant gut. *J. Appl. Microbiol.* 103, 2638–2644. doi: 10.1111/j.1365-2672.2007.03497.x

Martin, R., Jimenez, E., Heilig, H., Fernandez, L., Marin, M. L., Zoetendal, E. G., et al. (2009). Isolation of bifidobacteria from breast milk and assessment of the bifidobacterial population by PCR-Denaturing gradient gel electrophoresis and quantitative real-time PCR. *Appl. Environ. Microbiol.* 75, 965–969. doi: 10.1128/aem.02063-2068

McGuire, M. K., and McGuire, M. A. (2017). Got bacteria? The astounding, yet not-so-surprising, microbiome of human milk. *Curr. Opin. Biotech.* 44, 63–68. doi: 10.1016/j.copbio.2016.11.013

Meehan, C. L., Lackey, K. A., Hagen, E. H., Williams, J. E., Roulette, J., Helfrecht, C., et al. (2018). Social networks, cooperative breeding, and the human milk microbiome. *Am. J. Hum. Biol.* 30:e23131. doi: 10.1002/ajhb.23131

Milani, C., Mancabelli, L., Lugli, G. A., Duranti, S., Turroni, F., Ferrario, C., et al. (2015). Exploring vertical transmission of bifidobacteria from mother to child. *Appl. Environ. Microbiol.* 81, 7078–7087. doi: doi:10.1128/aem.02037-2015

Moossavi, S., Sepehri, S., Robertson, B., Bode, L., Goruk, S., Field, C. J., et al. (2019). Composition and variation of the human milk microbiota are influenced by maternal and early-life factors. *Cell Host Microbe* 25, 324–335. doi: 10.1016/j.chom.2019.01.011

Mueller, N. T., Bakacs, E., Combellick, J., Grigoryan, Z., and Dominguez-Bello, M. G. (2015). The infant microbiome development: mom matters. *Trends Mol. Med.* 21, 109–117. doi: 10.1016/j.molmed.2014.12.002

Murphy, K., Curley, D., O'callaghan, T. F., O'shea, C.-A., Dempsey, E. M., O'toole, P. W., et al. (2017). The composition of human milk and infant faecal microbiota over the first three months of life: a pilot study. *Sci. Rep.* 7:40597. doi: 10.1038/srep40597

Nyangahu, D. D., and Jaspan, H. B. (2019). Influence of maternal microbiota during pregnancy on infant immunity. *Clin. Exp. Immunol.* 198, 47–56. doi: 10.1111/cei.13331

Oh, J., Byrd, A. L., Park, M., Program, N. C. S., Kong, H. H., et al. (2016). Temporal stability of the human skin microbiome. *Cell* 165, 854–866. doi: 10.1016/j.cell.2016.04.008

Ojo-Okunola, A., Claassen-Weitz, S., Mwaikono, K. S., Gardner-Lubbe, S., Stein, D. J., Zar, H. J., et al. (2019). Influence of socio-economic and psychosocial profiles on the human breast milk bacteriome of South African women. *Nutrients* 11:1390. doi: 10.3390/nu11061390

Perez, P. F., Dore, J., Leclerc, M., Levenez, F., Benyacoub, J., Serrant, P., et al. (2007). Bacterial imprinting of the neonatal immune system: lessons from maternal cells? *Pediatrics* 119, e724–e732. doi: 10.1542/peds.2006-1649

Rao, C. R. (1984). *Convexity Properties of Entropy Functions and Analysis of Diversity*. Michigan, MICH: Institute of Mathematical Statistics.

Sakwinska, O., Moine, D., Delley, M., Combremont, S., Rezzonico, E., Descombes, P., et al. (2016). Microbiota in breast milk of Chinese lactating mothers. *PLoS One* 11:e0160856. doi: 10.1371/journal.pone.0160856

Schloss, P. D., and Westcott, S. L. (2011). Assessing and improving methods used in operational taxonomic unit-based approaches for 16S rRNA gene sequence analysis. *Appl. Environ. Microbiol.* 77, 3219–3226. doi: 10.1128/aem.02810-2810

Schnorr, S. L., Candela, M., Rampelli, S., Centanni, M., Consolandi, C., Basaglia, G., et al. (2014). Gut microbiome of the Hadza hunter-gatherers. *Nat. Commun.* 5:3654. doi: 10.1038/ncomms4654

Shenhav, L., Thompson, M., Joseph, T. A., Briscoe, L., Furman, O., Bogumil, D., et al. (2019). FEAST: fast expectation-maximization for microbial source tracking. *Nat. Methods* 16, 627–632. doi: 10.1038/s41592-019-0431-x

Sim, K., Cox, M. J., Wopereis, H., Martin, R., Knol, J., Li, M.-S., et al. (2012). Improved detection of bifidobacteria with optimised 16S rRNA-gene based pyrosequencing. *PLoS One* 7:e32543. doi: 10.1371/journal.pone.0032543

Soto, A., Martin, V., Jimenez, E., Mader, I., Rodriguez, J. M., and Fernandez, L. (2014). Lactobacilli and bifidobacteria in human breast milk: influence of antibiotherapy and other host and clinical factors. *J. Pediatr. Gastr. Nutr.* 59, 78–88. doi: 10.1097/mpg.0000000000000347

Subramanian, S., Huq, S., Yatsunenko, T., Haque, R., Mahfuz, M., Alam, M. A., et al. (2014). Persistent gut microbiota immaturity in malnourished Bangladeshi children. *Nature* 510, 417–421. doi: 10.1038/nature13421

Sundin, O. H., Mendoza-Ladd, A., Zeng, M., Diaz-Arevalo, D., Morales, E., Fagan, B. M., et al. (2017). The human jejunum has an endogenous microbiota that differs from those in the oral cavity and colon. *BMC Microbiol.* 17:160. doi: 10.1186/s12866-017-1059-1056

Tannock, G. W., Lawley, B., Munro, K., Pathmanathan, S. G., Zhou, S. J., Makrides, M., et al. (2013). Comparison of the compositions of the stool microbiotas of infants fed goat milk formula, cow milk-based formula, or breast milk. *Appl. Environ. Microbiol.* 79, 3040–3048. doi: 10.1128/aem.03910-3912

Tannock, G. W., Lee, P. S., Wong, K. H., and Lawley, B. (2016). Why don't all infants have bifidobacteria in their stool? *Front. Microbiol.* 7:834. doi: 10.3389/fmicb.2016.00834

Turroni, F., Berry, D., and Ventura, M. (2017). Editorial: bifidobacteria and their role in the human gut microbiota. *Front. Microbiol.* 7:2148. doi: 10.3389/fmicb.2016.02148

Turroni, F., Milani, C., Duranti, S., Mancabelli, L., Mangifesta, M., Viappiani, A., et al. (2016). Deciphering bifidobacterial-mediated metabolic interactions and their impact on gut microbiota by a multi-omics approach. *ISME J.* 10, 1656–1668. doi: 10.1038/ismej.2015.236

Turroni, F., Peano, C., Pass, D. A., Foroni, E., Severgnini, M., Claesson, M. J., et al. (2012). Diversity of bifidobacteria within the infant gut microbiota. *PLoS One* 7:e36957. doi: 10.1371/journal.pone.0036957

Urbaniak, C., Angelini, M., Gloor, G. B., and Reid, G. (2016). Human milk microbiota profiles in relation to birthing method, gestation and infant gender. *Microbiome* 4:1. doi: 10.1186/s40168-015-0145-y

Van Rossum, T., Ferretti, P., Maistrenko, O. M., and Bork, P. (2020). Diversity within species: interpreting strains in microbiomes. *Nat. Rev. Microbiol.* 18, 491–506. doi: 10.1038/s41579-020-0368-361

Vatanen, T., Plichta, D. R., Somani, J., Munch, P. C., Arthur, T. D., Hall, A. B., et al. (2019). Genomic variation and strain-specific functional adaptation in the human gut microbiome during early life. *Nat. Microbiol.* 4, 470–479. doi: 10.1038/s41564-018-0321-325

Ward, T. L., Hosid, S., Ioshikhes, I., and Altosaar, I. (2013). Human milk metagenome: a functional capacity analysis. *BMC Microbiol.* 13:116. doi: 10.1186/1471-2180-13-116

Yatsunenko, T., Rey, F. E., Manary, M. J., Trehan, I., Dominguez-Bello, M. G., Contreras, M., et al. (2012). Human gut microbiome viewed across age and geography. *Nature* 486, 222–227. doi: 10.1038/nature11053

Zacarias, M. F., Binetti, A., Laco, M., Reinheimer, J., and Vinderola, G. (2011). Preliminary technological and potential probiotic characterisation of bifidobacteria isolated from breast milk for use in dairy products. *Int. Dairy. J.* 21, 548–555. doi: 10.1016/j.idairyj.2011.03.007

Zhang, J., Zhang, N., Liu, Y.-X., Zhang, X., Hu, B., Qin, Y., et al. (2018). Root microbiota shift in rice correlates with resident time in the field and developmental stage. *Sci. China Life. Sci.* 61, 613–621. doi: 10.1007/s11427-018-9284-9284

Zhang, M., Hang, X., Tan, J., and Yang, H. (2015). The host genotype and environment affect strain types of *Bifidobacterium longum* subsp. longum inhabiting the intestinal tracts of twins. *Appl. Environ. Microbiol.* 81, 4774–4781. doi: 10.1128/AEM.00249-215

Zhang, X., Mushajiang, S., Luo, B., Tian, F., Ni, Y., and Yan, W. (2020). The composition and concordance of Lactobacillus populations of infant gut and the corresponding breast-milk and maternal gut. *Front. Microbiol.* 11:597911. doi: 10.3389/fmicb.2020.597911

Conflict of Interest: The authors declare that the research was conducted in the absence of any commercial or financial relationships that could be construed as a potential conflict of interest.

frontiers in Microbiology

ORIGINAL RESEARCH
published: 16 June 2021
doi: 10.3389/fmicb.2021.653587

Bifidobacterium breve Exopolysaccharide Blocks Dendritic Cell Maturation and Activation of CD4$^+$ T Cells

Ana Hickey[1,2], Panagiota Stamou[1], Sreeram Udayan[1,2], Ana Ramón-Vázquez[1], Maria Esteban-Torres[1,3], Francesca Bottacini[1,3], Jerzy Adam Woznicki[1], Owen Hughes[4], Silvia Melgar[1], Marco Ventura[5], Douwe Van Sinderen[1,3], Valerio Rossini[1†] and Ken Nally[1,2*†]*

[1] APC Microbiome Ireland, University College Cork, Cork, Ireland, [2] School of Biochemistry and Cell Biology, University College Cork, Cork, Ireland, [3] School of Microbiology, University College Cork, Cork, Ireland, [4] Luminex Corporation, Austin, TX, United States, [5] Life Sciences and Environmental Sustainability, University of Parma, Parma, Italy

OPEN ACCESS

Edited by:
Lifeng Zhu,
Nanjing Normal University, China

Reviewed by:
Koji Hosomi,
National Institutes of Biomedical Innovation, Health and Nutrition, Japan
Fabien P. Blanchet,
Institut National de la Santé et de la Recherche Médicale (INSERM), France
Aristobolo Mendes Da Silva,
Minas Gerais State University, Brazil

***Correspondence:**
Valerio Rossini
valerio.rossini@ucc.ie
Ken Nally
k.nally@ucc.ie

†These authors share senior authorship

Specialty section:
This article was submitted to Microbial Symbioses, a section of the journal Frontiers in Microbiology

Received: 14 January 2021
Accepted: 11 May 2021
Published: 16 June 2021

Citation:
Hickey A, Stamou P, Udayan S, Ramón-Vázquez A, Esteban-Torres M, Bottacini F, Woznicki JA, Hughes O, Melgar S, Ventura M, Van Sinderen D, Rossini V and Nally K (2021) Bifidobacterium breve Exopolysaccharide Blocks Dendritic Cell Maturation and Activation of CD4$^+$ T Cells. Front. Microbiol. 12:653587. doi: 10.3389/fmicb.2021.653587

Exopolysaccharide (EPS) is a bacterial extracellular carbohydrate moiety which has been associated with immunomodulatory activity and host protective effects of several gut commensal bacteria. *Bifidobacterium breve* are early colonizers of the human gastrointestinal tract (GIT) but the role of EPS in mediating their effects on the host has not been investigated for many strains. Here, we characterized EPS production by a panel of human *B. breve* isolates and investigated the effect of EPS status on host immune responses using human and murine cell culture-based assay systems. We report that *B. breve* EPS production is heterogenous across strains and that immune responses in human THP-1 monocytes are strain-specific, but not EPS status-specific. Using wild type and isogenic EPS deficient mutants of *B. breve* strains UCC2003 and JCM7017 we show that EPS had strain-specific divergent effects on cytokine responses from murine bone marrow derived macrophages (BMDMs) and dendritic cells (BMDCs). The *B. breve* UCC2003 EPS negative (EPS$^-$) strain increased expression of cytokine genes (*Tnfa, Il6, Il12a*, and *Il23a*) relative to untreated BMDCs and BMDCs treated with wild type strain. *B. breve* UCC2003 and JCM7017 EPS$^-$ strains increased expression of dendritic cell (DC) activation and maturation marker genes (*Cd80, Cd83*, and *Cd86*) relative to untreated BMDCs. Consistent with this, BMDCs co-cultured with *B. breve* UCC2003 and JCM7017 EPS$^-$ strains engineered to express OVA antigen activated OVA-specific OT-II CD4$^+$ T-cells in a co-culture antigen-presentation assay while EPS proficient strains did not. Collectively, these data indicate that *B. breve* EPS proficient strains use EPS to prevent maturation of DCs and activation of antigen specific CD4$^+$ T cells responses to *B. breve*. This study identifies a new immunomodulatory role for *B. breve* EPS and suggests it may be important for immune evasion of adaptive immunity by *B. breve* and contribute to host-microbe mutualism.

Keywords: *Bifidobacterium breve*, exopolysaccharides, host immune responses, macrophages, dendritic cells, antigen presentation

INTRODUCTION

Bifidobacteria elicit protective immunomodulatory effects on murine and human hosts including reduction of gastrointestinal (GI) diseases and potentially systemic effects (Sivan et al., 2015; Sarkar and Mandal, 2016; Riedel, 2018). However, mechanisms underpinning these effects are still poorly understood (Fischbach, 2018; Round and Palm, 2018). Identification and characterization of specific bifidobacterial microbe-associated molecular patterns (MAMPs), their corresponding host pattern recognition receptors (PRRs) (Round et al., 2011) and associated immune cell responses is needed in order to understand proposed immunomodulatory properties of bifidobacteria. One of these candidate bifidobacterial MAMPs is EPS, a surface-associated glycan which is used by pathogens and other microbiota members to manipulate host responses (Castro-Bravo et al., 2018b). There is large structural diversity in EPS polymers produced by bifidobacteria, even between strains of the same species (Bottacini et al., 2014; Hidalgo-Cantabrana et al., 2014; Ferrario et al., 2016). The genes responsible for EPS biosynthesis are clustered within one or two transcriptional units. Variations in monosaccharide components and quantities of such, in addition to differences in glycosidic linkages and the degree of branching have been observed for different bifidobacteria strains (Leivers et al., 2011; Hidalgo-Cantabrana et al., 2014; Inturri et al., 2017; Castro-Bravo et al., 2018a). This variation could, in principle, lead to a vast number of distinct EPS structures and, theoretically to different immunomodulatory effects on the host. Reports indicate that purified EPS from two different bifidobacterial species can be detected by host innate immune PRRs – toll like receptor (TLR) 2 and TLR4 (Schiavi et al., 2018; Castro-Bravo et al., 2019). Bifidobacterial EPS has also been shown to ameliorate inflammation in murine pulmonary and intestinal models of inflammation (Hidalgo-Cantabrana et al., 2016; Schiavi et al., 2018). Previously, our group showed that EPS deficient *B. breve* UCC2003 had profound immunomodulatory effects on the host with an increase in pro-inflammatory cytokines interferon (IFN)-γ, tumor necrosis factor (TNF)-α and IL-12 detected from splenocytes cultured with the bacteria. These effects were associated with an increase in neutrophils, macrophages, natural killer cells, B cells and IFN-γ^+, TNF-α^+, and IL-12$^+$ T cells (Fanning et al., 2012). Furthermore, the administration of EPS deficient *B. breve* to mice increased susceptibility to *Citrobacter rodentium* infection and reduced persistence of *B. breve* in the murine GIT (Fanning et al., 2012). Although many studies have used purified EPS to characterize host responses, this approach is susceptible to contamination with additional MAMPs derived from components of bacterial cell walls, membranes, or even cytoplasms (Alhudhud et al., 2018). An alternative reductionist approach is to investigate the effects of EPS using EPS deficient isogenic mutants of EPS producers and compare immune cell responses to both WT EPS proficient and mutant EPS deficient strains. EPS deficient mutants have been created for several bifidobacterial strains such as *Bifidobacterium longum* ssp. *longum* 35624 (Schiavi et al., 2016), *B. longum* 105-A (Tahoun et al., 2017), *Bifidobacterium breve* UCC2003 (Fanning et al., 2012), and *B. breve* JCM7017 (Alhudhud et al., 2018). Another consideration when investigating EPS-mediated effects is to use experimental cell-based systems from different host species as bifidobacteria are found and isolated from various ecological niches (Turroni et al., 2018). In this study, we analyzed a panel of 12 *B. breve* strains, which were isolated from humans, to assess EPS production. Two of these strains had matching isogenic EPS deficient mutant strains as previously described (*B. breve* UCC2003 and JCM7017) (Fanning et al., 2012; Alhudhud et al., 2018) and were used to determine the contribution of EPS to host immune cell responses. We found that *B. breve* EPS production was required to prevent maturation of dendritic cells and dendritic cell-mediated activation of CD4$^+$ T cells responses.

MATERIALS AND METHODS

Bacterial Culture Conditions and Plasmid Transformation

All bacterial strains used in this study are listed in **Table 1**. Strains were routinely cultured in reinforced clostridial medium (RCM; Oxoid cat. CM0149), sub-cultured into de Man Rogosa and Sharpe Medium (MRS; Becton Dickonson Difco cat. 288130) supplemented with 0.05% cysteine-HCl (Sigma) and incubated anaerobically at 37°C. Culture of bifidobacterial strains for growth curves was carried out in modified MRS (mMRS) medium, which was prepared from first principles (De Man et al., 1960) and supplemented with 0.05% cysteine-HCl (Sigma) and 1% glucose (Sigma). Cultures containing either *B. breve* UCC2003 EPS$^-$ or *B. breve* JCM7017 EPS$^-$ mutants were supplemented with 0.01 mg/mL tetracycline (Sigma) and cultures containing bacteria transformed with the pMG-mCherry-OVA plasmid were supplemented with 0.01 mg/mL chloramphenicol (Sigma). The pMG-mCherry-OVA plasmid was constructed from the pMG-mCherry plasmid as

TABLE 1 | List of B. breve strains used in study, their origin of isolation and genome accession number.

Strain	Origin	Accession number	References
UCC2003	Human infant feces	NC_020517	Bottacini et al., 2014
UCC2003_EPSneg	Mutant made in UCC		Fanning et al., 2012
JCM7017	Human adult feces	CP006712	Bottacini et al., 2014
JCM7017_EPSneg	Mutant made in UCC		Alhudhud et al., 2018
JCM7019	Human infant feces	CP006713	Bottacini et al., 2014
215W447A	Human infant feces	CP021558	Bottacini et al., 2017
017W439A	Human infant feces	CP021554	Bottacini et al., 2017
082W48	Human infant feces	CP021555	Bottacini et al., 2017
689b	Human infant feces	CP006715	Bottacini et al., 2014
NCTC 11815	Human infant feces	BBAO00000000	Bottacini et al., 2014
139W4	Human infant feces	CP021556	Bottacini et al., 2017
NCFB 2258	Human infant feces	CP006714	Bottacini et al., 2014
180W83	Human infant feces	CP021557	Bottacini et al., 2017
B12L	Human milk	CP006711	Bottacini et al., 2014

described by Grimm et al. (2014). Transformation of the pMG-mCherry-OVA plasmid into *B. breve* strains was achieved by electroporation with subsequent screening for chloramphenicol-resistant colonies on RCM agar plates containing 0.01 mg/mL chloramphenicol (Sigma). Further confirmation of mCherry-OVA expression was carried out by flow cytometry for mCherry expression (excitation at 545 ± 30 nm, emission at 610 ± 75 nm) using the BD FACSAria III Fusion Cell sorter, polymerase chain reaction and western blot. Flow cytometry data was further analyzed using FCS Express version 5 software (*De Novo*).

Electron Microscopy

Bacteria were prepared as described. Materials were directly adsorbed onto a carbon film membrane on a 300-mesh copper grid, stained with 1% uranyl acetate, dissolved in distilled water, and dried at room temperature. Grids were examined with Hitachi HT7700 electron microscope operated at 80 kV (Elexience – France), and images were acquired with a charge-coupled device camera (AMT). This work was carried out at the facilities and expertise of MIMA2 MET – GABI, INRA, Agroparistech (78352 Jouy-en-Josas, France).

In silico and *in vitro* Analysis of EPS Production

In silico analysis of *B. breve* fully sequenced strains was carried out using comparative genome analysis according to a previously described method (Bottacini et al., 2018). Whole genome sequences of 12 *B. breve* strains were retrieved from the National Centre for Biotechnology Information (NCBI) database. The genomic region previously described as associated to EPS biosynthesis in *B. breve* UCC2003 (Fanning et al., 2012; Bottacini et al., 2017), encoded between a priming glycosyl transferase (Bbr_0430) and a chain length determinant (Bbr_0474) was used as starting point for predicting homologous EPS-encoding regions in the 12 *B. breve* strains here analyzed. Presence/absence of homologous genes was retrieved by comparative genome analysis using "all-against-all," bi-directional BLASTP alignments49 (cut-off: *E*-value < 0.0001, with at least 50% identity across at least 50% of either protein sequence). Based on previous descriptions for the *B. breve* spp., each strain was classified as an EPS "producer" or "non-producer" based on the presence of: (a) an EPS locus larger than 30 Kb, (b) at least three glycosyltransferase (GTF)-encoding genes within the predicted EPS locus, (c) a priming glycosyltransferase, (d) a gene encoding a flippase, (e) a chain length determinant. EPS status was assessed *in vitro* by a sedimentation assay as previously described (Fanning et al., 2012; Tahoun et al., 2017). Briefly, optical density measurements ($OD_{600\ nm}$) of *B. breve* strains and EPS^- mutants were taken over a 6 h time period grown in mMRS medium, which was prepared from first principles (De Man et al., 1960) and supplemented with 0.05% cysteine-HCl and 1% glucose, lactose or maltose (Sigma) without agitation. A drop in OD values due to sedimentation is a characteristic of EPS non-producers.

Mice

Mice used for this study were 8–12 weeks old from a C57BL/6 background. WT C57BL/6 mice for isolation of bone marrow and generation of BMDMs and BMDCs were purchased from Envigo (Oxfordshire, United Kingdom). OT-II mice were acquired from Jackson Laboratories (Bar Harbor, United States) and breeding was maintained in house. All mice were housed in UCC Biological Services Unit under specific pathogen free (SPF) conditions. Standard housing conditions were maintained with 12 h darkness and 12 h light, temperature controlled at 21°C and 50% humidity. Animals were fed standard chow pellets and water was given *ad libitum*. The animal work was performed in accordance with EU legislation, in accordance with EU Directive 2010/63/EU, for the protection of animals used for scientific purposes and approved by the Animal Experimentation Ethics Committee of University College Cork, Euthanasia Only Application ID 2018/007.

THP-1 Human Monocytic NF-κB Reporter Cells

THP1-XBlue™ and THP1-XBlue™-defMyD (MyD88 deficient) NF-κB reporter cell lines were purchased from Invivogen. Cells were routinely cultured using Roswell Park Memorial Institute medium (RPMI 1640; Sigma cat. R8758) supplemented with 10% Fetal Bovine Serum (FBS; Sigma), 1% Penicillin-Streptomycin (P/S; Sigma), 100 μg/mL Normocin (Invivogen) and 200 μg/mL Zeocin (Invivogen). For the THP1-XBlue™-defMyD cells 100 μg/mL Hygromycin B Gold (Invivogen) was added to the medium. Cells were continuously maintained at a density between 7×10^5 cells/mL and 2×10^6 cells/mL. NF-κB activity in THP-1 reporter cell lines was assayed using Quanti-blue (Invivogen cat. rep-qb1), as per manufacturer's instructions.

GM-CSF-Derived Bone Marrow Derived Macrophages and Dendritic Cells

Bone marrow isolation was carried out using aseptic techniques. This method was based on the work of Helft et al. (2015). Briefly, bone marrow was isolated from the femurs and tibias of selected mice by flushing using RPMI and filtered through a 70 μm strainer. Cells were collected by centrifugation at $200 \times g$ at 4°C for 10 min. The cell pellet was resuspended in differentiation media – RPMI containing 10% FBS, 1% P/S and 20 ng/mL GM-CSF (PeproTech cat. 315-03). Cells were counted and 10^7 cells were seeded per well in 6 well plates with each well containing 4 mL of differentiation media. On day 2 half of the content was collected from each well, centrifuged and cells were resuspended in RPMI containing 10% FBS, 1% P/S and 40 ng/mL GM-CSF and added back to the 6 well plates. On day 3, all content from each well was harvested, centrifuged and cells were resuspended in RPMI containing 10% FBS, 1% P/S and 20 ng/mL GM-CSF before being added back to the 6 well plates. Both suspension cells (containing the DC fraction) and adherent cells (containing the macrophage fraction) were collected on day 6 and prepared for sorting. Prior to collection, adherent cells were harvested using Stempro Accutase (Thermo Scientific).

Cells were stained using anti-mouse CD11c Alexa Fluor 700 (BioLegend cat. 117320), anti-mouse I-A/I-E fluorescein isothiocyanate (BioLegend cat. 107606), anti-mouse CD11b R-phycoerythrin cyanine 7 (BioLegend cat. 101216) and anti-mouse CD115 Allophycocyanin (BioLegend cat. 135510). Cells were then analyzed using the BD FACSAriaIII Fusion Cell sorter and sorted into pure populations of BMDMs and BMDCs based on a gating strategy modified from Helft et al. (2015). Data was further analyzed using FCS Express version 5 software (*De Novo*).

Co-culture of Mammalian Cells and Bifidobacteria

For all experiments, after an overnight culture of bacteria an $OD_{600\ nm}$ of 1 corresponded to 10^9 CFU of bacteria. Bacteria were washed twice in sterile PBS and resuspended in the appropriate mammalian cell culture medium with no antibiotics and concentration was adjusted as required. For cytokine and NF-κB activity experiments, BMDMs, BMDCs and THP-1 monocytes were seeded in 96 well plates at a density of 5×10^4 cells/well in RPMI with 10% FBS and incubated with bacteria at a multiplicity of infection of 10:1 bacteria:cells. For BMDM and BMDCs experiments 100 ng/mL of LPS-B5 (Invivogen cat. tlrl-b5lps) and 5 μM of ODN 1585 CpG (Invivogen cat. tlrl-1585) were added as a positive controls, respectively. Co-cultures were incubated for 24 h at 37°C in 5% CO_2. After 24 h, cells were collected by centrifugation and supernatants analyzed for NF-κB activity (THP-1 cells only). For reverse transcription-quantitative polymerase chain reaction (RT-qPCR) BMDMs or BMDCs were seeded at 2.5×10^5 cells were seeded per well in 12 well plates in RPMI with 10% FBS and incubated with bacteria at a multiplicity of infection of 10:1. 100 ng/mL of LPS-B5 (Invivogen cat. tlrl-b5lps) was used as a positive control in BMDM cultures and 5 μM of ODN 1585 CpG (Invivogen cat. tlrl-1585) was used as a positive control in BMDCs cultures. Co-cultures were incubated for 4 or 8 h at 37°C in 5% CO_2. After 4 or 8 h, BMDMs were washed with ice cold PBS once and lysed using RLT lysis buffer (Qiagen). BMDCs were transferred to 1.5 mL tubes and centrifuged for 7 min at 400 × *g* at 4°C. Supernatants were removed and cells lysed in RLT lysis buffer. Both BMDM and BMDs lysates were immediately stored at −80°C until total RNA was extracted.

Cytokine ELISAs

BMDM and BMDCs co-culture supernatants were analyzed for secreted cytokines TNF-α and IL-10 using mouse TNF-alpha DuoSet ELISA (R&D Systems cat. DY410) and mouse IL-10 DuoSet ELISA (R&D Systems cat. DY417) as per manufacturer's instructions. Supernatants from T cell and BMDM or BMDCs co-cultures were analyzed for secreted cytokines TNF-α and IL-2 using mouse TNF-alpha DuoSet ELISA (R&D Systems cat. DY410) and mouse IL-2 DuoSet ELISA (R&D Systems cat. DY402) as per manufacturer's instructions. TNF-α production by THP-1 reporter cell lines was measured in supernatants from these experiments using human TNF-α ELISA Duoset (R&D Systems cat. DY210).

RT-qPCR

RNA was isolated from BMDMs and BMDCs using RNeasy Micro Kit (Qiagen cat. 74004) which included DNase treatment. Total RNA was quantified using Qubit RNA high sensitivity kit (Biosciences cat. Q32852). Complementary DNA (cDNA) was synthesized from 100 ng of total RNA using Transcriptor Reverse Transcriptase (Roche) and random hexamer primers (Roche) as per manufacturer's instructions. qPCR assays were designed using the Roche Universal Probe Library Assay Design Centre (**Table 2**). qPCR assays were carried out by using SensiFAST Probe No-ROX Kit (Bioline), 500 nM primers, 250 nM corresponding ProbeLibrary probe from Universal ProbeLibrary (Roche) and 2 ng of cDNA. PCR reactions were run on a LightCycler 480 instrument (Roche) and the $2^{-\Delta\Delta CT}$ method (Mar et al., 2009; McCall et al., 2014) was used to calculate relative gene changes in gene expression compared to β-actin which served as a housekeeping gene (Livak and Schmittgen, 2001).

Western Blotting

After an overnight culture, bacterial cells were resuspended in ice-cold 10 mM Tris-HCl pH 8, transferred to tubes containing glass microbeads and bead-beated three times. Lysates were centrifuged at maximum speed for 15 min at 4°C and supernatants were transferred to fresh 1.5 mL tubes. Protein was quantified using Pierce BCA Protein Assay Kit (Thermo Scientific) as per manufacturer's instructions. Fifty μg of protein for each sample was standardized and the appropriate volume of 4× LDS sample buffer and 10× sample reducing agent (Novex) was added to each sample. Protein was denatured by heating at 70°C for 10 min. Samples were separated on a 4–12% Bis-Tris Plus Gel (Invitrogen) alongside SeeBlue Plus2 Prestained Standard ladder (Invitrogen) and transferred onto a PVDF membrane (Millipore) for antibody detection. Membranes were stained with Ponceau S to confirm protein transfer, blocked for 1 h rocking at room temperature with 5% milk powder (Sigma) dissolved in 0.05% Tween-20 TBS (TBST), washed three times with TBST and incubated rocking overnight at

TABLE 2 | List of genes, Universal ProbeLibrary (UPL) probes and primers used for RT-qPCR.

Gene	Probe	Forward primer	Reverse primer
Il10	41	cagagccacatgctcctaga	tgtccagctggtcctttgtt
Tnfa	49	tcttctcattcctgcttgtgg	ggtctgggccatagaactga
Il6	6	gctaccaaactggatataatcagga	ccaggtagctatggtactccagaa
Il12a	62	ccaggtgtcttagccagtcc	gcagtgcaggaataatgtttca
Il12b	27	gactccaggggacaggcta	ccaggagatggttagcttctga
Il23a	19	tccctactaggactcagccaac	agaactcaggctgggcatc
H2/MHCII	110	ctctgattctgggggtcct	accataggtgcctacgtggt
Cd80	91	ttcgtctttcacaagtgtcttca	tgccagtagattcggtcttca
Cd86	107	gaagccgaatcagcctagc	cagcgttactatcccgctct
Adhl1a2	33	catggtatcctccgcaatg	gcgcatttaaggcattgtaac
Cd274	101	gttgttcctcattgtagtgtcca	cacatttctccacatctagcattc
Pdcd1lg2	17	gcatgttctggaatgctcac	ctttgggttccatccgact
Cd83	29	accgtggttctgaaggtgac	caaccagagagaagagcaacac
β-actin	64	ctaaggccaaccgtgaaaag	accagaggcatacagggaca

4°C with anti-OVA (Abbiotec cat. 250803) in 5% milk in TBST. Membranes were washed with TBST and incubated with HRP-conjugated goat anti-rabbit secondary antibody (Sigma) in 5% milk in TBST. Membranes were washed with TBST and WesternBright substrate (Advansta) was added. Images were acquired using Fujifilm LAS-3000 instrument and software.

Co-culture Antigen Presentation Assay With Bacterial – BMDC– $CD4^+$ T Cells

5×10^4 sorted BMDCs were seeded per well in 96 well plates in RPMI with 10% FBS but no antibiotics. Bacteria expressing mCherry-OVA were added at ratio 10:1. OVA protein (Sigma) was added at a final concentration of 150 μg/mL as a positive control. The cells were incubated with OVA protein or bacteria for 8 h at 37°C in a cell culture incubator at 5% CO_2. $CD4^+$ T cells were isolated from OT-II mice by spleen homogenization. Red blood cells were lysed using RBC lysis buffer (Invitrogen) and $CD4^+$ T cells separated magnetically using mouse $CD4^+$ T Cell Isolation Kit (Miltenyi cat. 130-104-454) as per manufacturer's instructions. Isolated T cells were then labeled with carboxyfluorescein succinimidyl ester (CFSE) Cell Division Tracker kit (BioLegend cat. 423801) as per manufacturer's instructions. After 8 h co-incubation with OVA protein or bacteria, media was removed from the BMDCs cultures and fresh media containing 200 μg/mL gentamicin (Sigma) was added for 30 min at 37°C. The cells were washed three times with PBS and fresh media was added along with CFSE-labeled $CD4^+$ T cells from OT-II mice at a ratio of 1:1 T cells:BMDCs. Plates were incubated at 37°C in 5% CO_2 for 5 days. T cells were then collected by centrifugation and stained with anti-mouse CD4 Brilliant Violet421 (BioLegend cat. 135510) and anti-mouse CD25 R-phycoerythrin cyanine 7 (BioLegend cat. 101916). T cell proliferation and activation was analyzed using the BD FACSCelesta Analyzer and data was further analyzed using FCS Express version 5 software (*De Novo*).

Image Stream Analysis

1×10^6 sorted BMDCs were seed in 6-well plates and co-cultured overnight at 37°C with *B. breve* EPS^+ and *B. breve* EPS^- at MOI 10:1. Cultured BMDCs alone were used as negative controls. Cells were washed and incubated with gentamicin (200 μg/mL) for 30 min at 37°C and then washed 3 times in 1 × PBS and stained with CD45 APC, as previously described. Cells were washed twice in wash buffer, fixed with 1% paraformaldehyde and re-suspended in 50 μl of wash buffer. Fixed and stained cell samples were analyzed with an Amnis ImageStreamX MkII cytometer running INSPIRE software version 200.1.620.0 At least 2000 CD45 positive cells were acquired from each experimental sample. Data was analyzed using IDEAS version 6.2.187.0.

Statistical Analysis

For every experiment at least three biological replicates with three technical replicates per experiment were performed. Statistical analysis was compiled using one way ANOVA with Dunnett's comparison in GraphPad Prism version 5.03. Statistical comparisons were completed using student's *t*-tests and *p*-values less than 0.05 were considered significant.

RESULTS

Heterogeneous Production of EPS by Human *B. breve* Strains

The EPS status (**Table 3**) of twelve *B. breve* strains (**Table 1**) was predicted by *in silico* analyses of *B. breve* genomes for presence of genes required for EPS production. We used the EPS^- mutant of *B. breve* UCC2003 as a positive control for an EPS sedimentation assay. Because the carbohydrate source can significantly impact EPS production we screened all *B. breve* strains in media supplemented with different carbohydrates (glucose, lactose, and maltose) (Raftis et al., 2011). *B. breve* UCC2003 and JCM7017 wild type (WT) strains did not sediment but their EPS^- mutants did over a period of 6 h (**Figure 1A**). *B. breve* JCM7019 was a consistent EPS producer while *B. breve* NCTC 11815 sedimented in both glucose and lactose but not in maltose, despite the fact that it was predicted not to produce EPS (**Figure 1A** and **Table 3**). *B. breve* strains 017W439A and 215W447A were EPS producers when cultured in all three carbohydrate sources while the 139W4 and NCFB 2258 strains were not (**Figure 1B**). *B. breve* strains 082W48 and 689b were EPS producers when cultured in all three carbohydrate sources while *B. breve* strains 180W83 and B12L were not (**Figure 1C**). Comparison between the predicted and actual EPS status of *B. breve* strains (based on EPS sedimentation assay) demonstrated that all predictions were correct except for strain 139W4 which was predicted to produce EPS but actually sedimented *in vitro* irrespective of the carbohydrate source used (**Table 3**).

Human THP-1 Monocyte Responses to *B. breve* Strains Are MyD88-Dependent

To investigate if EPS production by *B. breve* strains either positively or negatively affected recognition and response to the bacteria by monocytes, the panel of bacteria were co-cultured with WT and $MyD88^{-/-}$ human THP-1 monocyte nuclear factor (NF)-κB reporter cell lines (**Figure 2A**). NF-κB responses to the panel of *B. breve* strains showed that there was no clear EPS-dependent associated innate immune response. Although strains (*B. breve* 215W447A, 689b, and JCM7019) which stimulated highest activation of NF-κB were all EPS positive, the strain (017W439A) which stimulated lowest activation of NF-κB was also EPS positive (**Figure 2A**). There was decreased activation of NF-κB by *B. breve* UCC2003 and JCM7017 EPS^- isogenic mutant strains compared to their WT parental strains (**Figure 2A**). Production of TNF-α by THP-1 cells showed a similar trend to NF-κB responses (**Figure 2B**) for all strains. The lack of response to all strains in the $MyD88^{-/-}$ THP-1 cell line showed that NF-κB activation and TNF-α production was uniformly MyD88-dependent in this cell system (**Figure 2**). Overall, there was no correlation between EPS status and immune activation of human THP-1 monocytic cells, although all responses to *B. breve* were MyD88-dependent, regardless of strain.

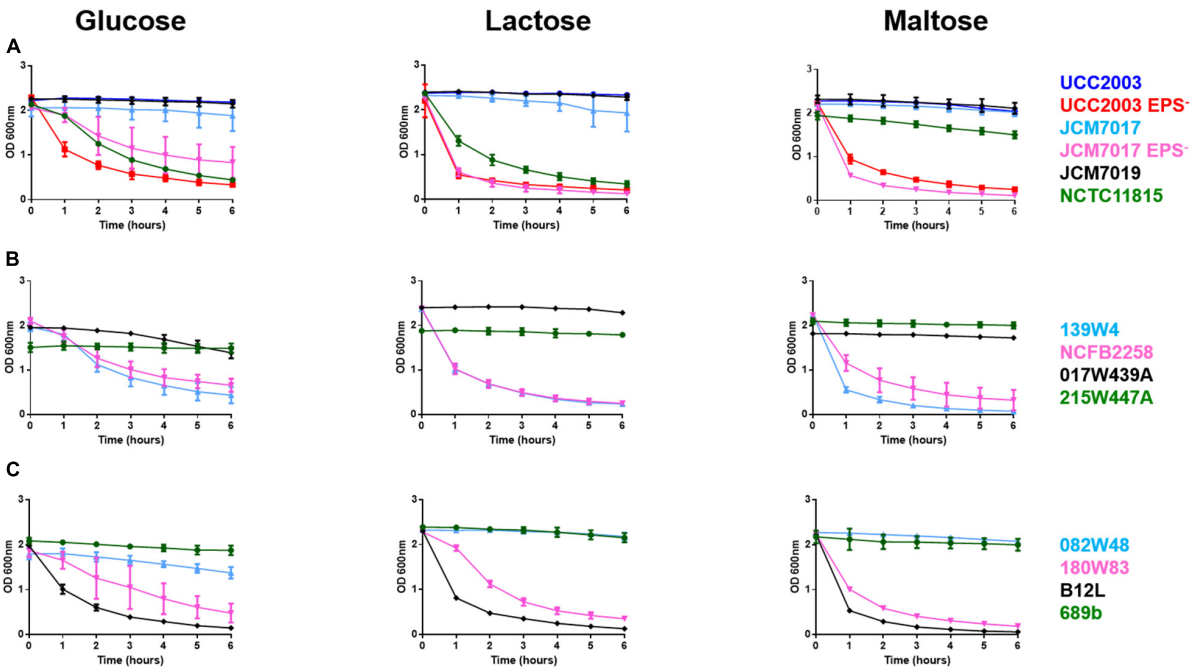

FIGURE 1 | Heterogeneity of EPS production by *B. breve* strains in different carbon sources. *B. breve* strains were cultured overnight, homogenized before OD readings were taken from cultures over 6 h with no disturbance to cultures at all. Bacteria were grown in media containing either glucose, lactose, or maltose as a carbon source. This was done for *B. breve* UCC2003, UCC2003 EPS$^-$, JCM7017, JCM7017 EPS$^-$, JCM7019 and NCTC 11815 **(A)**, 139W4, NCFB 2258, 215W447A and 017W439A **(B)**, 082W48, 180W83, B12L and 689b **(C)**. Data show the average of three independent experiments.

EPS Modulates Cytokine Response of BMDMs to *B. breve* UCC2003 and JCM7017

Because we observed no association between EPS production status and immunomodulation by different *B. breve* strains in THP-1 cells, we investigated the role of EPS on immunomodulation specifically by *B. breve* UCC2003 and JCM7017 using the EPS$^-$ isogenic mutants of both strains. EPS production by *B. breve* UCC2003 and JCM7017 parental strains and their respective isogenic EPS$^-$ mutants was first confirmed by transmission electron microscopy (TEM) (**Figure 3**). TEM images showed a noticeably thicker layer of EPS surrounding the WT *B. breve* UCC2003 strain compared with JCM7017 WT strain (**Figures 3A,C**). In addition TEM confirmed absence of EPS on the surface of both the *B. breve* UCC2003 EPS$^-$ and JCM7017 EPS$^-$ isogenic mutant strains (**Figures 3B,D**). To understand how EPS affects macrophage and DC cytokine responses to *B. breve* UCC2003 and JCM7017, primary BMDMs (**Figure 4A**) and BMDCs (**Figure 4B**) were co-cultured with the strains and their isogenic EPS$^-$ mutants for 24 h. The absence of EPS from *B. breve* UCC2003 enhanced BMDM TNF-α and IL10 cytokine responses, while the absence of EPS from *B. breve* JCM7017 reduced cytokine responses (**Figures 4C,D**). BMDCs did not produce significant TNF-α or IL10 in response to any bacterial strain (**Figures 4E,F**).

TABLE 3 | EPS status of *B. breve* strains.

Strain	Predicted EPS status	EPS status by assay
UCC2003	Positive	Positive
UCC2003_EPSneg	Negative (mutant)	Negative
JCM7017	Positive	Positive
JCM7017_EPSneg	Negative (mutant)	Negative
JCM7019	Positive	Positive
215W447A	Positive	Positive
017W439A	Unclear	Positive
082W48	Unclear	Positive
689b	Unclear	Positive
NCTC 11815	Negative	Negative
139W4	Positive	Negative
NCFB 2258	Negative	Negative
180W83	Unclear	Negative
B12L	Unclear	Negative

Strains were predicted in silico to be EPS producers or non-producers based on the presence of pGTF and chain length regulator genes. EPS status in vitro was evaluated using EPS sedimentation assays.

EPS Reduces Activation of BMDCs by *B. breve* UCC2003 and JCM7017

To further understand the innate immune response of phagocytes to *B. breve* UCC2003 and JCM7017 and how EPS can affect this, we co-cultured sorted BMDCs with the two WT bacterial strains and their EPS$^-$ isogenic mutants for 4 h (**Figure 5** and **Supplementary Table 1**) and 8 h (**Supplementary Figure 1**). We also co-cultured BMDMs with the strains for

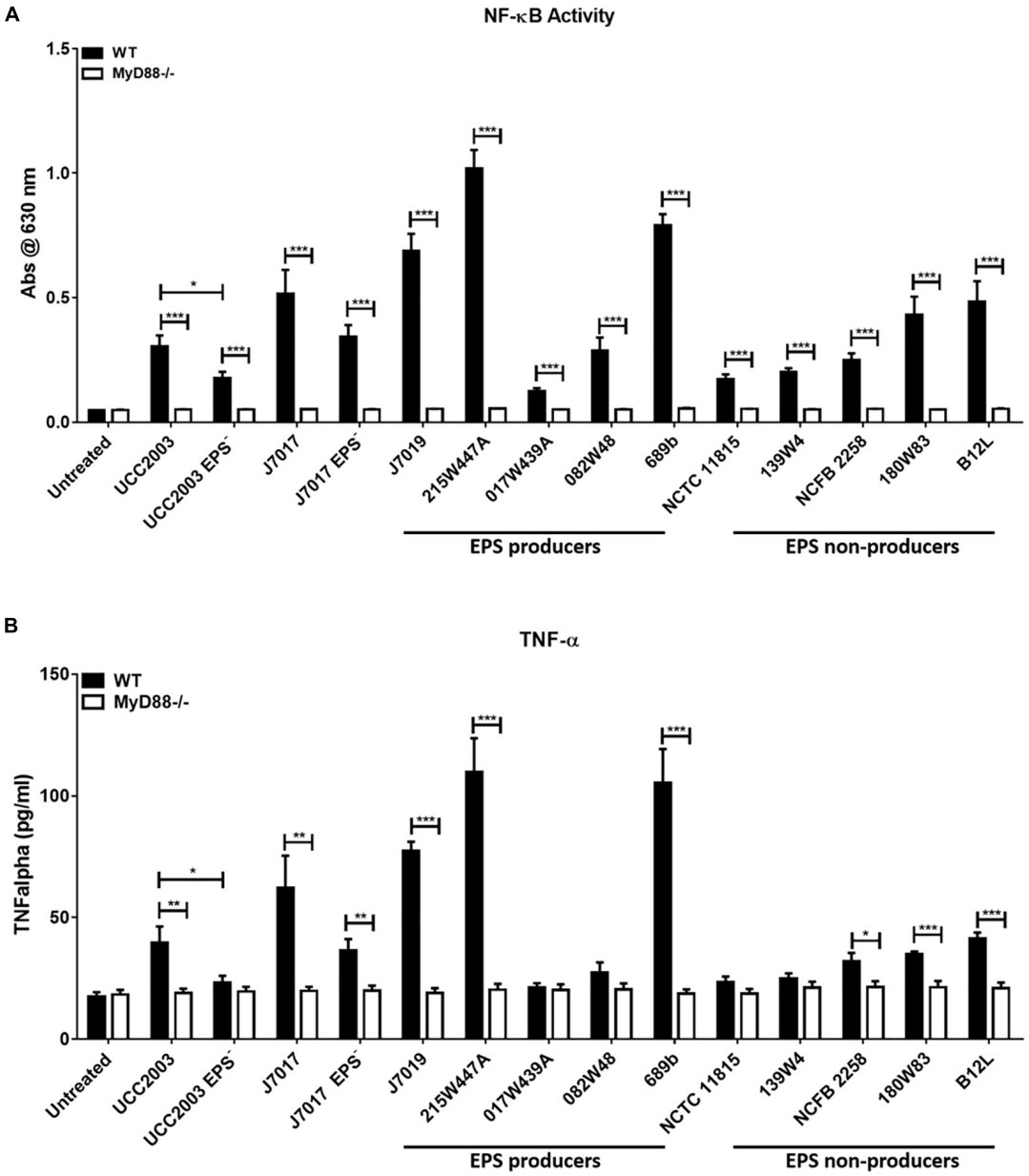

FIGURE 2 | Human THP-1 monocyte responses to *B. breve* strains are MyD88-dependent but EPS-independent. *B. breve* strains were incubated with THP1-XBlue and THP1-XBlue-defMyD reporter cell lines for 24 h. **(A)** NF-κB responses were assessed by measuring reporter gene production, secreted embryonic alkaline phosphatase. **(B)** TNF-α secretion was assessed by ELISA. Data shown is the average of three independent experiments performed in triplicate wells. Data are presented as mean ± SEM. Statistical analysis was assessed using the student *t*-test in GraphPad Prism where **p*-value < 0.05, ***p*-value < 0.005, and ****p*-value < 0.0005.

8 h (**Supplementary Figure 2**). RT-qPCR was performed for cytokine genes (*Il10, Tnfa, Il6, Il12a, Il12b*, and *Il23a*), antigen presentation and co-stimulatory genes (*H2/MHC-II, Cd80, Cd83*, and *Cd86*), and immune tolerogenic genes (*Aldh1a2, Cd274*, and *Pdcd1lg2*). *B. breve* UCC2003, JCM7017 strains and their EPS$^-$ mutants significantly increased the expression of cytokine genes *Il10, Tnfa, Il6* (**Figures 5A–C**) relative to untreated BMDCs at 4 h. *B. breve* UCC2003 EPS$^-$ also increased expression of both *Il12a/Il12p35* and *Il23a/Il12p19* compared to untreated cells (**Figure 5D**). However, no significant differences were observed between groups for the expression of *Il12b/Il12p40,* the gene coding for the other subunit of both IL-12p35/p40 and IL-23p19/p40 cytokines which are associated with Th1 and Th17 responses, respectively. No effects were seen on *H2*/MHC-II (**Figure 5G**) or *Pdcd1lg2*/PDL1 (**Figure 5K**) expression. Significantly, EPS$^-$ mutants of both *B. breve* UCC2003 and JCM7017 – but not EPS WT strains - increased the expression of the T cell co-stimulatory genes *Cd80* (**Figure 5H**) and

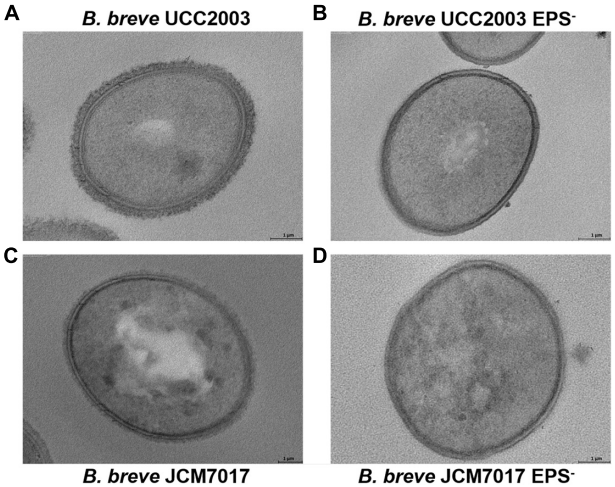

FIGURE 3 | Confirmation of EPS production by *B. breve* UCC2003, JCM7017 and EPS$^-$ mutants. Transmission electron microscopy images of *B. breve* UCC2003 **(A)**, *B. breve* UCC2003 EPS$^-$ **(B)**, *B. breve* JCM7017 **(C)**, and *B. breve* JCM7017 EPS$^-$ **(D)**.

Cd83 (**Figure 5M**), relative to untreated BMDCs while *Cd86* (**Figure 5I**) expression was increased by both *B. breve* UCC2003 EPS$^-$ and WT JCM7017. The absence of EPS from *B. breve* UCC2003 further enhanced expression of *Tnfa, IL6*, and *Il23a* relative to the WT parental strain (**Figures 5B,C,F**). No significant differences between the parental WT and EPS$^-$ mutant strains of *B. breve* JCM7017 were observed for any of the genes tested. After 8 h co-culture (**Supplementary Figure 1** and **Supplementary Table 1**), all four tested strains continued to significantly enhance *Il10* and *Il6* expression relative to untreated BMDCs (**Supplementary Figures 1A,C**). Expression of *Tnfa* was also significantly increased by all strains except WT *B. breve* UCC2003 (**Supplementary Figure 1B**). The absence of EPS from *B. breve* UCC2003 increased *Tnfa* transcription (**Supplementary Figure 1B**) and decreased Il6 transcription relative to its parental WT strain (**Supplementary Figure 1C**). Both EPS$^-$ mutants induced the expression of *Il23a* compared to untreated (**Supplementary Figure 1F**) and WT *B. breve* UCC2003 decreased expression of *H2*/MHC-II (**Supplementary Figure 1G**) and *Cd83* (**Supplementary Figure 1M**) relative to untreated cells. Importantly, absence of EPS from *B. breve* UCC2003 increased transcription of *Cd83* (**Supplementary Figure 1M**) at 8 h relative to its parental WT strain. In BMDM after 8 h of co-culture with the strains (**Supplementary Figure 2** and **Supplementary Table 1**), the absence of EPS from *B. breve* JCM7017 increased *Il10* (**Supplementary Figure 2A**), *Tnfa* (**Supplementary Figure 2B**), and *Il12a* (**Supplementary Figure 2D**) transcription. *B. breve* UCC2003 and its associated EPS$^-$ mutant showed a similar, non-significant trend for *Tnfa* and *Il12a* gene expression. EPS absence from *B. breve* UCC2003 increased Cd274 expression (**Supplementary Figure 2K**). No other significant differences were observed in the genes analyzed (**Supplementary Figures 2C,E–M**). Overall, this gene expression data indicate that the presence of EPS suppresses the expression of cytokine and co-stimulatory genes required for activation and maturation of dendritic cells in response to *B. breve* UCC2003 and JCM7017 strains.

B. breve EPS Blocks Antigen Specific Activation of CD4$^+$ T Cells by BMDCs

To further investigate how EPS impacts both the recognition and response of phagocytes to *B. breve* UCC2003 and JCM7017, an antigen presentation experiment was designed (Helft et al., 2015). *B. breve* UCC2003 and JCM7017 and their corresponding isogenic EPS$^-$ mutant strains were transformed with pMG-mCherry or pMG-mCherry OVA plasmid. FACS analysis validated expression of mCherry in the transformant bacteria (**Figure 6A** and **Supplementary Figure 3A**). Western blotting analysis confirmed that the bacteria expressed mCherry-OVA (**Figure 6B** and **Supplementary Figure 3B**). Bacterial growth profiles showed that strains were not seriously affected in any obvious manner by the presence of the plasmid (**Figures 6C,D**). Antigen presentation assays were set up as illustrated in **Figure 6E**. Sorted BMDCs were co-cultured with *B. breve* strains transformed or not with pMG-mCherry (used as negative control) or pMG-mCherry-OVA for 8 h. BMDCs were treated with OVA protein as a positive control. After this time, potential extracellular bacteria were killed with gentamicin and BMDCs were washed prior to co-culturing with OVA specific OT-II CD4$^+$ T cells for 5 days. T cell activation was determined by examining the numbers of proliferated (CFSE^{low}) CD25$^+$CD4$^+$ T cells. Flow cytometry analysis showed that the absence of EPS from both *B. breve* UCC2003 and JCM7017 significantly increased T cell activation (**Figure 6F** and **Supplementary Figure 4**). To investigate if EPS affected uptake of bacteria, BMDCs were co-cultured with *B. breve* UCC2003 strains transformed with pMG-mCherry. After this time, BMDCs were analyzed by Image Stream flow cytometry to identify and quantify uptake of bacteria by cells. *B. breve* UCC2003 EPS$^+$ and EPS$^-$ were detected inside CD45$^+$ (**Supplementary Figure 4B**). cells and no difference in similarity was observed between cells which had taken up these strains (**Supplementary Figure 4C**). To investigate persistence of viable *B. breve* UCC2003 and EPS$^-$ inside DCs, we co-cultured these bacteria with BMDCs for 2 h. Then, after a gentamicin step to kill extracellular bacteria, we lysed DCs at different time points and plated cell lysates on RCA plates (**Supplementary Figure 4D**). Colonies of *B. breve* UCC2003 were recovered at significantly higher levels compared to *B. breve* UCC2003 EPS$^-$ (**Supplementary Figure 4D**). Collectively, these results indicate that while EPS does not affect the uptake of bacteria by DCs, it does reduce processing and presentation of bacterial derived OVA antigen and activation of antigen specific CD4$^+$ T cells by DCs.

DISCUSSION

In this paper, we report on the production and immunomodulatory effects of EPS from a collection of human-isolated *B. breve* strains. EPS was produced differentially across a panel of strains and EPS status did not correlate with obvious

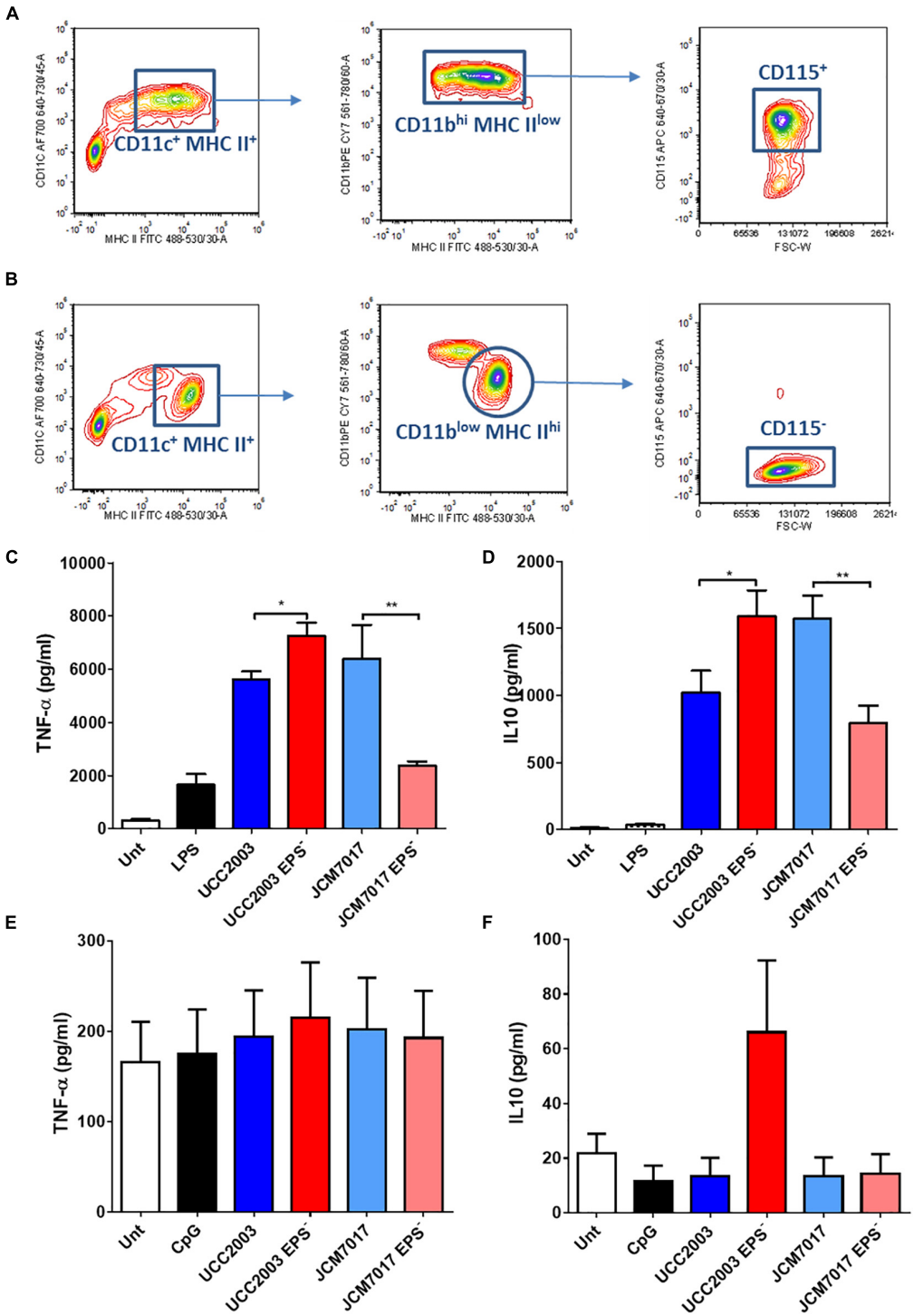

FIGURE 4 | Opposing effects of EPS on murine macrophage cytokine responses to *B. breve* strains. **(A,B)** Gating strategy to identify and sort BMDMs. The bone marrow cells were analyzed and sorted by multi-color flow cytometry. Cells were stained for MHC-II, CD11b, CD11c, and CD115. **(A)** For the adherent cells, MHC-II vs. CD11b contour plots were obtained by gating on MHC-II^{+}CD11c^{+} cells. Forward size scattered (FSC) vs. CD115 contour plots were obtained by gating on MHC-II^{low}CD11b^{high} cells. CD115^{+} cells were sorted and considered as pure macrophages population. **(B)** For the suspension cells MHC-II vs. CD11b contour plots were obtained by gating on MHC-II^{+}CD11c^{+} cells. FSC vs. CD115 contour plots were obtained by gating on MHC-II^{high}CD11b^{low} cells. CD115^{-} cells were sorted and considered as pure dendritic cells population. **(C,D)** TNF-α and IL10 secretion from BMDMs co-cultured with *B. breve* UCC2003, JCM7017 and their isogenic EPS^{-} mutants. **(E,F)** TNF-α and IL10 secretion from BMDCs co-cultured with B. breve UCC2003, JCM7017 and their isogenic EPS^{-} mutants. Cytokines were analyzed by ELISA. Data is the average of three independent experiments performed in triplicates. Statistical analysis was assessed using the student *t*-test in GraphPad Prism where **p*-value < 0.05 and ***p*-value < 0.005.

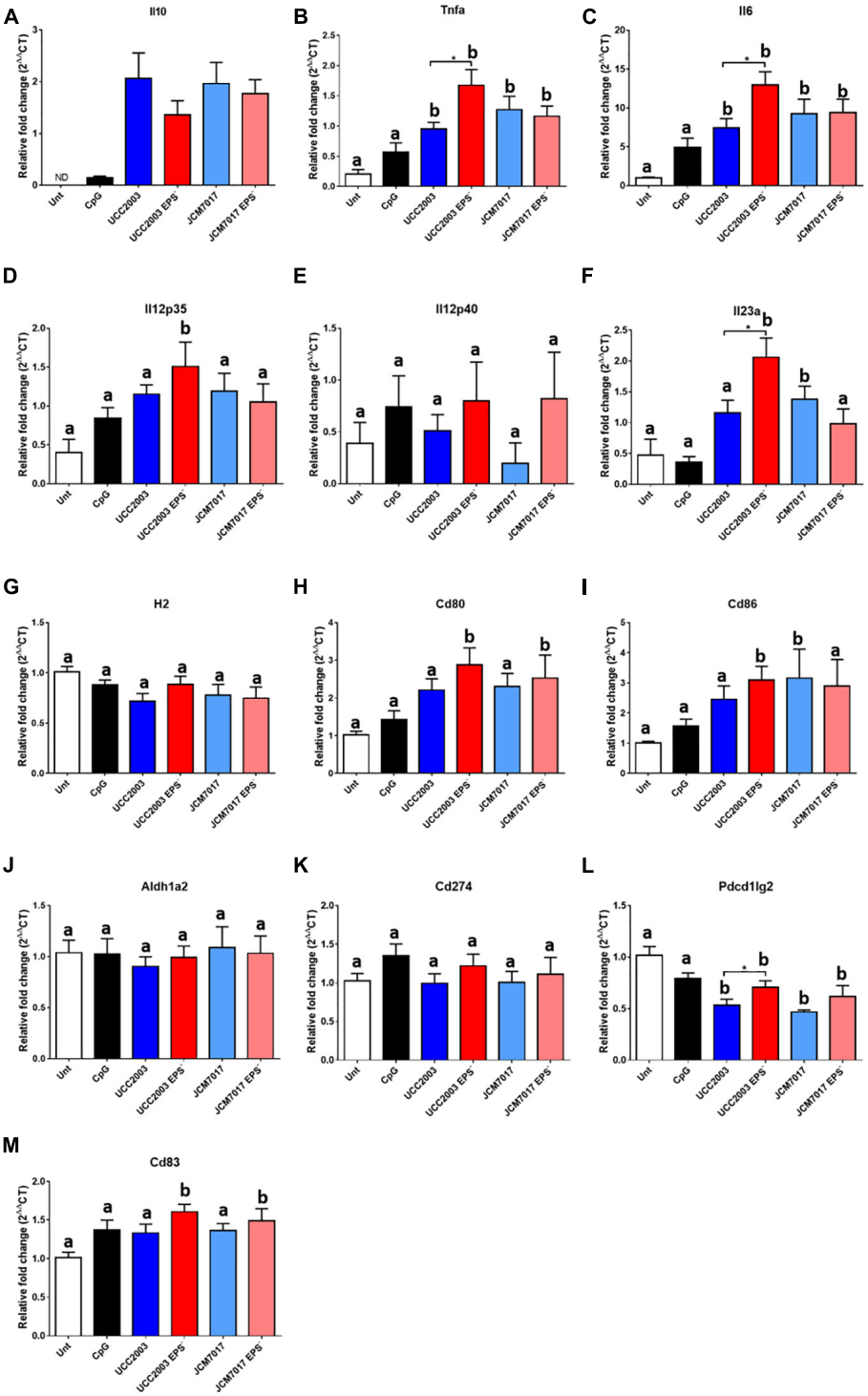

FIGURE 5 | EPS modulates the expression of immunomodulatory genes in BMDCs. Sorted BMDCs were co-cultured or not [untreated (Unt)] with *B. breve* strains as indicated (CpG was used as a positive control) for 4 h. RT-qPCR was carried out and the expression of **(A–F)** cytokine genes **(G–I)** antigen presentation and co-stimulatory genes and **(J–M)** tolerogenic genes were assessed. Expression changes are relative to β-actin. Data show the average of three independent experiments. Gene expression differences between the groups were compared first with the untreated control. Different letters (a and b) indicate statistical difference for each presented gene expression. Letter a indicates no statistical difference between the indicated group and the untreated control, letter b indicates significant differences between the indicated group and the untreated control ($p < 0.05$ of Dunnett's test). Then, the student *t*-test was used to compare wild type Bifidobacteria (both UCC2003 and JCM7017) with their isogenic EPS mutants (*p-value < 0.05 and **p-value < 0.005).

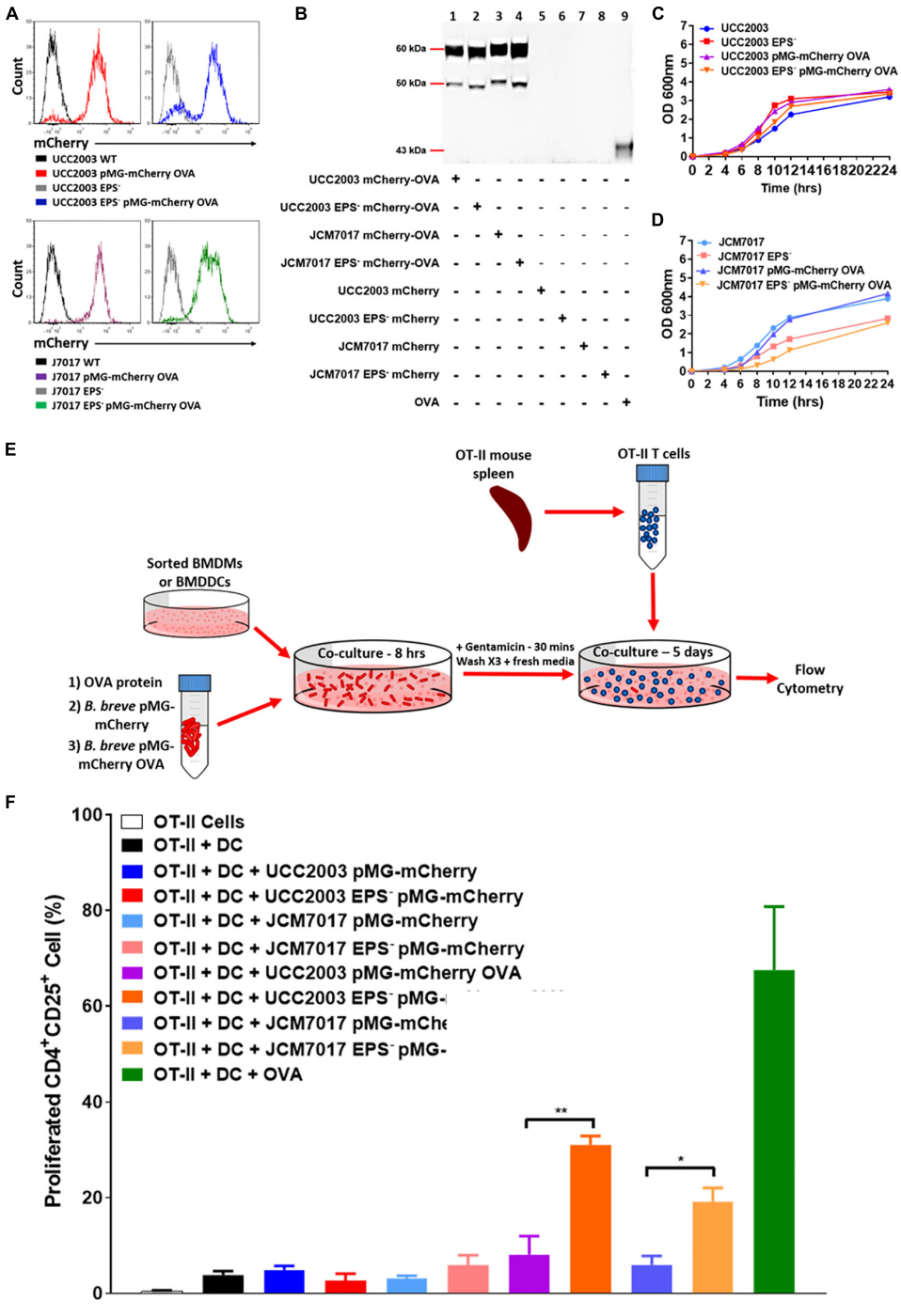

FIGURE 6 | EPS protects from antigen presentation of *B. breve* to OT-II CD4$^+$ T cells by DCs. **(A)** mCherry expression (pMG-mCherry OVA) in the indicated *B. breve* strains by flow cytometry. Histograms were obtained by gating on bacterial cells. Black and gray histograms were obtained from parental *B. breve* UCC2003 and JCM7017 wild type or EPS$^-$. Red and blue histograms were obtained from *B. breve* UCC2003 wt and *B. breve* UCC2003 EPS$^-$ transformed with the plasmid pMG-mCherry OVA. Purple and green histograms were obtained from *B. breve* JCM7017 wt and *B. breve* JCM7017 EPS$^-$ transformed with the plasmid pMG-mCherry OVA. **(B)** Western blot for OVA protein production by pMG-mCherry-OVA and pMG-mCherry transformed strains of *B. breve* as indicated. 0.025 μg of ovalbumin was used as a positive control. **(C,D)** Growth curves of strains transformed or untransformed with the pMG-mCherry-OVA plasmid over 24 h. Growth curves are representative of three experiments. **(E)** Schematic of the antigen presentation assay setup. **(F)** Sorted BMDCs were co-cultured or not with different bacterial strains expressing or not OVA (as indicated) for 8 h. OVA protein was used as positive control. mCherry only expressing bacteria were used as negative controls. Cells were then co-cultured with OT-II CD4$^+$ T cells for 5 days and analyzed by multi-color flow cytometry. T cells were stained for CD4, CD25, and CFSE. Percentage of proliferated CD4$^+$CD25$^+$ OT-II T cells was quantitated and presented as mean ± SEM. Data is the average of three independent experiments performed in triplicate wells. Statistical analysis was assessed using the student *t*-test in GraphPad Prism where $^*p$-value < 0.05 and $^{**}p$-value < 0.005.

immunomodulatory effects in a series of immune cell-based assay systems. However, *B. breve* EPS was required for suppression of gene expression associated with and required for full maturation of DCs. Consistent with this, EPS was necessary to prevent processing and presentation of antigen from the strains and antigen-specific activation of $CD4^+$ T cells by DCs. Overall, we have identified a new immunomodulatory role for EPS which indicates that EPS is utilized by *B. breve* for immune evasion perhaps as a mechanism to promote host-microbe mutualism.

The panel of *B. breve* strains screened appeared to represent a near equal number of EPS producers and non-producers. Heterogeneity in EPS production has been noted before for bifidobacteria and, taking into account the fact that the genes of EPS biosynthesis loci have a lower GC content than the average bifidobacterial genome, it is proposed that some species and strains acquired the ability to produce EPS by horizontal gene transfer (Hidalgo-Cantabrana et al., 2014; Ferrario et al., 2016). By assessing the phenotypic production of EPS by a panel of *B. breve* strains in different carbohydrate sources, we were able to identify consistent EPS producers and non-producers and compare this phenotypic behavior to *in silico* analysis. The carbohydrate source has previously been shown to impact on EPS production in both lactobacilli (Raftis et al., 2011) and bifidobacteria (Audy et al., 2010). For example lactose induced the highest production of the glycan in *B. longum* subsp. *longum* CRC 002 compared to glucose, galactose, and fructose (Audy et al., 2010) and perhaps this is because lactose itself is a source of glucose and galactose, the two major constituents of EPS in the strain. In addition to carbon source, EPS composition and production can be impacted by other environmental factors such as O_2, bacterial growth phase, temperature and pH (Degeest et al., 2001). Therefore, it is possible that strains that were phenotypically negative for EPS production in glucose, lactose and maltose-containing medium may be positive under different growth conditions. For example, *B. breve* 139W4 was predicted to produce EPS but did not do so in any of the prepared media under the experimental conditions used. It is possible that it is an EPS producer but that the growth conditions used were not optimal for EPS biosynthesis in this strain. Similarly, this may explain why *B. breve* NCTC 11815 sedimented as an EPS non-producer in glucose and lactose but not in maltose. A screen of bifidobacterial type strains showed that of the 48 (sub)species, 56% were EPS producers, 21% were non-producers and 23% displayed an intermediate phenotype (Ferrario et al., 2016). This variability could also be altered by growth in different media but the mechanistic reasons for this have yet to be explored.

When we assayed for immunomodulatory effects of EPS we found that NF-κB activation in THP-1 monocytes did not correlate with EPS status. This may be due to differences between EPS structures and/or composition of the EPS producers or the presence/absence of other MAMPs involved in triggering NF-κB responses. The fact that there was strain-specific modulation rather than EPS-associated modulation is not entirely surprising as strain-specific effects have been characterized for bifidobacteria (López et al., 2010, 2011, 2012). EPS from *Lactobacillus plantarum* can act in a TLR2-dependent manner to activate signal transducer and activator of transcription 3 (STAT3) independently of NF-κB (Zhou et al., 2018). It is certainly possible that there may be other mononuclear phagocyte responses to these strains which were not investigated here and that are associated with EPS status. In our study the TLR signaling adaptor MyD88 was necessary to activate the NF-κB pathway by all *B. breve* strains tested. This was not entirely surprising considering previous studies linking bifidobacterial immunomodulation to the TLR family and MyD88 (Jeon et al., 2012; Schiavi et al., 2018; Verma et al., 2018; Castro-Bravo et al., 2019). The absence of EPS from both *B. breve* UCC2003 and JCM7017 drove different cytokine responses by BMDMs. While the absence of EPS from *B. breve* UCC2003 increased the production and secretion of IL10 and TNF-α from BMDMs at 24 h the opposite effect was observed for responses to EPS deficient *B. breve* JCM7017 with decreased production and secretion of IL10 and TNF-α detected. It is possible that EPS acts as a cloaking MAMP, reducing the exposure of other bacterial MAMPs on the same cell to PRRs, or even that it shields other MAMPs completely. Any of these scenarios could explain why EPS from *B. breve* UCC2003 appears to modulate more anti-inflammatory effects while EPS from *B. breve* JCM7017 appears to induce more pro-inflammatory effects. It would be useful to understand the composition and structure of *B. breve* UCC2003 EPS in order to compare to the already characterized EPS of *B. breve* JCM7017 (Alhudhud et al., 2018), although TEM images did show significant differences in EPS density between the two strains with *B. breve* UCC2003 having a thicker EPS layer. However, a pure population of sorted BMDCs did not produce IL10 or TNF-α at all to *B. breve* UCC2003 or JCM7017 after 24 h of exposure. BMDCs generated and FACS purified using the approach by Helft et al. (2015) demonstrate a tolerogenic phenotype (Vander Lugt et al., 2017), and represent a pure population of DCs with no contaminating macrophages. This might explain why they did not show an obvious inflammatory response to our *B. breve* strains.

Because we detected EPS-dependent differences in cytokine response of BMDMs to *B. breve* UCC2003 and JCM7017, we analyzed the expression of a panel of immune genes in BMDMs and BMDCs co-cultured with the strains to further understand how EPS can modulate phagocyte immune responses. Our data indicates that both phagocyte populations sensed the presence of the bacteria and responded through PRR-mediated signaling pathways and transcriptional mechanisms to alter gene expression. In BMDCs, the absence of EPS from *B. breve* UCC2003 but not from JCM7017, significantly increased *Tnfa, Il6, and Il23a* expression after 4 h co-culture and decreased, *H2*/MHC-II, *Pdcd1lg2*/PD-L2, and *Cd83* expression after 8 h co-culture. The absence of EPS from *B. breve* JCM7017, but not from *B. breve* UCC2003, significantly increased *Il10* and *Il23a* expression after 8 h co-culture. Significantly, in BMDCs the absence of EPS increased the expression of genes for co-stimulatory molecules (*Cd80, Cd86* for UCC2003 and *Cd83* for both UCC2003 and JCM7017) typically associated with maturation of DCs. This data is consistent with similar suppressive effects of EPS on expression

of cytokine genes (*Il12a/Il12p35* and *Il23a/Il12p19*) associated with T cell differentiation and with suppression of T cell activation in our co-culture antigen presentation assay. In BMDMs, the absence of EPS in *B. breve* UCC2003 increased the expression of *Cd274* and the absence of EPS from *B. breve* JCM7017, but not from *B. breve* UCC2003, increased *Il10, Tnfa*, and *Il12a* expression after 8 h. Indeed, we noted an interesting discrepancy in BMDMs between cytokine (*Il10*/IL10 and *Tnfa*/TNF-α) protein data at 24 h and gene expression data at 8 h in response to the EPS deficient JCM7017 strain. While the strain increased *Il10* and *Tnfa* gene expression at 8 h it decreased IL10 and TNF-α cytokine production at 24 h. This curious finding may have an underlying biological mechanism associated with it that is particular to the JCM7017 EPS$^-$ strain and the kinetics of BMDM response to this strain. There is evidence in the literature of similar discrepancies and disconnect between cytokine mRNA expression and protein production and secretion. For example in the context of Crohn's disease it has been reported that despite macrophages showing normal levels and stability of cytokine mRNA intracellular levels of the protein and secretion were abnormally low (Smith et al., 2009). Interestingly, the WT *B. breve* JCM7017 strain did not induce *Il12b*/IL12p40 transcription at all in BMDMs. *Il12b*/IL12p40 encodes a subunit that can be used in conjunction with *Il12a*/IL12p35 to generate the IL-12 cytokine (an important inducer of T_H1 differentiation) or dimerise with *Il23a*/IL23p19 to create the IL-23 cytokine (an inducer for T_H17 differentiation). *Il12b*/IL12p40 can alternatively homodimerise to induce macrophage chemotaxis or encourage primed DC migration (Cooper and Khader, 2007). The fact that *B. breve* JCM7017 did not induce expression of the *Il12b*/IL12p40 subunit in BMDMs implies that the bacteria may not support differentiation of T_H1 or T_H17 T cells. It also implies that EPS is responsible for controlling this as the EPS$^-$ mutant upregulated the expression of *Il12b*/IL12p40 in BMDMs.

We used mCherry-Ova expressing *B. breve* UCC2003 and JCM7017 strains in a co-culture antigen presenting assay to investigate if BMDCs were able to present bacterially expressed antigens to T cells, or if they were just unresponsive to the tested bacterial strains. Although T cell activation was increased by both EPS$^-$ mutants expressing OVA, the *B. breve* UCC2003 EPS$^-$ mcherry-OVA strain induced stronger T cell activation than the *B. breve* JCM7017 EPS$^-$ mcherry-OVA strain. This suggests that EPS is more important for *B. breve* UCC2003 to avoid triggering T cell responses than it is for *B. breve* JCM7017. This observation also ties in with a previous report that the absence of EPS from *B. breve* UCC2003 increased T cell numbers from splenocytes cultured with the bacteria (Fanning et al., 2012). It appears that EPS in different strains may be involved in different functions, possibly because of differences in EPS composition and production. Indeed, higher molecular weight EPS is implicated in better bacterial survival but also reduces traits such as host cell adhesion and aggregation with other bacteria (Yu et al., 2019) and so there may be a trade-off between bacterial fitness and ability to affect cell–cell interactions with host and neighbors. This is possibly the reason for the heterogeneity in EPS production observed, even between EPS producers such as *B. breve* UCC2003 and JCM7017. The absence of EPS from these two strains revealed that it modulates host immune cell responses differently by the two strains but that it also elicits similar functions such as prevention of antigen presentation by BMDCs to T cells. While use of isogenic EPS$^-$ mutants offers a potential advantage over the use of purified EPS, observed responses to the bacteria did not clarify if the effect is directly because of the EPS binding a PRR, shielding other MAMP/MAMPs, altering binding affinity of other MAMPs to PRRs, reduction of intra-cellular processing of the bacteria through the phagolysosome or a combination of the above. Certainly EPS is able to shield MAMPs as an EPS$^-$ mutant of *Lactobacillus rhamnosus* GG revealed that the bacteria produced sortase-dependent pili on its surface (Lebeer et al., 2009) and a similar observation was made for *B. longum* 105-A (Tahoun et al., 2017). Additionally, it has been shown that while purified EPS from *B. animalis* subsp. *lactis* triggers TLR4 activation, the whole bacteria itself activates TLR2, TLR2/1 and TLR2/6 (Castro-Bravo et al., 2019). Our study shows that while EPS production was heterogeneous amongst human-isolated *B. breve* strains; EPS from *B. breve* UCC2003 and JCM7017 had similar effects on maturation and antigen presentation function of BMDCs. It is important to acknowledge that the biochemical composition and density of EPS observed in both WT strains may contribute to the differences observed in BMDM and BMDCs immune responses. Further detailed biochemical, molecular and cell-based investigations are required to understand the biochemistry and immunological effects of different EPS structures and their effects on dendritic cell biology. Our observations suggest that EPS may contribute to an important immunomodulatory effect of *B. breve* strains by blocking activation and antigen presentation function of DCs. This would allow these strains to manipulate DCs for immunomodulatory effects promoting immune evasion and host-microbe mutualism by these gut symbionts.

DATA AVAILABILITY STATEMENT

The original contributions generated for this study are included in the article/**Supplementary Material**, further inquiries can be directed to the corresponding authors.

ETHICS STATEMENT

Use of animals for this study was reviewed and approved by Animal Experimentation Ethics Committee of University College Cork.

AUTHOR CONTRIBUTIONS

VR, DV, SM, and KN: conceptualization. AH, VR, PS, SU, AR-V, ME-T, and FB: methodology and writing – original draft. AH, VR, PS, and AR-V: validation. AH, VR, PS, AR-V, JW, and OH: formal analysis. AH, VR, PS, SU, and AR-V: investigation. MV, DV, SM, and KN: resources. AH, VR, PS, and

AR-V: data curation. AH, VR, and KN: writing – review and editing. AH, VR, PS, and AR-V: visualization. KN, SM, and DV: supervision. KN: project administration. DV and KN: funding acquisition. All authors contributed to the article and approved the submitted version.

FUNDING

This work was supported by grants from Science Foundation Ireland – namely a research center grant (SFI-12/RC/2273) to APC Microbiome Ireland.

ACKNOWLEDGMENTS

We would like to acknowledge and thank the Flow Cytometry Platform, APC Microbiome Ireland located at University College Cork for assistance with flow cytometry analysis.

SUPPLEMENTARY MATERIAL

The Supplementary Material for this article can be found online at: https://www.frontiersin.org/articles/10.3389/fmicb.2021.653587/full#supplementary-material

REFERENCES

Alhudhud, M., Sadiq, S., Ngo, H., Hidalgo-Cantabrana, C., Ruas-Madiedo, P., Van Sinderen, D., et al. (2018). Extraction of the same novel homoglycan mixture from two different strains of *Bifidobacterium animalis* and three strains of *Bifidobacterium breve*. *Benef. Microbes* 9, 663–674. doi: 10.3920/bm2017.0145

Audy, J., Labrie, S., Roy, D., and LaPointe, G. (2010). Sugar source modulates exopolysaccharide biosynthesis in *Bifidobacterium longum* subsp. longum CRC 002. *Microbiology* 156, 653–664. doi: 10.1099/mic.0.033720-0

Bottacini, F., Morrissey, R., Esteban-Torres, M., James, K., van Breen, J., Dikareva, E., et al. (2018). Comparative genomics and genotype-phenotype associations in *Bifidobacterium breve*. *Sci. Rep.* 8:10633.

Bottacini, F., Morrissey, R., Roberts, R. J., James, K., van Breen, J., Egan, M., et al. (2017). Comparative genome and methylome analysis reveals restriction/modification system diversity in the gut commensal *Bifidobacterium breve*. *Nucleic Acids Res.* 46, 1860–1877. doi: 10.1093/nar/gkx1289

Bottacini, F., O'Connell Motherway, M., Kuczynski, J., O'Connell, K. J., Serafini, F., Duranti, S., et al. (2014). Comparative genomics of the *Bifidobacterium breve* taxon. *BMC Genomics* 15:170. doi: 10.1186/1471-2164-15-170

Castro-Bravo, N., Margolles, A., Wells, J. M., and Ruas-Madiedo, P. (2019). Exopolysaccharides synthesized by *Bifidobacterium animalis* subsp. lactis interact with TLR4 in intestinal epithelial cells. *Anaerobe* 56, 98–101. doi: 10.1016/j.anaerobe.2019.02.014

Castro-Bravo, N., Sánchez, B., Margolles, A., and Ruas-Madiedo, P. (2018a). "Biological activities and applications of Bifidobacterial Exopolysaccharides: from the bacteria and host perspective," in *The Bifidobacteria and Related Organisms*, eds P. Mattarelli, B. Biavati, W. H. Holzapfel, and B. J. B. Wood (Amsterdam: Academic Press), 177–193. doi: 10.1016/b978-0-12-805060-6.00010-7

Castro-Bravo, N., Wells, J. M., Margolles, A., and Ruas-Madiedo, P. (2018b). Interactions of Surface Exopolysaccharides From *Bifidobacterium* and *Lactobacillus* within the intestinal environment. *Front. Microbiol.* 9:2426. doi: 10.3389/fmicb.2018.02426

Cooper, A. M., and Khader, S. A. (2007). IL-12p40: an inherently agonistic cytokine. *Trends Immunol.* 28, 33–38. doi: 10.1016/j.it.2006.11.002

De Man, J. C., Rogosa, M., and Sharpe, M. E. (1960). A medium for the cultivation of lactobacilli. *J. Appl. Bacteriol.* 23, 130–135. doi: 10.1111/j.1365-2672.1960.tb00188.x

Degeest, B., Vaningelgem, F., and De Vuyst, L. (2001). Microbial physiology, fermentation kinetics, and process engineering of heteropolysaccharide production by lactic acid bacteria. *Int. Dairy J.* 11, 747–757. doi: 10.1016/s0958-6946(01)00118-2

Fanning, S., Hall, L. J., Cronin, M., Zomer, A., MacSharry, J., Goulding, D., et al. (2012). Bifidobacterial surface-exopolysaccharide facilitates commensal-host interaction through immune modulation and pathogen protection. *Proc. Natl. Acad. Sci. U.S.A.* 109, 2108–2113. doi: 10.1073/pnas.1115621109

Ferrario, C., Milani, C., Mancabelli, L., Lugli, G. A., Duranti, S., Mangifesta, M., et al. (2016). Modulation of the eps-ome transcription of bifidobacteria through simulation of human intestinal environment. *FEMS Microbiol. Ecol.* 92:fiw056. doi: 10.1093/femsec/fiw056

Fischbach, M. A. (2018). Microbiome: focus on causation and mechanism. *Cell* 174, 785–790. doi: 10.1016/j.cell.2018.07.038

Grimm, V., Gleinser, M., Neu, C., Zhurina, D., and Riedel, C. U. (2014). Expression of fluorescent proteins in bifidobacteria for analysis of host-microbe interactions. *Appl. Environ. Microbiol.* 80, 2842–2850. doi: 10.1128/aem.04261-13

Helft, J., Böttcher, J., Chakravarty, P., Zelenay, S., Huotari, J., Schraml, B. U., et al. (2015). GM-CSF mouse bone marrow cultures comprise a heterogeneous population of CD11c+ MHCII+ macrophages and dendritic cells. *Immunity* 42, 1197–1211. doi: 10.1016/j.immuni.2015.05.018

Hidalgo-Cantabrana, C., Algieri, F., Rodriguez-Nogales, A., Vezza, T., Martínez-Camblor, P., Margolles, A., et al. (2016). Effect of a ropy exopolysaccharide-producing *bifidobacterium animalis* subsp. lactis strain orally administered on DSS-Induced colitis mice model. *Front. Microbiol.* 7:868. doi: 10.3389/fmicb.2016.00868

Hidalgo-Cantabrana, C., Sánchez, B., Milani, C., Ventura, M., Margolles, A., and Ruas-Madiedo, P. (2014). Genomic overview and biological functions of exopolysaccharide biosynthesis in *Bifidobacterium* spp. *Appl. Environ. Microbiol.* 80, 9–18. doi: 10.1128/aem.02977-13

Inturri, R., Molinaro, A., Di Lorenzo, F., Blandino, G., Tomasello, B., Hidalgo-Cantabrana, C., et al. (2017). Chemical and biological properties of the novel exopolysaccharide produced by a probiotic strain of *Bifidobacterium longum*. *Carbohydr. Polym.* 174, 1172–1180. doi: 10.1016/j.carbpol.2017.07.039

Jeon, S. G., Kayama, H., Ueda, Y., Takahashi, T., Asahara, T., Tsuji, H., et al. (2012). Probiotic *Bifidobacterium breve* Induces IL-10-Producing Tr1 Cells in the Colon. *PLoS Pathog.* 8:e1002714. doi: 10.1371/journal.ppat.1002714

Lebeer, S., Verhoeven, T. L. A., Francius, G., Schoofs, G., Lambrichts, I., Dufrêne, Y., et al. (2009). Identification of a gene cluster for the biosynthesis of a long, galactose-rich exopolysaccharide in *Lactobacillus rhamnosus* GG and functional analysis of the priming glycosyltransferase. *Appl. Environ. Microbiol.* 75, 3554–3563. doi: 10.1128/aem.02919-08

Leivers, S., Hidalgo-Cantabrana, C., Robinson, G., Margolles, A., Ruas-Madiedo, P., and Laws, A. P. (2011). Structure of the high molecular weight exopolysaccharide produced by *Bifidobacterium animalis* subsp. lactis IPLA-R1 and sequence analysis of its putative eps cluster. *Carbohydr. Res.* 346, 2710–2717. doi: 10.1016/j.carres.2011.09.010

Livak, K. J., and Schmittgen, T. D. (2001). Analysis of relative gene expression data using real-time quantitative PCR and the $2^{-\Delta\Delta CT}$ method. *Methods* 25, 402–408. doi: 10.1006/meth.2001.1262

López, P., González-Rodríguez, I., Gueimonde, M., Margolles, A., and Suárez, A. (2011). Immune response to *Bifidobacterium* bifidum strains support Treg/Th17 plasticity. *PLoS One* 6:e24776. doi: 10.1371/journal.pone.0024776

López, P., Gueimonde, M., Margolles, A., and Suárez, A. (2010). Distinct *Bifidobacterium* strains drive different immune responses in vitro. *Int. J. Food Microbiol.* 138, 157–165. doi: 10.1016/j.ijfoodmicro.2009.12.023

López, P., Monteserín, D. C., Gueimonde, M., de los Reyes-Gavilán, C. G., Margolles, A., Suárez, A., et al. (2012). Exopolysaccharide-producing *Bifidobacterium* strains elicit different in vitro responses upon interaction with human cells. *Food Res. Int.* 46, 99–107. doi: 10.1016/j.foodres.2011.11.020

Mar, J. C., Kimura, Y., Schroder, K., Irvine, K. M., Hayashizaki, Y., Suzuki, H., et al. (2009). Data-driven normalization strategies for high-throughput quantitative RT-PCR. *BMC Bioinformatics* 10:110. doi: 10.1186/1471-2105-10-110

McCall, M. N., McMurray, H. R., Land, H., and Almudevar, A. (2014). On non-detects in qPCR data. *Bioinformatics* 30, 2310–2316. doi: 10.1093/bioinformatics/btu239

Raftis, E. J., Salvetti, E., Torriani, S., Felis, G. E., and O'Toole, P. W. (2011). Genomic diversity of *Lactobacillus salivarius*. *Appl. Environ. Microbiol.* 77, 954–965. doi: 10.1128/aem.01687-10

Riedel, C. U. (2018). "Chapter 13 - clinical significance of bifidobacteria," in *The Bifidobacteria and Related Organisms*, eds P. Mattarelli, B. Biavati, W. H. Holzapfel, and B. J. B. Wood (Cambridge, MA: Academic Press), 221–234. doi: 10.1016/b978-0-12-805060-6.00013-2

Round, J. L., Lee, S. M., Li, J., Tran, G., Jabri, B., Chatila, T. A., et al. (2011). The toll-like receptor 2 pathway establishes colonization by a commensal of the human microbiota. *Science* 332, 974–977. doi: 10.1126/science.1206095

Round, J. L., and Palm, N. W. (2018). Causal effects of the microbiota on immune-mediated diseases. *Sci. Immunol.* 3:eaao1603. doi: 10.1126/sciimmunol.aao1603

Sarkar, A., and Mandal, S. (2016). Bifidobacteria—Insight into clinical outcomes and mechanisms of its probiotic action. *Microbiol. Res.* 192, 159–171. doi: 10.1016/j.micres.2016.07.001

Schiavi, E., Gleinser, M., Molloy, E., Groeger, D., Frei, R., Ferstl, R., et al. (2016). The surface-associated exopolysaccharide of *Bifidobacterium longum* 35624 plays an essential role in dampening host proinflammatory responses and repressing local TH17 responses. *Appl. environ. Microbiol.* 82, 7185–7196. doi: 10.1128/aem.02238-16

Schiavi, E., Plattner, S., Rodriguez-Perez, N., Barcik, W., Frei, R., Ferstl, R., et al. (2018). Exopolysaccharide from *Bifidobacterium longum* subsp. longum 35624^{TM} modulates murine allergic airway responses. *Benef. Microbes* 9, 761–773. doi: 10.3920/bm2017.0180

Sivan, A., Corrales, L., Hubert, N., Williams, J. B., Aquino-Michaels, K., Earley, Z. M., et al. (2015). Commensal *Bifidobacterium* promotes antitumor immunity and facilitates anti–PD-L1 efficacy. *Science* 350, 1084–1089. doi: 10.1126/science.aac4255

Smith, A. M., Rahman, F. Z., Hayee, B., Graham, S. J., Marks, D. J., Sewell, G. W., et al. (2009). Disordered macrophage cytokine secretion underlies impaired acute inflammation and bacterial clearance in Crohn's disease. *J. Exp. Med.* 206, 1883–1897. doi: 10.1084/jem.20091233

Tahoun, A., Masutani, H., El-Sharkawy, H., Gillespie, T., Honda, R. P., Kuwata, K., et al. (2017). Capsular polysaccharide inhibits adhesion of *Bifidobacterium longum* 105-A to enterocyte-like Caco-2 cells and phagocytosis by macrophages. *Gut Pathog.* 9:27.

Turroni, F., Milani, C., Van Sinderen, D., and Ventura, M. (2018). "Chapter 12 - bifidobacteria: ecology and coevolution with the host," in *The Bifidobacteria and Related Organisms*, eds P. Mattarelli, B. Biavati, W. H. Holzapfel, and B. J. B. Wood (Cambridge, MA: Academic Press), 213–220. doi: 10.1016/b978-0-12-805060-6.00012-0

Vander Lugt, B., Riddell, J., Khan, A. A., Hackney, J. A., Lesch, J., DeVoss, J., et al. (2017). Transcriptional determinants of tolerogenic and immunogenic states during dendritic cell maturation. *J. Cell Biol.* 216, 779–792. doi: 10.1083/jcb.201512012

Verma, R., Lee, C., Jeun, E. J., Yi, J., Kim, K. S., Ghosh, A., et al. (2018). Cell surface polysaccharides of *Bifidobacterium bifidum* induce the generation of Foxp3(+) regulatory T cells. *Sci. Immunol.* 3:eaat6975.

Yu, R., Zuo, F., Ma, H., and Chen, S. (2019). Exopolysaccharide-Producing *Bifidobacterium* adolescentis strains with similar adhesion property induce differential regulation of inflammatory immune response in Treg/Th17 Axis of DSS-Colitis Mice. *Nutrients* 11:782. doi: 10.3390/nu11040782

Zhou, X., Qi, W., Hong, T., Xiong, T., Gong, D., Xie, M., et al. (2018). Exopolysaccharides from *Lactobacillus plantarum* NCU116 regulate intestinal barrier function via STAT3 signaling pathway. *J. Agric. Food Chem.* 66, 9719–9727. doi: 10.1021/acs.jafc.8b03340

Conflict of Interest: OH is employed by the company Luminex Corporation which manufactures the Amnis ImageStream flow cytometer used in this study.

The remaining authors declare that the research was conducted in the absence of any commercial or financial relationships that could be construed as a potential conflict of interest.

Advantages of publishing in Frontiers

OPEN ACCESS
Articles are free to read for greatest visibility and readership

FAST PUBLICATION
Around 90 days from submission to decision

HIGH QUALITY PEER-REVIEW
Rigorous, collaborative, and constructive peer-review

TRANSPARENT PEER-REVIEW
Editors and reviewers acknowledged by name on published articles

Frontiers
Avenue du Tribunal-Fédéral 34
1005 Lausanne | Switzerland

Visit us: www.frontiersin.org
Contact us: frontiersin.org/about/contact

REPRODUCIBILITY OF RESEARCH
Support open data and methods to enhance research reproducibility

DIGITAL PUBLISHING
Articles designed for optimal readership across devices

FOLLOW US
@frontiersin

IMPACT METRICS
Advanced article metrics track visibility across digital media

EXTENSIVE PROMOTION
Marketing and promotion of impactful research

LOOP RESEARCH NETWORK
Our network increases your article's readership